ISSN 2663-0419 (Online)
ISSN 2218-8754 (Print)

AZERBAIJAN NATIONAL ACADEMY OF SCIENCES

ANAS TRANSACTIONS

EARTH SCIENCES

www.journalesgia.com

2024
№1

Buraxılışına məsul: **Hafiz Abıyev**

Dizayn/Qrafika: **Kərim Nəbiyev**
Xəlil Nəbiyev

Veb-redaktor: **Tofiq Rəşidov**

Jurnal Azərbaycan MEA Geologiya və Geofizika İnstitutunda yığılmış və səhifələnmişdir

* * *

Responsible for the issue: **Hafiz Abiyev**

Design/Graphycs: **Karim Nabiyev**
Khalil Nabiyev

Web-editor: **Tofig Rashidov**

This journal has been prepead at the Geology and Geophysics Institute of Azerbaijan National Academy of Sciences

* * *

Ответственный за выпуск: **Хафиз Абиев**

Дизайн/графика: **Керим Набиев**
Халил Набиев

Веб-редактор: **Тофиг Рашидов**

Журнал набран и сверстан в Институте геологии и геофизики НАН Азербайджана

* * *

Ünvan: AZ1001, Bakı şəhəri, İstiqlaliyyət küçəsi 30, "ANAS Transactions, Earth Sciences"

Address: "ANAS Transactions, Earth Sciences" 30, Istiglaliyyat str., Baku, Azerbaijan, AZ1001

Адрес: AZ1001, г. Баку, Истиглалият, 30. Редакция "ANAS Transactions, Earth Sciences"

* * *

İcraçı redaktorlar: **A.A.İsrafilova, C.S.Qurbanova**
Executive Editors: **A.A.Israfilova, J.S.Gurbanova**
Исполнителные редакторы: **А.А.Исрафилова**
Дж.С.Курбанова

ELM NƏŞRİYYATI

Formatı: 60x84$^{1/8}$. Həcmi: 29 ç.v.
Tirajı: 300 nüsxə

Akif Alizade -90th
Happy Anniversary
Congratulations!

ANAS Transactions Earth Sciences 1 / 2024

http://www.journalesgia.com

DIFFICULT ASCENT TO THE PEAKS OF SCIENCE

Academician Akif Ali-Zadeh is known in Azerbaijan and far beyond its borders not only for his unique scientific achievements in the field of paleontology and other earth sciences, but also for his extensive scientific and organizational activity as director of the Institute of Geology and Geophysics of the National Academy of Sciences of Azerbaijan (1976 – present, currently Institute of Geology and Geophysics of the Ministry of Science and Education of Azerbaijan Republic) and President of the Azerbaijan National Academy of Sciences (2013-2019). The initial stage of this activity (1976-1990) became a real school for the young scientist at that time, who was appointed head of the largest Institute in the system of the Academy of Sciences at the age of 42 (!).

There were no ordinary lessons and textbooks in this "school", they were replaced by daily live communication with employees during which Akif Ali-Zadeh learned to listen to people and delve into their problems, no matter how insignificant they may seem at first glance, use any opportunities for providing them the necessary help and support, look for optimal ways out of occurring conflict situations, unite supporters around himself filling them with his inexhaustible enthusiasm, sparkle a favorable creative environment in the team, defend his position with arguments avoiding the use of dictate and volitional decisions, accept and analyze constructive criticism, admit and correct his mistakes and so on. This is how the talent inherent in today's leader of geological science of attentive and friendly attitude to the people around him was formed. His "philosophy of life"[1] was formed in such conditions.

It was a marvelous time, which is not by chance now called the "golden age of science", because it was then that the most important discoveries were made in the world science and after it in the "great Soviet science", which had a noticeable impact on the development of geological science.

It was necessary to intensify the creative process, concentrate the efforts of the team of scientists in priority (primarily interdisciplinary) directions, create new scientific schools and supply them with modern equipment, train new personnel, etc. in order to stay on track with the ongoing changes. All these issues were constantly in view of the head of the Institute – Akif Ali-Zadeh.

It was not only a difficult but also a very interesting time whereas during this period Akif Ali-Zadeh was lucky to work with many luminaries of the geological science of Azerbaijan. He remembers his teachers: academicians Musa Mirzoevich Aliyev, Azal Jafarovich Sultanov, Aliashraf Abdulguseinovich Alizade, Shamil Abduragimovich Azizbekov, Gambay Asgarovich Alizade, Shafayat Farkhadovich Mehdiyev, Edhem Shakhlarovich Shikhalibayli, Mirali Saidovich Kashkai, Abdulhamid Yusifovich Khalilov and others with special warmth and gratitude noting their help, valuable advice, constant support and friendly attitude towards him.

But, in fairness, it should be noted that, there were also detractors among the people surrounding Akif Ali-Zadeh which (either out of envy or from other motives) created artificial obstacles on his path.

Definitely, any leader can take decisive and even tough measures against such people in such situations to stop their slanderous fabrications. But Akif Ali-Zadeh as a human of honor is not capable of this. *"Personal honor, he says, is determined not so much by the individual's ability to tolerate insults and offences as by his inability to insult and offend anyone."*

This is how he has always been acting proving his ill-wishers his place and role in science on the obtained results among which we note the following: the discovery of a new family of belemnoids named after him – *Akifibelidae* (not many scientists receive such recognition!), determination of paleotemperatures in the Cretaceous basins of the Caucasus by the method of isotope paleothermometry, studying the mineral and geochemical composition of the Cretaceous belemnites in Azerbaijan, etc.

But the real test fell to Akif Ali-Zadeh in the early 90s of the last century, when the Soviet Union collapsed, established ties with the specialized scientific organizations of the former Soviet Republics that became independent states were broken, the amount of state budget funding of scientific research was sharply decreased, and the outflow of highly qualified personnel began and so on. During these

[1] Abbasova R. Philosophy of life (interview with Ak.A.Ali-Zadeh). "Kaspiy", May 30, 2015.

troubled times, some pseudo-patriots appeared from somewhere and called for "closing the Academy as an unnecessary appendage of the Soviet past". Akif Ali-Zadeh was among those who resolutely came to its defense. Based on knowledge and deep understanding of the trends in the development of world science, he urged: "*It is necessary not to close the Academy, but to reform and gradually develop the system of organizing fundamental scientific research, adapting it to the conditions of a market economy"*. These words testify a deep understanding of the role of science in modern society, its influence on the course of inevitable reforms in a market economy, and the necessity for progressive development in priority areas, one of which is science.

It should be admitted that in those years (the first years of independence of the Republic of Azerbaijan) there was not yet an appropriate regulatory and legal framework of laws, strategies, state programs, action plans, etc. for the progressive development of science. All these have already appeared in the next century. In the meantime, complete uncertainty has remained in the system of organizing scientific research gradually "corroding" like corrosion the creative potential of the Academy of Sciences especially among young specialists. Akif Ali-Zadeh – a scientist deeply devoted to science could not remain indifferent to such situation, so, it was necessary to find a way out of the situation. And he did everything possible to find and demonstrate how and in what directions basic science should develop in the near future.

Once Academician A.E.Fersman quite rightly remarked: "*One of the biggest challenges of science is its ability to predict and anticipate*". Akif Ali-Zadeh undoubtedly has such a talent based on high intelligence and extensive scientific outlook. This was especially clearly manifested in the project of the first national Concept of organization of Fundamental Scientific Research (FSR) in the Republic of Azerbaijan (hereinafter referred to as Concept' 92)[2] developed in 1992 on his initiative and direct participation, and in a number of articles published later in periodicals touching on key aspects of this Concept – state support of science, forms and financing mechanism of scientific research, the creation of a regulatory and legal framework for science, the development of international scientific cooperation, the introduction of scientific achievements (in modern interpretation – the development of mastering the innovative scientific developments), etc. It is interesting to note that many of the scientist's proposals expressed by him, in particular, in the fundamentally important article "What kind of Academy does Azerbaijan need?"[3] were reflected in one form or another in the conceptual document for domestic science "National Strategy for the Development of Science in the Republic of Azerbaijan for the period of 2009-2015 and the State Program for the implementation of this Strategy" (approved by Order of the President of the Republic of Azerbaijan, May 4, 2009, No. 255) and in a number of other program documents and regulatory and legal acts. Some of them will be briefly considered below on specific examples.

Sources of scientific research funding

The main source of funding of science was (and remains today) state budgetary funding, the various forms of which were not written clearly enough anywhere (in any official documents) for a long time. Akif Ali-Zadeh proposed to divide the state budgetary funding of science into two "channels" to eliminate this uncertainty in 1992: the channel of basic funding of large institutes, centers and other scientific infrastructure facilities and the channel of program-targeted allocations (in modern interpretation – The Targeted Funding Program) of research projects and programs of national importance[4], while the second channel also included grants allocated by state funds (which did not exist at that time!) to finance initiative scientific projects on a competitive basis.

24 years later (i.e. in 2016), the Law of the Republic of Azerbaijan "On Science" was adopted, in which the forms of state financing of scientific and scientific-technical activities in Article 34.4 were defined as follows: Basic Financing, The Targeted Financing Program and Grant Funding. The only difference between this article and the scientist's previously expressed proposal is the allocation of grant funding as a separate line, although this does not change the essence of the matter.

Akif Ali-Zadeh initiated the development of four state programs at the Institute of Geology and Geophysics, which were approved by the Cabinet of Ministers of the Republic of Azerbaijan (see: Resolutions of the Cabinet of Ministers of the Republic of Azerbaijan, June 18, 2007, No. 98; January 23, 2008, No. 22s; August 22, 2008, No. 299s; July 31, 2014, No. 236s) and were successfully implemented over the period of 2007 - 2018 following the principle "Test your ideas in practice to make sure they

[2] Ali-Zadeh Ak.A., Ibrahimov V.B. Organization of basic scientific research in the Republic of Azerbaijan: main directions of reform (Project Concept). "Elm", No. 11, 1992.

[3] Ali-Zadeh Ak.A. What kind of Academy does Azerbaijan need? "Bakinskiy Rabochiy" No. 48, 2001.

[4] Ali-Zadeh Ak.A., Ibrahimov V.B. "Lifesaver" for science. "Vishka", September 29, 1992.

work" within the channel "The Targeted Financing Program of Scientific Research" for the first time in the system of the Azerbaijan National Academy of Sciences. Akif Ali-Zadeh had already created a new Department "Coordination of innovative projects" related to the "grant financing" within the structure of the Institute of Geology and Geophysics in 2001 with information and methodological support of which the Institute's employees received about 150 grants from government funds (Science Development Foundation under the President of the Republic of Azerbaijan, Scientific Foundation under SOCAR), as well as foreign funds such as CRDF, INTAS, CARIPLO, DEFRA, SDC, NSF, WOTRO, etc.

But is the state budget the only source of funding for scientific research? "No, it is not," Akif Ali-Zadeh convinces. He notes the significant share of private companies in the total amount of funding for scientific research analyzing foreign experience and decides to use this factor anticipating an interest of the western oil companies in the development of oil and gas fields in the Azerbaijani sector of the Caspian Sea. A group of highly qualified specialists of the Institute began working with the alliance of "BP-Statoil" (Great Britain - Norway) companies providing for joint scientific research (with the financial support of the alliance) in the field of studying geology and geochemistry of mud volcanoes, as well as biostratigraphy of the Neogene of Azerbaijan and, in particular, the South Caspian basin in 1992 before the sign of the famous "Contract of the Century" on Akif Ali-Zadeh's initiative. Hereafter the Institute carried out more than 50 works (!) on a contract basis for such oil companies as *ConocoPhilips*, *Statoil*, *ChevronTexaco*, *ExxonMobil*, *Shell*, *Unocal*, *Total*, *Elf*, *Agip*, *Lukoil*, etc. over the next two decades. All this made it possible not only to stabilize the financial situation of the Institute at certain stages, but also to accumulate invaluable experience in business interaction with similar western companies, as well as significantly expand the knowledge and practical skills of individual employees who have become real experts of the European level in the relevant fields of oil and gas geology.

The gradual transition from predominantly state to decentralized (multiple) funding of scientific research and development began from this period which was predicted by Akif Ali-Zadeh.

Commercialization in the scientific and technical field

Akif Ali-Zadeh urged scientists to learn how to earn money themselves e.g., using various forms of entrepreneurial activity noting the limited and constantly decreasing amount of state budget funding for science (it amounts to 0.1-0.2% of GDP in Azerbaijan, and fluctuates between 2-5% of GDP while abroad). He wrote in the above-mentioned Concept' 92 back in the early 90s of the last century: "The new organizational structure of the Academy of Sciences should include commercial subdivisions intended to create a specific "nutrient medium" for the interaction of science and subjects of a market economy. This includes well-established *technology parks* in other countries, as well as small forms of entrepreneurial activity in the scientific and technical field – small and medium-sized enterprises, consulting, marketing, intermediary, information and other service firms forming a network of so-called "*small research business*". As expected, numerous skeptics objected: they say that scientists should only be concerned with obtaining new knowledge, and let businessmen and their commercial structures deal with entrepreneurship. But Akif Ali-Zadeh stood firm in his position and was right. The right of scientists and specialists of scientific organizations and universities to engage in scientific entrepreneurial activities were clearly established in the Article 38 of the Law of the Republic of Azerbaijan "On Science" adopted in 2016. Hereafter the Resolution of the Cabinet of Ministers of the Republic of Azerbaijan, June 20, 2017, No. 266 specified the types of entrepreneurial activities allowed for research institutes, – production and sale of high-tech products, consulting services, laboratory tests (analyses) on a paid basis, information services, carrying out scientific research based on orders, etc. It is not difficult to see that all these types cover the above-mentioned "small research business".

But Akif Ali-Zadeh considered that the creation of larger structures – technology parks is the most perspective organizational form of integration of science and production for the purpose of development (commercialization) of scientific achievements. In his article "Science on the Path to the Market" published in 1993[5], he confidently stated: "I consider it is advisable to immediately begin preparations for the creation of the first of them in Azerbaijan (at least as an experiment) on the basis of the Academy of Sciences". This proposal of the scientist remained unclaimed for a long time until 2016 when High Technology Park of the Azerbaijan National Academy of Sciences was created by Order of the President of the Republic of Azerbaijan, November 8, 2016, No. 2425. Thus, Akif Ali-Zadeh's this prediction based on deep knowledge of the trends in the development of world science in a market economy came true.

[5] Ali-Zadeh Ak. A., Ibrahimov V.B. Science on the path to the market. "Bakinskiy Rabochiy", March 13, 1993.

Possessing a pronounced innovative mindset, Akif muallim foresaw the innovative path of development of Azerbaijan and prepared for it: "I see a way out of the current situation (with the development and commercialization of scientific developments)," he said in 2001, "on the way of transition (of the institutes of the Academy of Sciences) to active innovation." And this "transition" began with the creation of the first specialized Department "Coordination of innovative projects" at the Institute of Geology and Geophysics in the system of Azerbaijan National Academy of Sciences, where four innovative projects were developed by the employees of the Institute in a short time. The final product of one of them, "Atlas of lithologic-paleogeographical maps of the territory of Azerbaijan and the Azerbaijani sector of the Caspian Sea" was acquired by BP (British Petroleum). Thus, it was proven that the scientific developments of the Institute of an innovative nature can be of not only scientific, but also commercial interest.

Academician Akif Alizadeh turned 90 years. But, despite such a venerable age he does not stop and continues the "difficult ascent to the peaks of science". He is still full of new ideas and plans. And we believe that they will all realize.

d.t.s. Vagif Ibrahimov

ANAS Transactions **Earth Sciences** **1 / 2024**

http://www.journalesgia.com

CURRENT STATUS OF PALEONTOLOGICAL-STRATIGRAPHIC STUDIES IN AZERBAIJAN*

Alizadeh Ak.A.

Ministry of Science and Education of the Republic of Azerbaijan,
Institute of Geology and Geophysics,
119, H.Javid ave., Baku, AZ1143

Keywords: *Paleontology, stratigraphy, Azerbaijan, Productive Series, climato-stratigraphic scheme, Azykh*

Summary. The history of the study of fossil paleontological remains in Azerbaijan is divided into several stages depending on the degree of research intensity, the scale of stratigraphic coverage, and the participation of national personnel. In the 50-80s of the twentieth century, the priority was to unite specialists according to age groups of fossil remains (e.g., Jurassic ammonites, Cretaceous inoceramas, ammonites and belemnites, Paleogene nummulites, Miocene pelecypods, etc.). Later, by the end of the nineties of the last century, the priorities of fundamental research shifted somewhat to the study of ecosystem evolution, paleobiology, event biostratigraphy, etc.

Such coryphees as academicians: M.M.Aliyev, G.A.Alizadeh, professors A.G.Khalilov, D.M.Khalilov, D.A.Agalarova stood at the origins of development of paleontological and stratigraphic researches in Azerbaijan. Activity of these scientists was accompanied by rapid development of paleontological and stratigraphic ideas, study of invertebrate fossil fauna, phytofossils (including nanofossils). Thus, by the end of the twentieth century, almost all archistratigraphic groups of fauna, their evolution, as well as paleoecological, paleobiological, paleobiogeochemical and other aspects of their habitat conditions had already been studied in detail.

As they say today, it really was the "golden age" of science, including paleontological and stratigraphic one. The main actor of this progress in science and its practical affairs, of course, was a researcher – an expert in his field, and only highly qualified personnel of Azerbaijani paleontological and stratigraphic science dynamically raised the bar of its achievements higher and higher. Among them are prominent paleontologists: T.A.Gasanov, K.M.Sultanov, H.Aliulla, B.G.Vekilov, A.B.Abbasov, R.G.Babaev, Sh.A.Babaev, M.R.A. Abdulkasumzadeh, G.A.Aliev, R.A.Aliev, R.O.Koshkarly, R.N.Mamedzadeh, O.B.Aliev, E.Z.Ataeva, H.Sh.Aliyev and others.

Thus, the wide scope of fundamental paleontological and stratigraphic research allowed Azerbaijani scientists to create a serious paleontological and stratigraphic base of geological research in Azerbaijan. The continuation of the systematic and systematic development of the regional geological study of the territory of Azerbaijan ultimately led to the creation of a fundamental formation-stratigraphic and geochronological basis, based on a set of modern methods and achievements in the field of paleontology, stratigraphy, isotope geochronology, facies-paleogeographic analysis and historical and geological synthesis.

For over thirty years of the independence, Azerbaijani scientists have travelled a difficult and complex path in the field of paleontological and stratigraphic research. 1990s were marked by a stagnation experienced by all activity spheres of the country, including politics, culture, education, and science. The scientific sector of Azerbaijan, including academic studies, had unexpectedly become challenged by a number of difficulties, such as the shortage of funding, the outflow of talented young researchers, the transition of adventurous people to the business sector, and the breakage of ties with research organizations and scientists in Russia and the CIS countries. In general, the Azerbaijani science lived a deep crisis in the last decade of the 20th century. In their efforts to overcome the emerging problems, the local scientists, of course, including geologists-paleontologists, tried to maintain cooperation with their colleagues from the post-Soviet states, and to gain new partners overseas. Both efforts aimed at the integration with global scientific community – fundamental purpose of the national science of that period.

* Paper presented during LXX Anniversary Session of the Paleontological Society of Russia, 2024

Historians will probably more accurately determine the formation period, development stages and the "Golden Age" of the geological and paleontological science of Azerbaijan. In our opinion, the paleontological-stratigraphic research in Azerbaijan reached its' peak in the second half of the 20th century, when, through the efforts of several generations of specialists, the main features of the dynamics of paleontological and stratigraphic studies had been formulated. Based on these fundamental achievements, the local paleontologists and stratigraphers established a standard stratigraphic basis for large-scale geological surveys, deep and ultra-deep (Saatli well) formation drilling in the region (Alizade et al., 1999).

Moreover, rapid development of the national oil industry at that period also occurred thanks to the efforts of the Azerbaijani geologists, with essential contribution of paleontologists and stratigraphers. Starting from the hard times of 1990s, local researchers have managed to intensify the integration process of the Azerbaijani paleontological-stratigraphic science into the world scientific network. With signing of the "Contract of the Century" in 1994, new opportunities were created for a joint work with the world's largest oil corporations, such as British Petroleum, Unocal, Exxon, Shell, Amoco, Mobil, Statoil, Total, Agip, etc.

For the Azerbaijani geologists, stratigraphers and paleontologists this was a breakthrough into the international research auditorium. During this period, a relatively small team of scientists, mostly young specialists, completed over 50 research projects in geology, oil and gas problems, geochemistry and, of course, paleontology and stratigraphy. Joint desktop and field studies, followed by the analysis and interpretation of the produced data at the different foreign scientific centres and universities, have made it possible to quickly learn new research methods, software and standards used in the Western countries on the one hand, and to intensify training of local scientists on the other.

Historically, increased attention paid since the 1930-40s to the paleontological and stratigraphic research in Azerbaijan was primarily associated with the growing demands of oil-gas search and exploration. This had determined stricter requirements set against stratigraphic-paleontological studies implemented using various complex methodologies. You are all well aware that the territory of Azerbaijan has diverse geological and tectonic evolution record, resulting in the emergence of the Absheron Peninsula, Caspian shelf, Middle Kur Depression (Fig. 1) and the other world-famous oil and gas provinces.

The list of the pioneers of the Azerbaijani paleontology and stratigraphy contains the names of such famous scientists as academicians Musa Aliyev, Aliashraf Alizadeh, Gambay Alizadeh, Professors Dunya Agalarova, Jalil Khalilov, Damir Gadjiyev and others (Fig. 2).

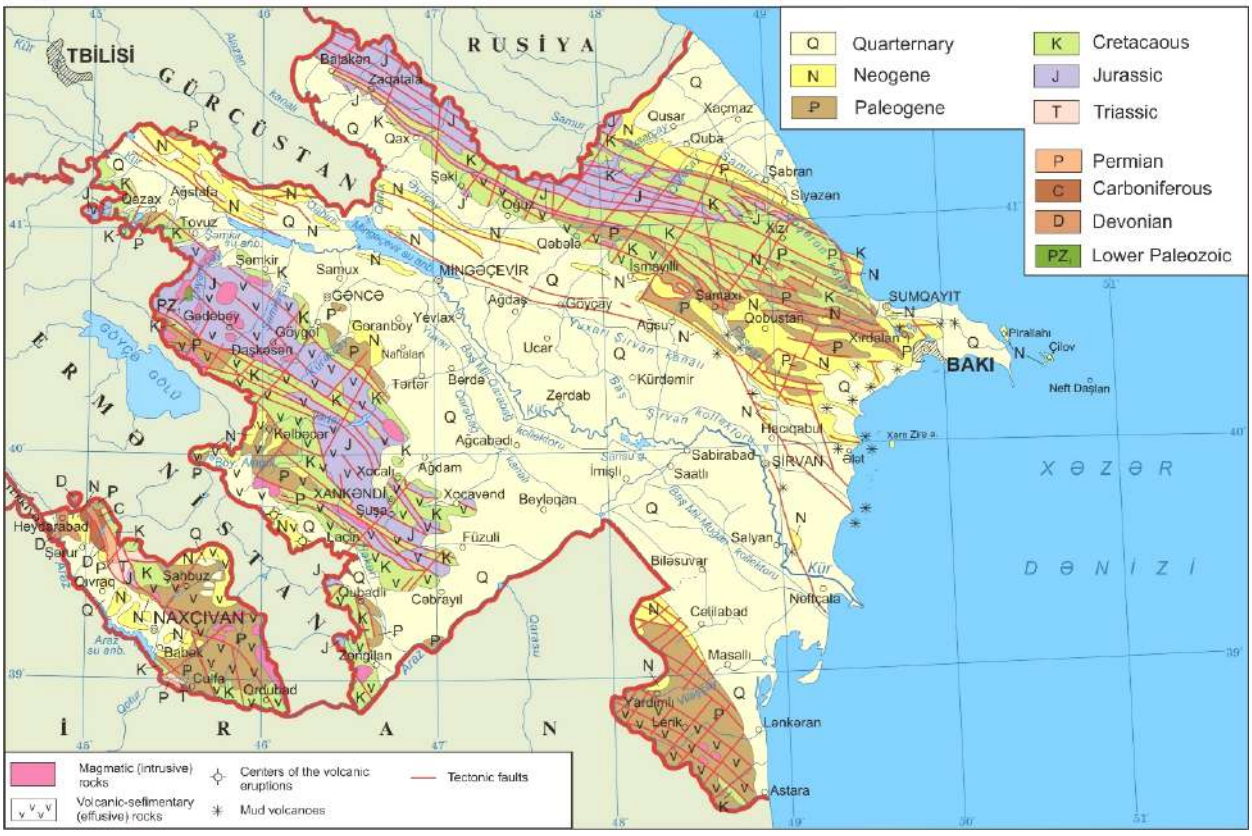

Fig. 1. Geological map of Azerbaijan

Fig. 2. The famous palaeontologists of Azerbaijan: 1 – Musa Aliyev; 2 – Aliashraf Alizadeh; 3 – Gambay Alizadeh; 4 – Dunya Agalarova; 5 – Jalil Khalilov; 6 – Damir Gadjiyev

Over the course of 70 years of the history of the Soviet Azerbaijan, local scientists conducted fundamental scientific research and published important findings in the fields of the Phanerozoic paleontology and stratigraphy (mollusks, brachiopods, foraminifera, ostracods, spores-pollen, etc.). Great contribution to the formation and development of this research area in Azerbaijan had been made by the outstanding Russian and Soviet scientists, such as I.M.Gubkin, N.B.Vassoevich, V.V.Weber, V.V.Bogachev, D.V.Nalivkin, Yu.A.Orlov, B.S.Sokolov, V.I.Zhamoida, N.P.Luppov, V.V.Drushchits, V.A.Vakhrameev, V.I.Kacharava, L.Sh.Davitashvili, etc. Regional stratigraphers compiled stratigraphic schemes of different-scale geological surveys which had covered the entire territory of Azerbaijan.

These schemes (Халилов, 1978) were developed based on the results of complex studies implemented by the Azerbaijani macro- and micropaleontologists. These scientists developed detailed reference sections of the Devonian, Cretaceous, Paleogene and Neogene stratigraphy of the Lesser and Greater Caucasus systems. Also, they prepared detailed stratigraphic schemes (up to the identification of faunal zones) of the Mesozoic, Paleogene and Neogene sequences of both systems (Ализаде Ак.А., 1972; Ализаде К.А., 1977; Алиюлла, 1970, 1977; Халилов и др., 1973; Халилов, Ализаде Ак.А., 1970; Касимова, 1970; Ализаде, Мамедов, 1970 a, b; Ализаде, Гаджиев, 1975; Бабаев, 1970). Another important achievement of the Azerbaijani stratigraphers was the creation of a biostratigraphic scheme of the country's Quaternary deposits. The Azerbaijani scientists have published the results of important studies dedicated to the micromorphology of foraminifers, ostracods, mollusks, brachiopods and pollen spores (Мамедов, 1992; Векилов, 1969, 1962; Атаева, 2007; Агаларова и др., 1961; Джабарова, 1967; Джафарова, 2006; Касумова, 1966). Using scanning electron microscope (SEM) in the carried-out investigations helped identify new micromorphological features and trace onto-phylogeny of the morphological elements of a number of studied micropaleontological groups of the fauna, such as ostracods, nanoplankton, etc. (Koshkarly, Mamedova, 1997).

Analysis of the micromorphological evolution of various micropaleontological fauna groups allowed establishing the taxonomic rank of the studied signs which had represented a value for the stratigraphy of oil and gas deposits.

In 1990s, the Institute of Geology of Azerbaijan had continued biostratigraphic studies of the main oil-gas deposits. In particular, investigation of the Neogene deposits of the Eastern Azerbaijan and the South Caspian basin has provided evidences to an assumption that the basement of the Productive Series should be located at a glacio-eustatically low sea level. Study of the Azerbaijan's famous Pliocene Productive Series which contains about 26 billion barrels of the oil equivalent, allowed characterizing its' stratotype section covering the time interval between 3.4 Ma (upper boundary) and 5.5 Ma (lower boundary) (Fig. 3).

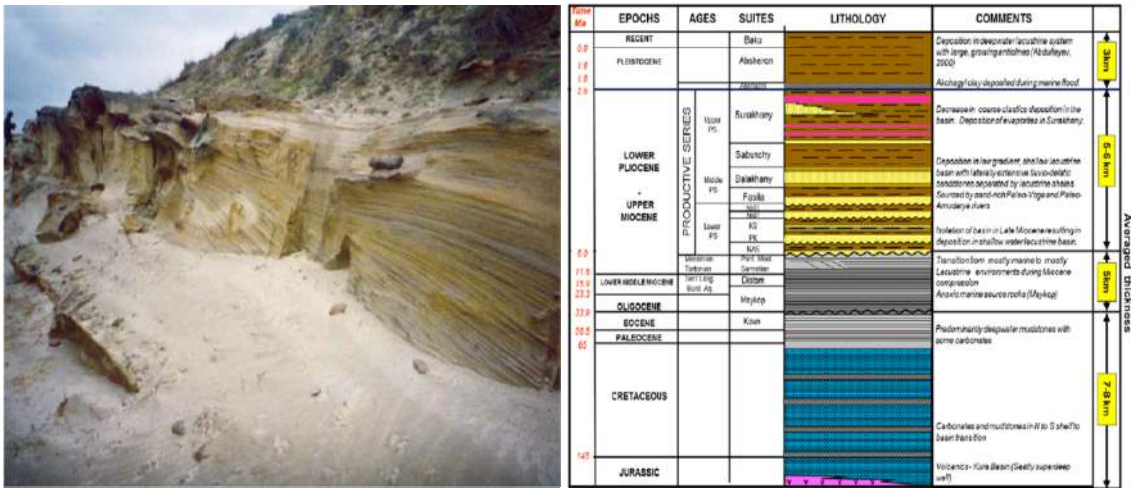

Fig. 3. Kirmaky section, Stratotype of Productive Series of Azerbaijan.
Stratigraphic column for South Caspian Basin (Javanshir et al., 2014)

The study outcomes were summarized in a monograph "Productive Series of Azerbaijan" (Ализаде и др., 2018, Vol. 1, 2).

The Paleogene of Azerbaijan has been sufficiently studied. The stratigraphic division of the Paleogene deposits is based on macrofauna, plankton foraminifers and nanofossils (more than 10 biozones of the standard Martini's scale (Martini, 1970) have been discovered in Azerbaijan). Several detailed nano-zone sequences have been identified among Eocene and Oligocene deposits. The biostratigraphic studies of Neogene, Paleogene and Cretaceous formation were implemented based on a program developed in Azerbaijan back in 1978 for the biostratigraphic studies of the calcareous nanofossils. Several interesting papers on nanofossils were published in 1990, such as "Regional Paleogene stratigraphic scheme of the Azerbaijan" (Ализаде К.А. и др., 1989), "Biostratigraphic and stratigraphic Atlas of the Cretaceous, Paleogene, Neogene, and Quaternary strata of Azerbaijan and South Caspian basin" (Koshkarly, Mamedova, 1997), "Geology of Azerbaijan. Stratigraphy. Volumes 1, 2" (2007), "Geosciences of Azerbaijan" (Alizadeh et al., 2016).

Special mention should be made of a radiometric scale of the Azerbaijan's Late Cenozoic, developed by Azerbaijani specialists in close collaboration with scientists and specialists of St. Petersburg State University specialized in absolute geochronology. These studies brought significant clarifications into the understanding of the Neogene stratigraphy of Azerbaijan and the Caspian region (Fig. 4), dating the Pontian regiostage as Upper Miocene, and the Productive Series as Lower Pliocene deposits (Чумаков и др., 1988 a, b).

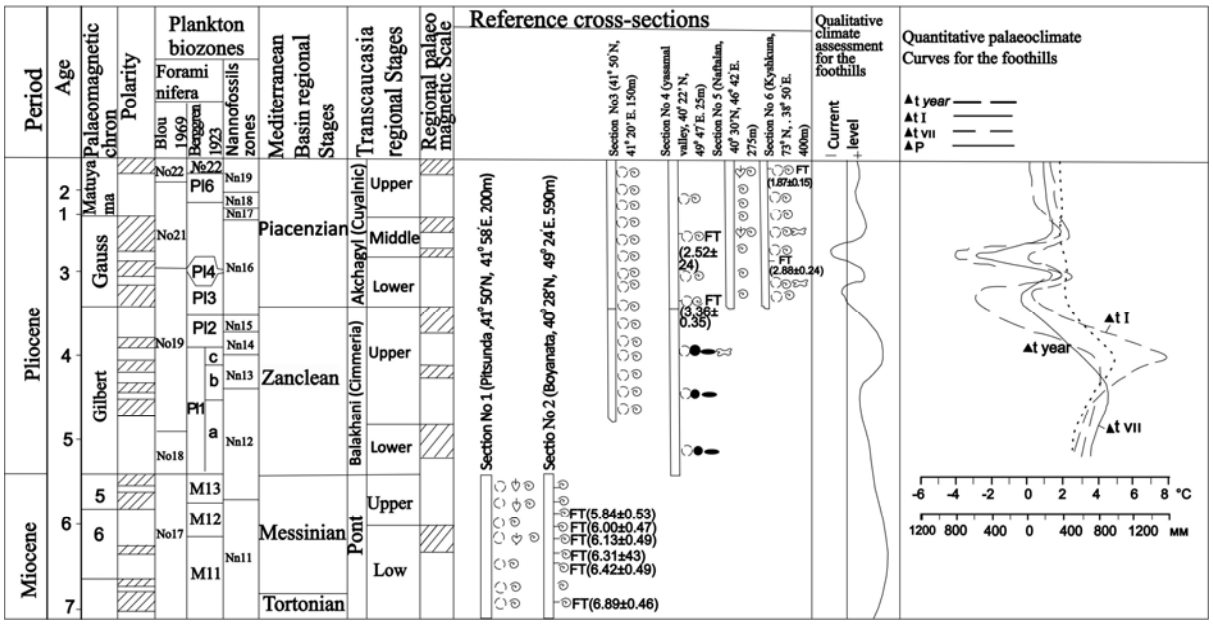

Fig. 4. Chronostratigraphic scale of Pliocene of South Caucasus (Мамедов, 1991)

Based on the latest data on the origin of the Caspian Sea and the formation of its main structures, 18 paleogeographic maps were compiled and included in the zootomic atlas "Paleogeographic atlas of shelf regions of Eurasia for the Mesozoic and Cenozoic shelves of Eurasia" (Атлас палеогеографических карт, 1992).

Many works of the Azerbaijani paleontologists are devoted to Quaternary period of Azerbaijan (2.5 Ma). This interest is due to a decisive role of this period in the formation of modern Earth's surface. As is known, the Quaternary period is generally very contrasting due to sharp climatic transformations (Fig. 5), multiple continental glaciation events and repeated changes in landscape and climatic belts of the region.

The data produced as a result of many years of the studies had made it possible to develop a Pleistocene climate-stratigraphic division chart of the Caspian Sea and correlate it with the paleogeographic events of the Black Sea and the European continent. Azerbaijani specialists have revealed a close connection between the Quaternary transgressions and regressions of the Caspian Sea and the climatic events in the northern latitudes. It has been established that the scale of the Caspian Sea's transgression and regression, as well as of the glaciation area of the East European Plain, tends to decrease from more ancient

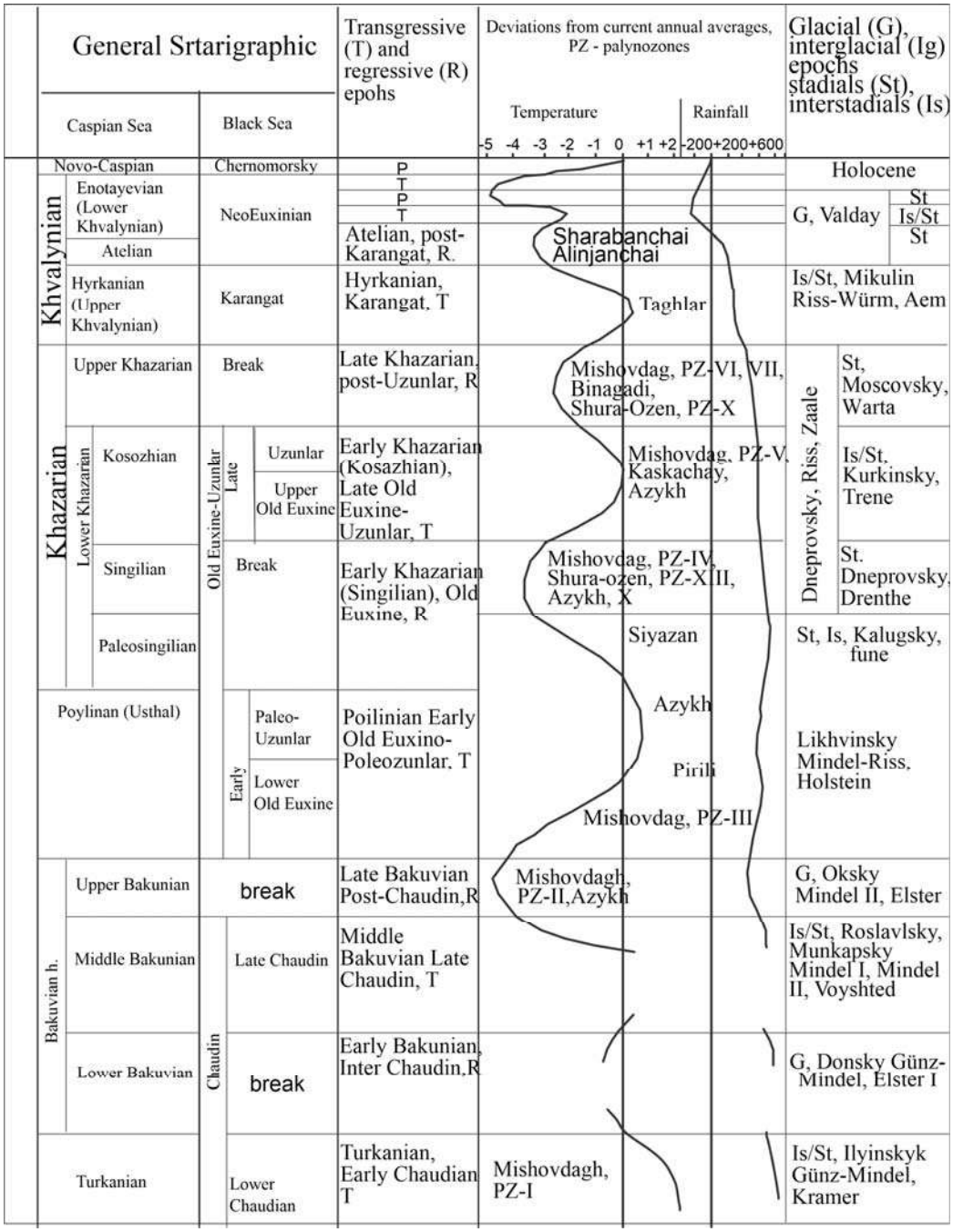

Fig. 5. Climatostratigraphic scheme of the Caspian Sea Pleistocene (Велиев и др., 2004)

to more recent epochs. Generalization of accumulated factual material on macro- (remains and imprints) and micro- (pollen and spores) remains of the plants playing a leading role in the interpretation of paleolandscape and paleoclimatic reconstructions, made it possible to identify the main evolution stages of landcover and climate for the territories of the Caucasus (Early epochs of the Cenozoic – Eocene, Oligocene, Miocene) and Azerbaijan (Late Cenozoic – Pliocene, Pleistocene). 1:2500000 scale vegetation maps were compiled for individual chronological sections of the Cenozoic era, 8 of which were included in the National Atlas of Azerbaijan (Tağıyeva və b., 2014).

Restored landscapes formed due to the climatic changes of the Pleistocene interglacial periods, provide valuable information about changes in modern landscape components and can be used to make climate change and anthropogenic intervention based forecasts. These studies resulted in preparing and publishing of the "Palaeontological Atlas of Quaternary Systems of Azerbaijan" (2017). Serving as a summary of the past studies, the Atlas presented results of the stratigraphical study of Azerbaijan's Quaternary deposits based on the analysis of macro- and microfauna remains of Pleistocene and Holocene.

Another noteworthy important international initiative pursuing the study of Azerbaijan paleogeography was implemented within the framework of the program "The dynamics of the interaction between the Natural environment and Primitive Man" (Беличко и др., 1980; Гаджиев и др., 1979; Мамедов и др., 1982; Сулейманов, 1979, 1982). The basis for carrying out these studies was laid back in 1960s by a discovery of the Paleolithic men's sites (Damdzhily, Azykh, Taglar) in the territory of the Garabagh region of Azerbaijan. Azykh site is a unique archaeological monument illustrating more than 1 Ma of the Paleolithic Human evolution in a single cave complex. Discussions about it continue to this day. Located at one of the migration routes of the *Homo erectus* from Africa to Europe, the Garabagh region surpasses all other parts of the South Caucasus in terms of the number of discovered archaeological sites. Today, prehistorical sites of the Lesser Caucasus region are studied together by paleogeographers and archaeologists from the Azerbaijan National Academy of Sciences, and the scientists from Japan and Germany. The research project called "Absolute and relative chronology of the Neolithic monuments of Garabagh" is implemented together with the German Archaeological Institute.

Within the Cenozoic Era, the Neogene (Miocene and Pliocene) are the two most interesting periods in the history of the Earth's evolution. Azerbaijani scientists have implemented comprehensive palaeobotanical (spores-pollen, dinoflagellates, diatoms) and microfaunistic studies of marine sediments on the western flange of the South Caspian Basin (part of the Eastern Paratethys), in order to elaborate on and clarify its' stratigraphy (Fig. 6) (Байрамова и др., 2021).

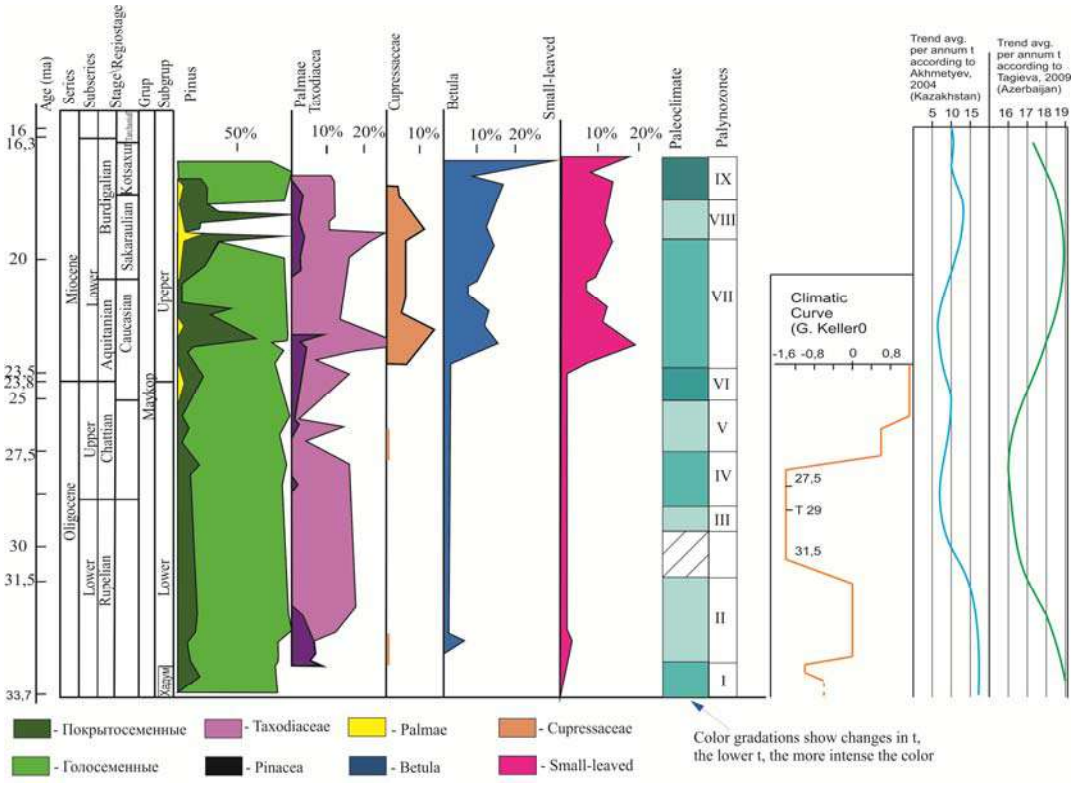

Fig. 6. Changes in the paleogeographic conditions of the Maykop time of the Shamakhi-Gobustan region by palynological data (Байрамова и Тагиева, 2023)

The research carried out in this area has allowed correlating and identifying paleopalynological zones of the oil-gas bearing, Maykopian and Diatom formation of Azerbaijan, as well as to study the change in environmental conditions and vegetation in the stratigraphic sequences of geological periods. Based on the phytoplankton study results, the origin of dispersed organic matter and changes in its catagenesis degree have been studied. To make these studies efficient, the Institute of Geology has been equipped with a full set of up-to-date equipment, including optical and scanning electron microscopes and the required computer software.

A few words should be said about the current state of paleontological studies of vertebrates. The history of these studies in Azerbaijan covers a period of 150 years (since 1870). Stratigraphically, the studies cover the time interval from the Cretaceous to the Holocene. In total, remains of more than 500 vertebrate species have been identified in Azerbaijan, including more than 140 fishes, 10 amphibians, 12 reptiles, 140 birds and 205 mammal species.

The studies resulted in the development of a special catalogue characterizing more than 500 species and subspecies belonging to 5 classes. The catalogue reflects the systematic confinement of different species in the sequence of their appearance in the evolution process. To the extent possible, each of the catalogued fossils was provided by a card index identifying the location of the discovery and storage place of the fossil, as well as the people who found and characterized the discovery. It should be noted that this is only the first stage of research and work on the catalogue will be continued, since a large amount of the discovered fossil vertebrates must be re-identified and placed in the collection funds of the Natural History Museum of Azerbaijan (NHM).

Intensive systematic excavations on the paleontology of vertebrate animals were carried out by employees of the NHM of Azerbaijan, as a result of which the museum's collections were replenished with new fossil materials from the Binagadi burials (suburbs of Baku), the Mingachevir reservoir (west of Azerbaijan) and other sites. Thus, tens of thousands of the bones belonging to different vertebrate species (reptiles, birds, mammals), as well as a large number of plant and arthropod remains were discovered at the Binagadi site (Fig. 7) only. Recently, the collection has been further enriched by new, previously undescribed species of birds, bats and plants.

During excavations in the vicinity of the Mingachevir reservoir, a whole skull (without the lower jaw) of a southern elephant (Fig. 8) was discovered.

After a sharp drop in the water level of the reservoir, numerous bones remain of the postcranial skeletons and skulls of the southern and forest elephants (Fig. 9) were discovered.

There is a large accumulation of different vertebrate species discovered for the first time since 2012 in the vicinity of the Mingachevir reservoir, on the spurs of the Bozdagh and Garaja ranges (composed of Absheronian and Bakunian deposits) (Fig. 10).

The discovered species include primitive bull *Bos* sp. (Fig. 13), bison – *Bison* sp., buffalo – *Bubalus* sp. (Fig. 11), forest elephant – *Palaeoloxodon antiquus* (Fig. 12), ancestor of the giant deer – *Praemegaceros verticornis* (Fig. 15) (both species were first discovered in Azerbaijan); two species of the ancient Merki rhinoceros (Fig. 16) – *Stephanorhinus hundsheimensis* and *Stephanorhinus kirchbergensis*, skull of a trogonteria elephant or Wüsti elephant bones of the postcranial and cranial skeleton of the Stenon horse – *Equus stenonis*, ancient cabaloid horse *Equus* sp., giant deer *Megaloceros giganteus*, red deer *Cervidae* (Fig. 14.)

Together with bone remains, there are many Early Paleolithic Man's tools (Fig. 17), discovered in the Mingachevir site.

As a result of the studies, it was established that the surroundings of the Mingachevir reservoir are unique, having no analogues in the world in terms of the area, relief and the annual number of discovered fossils. It was concluded that to organize its' protection, the site must be given the status of a "Natural Monument" of global significance.

Research has shown that the Merk's rhinoceros (Fig. 16) from the Garaja site (*Stephanorhinus kirchbergensis*) is a typical species of the Late Villafrancian – Early Galerian complexes of the Western Europe (analogues of the Tamanian faunal complex).

Stratigraphic spread of this taxon in the Eastern Europe is currently unknown due to the fragmentation of previously identified Early Pleistocene rhinoceroses in this area.

In 2021, a large skull fragment belonging to a forest straight-tusked elephant, as well as more than 2 m long tusk fragment of a forest elephant (Fig. 18) were discovered in the Garaja site.

Along with the abundance of animal bone remains, the Mingachevir site is characterized by rich variety of various Pleistocene flora species, represented by fossilized trunks (Fig. 19) of large and small trees and shrubs (typical forest vegetation). This speaks for the assumption that during the described period, the area represented a habitat with semi-open forest-steppe type landscapes dominated by the steppe areas interspersed with tree and shrub vegetation.

Fig. 7. Binagadi burial of the Quaternary fauna and flora. Turtles bones

Fig. 8. Southern elephant *Archidiscodon meridionalis*

Fig. 9. Forest elephants *Mammuthus trogontherii*

Fig. 10. Mingachevir reservoir. Bozdagh and Garaja

Fig. 11. Fragment of the skull of the fossil buffalo *Bubalus* sp. from the Upper Bakunian deposits

Fig. 12. Forest elephant *Paleoloxodon antiquus*

Fig. 13. Fragments of the horns and lower jaw of the bull *Bos* sp.

Fig. 14. Ancient cabaloid horse *Equus* sp.; Giant deer *Megaloceros giganteus*; Red deer *Cervidae*

Fig. 15. The ancestor of the giant deer *Praemegaceros verticornis*

Fig. 16. Merki rhinoceros *Stephanorhinus hundsheimensis, Stephanorhinus kirchbergensis*

Fig. 17. Early Paleolithic Man's tools. Garadja

Fig. 18. Tusk of a straight-tusked elephant *Paleoloxodon antiquus.* Mingachevir, Garadja site

Spine paleontologists continued their studies in the vicinity of Pirakashkul village located on the south-eastern termination of the Greater Caucasus mountains. There, in the upper parts of the southern slope of Gara-Islam Mountain, numerous whale bone fragments were first discovered in the diatomic deposits.

In 2012-2013, in the vicinity of the Shamkir reservoir (Fig. 20), lower jaw fragments of a Stenon horse, and a tooth of a Southern elephant (Fig. 21) were discovered.

Fig. 19. Fossilized trunks of trees. Garadja

Fig. 20. Shamkir reservoir

Fig. 21. Lower jaw fragments of a Stenon horse. A tooth of a Southern elephant

In 2020, specialists of the NHM discovered a large new deposit of the Maykopian flora (tree trunks) and vertebrate fauna (cetaceans, cartilaginous bony fishes) (Fig. 22), located in Greater Caucasus at the foothills of Jangi Mountain.

As to international relations, Azerbaijani scientists continue to actively participate in the implementation of international programs, conducting joint research with several foreign institutions. Thus, the Institute of Geology and Geophysics, together with the Institute of Geography (Azerbaijan), as well as the Institute of Applied Geosciences, University Montan Leoben and Geocentre NAWI Graz Austria, are conducting joint micropaleontological, mineralogical and geochemical investigation of the previously unstudied Miocene deposits of Azerbaijan (Gobustan). Close ties are also maintained with the Paleontological Institute and the Geological Institute of the Russian Academy of Sciences (Fig. 23).

Azerbaijani palaeogeographers work closely with the evolutionary geography department of the Institute of Geography of the Russian Academy of Sciences, conducting joint research consisting in the study of changes in natural environment and the correlation of events that occurred during the Quaternary period in Azerbaijan and Eastern Europe. It is known that the development of new research methods requires the training of qualified personnel. In this regard, Azerbaijani young scientists acquire grants for conducting scientific research and opening startups to implement new projects. They are also gaining internships at leading universities in Europe and Russia. Another noteworthy example of the international cooperation is the research conducted jointly by the Azerbaijani paleontologists and stratigraphers, and the geological services of Russia, Kazakhstan, Central Asian states, and China.

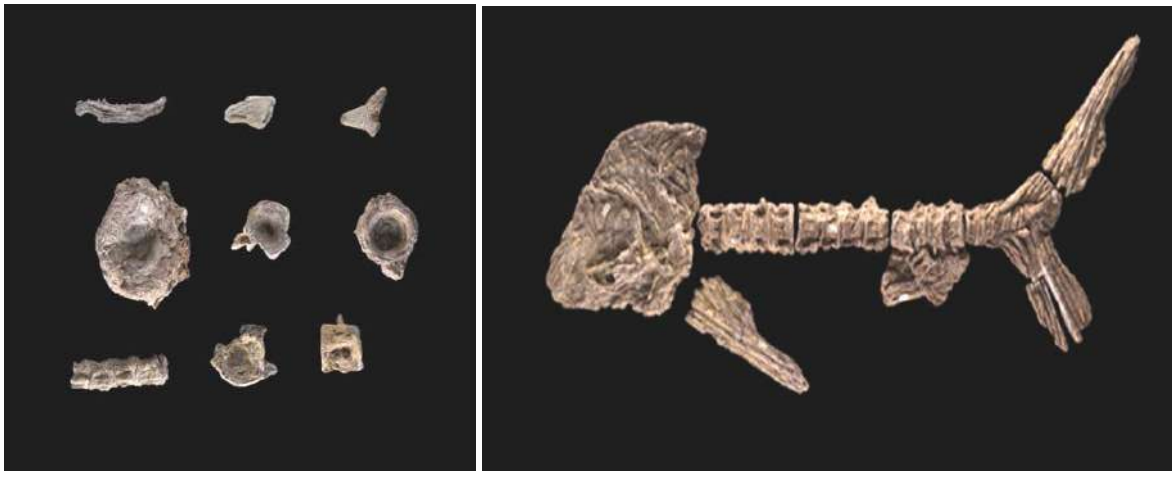

Fig. 22. Cetaceans, cartilaginous bony fishes. Tunes. Jangi

Fig. 23. Scientist from Azerbaijan, Austria, and Russia

Thus, over the past 30-40 years, fundamental research has been carried out in the field of stratigraphy and paleontology in Azerbaijan, producing interesting scientific results. At the same time, the ongoing complex global study of the oceans – the Earth's superstructures, has allowed geologists, including stratigraphers and paleontologists, to take a new look at the World Ocean, which occupies 3/4 of the Earth's surface. This branch of geology – the geology of the bottoms of the seas and oceans, had almost fallen out of the specialists' interest before drilling of "Challenger" 1968 allowed judging about the ocean's lithosphere. This, of course, was a revolution in geology, giving rise to a plenty of thoughts and forecasts for the future. Knowledge of the World Ocean's floor made it possible to pose and solve problems of global stratigraphic correlation within the time interval of the Mesozoic through the Quaternary. Tremendous role in this progress was played by a monographic study of nanofossils, microfauna, and the salt content of the waters.

Nowadays, the scientific community of Azerbaijan is focused on this type of the correlative stratigraphic studies. It is planned to pay close attention to determining the stratotypes of the boundaries – large Phanerozoic stratons. One of such stratotype sections is the Dorasham section (Fig. 24) in Nakhchivan (Julfa canyon). It is useful for studying the Permian-Triassic boundary on the territory of Azerbaijan.

This section (Fig. 24) has got everything to be recognized by the international scientific stratigraphic community as a reference for solving the problem of stratigraphic boundaries between Permian and Triassic periods.

The most important problem of the Azerbaijani stratigraphy and paleontology remains the solution of some unsolved problems of the Quaternary stratigraphy. In this regard, it is important to thoroughly study the relationships and the places of transition of the continental Quaternary sediments to marine facies. It is necessary to implement more detailed investigation of the problem of accurate identification of the distribution boundaries of marine Caspian transgressions, starting from the Bakunian stage and up to the Khazarian, Khvalynian and other transgressions. Comparisons of faunistically characterized Caspian terraces with similar modern continental deposits are also of great interest. Finally, we believe it is important to begin a detailed dissection of the Quaternary lavas of the Garabagh plateau and the river basin of Tartar.

Fig. 24. Julfa canyon. Stratotype of the Upper Permian

In the future, serious attention should be paid to conducting modern research on basin stratigraphy – sequence-stratigraphy with mandatory paleobiogeochemical and facies analysis. As is known, the latter is associated with the study and modelling of the sedimentation stages.

As before, there is a high demand for the development of seismostratigraphic studies in the geosciences, as this is one of the key methods of theoretical stratigraphy enabling the wide use of mathematical and IT methodology in solving specific geological tasks. Very important is the correlation of continental, terrigenous and volcanic formations on a biostratigraphic basis. Paleontologists and stratigraphers of Azerbaijan are planning to implement interesting studies of the stratigraphy of the Caspian shelf sediments.

It is an urgent task to study the stratigraphic layers illustrating various stages of the development of life throughout the Phanerozoic. Today, Azerbaijani paleontologists pay special attention to the study of the evolution of ecosystems, problems of paleobiogeography, evolutionary morphology, regularities of the evolution process and problems of biomineralization. In the coming years, Azerbaijan National Academy of Sciences is planning to implement the Program "Evolution of the Biosphere" (2024-2030). These studies will be carried out at the intersection of paleontology, geochemistry, biogeochemistry, and lithology. As it comes to how purely paleontological and paleobiogeographic problems are addressed in Azerbaijan, special mention should be made of the studies covering the evolution of a biota. It is important to create section-by-section chronostratigraphic and paleogeographic reconstructions of the territory of Azerbaijan with clarification of cause-and-effect relations, as well as to implement quantitative and qualitative assessment of the nature-climatic changes. Studies of the prehistorical ecology shall target the reconstruction of natural and climatic conditions that existed on the territory of the Paleolithic sites of Azerbaijan, and the study of interaction between the natural environment and the primitive societies.

In conclusion, let me say a few words about how almost the entire toolkit of a geologist, paleontologist-stratigrapher has changed in the 21st century. Today, this toolkit is based on automated research systems that are embodied in specialized user-friendly software, freeing a researcher from a routine manual work. Recent years were marked by a significant increase in the intensity of scientific contacts and exchanges within the global scientific network. Global international projects with the participation of scientists from many countries, including Azerbaijan, have become more common. High reputation of the Institute of Geology and Geophysics gained from its' participation in dozens of international contracts, guarantees that the institute will successfully meet the today's requirements and initiate several of its' own projects.

I would like to recall the words of the outstanding Austrian biologist and ethologist Konrad Lorenz: "*When we scientifically explain one of the wonderful phenomena of nature, this explanation is in no way like an unmasked wizard. The true reasons are grander and more amazing than the most beautiful myth.*"

Therein lies all our love of science!

REFERENCES

Agalarova D.A., Kadyrova Z.M., Kulieva S.K. Ostracods of Pliocene and post-Pliocene deposits of Azerbaijan. Azernesh. Baku, 1961, 420 p. (in Russian).

Aliulla H. Upper Cretaceous and development of foraminifera of the Lesser Caucasus (Azerbaijan). Elm. Baku, 1977, 237 pp. (in Russian).

Aliyulla H. Evolution rates of Late Cretaceous planktonic foraminifera of the eastern part of the Lesser Caucasus. In: Biostratigraphic and paleobiofacial studies and their practical significance. Nedra. Moscow, 1970, pp. 26-31 (in Russian).

Alizadeh Ak. A. et al. Saatli superdeep SG-1. Nafta Press. Baku, 1999, 242 p. (in Russian).

Alizadeh Ak.A. Cretaceous belemnites of Azerbaijan Nedra. Moscow, 1972, 279 p. (in Russian).

Alizadeh Ak.A. et al. Productive strata of Azerbaijan. In 2 volumes. "Nedra Publishing House". Moscow, 2018 (in Russian).

Alizadeh Ak.A., Guliyev I.S., Kadirov F.A., Eppelbaum L.V. Geosciences of Azerbaijan: Volume I: Geology. Springer. Cham, 2016, 237 p., DOI: 10.1007/978-3-319-27395-2.

Alizadeh K.A. Cenozoic of Azerbaijan by results of the newest researches. Proceedings of the Academy of Sciences of AzSSR, ser. The Sciences of Earth, 1977, No. 5, p. 42-47 (in Russian).

ЛИТЕРАТУРА

Агаларова Д.А., Кадырова З.М., Кулиева С.К. Остракоды плиоценовых и постплиоценовых отложений Азербайджана. Азернешр. Баку,1961, 420 с.

Ализаде А.А. и др. Продуктивная толща Азербайджана. В 2-х томах. "Издательский дом Недра". Москва, 2018.

Ализаде Ак.А. и др. Саатлинская сверхглубокая СГ-1. Nafta-Press. Баку, 1999, 242 с.

Ализаде Ак.А. Меловые белемниты Азербайджана. Недра. Москва, 1972, 279 с.

Ализаде К.А. и др. Региональная стратиграфическая схема палеогена Азербайджана. Элм. Баку, 1989, 308 с.

Ализаде К.А. Кайнозой Азербайджана по результатам новейших исследований. Изв. АН АзССР, сер. наук о Земле, 1977, No. 5, с. 42-47.

Ализаде К.А., Гаджиев Т.М. Распределение моллюсковой остракодовой фауны в антропогеновых отложениях акватории Бакинского архипелага. Изв. АН АзССР, сер. наук о Земле, 1975, No. 4, с. 85-94.

Ализаде К.А., Мамедов Т.А. О границах между стратиграфическими единицами палеогена и неогена Азербайджана. Изв. АН АзССР, сер. наук о Земле, 1970а, No. 3-4, с. 72-80.

Alizadeh K.A. et al. Regional stratigraphic scheme of the Paleogene of Azerbaijan. Elm. Baku, 1989, 308 p. (in Russian).

Alizadeh K.A., Hajiyev T.M. Distribution of molluskan ostracod fauna in anthropogenic sediments of the Baku Archipelago water area. Proceedings of the Academy of Sciences of the AzSSR, ser. The Sciences of Earth, 1975, No. 4, pp. 85-94 (in Russian).

Alizadeh K.A., Mammadov T.A. About boundaries between stratigraphic units of Paleogene and Neogene of Azerbaijan. Proceedings of the Academy of Sciences of the AzSSR, ser. The Sciences of Earth, 1970a, No. 3-4, pp. 72-80 (in Russian).

Alizadeh K.A., Mammadov T.A. Evolution of the Upper Pliocene mollusk fauna of Azerbaijan. Proceedings of the Academy of Sciences of the Azerbaijan SSR, ser. The Sciences of Earth, 1970b, No. 1, pp. 105-113 (in Russian).

Atayeva E.Z. Miocene (without Pontic Stage). In: Geology of Azerbaijan, Vol. 1 – Stratigraphy, part 2. Nafta-Press. Baku, 2007, pp. 322-381 (in Russian).

Atlas of paleogeographic maps. Shelves of Eurasia in the Mesozoic and Cenozoic. T. 2. Ed. by ROBERTSON GROUP plc, Llandudno, Gwynedd, UK, Geological Institute of the USSR Academy of Sciences. 1992,104 c.

Babayev R.G. Biostratigraphy of the Upper Jurassic sediments of the Lesser Caucasus (Azerbaijan) by scleractinia. In: Mesozoic Corals of the USSR, Issue 4, Nauka. Moscow, 1970, pp. 81-92 (in Russian).

Bayramova Sh.S., Tagieva E.N., Babazade A.D. Micropaleontological studies of the Maikop series sediments of the southeastern end of the Greater Caucasus (Azerbaijan). ANAS Transactions, Earth Sciences, No. 1, 2021, pp. 56-74, DOI: 10.33677/ggianas20210100055 (in Russian).

Bayramova Sh.S., Tagieva E.N. Palynoflora of the Maikop formation (Late Oligocene – Early Miocene) and its significance for stratigraphy and paleogeography of Azerbaijan. ANAS Transactions, Earth Sciences, No. 1, 2023, pp. 25-41, DOI:10.33677/ggianas20230100091 (in Russian).

Chumakov I.S., Byzova S.L., Ganzey S.S., Mamedov A.V. et al. Radiometric scale of the Late Cenozoic of Azerbaijan. Azerb.Neftyanoe Khozyaystvo, No. 2, 1988a (in Russian).

Chumakov I.S., Mammadov A.V., Ganzey S.S., Aleskerov V.D, Byzova S.L., Chronology of the Late Cenozoic of Azerbaijan. Proceedings of the Academy of Sciences of Azerbaijan, ser. The Sciences of Earth, 1988b, No. 3, pp. 50-57 (in Russian).

Geology of Azerbaijan. Stratigraphy. Nafta-press. Baku, 2007, 636 p. (in Russian).

Hajiyev D.V., Huseynov M.M., Mamedov A.V., Shirinov N.Sh. Short results of complex studies of the Azykh ancient Paleolithic site. Proceedings of the AS of the Az.SSR, ser. The Sciences of Earth, 1979, No. 3, pp. 20-35 (in Russian).

Jabarova H.S. Flora and vegetation of Western Azerbaijan in the Upper Miocene. Publishing house of the Academy of Sciences of the Azerbaijan SSR. Baku, 1967, 95 p. (in Russian).

Jafarova J.D. Neogene Otolites of Azerbaijan (edited by G.A. Aliev). Nafta-Press. Baku, 2006, 168 p. (in Russian).

Javanshir R.J., Riley G.W., Duppenbecker S.J., Abdullayev N. Validation of lateral fluid flow in an overpressured sand-shale sequence during development of Azeri-Chirag-Gunashli oil field and Shah Deniz gas field: South Caspian Basin, Azerbaijan. Marine and Petrolium geology, Vol. 59, 2015, pp. 593-610.

Kasimova G.K., Aliyeva D.G. New representatives of the genera Verneuilina and Marssonella from Middle Jurassic sediments of Azerbaijan. Proceedings of the Academy of Sciences of the Azerbaijan SSR, ser. The Sciences of Earth, 1970, No. 5, pp. 36-42 (in Russian).

Kasumova G.M. Flora of Oligocene deposits of the northeastern foothills of the Lesser Caucasus. AS Azerb. SSR Publishing House. Baku, 1966 (in Russian).

Khalilov A.G. Stratigraphy of Azerbaijan: reference book. Elm. Baku, 1978, 161 pp. (in Russian).

Ализаде К.А., Мамедов Т.А. Эволюция верхнеплиоценовой фауны моллюсков Азербайджана. Изв. АН Азерб. ССР, сер. наук о Земле, 1970b, No. 1, с. 105-113.

Алиюлла Х. Верхний мел и развитие фораминифер Малого Кавказа (Азербайджан). Элм. Баку, 1977, 237 с.

Алиюлла Х. Темпы эволюции позднемеловых планктонных фораминифер восточной части Малого Кавказа. В сб.: Биостратиграф. и палеобиофациальн. исслед. и их практич. значение. Недра. Москва, 1970, с. 26-31.

Атаева Э.З. Миоцен (без понтического яруса). В кн.: Геология Азербайджана, Том 1 – Стратиграфия, часть 2. Nafta-Press. Баку, 2007, с. 322-381.

Атлас палеогеографических карт. Шельфы Евразии в мезозое и кайнозое. Т. 2. Изд. РОБЕРТСОН ГРУП плк, Лландидно, Гвинедд, Великобритания, Геологический институт АН СССР. 1992, 104 с.

Бабаев Р.Г. Биостратиграфия верхнеюрских отложений Малого Кавказа (Азербайджан) по склерактиниям. В сб.: Мезозойск. кораллы СССР, Вып. 4, Наука. Москва, 1970, с. 81-92.

Байрамова Ш.Ш., Тагиева Е.Н., Бабазаде А.Д. Микропалеонтологические исследования майкопской серии Юго-Восточного окончания Большого Кавказа (Азербайджан). ANAS Transactions, Earth Sciences, No. 1, 2021, с. 56-74, DOI: 10.33677/ggianas20210100055.

Байрамова Ш.Ш., Тагиева Е.Н. Палинофлора майкопского времени (поздний олигоцен-ранний миоцен) и ее значение для стратиграфии и палеогеографии Азербайджана. ANAS Transactions, Earth Sciences, No. 1, 2023, с. 25-41, DOI:10.33677/ggianas20230100091.

Векилов Б.Г. Антропогеновые отложения Северо-Восточного Азербайджана. Элм. Баку, 1969, 220 с.

Векилов Б.Г. Понтический ярус Восточного Азербайджана. Изд-во АН Азерб. ССР. Баку, 1962, 223 с.

Велиев С.С., Тагиева Е.Н., Алекперова Х.А., Атакишиев Р.М. Палеогеографические условия формирования четвертичных (послеапшеронских) осадков Каспийского моря. Известия НАН Азербайджана. Науки о Земле, 2004, No. 4, с. 195-202.

Величко А.А., Антонова Г.В., Зеликсон Э.М., Маркова А.К., Моносзон М.Х., Морозова Т.Д., Певзнер М.А., Сулейманов М.Б., Халчева Т.А. Палеогеография стоянки Азых – древнейшего поселения первобытного человека на территории СССР. Известия АН СССР, серия геогр., 1980, No. 3, с. 20-35.

Гаджиев Д.В., Гусейнов М.М., Мамедов А.В., Ширинов Н.Ш. Краткие результаты комплексных исследований Азыхской древнепалеолитической стоянки. Известия АН Аз.ССР, серия наук о Земле, 1979, No. 3, с. 20-35.

Геология Азербайджана. Стратиграфия. Nafta-press. Баку, 2007, 636 с.

Джабарова Х.С. Флора и растительность Западного Азербайджана в верхнемиоценовое время. Изд-во АН Азерб. ССР. Баку, 1967, 95 с.

Джафарова Ж.Д. Отолиты неогена Азербайджана (под ред. Г.А.Алиева). Nafta-Press. Баку, 2006, 168 с.

Касумова Г.М. Флора олигоценовых отложений северо-восточных предгорий Малого Кавказа. Изд. АН Азерб. ССР. Баку, 1966.

Касимова Г.К., Алиева Д.Г. Новые представители родов Verneuilina и Marssonella из среднеюрских отложений Азербайджана. Изв. АН Азерб. ССР, серия наук о Земле, 1970, No. 5, с. 36-42.

Мамедов А.Б. Стратиграфия и брахиоподы девона Нахичеванской Автономной республики (Южное Закавказье). Докторская диссертационная работа. Баку, 1992, 568 с.

Мамедов А.В. Палеогеография Закавказья в климатическом оптимуме плиоцена. Палеоклиматы в плиоцене: Совет-

Khalilov A.G., Aliev G.A., Askerov R.B. About the age of limestones of Shusha plateau. Proceedings of the AS of the Azerb. SSR, ser. The Sciences of Earth, No. 52, 1973 (in Russian).

Khalilov A.G., Alizadeh A.A. Stratigraphy. Lower Cretaceous. Upper Cretaceous. Cretaceous sediments of Kobystan and prospects of their oil and gas bearing capacity. Elm. Baku, 1970, pp. 6-18 (in Russian).

Koshkarly R., Mamedova D. Biostratigraphic and stratigraphic atlas of the Cretaceous, Paleogene, Neogene, and Quaternary strata of Azerbaijan and the South Caspian Basin, Baku, 1997.

Mamedov A.V. Paleogeography of Transcaucasia in the Pliocene climatic optimum. Paleoclimates in the Pliocene: Soviet-American Symposium (Moscow, April 20-24, 1990). Preprint Publishing House. Moscow, 1991.

Mamedov A.V., Aleskerov B.D., Suleimanov M.A., Suleimanov M.B. Paleogeography of the area of the ancient Paleolithic site of Azykh in the Eopleistocene and Pleistocene. In: Physical Geography and Geomorphology. Publishing house of ASU named after S.M.Kirov. Baku, 1982 (in Russian).

Mammadov A.B. Stratigraphy and brachiopods of the Devonian of the Nakhichevan Autonomous Republic (South Transcaucasia). Doctoral thesis. Baku, 1992, 568 p.

Martini E. Standard Palaeogene calcareous nanno-plankton zonation. Nature, Vol. 226, 1970, pp. 560-561.

Paleontological atlas of the Quaternary (quarter) system of Azerbaijan. Nafta Press. Baku, 2017, 384 p. (in Azerbaijani).

Suleymanov M.B. Current state of complex research in the Paleolithic caves of Azykh and Taglar (Azerbaijan SSR). Proceedings of the AS of the Azerb. SSR, ser.The Sciences of Earth, No. 56, 1979 (in Russian).

Suleymanov M.B. Habitat of primitive man in the south-east of the Lesser Caucasus (on the data of the paleolithic caves Azykh and Taglar. Abstract of dissertation of candidate of geological sciences, Moscow, 1982.

Tagieva Yu.N., Valiev S.S., Aleskerov B.Ch. Maps of the Paleobite cover of the Cenozoic era. In: National Atlas of the Republic of Azerbaijan. State Committee on Land and Cartography. Baku, 2014, pp. 245-247 (in Azerbaijani).

Vekilov B.G. Anthropogenic sediments of North-Eastern Azerbaijan. Elm. Baku, 1969, 220 p. (in Russian).

Vekilov B.G. Pontic Stage of Eastern Azerbaijan. Publishing house of the Academy of Sciences of the Azerbaijan SSR. Baku, 1962, 223 p. (in Russian).

Velichko A.A., Antonova G.V., Zelikson E.M., Markova A.K., Monoszon M.X., Morozova T.D., Pevzner M.A., Suleimanov M.B., Khalcheva T.A. Paleogeography of the Azykh site – the oldest settlement of primitive man on the territory of the USSR. Izvestia AS USSR, series of geography, 1980, No. 3, pp. 20-35 (in Russian).

Veliyev S.S., Taghiyeva E.N., Alekperova H.A., Atakishiev R.M. Paleogeographic conditions of formation of Quaternary (post-Apsheron) sediments of the Caspian Sea. Proceedings of the National Academy of Sciences of Azerbaijan. The Sciences of Earth, 2004, No. 4, pp. 195-202 (in Russian).

ско-Американский симпозиум (Москва, 20-24 апреля 1990). Изд-во «Препринт». Москва, 1991.

Мамедов А.В., Алескеров Б.Д., Сулейманов М.А., Сулейманов М.Б. Палеогеография района древнепалеолитической стоянки Азых в эоплейстоцене и в плейстоцене. В сб.: Физическая география и геоморфология. Изд. АГУ им. С.М.Кирова. Баку, 1982.

Сулейманов М.Б. Современное состояние комплексных исследований в палеолитических пещерах Азых и Таглар (Азербайджанская ССР). Известия АН Азерб. ССР, серия наук о Земле, No. 56, 1979.

Сулейманов М.Б. Среда обитания первобытного человека на юго-востоке Малого Кавказа (по данным палеолитических пещер Азых и Таглар. Автореферат дисс. канд. геол. наук, Москва,1982.

Халилов А.Г. Стратиграфия Азербайджана: справочник. Элм. Баку, 1978, 161 с.

Халилов А.Г., Алиев Г.А., Аскеров Р.Б. О возрасте известняков Шушинского плато. Изв.АН Азерб.ССР, серия наук о Земле, No. 52, 1973.

Халилов А.Г., Ализаде Ак.А. Стратиграфия. Нижний мел. Верхний мел. Меловые отложения Кобыстана и перспективы их нефтегазоносности. Элм. Баку, 1970, с. 6-18.

Чумаков И.С., Бызова С.Л., Ганзей С.С., Мамедов А.В. и др. Радиометрическая шкала позднего кайнозоя Азербайджана. Азербайджанское нефтяное хозяйство, No. 2, 1988a.

Чумаков И.С., Мамедов А.В., Ганзей С.С., Алескеров В.Д, Бызова С.Л., Хронология позднего кайнозоя Азербайджана. Известия АН Азербайджана. Серия наук о Земле, 1988b, No. 3, с. 50-57.

Alizadeh Ak.A., Guliyev I.S., Kadirov F.A., Eppelbaum L.V. Geosciences of Azerbaijan: Volume I: Geology. Springer. Cham, 2016, 237 p., DOI: 10.1007/978-3-319-27395-2.

Koshkarly R., Mamedova D. Biostratigraphic and stratigraphic atlas of the Cretaceous, Paleogene, Neogene, and Quaternary strata of Azerbaijan and the South Caspian Basin, Baku, 1997.

Javanshir R.J., Riley G.W., Duppenbecker S.J., Abdullayev N. Validation of lateral fluid flow in an overpressured sand-shale sequence during development of Azeri-Chirag-Gunashli oil field and Shah Deniz gas field: South Caspian Basin, Azerbaijan. Marine and Petrolium geology, Vol. 59, 2015, pp. 593-610.

Martini E. Standard Palaeogene calcareous nanno-plankton zonation. Nature, Vol. 226, 1970, pp. 560-561.

Azərbaycanın Dördüncü dövr (kvarter) sisteminin paleontoloji atlası. Nafta-Press. Bakı, 2017, 384 s.

Tağıyeva Y.N., Vəliyev S.S., Ələsgərov B.C. Kaynozoy erasının paleobitki örtüyü xəritələr. Azərbaycan Respublikası Milli Atlas. Dövlət torpaq və xəritəçəkmə komitəsi. Bakı, 2014, s. 245-247.

СОВРЕМЕННОЕ СОСТОЯНИЕ ПАЛЕОНТОЛОГО-СТРАТИГРАФИЧЕСКИХ ИССЛЕДОВАНИЙ В АЗЕРБАЙДЖАНЕ

Али-Заде Ак.А.

Министерство науки и образования Азербайджанской Республики, Институт геологии и геофизики, Азербайджан AZ1143, Баку, просп. Г.Джавида, 119

Резюме. История изучения ископаемых палеонтологических остатков в Азербайджане подразделяется на несколько этапов в зависимости от степени интенсивности исследований, масштаба стратиграфического охвата, а также участия в них национальных кадров. В 50-80-е годы XX века приоритетом было объединение специалистов по возрастным группам ископаемых остатков (например, юрские аммониты, меловые иноцерамы, аммониты и белемниты, палеогеновые нуммулиты, миоценовые

пелециподы и т.д.). Позднее, к концу девяностых годов прошлого столетия приоритеты фундаментальных исследований несколько сместились в область изучения эволюции экосистем, палеобиологии, событийной биостратиграфии и т.д.

У истоков развития палеонтолого-стратиграфических исследований в Азербайджане стояли такие корифеи, как академики: М.М.Алиев, Г.А.Ализаде, профессора А.Г.Халилов, Д.М.Халилов, Д.А.Агаларова. Деятельность этих учёных сопровождалась бурным развитием палеонтологических и стратиграфических идей, изучением беспозвоночной ископаемой фауны, фитоостатков (включая нанофоссилии). Так, к концу XX века детально были уже изучены почти все архистратиграфические группы фауны, их эволюция, а также палеоэкологические, палеобиологические, палеобиогеохимические и другие аспекты условий их обитания.

Как сегодня принято говорить, это действительно был «золотой век» науки, в том числе и палеонтолого-стратиграфической. Главным действующим лицом этого прогресса в науке и её практических делах, конечно, был исследователь – классный специалист, и только высококвалифицированные кадры азербайджанской палеонтолого-стратиграфической науки динамично поднимали планку её достижений всё выше. Среди них видные специалисты палеонтологи: Т.А.Гасанов, К.М.Султанов, Х.Алиюлла, Б.Г.Векилов, А.Б.Аббасов, Р.Г.Бабаев, Ш.А.Бабаев, М.Р.Абдулкасумзаде, Г.А.Алиев, Р.А.Алиев, Р.О.Кошкарлы, Р.Н.Мамедзаде, О.Б.Алиев, Э.З.Атаева, Х.Ш.Алиев и другие.

Таким образом, широкий размах фундаментальных палеонтолого-стратиграфических исследований позволил азербайджанским учёным создать серьезную палеонтолого-стратиграфическую базу геологических исследований в Азербайджане. Продолжение планомерного и систематического развития регионального геологического изучения территории Азербайджана привело в итоге к созданию фундаментальной формационно-стратиграфической и геохронологической основы, опирающейся на комплекс современных методов и достижений в области палеонтологии, стратиграфии, изотопной геохронологии, фациально-палеогеографического анализа и историко-геологического синтеза.

Ключевые слова: *Палеонтология, стратиграфия, Азербайджан, продуктивная серия, климатостратиграфическая схема, Азых*

AZƏRBAYCANDA PALEONTOLOJİ-STRATİQRAFİK TƏDQİQATLARIN MÜASİR VƏZİYYƏTİ

Əlizadə Ак.А.

[1]*Azərbaycan Respublikasının Elm və Təhsil Nazirliyi, Geologiya və Geofizika İnstitutu*
AZ1143, Bakı şəh., H.Cavid pr., 119

Xülasə. Azərbaycanda paleontoloji qalıqların öyrənilmə tarixi müvafiq tədqiqatların intensivliyi, stratiqrafik yaş intervalı, həmçinin bu tədqiqatlarda milli kadrların iştirakı dərəcəsindən asılı olaraq bir neçə mərhələyə bölünür. XX əsrin 50-80-ci illərində paleontoloji qalıqların tədqiqatı zamanı mütəxəssislərin geoloji yaş qrupları üzrə birləşməsi prioritet idi (məsələn, Yura ammonitləri, Təbaşir inoseramları, ammonit və belemnitləri, Paleogen nummulitləri, Miosen pelesipodları və s.). Daha sonra ötən yüzilliyin doxsanıncı illərinin sonunda fundamental tədqiqatların prioritetləri bir qədər dəyişərək ekosistemlərin təkamülünün, paleobiologiyanın, biostratiqrafik hadisələrin öyrənilməsi kimi sahələrə üstünük verildi.

Azərbaycanda paleontoloji-stratiqrafik tədqiqatların təməli akademiklər Musa Mirzə oğlu Əliyev, Qambay Əsgər oğlu Əlizadə, professorlar Əbdülhəmid Yusif oğlu Xəlilov, Cəlil Mustafa oğlu Xəlilov, Dünya Ələkbər qızı Ağalarova kimi korifeylər tərəfindən qoyulmuşdur. Bu alimlərin fəaliyyəti paleontoloji və stratiqrafik ideyaların sürətli inkişafı, qədim onurğasız faunanın və floranın (nanofossillər də daxil) öyrənilməsi ilə müşayiət olunurdu. Beləliklə, XX əsrin sonuna qədər, demək olar ki, bütün arxistratiqrafik fauna qrupları, onların təkamülü, həmçinin onların yaşam şəraitinin paleoekoloji, paleobioloji, paleobiogeokimyəvi və başqa aspektləri ətraflı öyrənilmişdi.

Bu dövr, həqiqətən, elmin, o cümlədən paleontologiya-stratiqrafiya elminin "qızıl əsri" – intibah dövrü idi. Elmdə və onun praktiki tətbiqində bu tərəqqinin əsas hərəkətverici qüvvəsi, əlbəttə, tədqiqatçılar – yüksəkixtisaslı mütəxəssislər idi. Yüksəkixtisaslı kadrlar Azərbaycanın paleontologiya-stratiqrafiya elminin nailiyyətlərinin dinamik inkişafının təkanverici qüvvəsi idi. Onların arasında paleontologiya üzrə görkəmli mütəxəssislər T.A.Həsənov, Q.M.Sultanov, X.Əliyulla, B.Q.Vəkilov, A.B.Abbasov, R.Q.Babayev, Ş.Ə.Babayev, M.R.Əbdülqasımzadə, Q.A.Əliyev, R.Ə.Əliyev, R.O.Qoşqarlı, R.N.Məmmədzadə, O.B.Əliyev, E.Z.Atayeva, X.Ş.Əliyev, V.B.Ağayev, Ç.Ə.Tahirov və başqalarının adları xüsusi qeyd edilməlidir.

Beləliklə, fundamental paleontoloji-stratiqrafik tədqiqatların geniş miqyas alması sayəsində Azərbaycan alimləri respublikada geoloji tədqiqatların ciddi paleontoloji-stratiqrafik bazasını yaratmaq imkanı əldə etdilər. Azərbaycan ərazisinin regional geoloji tədqiqinin planauyğun və sistematik şəkildə davam və inkişaf etdirilməsi yekunda müasir metodlara və paleontologiya, stratiqrafiya, izotopların geoxronologiyası, fasial-paleocoğrafi analiz və tarixi-geoloji sintez sahələrində nailiyyətlərə söykənən fundamental formasion-stratiqrafik və geoxronoloji təməlin yaradılması ilə nəticələndi.

Açar sözlər: *paleontologiya, stratiqrafiya, Azərbaycan, Məhsuldar seriya, iqlimstratiqrafiya sxemi, Azıx*

ANAS Transactions Earth Sciences 1 / 2024

http://www.journalesgia.com

RESULTS FROM 25 YEARS (1998-2022) OF CRUSTAL DEFORMATION MONITORING IN AZERBAIJAN AND ADJACENT TERRITORY USING GPS

Kadirov F.[1], Yetirmishli G.[3], Safarov R.[1], Mammadov S.[1], Kazimov I.[3], Floyd M.[2], Reilinger R.[2], King R.[2]

[1]*Ministry of Science and Education of the Republic of Azerbaijan, Institute of Geology and Geophysics, Azerbaijan 119, H.Javid ave., Baku, AZ1143*

[2]*Department of Earth, Atmospheric and Planetary Sciences, Massachusetts Institute of Technology 77 Massachusetts Ave., 54-918 Cambridge MA USA*

[3]*Republican Seismic Survey Center, Azerbaijan National Academy of Sciences 25, Rafibeyli str.,Baku, AZ1001*

Keywords: *Deformation, tectonic structures, monitoring, GPS, earthquake, seismic hazard*

Summary. We present GPS observations of crustal deformation monitoring in Azerbaijan and adjacent territory which carried out since 1998. Unlike our previous studies there are more permanent GPS station and survey mode data aggregated, which accordingly allowed us more accurately determine the dynamics of the main tectonic structures.

Eight permanent stations were established by the Institute of Geology and Geophysics since 2006.In 2012, Republican Seismological Survey Center of Azerbaijan National Academy of Sciences started to construct permanent GPS stations, where totally 24 stations were established. Over 35 survey mode sites were measured repeatedly starting from 1998 to 2022.

On a broad scale, the GPS velocity field clearly illustrates the NNE motion of Caucasus and adjacent regions with respect to Eurasia south of the Main Caucasus Thrust Fault (MCT). An important note here is the sharp decrease in site velocities, and the clockwise rotation, between sites located to the west of West Caspian Fault (WCF) in Kura Depression and Talish region and sites to the east of WCF in Absheron Peninsula. This decrease and difference in GPS vector directions indicate high strain accumulation rates ~6 mm/yr south to Absheron Peninsula. We believe that the significant accumulation of elastic energy is responsible for the activation of seismic events and ofmud volcanoes in this region. Thus, spatial densification of the GPS observations is needed to better resolve localized deformation, and consequently the seismic hazard in the eastern Caucasus, Kur Depression, and Absheron area.

Introduction

Azerbaijan is caught in the active continent-continent collision of the Arabian plate with Eurasia (Mckenzie, 1972; Sengor et al., 1985; Philip et al., 1989). Plate tectonic reconstructions provide only broad constraints on the timing of the initial collision of the Arabian Plate with Eurasia of between 10-30 Ma BP (e.g., Robertson, 2000; Allen et al., 2004), and indicate that the rate of northward motion of Arabia relative to Eurasia has remained more or less constant at about 20 mm/yr since collision began (McQuarrie et al., 2003; Reilinger et al., 2006). These reconstructions imply that Arabia has progressed from 200-600 km "into" space formerly occupied by Eurasian continental lithosphere. This continuing "invasion" of the Arabian Plate into the Eurasian Plate determines the lithospheric shortening along the Main Caucasian Thrust (MCT), which extends in the meridional direction, and horizontal displacement of the lithosphere (McKenzie, 1972; Sengor et al., 1985; Jackson, 1992; Shevchenko et al., 1999; Guliev et al., 2002; Reilinger et al., 2006; Kadirov et al., 2008, 2012, 2023; Kadirov, 2004).

Since the Arabian Plate is moving north relative to Africa at a rate of 1.1-2.0 cm/year, a strong movement of the Arabian Plate towards Eurasia can be expected in advance. This causes the Caucasus to form a raised bridge separating two deep-water basins: the Black Sea and the South Caspian. Being responsible for crustal deformations, these regional

tectonic processes cause earthquakes, which are historically documented throughout the entire Caucasus (Зоненшайн и Савостин, 1979; McKenzie, 1972).

In this paper we use Global Positioning System (GPS) observations in and around Azerbaijan in the period 1998-2022 to estimate present-day surface motions. The observed motions (site velocities) allow us to identify zones of rapid strain accumulation that we interpret as resulting from deep slip on faults that are presently locked at crustal depths and will likely give rise to future earthquakes. The GPS-derived surface motions allow estimation of fault geometry, slip rates, and locking depths (e.g., Okada, 1992), thereby providing an improved physical basis for estimating regional earthquake hazards. For example, the estimated rate of slip on the deep, freely sliding section of the Main Caucasus Thrust Fault (MCT) determined by GPS observations of surface motion, and estimates of slip in prior earthquakes (from study of historic and pre-historic earthquakes) allows estimation of the time required to accumulate sufficient strain to generate an earthquake, or equivalently, the earthquake recurrence time for individual fault segments (assuming the time-predictable earthquake model; Shimazaki and Nakata, 1980). Furthermore, the total coseismic slip from prior earthquakes, together with estimates of the locking depth of the fault (from the wavelength of the GPS deformation field), and the length of fault segments (from geological and geophysical studies) allow estimation of the magnitude of future events. Thus, our GPS observations have the potential to constrain the timing and magnitude of future earthquakes.

1. Tectonic Settings of the Caucasus Mountains

In the broadest context, the Lesser and Greater Caucasus Mountains lie within the zone of plate interaction where the African and Arabian plates are actively converging with the Eurasian Plate (Fig.1). McKenzie et al. (1970), McKenzie (1972), and Jackson and McKenzie (1984, 1988) provided a plate tectonic description of the region, recognizing active continental collision in eastern Turkey, the Caucasus, and the Zagros; lateral transport of Anatolia (Turkey) towards the west; subduction of African oceanic lithosphere (i.e., Neotethys) along the Hellenic and Cyprus trenches; N-S extension in the Aegean and western Turkey; and ocean rifting along the Red Sea and Gulf of Aden. Convergence of Arabia and Africa with Eurasia has been occurring for > 100 Ma as the intervening Neotethys Ocean lithosphere has been subducting beneath Eurasia. While ocean subduction continues at present along the Hellenic and Cyprus trenches, complete ocean closure north of the Arabian plate occurred ~27 Ma (e.g. McQuarrie and van Hindsbergan, 2013).

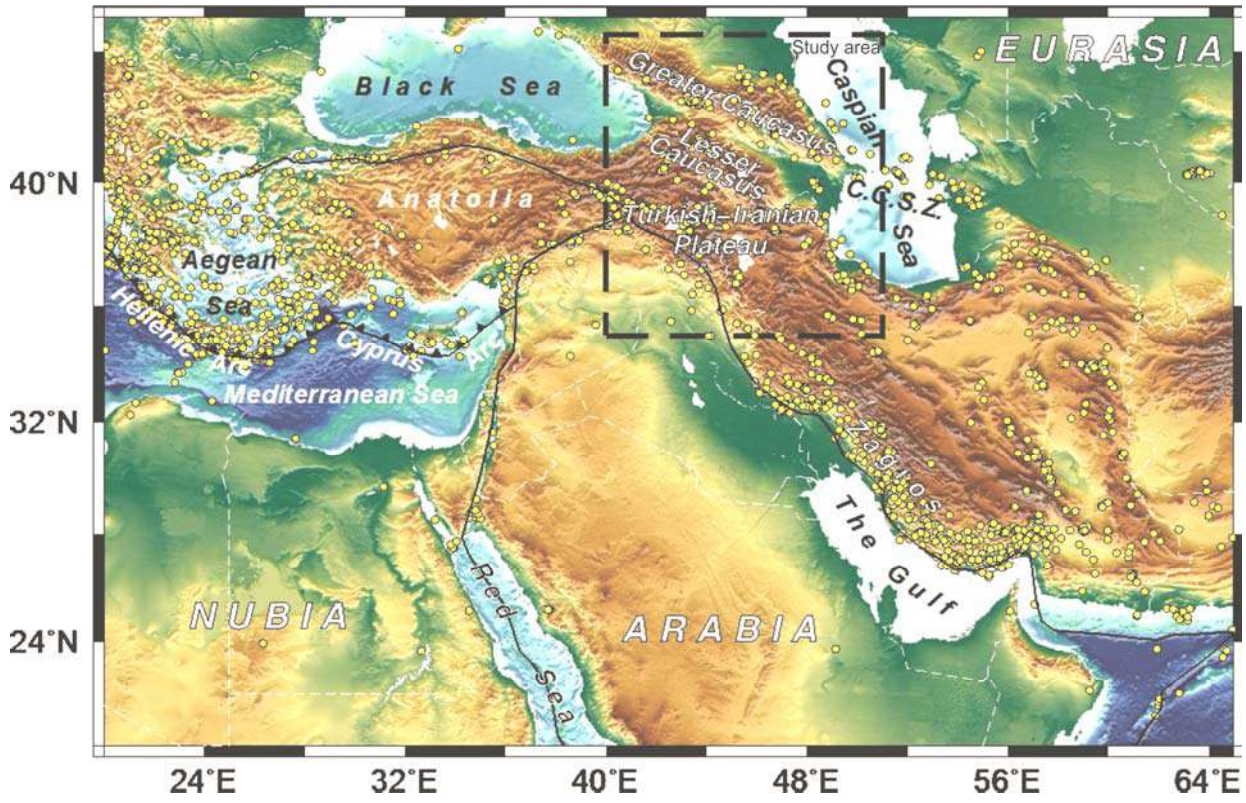

Fig. 1. Tectonic overview of the Arabia-Eurasia Collision Zone. Yellow dots are earthquakes from the EHB catalog (Engdahl et al., 1998) and updates thereof to 2008, plus ISC locations from 2009 onwards. Major plate boundaries are from Bird (2003)

Subsequent seismological, geophysical and geological studies added important refinements to this plate tectonic characterization, including the westward "extrusion" of Anatolia accommodated by the North and East Anatolian faults (Sengor et al., 1985), partitioning of crustal deformation in the eastern Turkey/Caucasus continental collision zone (Jackson, 1992; Allen et al., 2004;Copley and Jackson, 2006), the influence of slab detachment on uplift and volcanism of the Turkish Iranian Plateau (e.g.,Sengor et al., 2004;Barazangi et al., 2006), and early subduction of the S Caspian oceanic basin beneath the N Caspian Eurasian continental lithosphere along the central Caspian Seismic Zone (e.g., Jackson et al., 2002).

The Greater Caucasus Mountains are thought to have formed by tectonic inversion of a former back-arc ocean that opened during north-dipping subduction of the Neotethys (e.g. Zonenshain and Le Pichon, 1986; Forte et al., 2012; Alizadeh et al., 2016, 2017; Tye et al., 2021, 2022; Kangarli et al., 2018, 2021, 2022), where the eastern Black Sea, Kur Depression in Azerbaijan, and southern Caspian Sea are the remaining remnants of the back-arc basin. Both the timing and spatial evolution of shortening and exhumation remain uncertain, with preferred estimates of the timing being Late Miocene to Early Pliocene (e.g. Kopp and Shcherba, 1985; Philip et al., 1989; Vincent et al., 2007). Total shortening across the Greater Caucasus is also uncertain with estimates ranging from 150-400 km (e.g. McQuarrie and van Hindbergen, 2013), and an increase in total shortening from west to east (e.g. Kral and Gurbanov, 1996; Avdeev and Niemi, 2008; Forte et al., 2012).

2. Tectonics of the Africa–Arabia–Eurasia Plate System and GPS

During the past ~30 years, the active tectonics of theAfrica–Arabia–Eurasia plate system has been measured directly by geodetic observations, most importantly the GPS (Hager et al., 1991; Dixon, 1991). GPS consists of a system of 32 satellites 20,000 km above the Earth's surface that complete 2 orbits of the Earth each 24 h (http://tycho.usno.navy.mil/gpscurr.html). The satellites are operated by the US Department of Defense in cooperation with the Interagency GPS Executive Board. Other Global Navigation Satellite Systems (GNSS) have been developed by Russia (GLONASS), a European consortium (Galileo), Japan (QZSS), and China (Beidou), but these systems are not used in the results we report.

There are three components to use the GPS system for precise positioning: the satellite constellation, a global network of GPS tracking stations (Mueller and Beutler, 1992), and data processing involving applying physical models and parameter estimation. Most importantly for this chapter, positions are determined with an accuracy of ~2 mm in horizontal coordinates and 3-10 mm in heights by recording data over a 24-h period. These precisions are possible because of highly accurate timing provided by atomic clocks on the GPS satellites, precise orbital positions for the satellites provided by the International GNSS Service (http://igs.org/) (determined from the global network of observing stations), and processing software that uses advanced mathematical models to account for the Earth's rotation, solid Earth and ocean tides, and the ionospheric and atmospheric delays of the GPS signal, among other factors that influence position estimates (e.g., Herring et al., 2010).

3. Combined Azerbaijan – US Investigations: A Short Background

The Geology and Geophysics Institute of the Ministry of Science and Education of the Republic of Azerbaijan and Republican Seismic Survey Center of the Azerbaijan National Academy of Sciences and the Department of Earth, Atmospheric, and Planetary Sciences at Massachusetts Institute of Technology have been using the Global Positioning System (GPS) to monitor crustal deformation in the territory of Azerbaijan since 1998 (Reilinger et al., 2006; Kadirov et al., 2008,2009, 2013, 2014, 2015; Kadirov and Safarov, 2014; Ahadov and Kadirov, 2021; Ahadov and Jin, 2017; Ahadov and Jin, 2021; Ismail-Zadeh et al., 2020). These studies, coordinated and integrated with GPS studies in neighboring parts of the Arabia–Eurasia collision zone, provide new constraints on the fundamental geodynamic processes that are actively deforming the collision zone (e.g., Reilinger et al., 2006; Kadirov et al., 2012, 2015; Forte et al., 2012; Eppelbaum and Katz, 2022; Eppelbaum and Keshin, 2012). These geodynamic processes produced and maintain the high elevation of the Turkish–Iranian Plateau (Fig.1) and are the cause of the volcanic and earthquake activities that characterize this region.

The question of earthquake hazards has played a central role in our research because of the increasing vulnerability of the growing population and rapid infrastructure development expected maximum magnitude, and their likelihood of occurrence. This information is necessary in order to take appropriate preparedness and mitigation measures to reduce the risk to the population and infrastructure, including the vulnerable facilities associated with the petroleum industry that are critical to the economy of Azerbaijan.

In this chapter, we use GPS observations to constrain Arabia–Eurasia relative plate motions and the character of interplate deformations in the Ara-

bia–Eurasia collision zone. Within this broader context, we focus on earthquake hazards in the Azerbaijan Caucasus and SW Caspian Basin.

4. Seismicity of Azerbaijan Territory. A Brief Background

Territory of Azerbaijan is located within the central part of the Mediterranean tectonic belt seismicity of which is caused by intensive geodynamic interaction of the Eurasian and Arabian lithospheric plates (Хаин, 2001; Азизбеков, 1968; Yetirmishli, 2020). Territory of Azerbaijan is characterized by high seismic activity where during historical period (registered), strong and catastrophic earthquakes with magnitude M ≥ 6 were observed. Azerbaijan territory may be subdivided by the level of seismic activity and character of space distribution of strong and weak earthquakes into the following manner:(1) Southern slope of the eastern part of the Greater Caucasus, (2) Kur Depression, (3) Talysh Mts., (4) Gusar-Shabran depression, (5) Northern slope of Lesser Caucasus, (6) Absheron Peninsula and (7) Caspian Sea (Telesca et al., 2017).

The history of seismic studies in Azerbaijan can be divided into two main periods: (1) pre-instrumental (historical)including all the information from ancient times reflected in the historical Arab chronicles, manuscripts, travel notes of travelers, etc., and (2) instrumental (contemporary) period which includes information about earthquakes from the beginning of the twentieth century (when after strong Shamakhi earthquake in 1902, the first seismic station in Azerbaijan "Shamakhi" was founded) till the present time.

Among the strong (historical) earthquakes, we can note such events as Azerbaijan earthquake of 427, Goygol of 1139,Ganja of 1235, Eastern Caucasian of 1668, Mashtaga of 1842,numerous Shamakhi events (1192, 1667, 1669, 1828, 1859,1868, 1872, 1902), Ardebil of 1924, Lankaran of 1913, and Caspian earthquakes (957, 1812, 1842, 1852, 1911, 1935,1961, 1963, 1986, 1989, 2000) triggered earth relief changing, building destructions, and numerous casualties.

One of the largest seismic events in Azerbaijan in twentieth century was a Shamakhi earthquake on February 13, 1902 (lat., 40.7 and long., 48.6; magnitude ≈ 7; depth offocus, 15 km; intensity of motions in the center, VIII–IX).

5. Role of GPS measurements on seismological studies in Azerbaijan

GPS observations play an important role in studying crustal deformation in the Arabia-Eurasia zone of plate interaction, and use these observations to constrain broad-scale tectonic processes within the collision zone of the Arabian and Eurasian plates. Within this plate tectonics context, we examine deformation of the Caucasus system (Lesser and Greater Caucasus and intervening Caucasian Isthmus), and show that most crustal shortening in the collision zone is accommodated by the Greater Caucasus Fold-and-Thrust Belt (GCFTB) along the southern edge of the Greater Caucasus Mountains. The eastern GCFTB appears to bifurcate west of Baku, with one branch following the arcuate geometry of the Greater Caucasus, turning towards the south and traversing the Neftchala Peninsula. A second branch (or branches) may extend directly into the Caspian Sea south of Baku, likely connecting to the Central Caspian Seismic Zone (CCSZ). Our studies indicate that strain is actively accumulating on the fault along the ~200 km segment of the fault west of Baku (approximately between longitudes 47-49°E). Parts of this segment of the fault broke in major earthquakes historically (1191, 1859, 1902) suggesting that significant future earthquakes (M~6-7) are likely on the central and western segment of the fault. We observe a similar deformation pattern across the eastern end of the GCFTB along a profile crossing the Kur Depression and Greater Caucasus Mountains in the vicinity of Baku. Along this eastern segment, a branch of the fault changes from a NW-SE striking thrust to an ~ N-S oriented strike-slip fault (or in multiple splays). The similar deformation pattern along the eastern and central GCFTB segments raises the possibility that major earthquakes may also occur in eastern Azerbaijan. However, the eastern segment of the GCFTB has no record of large historic earthquakes, and is characterized by thick, highly saturated and over-pressured sediments within the Kur Depression and adjacent Caspian Basin that may inhibit elastic strain accumulation in favor of fault creep, and/or distributed faulting and folding. Thus, while our analyses suggest that large earthquakes are likely in central and western Azerbaijan, it is still uncertain whether significant earthquakes are also likely along the eastern segment, and on which structure. Ongoing and future focused studies of active deformation promise to shed further light on the tectonics and earthquake hazards in this highly populated and developed part of Azerbaijan.

6. Estimating Surface Motions from GPS Observations

The GPS measurements presented in this paper include both continuously recording stations (cGPS) that remain in place indefinitely and survey-mode (sGPS) observations where the GPS antenna is positioned temporarily over a survey marker (Fig. 2). Over 35 survey mode sites were measured repeatedly starting from 1998 to 2022. By repeating the

sGPS measurements episodically, we are able to estimate how the position has changed during the observation period.

Eight permanent stations were established by the Institute of Geology and Geophysics since 2006. In 2012, Republican Seismological Survey Center of Azerbaijan National Academy of Sciences started to construct permanent GPS stations, where totally 24 stations were established. Continuous GPS observations allow estimation of position on a daily basis or more frequently. However, reliable estimates of long-term, secular site velocities require a minimum of 2.5 years of observations even for cGPS because annual and semiannual systematic errors can bias estimates of steady-state motion (Blewitt and Lavellee, 2002).

While the precision of our site velocities varies with observation period, the GPS horizontal velocities we determine using the GAMIT-GLOBK processing software (Herring, 2004; Herring et al., 2010) have 1-sigma uncertainties in the range of0.2-0.9 mm/year, with most sites <0.5 mm/year. Because deformation rates across the Greater Caucasus Mountains vary from 2 to 14 mm/year from northwest to southeast, these precisions allow us to investigate details of the mountain building processes and associated earthquake hazards.

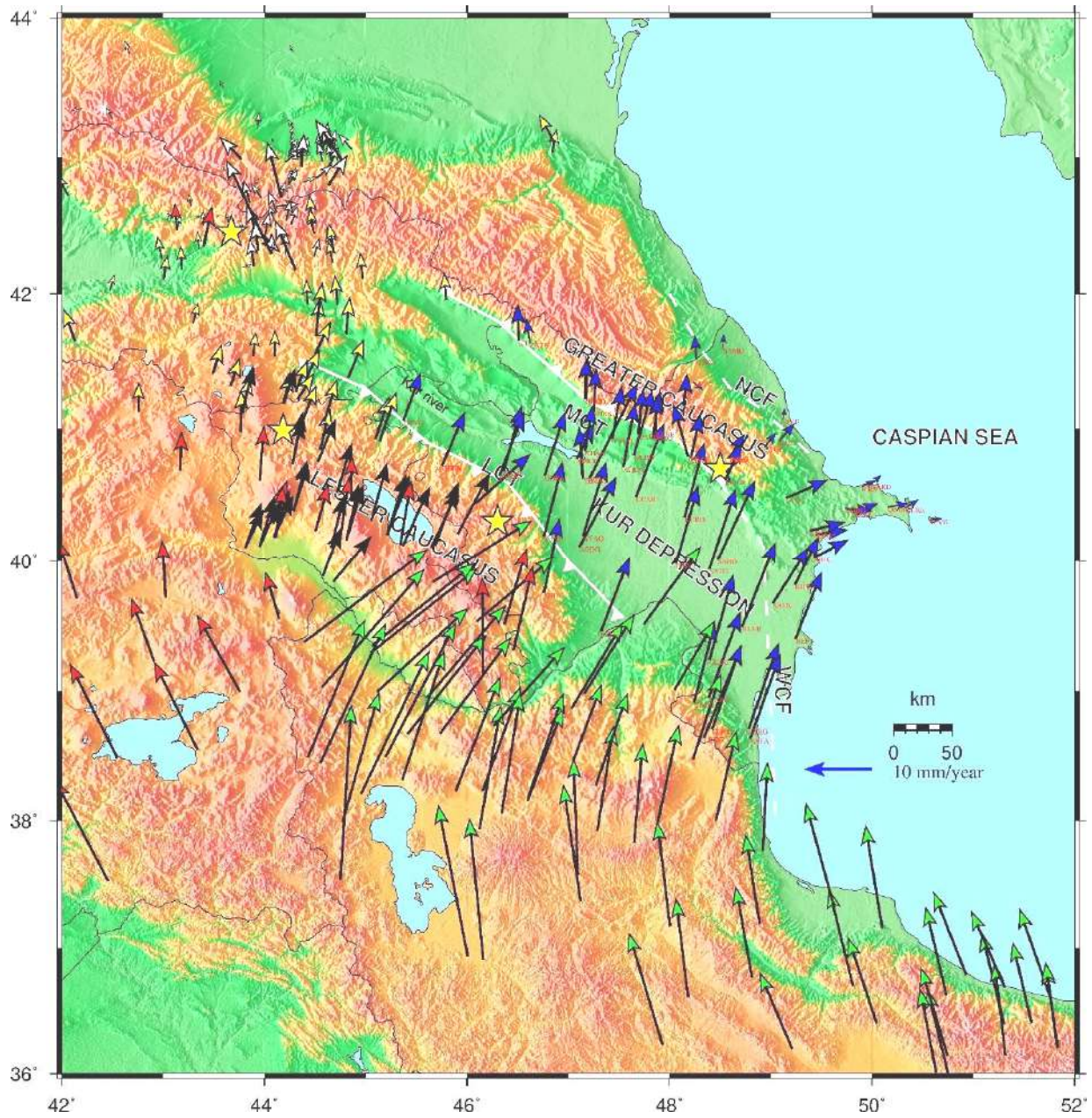

Fig. 2. GPS velocities with respect to Eurasia for the eastern AR-EU collision zone. Orange stars shows 1902, M6.9 Shamakhi; 1139, M7.3 Ganja; 1988, M6.8 Spitak and 1991, M7.0 Racha earthquake epicenters. Four character codes indicate survey and permanent GPS site names. Blue arrows indicate Azerbaijan GPS sites from these study, green arrows – Iranian GPS sites (Raeesi et al.,2017), Red arrows – Armenian GPS sites (Karakhanyan et al.,2013), Yellow arrows – Georgian GPS sites (Sokhadze et al., 2018), White arrows – Russian GPS sites (Milyukov et al.,2015), Black arrows are velocities from Reilinger et al., 2006.

Velocity estimates are determined in a global reference frame, that is, with respect to the global network of tracking stations. The reference frame is determined and maintained (updated) by the International Terrestrial Reference Frame (ITRF2014) Service (Altamimi et al., 2016) using well-positioned stations, with a long history of well-behaved observations, located around the globe and accounting for motions of the Earth's tectonic plates. We determine site velocities from Altamimi et al. (2016), but we present them in a reference frame fixed to the Eurasian Plate. It is important to bear in mind that the relative motion between measurement sites (i.e., deformation or strain rate) is invariant to changes in reference frame.

7. Present-Day Arabia–Eurasia Continental Collision

Fig.2 shows the velocities of GPS sites in the zone of interaction of the African, Arabian, and Eurasian plates (Reilinger et al., 2006 and updates thereof for sites in Azerbaijan). Virtually all major active tectonic processes are well resolved and quantified by the GPS observations, including the northward motion and counterclockwise (CCW) rotation of the Arabian Plate as a result opening of the Red Sea (e.g., ArRajehi et al., 2010), crustal shortening of the Zagros fold-and-thrust zone in Iran (e.g., Djamour et al., 2010), motion of the African Plate with respect to Eurasia (McClusky et al., 2003), and the change from NNW motion of Arabia to NNE motion of the Caucasus system (Reilinger et al., 2006; Vernant and Chery, 2006).

Reilinger et al. (2006) used the GPS velocity field to estimate how AR-EU convergence is partitioned between lateral "extrusion" of crustal blocks and crustal shortening. They found that a large majority (~70 %) of the convergence is accommodated by lateral transport, and ~15 %by shortening along the GCFTB (Greater Caucasus Fold-and-Thrust Belt), with the remainder being accommodated by other structures or distributed strain. The only slightly thickened crust in the Lesser Caucasus—E Turkey Plateau (Gok et al., 2003; Barazangi et al., 2006), in spite of 150–400 km of continental convergence (McQuarrie and van Hindbergen, 2013) – indicates that the geodetic results reflect long-term, tectonic deformation processes in the collision zone (i.e., if not for lateral transport, the crust would be expected to be much thicker). The utility of geodetic studies for constraining long-term geodynamic processes finds further support from comparison between present-day, geodetically derived Arabia–Eurasia convergence rates and longer-term plate convergence rates derived from plate tectonic reconstructions (e.g., McQuarrie et al., 2003) that indicate that these plate motions have been remarkably constant (±10–15 %) since the onset of continental collision in the Early Miocene (e.g., ArRajehi et al., 2010).

Results and discussion

Unlike previous years, in this study there are more permanent GPS station data and accordingly moreaccurate GPS observations made along the MCT (Reilinger et al., 2006; Kadirov et al., 2008, 2009, 2013, 2014, 2015; Kadirov and Safarov, 2014; Ahadov and Kadirov, 2021; Ahadov and Jin, 2017; Ahadov and Jin, 2021; Ismail-Zadeh et al., 2020; Yetirmishli et al., 2021, 2022a,b; Kazimov, 2021). Therefore it is possible to accurately track how the dynamics of the MCT changes from west to the east. Fig.3 shows a close-up of the GPS velocity field around the Greater and Lesser Caucasus, providing a quantitative basis to estimate the locations and slip rates and directions on the major structures that accommodate deformation.

On a broad scale, the GPS velocity field clearly illustrates the NNE motion of Caucasus and adjacent regions with respect to Eurasia south of the MCT (Fig.3).

The main shortening here in collision zone occurs along the southern boundary of the Greater Caucasus near the seismically active Greater Caucasus Fold-and-Thrust Belt (GCFTB).

This is well illustrated in the series of velocity profiles in Figs.4, 5 and 6, which show the rate of motion versus distance along profiles parallel to ($AA^{/}$) and traversing (B-C) the Caucasus system (profile locations on Fig. 3). Fig. 4a shows the component of velocity parallel to the direction of the profile; Fig. 4b shows the component normal to the direction of the profile (i.e. shortening or lengthening).

The plot in Fig.4b for the profile aligned along strike of the Greater Caucasus demonstrates the progressive increase in convergence rate with Eurasia from west to east, from 1-2 mm/yr in Georgia, to 13-14 mm/yr south of Absheron peninsula. The absence of any consistent change in rates in the direction of the profile traversing the Lesser Caucasus (i.e., Figs 5a and 6a) constrains active shortening in the Lesser Caucasus to < 2 mm/yr. These observations, and the low level of significant seismicity in the Lesser Caucasus (Fig. 3; the M6.8, 1988, Spitak, Armenia Earthquake being a notable exception), suggest that, within the resolution of our GPS observations, the Lesser Caucasus behaves like a coherent block rotating in a counterclockwise sense with respect to Eurasia, around a pole near the eastern end of the Black Sea (e.g. Lawrence, 2003; Reilinger et al., 2006; Copley and Jackson, 2006). Rotation may be related to the closure of an inter-continental back-arc basin separating the Lesser and Greater Caucasus, with the Caucasian Isthmus (Kur Depression in Azerbaijan) being

the last remnants currently undergoing the final stages of subduction/closure (e.g. Cowgill et al., 2012).

However, when looking in more detail, we can see that along the MCT, the direction of the GPS velocity vectors west and east of the 48^0E -longitude changes from NNW to NNE, respectively. This can be explained by the separation of the MCT into a segment with more different dynamics near its intersection with 48^0E and/or by the presence of an active fault normal to the strike of MCT.

Along the southern slope of the Greater Caucasus, from west to east highest velocities are observed in KATE (5.51 mm/yr), OKUD (6.11 mm/yr), SEKC (6.10 mm/yr), YAGB (7.91 mm/yr), QABL (6.83 mm/yr), KEBE (5.46 mm/yr), ISMA (6.77 mm/yr) and IMLG (8.04 mm/yr) stations. The direction of the GPS velocity vectors at these points is mainly to the NNW, except for ISMA. Starting from GPS station MEDR (6.00 mm/yr) eastward from the epicenter of historical Shamakhi earthquake to Absheron Peninsula, the values of velocity vectors gradually decrease and reach 1.70 mm/yr at station JLVG, while the directions of movement are towards NNE.

Relatively smaller velocities are observed in the stations located on the northern slope of the Greater Caucasus and the northern part of the NCF. Thus, the earth's crust horizontal rates at QSRG, SAMU, SIYE stations are equal to 3.65, 2.19 and 1.71 mm/yr, respectively. Although the direction of motion is NNE at station XNQG (4.85 mm/yr), which is located slightly to the south, the velocity at station ANIX is 1.90 mm/yr, and the direction of motion is SW. Thesmall, but sharp difference from the regional crustal motion sense at the ANIX station may be a sign of the presence of a local active fault perpendicular to the strike of the Great Caucasus trust andfold system. This can be observed from the topographic structure of the area, as well.

We can observe how the Earth's crust horizontal movement ratesare gradually increase from west to east, in the GPS stations located in the northern slope of the Lesser Caucasus, the Kura depression and the Talish zone. In general, unlike the Greater Caucasus,here the velocities are higher. Thus, the horizontal crustal movement velocities starting from the territory of Georgia in the west, from the station QZXG (7.65 mm/yr) located in the territory of Azerbaijan increase towards the east, at stations BLVR (13.54 mm/yr), ASTA (13.40 mm/yr), and LKRG (13.54 mm/yr). In addition, it is observed that the Earth's crust movement direction along the Kura depression is towards the NNE in all the stations, except for the YEVL station, which suggests that the Lesser Caucasus, the Kura depression and the Talysh zone move as a coherentand single block. The same pattern is observed in the neighboring territories of Georgia and Armenia.

We believe that the observed NNW movement at the YEVL site is caused by the large number of multi-trajectory errors and the higher signal-to-noise ratio at this site (due to the presence of tall buildings and trees near the antenna).

In the areas located south of Goycha Lake and the Iran-Azerbaijani border, we encounter a more complex velocity field, which indicates the existence of an active fault system parallel to each other in the SE-NW direction, which is also observed in the territories of Armenia and Iran in the south, starting from the Hekari river valley.

It can be observed that the crustal movement velocities at the GPS stations located south of the Absheron Peninsula (starting from SALN)decrease from the WCF to the east and, at the same time, the movement directions change from NNE (SALN, KHİD) to East (SHİK, SANG, JANG, BAKU, GOBG, QALG, GURK, JLVG, PIERCE, NARD) (Figs 3, 6).

In addition, small azimuth differences are noticeable in the direction of PIRS and NARD GPS vectors located in the north of the Absheron Peninsula and GOBG, BAKU, QALG, GURK and JLVG stations located in the south. This can be explained by the dynamics of the fault, which is characterized by weak activity passing in the subparallel direction from the northern part of the Absheron Peninsula, suggesting that significant deformational energy can be accumulated here along the boundary.

We estimate shortening across the eastern segment of the MCT from the velocity difference between site KURD in the Kura Depression and SAMU on the northernmost site of the Pre-Caspian-Guba region (Fig. 2). The total velocity difference is 9 ± 1 mm/yr, corresponding to the rate of shortening across the MCT at ~48° E longitude. The total velocity difference between SATG in the central Kura Depression and SIYE on the north of the Absheron peninsula is almost 11 ± 1 mm/yr (Fig. 2). In western Azerbaijan the rate of crustal shortening derived from QZXG and ZKTG GPS site velocity differences is about 4 ± 1 mm/yr, indicating that the strain accumulation rates across the MCT is different from west to east.

An important note here is the sharp decrease in site velocities, and the clockwise rotation, between sites located to the west of WCF in Kura Depression and Talish region (GOSM, YARD, BILE, SATG, SABD) and sites to the east of WCF in Absheron Peninsula (SHIK, SANG, GOBG, BAKU and further to the east) (Fig. 2). This decrease and difference in GPS vector directions indicate high strain accumulation rates ~6 mm/yr south to Absheron Peninsula.

This is best illustrated by the GPS velocity profiles shown in Fig.6a, and b. The location of the profile CC/is shown on Fig. 3. Fig.6a shows the component of site velocity parallel to the WCF at this loca-

tion (rate of right-lateral strike slip), and Fig.6b the component of site velocity normal to the WCF (i.e., rate of fault-normal motion). Fig.6a indicates11 ± 1 mm/yr right-lateral strike slip motion across the WCF, while Fig.6b indicates 3 ± 1 mm/yr fault-normal motion along the segment of the MCT/WCF south of the Absheron Peninsula.

As noted earlier, the small difference on crustal motions for sites in northern Absheron (PIRS, NARD) and those located in southern side indicates left lateral, strike slip on the fault, which is probably the southern segment of NCT, where it turns to the south inland from the Caspian coast line and crosses the peninsula from west and continues eastward to the Caspian Sea. This geometry for the NCT is roughly consistent with some earlier interpretations of the regional tectonics (e.g., Philip et al., 1989), and indicates that the Baku area is located at a highly complex junction between four fault systems, the MCT, the Central Caspian Seismic Zone, the North Caspian Fault, and the West Caspian Fault.

A decrease in the velocity and a significant accumulation of elastic energy in the southern Absheron Peninsula is responsible for the activation of seismic events and of mud volcanoes in this region. The strong earthquake in the Caspian Sea at the end of 2000 and its aftershocks probably represent a response to the deformational processes which continue in recent years, and the related stress accumulation at foothills of the Greater Caucasus and the Absheron Peninsula and middle Caspian regions (Kadirov et al. 2005).

While the available GPS data provide fundamentally new constraints on fault geometry and rates of strain accumulation, spatial densification of the GPS observations is needed to better resolve localized deformation, and consequently the seismic hazard in the eastern Caucasus, Kura Depression, and Absheron area.

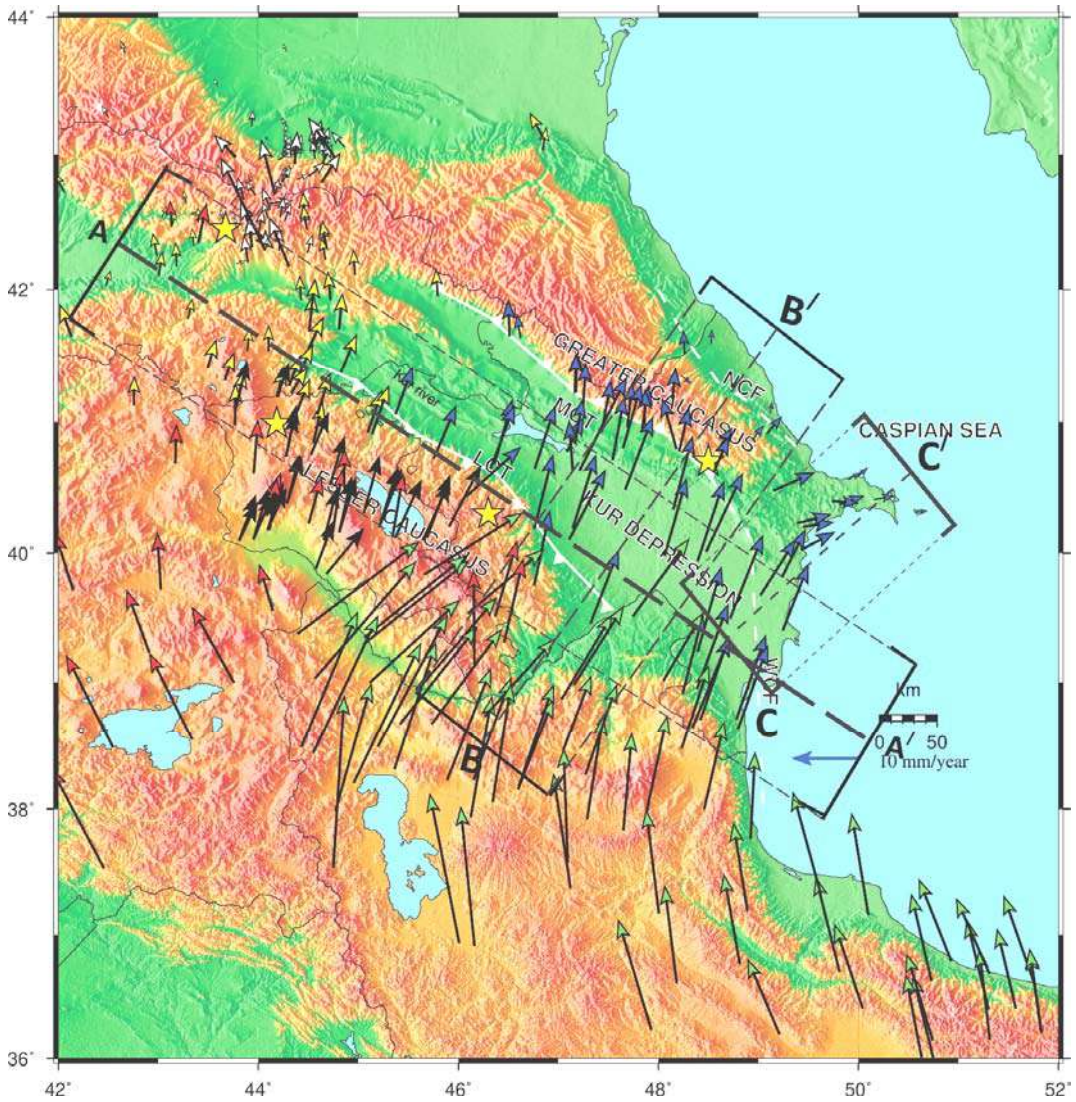

Fig. 3. GPS velocities with respect to Eurasia for the eastern AR-EU collision zone. Orange stars shows 1902, M6.9 Shamakhi; 1139, M7.3 Ganja; 1988, M6.8 Spitak and 1991, M7.0 Racha earthquake epicenters. Velocity profiles A-C are shown in Fig. 4-6. Locations and widths (brackets) of velocity profiles crossing the Kura Basin (A–A′) across strike of the Greater Caucasus (B-B′), and Absheron Peninsula (C-C′), respectively.

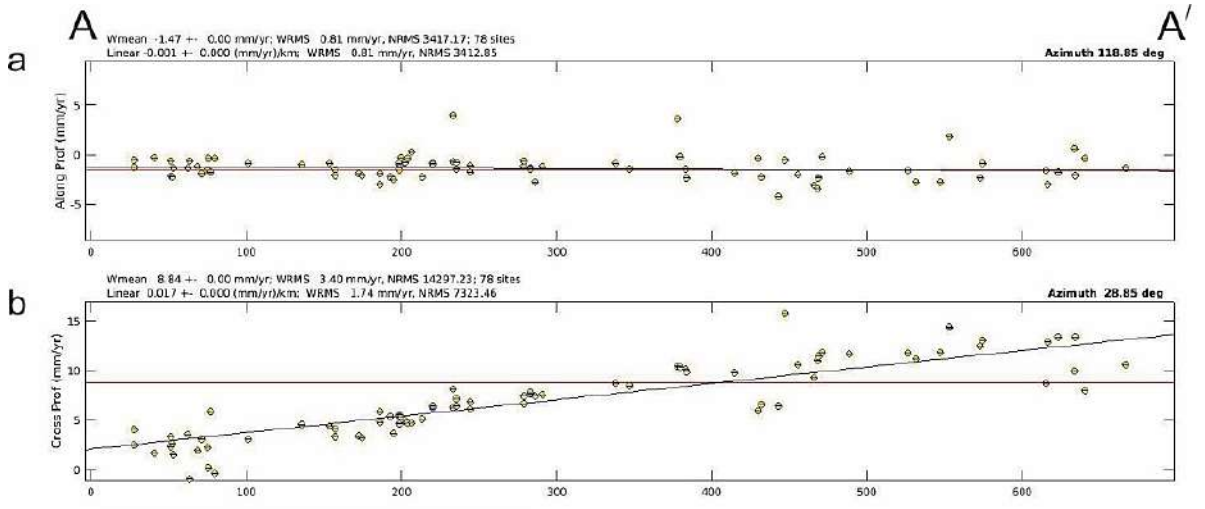

Fig. 4.GPS velocities with respect to Eurasia plotted versus distance along profile A-A/ shown in Fig. 3. The widths ofthe profile is indicated by brackets in Fig. 3. (a) The component of motionparallel to the profile, (b) The component of motion normal to the strike of the profile.

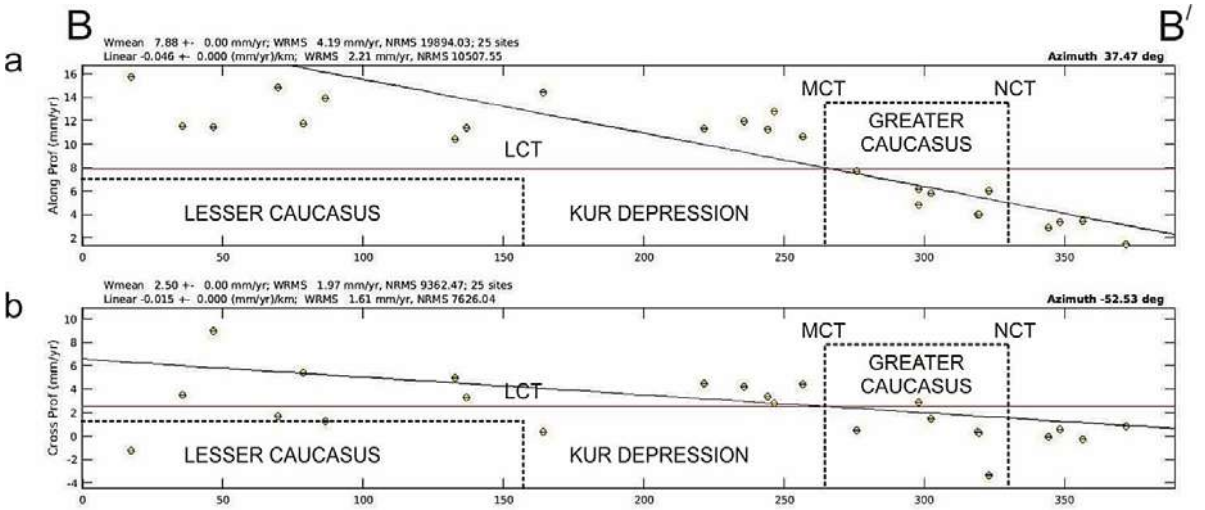

Fig. 5. GPS velocities with respect to Eurasia plotted versus distance along profile B-B/ shown in Fig. 3. The widths of the profile is indicated by brackets in Fig. 3. (a) The component of motion parallel to the profile, (b) The component of motion normal to the strike of the profile.

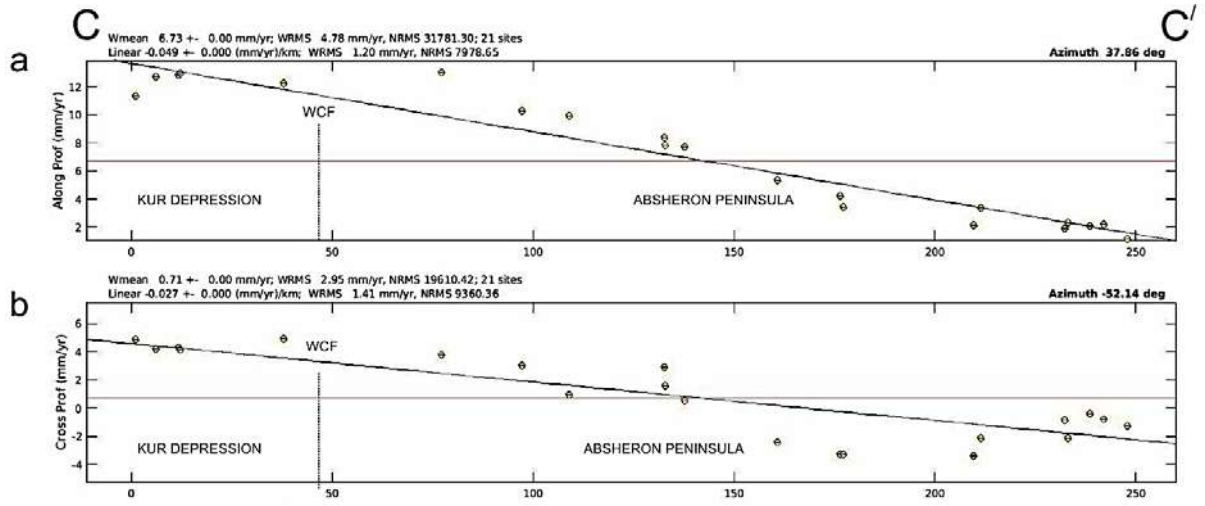

Fig. 6. GPS velocities with respect to Eurasia plotted versus distance along profile C-C/ shown in Fig. 3. The widths of the profile are indicated by brackets in Fig. 3. (a) The component of motion parallel to the profile, (b) The component of motion normal to the strike of the profile

Structures accommodating deformation may merge offshore with the thick, folded sediments south of the Absheron Peninsula. This offshore geometry is supported by GPS velocities in the SW corner of the Caspian Basin in Iran (Djamour et al., 2010) that indicate northerly motion with rates similar to those in the adjacent Lesser Caucasus to the west.

Conclusions

Repeated GPS surveys in Azerbaijan and more permanent station data for the period 1998 – 2022 are providing direct observations of present-day surface motions. They clearly define active convergence between the Lesser Caucasus/Kura Depression and the Greater Caucasus with strain concentrated along the Main Caucasus Thrust Fault (MCT).

On a broad scale, the GPS velocity field clearly illustrates the NNE motion of Caucasus and adjacent regions with respect to Eurasia south of the MCT.

Present-day slip rates on the MCT decrease from 10 ± 1 mm/yr in eastern Azerbaijan to 4 ± 1 mm/yr in western Azerbaijan. These new observations further indicate that the strain accumulation rates along MCT gradually changes from west in Georgia, to the east of the Absheron Peninsula.

GPS velocity vectors west and east of the 48^0E suggests that MCT separates into a segments byan active fault normal to the strike of MCT characterized by different dynamics near its intersection with 48^0E.

It is observed that the earth's crustal movement direction along the Kura depression is towards the NNE in all the stations, except for the YEVL station, which suggests that the Lesser Caucasus, the Kura depression and the Talysh zone move as a coherentand single block.

WCF is a predominantly right lateral strike slip fault with a slip rate of 11± 1 mm/yr south of the Absheron Peninsula.

GPS-derived motions in the northern slope of Greater Caucasus and along the Caspian coast in Azerbaijan north of the Absheron Peninsula require that thrust faulting along the south-dipping North Caucasus. Thrust turns to the south inland of the Caspian coast, crosses the peninsula from west and continues eastward to the Caspian Sea, presumably accommodating left-lateral strike slip motion on this segment.

These interpretations of the GPS velocity field place Baku at the junction of four active fault systems, the MCT, the North and West Caspian faults (likely left and right-lateral, strike slip respectively), and the Central Caspian Seismic Zone. More focused geodetic monitoring of surface motions are needed in the Absheron region and Kura Depression, as well as in the immediate vicinity of other active faults and mud volcanoes.

The geodetic observations presented in this study demonstrate that strain is accumulating along all segments of the Greater Caucasus Fold-and-Thrust Belt from the Shamakhi region (~70 km west of Baku) to the Azerbaijan-Georgian border.

Geodetic observations across the Kur Depression and Absheron Peninsula in the densely populated and highly developed easternmost part of Azerbaijan show a similar deformation pattern across the GCFTB as the observations crossing the central and eastern segments of the fault. While this may indicate active strain accumulation that could generate earthquakes, the absence of large historic earthquakes, the change in strike of the fault west of Baku, and the thick highly saturated sediments in the eastern Kur Depression and south Caspian Basin may preclude large events like those known to occur on the fault further east.

However, given the rapid increase in the population and the extensive infrastructural development in this part of Azerbaijan, and the likelihood of gaining new insights from additional geodetic observations and complex fault models, it is essential that further studies be focused on the possibility and effects of damaging earthquakes along the eastern segment of the GCFTB. In particular, densifying GPS coverage along and across the eastern Caucasus, Kur Basin, and Greater Caucasus, constraining the subsurface geometry of the GCFTB and it's extension into the Caspian Sea with seismic studies, and investigating the historic earthquake record and paleoseismic observations to extend the earthquake record will provide the constraints needed to clarify better earthquake hazards in Azerbaijan.

Acknowledgments

We are grateful to the survey personnel who assisted with the field observations in Azerbaijan, and many individuals that maintain the global IGS stations used in our analysis. The maps in this paper were generated using the public domain Generic Mapping Tools (GMT) software (Wessel and Smith, 1995). Velocity profiles were generated using velview matlab tools provided by T.Herring, 2003. This work was supported in part by the Geology and Geophysics Institute, Azerbaijan Science and Education Ministry and MIT.

REFERENCES

Ahadov B. and Jin S. Present-day kinematics in the Eastern Mediterranean and Caucasus from dense GPS observations. Physics of the Earth and Planetary Interiors, Vol. 268, 2017, pp.54-64.

Ahadov B. and Jin S. Slip rates and seismic potential along main faults in the Eastern Mediterranean and Caucasus from dense GPS observations and seismic data. Pure and Applied Geophysics, Vol. 178, 2021, pp. 39-54.

Ahadov B.G., Kadirov F. A. Insar analysis of the Ayazakhtarma mud volcano and its response to the 2021 Shamakhi earthquake: understanding seismo-volcanic interactions. SOCAR Proceedings, No.4, 2023, pp. 007-012, DOI: 10.5510/OGP20230400911.

Alizadeh A.A., Guliyev I.S., Kadirov F.A., Eppelbaum L.V. Geosciences of Azerbaijan. Volume I: Geology. Springer International Publishing. 2016, 340 p.

Alizadeh A.A., Guliyev I.S., Kadirov F.A., Eppelbaum L.V. Geosciences of Azerbaijan. Volume II: Economic Geology and Applied Geophysics. Springer International Publishing. 2017, 351 p.

Allen M., Jackson J. and Walker R. Late Cenozoic reorganization of the Arabia-Eurasia collision and the comparison of short-term and long-term deformation rates. Tectonics, Vol. 23, No. 2, 2004, DOI: 10.1029/2003TC001530.

Altamimi Z., Rebischung P., Métivier L., Collilieux X. ITRF2014: A new release of the International Terrestrial Reference Frame modeling nonlinear station motions. Journal of Geophysical Research: Solid Earth, Vol. 121(8), 2016, pp. 6109-6131.

ArRajehi A., McClusky S., Reilinger R.E., Daoud M., Alchalbi A., Ergintav S., Gomez F., Sholan J., Bou-Rabee F., Ogubazghi G., Haileab B., Fisseha S., Asfaw L., Mahmoud S., Rayan A., Bendik R., Kogan L. Geodetic constraints on present-day motion of the Arabian Plate: Implications for Red Sea and Gulf of Aden rifting. Tectonics, Vol. 29, TC3011, 2010, DOI:10.1029/2009TC002482.

Avdeev B., Niemi N.A. Constraints on the rates and timing of exhumation of the Greater Caucasus from low temperature thermochronology. Eos, Trans. Am. Geophys. Union, Vol. 89, 2008, 53.

Azizbekov S.A. Tectonic structure of Azerbaijan and the Caspian depression. In International Geophysical Congress, Tectonic Maps of Europe and the World (p. 4). Baku, Academy of Sciences of the Azerbaijan SSR, Department of Earth Sciences, 1968 (in Russian).

Barazangi M., Sandvol E., Seber D. Structure and tectonic evolution of the Anatolian plateau in eastern Turkey. Geol. Soc. Am., Special Paper 409, pp. 463-473, 2006, DOI:10.1130/2006.2409(22)

Bird P. An updated digital model of plate boundaries. Geochemistry, Geophysics, Geosystems, Vol. 4, No. 3, 2003, pp. 1-52, DOI: 10.1029/2001GC000252.

Blewitt G. and Lavallee D. Bias in geodetic site velocity due to annual signals. In “Vistas for Geodesy in the New Millenium”, Int.Assoc. Geod. Symposia, Vol. 125, 2002, pp. 499-500.

Copley A. and Jackson J. Active tectonics of the Turkish-Iranian Plateau. Tectonics, Vol. 25, TC6006, 2006, DOI:10.1029/2005TC001906.

Cowgill E., Niemi N.A., Forte A.M., Elashvili M., Javakishvili Z. and Mumladze T. Orogen-scale structural architecture and potential seismic sources resulting from Cenozoic closure of a relict Mesozoic ocean basin in the Greater Caucasus. S43 J-07, 2012 Spring AGU Meeting.

Dixon T. An introduction to the Global Positioning System and some geological applications. Reviews of Geophys., Vol. 29, 1991, pp. 249-276.

ЛИТЕРАТУРА

Ahadov B. and Jin S. Present-day kinematics in the Eastern Mediterranean and Caucasus from dense GPS observations. Physics of the Earth and Planetary Interiors, Vol. 268, 2017, pp.54-64.

Ahadov B. and Jin S. Slip rates and seismic potential along main faults in the Eastern Mediterranean and Caucasus from dense GPS observations and seismic data. Pure and Applied Geophysics, Vol. 178, 2021, pp. 39-54.

Ahadov B.G., Kadirov F. A. Insar analysis of the Ayazakhtarma mud volcano and its response to the 2021 Shamakhi earthquake: understanding seismo-volcanic interactions. SOCAR Proceedings, No. 4, 2023, pp. 007-012, DOI: 10.5510/OGP20230400911.

Alizadeh A.A., Guliyev I.S., Kadirov F.A., Eppelbaum L.V. Geosciences of Azerbaijan. Volume I: Geology. Springer International Publishing. 2016, 340 p.

Alizadeh A.A., Guliyev I.S., Kadirov F.A., Eppelbaum L.V. Geosciences of Azerbaijan. Volume II: Economic Geology and Applied Geophysics. Springer International Publishing. 2017, 351 p.

Allen M., Jackson J. and Walker R. Late Cenozoic reorganization of the Arabia-Eurasia collision and the comparison of short-term and long-term deformation rates. Tectonics, Vol. 23, No. 2, 2004, DOI: 10.1029/2003TC001530.

Altamimi Z., Rebischung P., Métivier L., Collilieux X. ITRF2014: A new release of the International Terrestrial Reference Frame modeling nonlinear station motions. Journal of Geophysical Research: Solid Earth, Vol. 121(8), 2016, pp. 6109-6131.

ArRajehi A., McClusky S., Reilinger R.E., Daoud M., Alchalbi A., Ergintav S., Gomez F., Sholan J., Bou-Rabee F., Ogubazghi G., Haileab B., Fisseha S., Asfaw L., Mahmoud S., Rayan A., Bendik R., Kogan L. Geodetic constraints on present-day motion of the Arabian Plate: Implications for Red Sea and Gulf of Aden rifting. Tectonics, Vol. 29, TC3011, 2010, DOI:10.1029/2009TC002482.

Avdeev B., Niemi N.A. Constraints on the rates and timing of exhumation of the Greater Caucasus from low temperature thermochronology. Eos, Trans. Am. Geophys. Union, Vol. 89, 2008, 53.

Barazangi M., Sandvol E., Seber D. Structure and tectonic evolution of the Anatolian plateau in eastern Turkey. Geol. Soc. Am., Special Paper 409, pp. 463-473, 2006, DOI:10.1130/2006.2409(22).

Bird P. An updated digital model of plate boundaries. Geochemistry, Geophysics, Geosystems, Vol. 4, No. 3, 2003, pp. 1-52, DOI: 10.1029/2001GC000252.

Blewitt G. and Lavallee D. Bias in geodetic site velocity due to annual signals. In “Vistas for Geodesy in the New Millenium”, Int.Assoc. Geod. Symposia, Vol. 125, 2002, pp. 499-500.

Copley A. and Jackson J. Active tectonics of the Turkish-Iranian Plateau. Tectonics, Vol. 25, TC6006, 2006, DOI:10.1029/2005TC001906.

Cowgill E., Niemi N.A., Forte A.M., Elashvili M., Javakishvili Z. and Mumladze T. Orogen-scale structural architecture and potential seismic sources resulting from Cenozoic closure of a relict Mesozoic ocean basin in the Greater Caucasus. S43 J-07, 2012 Spring AGU Meeting.

Dixon T. An introduction to the Global Positioning System and some geological applications. Reviews of Geophys., Vol. 29, 1991, pp. 249-276.

Djamour Y., Vernant P., Bayer R., Nankali H.R., Ritz J.F., Hinderer J., Hatam Y., Luck B., Le Moigne N., Sedighi M., Khorrami F. GPS and gravity constraints on continental deformation in the Alborz mountain range, Iran. Geophys. Jour. Int., Vol. 183, 2010, pp. 1287-1301.

Engdahl E.R., van der Hilst R., Buland R. Global teleseismic earthquake relocation with improved travel times and procedures for depth determination. Bull. Seismol. Soc. Am., Vol. 88, 1998, pp. 722-743.

Djamour Y., Vernant P., Bayer R., Nankali H.R., Ritz J.F., Hinderer J., Hatam Y., Luck B., LeMoigne N., Sedighi M., Khorrami F. GPS and gravity constraints on continental deformation in the Alborz mountain range, Iran. Geophys. Jour. Int., Vol. 183, 2010, pp.1287-1301.

Engdahl E.R., van der Hilst R., Bul and R. Global teleseismic earthquake relocation with improved travel times and procedures for depth determination. Bull. Seismol. Soc. Am., Vol. 88, 1998, pp. 722-743.

Eppelbaum L. and Katz Y. Tectonic magnetic-paleomagnetic mapping of heterogeneous media: implication for the Easternmost Mediterranean (Northern Israel). ANAS Transactions, Earth Sciences, No. 2, 2022, pp. 3-26, DOI: 10.33677/ggianas20220200079.

Eppelbaum L.V. and Khesin B.E. Geophysical studies in the Caucasus. Springer. Heidelberg – N.Y. – London, 2012.

Forte A., Cowgill E. Bernardin T., Kreylos O., Hamann B. Late Cenozoic deformation of the Kur fold-thrust belt, southern Greater Caucasus. Geological Society of America Bulletin, Vol. 122(3), 2012, pp.465-486, DOI:10.1130/B26464.1.

Gok R., Sandvol E., Turkelli N., Seber D., Barazangi M. Sn attenuation in the Anatolian and Iranian plateau and surrounding regions. Geophys. Res. Lett., Vol. 30, No. 24, 2003, DOI: 10.1029/2003GL018020.

Guliev I.S., Kadirov F.A., Reilinger R.E., Gasanov R.I., Mamedov A.R. Active tectonics in Azerbaijan based on geodetic, gravimetric and seismic data. Transactions of the Russian Academy of Sciences. Earth Sciences Section, Vol. 383, No. 2, 2002, pp. 174-177.

Hager B.H., King R.W., Murray M.H. Measurements of crustal deformation using the Global Positioning System. Ann. Rev. Earth Planet Sci., Vol. 19, 1991, pp. 351-382.

Herring T. MATLAB Tools for viewing GPS velocities and time series. GPS Solutions, Vol. 7, 2003, pp. 194-199, https://doi.org/10.1007/s10291-003-0068-0.

Herring T.A. GLOBK: Global Kalman filter VLBI and GPS analysis program version 4.1, Massachusetts Institute of Technology, Cambridge. MA, 2004.

Herring T.A., King R.W., McClusky S.M. Introduction to GAMIT/GLOBK Release 10.4. Mass. Inst. Of Technology, 2010, 48 p.

Ismail-Zadeh A., Adamia Sh., Chabukiani A., Chelidze T., Cloetingh S., Floyd M., Gorshkov A., Gvishiani A., Ismail-Zadeh T., Kaban M.K., Kadirov F., Karapetyan J., Kengerli T., Kiria J., Koulakov I., Mosar J., Mumladze T., Müller B., Sadradze N., Safarov R., Schilling F., Soloviev A. Geodynamics, seismicity, and seismic hazards of the Caucasus. Earth-Science Reviews, Vol. 207, 2020,103222, https://doi.org/10.1016/j.earscirev.2020.103222.

Jackson J. Partitioning of strike-slip and convergent motion between Eurasia and Arabia in eastern Turkey. J. Geophys. Res., Vol. 97, 1992, pp. 1247-12479.

Jackson J., McKenzie D. Active tectonics of the Alpine-Himalayan belt between western Turkey and Pakistan. Geophys. J. R. Astr. Soc., Vol. 77, 1984, pp.185-246.

Jackson J., McKenzie D.P. The relationship between plate motions and seismic moment tensors, and the rates of active deformation in the Mediterranean and Middle East. Geophysical Journal International, Vol. 93, 1988, pp. 45-73, https://doi.org/10.1111/j.1365-246X. 1988.tb01387.x.

Jackson J., Priestley K., Allen M., Berberian M. Active tectonics of the south Caspian Basin. Geophys. J. I., Vol. 148, No. 2, 2002, pp. 214-245.

Kadirov F., Floyd M., Alizadeh A. et al. Kinematics of the eastern Caucasus near Baku, Azerbaijan. Nat Hazards, Vol. 63, 2012, pp. 997-1006, https://doi.org/10.1007/s11069-012-0199-0.

Kadirov F., Gadirov A., Safarov R., Reilinger R., McClusky S. Global Positioning system measurements of present-day

Eppelbaum L. and Katz Y. Tectonic magnetic-paleomagnetic mapping of heterogeneous media: implication for the Easternmost Mediterranean (Northern Israel). ANAS Transactions, Earth Sciences, No. 2, 2022, pp. 3-26, DOI: 10.33677/ggianas20220200079.

Eppelbaum L.V. and Khesin B.E. Geophysical studies in the Caucasus. Springer. Heidelberg – N.Y. – London, 2012.

Forte A., Cowgill E. Bernardin T., Kreylos O., Hamann B. Late Cenozoic deformation of the Kur fold-thrust belt, southern Greater Caucasus. Geological Society of America Bulletin, Vol. 122(3),2012, pp.465-486, DOI:10.1130/B26464.1.

Gok R., Sandvol E., Turkelli N., Seber D., Barazangi M. Sn attenuation in the Anatolian and Iranian plateau and surrounding regions. Geophys. Res. Lett., Vol. 30, No. 24, 2003, DOI: 10.1029/2003GL018020.

Guliev I.S., Kadirov F.A., Reilinger R.E., Gasanov R.I., Mamedov A.R. Active tectonics in Azerbaijan based on geodetic, gravimetric and seismic data. Transactions of the Russian Academy of Sciences. Earth Sciences Section, Vol. 383, No. 2, 2002, pp. 174-177.

Hager B.H., King R.W., Murray M.H. Measurements of crustal deformation using the Global Positioning System. Ann. Rev. Earth Planet Sci., Vol. 19, 1991, pp. 351-382.

Herring T. MATLAB Tools for viewing GPS velocities and time series. GPS Solutions, Vol. 7, 2003, pp. 194-199, https://doi.org/10.1007/s10291-003-0068-0.

Herring T.A. GLOBK: Global Kalman filter VLBI and GPS analysis program version 4.1, Massachusetts Institute of Technology, Cambridge. MA, 2004.

Herring T.A., King R.W., McClusky S.M. Introduction to GAMIT/GLOBK Release 10.4. Mass. Inst. Of Technology, 2010, 48 p.

Ismail-Zadeh A., Adamia Sh., Chabukiani A., Chelidze T., Cloetingh S., Floyd M., Gorshkov A., Gvishiani A., Ismail-Zadeh T., Kaban M.K., Kadirov F., Karapetyan J., Kengerli T., Kiria J., Koulakov I., Mosar J., Mumladze T., Müller B., Sadradze N., Safarov R., Schilling F., Soloviev A. Geodynamics, seismicity, and seismic hazards of the Caucasus. Earth-Science Reviews, Vol. 207, 2020,103222, https://doi.org/10.1016/j.earscirev.2020.103222.

Jackson J. Partitioning of strike-slip and convergent motion between Eurasia and Arabia in eastern Turkey. J. Geophys. Res., Vol. 97, 1992, pp. 1247-12479.

Jackson J., McKenzie D. Active tectonics of the Alpine-Himalayan belt between western Turkey and Pakistan. Geophys. J. R. Astr. Soc., Vol. 77, 1984, pp.185-246,

Jackson J., McKenzie D.P. The relationship between plate motions and seismic moment tensors, and the rates of active deformation in the Mediterranean and Middle East. Geophysical Journal International, Vol. 93, 1988, pp. 45-73,https://doi.org/10.1111/j.1365-246X. 1988.tb01387.x.

Jackson J., Priestley K., Allen M., Berberian M. Active tectonics of the south Caspian Basin. Geophys. J. I., Vol. 148, No. 2, 2002, pp. 214-245.

Kadirov F., Floyd M., Alizadeh A. et al. Kinematics of the eastern Caucasus near Baku, Azerbaijan. Nat Hazards, Vol. 63, 2012, pp. 997-1006, https://doi.org/10.1007/s11069-012-0199-0.

Kadirov F., Gadirov A., Safarov R., Reilinger R., McClusky S. Global Positioning system measurements of present-day cructal movements in the Azerbaijan. Science without borders. Transactions of the International Academy of science H&E. Innsbruck, Vol.3, 2009,pp. 448-459.

Kadirov F., Mammadov S., Reilinger R., McClusky S. Some new data on modern tectonic deformation and active faulting in Azerbaijan (according to Global Positioning System measurements). Proceedings of Azerbaijan National Academy of Sciences, the Sciences of Earth, No. 1, 2008, pp. 82-88.

Kadirov F.A. Gravity model of lithosphere in the Caucasus-Caspian Region. In: South Caspian Basin: Geology, geo-

cructal movements in the Azerbaijan. Science without borders. Transactions of the International Academy of science H&E. Innsbruck, Vol. 3, 2009, pp. 448-459.

Kadirov F., Mammadov S., Reilinger R., McClusky S. Some new data on modern tectonic deformation and active faulting in Azerbaijan (according to Global Positioning System measurements). Azerbaijan National Academy of Sciences, Proceedings, the Sciences of Earth, No. 1, 2008, pp. 82-88.

Kadirov F.A. Gravity model of lithosphere in the Caucasus-Caspian Region. In: South Caspian Basin: Geology, geophysics, oil and gas content, Geology Institute, Azerbaijan National Academy of Sciences, Nafta Press. Baku, Azerbaijan, 2004, 333 p.

Kadirov F.A., Floyd M., Reilinger R., Alizadeh Ak.A., Guliyev I.S., Mammadov S.G., Safarov R.T. Active geodynamics of the Caucasus region: implications for earthquake hazards in Azerbaijan. Proceedings of Azerbaijan National Academy of Sciences, The Sciences of Earth, No. 3, 2015, pp. 3-17.

Kadirov F.A., Gadirov A.G., Babayev G.R., Agayeva S.T., Mammadov S.G., Garagozova N.R., Safarov R.T. Seismic zoning of the southern slope of Greater Caucasus from the fractal parameters of the earthquakes, stress state, and GPS velocities. Izvestiya, Physics of the Solid Earth, Vol. 49, No. 4. July 2013, pp. 554-562.

Kadirov F.A., Guliyev I.S., Feyzullayev A.A., Safarov R.T., Mammadov S.K., Babayev G.R., Rashidov T.M. GPS-based crustal deformations in Azerbaijan and their influence on seismicity and mud volcanism. Izvestiya, Physics of the Solid Earth, Vol. 50, No. 6. 2014, pp. 814-823.

Kadirov F.A., Klokočník J., Eppelbaum L.V., Kostelecký J., Bezděk A. Bouguer gravity data and satellite gravity transformation integration in the Caspian region: an introduction. ANAS Transactions, Earth Sciences No.1, 2023, pp. 11-16, DOI: 10.33677/ggianas20230100089.

Kadirov F.A., Safarov R.T. Current crustal deformation within the Azerbaijan territory. Seismoprognosis observations in the territory of Azerbaijan, Vol. 11, No. 1, 2014, pp. 34-37.

Kangarli T., Mammadli T., Aliyev F., Safarov R., Kazimova S. Revelation of potentially seismic dangerous tectonic structures in a view of modern geodynamics of the Eastern Caucasus (Azerbaijan), Earth's crust and its evolution – from Pangea to the Present Continents. IntechOpen, Oct. 12, 2022, DOI: 10.5772/intechopen.101274.

Kangarli T., Mammadli T., Aliyev F., Safarov R., Kazimova S. Revelation of potentially seismic dangerous tectonic structures in a view of modern geodynamics of the Eastern Caucasus (Azerbaijan). IntechOpen: Book Chapter, 2021, pp.1-16, DOI: http://dx.doi.org/10.5772 /intechopen.101274.

Kangarli T.N., Kadirov F.A., Yetirmishli G.J., Aliyev F.A., Kazimova S.E., Aliyev A.M., Safarov R.T., Vahabov U.G. Recent geodynamics, active faults and earthquake focal mechanisms of the zone of pseudosubduction interaction between the Northern and Southern Caucasus microplates in the southern slope of the Greater Caucasus (Azerbaijan). Geodynamics and Tectonophysics, published by the Institute of the Earth's Crust Siberian branch of Russian Academy of Sciences, Vol. 9, No. 4, 2018, pp. 1099-1126, https://doi.org/10.5800/GT-2018-9-4-0385.

Karakhanyan A., Vernant P., Doerflinger E., Avagyan A., Philip H., Aslanyan R., Champollion C., Arakelyan S., Collard P., Baghdasaryan H., Peyret M., Davtyan V., Calais E., Masson F. GPS constraints on continental deformation in the Armenian region and Lesser Caucasus, Tectonophysics, Vol. 592, 2013, pp. 39-45, ISSN 0040-1951, https://doi.org /10.1016/j.tecto.2013.02.002.

Kazimov I.E. Geodynamics of the territory of Azerbaijan on the basis of GPS data in 2017-2019 yy. Geotectonics and geodynamics. Geology and Geophysics of Russian South, Vol. 11(2), 2021, pp. 51-62.

physics, oil and gas content, Geology Institute, Azerbaijan National Academy of Sciences, Nafta Press. Baku, Azerbaijan, 2004, 333 p.

Kadirov F.A., Floyd M., Reilinger R., Alizadeh Ak.A., Guliyev I.S., Mammadov S.G., Safarov R.T. Active geodynamics of the Caucasus region: implications for earthquake hazards in Azerbaijan. Proceedings of Azerbaijan National Academy of Sciences, The Sciences of Earth, No. 3, 2015, pp. 3-17.

Kadirov F.A., Gadirov A.G., Babayev G.R., Agayeva S.T., Mammadov S.G., Garagozova N.R., Safarov R.T. Seismic zoning of the southern slope of Greater Caucasus from the fractal parameters of the earthquakes, stress state, and GPS velocities. Izvestiya, Physics of the Solid Earth, Vol. 49, No. 4. July 2013, pp. 554-562.

Kadirov F.A., Guliyev I.S., Feyzullayev A.A., Safarov R.T., Mammadov S.K., Babayev G.R., Rashidov T.M. GPS-based crustal deformations in Azerbaijan and their influence on seismicity and mud volcanism. Izvestiya, Physics of the Solid Earth, Vol. 50, No. 6. 2014, pp. 814-823.

Kadirov F.A, Lerche I., Guliyev I.S., Kadyrov A.G., Feyzullayev A.A., Mukhtarov A.Sh. 2005. Deep structure model and dynamics of mud volcanoes, Southwest Absheron Peninsula (Azerbaijan). Energy exploration & exploitation. Volume 23, Issue 5. 2005, pp. 307-332. https://doi.org/10.1260/014459805775992717

Kadirov F.A., Klokočník J., Eppelbaum L.V., Kostelecký J., Bezděk A. Bouguer gravity data and satellite gravity transformation integration in the Caspian region: an introduction. ANAS Transactions, Earth Sciences No.1, 2023, pp. 11-16, DOI: 10.33677/ggianas20230100089.

Kadirov F.A., Safarov R.T. Current crustal deformation within the Azerbaijan territory. Seismoprognosis observations in the territory of Azerbaijan, Vol. 11, No. 1, 2014, pp. 34-37.

Kangarli T., Mammadli T., Aliyev F., Safarov R., Kazimova S. Revelation of potentially seismic dangerous tectonic structures in a view of modern geodynamics of the Eastern Caucasus (Azerbaijan), Earth's crust and its evolution – from Pangea to the Present Continents. IntechOpen, Oct. 12, 2022, DOI: 10.5772/intechopen.101274.

Kangarli T., Mammadli T., Aliyev F., Safarov R., Kazimova S. Revelation of potentially seismic dangerous tectonic structures in a view of modern geodynamics of the Eastern Caucasus (Azerbaijan). IntechOpen: Book Chapter, 2021, pp.1-16, DOI: http://dx.doi.org/10.5772 /intechopen.101274.

Kangarli T.N., Kadirov F.A., Yetirmishli G.J., Aliyev F.A., Kazimova S.E., Aliyev A.M., Safarov R.T., Vahabov U.G. Recent geodynamics, active faults and earthquake focal mechanisms of the zone of pseudosubduction interaction between the Northern and Southern Caucasus microplates in the southern slope of the Greater Caucasus (Azerbaijan). Geodynamics and Tectonophysics, published by the Institute of the Earth's Crust Siberian branch of Russian Academy of Sciences, Vol. 9, No. 4, 2018, pp. 1099-1126, https://doi.org/10.5800/GT-2018-9-4-0385.

Karakhanyan A., Vernant P., Doerflinger E., Avagyan A., Philip H., Aslanyan R., Champollion C., Arakelyan S., Collard P., Baghdasaryan H., Peyret M., Davtyan V., Calais E., Masson F. GPS constraints on continental deformation in the Armenian region and Lesser Caucasus, Tectonophysics, Vol. 592, 2013, pp. 39-45, ISSN 0040-1951, https://doi.org /10.1016/j.tecto.2013.02.002.

Kazimov I.E. Geodynamics of the territory of Azerbaijan on the basis of GPS data in 2017-2019 yy. Geotectonics and geodynamics. Geology and Geophysics of Russian South, Vol. 11(2), 2021, pp. 51-62.

Kopp M.L., Shcherba I.G. Late Alpine development of the east Caucasus. Geotectonics, Vol. 19(6), 1985, pp. 497-507.

Kral J., Gurbanov A.G. Apatite fission track data from the

Khain V.E. Tectonics of continents and oceans (year 2000). Nauchniy mir. Moscow, 2001, 606 p. (in Russian).

Kopp M.L., Shcherba I.G. Late Alpine development of the east Caucasus. Geotectonics, Vol. 19(6), 1985, pp. 497-507.

Kral J., Gurbanov A.G. Apatite fission track data from the Greater Caucasus pre-Alpine basement. Chemieder Erde, Vol. 56, 1996, pp. 177-192.

Lawrence S.A. Kinematically consistent, elastic block model of the Eastern Mediterranean constrained by GPS measurements. M.S. Thesis, Massachusetts Institute of Technology, Cambridge, MA,2003.

McClusky S., Reilinger R., Mahmoud S., Ben Sari D., Tealeb A. GPS constraints on Africa (Nubia) and Arabia plate motion. Geophys. J. Int., Vol. 155, 2003, pp. 126-138.

McKenzie D. Active tectonics of the Mediterranean region. Geophys. J.I., Vol. 30(2), 1972, pp. 109-185.

McKenzie D.P., Davies D., Molnar P. Plate tectonics of the Red Sea and East Africa. Nature, Vol. 226, 1970, pp. 243-248.

McQuarrie N., Stock J., Verdel C., Wernicke B.P. Cenozoic evolution of Neotethys and implications for the causes of plate motions. Geophys. Res. Lett., Vol. 30(20), 2003, 2036, DOI:10.1029/2003GL017992.

McQuarrie N., Van Hinsbergen D.J.J. Retrodeforming the Arabia-Eurasia collision zone: Age of collision versus magnitude of continental subduction. Geology, Vol. 41, 2013, pp. 315-318.

Milyukov V.K., Mironov A.P., Rogozhin E.A.et al. Velocities of contemporary movements of the Northern Caucasus estimated from GPS observations. Geotecton., Vol. 49, 2015, pp. 210-218, https://doi.org/10.1134/S0016852115030036.

Mueller I.I., Beutler G. The International GPS Service for geodynamics – development and current structure. Proceedings of the 6th Symposium on Satellite Positioning, Ohio State University, Columbus, Ohio, 1992.

Okada Y. Internal deformation due to shear and tensile faults in a half-space. Bull. Seismol. Soc. Am., Vol. 82, 1992, pp. 1018-1040.

Philip H., Cisternas A., Gviskiani A., Gorshkov A. The Caucasus: An actual example of the initial stages of continental collision. Tectonophysics, Vol. 161, 1989, pp. 1-21.

Raeesi M., Zarifi Z., Nilfouroushan F.et al. Quantitative analysis of seismicity in Iran. Pure Appl. Geophys., Vol. 174, 2017, pp. 793-833, https://doi.org/10.1007/s00024-016-1435-4.

Reilinger R.S., and 22 others. GPS constraints on continental deformation in the Africa-Arabia-Eurasia continental collision zone and implications for the dynamics of plate interactions. J. Geophys. Res., 2006, Vol. 111, BO5411, DOI: 10.1029/2005JB004051.

Robertson A.H.F. Mesozoic-Tertiary tectonic evolution of a south Tethyan ocean basin and its margins in southern Turkey. In: Tectonics and Magmatism in Turkey and the Surrounding Area, (Bozkurt E., Winchester J.A., Piper J.D.A., eds.), Geol. Soc. Spec. Pub. London, Vol. 173, 2000, pp. 97-138.

Sengor A.M.C., Gorur N., Saroglu F. Strike-slip faulting and related basin formation in zones of tectonic escape: Turkey as a case study. In: Strike-slip Faulting and Basin Formation (Biddle K.T. and Christie-Blick N., eds.), Society of Econ. Paleont. Min. Sec. Pub., Vol. 37, 1985, pp. 227-264.

Sengor A.M.C., Tuysuz O., Imren C., Sakinc M., Eyidogan H., Gorur N., Le Pichon X., Rangin C. The North Anatolian fault: A new look. Ann. Rev. Earth Planet. Sci., Vol. 33, 2004, pp. 1-75.

Shevchenko V.I., Guseva T.V., Lukk A.A., Mishin A.V., Prilepin M.T., Reilinger R.E., Hamburger M.W., Shempelev A.G., Unga S.L. Modern geodynamics of Caucasus (based on GPS measurements and seismological data). Physics of the Earth, No. 9, 1999, pp. 3-18.

Shimazaki K. and NakataT. Time-predictable recurrence model for large earthquakes. Geophys. Res. Lett., Vol. 7, 1980, pp. 279-282.

Greater Caucasus pre-Alpine basement. Chemieder Erde, Vol. 56, 1996, pp.177-192.

Lawrence S.A. Kinematically consistent, elastic block model of the Eastern Mediterranean constrained by GPS measurements. M.S. Thesis, Massachusetts Institute of Technology, Cambridge, MA,2003.

McClusky S., Reilinger R., Mahmoud S., Ben Sari D., Tealeb A. GPS constraints on Africa (Nubia) and Arabia plate motion. Geophys. J. Int., Vol. 155, 2003, pp. 126-138.

McKenzie D. Active tectonics of the Mediterranean region. Geophys. J.I.,Vol. 30(2), 1972, pp. 109-185.

McKenzie D.P., Davies D., Molnar P. Plate tectonics of the Red Sea and East Africa. Nature, Vol. 226, 1970,pp. 243-248.

McQuarrie N., Stock J., Verdel C., Wernicke B.P. Cenozoic evolution of Neotethys and implications for the causes of plate motions. Geophys. Res. Lett., Vol. 30(20), 2003, 2036, DOI:10.1029/2003GL017992.

McQuarrie N., Van Hinsbergen D.J.J. Retrodeforming the Arabia-Eurasia collision zone: Age of collision versus magnitude of continental subduction. Geology, Vol. 41, 2013, pp.315-318.

Milyukov V.K., Mironov A.P., Rogozhin E.A.et al. Velocities of contemporary movements of the Northern Caucasus estimated from GPS observations. Geotecton., Vol. 49, 2015, pp. 210-218, https://doi.org/10.1134/S0016852115030036.

Mueller I.I., Beutler G. The International GPS Service for Geodynamics – Development and Current Structure. Proceedings of the 6th Symposium on Satellite Positioning, Ohio State University, Columbus, Ohio, 1992.

Okada Y. Internal deformation due to shear and tensile faults in a half-space. Bull. Seismol. Soc. Am., Vol. 82, 1992, pp. 1018-1040.

Philip H., Cisternas A., Gviskiani A., Gorshkov A. The Caucasus: An actual example of the initial stages of continental collision. Tectonophysics, Vol. 161, 1989, pp.1-21.

Raeesi M., Zarifi Z., Nilfouroushan F.et al. Quantitative analysis of seismicity in Iran. Pure Appl. Geophys., Vol. 174, 2017, pp. 793–833, https://doi.org/10.1007/s00024-016-1435-4.

Reilinger R.S. and 22 others. GPS constraints on continental deformation in theAfrica-Arabia-Eurasia continental collision zone and implications for the dynamics of plate interactions. J. Geophys. Res., 2006, Vol. 111, BO5411, DOI: 10.1029/2005JB004051.

Robertson A.H.F. Mesozoic-Tertiary tectonic evolution of a south Tethyan ocean basin and its margins in southern Turkey. In: Tectonics and Magmatism in Turkey and the Surrounding Area, (Bozkurt E., Winchester J.A., Piper J.D.A., eds.), Geol. Soc. Spec. Pub. London, Vol. 173, 2000, pp. 97-138.

Sengor A.M.C., Gorur N., Saroglu F. Strike-slip faulting and related basin formation in zones of tectonic escape: Turkey as a case study. In: Strike—slip Faulting and Basin Formation (Biddle, K.T. and Christie-Blick N., eds.), Society of Econ. Paleont. Min. Sec. Pub., Vol. 37, 1985, pp. 227-264.

Sengor A.M.C., Tuysuz O., Imren C., Sakinc M., Eyidogan H., Gorur N., Le Pichon X., Rangin C. The North Anatolian fault: A new look. Ann. Rev. Earth Planet. Sci., Vol. 33, 2004, pp. 1-75.

Shevchenko V.I., Guseva T.V., Lukk A.A., Mishin A.V., Prilepin M.T., Reilinger R.E., Hamburger M.W., Shempelev A.G., Unga S.L. Modern geodynamics of Caucasus (based on GPS measurements and seismological data). Physics of the Earth, No. 9,1999, pp. 3-18.

Shimazaki K. and Nakata T. Time-predictable recurrence model for large earthquakes. Geophys. Res. Lett.,Vol. 7, 1980, pp. 279-282.

Sokhadze G., Floyd M., Godoladze T., King R., Cowgill E.S., Javakhishvili Z., Hahubia G., Reilinger R. Active convergence between the Lesser and Greater Caucasus in Georgia: Constraints on the tectonic evolution of the Lesser–Greater Caucasus continental collision. Earth and Planetary Science Letters, Vol. 481, 2018, pp. 154-161.

Telesca L., Kadirov F., Yetirmishli G. et al. Statistical analysis of the 2003–2016 seismicity of Azerbaijan and sur-

Sokhadze G., Floyd M., Godoladze T., King R., Cowgill E.S., Javakhishvili Z., Hahubia G., Reilinger R. Active convergence between the Lesser and Greater Caucasus in Georgia: Constraints on the tectonic evolution of the Lesser–Greater Caucasus continental collision. Earth and Planetary Science Letters, Vol. 481, 2018, pp. 154-161.

Telesca L., Kadirov F., Yetirmishli G. et al. Statistical analysis of the 2003–2016 seismicity of Azerbaijan and surrounding areas. J. Seismol., Vol. 21, 2017, pp. 1467-1485, https://doi.org/10.1007/ s10950-017-9677-x.

Tye A.R., Niemi N.A., Cowgill E., Kadirov F.A., Babayev G.R.. Diverse deformation mechanisms and lithologic controls in an active orogenic wedge: structural geology and thermochronometry of the Eastern Greater Caucasus. Tectonics, Vol. 41(12), 2022, DOI:10.1029/2022TC007349.

Tye A.R., Niemi N.A., Safarov R.T., Kadirov F.A., Babayev G.R. Sedimentary response to a collision orogeny recorded in detrital zircon provenance of Greater Caucasus foreland basin sediments. Basin Research, Vol. 33, No. 2, 2021, pp. 933-967, https://doi. org/10.1111/bre.12499.

Vernant P., Chery J. Low fault friction in Iran implies localized deformation for the Arabia–Eurasia collision zone. Earth and Planetary Sci. Lett., Vol. 246, 2006, pp. 197-206.

Vincent S.J., Morton A.C., Carter A., Gibbs S., Teimuraz G.B. Oligocene uplift of the Western Greater Caucasus: An effect of initial Arabia-Eurasia collision. Terra Nova, Vol. 19, 2007, pp. 160-166, DOI:10.1111/j.1365-3121.2007.00731.x.

Wessel R. and Smith W.H.F. New version of the Generic Mapping Tools released. EOS Trans. AGU, Vol. 76, 1995, p. 329.

Yetirmishli G.J., Kazimov I.E. Modern GPS geodynamics of Azerbaijan. Geotectonics and geodynamics. Geology and Geophysics of Russian South, Vol. 12(4), 2022a, pp. 19-30.

Yetirmishli G.J., Kazimov I.E., Kazimova A.F. Analysis of modern movements of Earth crust blocks in Azerbaijan according to the data of GPS stations in 2020-2021. Seismoprognosis observations in the territory of Azerbaijan, Vol. 21, No. 1, 2022b, pp. 19-24

Yetirmishli G.J., Kazimov I.E., Kazimova A.F. Contemporary geodynamics of the eastern Mediterranean. Seismoprognosis observations in the territory of Azerbaijan, V. 20, No. 2, 2021, pp. 3-10.

Zonenshain L.P., Le Pichon X. Deep basins of the Black Sea and Caspian Sea as remnants of Mesozoic back-arc basins. Tectonophysics, Vol. 123, 1986, pp. 181-211, DOI: 10.1016/0040-1951(86)90197-6.

Zonenshain L.P., Savostin L.A. Introduction to geodynamics. Nedra. Moscow, 1979, 311 p. (in Russian).

rounding areas. J. Seismol., Vol. 21, 2017, pp. 1467-1485, https://doi.org/10.1007/ s10950-017-9677-x.

Tye A.R., Niemi N.A., Cowgill E., Kadirov F.A., Babayev G.R.. Diverse deformation mechanisms and lithologic controls in an active orogenic wedge: structural geology and thermochronometry of the Eastern Greater Caucasus. Tectonics, Vol. 41(12), 2022,DOI:10.1029/2022TC007349.

Tye A.R., Niemi N.A., Safarov R.T., Kadirov F.A., Babayev G.R. Sedimentary response to a collision orogeny recorded in detrital zircon provenance of Greater Caucasus foreland basin sediments. Basin Research, Vol. 33, No. 2, 2021, pp.933-967, https://doi. org/10.1111/bre.12499.

Vernant P., Chery J. Low fault friction in Iran implies localized deformation for the Arabia–Eurasia collision zone. Earth and Planetary Sci. Lett., Vol. 246, 2006, pp. 197-206.

Vincent S.J., Morton A.C., Carter A., Gibbs S., Teimuraz G.B. Oligocene uplift of the Western Greater Caucasus: An effect of initial Arabia-Eurasia collision. Terra Nova, Vol. 19, 2007, pp. 160-166, DOI:10.1111/j.1365-3121. 2007.00731.x.

Wessel R. and Smith W.H.F. New version of the Generic Mapping Tools released. EOS Trans. AGU, Vol. 76, 1995, p. 329.

Yetirmishli G.J. Tangible earthquakes occurred in Azerbaijan for the period of 2003-2018 years. Elm, 2020. 415 p. (in Russian)

Yetirmishli G.J., Kazimov I.E. Modern GPS geodynamics of Azerbaijan. Geotectonics and geodynamics. Geology and Geophysics of Russian South, Vol. 12(4), 2022a, pp. 19-30.

Yetirmishli G.J., Kazimov I.E., Kazimova A.F. Analysis of modern movements of Earth crust blocks in Azerbaijan according to the data of GPS stations in 2020-2021. Seismoprognosis observations in the territory of Azerbaijan, Vol. 21, No. 1, 2022b, pp. 19-24

Yetirmishli G.J., Kazimov I.E., Kazimova A.F. Contemporary geodynamics of the eastern Mediterranean. Seismoprognosis observations in the territory of Azerbaijan, V. 20, No. 2, 2021, pp. 3-10.

Zonenshain L.P., Le Pichon X. Deep basins of the Black Sea and Caspian Sea as remnants of Mesozoic back-arc basins. Tectonophysics, Vol. 123, 1986, pp. 181-211, DOI: 10.1016/0040-1951(86)90197-6.

Азизбеков С.А. Тектоническое строение Азербайджана и Прикаспийской впадины. В сборнике: Международный геофизический конгресс, Тектонические карты Европы и мира (с. 4). Баку, Академия наук Азербайджанской ССР, Отделение наук о Земле, 1968.

Зоненшайн Л.П., Савостин Л.А. Введение в геодинамику. Недра. Москва, 1979, 311 с.

Хаин В.Е. Тектоника континентов и океанов (год 2000). Научный мир. Москва, 2001, 606 с.

РЕЗУЛЬТАТЫ 25-ЛЕТНЕГО (1998-2022) МОНИТОРИНГА ДЕФОРМАЦИИ ЗЕМНОЙ КОРЫ В АЗЕРБАЙДЖАНЕ И НА СОПРЕДЕЛЬНОЙ ТЕРРИТОРИИ С ИСПОЛЬЗОВАНИЕМ GPS

Кадиров Ф.[1], Етирмишли Г.[3], Сафаров Р.[1], Мамедов С.[1], Казимов И.[3], Флойд М.[2], Рейлингер Р.[2], Кинг Р.[2]

[1]Министерство науки и образования Азербайджанской Республики, Институт геологии и геофизики, Азербайджан AZ1143, Баку, просп. Г.Давида, 119

[2]Факультет наук о Земле, атмосфере и планетах, Массачусетский технологический институт 54-918 Кембридж, Массачусетс, США, Массачусетс авеню, 77

[3]Республиканский центр сейсморазведки Национальной академии наук Азербайджана Азербайджан, Баку Az 1001, ул. Н.Рафибейли 25

Резюме. Мы представляем GPS-наблюдения за мониторингом деформаций земной коры в Азербайджане и на прилегающей территории, которые проводились с 1998 года. В отличие от наших предыдущих исследований, здесь собрано еще больше данных постоянных GPS-станций и съемки, что, соответственно, позволило нам более точно определить динамику основных тектонических структур.

С 2006 года Институтом геологии и геофизики было создано восемь постоянных станций. В 2012 году Республиканский центр сейсмологической службы Национальной академии наук Азербайджана приступил к строительству постоянных стан-

ций GPS, всего было установлено 24 станции. С 1998 по 2022 год неоднократно проводились измерения на более чем 35 пунктах наблюдения.

В широком масштабе поле скоростей GPS четко иллюстрирует движение Кавказа и прилегающих регионов в северо–северо-восточном направлении относительно Евразии к югу от Главного Кавказского надвига (ГКН). Здесь важно отметить резкое уменьшение скоростей на пунктах измерения и вращение по часовой стрелке между пунктами, расположенными к западу от Западно-Каспийского разлома (ЗКР) в Куринской впадине и Талышском районе, и участками к востоку от ЗКР на Абшеронском полуострове. Такое уменьшение и различие в направлениях GPS-векторов указывает на высокие скорости накопления деформации – ~6 мм/год к югу от Абшеронского полуострова. Мы полагаем, что значительное накопление упругой энергии является одной из основных причин активизации сейсмических событий и грязевых вулканов в этом регионе. Таким образом, пространственное уплотнение GPS- наблюдений необходимо для лучшего разрешения локализованных деформаций и, следовательно, сейсмической опасности на Восточном Кавказе, в Куринской впадине и на Абшероне.

Ключевые слова: *Деформация, тектонические структуры, мониторинг, GPS, землетрясение, сейсмическая опасность*

AZƏRBAYCAN VƏ QONŞU ƏRAZİLƏRDƏ GPS VASİTƏSİLƏ YER QABIĞI DEFORMASİYALARININ 25 İLLİK (1998-2022) MONİTORİNQİNİN NƏTİCƏLƏRİ

Qədirov F.[1], Yetirmişli Q.[3], Səfərov R.[1], Məmmədov S.[1], Kazımov I.[3], Floyd M.[2], Reylinger R.[2], Kinq R.[2]

[1]Azərbaycan Respublikasının Elm və Təhsil Nazirliyi, Geologiya və Geofizika Institutu, Azərbaycan AZ1143, Bakı, H.Cavid prosp., 119

[2]Yer, atmosfer və planetlər elmləri fakültəsi, Massaçusets Texnologiya Institutu 54-918, ABŞ, Massaçusets, Kembric, Massaçusets Avenyu, 77

[3]Azərbaycan Milli Elmlər Akademiyasının Seysmik Kəşfiyyat Mərkəzi AZ1001, Bakı, N.Rəfibəyli küç., 25

Xülasə. 1998-ci ildən Azərbaycanda və ona bitişik ərazilərdə aparılan yer qabığı deformasiyalarının GPS monitorinq nəticələri təqdim edilmişdir. Əvvəlki tədqiqat işlərindən fərqli olaraq, burada daha çox fasiləsiz işləyən GPS stansiyaları və ölçü məntəqə məlumatları cəmlənmişdirki, bu da regionun əsas tektonik strukturlarının dinamikasını daha dəqiq müəyyən etməyə imkanvermişdir.

2006-cı ildən başlayaraq, Geologiya və Geofizika İnstitutu tərəfindən səkkiz fasiləsiz işləyən stansiya qurulmuşdur. 2012-ciildənisə Azərbaycan Milli Elmlər Akademiyası nəzrində Respublika Seysmoloji Xidmət Mərkəzi tərəfindən GPS stansiyalarının qurulmasına başlanmış və burada ümumilikdə 24 stansiya yaradılmışdır. 1998-ciildən 2022-ciilə qədər 35-dən çox ölçü məntəqəsində dəfələrlə müşahidələr aparılmışdır.

Böyük miqyasda, GPS sürət sahəsi Əsas Qafqaz Üstəgəlmə Qırılmasından (MCT) cənubda olmaqla Qafqaz və ona bitişik rayonların Avrasiyaya nəzərən şimal-şimal-şərq istiqamətində hərəkətini aydın şəkildə təsvir edir. Burada qeyd edilməli mühüm məqam Kür çökəkliyi və Talış bölgəsində Qərbi Xəzər qırılmasından (QXQ) qərbdə yerləşən məntəqələrlə QXQ-nin şərqində Abşeron yarımadasında yerləşən məntəqələr arasında sürətlərin kəskin azalması və saat əqrəbi istiqamətində fırlanmadır. GPS vektor istiqamətlərindəki bu azalma və fərq Abşeron yarımadasının cənubunda ~6 mm/il olmaqla deformasiyaların yüksək sürətlə toplanmasını göstərir. Belə hesab edirik ki, elastik enerjinin əhəmiyyətli dərəcədə toplanması bu regionda seysmik hadisələrin və palçıq vulkanlarının aktivləşməsinin səbəblərindəndir. Beləliklə, Şərqi Qafqazda, Kür çökəkliyində və Abşeron ərazisində toplanmış deformasiyanı və nəticədə seysmik təhlükəni daha dolğun qiymətləndirmək məqsədilə GPS müşahidə məntəqələrinin sıxlığının artırılmasına ehtiyac vardır.

Açar sözlər: *Deformasiya, tektonik strukturlar, monitorinq, GPS, zəlzələ, seysmik təhlükə*

ANAS Transactions Earth Sciences 1 / 2024

http://www.journalesgia.com

HEAVY CARBON ISOTOPE COMPOSITION OF THE MIOCENE DIATOMITES AND OILS IN THE SOUTH CASPIAN BASIN AS A POSSIBLE GLOBAL PHENOMENON

Feyzullayev A.A.[1,2]

[1]*Ministry of Science and Education of the Republic of Azerbaijan, Institute of Geology and Geophysics, Azerbaijan*
119, H.Javid ave., Baku, AZ1143: fakper@gmail.com
[2]*Ministry of Science and Education of the Republic of Azerbaijan, Institute of Oil and Gas, Azerbaijan*
9, F.Amirov str., Baku, AZ1000

Keywords: *carbon isotope composition, organic matter, oil, sedimentary basins, Miocene, Pre-Miocene*

Summary. The paper provides an analysis of the results of isotope-geochemical studies of rocks and oils of the Cenozoic-Mesozoic section of the South Caspian Basin (SCB) over the past 30 years. As a result, the previously established fact of the heavy carbon isotope composition (ICC) of organic matter (OM) of Miocene rocks (Diatom Formation), as well as its derivative oils accumulated in the main (Lower Pliocene) reservoir of the SCB, were confirmed. To verify the global nature of this phenomenon, a comparative analysis of isotope-geochemical data on sedimentary basins of 18 countries was carried out. A generalized diagram showing the limits of change in the ICC of kerogen and oils and their average values for various stratigraphic complexes for all considered basins has been constructed. It has been established that this phenomenon is also characteristic of other basins of the world. Based on this, a conclusion was made about the global nature of this phenomenon. The reasons that led to the isotopic shift in the global carbon budget that occurred in the Miocene are not completely understood. The existing ideas about its possible nature are considered. The results once again confirmed the effectiveness of using $\delta^{13}C$ for oil-oil and oil-source rock correlation in combination with other geochemical criteria.

Introduction

The South Caspian basin (SCB) is a large tectonic element of the Earth's crust in the central segment of the Alpine-Himalayan mobile belt, which includes the deepest depression on Earth – the South Caspian Depression (SCD). The SCB is characterized by very rapid Pliocene- Quaternary subsidence and sedimentation (1.2-3.0 km/Ma). The sedimentary fill of the SCB reaches a thickness up to 25 km and is formed by deposits of Middle Jurassic to Quaternary age.

The SCB is among the oldest oil and gas bearing provinces in the world. Oil and gas is produced from reservoirs over a wide stratigraphic range: from the Upper Cretaceous to the Quaternary. The majority of commercial oil reserves, however, are located in the Lower Pliocene – Productive Series (>75%), with the remainder in the Miocene-Paleogene (15%) and the Upper Cretaceous (10%) (Feyzullayev et al., 2001).

Over the past 30 years, a large amount of research has been carried out to study the generation potential of the Mesozoic-Cenozoic rocks from outcrops and wells, as well as the carbon isotope composition (ICC) of reservoir oils. Oil-to-oil and source rocks-to-oil correlations based on carbon isotopic ratios suggest that the Miocene interval (Diatom, Chokrak and Upper Maykop strata) has played the principal role in the formation of commercial oil accumulations in Lower Pliocene – Productive Series (PS) reservoirs (Guliyev et al., 1997; Feyzullayev et al., 2001; Guliyev et al., 2001; Feyzullayev, 2019).

Based on the ICC of organic matter (OM), two groups of rocks were clearly identified in the sedimentary section of the SCB: diatoms and pre-diatoms. OM of diatom rocks, as well as its derivative oils, is characterized by relatively heavier ICC (Fig. 1 and 2).

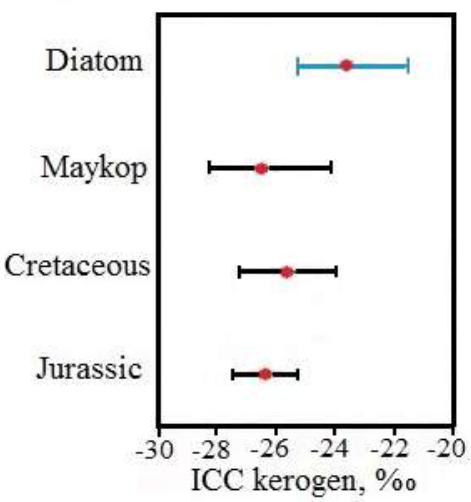

Fig. 1. SCB. Limits of change and average values of $\delta^{13}C$ in kerogen of rocks of different ages (Feyzullayev et al., 2001)

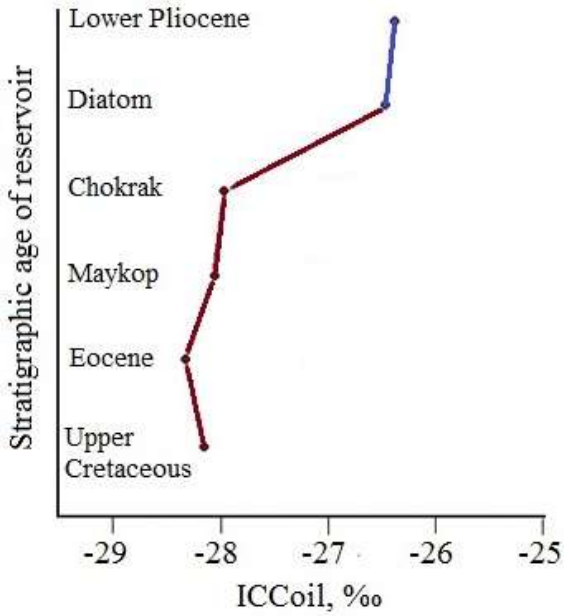

Fig. 2. Average values of carbon isotope ratios in the alkane fraction of oils from different age reservoirs in the South Caspian Basin (Guliyev et al., 2001)

The source of oils of the main (Lower Pliocene) SCB reservoir is mainly the diatomaceous formation (Feyzullayev, Aliyeva, 2003) and therefore they are also characterized by relatively heavy ICC.

The Diatom suite belongs to the Middle-Upper Miocene stratigraphic interval and includes 4 horizons namely: Konk, Karagan, Sarmat and Meotis. This formation is distinguished by a high Total Organic Carbon (TOC) content (on average 4.35 wt.%) with type II-I kerogen (HI up to 770 mg HC/g TOC) and a high generation potential (~3 t. HC/m^2).

As the name of the formation suggests, it consists of more than 50% diatom shells and is represented by loose or cemented siliceous deposits of light gray or yellowish color (Diatomite, 1978; Zhuze, 1973).

The diatomite is a porous rock, light-weight, siliceous, being a result of accumulation and compactions of diatom remains, clay and silt. The diatoms accumulate in areas where the rate of deposition of diatoms frustule is higher than the deposition of other sediments (e.g., Berger, 1970; Barron 1987). Diatomites are of marine, less often freshwater (lake) origin and contain 70-98% silica (Jordan, Stickley, 2010).

Diatomites are prolific hydrocarbon source rocks in many basins worldwide (Schwartz, 1987; Aoyagi, Iijima, 1987; Aoyagi, Omokawa, 1992; Bailey et al., 1996; Bazhenova, 2002; Mayer et al., 2018; Sachsenhofer et al., 2018; Tulan et al., 2020).

Examples include the Miocene Monterey Formation in California (Isaacs and Rullkötter, 2001). Several Miocene diatomaceous deposits are documented in Central Europe. In the Pannonian Basin the Middle Miocene diatom-rich rocks are associated with volcanic activity (Dill et al., 2008).

They are distributed mainly in Paleogene-Neogene and Quaternary geological deposits (Tomkeev, 1986). Diatomites acquire a particularly important significance in the Tertiary period; in Paleogene diatomites, silica is often replaced by pyrite (Maslov, 1974).

The starting discovery of a similar phenomenon (heavy ICC of the Miocene OM and oils) in some other sedimentary basins motivated this study (Kennett, 1986; Chung et al., 1992; Magoon et al., 1995; Lillis et al., 2001; Younes, 2012; Philip, Jarde, 2015).

In this regard, the main objective of this study was to collect, summarize and compare the ICC of kerogen and oils of the Miocene and older rocks/reservoirs of various sedimentary basins of the world. The main purpose is to test the assumption about the global nature of the phenomenon of heavy ICC of OM and oils of the Miocene identified in the SCB.

Analytical database

The data on the carbon isotope composition of OM (kerogen/extract of rocks) and SCB oils used in the paper represent the most complete summary of research results over the past 30 years. For a comparative analysis with other basins of the world, data on Miocene (Diatom Formation) and relatively older Oligocene-Lower Miocene (Maykop Series), Eocene and Cretaceous sediments were used. The amount of this data is reported in Table 1.

Results from other basins in the world are divided into two groups in Table 2 based on their age (Miocene and Pre-Miocene).

Table 1

Number of analyzes ICC of OM and oils in the SCB

Age of oil source and reservoir rocks	Diatom		Maykop		Eocene		Cretaceous	
Analyzed objects	OM	Oil	OM	Oil	OM	Oil	OM	Oil
Number of analyses	31	64	52	29	12	28	14	10

Table 2

Number of analyzes ICC of OM and oils for various basins of the world

Country	**Basins / Province**	**Number of ICC**				**Source**
		Miocene		**Pre-Miocene**		
		OM	**Oil**	**OM**	**Oil**	
Azerbaijan	South Caspian – Kura basin	31	64	78	57	Guliyev et. al., 1997; Guliyev et al., 2001
USA	San Joaquin and Santa Clara basins, California; Pismo, Santa Maria and Hartford basins; Denver and Powder River basins; Gulf of Mexico.	29	152	57	88	Clayton et al., 1992; Magoon et al., 1995; Lillis et al., 2001; Lillis and Magoon, 2007; Peters et al., 2018; Andrusevich et al., 1998; Schouten et al., 1997; Johnson, 1998; Spiker et al., 1988; Komada et al., 2005; Froelich, Robinson, 1988;
Russia	Eastern and Western Siberia basins, Yenisei-Khatanga OGR, Sakhalin, Kamchatka, Crimea-Caucasus region, Caspian depression.		28	77	206	Kontorovich et al., 2011; Leushina et al., 2021; Afanasenkov et al., 2019; Oblasova et al., 2020; Andrusevich et al., 1998; Timoshina, 2005
Canada	Saanich Inlet, British Columbia	30				Johnson, 1998
Norway	Wring Plateau, Nothern Sea.	8			11	Morris, 1976; Andrusevich et al., 1998
Hungary	Pannonian basin	20		4		Körmös et al., 2021; Veto et al., 2016
Poland / Ukraine	Outer and CisCarpathia (Polish-Ukrainian segment)			14	20	Kotarba, Koltun, 2006; Kotarba et al., 2021; Wieclaw et al., 2012
Austria	Alpine foreland basin				41	Gratzer et al., 2011
Lithuania	Baltic Syneclise				12	Zdanaviciute, Bojesen–Koefoed, 1997
Kazakhstan	Aryskum trough				14	Golyshev et al., 2020; Madisheva, 2020
Oman	Salt basin			40		Grosjean et al., 2009
Libya	East Sirte Basin				16	Aboglila, 2010
Guinea	Niger Delta Basin			12	39	Ogbesejana et al., 2020
Egypt	Gulf of Suez		4			Younes, 2012
Turkiye	Gulf of Edremit, northwestern Anatolia	3				Bozcu, 2015
India	Indus Fan (Laxmi basin in the eastern Arabian Sea)	7				Khim et al., 2020
Malaysia	North Sabah Basin	3				Anuar, 1994
TOTAL		**131**	**248**	**282**	**504**	

The Pre-Miocene data presented in Table 2 covers a wide stratigraphic interval spanning from the Oligocene to the Cambrian. These data include the results of the determination of the ICC of both kerogen/extract and oil as a whole, as well as their saturated and aromatic fractions.

Data processing and graphical constructions were performed using standard computer programs.

Results

The South Caspian Basin

The fact of isotope-heavy carbon of OM of Neogene rocks and oils of the SCB in comparison with underlying rocks and reservoirs was first noted in previous studies (Guliyev, Feyzullayev, 1996; Guliyev et al., 1997), and later in the works (Feyzullayev et al., 2001 and Guliyev et al., 2001).

In order to consider this problem from a global scale, the results of a profound analysis of ICC of OM and oils in SCB based on the most complete summary of data are given below.

Figure 3 shows histograms of the distribution of ICC values of OM and oils of Miocene and pre-Miocene rocks and reservoirs, according to which an isotopic difference between these two age groups is obvious with a boundary value of -27.0‰.

Isotopic differences in OM and oils of the two age groups under consideration are clearly reflected in the graphs of the relationship between their saturated and aromatic fractions (Fig. 4).

There is an interesting feature in the change of ICC values with depth: the values of oils from Miocene reservoirs shift upward (mainly above a depth of 3 km) compared to the ICC of OM of Miocene rocks, which is apparently associated with subvertical migration processes (Fig. 5). Due to these processes, the oils of the main reservoir of the SCB (Productive Series), which have an epigenetic nature and are derivatives of predominantly Miocene source rocks, have also a heavy carbon isotope (Guliyev et al., 2001).

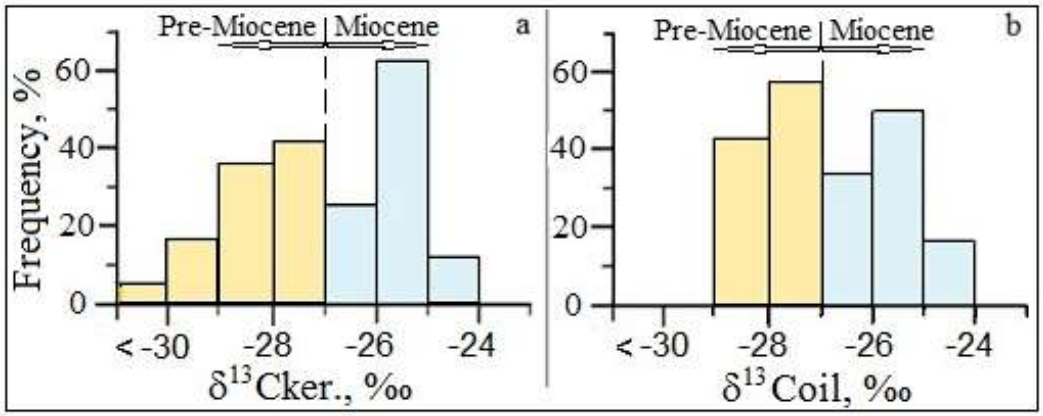

Fig. 3. Distribution of ICC values of Miocene and Pre-Miocene OM (a) and oils (b) in the SCB

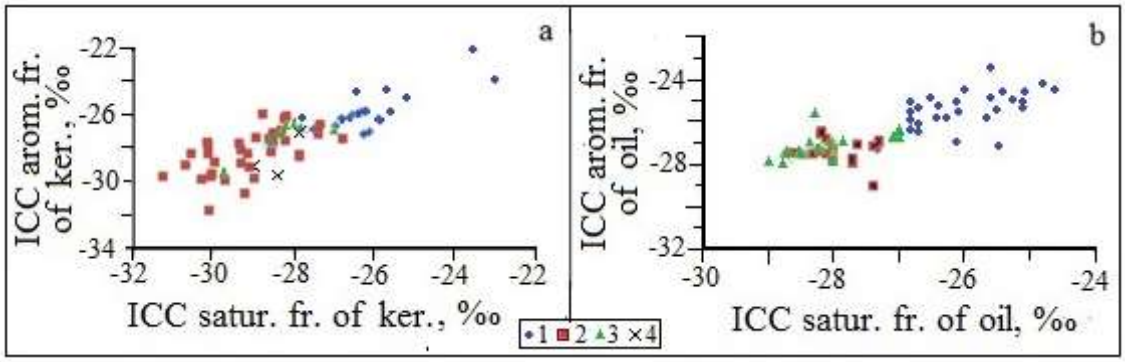

Fig. 4. Graphs showing the relationship between ICC of saturated and aromatic fractions of OM and oils of rocks and reservoirs of different stratigraphic age: 1-Miocene; 2-Maykop; 3-Eocene; 3- Cretaceous

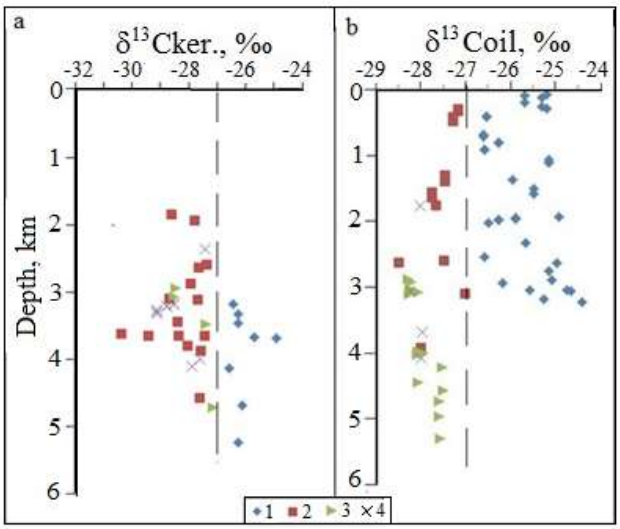

Fig. 5. SCB. ICC values of OM and oils of different stratigraphic units vs. depth: 1-Miocene; 2-Maykop; 3-Eocene; 4-Cretaceouse.

Results for other basins around the world

Before conducting a comparative analysis for all basins of the world as a whole, we will first consider the example of basins in America and Russia, for which (see Table 2), as well as for the SCB, there is a more complete and statistically significant amount of information. All charts below were compiled by the author of this paper based on the sources listed in Table 2.

San Joaquin basin (USA)

Histograms of ICC values of the saturated and aromatic fractions of kerogen in the OM of Miocene and pre-Miocene rocks of the San Joaquin basin show clear isotopic differences between these two age groups (Fig.6). A similar pattern is also observed in the histograms of the ICC values distribution of the saturated and aromatic fractions of oils from the San Joaquin reservoirs (fig. 7). The ICC boundary values between Miocene and Pre-Miocene reservoirs are: for OM – within -26.0/-25.0‰ and for oils – -25.0‰.

Obvious differentiation in the plots of the relationship between carbon isotopes of the saturated and aromatic fractions of kerogen and oils can also be observed in the San Joaquin basin (Fig. 8).

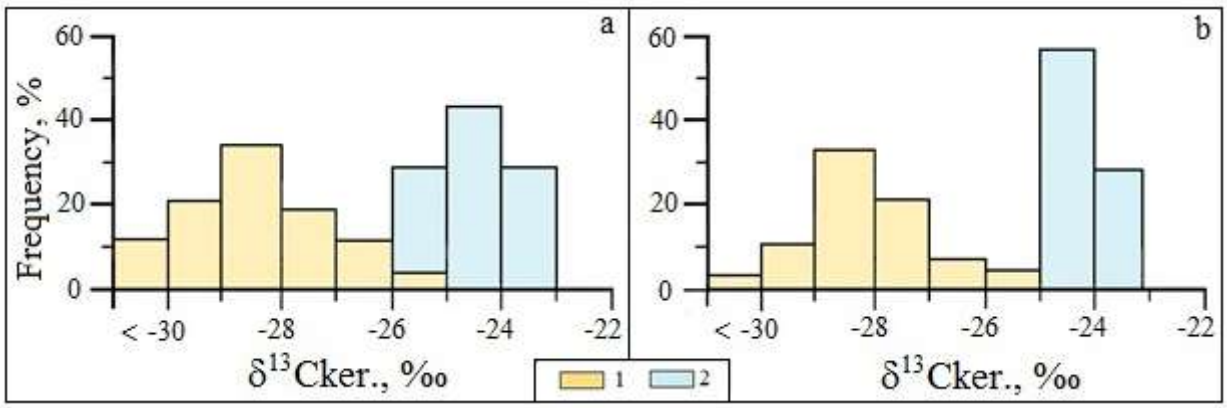

Fig. 6. Histograms of distribution of ICC values of the saturated (a) and aromatic (b) fractions of kerogen in OM of Pre-Miocene (1) and Miocene (2) rocks in San Joaquin basin (USA)

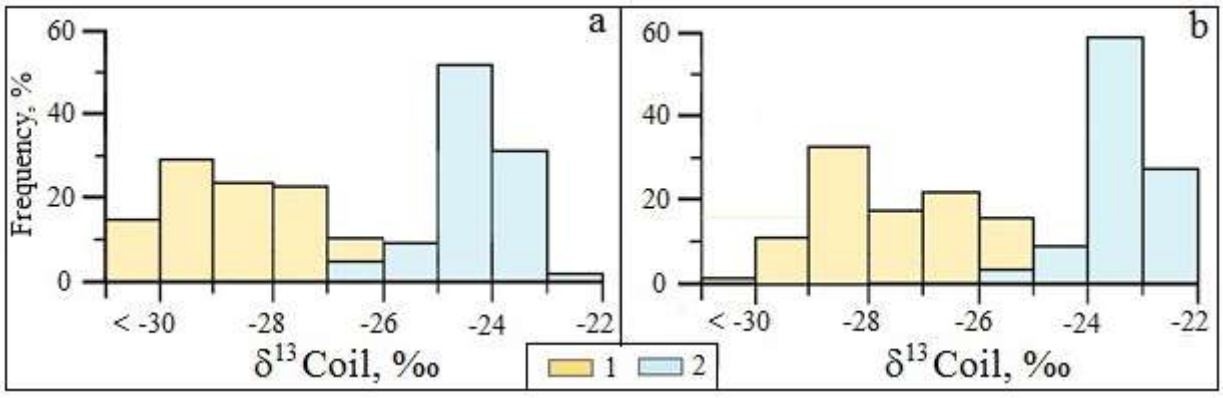

Fig. 7. Histograms of distribution of ICC values of the saturated (a) and aromatic (b) fractions of oils of Pre-Miocene (1) and Miocene (2) reservoirs in San Joaquin basin (USA)

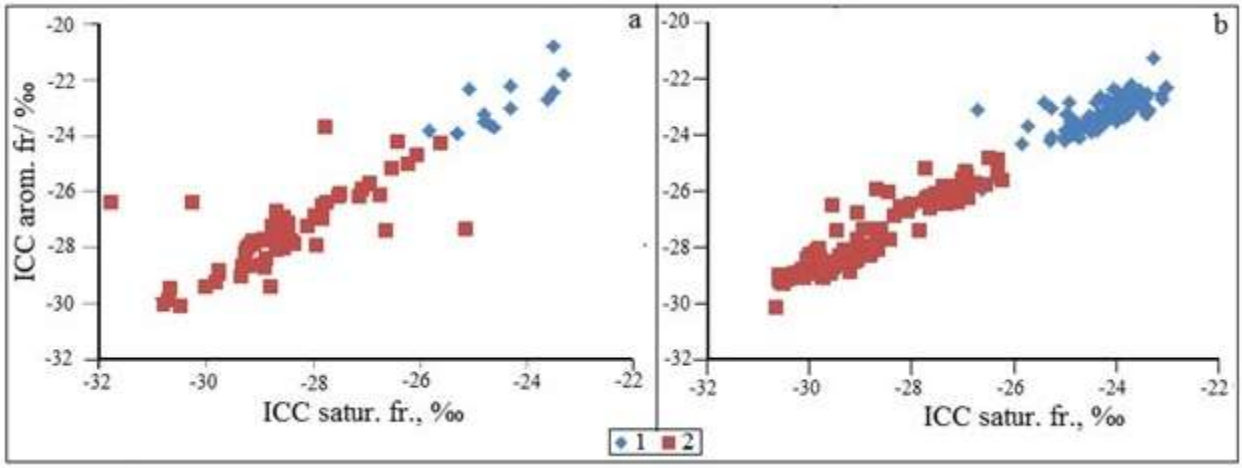

Fig. 8. Graphs of the relationship between ICC of saturated (a) and aromatic (b) fractions of OM and oils of Miocene (1) and Pre-Miocene (2) rocks and reservoirs in San Joaquin basin (USA)

East Siberian basins

For this region, a comparative analysis was performed using ICC for both saturated and aromatic fractions of oils. According to the histograms, although the differences in ICC in fractions of Miocene and Pre-Miocene oils is obvious, the boundary values between these two age groups are less clear, the saturated fraction is situated in the range -29.0/ – -27.0‰, and in the aromatic fraction it lies in the range - 28.0/ – -26.0‰ (Fig. 9). An obvious difference between the two age groups can also be found in the graph of the saturated fraction versus the aromatic fraction of the oil (Fig. 10).

Gulf of Suez province

According to bibliographic sources (Younes, 2012) a differentiation between oils of Miocene and Pre-Miocene reservoirs was also identified in the southern *Gulf of Suez province* (Fig. 11).

Generalization for all considered basins of the world

Based on the data reported in Table 2, a general diagram of the limits of change and average values for ICC of OM and crude oils along the stratigraphic section was compiled (Fig. 12).

Discussion

The problem of identifying of the source of oil is one of the most current in organic geochemistry. The informative value of stable carbon isotopes in solving this problem was indicated in the earliest works of geochemists (for ex., Silverman, Epstein, 1958), which was confirmed by the results of numerous subsequent studies.

The vast majority of geochemists admit that $\delta^{13}C$ values of oils are useful for determining oil-oil and oil-source rock correlation and, in conjunction with other geochemical properties, can indicate the possible age and depositional environment of source rocks.

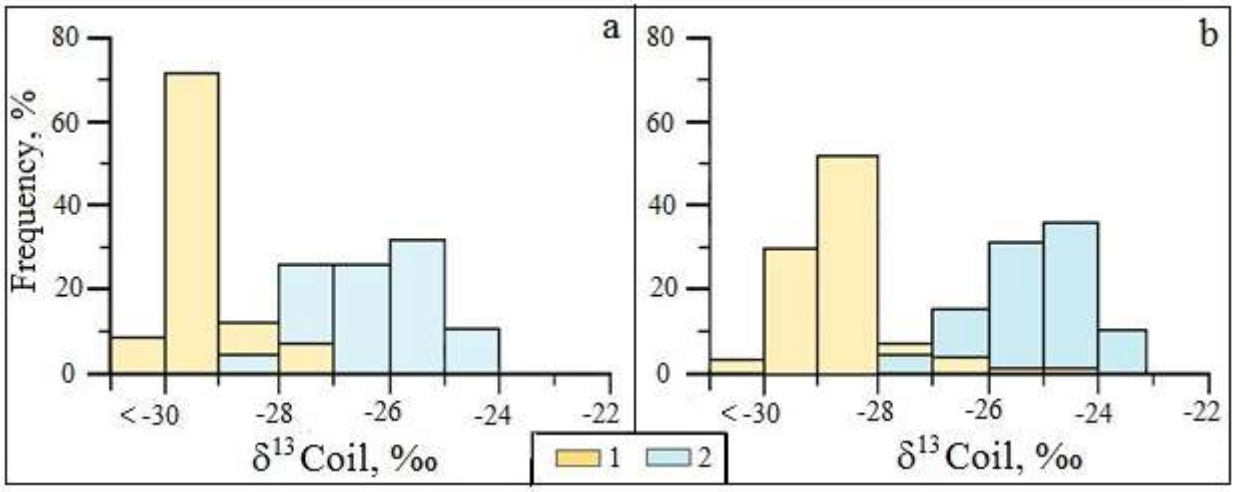

Fig. 9. Histograms of distribution of ICC values of the saturated (a) and aromatic (b) fractions of Pre-Miocene and (1) Miocene (2) reservoir oils in the East Siberian basins

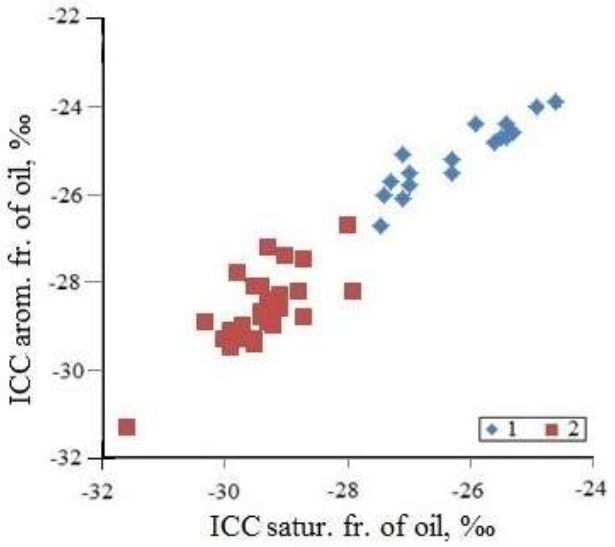

Fig. 10. ICC of saturated vs. aromatic fractions of oils from Miocene (1) and Pre-Miocene (2) resevoirs in the East Siberian basins

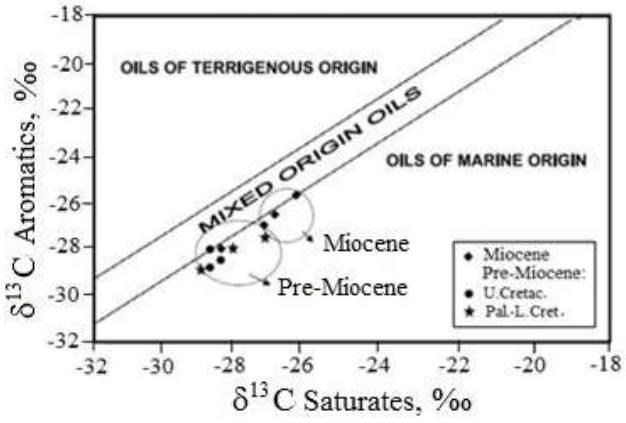

Fig. 11. Relation between ICC of the satureted and aromatic fractions for crude oils from Miocene and Pre-Miocene reservoirs in the southern Gulf of Suez province (Younes, 2012)

The similarities or differences in $\delta^{13}C$ values of OM and their derivative oils observed on a global scale are primarily due to the conditions of their formation. During certain geological periods, general conditions for oil and gas formation existed in many regions of the Earth, such as the widespread formation of a heavy carbon isotope composition in the Miocene.

Based on the diagram presented in Figure 12, as well as the results of numerous independent studies of various basins of the world addressing this problem, we conclude supporting the global nature of the phenomenon of heavier carbon in the Miocene.

The reasons that led to the isotopic shift in the global carbon budget that occurred in the Miocene are not completely understood. Numerous hypotheses have been proposed for the cause of such carbon isotope shift.

According to one hypothesis, the nature of this phenomenon is glacioeustatic lowering of sea level (Loutit, Kennett, 1979; Mercer, Sutter, 1982) in the latest Miocene, caused by global regression (Kennett, 1986; Adams et al., 1977; Vail, Hardenbol, 1979).

Chung et al. (1992) believe that Miocene oils are isotopically heavier because of decreased atmospheric CO_2 concentration, which has resulted in decreased isotope fractionation by marine plankton during photosynthesis. However, Mejia et al. (2017) suppose that the role of atmospheric CO_2 in forcing Late Miocene climate remains unclear, with some proxy records suggesting a sharp decrease in CO_2 associated with decreasing extra-tropical Sea surface temperature. Other authors (Pagani et al. 1999; LaRivere et al., 2012) instead suggest a decoupling of CO_2 and global climate during this time interval.

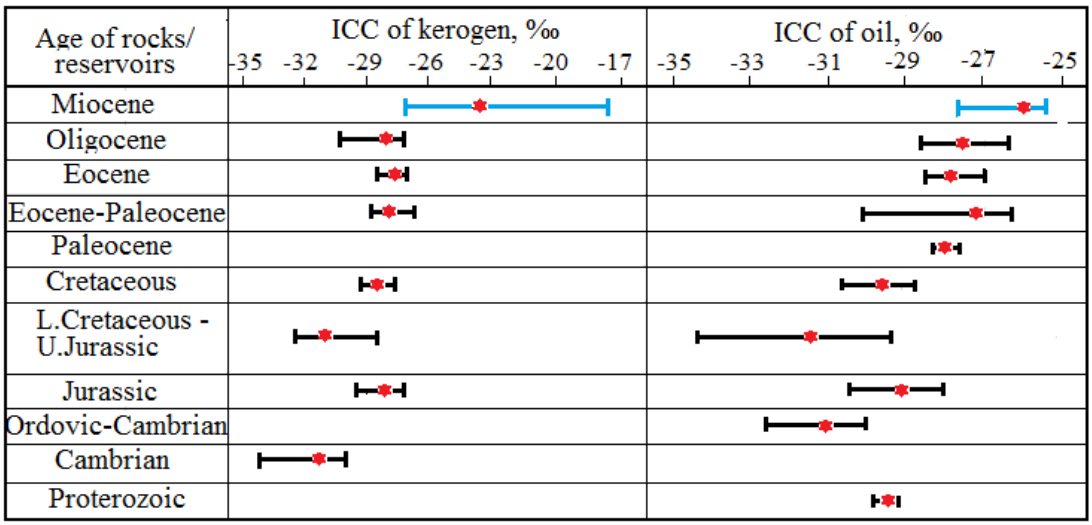

Fig. 12. Generalized diagram showing the limits of change in ICC of kerogen and oils and their average values for various stratigraphic complexes for all the considered basins (The diagram was compiled by the author of the paper based on bibliographic sources given in Table 2)

According to another, most followed model, the Miocene was a period of progressive climatic change, during which the Earth's climate system underwent a remarkable cooling associated with the expansion of the East Antarctic Ice Sheet. This resulted in a marked increase in $\delta^{18}O$ of benthic foraminiferal calcite (Zachos et al., 2001; Miller et al., 1987; Shackleton, Kennett, 1975). Such a climate change may have reduced the amount of water vapor held in the atmosphere, thereby leading to further restrain of moisture source (Li et al., 2014). Middle Miocene cooling was clearly a profound period of climatic change worldwide (Mitchison, 2019).

Conclusion

Based on the collection, generalization and comparative analysis of data gathered from literary sources on the carbon isotope of OM and oils from various basins of the world, as well as the results of own and co-authors researches on the SCB, the following main conclusions can be made:

– the occurrence of isotope-heavy carbon in Miocene OM and oils revealed in the SCB is also characteristic for other basins of the world;

– the global nature of the identified phenomenon is substantiated;

– existing hypotheses about the reasons of this natural appearance are considered;

– the results once again confirm that $\delta^{13}C$ values are useful for oil-oil and oil-source rock correlation in conjunction with other geochemical properties;

– in petroleum exploration, the diatom-bearing sediments can be used as an indicator of the depositional setting.

Acknowledgments

The author expresses his gratitude to the co-authors of previously published joint papers related to the problem under consideration.

The author is also grateful to the reviewers for their efforts in analyzing and editing the paper. The objective comments of the reviewers significantly improved the quality of the paper.

REFERENCES

Aboglila S. Organic and isotopic geochemistry of source-rocks and crude oils from the East Sirte Basin (Libya). Thesis for the Degree of Doctor of Philosophy of Curtin University of Technology, Western Australia. 30 June 2010, 113 p.

Adams C.G., Benson R.H., Kidd R.B., Ryan W.F.B., Wright R.C. The Messinian salinity crisis and evidence of late Miocene eustatic changes in the world ocean. Nature, Vol. 269, 1977, pp. 383-386.

Afanasenkov A.P., Zheglova T.P., Petrov A.L. Hydrocarbons-biomarkers and carbon isotope composition of bitumoids and oils of Mesozoic sediments in the western part of the Yenisei-Khatanga oil and gas region. Georesources, Vol. 21, No. 1, 2019, pp. 47-63, DOI: https://doi.org/10.18599/grs.2019.1.47-63 (in Russian).

Andrusevich V.E., Engel M.H., Zumberge J.E., Brothers L.A. Secular, episodic chances in stable carbon isotope composition of crude oils. Chemical Geology, Vol. 152, 1998, pp. 59-72.

Anuar A. Source rock evaluation of Middle-Late Miocene sequences, north Sabah basin, Malaysia. A dissertation submitted for the degree of Doctor of Philosophy. Petroleum Geology Group, Department of Geology, Royal School of Mines Imperial College, London, 1994, 316 p.

Aoyagi K., Iijima A. Petroleum occurrence, generation, and accumulation in the Miocene siliceous deposits of Japan. In: Siliceous sedimentary rock-hosted ores and petroleum, (J.R Hein, ed.), Van Nostrand Reinhold Co. New York, 1987, pp. 117-137.

Aoyagi K., Omokawa M. Neogene diatoms as the important source of petroleum in Japan. Journal of Petroleum Science and Engineering, Vol. 7, No. 3-4, 1992, pp. 247-262.

Bailey N.J.L., Guliyev I.S., Feyzullayev A.A. Source rocks in the South Caspian. AAPG/ASPG research symposium “Oil and gas petroleum systems in rapidly-subsiding basins”. Book of abstracts. Baku, Azerbaijan, October 6-9 1996.

Barron J.A. Diatomite: environmental and geological factors affecting its distribution. In: Siliceous sedimentary rock-hosted ores and petroleum (J.R.Hein, ed.), Van Nostrand Reinhold Co. New York, 1987, pp. 164-78.

ЛИТЕРАТУРА

Aboglila S. Organic and isotopic geochemistry of source-rocks and crude oils from the East Sirte Basin (Libya). Thesis for the Degree of Doctor of Philosophy of Curtin University of Technology, Western Australia. 30 June 2010, 113 p.

Adams C.G., Benson R.H., Kidd R.B., Ryan W.F.B., Wright R.C. The Messinian salinity crisis and evidence of late Miocene eustatic changes in the world ocean. Nature, Vol. 269, 1977, pp. 383-386.

Andrusevich V.E., Engel M.H., Zumberge J.E., Brothers L.A. Secular, episodic chances in stable carbon isotope composition of crude oils. Chemical Geology, Vol. 152, 1998, pp. 59-72

Anuar A. Source rock evaluation of Middle-Late Miocene sequences, north Sabah basin, Malaysia. A dissertation submitted for the degree of Doctor of Philosophy. Petroleum Geology Group, Department of Geology, Royal School of Mines Imperial College, London, 1994, 316 p.

Aoyagi K., Iijima A. Petroleum occurrence, generation, and accumulation in the Miocene siliceous deposits of Japan. In: Siliceous sedimentary rock-hosted ores and petroleum, (J.R Hein, ed.), Van Nostrand Reinhold Co. New York, 1987, pp. 117-137.

Aoyagi K., Omokawa M. Neogene diatoms as the important source of petroleum in Japan. Journal of Petroleum Science and Engineering, Vol. 7, No. 3-4, 1992, pp. 247-262.

Bailey N.J.L., Guliyev I.S., Feyzullayev A.A. Source rocks in the South Caspian. AAPG/ASPG research symposium “Oil and gas petroleum systems in rapidly-subsiding basins”. Book of abstracts. Baku, Azerbaijan, October 6-9 1996.

Barron J.A. Diatomite: environmental and geological factors affecting its distribution. In: Siliceous sedimentary rock-hosted ores and petroleum (J.R.Hein, ed.), Van Nostrand Reinhold Co. New York, 1987, pp. 164-78.

Berger W.H. Planktonic foraminifera: selective solution and the Lysocline. Marine Geology, Vol. 8, No. 2, 1970, pp. 111-138, http://dx.doi.org/10.1016/0025-3227(70)90001-0.

Bozcu A. Source rock potential of Lower-Middle Miocene lacustrine deposits: example of the Küçükkuyu formation, Nw Turkey. Oil Shale, Vol. 32, No. 4, 2015, pp. 313-334, DOI:10.3176/oil.2015.4.03.

Bazhenova O.K. Oil and gas source rock potential and the presence of oil and gas in Sakhalin. In: The Cenozoic geology and the oil and gas presence in Sakhalin (Gladenkov Y.B., Bazhenova O.K., Grechin V.I., Margulis L.S. and Salnikov B.A., eds.). GEOS. Moscow, 2002, pp. 137-194 (in Russian).

Berger W.H. Planktonic foraminifera: selective solution and the Lysocline. Marine Geology, Vol. 8, No. 2, 1970, pp. 111-138, http://dx.doi.org/10.1016/0025-3227(70)90001-0.

Bozcu A. Source rock potential of Lower-Middle Miocene lacustrine deposits: example of the Küçükkuyu formation, Nw Turkey. Oil Shale, Vol. 32, No. 4, 2015, pp. 313-334, DOI:10.3176/oil.2015.4.03.

Chung H.M., Rooney M.A., Toon M.B., Claypool G.E. Carbon isotope composition of marine crude oils. AAPG Bulletin, Vol. 76, No. 7, 1992, pp. 1000-1007, https://doi.org/10.1306/BDFF8952-1718-11D7-8645000102C1865D.

Clayton J.L., Warden A., Daws T.A., Lillis P.G., Michael G.E., Dawson M. Organic Geochemistry of black shales, marlstones, and oils of Middle Pennsylvanian rocks from the Northern Denver and Southeastern Powder River Basins, Wyoming, Nebraska, and Colorado.US Geological Survey Bulletin 1917-K, US Government Printing Office, Denver, 1992, 52 p.

Diatomite. Geological Dictionary. Vol. 1. Nedra. Moscow, 1978, 227 p. (in Russian).

Dill H.G., Sachsenhofer R.F., Grecula P., Sasvári T., Palinkas L.A., Borojevic-Šostaric S., Strmic-Palinkas S., Prochaska W., Garuti, G., Zaccarini F., Arbouille D., Schulz H.-M. Fossil fuels, ore and industrial minerals. In: The Geology of Central Europe (T.McCann, ed.), Vol. 2: Mesozoic and Cenozoic. Geological Society. London, 2008, pp. 1341-1449, https://doi.org/10.1144/cev2p.9.

Feyzullayev A., Aliyeva Es.A. Estimation of the various source rocks contribution in oil pools formation. EAGE 65 Conference and Exhibition, Stavanger, The Norway, 2-5 June 2003, Extended Abstracts on CD, P 026, 4 p.

Feyzullayev A., Guliyev I., Tagiyev M. Source potential of the Mesozoic-Cenozoic rocks in the South Caspian Basin and their role in forming the oil accumulations in the Lower Pliocene reservoirs. Petroleum Geoscience, Vol. 7, No. 4, 2001, pp. 409-417.

Feyzullayev A.A. Isotope-geochemical characteristics of hydrocarbons on the north-western flank of South Caspian basin. ANAS Transactions, Earth Sciences, Vol. 1, 2019, pp. 3-10.

Froelich A.J., Robinson G.R. (eds.). Studies of the Early Mesozoic Basins of the Eastern United States. Geological Survey Bulletin, Vol. 1776, 1988, pp. 63-68.

Golyshev S.I., Padalko N.L., Madisheva R.K., Ozdoev S.M., Portnov V.S., Isaev V.I. Isotopic composition of the Aryskum depression oil (South Kazakhstan). Bulletin of the Tomsk Polytechnic University, Geo Assets engineering, V. 331, No. 3, 2020, pp. 80-89 (in Russian).

Gratzer R., Bechtel A., Sachsenhofer R.F., Linzer H.-G., Reischenbacher D., Schulz H.-M. Oil- oil and oil-source rock correlations in the Alpine Foreland Basin of Austria: insights from biomarker and stable carbon isotope studies. Marine and Petroleum Geology, Vol. 28, 2011, pp. 1171-1186.

Grosjean E., Love G.D., Stalvies C., Fike D.A., Summons R.E. Origin of petroleum in the Neoproterozoic-Cambrian South Oman Salt Basin. Org. Geochem., Vol. 40, 2009, pp. 87-110, DOI:10.1016/j.orggeochem.2008.09.011.

Guliyev I., Feyzullayev A. Geochemistry of hydrocarbon seepages in Azerbaijan. In: Hydrocarbon migration and its near-surface expression (D.Shumacher and M.Abrams, eds). AAPG Memoir, Vol. 66, 1996, pp. 63-70.

Guliyev I., Feyzullayev A., Tagiyev M. Isotope-geochemical characteristics in the South Caspian basin. Energy Exploration and Exploitation, Vol. 15, No. 4/5, 1997, pp. 311-368.

Chung H.M., Rooney M.A., Toon M.B., Claypool G.E. Carbon isotope composition of marine crude oils. AAPG Bulletin, Vol. 76, No. 7, 1992, pp. 1000-1007, https://doi.org/10.1306/BDFF8952-1718-11D7-8645000102C1865D.

Clayton J.L., Warden A., Daws T.A., Lillis P.G., Michael G.E., Dawson M. Organic Geochemistry of black shales, marlstones, and oils of Middle Pennsylvanian rocks from the Northern Denver and Southeastern Powder River Basins, Wyoming, Nebraska, and Colorado.US Geological Survey Bulletin 1917-K, US Government Printing Office, Denver, 1992, 52 p.

Dill H.G., Sachsenhofer R.F., Grecula P., Sasvári T., Palinkas L.A., Borojevic-Šostaric S., Strmic-Palinkas S., Prochaska W., Garuti, G., Zaccarini F., Arbouille D., Schulz H.-M. Fossil fuels, ore and industrial minerals. In: The Geology of Central Europe (T.McCann, ed.), Vol. 2: Mesozoic and Cenozoic. Geological Society. London, 2008, pp. 1341-1449, https://doi.org/10.1144/cev2p.9.

Feyzullayev A., Aliyeva Es.A. Estimation of the various source rocks contribution in oil pools formation. EAGE 65 Conference and Exhibition, Stavanger, The Norway, 2-5 June 2003, Extended Abstracts on CD, P 026, 4 p.

Feyzullayev A., Guliyev I., Tagiyev M. Source potential of the Mesozoic-Cenozoic rocks in the South Caspian Basin and their role in forming the oil accumulations in the Lower Pliocene reservoirs. Petroleum Geoscience, Vol. 7, No. 4, 2001, pp. 409-417.

Feyzullayev A.A. Isotope-geochemical characteristics of hydrocarbons on the north-western flank of South Caspian basin. ANAS Transactions, Earth Sciences, Vol. 1, 2019, pp. 3-10.

Froelich A.J., Robinson G.R. (eds.). Studies of the Early Mesozoic Basins of the Eastern United States. Geological Survey Bulletin, Vol. 1776, 1988, pp. 63-68.

Gratzer R., Bechtel A., Sachsenhofer R.F., Linzer H.-G., Reischenbacher D., Schulz H.-M. Oil- oil and oil-source rock correlations in the Alpine Foreland Basin of Austria: insights from biomarker and stable carbon isotope studies. Marine and Petroleum Geology, Vol. 28, 2011, pp. 1171-1186.

Grosjean E., Love G.D., Stalvies C., Fike D.A., Summons R.E. Origin of petroleum in the Neoproterozoic-Cambrian South Oman Salt Basin. Org. Geochem., Vol. 40, 2009, pp. 87-110, DOI:10.1016/j.orggeochem.2008.09.011.

Guliyev I., Feyzullayev A. Geochemistry of hydrocarbon seepages in Azerbaijan. In: Hydrocarbon migration and its near-surface expression (D.Shumacher and M.Abrams, eds). AAPG Memoir, Vol. 66, 1996, pp. 63-70.

Guliyev I., Feyzullayev A., Tagiyev M. Isotope-geochemical characteristics in the South Caspian basin. Energy Exploration and Exploitation, Vol. 15, No. 4/5, 1997, pp. 311-368.

Guliyev I.S., Feyzullayev A.A., Guseynov D.A. Carbon isotopic composition of the hydrocarbon fluids of the South Caspian Megadepression. Geochemistry International, Vol. 39, No. 3, 2001, pp. 237-243.

Isaacs C.M., Rullkötter J. (eds.). The Monterey Formation: from rocks to molecules. Columbia University Press. New York, 2001, pp. 268-295, https://doi.org/10.1017/S0016756802246506.

Johnson K.M. Multi-tracer geochemical investigation of laminated diatomaceous sediments: Miocene Monterey formation and Holocene marine environments (Saanich Inlet and Santa Barbara basin). A thesis for the degree of Master of science. The University of British Columbia, Vancouver, Canada. March, 1998, 106 p.

Jordan R.W., Stickley C.E. Diatoms as indicators of paleoceanographic events. In: The diatoms: applications for the Environmental and Earth Sciences. Cambridge University Press. Cambridge, 2010, pp. 423-452.

Kennett J.P. Miocene to early Pliocene oxygen and carbon isotope stratigraphy in the southwest Pacific, deep sea drilling

Guliyev I.S., Feyzullayev A.A., Guseynov D.A. Carbon isotopic composition of the hydrocarbon fluids of the South Caspian Megadepression. Geochemistry International, Vol. 39, No. 3, 2001, pp. 237-243.

Isaacs C.M., Rullkötter J. (eds.). The Monterey Formation: from rocks to molecules. Columbia University Press. New York, 2001, pp. 268-295, https://doi.org/10.1017/S0016756802246506.

Johnson K.M. Multi-tracer geochemical investigation of laminated diatomaceous sediments: Miocene Monterey formation and Holocene marine environments (Saanich Inlet and Santa Barbara basin). A thesis for the degree of Master of science. The University of British Columbia, Vancouver, Canada. March, 1998, 106 p.

Jordan R.W., Stickley C.E. Diatoms as indicators of paleoceanographic events. In: The diatoms: applications for the Environmental and Earth Sciences. Cambridge University Press. Cambridge, 2010, pp. 423-452.

Kennett J.P. Miocene to early Pliocene oxygen and carbon isotope stratigraphy in the southwest Pacific, deep sea drilling project LEG 90[1]. Graduate School of Oceanography, University of Rhode Island, 1986, pp. 1383-1411.

Khim B.-K., Lee J., Ha S., Park J., Pandey D.K., Clift P.D., Kulhanek D.K., Steinke S., Griffith E.M., Suzuki K., Xu Z., IODP Expedition 355 Scientists. Variations in $\delta^{13}C$ values of sedimentary organic matter since late Miocene time in the Indus Fan (IODP Site 1457) of the eastern Arabian Sea. Geological Magazine, Vol. 157, No. 6, 2020, pp. 1012-1021, https://doi.org/10.1017/S0016756818000870.

Komada T., Druffel E.R.M., Hwang J. Sedimentary rocks as sources of ancient organic carbon to the ocean: An investigation through Δ14C and δ13C signatures of organic compound classes. Global Biogeochem. Cycles, Vol. 19, No. 2, 2005, GB2017, DOI:10.1029/2004GB002347.

Kontorovich A.E., Kostyreva E.A., Saraev S.V., Melenevskii V.N., Fomin A.N. The geochemistry of Cambrian organic matter from the Cis-Yenisei subprovince (evidence from the wells Vostok-1 and Vostok-3). Russian Geology and Geophysics, Vol. 52, No. 6, 2011, pp. 571-582 (in Russian).

Körmös S., Sachsenhofer R.F., Bechtel A., Geza Radovics B., Milota K., Schubert F. Source rock potential, crude oil characteristics and oil-to-source rock correlation in a Central Paratethys sub-basin, the Hungarian Palaeogene Basin (Pannonian basin). Marine and Petroleum Geology, Vol. 127, 104955, 2021, DOI:10.1016/j.marpetgeo.2021.104955.

Kotarba M.J., Bilkiewicz E., Jurek K., Wieclaw D., Machowski G. Origin, migration and secondary processes of oil and natural gas in the western part of the Polish Outer Carpathians: geochemical and geological approach. International Journal of Earth Sciences, Original paper, Vol. 110, 2021, pp. 1653-1679, DOI:10.1007/s00531-021-02035-7.

Kotarba M.J., Koltun Y.V. The origin and habitat of hydrocarbons of the Polish and Ukrainian parts of the Carpathian Province. In: The Carpathians and Their Foreland: Geology and Hydrocarbon Resources (J.Golonka, F.J.Pícha, eds.). American Association of Petroleum Geologists Memoirs, Vol. 84, 2006, pp. 395-442, https://doi.org/10.1306/985614m843074.

Krebs W.N., Gladenkov A.Y., Jones G.D. Diatoms in oil and gas exploration. In: The diatoms: applications for the environmental and earth sciences (J.P.Smol, E.F.Stoermer, eds.), Cambridge University Press. 2010, pp. 402-412.

LaRiviere J.P., Ravelo A.C., Crimmins A., Dekens P.S., Ford H.L., Lyle M., Wara M.W. Late Miocene decoupling of oceanic warmth and atmospheric carbon dioxide forcing. Nature, Vol. 486, No. 7401, 2012, pp. 97-100.

Leushina E., Bulatov T., Kozlova E., Panchenko I., Voropaev A., Karamov T., Yermakov Y., Bogdanovich N., Spasennykh M. Upper Jurassic-Lower Cretaceous source rocks in the North of Western Siberia: comprehensive geochemical project LEG 90[1]. Graduate School of Oceanography, University of Rhode Island, 1986, pp. 1383-1411.

Khim B.-K., Lee J., Ha S., Park J., Pandey D.K., Clift P.D., Kulhanek D.K., Steinke S., Griffith E.M., Suzuki K., Xu Z., IODP Expedition 355 Scientists. Variations in $\delta^{13}C$ values of sedimentary organic matter since late Miocene time in the Indus Fan (IODP Site 1457) of the eastern Arabian Sea. Geological Magazine, Vol. 157, No. 6, 2020, pp. 1012-1021, https://doi.org/10.1017/S0016756818000870.

Komada T., Druffel E.R.M., Hwang J. Sedimentary rocks as sources of ancient organic carbon to the ocean: An investigation through Δ14C and δ13C signatures of organic compound classes. Global Biogeochem. Cycles, Vol. 19, No. 2, 2005, GB2017, DOI:10.1029/2004GB002347.

Körmös S., Sachsenhofer R.F., Bechtel A., Geza Radovics B., Milota K., Schubert F. Source rock potential, crude oil characteristics and oil-to-source rock correlation in a Central Paratethys sub-basin, the Hungarian Palaeogene Basin (Pannonian basin). Marine and Petroleum Geology, Vol. 127, 104955, 2021, DOI:10.1016/j.marpetgeo.2021.104955.

Kotarba M.J., Bilkiewicz E., Jurek K., Wieclaw D., Machowski G. Origin, migration and secondary processes of oil and natural gas in the western part of the Polish Outer Carpathians: geochemical and geological approach. International Journal of Earth Sciences, Original paper, Vol. 110, 2021, pp. 1653-1679, DOI:10.1007/s00531-021-02035-7.

Kotarba M.J., Koltun Y.V. The origin and habitat of hydrocarbons of the Polish and Ukrainian parts of the Carpathian Province. In: The Carpathians and Their Foreland: Geology and Hydrocarbon Resources (J.Golonka, F.J.Pícha, eds.). American Association of Petroleum Geologists Memoirs, Vol. 84, 2006, pp. 395-442, https://doi.org/10.1306/985614m843074.

Krebs W.N., Gladenkov A.Y., Jones G.D. Diatoms in oil and gas exploration. In: The diatoms: applications for the environmental and earth sciences (J.P.Smol, E.F.Stoermer, eds.), Cambridge University Press. 2010, pp. 402-412.

LaRiviere J.P., Ravelo A.C., Crimmins A., Dekens P.S., Ford H.L., Lyle M., Wara M.W. Late Miocene decoupling of oceanic warmth and atmospheric carbon dioxide forcing. Nature, Vol. 486, No.7401, 2012, pp. 97-100.

Leushina E., Bulatov T., Kozlova E., Panchenko I., Voropaev A., Karamov T., Yermakov Y., Bogdanovich N., Spasennykh M. Upper Jurassic-Lower Cretaceous source rocks in the North of Western Siberia: comprehensive geochemical characterization and reconstruction of paleo-sedimentation conditions. Geosciences, Vol. 11, No. 8, 2021, pp. 320, https://doi.org/10.3390/geosciences11080320.

Li H.J., Song C., Zhang J., Hui Z., Chen S., Xian F. Understanding Miocene climate evolution in Northeastern Tibet: stable carbon and oxygen isotope records from the Western Tianshui Basin, China. Journal of Earth Science, Vol. 25, No. 2, 2014, pp. 357-365, DOI: 10.1007/s12583-014-0416-8.

Lillis P., Magoon L.B., Stanley R.G., McLaughlin R.J. Warden A. Characterization of Northern California Petroleum by stable carbon isotopes. Open-File Report 99-164, U.S. Geological Survey, California, 2001, 13 p., DOI: 10.3133/ofr99164.

Lillis P.G., Magoon L.B. Petroleum systems of the San Joaquin Basin Province, California –geochemical characteristics of oil types. In: Petroleum systems and geologic assessment of oil and gas in the San Joaquin Basin Province, California (Allegra Hosford Scheirer, ed.). U.S. Geological Survey. Professional Paper 1713, 2007, pp. 1713-1765, DOI:10.3133/pp1713.ch09.

Loutit T.S., Kennett J.P. Application of carbon isotope stratigraphy to late Miocene shallow marine sediments, New Zealand. Science, Vol. 204, 1979, pp. 1196-1199.

Magoon L.B., Lillis P.G., Warden A., Stanley R.G., MacKevett N.H. and Castaño J. Carbon isotopic composition identify

characterization and reconstruction of paleo-sedimentation conditions. Geosciences, Vol. 11, No. 8, 2021, pp. 320, https://doi.org/10.3390/geosciences11080320.

Li H.J., Song C., Zhang J., Hui Z., Chen S., Xian F. Understanding Miocene climate evolution in Northeastern Tibet: stable carbon and oxygen isotope records from the Western Tianshui Basin, China. Journal of Earth Science, Vol. 25, No. 2, 2014, pp. 357-365, DOI: 10.1007/s12583-014-0416-8.

Lillis P., Magoon L.B., Stanley R.G., McLaughlin R.J. Warden A. Characterization of Northern California Petroleum by stable carbon isotopes. Open-File Report 99-164, U.S. Geological Survey, California, 2001, 13 p., DOI: 10.3133/ofr99164.

Lillis P.G., Magoon L.B. Petroleum systems of the San Joaquin Basin Province, California –geochemical characteristics of oil types. In: Petroleum systems and geologic assessment of oil and gas in the San Joaquin Basin Province, California (Allegra Hosford Scheirer, ed.). U.S. Geological Survey. Professional Paper 1713, 2007, pp. 1713-1765, DOI:10.3133/pp1713.ch09.

Loutit T.S., Kennett J.P. Application of carbon isotope stratigraphy to late Miocene shallow marine sediments, New Zealand. Science, Vol. 204, 1979, pp. 1196-1199.

Madisheva R.K. Study of the geodynamic situation of sedimentation and formation of oil and gas content of the pre-Jurassic complex of the Aryskum trough. Dissertation for the degree of Doctor of Philosophy. Karaganda Technical University, The Republic of Kazakhstan, Karaganda, 2020, 99 p. (in Russian).

Magoon L.B., Lillis P.G., Warden A., Stanley R.G., MacKevett N.H. and Castaño J. Carbon isotopic composition identify four hydrocarbon types in northern California. AAPG Bulletin, Vol. 79, 1995, p. 592.

Maslov V.P. Siliceous organisms: general comments. Atlas of rock-building organisms (calcareous and siliceous). Nauka. Moscow, 1973, 89 p. (in Russian).

Mayer J., Rupprecht B.J., Sachsenhofer R.F., Tari G., Bechtel A. et al. Source potential and depositional environment of Oligocene and Miocene rocks offshore Bulgaria. Geological Society of London, Special Publications, Vol. 464, No. 1, 2018, pp. 307-328, DOI:10.1144/sp464.2.

Mejia L.M., Mendez-Vicente A., Abrevaya L., Lawrence K.T., Ladlow C., Bolton C., Stoll H. A diatom record of CO_2 decline since the late Miocene. Earth and Planetary Science Letters, Vol. 479, 2017, pp. 18-33.

Mercer J.H., Sutter J.F. Late Miocene-Earliest Pliocene glaciation in southern Argentina: implications for global ice-sheet history. Palaeogeogr., Palaeoclimatol., Palaeoecol., Vol. 38, 1982, pp. 185-206.

Miller K.G., Faribanks R.G., Mountain G.S. Tertiary oxygen isotope synthesis, sea level history, and continental margin erosion. Paleoceanography, Vol. 2, 1987, pp. 1-19.

Mitchison F.L. Neogene diatoms from the Southern Ocean; tiny fossils, big questions. Thesis submitted for the Degree of Doctor of Philosophy. Cardiff University, August 2019, 303 p.

Morris D.A. Organic diagenesis of Miocene sediments from Site 341, Wring Plateau, Norway. In: M.Talwani, G.Udintsev et al., Initial Reports of the DSDP, Vol. 38, Washington (U.S. Government Printing Office), 1976, pp. 809-814.

Oblasova N.V., Goncharova I.V., Derduga A.V., Kunitsyna I.V. Genetic types of oils in the eastern part of the Crimean-Caucasian Region. Geochemistry, Vol. 65, No. 11, 2020, pp. 1129-1150 (in Russian).

Ogbesejana A.B., Bello O.M., Ali T. Origin and depositional environments of source rocks and crude oils from Niger Delta Basin: Carbon isotopic evidence. China Geology, Vol. 3, No. 4, 2020, pp. 602-610.

Pagani M., Freeman K.H., Arthur M.A. Late Miocene atmospheric CO_2 concentrations and the expansion of C_4 grasses. Science, Vol. 285, No. 5429, 1999, pp. 876-879.

four hydrocarbon types in northern California. AAPG Bulletin, Vol. 79, 1995, p. 592.

Mayer J., Rupprecht B.J., Sachsenhofer R.F., Tari G., Bechtel A. et al. Source potential and depositional environment of Oligocene and Miocene rocks offshore Bulgaria. Geological Society of London, Special Publications, Vol. 464, No. 1, 2018, pp. 307-328, DOI:10.1144/sp464.2.

Mejia L.M., Mendez-Vicente A., Abrevaya L., Lawrence K.T., Ladlow C., Bolton C., Stoll H. A diatom record of CO_2 decline since the late Miocene. Earth and Planetary Science Letters, Vol. 479, 2017, pp. 18-33.

Mercer J.H., Sutter J.F. Late Miocene-Earliest Pliocene glaciation in southern Argentina: implications for global ice-sheet history. Palaeogeogr., Palaeoclimatol., Palaeoecol., Vol. 38, 1982, pp. 185-206.

Miller K.G., Faribanks R.G., Mountain G.S. Tertiary oxygen isotope synthesis, sea level history, and continental margin erosion. Paleoceanography, Vol. 2, 1987, pp. 1-19.

Mitchison F.L. Neogene diatoms from the Southern Ocean; tiny fossils, big questions. Thesis submitted for the Degree of Doctor of Philosophy. Cardiff University, August 2019, 303 p.

Morris D.A. Organic diagenesis of Miocene sediments from Site 341, Wring Plateau, Norway. In: M.Talwani, G.Udintsev et al., Initial Reports of the DSDP, Vol. 38, Washington (U.S. Government Printing Office), 1976, pp. 809-814.

Ogbesejana A.B., Bello O.M., Ali T. Origin and depositional environments of source rocks and crude oils from Niger Delta Basin: Carbon isotopic evidence. China Geology, Vol. 3, No. 4, 2020, pp. 602-610.

Pagani M., Freeman K.H., Arthur M.A. Late Miocene atmospheric CO_2 concentrations and the expansion of C_4 grasses. Science, Vol. 285, No. 5429, 1999, pp. 876-879.

Peters K.E., Lillis P.G., Lorenson T.D., Zumberge J.E. Organofacies and paleoclimate controlled genetic oil families in the onshore/offshore Santa Maria Basins, California. Schlumberger-Stanford University–U.S. Geological Survey–Geomark Research LLC, 2018.

Philp R.P., Jarde E. Application of stable isotopes and radioisotopes. In: Introduction to environmental forensics (B.Murphy, R.Morrison, eds.). Elsevier. New York, NY, USA, 2015, pp. 455-512, DOI:10.1016/B978-0-12-404696-4.

Sachsenhofer R.F., Popov S.V., Ćorić S., Mayer J., Misch D. et al. Paratethyan petroleum source rocks: an overview. Journal of Petroleum Geology, Vol. 41, No. 3, 2018, pp. 219-245, DOI:10.1111/jpg.12702.

Schouten S., Schoell M., Rijpstra W.I.C., Damste S J.S., De Leeuw J.W. A molecular stable carbon isotope study of organic matter in immature Miocene Monterey sediments, Pismo basin. Geochimica et Cosmochimica Acta, Vol. 61, No. 10, 1997, pp. 2065-2082.

Schwartz D.E. Lithology, petrophysics, and hydrocarbons in cyclic Belridge Diatomite, south Belridge oil field, Kern Co., California. Fourth International Congress on Pacific Neogene Stratigraphy, Berkeley, CA, July 29-31 1987, Abstract 102.

Shackleton N.J., Kennett J.P. Paleotemperature history of the Cenozoic and the initiation of Antarctic glaciation: Oxygen and carbon isotope analyses in DSDP Sites 277, 279, and 281. In: (J.P.Kennett, R.E.Houtz et al.) Init. Repts. DSDP, 29, Washington (U.S. Government Printing Office), 1975, pp. 743-755.

Silverman S.R., Epstein S. Carbon isotopic compositions of petroleums and other sedimentary organic materials. AAPG Bulletin, Vol. 42, 1958, pp. 998-1012.

Spiker E.C., Kotra R.K., Hatcher P.G., Gottfried R.M., Horan M.F., Olsen P.E. Source of kerogen in Black shales from the Hartford and Newark basins, eastern United States. In: Studies of the Early Mesozoic Basins of the Eastern United States U.S. (A.J.Froelich, G.R.Robinson, eds.). Geological Survey Bulletin, Vol. 1776, 1988, pp. 63-68.

Peters K.E., Lillis P.G., Lorenson T.D., Zumberge J.E. Organofacies and paleoclimate controlled genetic oil families in the onshore/offshore Santa Maria Basins, California. Schlumberger-Stanford University–U.S. Geological Survey–Geomark Research LLC, 2018.

Philp R.P., Jarde E. Application of stable isotopes and radioisotopes. In: Introduction to environmental forensics (B.Murphy, R.Morrison, eds.). Elsevier. New York, NY, USA, 2015, pp. 455-512, DOI:10.1016/B978-0-12-404696-4.

Sachsenhofer R.F., Popov S.V., Ćorić S., Mayer J., Misch D. et al. Paratethyan petroleum source rocks: an overview. Journal of Petroleum Geology, Vol. 41, No. 3, 2018, pp. 219-245, DOI:10.1111/jpg.12702.

Schouten S., Schoell M., Rijpstra W.I.C., Damste S J.S., De Leeuw J.W. A molecular stable carbon isotope study of organic matter in immature Miocene Monterey sediments, Pismo basin. Geochimica et Cosmochimica Acta, Vol. 61, No. 10, 1997, pp. 2065-2082.

Schwartz D.E. Lithology, petrophysics, and hydrocarbons in cyclic Belridge Diatomite, south Belridge oil field, Kern Co., California. Fourth International Congress on Pacific Neogene Stratigraphy, Berkeley, CA, July 29-31 1987, Abstract 102.

Shackleton N.J., Kennett J.P. Paleotemperature history of the Cenozoic and the initiation of Antarctic glaciation: Oxygen and carbon isotope analyses in DSDP Sites 277, 279, and 281. In: (J.P.Kennett, R.E.Houtz et al.) Init. Repts. DSDP, 29, Washington (U.S. Government Printing Office), 1975, pp. 743-755.

Silverman S.R., Epstein S. Carbon isotopic compositions of petroleums and other sedimentary organic materials. AAPG Bulletin, Vol. 42, 1958, pp. 998-1012.

Spiker E.C., Kotra R.K., Hatcher P.G., Gottfried R.M., Horan M.F., Olsen P.E. Source of kerogen in Black shales from the Hartford and Newark basins, eastern United States. In: Studies of the Early Mesozoic Basins of the Eastern United States U.S. (A.J.Froelich, G.R.Robinson, eds.). Geological Survey Bulletin, Vol. 1776, 1988, pp. 63-68.

Timoshina I.D. Geochemistry of organic matter of oil-producing rocks and oils of the Upper Precambrian in the south of Eastern Siberia. Publishing House SB RAS. Novosibirsk, branch"Geo", 2005, 166 p.

Tomkeev S.I. Petrological English-Russian explanatory dictionary. In 2 volumes. T. 1. Mir. Moscow, 1986, 285 p. (in Russian).

Tulan E. Evaluation of diatom-rich Oligocene to Miocene hydrocarbon source rocks in the Paratethys. Doctoral Thesis. Montan Univercity Leoben, 2020, 210 p.

Vail P.R., Hardenbol J. Sea-level changes during the Tertiary. Oceanus, Vol. 22, 1979, pp. 71-79.

Veto I., Báldi K., Coric S., Hetényi M., Demény A., Futo I. (2016) Benthic algae as major precursors of oil-prone kerogen – A case study from the Hungarian Middle Miocene. Central European Geology, Vol. 59, No.1-4, 1979, pp. 87-107, DOI: 10.1556/24.59.2016.004.

Więcław D., Kotarba M.J., Kowalski A., Koltun Y.V. Origin and maturity of oils in the Ukrainian Carpathians and their Mesozoic basement. Geological Quarterly, Vol. 56, No. 1, 2012, pp. 158-168.

Younes M.A. Crude oil geochemistry dependent biomarker distributions in the Gulf of Suez, Egypt. In: Crude oil exploration in the world (M.Younes, ed.). ISBN: 978-953-51-0379-0, InTech., 2012, 220 p.

Zachos J., Pagani M., Sloan L. et al. Trends, rhythms, and aberrations in global climate 65 Ma to present. Science, Vol. 292, 2001, pp. 686-693.

Zdanaviciutė O., Bojesen-Koefoed J.A. Geochemistry of Lithuanian oils and source rocks: preliminary assessment. Journal of Petroleum Geology, Vol. 20, No. 4, 1997, pp. 381-402.

Zhuze A.P. Diatoms. Atlas of rock-forming organisms (calcareous and siliceous). Nauka. Moscow, 1973, pp. 89-91 (in Russian).

Timoshina I.D. Geochemistry of organic matter of oil-producing rocks and oils of the Upper Precambrian in the south of Eastern Siberia. Publishing House SB RAS. Novosibirsk, branch"Geo", 2005, 166 p.

Tulan E. Evaluation of diatom-rich Oligocene to Miocene hydrocarbon source rocks in the Paratethys. Doctoral Thesis. Montan Univercity Leoben, 2020, 210 p.

Vail P.R., Hardenbol J. Sea-level changes during the Tertiary. Oceanus, Vol. 22, 1979, pp. 71-79.

Veto I., Báldi K., Coric S., Hetényi M., Demény A., Futo I. (2016) Benthic algae as major precursors of oil-prone kerogen – A case study from the Hungarian Middle Miocene. Central European Geology, Vol. 59, No.1-4, 1979, pp. 87-107, DOI: 10.1556/24.59.2016.004.

Więcław D., Kotarba M.J., Kowalski A., Koltun Y.V. Origin and maturity of oils in the Ukrainian Carpathians and their Mesozoic basement. Geological Quarterly, Vol. 56, No. 1, 2012, pp. 158-168.

Younes M.A. Crude oil geochemistry dependent biomarker distributions in the Gulf of Suez, Egypt. In: Crude oil exploration in the world (M.Younes, ed.). ISBN: 978-953-51-0379-0, InTech., 2012, 220 p.

Zachos J., Pagani M., Sloan L. et al. Trends, rhythms, and aberrations in global climate 65 Ma to present. Science, Vol. 292, 2001, pp. 686-693.

Zdanaviciutė O., Bojesen-Koefoed J.A. Geochemistry of Lithuanian oils and source rocks: preliminary assessment. Journal of Petroleum Geology, Vol. 20, No. 4, 1997, pp. 381-402.

Афанасенков А.П., Жеглова Т.П., Петров А.Л. Углеводороды-биомаркеры и изотопный состав углерода битумоидов и нефтей мезозойских отложений западной части Енисей-Хатангской нефтегазоносной области. Георесурсы, 2019, Том. 21, No. 1. с. 47-63.

Баженова О.К. Нефтегазоматеринский потенциал и нефтегазоносность. В кн.: Кайнозой Сахалина и его нефтегазоносность (под ред. Ю.Б.Гладенкова). ГЕОС, Москва, 2002, с. 137-194.

Голышев С.И., Падалко Н.Л., Мадишева Р.К., Оздоев С.М., Портнов В.С., Исаев В.И. Изотопный состав нефтей Арыскумского прогиба (Южный Казахстан). Известия Томского политехнического университета, Инжиниринг георесурсов, Том 331, No. 3, 2020, с. 80-89.

Диатомит. Геологический словарь. Том 1. Недра. Москва, 1978, 227 с.

Жузе А.П. Диатомовые водоросли. В: Атлас породообразующих организмов (известковых и кремнёвых). Наука. Москва, 1973, с. 89-91.

Конторович А.Э., Костырева Е.А., Сараев С.В., Меленевский В.Н., Фомин А.Н. Геохимия органического вещества кембрия Предъенисейской субпровинции (по результатам бурения скважин Восток-1 и Восток-3). Геология и геофизика, Том 52, No. 6, 2011, с. 737-750.

Мадишева Р.К. Исследование геодинамической обстановки осадконакопления и формирования нефтегазоносности доюрского комплекса Арыскумского прогиба. Диссертация на соискание степени доктора философии. Карагандинский Технический Университет. Республика Казахстан. Караганда. 2020, 99 с.

Маслов В.П. Кремневые организмы: общие замечания. Атлас породообразующих организмов (известковых и кремневых). Наука. Москва, 1973, 89 с.

Обласова Н.В., Гончарова И.В., Дердуга А.В., Куницына И.В. Генетические типы нефтей восточной части Крымско-Кавказского региона. Геохимия, Том. 65, No. 11, 2020, с. 1129-1150.

Томкеев С.И. Петрологический англо-русский толковый словарь. В 2-х томах. Т. 1. Мир. Москва, 1986, 285 с.

ТЯЖЕЛЫЙ ИЗОТОПНЫЙ СОСТАВ УГЛЕРОДА ДИАТОМИТОВ И НЕФТЕЙ МИОЦЕНА В ЮЖНО-КАСПИЙСКОМ БАССЕЙНЕ КАК ВОЗМОЖНОЕ ГЛОБАЛЬНОЕ ЯВЛЕНИЕ

Фейзуллаев А.А. [1,2]
[1] *Министерство науки и образования Азербайджанской Республики, Институт геологии и геофизики, Азербайджан AZ1143, Баку, просп. Г.Джавида, 119*: fakper@gmail.com
[2] *Министерство науки и образования Азербайджанской Республики, Институт нефти и газа, Азербайджан AZ 1000, Баку, ул. Ф.Амирова, 9*

Резюме. В статье представлен анализ результатов изотопно-геохимических исследований пород и нефтей кайнозойско-мезозойского разреза Южно-Каспийского бассейна (ЮКБ) за последние 30 лет. Подтвержден ранее установленный факт накопления тяжелого изотопного состава углерода (ИСУ) органического вещества (ОВ) миоценовых пород (Диатомовая свита), а также его производных нефтей в главном (нижнеплиоценовом) резервуаре ЮКБ. Для проверки глобального характера этого явления был проведен сравнительный анализ изотопно-геохимических данных по осадочным бассейнам 18 стран. Построена обобщенная диаграмма, показывающая пределы изменения ИСУ керогена и нефтей и их средние значения для различных стратиграфических комплексов всех рассмотренных бассейнов. Установлено, что это явление свойственно и другим бассейнам мира, на основании чего сделан вывод о его глобальном характере. Причины, которые привели к изотопному сдвигу в глобальном балансе углерода, произошедшему в миоцене, до конца не выяснены. Рассмотрены существующие представления о его возможной природе. Полученные результаты еще раз подтвердили эффективность использования геохимического параметра $\delta^{13}C$ для корреляции нефть-порода и нефть-нефть в сочетании с другими геохимическими критериями.

Ключевые слова: *изотопный состав углерода, органическое вещество, нефть, осадочные бассейны, миоцен*

CƏNUBİ XƏZƏR HÖVZƏSİNDƏ MİOSEN DİATOMİTLƏRİNİN VƏ NEFTİNİN AĞIR KARBON İZOTOP TƏRKİBİ MÜMKÜN QLOBAL HADİSƏ KİMİ

Feyzullayev A.A.[1,2]
[1] *Azərbaycan Respublikasının Elm və Təhsil Nazirliyi, Geologiya və Geofizika İnstitutu, Azərbaycan AZ1143, Bakı, H. Cavid pr., 119: fakper@gmail.com*
[2]*Azərbaycan Respublikası Elm və Təhsil Nazirliyi, Neft və Qaz İnstitutu, Azərbaycan AZ 1000, Bakı, F.Əmirov küç., 9*

Xülasə. Məqalədə Cənubi Xəzər hövzəsinin (CXH) kaynozoy-mezozoy kəsilişinin süxur və neftlərinin son 30 ildə izotop-geokimyəvi tədqiqatlarının nəticələrinin təhlili təqdim olunur. Miosen süxurlarının (Diatom Formasiyası) üzvi maddələrinin (ÜM) və onun törəməsi olan CXH -nin əsas (Aşağı Pliosen) rezervuarında toplanan neftlərının əvvəllər müəyyən edilmiş karbon izotop tərkibinin (CİT) ağır olduğu faktı təsdiq edilmişdir. Bu hadisənin qlobal xarakterini yoxlamaq üçün 18 ölkənin çöküntü hövzələrinin izotop-geokimyəvi məlumatlarının müqayisəli təhlili aparılmışdır. Bütün baxılan hövzələrin müxtəlif stratiqrafik komplekslərə aid kerogen və neftin CİT-nin dəyişmə hüdudlarını və onların orta qiymətlərini göstərən ümumiləşdirilmiş diaqram tərtib edilmişdir. Müəyyən edilmişdir ki, bu hadisə dünyanın digər hövzələri üçün də xarakterikdir. Bunun əsasında onun qlobal mahiyyəti haqqında nəticə çıxarılmışdır. Miosendə baş verən qlobal karbon balansında izotop dəyişikliyinə səbəb hələ tam müəyyən edilməməşdir. Onun mümkün mənşəyi haqqında mövcud fikirlər nəzərdən keçirilir. Alınan nəticələr neft-süxur və neft-neft korrelyasiyası üçün $\delta^{13}C$ parametrin, digər geokimyəvi meyarlarla birlikdə, istifadə səmərəliliyi bir daha sübuta gətirilmişdir.

Açar sözlər: *karbonun izotop tərkibi, üzvi maddə, neft, çöküntü hövzələri, Miosen*

ANAS Transactions Earth Sciences 1 / 2024

http://www.journalesgia.com

THE RELATIONSHIP BETWEEN THE PALEOBIOGEOGRAPHY OF THE NORTHERN AND SOUTHERN SIDES OF THE NEOTETHYS AND THE DEEP GEODYNAMIC PROCESSES

Eppelbaum L.[1,2], Katz Y.[3], Kadirov F.[4]

[1]Dept. of Geophysics, Faculty of Exact Sciences, Tel Aviv University, Israel
Ramat Aviv 6997801, Tel Aviv
[2]Azerbaijan State Oil and Industry University, Azerbaijan
20 Azadlig Ave., Baku AZ1010
[3]Steinhardt Museum of Natural History & National Research Center,
Faculty of Life Sciences, Tel Aviv University, Israel
Ramat Aviv 6997801, Tel Aviv
[4]Ministry of Science and Education of the Azerbaijan Republic,
Institute of Geology and Geophysics, Azerbaijan
119, H. Javid Ave. Baku, AZ1143

Keywords: *geodynamics, deep rotating structure, paleobiogeographical maps, tectonophysical analysis, Neotethys Ocean*

Summary. Several of our previous studies substantiated the discovery of the phenomenon of a deep mantle structure rotating counterclockwise, influencing tectonics and various geological-environmental processes in the South Caucasus and the Eastern Mediterranean. This study made it possible to estimate the onset of the influence of the deep structure and characterize the structural-tectonic changes that occurred in different geological eras. The widespread use of paleontological data has made it possible to classify the migration of organisms from distant provinces and obtain data on the formation of basins based on the study of the geodynamics of terrane belts, island arcs, shear zones, and deep movements determined by the nature of mantle convection. The role of paleobiogeography, sedimentation tectonics, and paleogeography in assessing autochthonous and allochthonous structures is essential to the deep geodynamics of past and present geological eras. The geodynamic evolution of the Mesozoic Terrane Belt (MTB) located on the Neotethys southern side (the Gondwana northern part) was investigated. Our comprehensive studies showed the MTB's allochthonous nature and confirmed previous data on the terrane nature and the Mesozoic age of the displaced tectonic blocks. In the Lesser Caucasus, biogeographical and tectonophysical studies sharply separated the eastern (Azerbaijanian) part of the Lesser Caucasus from the ophiolite belt in its southwestern continuation. The structural-geodynamic uniqueness of the mixed Late Cretaceous fauna of the Garabakh region (western Azerbaijan) has received a comprehensive justification. An assessment was made of the beginning of the influence of the mantle structure on near-surface tectonic-structural elements.

1. Introduction

Hallam (1975) was among the first to point out an essential relationship between the Jurassic paleobiogeographical indicators and geodynamic processes. The distribution of Mesozoic Tethys biocenoses in connection with changes in biotic and abiotic environmental factors is a crucial problem. It is being developed as a factor in solving practical problems of the geological survey (Dixon and Robertson, 1984; Khain, 1994; Hall et al., 2005; Krasheninnikov et al., 2005; Leonov, 2007; Alizadeh et al., 2016, 2024), as well as theoretical problems of geosciences and issues for monitoring of natural processes (e.g., Gamkrelidze, 1986; Khain, 2000; Ben-Avraham et al., 2002; Golonka, 2004; Zakariadze et al., 2007; Şengör, 2009; Le Pichon and Kreemer, 2010; Eppelbaum and Khesin, 2012; Kadirov et al., 2013; Faccenna et al., 2014; Kadirov and Gadirov, 2014; Alizadeh et al., 2016; Said, 2017; Eppelbaum et al., 2018, 2023b).

In this regard, two crucial regions of practical importance are distinguished: (1) the Near and Mid-

dle East and (2) the Transcaucasus. The first marks the processes of geological development on the southern (Gondwana) side of the Neotethys, and the second marks the northern (Eurasian) frame of this Mesozoic Ocean. Both mentioned structural-biogeographic zones form the most constricted part of the collisional Alpine-Himalayan Fold Belt (AHFB) (Eppelbaum and Katz, 2023) (Fig. 1). It successively articulates three structures of different ages: (1) the ancient Precambrian Arabian Platform, (2) the folded-metamorphic Neoproterozoic belt, and (3) the blocky Mesozoic Terrane Belt (MTB). The same map illustrates another significant similarity between the two marked regions: they are dissected by two deep faults (cutting belts of different ages), creating their structural-geodynamic contrast. The first case is the Eastern Mediterranean-Nubian Fault (EMNF), which is seismically active and marked by the Meso-Cenozoic traps with the manifestations of the alkali-kimberlite mantle intrusions (Eppelbaum and Katz, 2012). The second major fault, Main Eastern European Fault (MEEF), is also seismically and tectonic-thermally active. It is significant that it discordantly cuts the Caucasus in half – into East and West. The generalized paleomagnetic data (Eppelbaum et al., 2021) shown in Fig. 1 indicate their geodynamic differences: the structures of the Western Caucasus rotate in a counterclockwise direction, and those of the Eastern Caucasus rotate clockwise.

This map indicates that the zone of the catastrophic Turkish earthquakes of 06.02.2023 is at the boundary between the MTB and AHFB. Besides this, a fold-block arc of the MTB deeply advanced to the north into the zone of the AHFB (Eppelbaum and Katz, 2023). Its distal part is shown with the corresponding designation (Fig. 1). It is significant that in the zone of this joint, the width of the Alpine belt of the Pontic-Caucasian zone is reduced to a minimum (Tye et al., 2022) – of about 500 km. Furthermore, to the west, from the Cyprus arc to Eastern Crimea, the width of the Alpine belt exceeds 1,200 km.

2. Brief Tectonic-Geophysical Background

The Easternmost Mediterranean (EMM) is a region belonging to the transition zone of the most prominent tectonic structures of the Earth – Eurasia and Gondwana (McKenzie, 1972; Ben-Avraham et al., 2002, 2006; Muttoni et al., 2003; Stern and Johnson, 2010). In the Cenozoic, four lithospheric plates were formed here: Nubian, Arabian, Aegean-Anatolian, and Sinai (Ben-Avraham et al., 2006). The area is characterized by unique geodynamics, which simultaneously expresses the elements of the geodynamic collision associated with the Tethys Ocean evolution (Le Pichon and Kreemer, 2010; Stampfli et al., 2013) and the Red Sea rift system's initial spreading (Bosworth et al., 2005). However, until now, the EMM's paleogeodynamics has not been entirely understood. The foreland sediments of Northern Arabia and Eastern Nubia are tectonically discordantly connected to the allochthonous Mesozoic Terrane Belt, which rotated counterclockwise in the direction of the Gondwana paleocontinent (Eppelbaum and Katz, 2015a, 2015b; Eppelbaum et al., 2021).

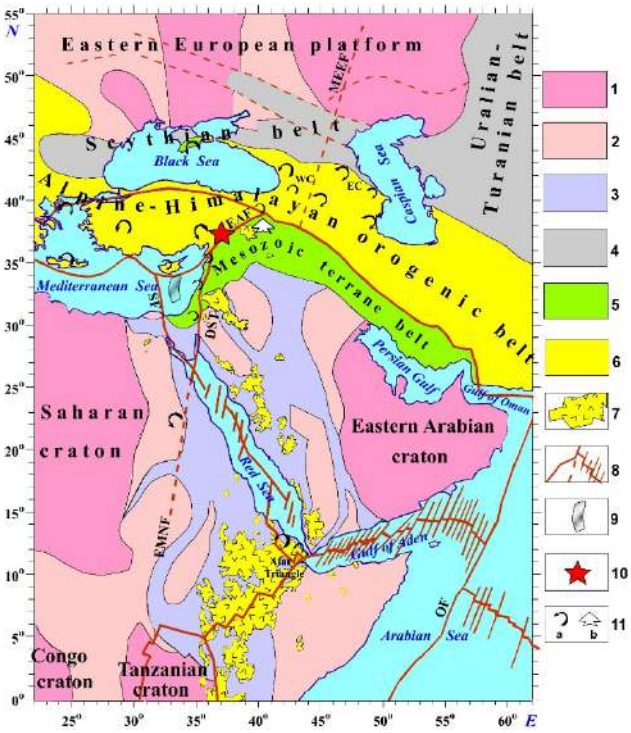

Fig. 1. The tectonic-geodynamic scheme of the region under study (modified after (Eppelbaum et al. (2021)).

(1) Archean cratons, (2-4) folded belts: (2) Paleo-Middle-proterozoic, (3) Neoproterozoic, (4) Late Paleozoic (Hercynian), (5) Mesozoic Terrane Belt (MTB), (6) Alpine-Himalayan orogenic belt, (7) Cenozoic traps of the African-Arabian rift belt, (8) main fault systems, (9) contour of the Kiama paleomagnetic hyperzone of inverse polarity (Eppelbaum et al., 2014; Eppelbaum and Katz, 2015b), (10) high magnitude seismogenic zone in Eastern Turkey (February 06, 2023), (11) **a**: rotational geodynamic elements derived from paleomagnetic data, **b**: distal part of the MTB. SF, Sinai Fault, DST, Dead Sea Transform, MEEF, Main Eastern European Fault, EMNB, Eastern Mediterranean Nubian Belt, OF, Owen Fault, WC, Western Caucasus, EC, Eastern Caucasus, EAF, Eastern Anatolian Fault.

Since the processes of plate geodynamics controlled the facies and structures of the habitat zones of ancient biocenoses, one should consider the actualistic model shown in Fig. 2. Here, for example, three geophysical fields are summarized (in fact, there are many more of them (Eppelbaum et al., 2024)): (1) smoothly averaged magnetic field ΔZ recalculated to one common level of 2.5 km over the msl, (2) residual gravity field map obtained from the satellite gravimetric observations, (3) GPS vector distribution from the satellite triangulation data

(Mahmoud, 2003; Reilinger et al., 2006; Khaffou et al., 2023; Eppelbaum and Katz, 2023).

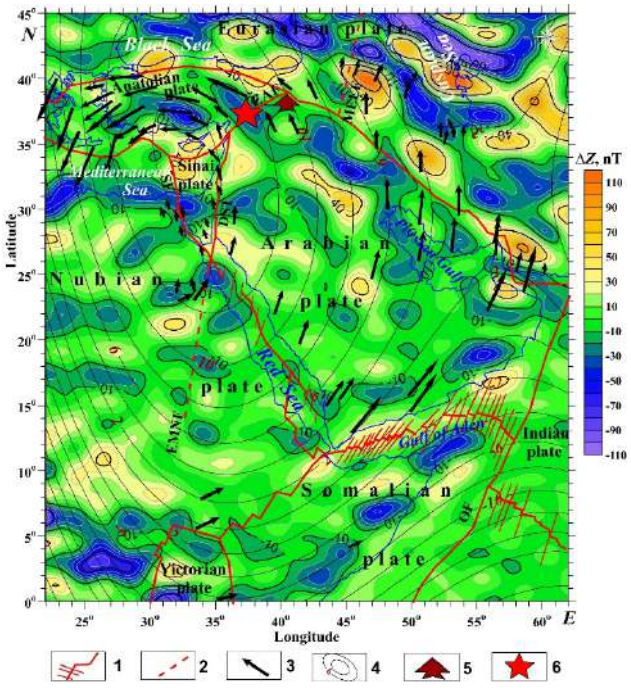

Fig. 2. Smoothly averaged magnetic ΔZ map recalculated to one common level of 2.5 km over the msl (initial data from https://geomag.colorado.edu/magnetic-field-model-mf7.html) for African-Arabian region with the main tectonic elements (Eppelbaum et al., 2024), the behavior of the GPS vectors (after Mahmoud, 2003; Reilinger et al., 2006; Khaffou et al., 2023) and overlaid residual gravity anomaly (Eppelbaum et al. (2021)).

(1) intraplate faults, (2) interplate faults, (3) GPS vectors, (4) residual satellite-gravity field isolines, (5) distal part of the Mesozoic Terrane Belt, (6) epicenters of two main catastrophic earthquakes in Eastern Turkey (February 06, 2023).

The geophysical map (Fig. 2) goes well with the tectonic map (Fig. 1). For explaining the paleogeography and biogeography of the geological past, important not only the structural-facial features of the development of ancient biocenoses but also various factors of the geodynamics of their formation since they reflect different levels of their intensity and significance in the migration and ecosystem biosphere process. In this regard, the geodynamic factors have long been taken into account, which has been well developed in the analysis of the relationships between ophiolitic, island-arc, and terrane associations in the aspect of correlation with the biocenoses of deep- and shallow-water zones (Dixon and Robertson, 1984; Katz, 1986; Ben-Avraham and Ginzburg, 1990; Lapkin and Katz, 1990; Kazmer, 1993; Hall et al., 2005; Alizadeh et al., 2016; Eppelbaum et al., 2021).

In the case of our research, an important role is played by the assessment of innovative geophysical studies that complement plate geodynamics, in particular, geoid, rotational, and mantle-convective factors that determine changes in the abiotic and biotic environment (Katz, 1986; Reilinger et al., 2006; Kadirov et al., 2012, 2013; Eppelbaum and Katz, 2021a, 2021b; Eppelbaum et al., 2024). First, we must pay attention to the development of a deep mantle sub-oval structure in the Arabian-Caucasian region, manifested in no less than fifteen anomalous geophysical and geological factors (Eppelbaum et al., 2024). Examples of the distribution of three anomalous fields: GPS vectors, magnetic field, and residual gravity field anomalies both in the Eastern Mediterranean and the Ponto-Caspian and Caucasus are shown in Fig. 2. This geodynamic factor can undoubtedly be very significant in assessing complex and inexplicable biogeographical phenomena identified in the Caucasian Mesozoic (Alizadeh, 1972; Alizadeh et al., 1983; Abdulkasumzadeh, 1988), which was traced based on geological and geophysical analysis of the formation of water areas and biocenoses of the Akchagylian stage in the Late Cenozoic basins of the Mediterranean and Ponto-Caspian Sea (Eppelbaum and Katz, 2021a, 2022, 2024).

The methodology for the linking between the biosphere and anthroposphere processes in connection with deep geophysical phenomena was developed using the example of the Akchagylian phenomenon, which manifested itself both in different facies basins of the Crimean-Caucasus region and in the Middle East – in the Levant and Nubia (Chumakov, 1967; Alizadeh et al., 2016; Eppelbaum and Katz, 2021a, 2024). Therefore, it is advisable to consider the features of the Mesozoic biogeography manifested in the phenomenon of sharp faunal differences between the Lesser Caucasus and the Levant in the same tectonic-geodynamic aspect.

Based on the above, the present study needs to pay attention to the Cenozoic stage when the Neotethys Ocean began to shrink under the influence of collision phenomena and was divided into two isolated residual basins: the southern Mediterranean and the northern Paratethys. The biogeographical and tectonophysical processes were in sharp contrast and incompatible with the stage of spreading geodynamics between Laurasia and Gondwana in the Mesozoic era.

3. Analysis of the Geodynamic Movements Combined with the Paleontological and Paleobiogeographical Data

Tectonic-geodynamic reconstructions of the transitional region between Eurasia and Gondwana (Scotese, 1991; Stampfli and Kozur, 2006), supplemented by paleobiogeographic and geodynamic data (Eppelbaum et al., 2024) show that in the Jurassic period, there were the most incredible distances between these supercontinents. The northern side of the

Neotethys adjoined Laurasia, and the southern side adjoined Gondwana. These two boundary zones differed biogeographically (Makridin et al., 1968; Hallam, 1975; Hirsch, 1988).

With the evolution of the Neotehys Ocean, the pelagic facies and nektonic organisms reached their maximum dominance. However, the ecosystems of the Boreal and Ethiopian provinces were located on the continental shelf and bordered the vast expanses of land in the northern and southern parts of Pangea (Fig. 3). At the present stage of the Mesozoic Ocean collision, the northern and southern sides of the Neotethys are geodynamic connected to a single structure associated with the deep mantle uplift. It is manifested in the numerous GPS studies in the Caucasus and surrounding regions (e.g., Reilinger et al., 2006; Kadirov et al., 2012, 2013; Eppelbaum et al., 2021a, 2023b).

In the Jurassic period, the southern Arabian-Levantine and northern Crimean-Caucasian sides of the Neotethys were at a considerable distance and could not be geodynamically connected. The present studies tested this indirect conclusion based on a comparative paleobiogeographic analysis of the Tethyan faunas of the western and eastern (Caucasian) parts of the Neotethys. In Fig. 3, we show the development of a specific fauna of the Late Jurassic (Kimmeridgian-Tithonian) *Pygope* brachiopods, indicators of the relatively deep-sea Neotethys zone (Kazmer, 1993), and widespread throughout the western part of this basin from the Rif Mts. to the Alpine-Carpathian Basin and Greece (Barczyk, 1972; Dibni and Middlemiss, 1981; Sandy, 1988, 1991; Vörös, 1993; Benzaggargh and Atrops, 1997; Énay et al., 2005; Bujtor et al., 2020). The significant factor is the discovery of this critical Tethys biogeographical indicator in the east – in various points of the Lesser Caucasus, carried out by Askerov (1965) (see Abdulkasumzade (1988)). Along with the *Pygope* finds, a typically Mediterranean complex of the Upper Jurassic brachiopods was identified here: *Lacunosella*, *Cheirothyris*, *Ismenia*, *Goniothyris*, *Sphaeroidothyris*, *Ptyctothyris, Aulacothyris* and some others (Askerov, 1965; Abdulkasumzade, 1988).

Examining paleobiogeographic data confirms the deep structure rotation and its relationship with the near-surface structures (Eppelbaum et al., 2024). Like the paleomagnetic ones, they show earlier stages of deep structure rotation and its reflection in surface geology. The region under consideration is essential for analyzing the development spreading stage (mainly Mesozoic) of the development of the Neotethys Ocean and adjacent parts of Gondwana and Laurasia. Special attention is drawn to anomalous biogeographic indicators, particularly shell remains of giant Late Jurassic brachiopods *Septirhynchia–Somalirhynchia*, Late Cretaceous brachiopods *Praeneothyris* and giant shells of Triassic endemic myalinid bivalves *Ramonalina*, (Katz, 1962; Makridin et al., 1966, 1968; Feldman, 1987; Cooper, 1989; Yancey et al., 2009; Feldman et al., 2014; Eppelbaum et al., 2024).

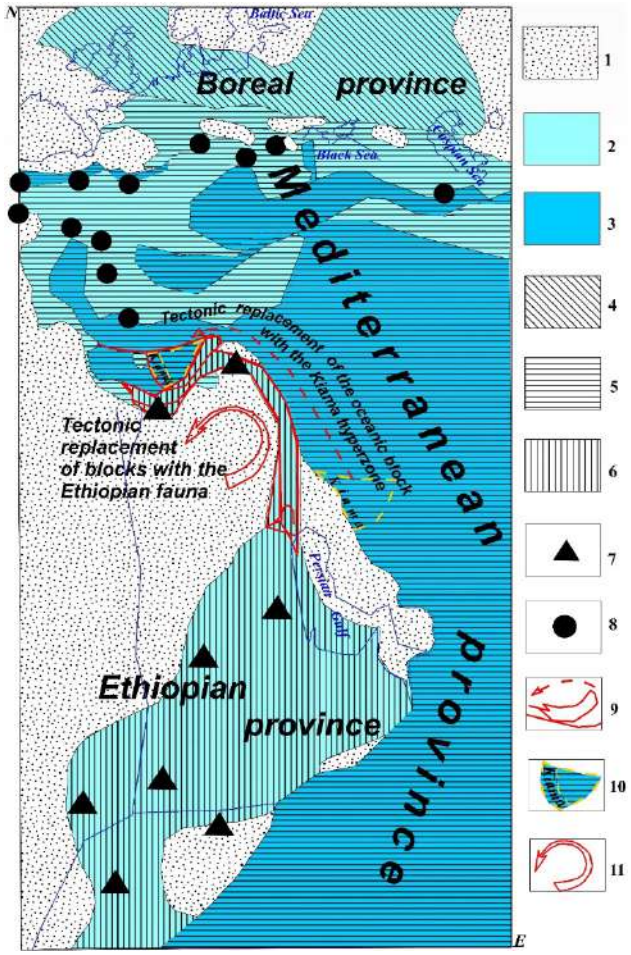

Fig. 3. The schematic Late Jurassic paleobiogeographical map of the transitional region of Eurasia and Gondwana with the elements of the subsequent Early Cretaceous geodynamics of the Mesozoic Terrane Belt. The blue lines show the modern boundaries between the seas and land.

(1) land, (2) continental shields and arcs, (3) oceanic plateaus and rifts, (4) Boreal paleobiogeographic province, (5) Mediterranean paleobiogeographic province, (6) Ethiopian paleobiogeographic province, (7) location points with the Ethiopian brachiopods *Septirhynchia-Somalirhynchia*, (8) location points with the Mediterranean brachiopods *Pygope*, (9) tectonic lines of discordant paleobiogeographic replacements, (10) block of the oceanic crust with the Kiama hyperzone, (11) counterclockwise rotated tectonic blocks.

This map was constructed using paleobiogeographic data from Arkell (1956), Askerov (1965), Makridin et al., 1968; Barczyk, 1972; Tchoumatcuenko, 1978; Feldman, 1987; Abdulkasumzade, 1988; Hirsch, 1988; Hirsch and Picard, 1988; Cooper, 1989; Golonka and Ford, 2000; Hall et al., 2005; Énay et al., 2005; Kazmer, 1993; Bujtor et al., 2020; Eppelbaum and Katz, 2023) and tectonic-geodynamic data from Scotese (1991), Stampfli and Kozur (2006), Eppelbaum et al. (2021), Eppelbaum and Katz (2023).

3.1 Late Jurassic paleobiogeographical map

The biogeographical mapping was based on the works of Scotese (1991), Stampfli and Kozur (2006), and previous authors' investigations (Eppelbaum and Katz, 2015b, 2020). In the region under study (Arkell, 1956; Makridin and Katz, 1966; Feldman, 1987; Hirsch, 1997; Hirsch and Picard, 1988; Cooper, 1989; Alizadeh et al., 2016), three paleobiogeographical provinces were selected (Fig. 3): Boreal (Eurasian shelf), (2) Mediterranean (Mediterranean Basin), and (3) Ethiopian (Arabia – Southeastern Africa).

At the same time, the ecosystems of the Boreal and Ethiopian provinces were located on the continental shelf and bordered by vast expanses of land in the northern and southern parts of Pangea. The constructed map (Fig. 3) shows the phenomenon (see the red arrow rotating counterclockwise) of the geodynamic transfer of tectonic blocks with the remains of the Ethiopian fauna from the present position of the Persian Gulf to the Levant (up to the Egyptian Western Desert). This fact proves the counterclockwise movement of the eastern and central parts of near-surface projections of the anomalous deep structure in the Jurassic and Early Cretaceous.

All of those mentioned above enabled us first to use geophysical and geodynamic characteristics to explain the uniqueness of the biogeographically anomalous zone of terrane block attachment to the Gondwana paleocontinent in the middle of the Early Cretaceous in the Levantine phase of tectogenesis (Eppelbaum and Katz, 2015b; Eppelbaum et al., 2024).

These studies are critical in terms of the separation of Tethys and Ethiopian Late Jurassic basins. Their biogeographical contact in the Levant in the context of the existence of an extensive barrier of the Western Arabian land (Makridin et al., 1968) was inexplicable for many decades until the development of tectonic-geodynamic studies in the region using deep geophysical studies (Ben Avraham and Ginzburg, 1990; Ben Avraham et al., 2002, 2006; Eppelbaum and Katz, 2011, 2015b, 2023), when the tectonically allochthonous nature of terrane blocks with the Ethiopian fauna was proven displaced in a counterclockwise rotation direction over a distance of more than 1,500 km from the area adjacent to the northwestern part of the modern Persian Gulf position. Similarly, the Neotethys terrane block of the primary oceanic crust, containing the oldest discovered oceanic crust of the Kiama paleomagnetic zone, was moved into the Levant (Eppelbaum et al., 2014).

In the plate-tectonic reconstruction of the Jurassic location of the MTB (Fig. 4), the identified theoretical data of a biogeographical and structural-paleogeographical nature are essential as a secondary criterion of a qualitative nature. It is significant that they are complemented by precise criteria for the primary orientation of the terrane blocks and are very important for analyzing the relationship of the Mesozoic Terrane Belt with the Gondwana foreland and the deep-sea basins of the Neotethys Ocean.

3.2 Geodynamics of the Mesozoic Terrane Belt in the Jurassic period

Biogeographical, deep structural-geophysical, and geodynamic data are the most critical regional aspects in the plate-tectonic position of the terrane belts. However, their direct paleotectonic mapping requires a criterion for the local relative position and orientation of terrane blocks, as shown in mapping the Hercynian belt of Avalonia (Cope et al., 1992). No less elegant works were performed in the Middle East for localization of the Neoproterozoic belt of the Arabian-Nubian region (Stern, 1994; Al-Husseini, 2000; Stern et al., 2004; Johnson and Kattan, 2008) where, in a complex range of the collision belt structures, multi-scale, including striped, terrane blocks appear.

We correct their relative position and orientation in pre-collision plate-tectonic reconstructions using three criteria: (1) the sequence of the final collision junction (Eppelbaum and Katz, 2015b), (2) the combination and nature of the relationship between the zones of syn-sedimentary uplifts and troughs, which we developed earlier (Eppelbaum and Katz, 2011, 2015b), and (3) data paleomagnetic-geodynamic mapping of terrane blocks indicating their rotation based on the orientation data of dike swarms of different ages (Eppelbaum et Katz, 2015a) and consistent reconstruction of the orientations of the terrane blocks themselves over time (Eppelbaum and Katz, 2022; Eppelbaum et al., 2023a).

In this work, we study the Middle East – Caucasus geodynamics problem in more detail, using the plate tectonic analysis of the terrane block movement, both MTB and the more ancient Tauride Belt (Channell et al., 1996; Golonka, 2004; Zakariadze et al., 2007), to explain several Mesozoic biogeographical paradoxes of the Middle East and the Caucasus (Alizadeh, 1972; Alizadeh et al., 2016; Eppelbaum and Katz, 2020, 2021b). These data are considered below.

In this work, we study the Middle East – Caucasus geodynamics problem in more detail, using the plate tectonic analysis of the terrane block movement, both MTB and the more ancient Tauride Belt (Channell et al., 1996; Golonka, 2004; Zakariadze et al., 2007). This analysis explains several Mesozoic biogeographical paradoxes of the Middle East and the Caucasus (Alizadeh, 1972; Alizadeh et al., 2016; Eppelbaum and Katz, 2020, 2021b). These data are considered below.

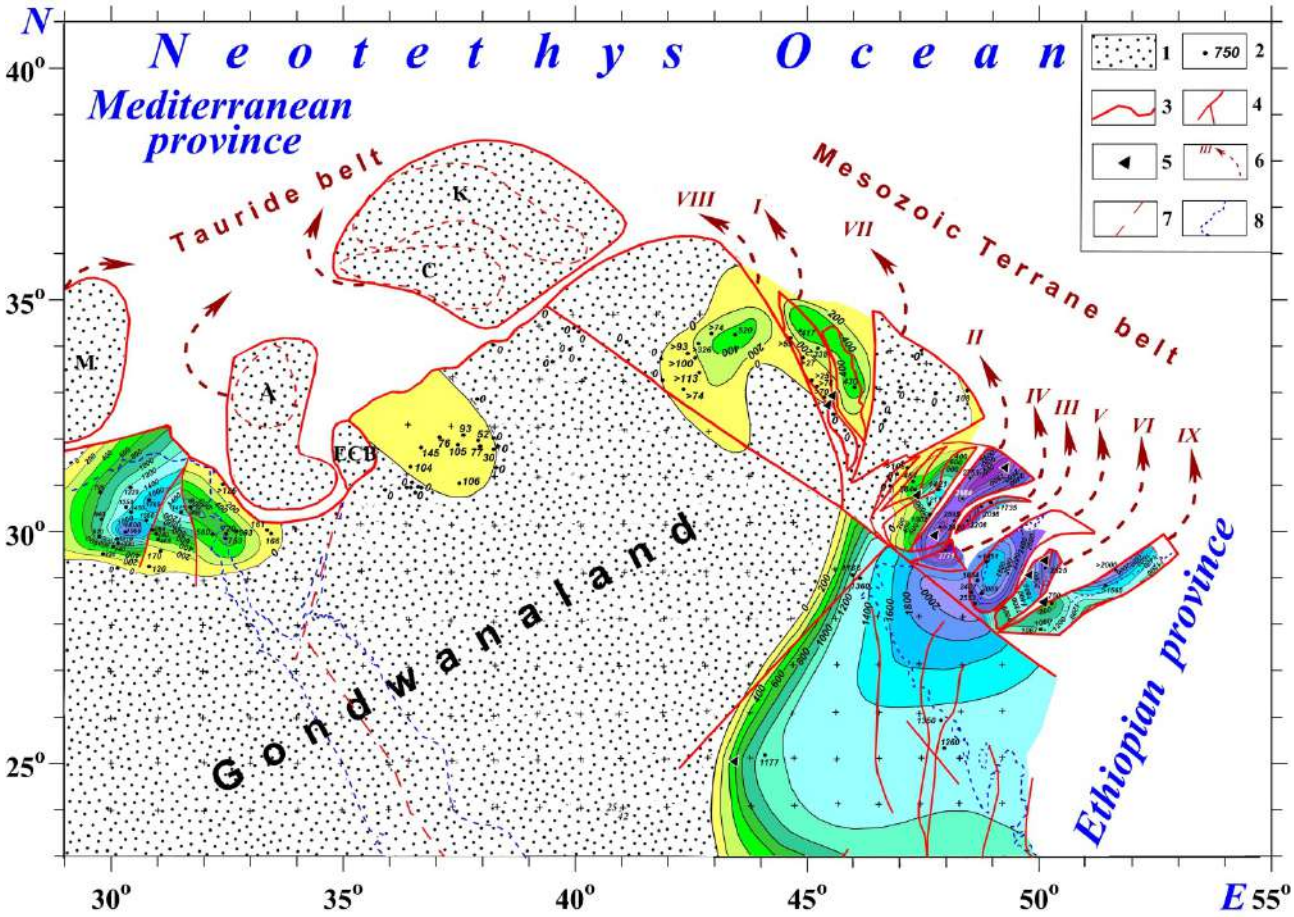

Fig. 4. Geodynamics of the Mesozoic Terrane belt (MTB) in the Jurassic period with elements of the Gondwana-Neotethys paleogeography and biogeography. The following primary sources were used for this map development: Arkell, 1956, Dixon and Robertson, 1984; Feldman, 1987; Cooper, 1989; Al-Husseini, 2000; Dercourt et al., 2000; Hall et al., 2005; Zakariadze et al., 2007; Feldman et al., 2014; Eppelbaum and Katz, 2015b; Said, 2017; Eppelbaum and Katz, 2023.

(1) Gondwanaland and MTB, (2) boreholes and outcrops with the Jurassic sediment thicknesses, (3) boundary of the Gondwana and MTB blocks, (4) syn-sedimentary Jurassic faults, (5) outcrops of the Ethiopian fauna *Somalirhynchia-Septirhynchia*, (6) counter-clockwise rotating of the MTB concerning to the Jurassic collision system (the Roman numbers designate an order of the conjunction with the west Arabian part of Gondwana), (7) postcollisional faults, (8) modern land-sea boundaries.

ECB, Eratosthenes continental block. Precambrian massifs in the Tauride belt terranes: A – Alanya, C – Central Tauride, K – Kirsehir, M – Menderes.

Classic plate tectonic reconstructions are dominated by planetological methods considering the position of expansion and rotation poles of major tectonic plates and paleomagnetic measurements aimed at reconstruction of paleolatitudes and paleolongitudes (e.g., Van der Voo et al., 1991; McElhinny and McFadden, 2000; Tauxe, 2002). In addition to mentioned, various data from paleogeography, sedimentology, and palinspastic reconstructions are used (Khramov et al., 1974; Cope et al., 1992; Dercourt et al., 2000; Golonka and Ford, 2000; Stampfli and Borel, 2002; Muttoni et al., 2003; Khramov and Iosifidi, 2012; Stampfli et al., 2013; Uzel et al., 2015; Eppelbaum and Katz, 2021a, 2024; Le Pichon et al., 2023). In our case of the extraordinary structural complexity of the region under study, we used combined data for tectonic-geodynamic reconstructions with the attracting of paleobiogeography, syn-sedimentary tectonics, regional geodynamics, and detailed paleomagnetic mapping (Eppelbaum and Katz, 2015b, 2020, 2024; Eppelbaum et al., 2014, 2021, 2023a).

According to these studies, the allochthonous nature of most parts of the tectonic structures of the continental and oceanic crust of the Eastern Mediterranean was proven. An analysis of the relationship between the boundary structures of the Gondwana continent and the Neotethys Ocean indicates that in the Jurassic, the northwestern part of its Arabian segment was uplifted relative to the southeastern margin adjacent to the modern Persian Gulf (Fig. 4). Therefore, during the reconstruction, blocks of the Tauride ophiolite belt were placed in the northwestern part of the region. Blocks of the MTB were placed in the southwestern part by their syn-sedimentary and biogeographical sequence, which is depicted on the developed map. Paleobiogeographic data also confirm this phenomenon. In the Upper

Jurassic, in the sections of the Arabian Plate and the Negev, Galilee-Lebanon, Anti-Lebanon, and Palmyrides terranes, remains of **Somalirhynchia-Septirhynchia** of the Ethiopian province are widely developed (Fig. 4).

The most essential element of the reconstruction is the location of the MTB directly on the northern shore of the Persian Gulf's current position. Now, it is the boundary between the ancient Precambrian Arabian platform and the Zagros terrane. Consensus data (Bordenave, 2008) indicate that the Zagros terrane is allochthonous (Eppelbaum and Katz, 2017). While thick strata of the Jurassic sediments are developed in the Persian Gulf region, Jurassic sediments are practically absent throughout the vast Zagros terrane (Bordenave, 2008). Thus, the primary location of the small linear MTB terranes looks tectonically correct. Their orientation, which differs from the modern one, was revealed earlier during paleomagnetic-geodynamic mapping (Eppelbaum et al., 2023a), the results of which are discussed in Section 3.3.

Paleo-structurally, analysis of the MTB demonstrates its connection with the geodynamics of the eastern end of the Arabian Gondwana (Eppelbaum and Katz, 2017), adjacent to the sharply subsided margin of the Mesozoic Neotethys Ocean. An active zone of graben-like structures developed here, which appeared in the Late Jurassic as favorable oil and gas deposits and seals of the world's largest fields in Saudi Arabia, Qatar, and Kuwait (Al-Husseini, 2000). These submeridional faults continue in the terrane belt outside Gondwana, creating an extraordinary contrast of syn-sedimentary uplifts and troughs. Moreover, these unusual structures are complicated by the mantle alkali-basalt and alkaline intrusions – swarms of the Jurassic dikes and stocks of different ages (Eppelbaum and Katz, 2015b; Eppelbaum et al., 2023a).

The unusual, banded junction of terrane blocks adjacent to the ancient Precambrian Arabian Platform is because the belt is allochthonous (Eppelbaum and Katz, 2015b) and is composed of the relatively young Late Precambrian crust covered by the Paleozoic and younger sedimentary rocks and trap complexes. The fact that the most minor and narrowest blocks, such as the Heletz terrane and the Hameishar, Ramon, and Avdat subterranes of the Negev terrane, are adjacent to the sharply lowered western flank of the Jurassic trough of the eastern margin of Gondwana indicates that at that time, the axial part of the deep mantle uplift was located here. Judging by the sedimentation data (the age of sedimentary rocks of the Gondwana foreland), it was formed at the Carboniferous-Permian boundary, and at the end of the Jurassic period, it began to rotate in a counterclockwise direction.

3.3 Geodynamic-paleomagnetic map of the Makhtesh Ramon area (southern Israel)

In the process of innovative geoscience mapping using remote sensing techniques and comprehensive modeling aspects, we are faced with the analysis of complex geological structures with the need to use well-developed criteria of a multidisciplinary methodology, where the numerical data of the exact sciences are well-combined with the versatile qualitative data of basic research in the field of evolutionary paleontology and careful ecological and taxonomic research. The developed geodynamic-paleomagnetic map of the Makhtesh Ramon Canyon (southern Israel) is entirely unexpected and indicative (Fig. 5).

Our comprehensive analysis indicates that the Negev terrane (based on the results of paleomagnetic-geodynamic analysis of the dike complex in the Makhtesh Ramon subterrane (Fig. 5B)) has rotated from the mid-Jurassic period in a counterclockwise direction by more than 90 degrees compared to its modern orientation (Eppelbaum et al., 2023a). This process's global character is confirmed by Cyprus's counterclockwise rotation in the Eastern Mediterranean (Eppelbaum et al., 2024; Hepworth et al., 2024).

3.4 Geodynamics of the Mesozoic Terrane Belt on the accretion stage

The developed tectonic-paleobiogeographic maps (Figs. 3-5) allow us to construct a geodynamic map of the Mesozoic Terrane Belt (MTB) during the accretion stage (Fig. 6). By the middle of the Early Cretaceous (at the boundary of the Early and Late Hauterivian), during the Levantine phase of tectogenesis, the rotating blocks of the MTB were attached along a system of transform arcuate faults to the western Arabian-Nubian part of Gondwana (Eppelbaum and Katz, 2015b). The sequence of the discordant junction of the terranes of the MTB with Western Gondwana is indicated in Fig. 6. Here, this sequence is illustrated both in the structural-geodynamic and paleobiogeographic terms in the form of paleo-faunistic indicators, indicators (inline form) belonging to certain biogeographic provinces of the Jurassic Sea basins, developed in the zone of development of both continental and oceanic crust. In this form, we, for the first time, consider together the relationship of tectonic and paleobiogeographic mapping, indicating the movement of terranes embedded in both continental and oceanic crust. By a complex movement in the counterclockwise direction along a system of transform faults, these terranes formed the complex collisional structure of the Eastern Mediterranean.

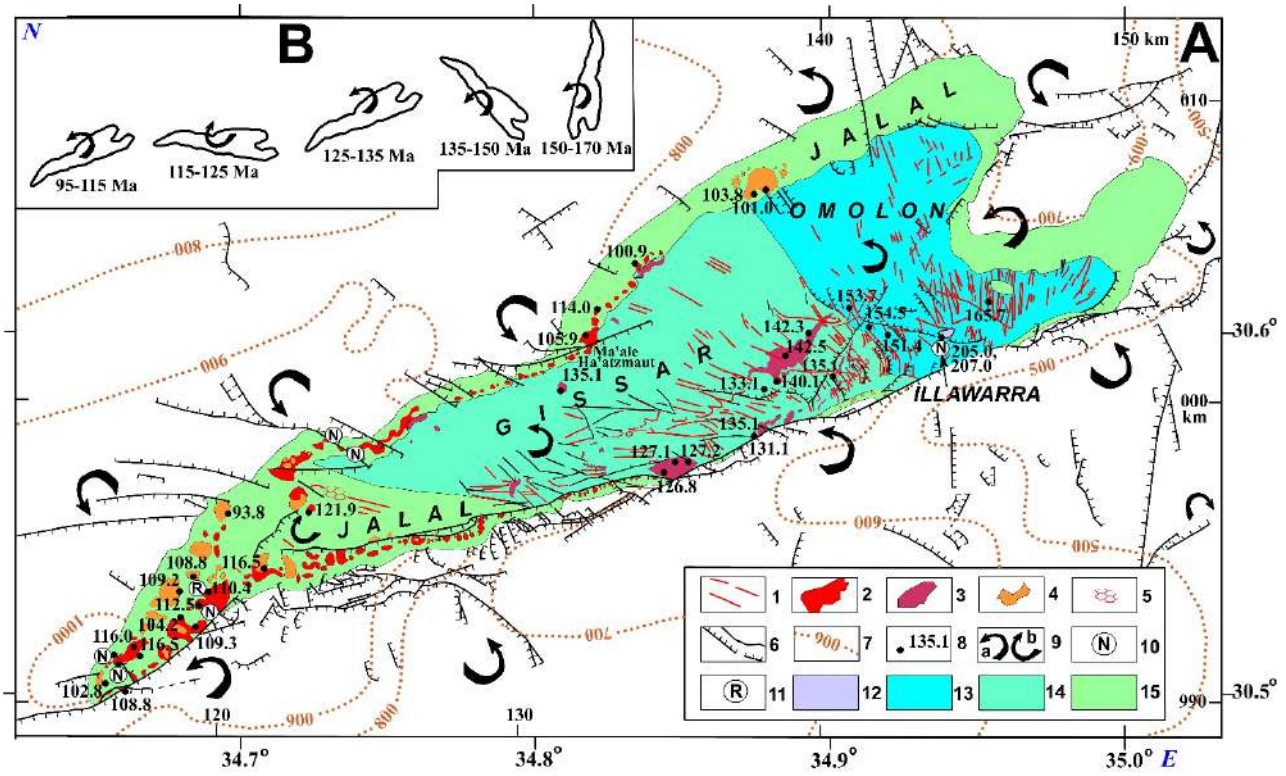

Fig. 5. Geodynamic-paleomagnetic map of the Makhtesh Ramon Canyon (southern Israel) (modified and supplemented after Eppelbaum and Katz, 2015b). **A**: Geodynamic-paleomagnetic indicators. **B**: Geodynamic changes of the Makhtesh Ramon subterrane displacement in the Middle Mesozoic.

(1) precollisional-collisional basalt dikes, (2) postcollisional alkali olivine basalt flows and volcanoclastic rocks, (3) precollisional association of alkali olivine gabbro, monzogabbro and syenites, (4) postcollisional association of basanites and nefelinites, (5) quartzitic hexagonal prisms, (6) faults, (7) hypsometric isolines within the Makhtesh Ramon plateau (1-7 from Garfunkel and A. Katz (1967), Zak (1968), Baer and Reshes (1991), Baer (1993), Sneh et al. (1998), Avni (2001), Zilberman and Avni (2004a, 2004b); Vapnik et al. (2007), Yudalevich et al. (2014), Eppelbaum and Y. Katz (2015b), Avni et al. (2016, 2017), Baer et al. (2017), Yudalevich and Vapnik (2018), (8) radiometric age of the magmatic rocks (from Lang and Steinitz (1989), Segev (2000), Segev et al. (2005)), (9) counterclockwise (a) and clockwise (b) rotation of the linear structures (faults, dykes and volcanic ridges), (10)-(11) magmatic rocks with normal (10), and reversal (11) paleomagnetic polarity (from Ron and Baer (1988), Gvirtzman et al. (1996), Baer et al. (1995), (12)-(15) paleomagnetic zonation within the magmatic complexes: (12) Illawarra, (13) Omolon, (14) Gissar, (15) Jalal.

Tectonic-geodynamic mapping of the study area was expanded to include other stages of development for the region under study. First, the connection between the deep geodynamics and the development of its structures, basins, and ecosystems in other periods of geological history is fascinating.

3.5 Geodynamics of the Mesozoic Terrane Belt in the Triassic period

For comparison with the Jurassic period of development of the MTB's structures and sedimentary basins of the Gondwana foreland, a Triassic plate-tectonic reconstruction was carried out using a similar methodology (Fig. 7). According to the data of syn-sedimentary paleotectonic analysis (Eppelbaum and Katz, 2011; 2015a, 2015b, 2023; Eppelbaum et al., 2021, 2023a) and paleomagnetic-geodynamic mapping with associated identification of the tectonothermal activity cycles, there is an insignificant contrast of tectonic-magmatic phenomena in the Permian and the Triassic in the Arabian segment of Gondwana. In this regard, the conclusion that the deep mantle structure, which determined this region's rich and very complex geodynamics in the Late Mesozoic and Cenozoic, was still in its infancy looks understandable. The Permian formations in the pericratonic depressions of the described part of Gondwana and within the MTB were very shallow and thin – up to 600-800 m, and igneous formations lie at their base and correspond to the Kiama paleomagnetic hyperzone. The Permian strata are broken through by younger intrusions (Hall et al., 2005). The picture for the Triassic is almost similar; however, during this period, the intensity of the amplitude of the sedimentation tectonics processes increases more than twice compared to the Permian stage. Meanwhile, the contrast of troughs and uplifts is not comparable to the Jurassic period's tectonics. In addition, the intensity of magmatism development was almost not manifested.

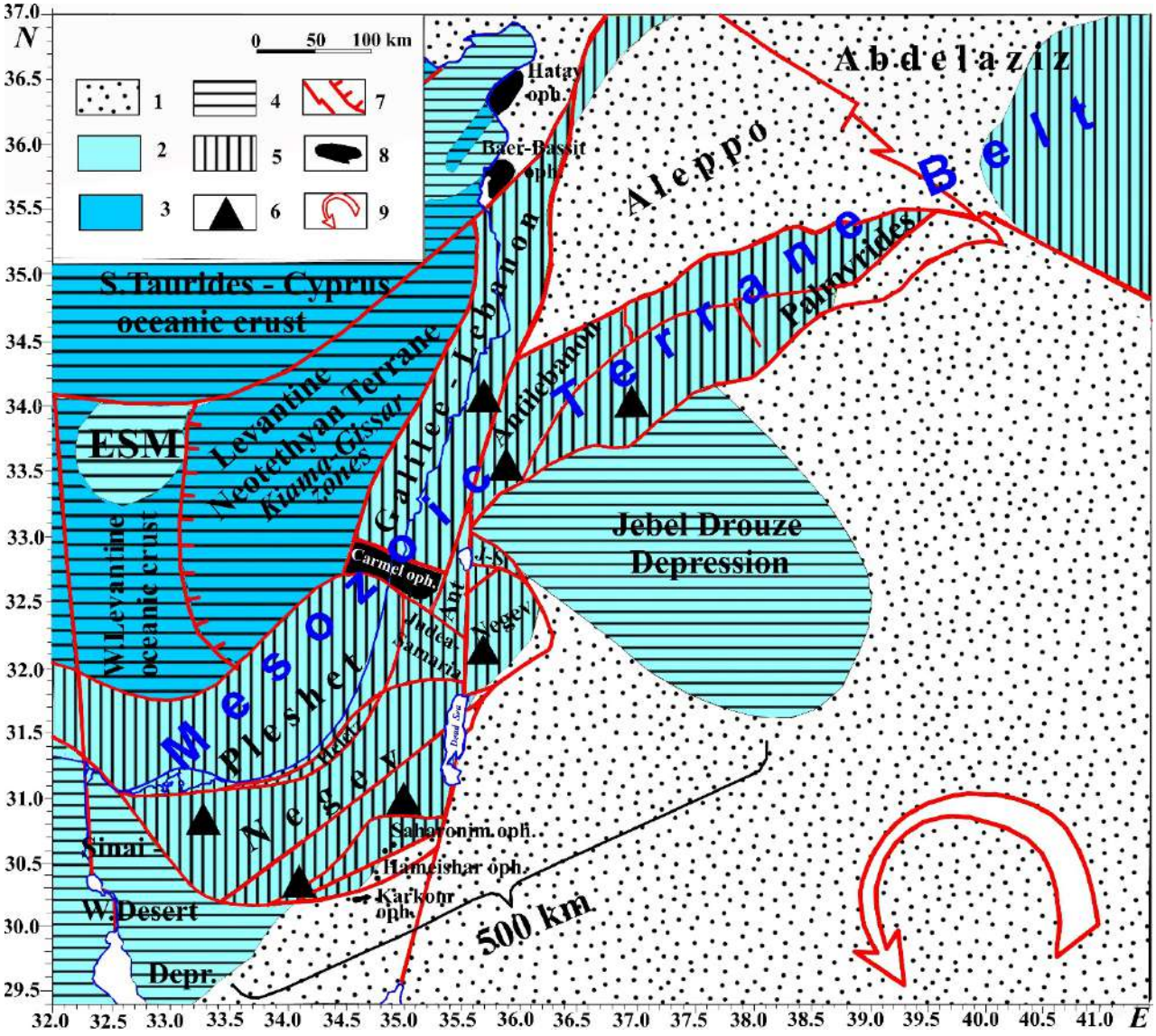

Fig. 6. Geodynamics of the Mesozoic Terrane Belt (MTB) on the accretion stage with the Gondwana-Mediterranean tectonic-paleobiogeographical elements. The following main sources were used for this map development: Feldman, 1987; Hall et al., 2005; Feldman et al., 2014; Eppelbaum and Katz, 2015b, 2023; Eppelbaum et al., 2024.

(1) Jurassic land, (2) Jurassic aquatics with the continental crust' structures, (3) Jurassic aquatics in the structures with oceanic crust, (4) Mediterranean province, (5) Ethiopian province, (6) outcrops of the Ethiopian fauna *Somalirhynchia-Septirhynchia*, (7) faults, (8) ophiolites, (9) MTB counterclockwise rotating. ESM, Eratosthenes Seamount.

Therefore, when constructing a tectonic map of the Triassic period (Fig. 7), we located terrane blocks in almost the same places and with the same orientation as in the Jurassic period reconstruction. The actual data coincided with the mapping data of the syn-sedimentary structures of the MTB and the Gondwana foreland. It is new that the maximum of the belt subsidence (almost up to 2,600 m) is confined to the Galilee-Lebanon terrane near its border in the Neotethys oceanic trough. The second element is the reconstruction of the proposed axis of formation of the deep mantle structure, which is confirmed by the development of ring alkaline intrusions (220 and 229 Ma) in the South Eastern Desert of Nubia (Said, 2017) and almost coeval magmatic manifestations (231 Ma) in the southernmost part of the Negev terrane in the Hameishar borehole in the boundary zone between the terrane and the Sinai uplift of the Neoproterozoic belt (Eppelbaum and Katz, 2015b).

These points of development of Triassic magmatism probably mark the formation of a deep mantle structure, the presumed axial line of which is depicted as a conditional fault with the supposed appearance of the first hot spots. In biogeographical terms, in the Triassic, there was no significant differentiation of data on cephalopods and conodonts of different parts of the Neotethys are very similar (Hirsch, 1997; Le Nindre et al., 2023). Undoubtedly, the marine biocenoses of the Neotethys basin con-

tain a significant number of endemics, among which giant shells of myalinid bivalves, assigned to the new genus **Ramonalina**, were described in the Triassic of the Negev terrane in outcrops of the Makhtesh Ramon basin (Yancey et al., 2009). Significantly, these authors described these large bivalves discovered in reef facies; over the past fifteen years, their remains have not been found anywhere else.

3.6 Paleobiogeographical map of the Maastrichtian basins of the Neotethys Ocean's western part

Of significant interest in paleobiogeography and geodynamics is the analysis of the marginal Neotethys basins in the Late Cretaceous and especially at its end – in the Maastrichtian (Fig. 8). At this time, the ocean basin of both the North and South Atlantic had already opened widely (Zonenshain and Savostin, 1979), the Indian Ocean had expanded significantly (Ali and Krause, 2011), and the Hindustan platform with a colossal area of Maastricht basalt traps approached the northern side of the Neotethys. The extensive Maastrichtian Neotethys shelf was represented by typically Mediterranean biotas, among which the most striking indicators were goblet-shaped bivalves (rudists) homeomorphic to corals, which only occasionally formed biocenoses in the southern margins of the basins of the European province. However, its most crucial paleobiogeographic indicator was the intrashell cephalopods – belemnites (Alizadeh, 1972). Through the Turgai Strait, there was an exchange between the biotas of the European and Boreal-Pacific provinces, which was clearly shown based on the distribution of the brachiopod fauna (Katz, 1986).

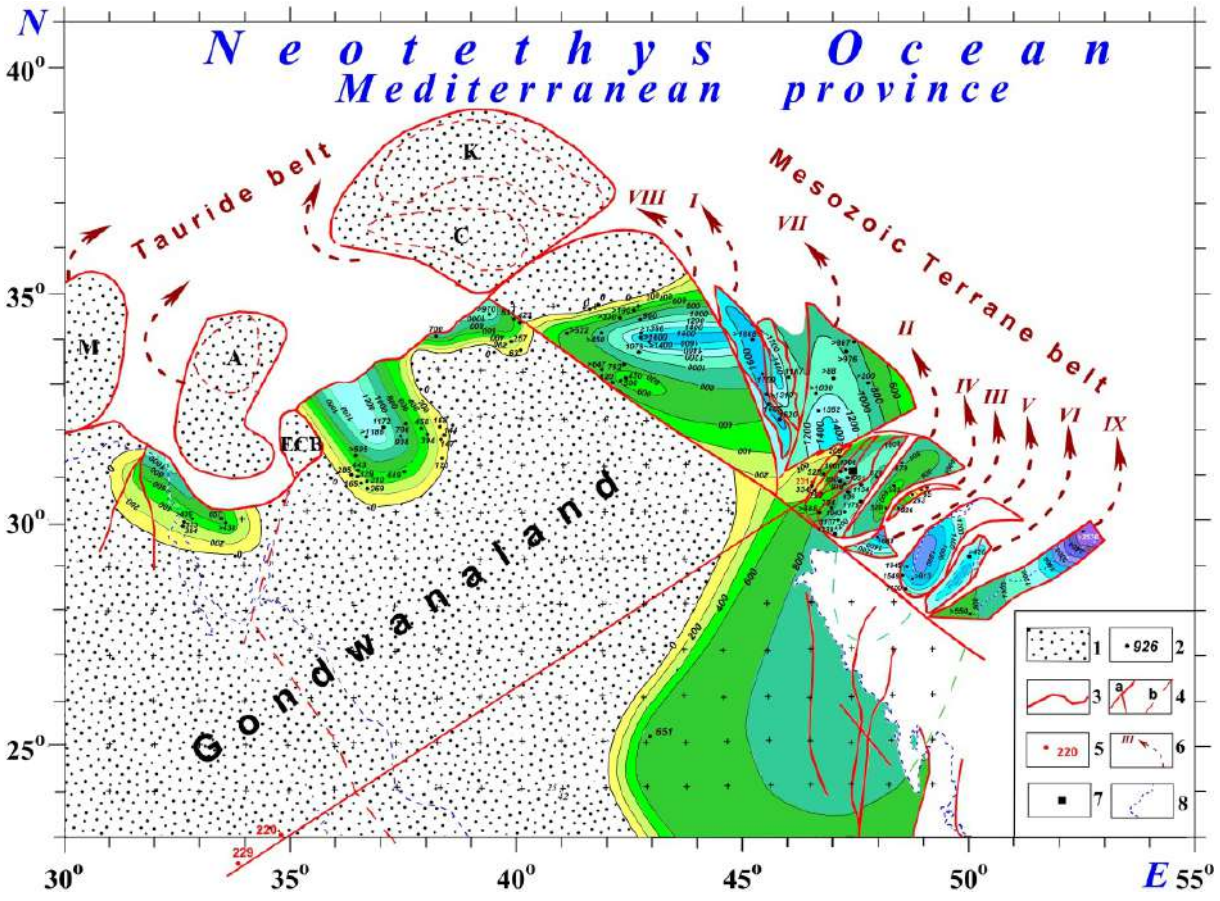

Fig. 7. Geodynamics of the Mesozoic Terrane Belt (MTB) in the Triassic period with the elements of Gondwana-Neotethys tectonic and paleobiogeographical elements. The following main sources were used for this map development: Al-Husseini, 2000; Hall et al., 2005; Krasheninnikov et al., 2005; Yancey et al., 2009; Eppelbaum and Katz, 2015b; Said, 2017.

(1) land of the Gondwana and MTB, (2) boreholes and outcrops with thickness of Triassic sediment thicknesses, (3) boundary of the Gondwana and MTB blocks, 4(**a**, **b**): **a**: syn-sedimentary Triassic and Jurassic faults, **b**: postcollisional faults, (5) boreholes and outcrops with radiometric dating of the Triassic magmatic rocks, (6) counterclockwise rotating of the MTB concerning to the Jurassic – Early Cretaceous collision system (the Roman numbers designate the conjunction order with the western Arabian part of Gondwana), (7) outcrop of the endemic bivalvia *Ramonalina* in the MTB, (8) modern land-sea boundaries.

ECB, Eratosthenes continental block. Precambrian massifs in the Tauride belt terranes: A – Alanya, C – Central Tauride, K – Kirsehir, M – Menderes.

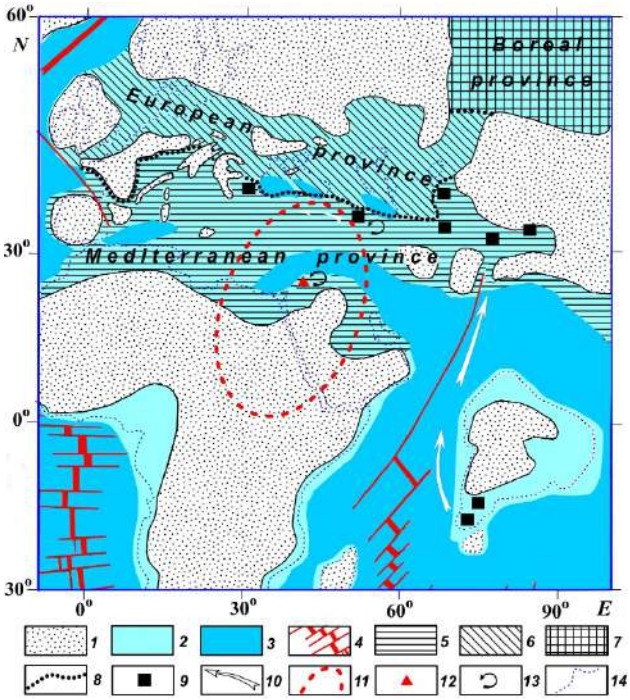

Fig. 8. Paleobiogeographic map of the Maastrichtian basins of the Neotethys Ocean's western part and the adjacent shelf seas of Eurasia and Gondwana with the elements of deep geodynamics. The following main sources were used for this map development: Tzankov, 1930; Katz, 1962; Makridin and Katz, 1966; **Zonenshain and Savostin, 1979;** Alizadeh et al., 1983; Gasanov, 1986; Nur et al., 1989; Golonka, 2004; Khalafly, 2006; Adamia et al., 2011; Ali and Krause, 2011; Alizadeh et al., 2016; Eppelbaum et al., 2023a.

(1) land, (2) areas of shelf seas of continental margins and intra-oceanic rises, (3) intra-oceanic troughs and rises with the oceanic crust, (4) oceanic rift zones, (5-7) paleobiogeographic provinces: (5) Mediterranean, (6) European, (7) Boreal, (8) boundaries between provinces, (9) outcrops of the giant Tethyan brachiopods *Praeneothyris spp*., (10) directions of migration of *Praeneothyris* within the Neotethys basins, (11) boundaries of the outlines of the suboval deep mantle structure, (12) Mt. Carmel (northern Israel) geodynamic block in the apical part of the deep mantle structure, (13) identified paleomagnetic counterclockwise rotation zones of the Levant (Mt. Carmel) and the Lesser Caucasus (Garabakh, Azerbaijan) regions, (14) outline of the modern boundaries of land and sea and the intracontinental margins of discordant zones of continental platforms.

4. Discussion

The distant migration of paleontological species (see previous section) makes us turn to the interaction of biotas emerging in the Cretaceous period in the Indian and Southern Oceans with more northern biotas of the Mesozoic Neotethys Ocean. Bulgarian paleontologists discovered shells of the giant Maastrichtian brachiopods (e.g., Tzankov, 1930) on its northern side, like modern inhabitants of the southern (Notal) biogeographical province. In South India, in the same Maastrichtian deposits, paleontological forms very similar to them were identified. Special studies in Central Asia at the turn of the 50-60s revealed the widespread development in this region of the described southern migrants from the opening Indian Ocean basin, assigned to the new genus *Praeneothyris* (Katz, 1962). However, findings identified for these southern migrants are extended in a submeridional direction from Hindustan to Central Asia. A biogeographic hiatus existed between this range and a scattered locality in Bulgaria. It was filled more than 20 years later (Alizadeh et al., 1983) when an extensive complex of organisms was discovered and studied in the Lesser Caucasus, including a unique composition of biotas of the Mediterranean, European type (Alizadeh, 1972), along with those migrating from the south migrants *Praeneothyris*.

The biogeographical paradox of mixing various biotas in the Lesser Caucasus requires an explanation from the standpoint of paleogeography and plate geodynamics. First, the Lesser Caucasus is in the narrowest place of the collisional Alpine belt between the Eurasian and Arabian plates, where the processes of collision of the Neotethys Ocean are most active. In addition, the zone of the oceanic trench at the intersection of the end of the Neotethys and the Indian Ocean rift comes closest here. The third geodynamic factor is the location of the Lesser Caucasus near the most active northern end of the deep mantle uplift, which rotated counterclockwise. The apical part of this uplift was located near the modern horst of Mt. Carmel (Israel). A system of ring concentric faults complicates the structure of the mentioned horst and, according to paleomagnetic data (Ron et al., 1984; Nur et al., 1989), rotates in a counterclockwise direction. The modern GPS data (Reilinger et al., 2006; Le Pichon and Kreemer, 2010) show that these movements, developed in the Aegean-Anatolian lithospheric plate, are geodynamic most intense in the northern zone.

Paleomagnetic data for the Upper Cretaceous of the Azerbaijani part of the Lesser Caucasus (e.g., Khalafly, 2006) indicate that this area experienced counterclockwise rotation, which contributed to the further migration of ecosystems and biocenoses of the Lesser Caucasus to the west. The mixed nature of the Maastrichtian biotas of the Lesser Caucasus is because to the east of it, like the modern geodynamic situation (based on analysis of GPS data (e.g., Reilinger et al., 2006; Kadirov et al., 2013)) in the meridional zone between the Pontus and the Caspian, there is a divergence in rotation directions (Eppelbaum et al., 2021, 2024). A similar picture is observed in the Maastrichtian age when the belemnites and brachiopod fauna moved from the nearest basins of the European province of Transcaucasia to the Mediterranean Basin of the Lesser Caucasus. At the same time, the Indian Ocean brachiopods *Preneothyris* at the larval stage experience migration diverging near the marginal part of the projection of

the deep mantle structure slope both counterclockwise and clockwise (Fig. 8).

This study attempts to explain the paleobiogeography of the Mesozoic Neotethys Ocean based on a combination of methods of structural-geological analysis and geophysical surveys using data from satellite technologies and advanced modeling. Based on the synthesis of paleobiogeography and tectonophysical studies, we have proposed a new methodology for complex dynamic cartography. It significantly expands the boundaries of the previous plate tectonics and allows us to identify new branches of geodynamics. This is primarily: (1) analysis of tectonothermal processes in the zone of development of local deep mantle structures, (2) geodynamics of surface (crustal and crust-mantle) terrane belts, ophiolite plates, mantle diapirs, and trap complexes, (3) geodynamics of shear zones, transform rotation structures and ring tectonic-magmatic structures. In addition, it is planned to develop new methods of paleomagnetic mapping using palinspastic reconstructions, cyclic analysis of trap complexes and facies heterogeneities determined by deep geodynamics and the completeness of the section of sedimentary strata as elements of hydrosphere disturbances.

In our work, we showed the relationship between the biogeographical phenomena of the Neotethys Ocean ecosystems and its geodynamic evolution – from initial spreading to the widespread development of collision processes towards the end of the Mesozoic era (Gasanov, 1986; Adamia et al., 2011). These relationships, along with other factors, made it possible to explain the phenomenon of biogeographical heterogeneity of the Maastrichtian faunas of the Garabakh region (western Azerbaijan), where associations of three paleobiogeographical provinces were paradoxically combined: Mediterranean, European, and Indian. Tectono-geodynamic mapping made it possible to elucidate the evolution of the deep mantle structure for the first time. The biogeographical allochthonous nature of the Mesozoic Terrane Belt, containing the *Somalirhynchia-Septirhynchia* fauna and the Levantine oceanic terrane, including the Kiama and Illawarra-Gissar paleomagnetic zones, was finally proven.

However, the most important conclusion is the significant paleobiogeographic differentiation of the Jurassic and Cretaceous ecosystems of the northern and southern sides of the Neotethys (see Figs. 3, 4, and 8), which allows us to draw a meaningful conclusion about the time when the influence of the deep structure on the near-surface blocks of the Earth's crust began. According to our estimates, this time can be 160-180 Ma.

Conclusions

The most significant research results boil down to the following conclusions.

(1) A new methodology for combined dynamic cartography is proposed based on synthesizing tectonic-geodynamic characteristics with paleomagnetic mapping, palinspastic reconstructions, and consolidated structural analysis.

(2) The age of activation of the influence of the deep mantle structure on the near-surface (surface) tectonic-structural elements of the studied region was estimated.

(3) The connection between the biogeographical phenomena of the Neotethys Ocean ecosystems and its geodynamic evolution is shown, starting from initial spreading to the widespread development of collision processes towards the end of the Mesozoic era.

(4) The biogeographical heterogeneity of the Maastrichtian faunas of the Garabakh region of Azerbaijan is explained.

Acknowledgment

The formulation of very unconventional research between the migration-ecosystem (biogeographic) and deep-geodynamic processes became possible only thanks to multidisciplinary research conducted over many decades by specialists from various fields of knowledge as part of fundamental projects set up and implemented by Professor Academician Akif Agamekhti Alizadeh. We consider him our teacher and, therefore, tried to explain several biogeographical paradoxes identified during his research from the standpoint of tectonophysics. Naturally, it is a great honor for us to dedicate this work to his 90th anniversary.

The authors would like to thank two anonymous reviewers who thoroughly reviewed the manuscript and provided valuable suggestions that helped us to prepare this paper.

REFERENCES

Abdulkasumzadeh M.P. Upper Jurassic of the Lesser Caucasus within the Azerbaijan Republic. Elm. Baku, 1988,184 p. (in Russian).

Adamia S., Zakariadze G., Chkhotva T., Sadradze N., Tsereteli N., Chabukiani A., Gventsadze A. Geology of the Caucasus: A Review. Turkish Journal of Earth Sciences, Vol. 20, No. 5, 2011, pp. 489-544.

ЛИТЕРАТУРА

Adamia S., Zakariadze G., Chkhotva T., Sadradze N., Tsereteli N., Chabukiani A., Gventsadze A. Geology of the Caucasus: A Review. Turkish Journal of Earth Sciences, Vol. 20, No. 5, 2011, pp. 489-544.

Al-Husseini M.I. Origin of the Arabian Plate structures: Amar Collision and Najd Rift. Geo-Arabia, Vol. 5, No. 4, 2000, pp. 527-542.

Al-Husseini M.I. Origin of the Arabian Plate structures: Amar Collision and Najd Rift. Geo-Arabia, Vol. 5, No. 4, 2000, pp. 527-542.

Ali J.R., Krause D.W. Late Cretaceous bioconnections between Indo-Madagascar and Antarctica: refutation of the Gunnerus Ridge causeway hypothesis. Journal of Biogeography, Vol. 38, 2011, pp.1855-1872.

Alizadeh A.A. Cretaceous Belemnites of Azerbaijan. Nedra. Moscow, 1972, 280 p. (in Russian).

Alizadeh A.A., Aliyev S.A., Katz Y.I., Gamzayev G.A., Mamedzade A.M. New data on the presence of the Danian stage between the Khacinchai and Terterchai rivers (Lesser Caucasus). Reports of Acad. Sci. Azerb., Vol. 39, No. 1, 1983, 49-51 (in Russian).

Alizadeh A.A., Guliyev I.S., Kadirov F.A., Eppelbaum L.V. Geosciences in Azerbaijan. Vol. 1. Geology. Springer. Heidelberg, N.Y., 2016, 239 p.

Alizadeh A.A., Guliyev I.S., Mamedov P.Z., Aliyeva E.G.-M., Feyzullayev A.A., Huseynov D.A., Eppelbaum L.V. Pliocene hydrocarbon sedimentary series of Azerbaijan. Springer. Heidelberg – N.Y., 2024, 514 p.

Arkell W.J. Jurassic geology of the world. Olivier and Boyd. London, 1956, 808 p.

Askerov R.B. The Upper Jurassic brachiopods of the Azerbaijan part of the Lesser Caucasus and their stratigraphic significance. PhD Thesis, Baku, Inst. of Geology of the Acad. Sci. of Azerbaijan, 1965, 18 p. (in Russian).

Avni Y. Har Loz, Sheet 21-III. Geological Map of Israel 1:50,000. Geol. Survey of Israel. Jerusalem, 2001.

Avni Y., Bartov Y., Shen A. Har Ardon, Sheet 22-I. Geological map of Israel 1:50,000. Geol. survey of Israel, Jerusalem, 2016.

Avni Y., Beker A., Zilberman E. Be'erot Oded, Sheet 21-IV. Geological map of Israel 1:50,000. Geol. Survey of Israel, Jerusalem, 2017.

Baer G. Flow directions in sills and dikes and formation of cauldrons in eastern Makhtesh Ramon. Israel Jour. of Earth Sci., Vol. 42, 1993, pp. 133-148.

Baer G., Heimann A., Eshet Y., Weinberger R., Mussett A., Sherwood G., The Saharonim basalt: A Late Triassic – Early Jurassic intrusion in southeastern Makhtesh Ramon, Israel. Israel Jour. of Earth Sci., Vol. 44, 1995, pp. 1-10.

Baer G. and Reches Z. Mechanics of emplacement and tectonic implications of the Ramon dike systems, Israel. Jour. of Geophysical Research, Vol. 96(B7), 1991, pp.11895-11910.

Baer Y., Soudry D., Bar O., Shen A. Zofar. Sheet 22-III, IV. Geological Map of Israel 1:50,000, Geol. Survey of Israel, Jerusalem. 2017.

Barczyk W. Some representatives of the family Pygopidae (Brachiopoda) from the Tithonian of the Pieniny Klippen Belt. Acta Geologica Polonica, Vol. 22, 1972, pp. 507-513.

Ben-Avraham Z. and Ginzburg A. Displaced terranes and crustal evolution of the Levant and the eastern Mediterranean. Tectonics, Vol. 9, 1990, pp. 613-622.

Ben-Avraham Z., Ginzburg A., Makris J., Eppelbaum L. Crustal structure of the Levant basin, eastern Mediterranean. Tectonophysics, Vol. 346, 2002, pp. 23-43.

Ben-Avraham Z., Schattner U., Lazar M., Hall J.K., Ben-Gai Y., Neev D., Reshef M. Segmentation of the Levant continental margin, eastern Mediterranean. Tectonics, TC5002, Vol. 25, 2006, pp. 1-17.

Benzaggagh M. and Atrops F. Stratigraphy and ammonite fauna association of the Kimmeridgian, Tithonian and Berriasian basal areas in the Internal Prerif (Rif, Morocco). Newsletters on Stratigraphy, Vol. 35 (3), 1997, pp. 127-163 (in French).

Bordenave M.L. The origin of the Permo-Triassic gas accumulations in the Iranian Zagros foldbelt and contiguous offshore areas: a review of the Paleozoic petroleum system. Jour. of Petroleum Geology, Vol. 31, No. 1, 2008, pp. 3-42.

Ali J.R., Krause D.W. Late Cretaceous bioconnections between Indo-Madagascar and Antarctica: refutation of the Gunnerus Ridge causeway hypothesis. Journal of Biogeography, Vol. 38, 2011, pp.1855-1872.

Alizadeh A.A., Guliyev I.S., Kadirov F.A., Eppelbaum L.V. Geosciences in Azerbaijan. Vol. 1. Geology. Springer. Heidelberg, N.Y., 2016, 239 p.

Alizadeh A.A., Guliyev I.S., Mamedov P.Z., Aliyeva E.G.-M., Feyzullayev A.A., Huseynov D.A., Eppelbaum L.V. Pliocene hydrocarbon sedimentary series of Azerbaijan. Springer. Heidelberg – N.Y., 2024, 514 p.

Arkell W.J. Jurassic geology of the world. Olivier and Boyd. London, 1956, 808 p.

Avni Y. Har Loz, Sheet 21-III. Geological Map of Israel 1:50,000. Geol. Survey of Israel. Jerusalem, 2001.

Avni Y., Bartov Y., Shen A. Har Ardon, Sheet 22-I. Geological map of Israel 1:50,000. Geol. survey of Israel, Jerusalem, 2016.

Avni Y., Beker A., Zilberman E. Be'erot Oded, Sheet 21-IV. Geological map of Israel 1:50,000. Geol. Survey of Israel, Jerusalem, 2017.

Baer G. Flow directions in sills and dikes and formation of cauldrons in eastern Makhtesh Ramon. Israel Jour. of Earth Sci., Vol. 42, 1993, pp. 133-148.

Baer G., Heimann A., Eshet Y., Weinberger R., Mussett A., Sherwood G., The Saharonim basalt: A Late Triassic – Early Jurassic intrusion in southeastern Makhtesh Ramon, Israel. Israel Jour. of Earth Sci., Vol. 44, 1995, pp. 1-10.

Baer G. and Reches Z. Mechanics of emplacement and tectonic implications of the Ramon dike systems, Israel. Jour. of Geophysical Research, Vol. 96(B7), 1991, pp.11895-11910.

Baer Y., Soudry D., Bar O., Shen A. Zofar. Sheet 22-III, IV. Geological Map of Israel 1:50,000, Geol. Survey of Israel, Jerusalem. 2017.

Barczyk W. Some representatives of the family Pygopidae (Brachiopoda) from the Tithonian of the Pieniny Klippen Belt. Acta Geologica Polonica, Vol. 22, 1972, pp. 507-513.

Ben-Avraham Z. and Ginzburg A. Displaced terranes and crustal evolution of the Levant and the eastern Mediterranean. Tectonics, Vol. 9, 1990, pp. 613-622.

Ben-Avraham Z., Ginzburg A., Makris J., Eppelbaum L. Crustal structure of the Levant basin, eastern Mediterranean. Tectonophysics, Vol. 346, 2002, pp. 23-43.

Ben-Avraham Z., Schattner U., Lazar M., Hall J.K., Ben-Gai Y., Neev D., Reshef M. Segmentation of the Levant continental margin, eastern Mediterranean. Tectonics, TC5002, Vol. 25, 2006, pp. 1-17.

Bordenave M.L. The origin of the Permo-Triassic gas accumulations in the Iranian Zagros foldbelt and contiguous offshore areas: a review of the Paleozoic petroleum system. Jour. of Petroleum Geology, Vol. 31, No. 1, 2008, pp. 3-42.

Bosworth W., Huchon P., McClay K. The Red Sea and Gulf of Aden basins. Jour. of African Earth Sci., Vol. 43, 2005, pp. 334-378.

Bujtor L., Albrecht R., Maróti D., Miklósy A. Lower Tithonian and Lower Berriasian brachiopods from the Márévár Limestone Formation, Zengővárkony (Mecsek Mountains Hungary), and remarks on their palaeoenvironment. Paläontologische Zeitschrift, Vol. 95, 2020, pp. 85-95.

Channell J.E.T., Tüysüz O., Bektas O., Sengör A.M.C. Jurassic-Cretaceous paleomagnetism of the Pontides (Turkey). Tectonics, Vol. 15, 1996, pp. 201-212.

Cooper G.A. Jurassic Brachiopods of Saudi Arabia. Smithsonian Contributions to Paleobiology. Vol. 65, 1989, 213 p.

Cope J.C.W., Ingham J.K., Rawson P.F. (eds.). Atlas of Palaeogeography and Lithofacies. Geological Society Memoir, London, No. 13, 1992.

Bosworth W., Huchon P., McClay K. The Red Sea and Gulf of Aden basins. Jour. of African Earth Sci., Vol. 43, 2005, pp. 334-378.

Bujtor L., Albrecht R., Maróti D., Miklósy A. Lower Tithonian and Lower Berriasian brachiopods from the Márévár Limestone Formation, Zengővárkony (Mecsek Mountains Hungary), and remarks on their palaeoenvironment. Paläontologische Zeitschrift, Vol. 95, 2020, pp. 85-95.

Channell J.E.T., Tüysüz O., Bektas O., Sengör A.M.C. Jurassic-Cretaceous paleomagnetism of the Pontides (Turkey). Tectonics, Vol. 15, 1996, pp. 201-212.

Chumakov I.S. Pliocene and Pleistocene deposits of the Nile Valley in Nubia and Upper Egypt. Trans. of the Geol. Inst., Russ. Acad. of Sci., Vol. 170, Nauka. Moscow, 1967, 119 p. (in Russian).

Cooper G.A. Jurassic Brachiopods of Saudi Arabia. Smithsonian Contributions to Paleobiology. Vol. 65, 1989, 213 p.

Cope J.C.W., Ingham J.K., Rawson P.F. (eds.). Atlas of Palaeogeography and Lithofacies. Geological Society Memoir, London, No. 13, 1992.

Dercourt J., Gaetani M., Vrielinck B., Barrier E., Biju-Duval B., Brunet V.F., Cadet J.P., Crasquin S., Sandylescu M. (eds). Peri-Tethys Paleogeographical Atlas. CCGM/CGMW, Paris, 2000.

Dibni I. and Middlemiss F.A. Pygopid brachiopods from the Venetian Alps. Boll. della Societa Paleontologica Italiana, Vol. 20, 1981, pp. 19-48.

Dixon J.E. and Robertson A.H.F. (eds.). The Geological evolution of the Eastern Mediterranean. Geol. Soc. Spec. Publ., No. 17, Bl. Publ. Oxford, UK, 1984, 832 p.

Énay R., Hantzpergue P., Soussi M., Mangold C. The Kimmeridgian-Tithonian boundary and the age of the formations of the Upper Jurassic of the Tunisian Ridge, comparisons with Algeria and Sicily. Géobios, Vol. 38, 2005, pp. 437-450 (in French).

Eppelbaum L.V., Ben-Avraham Z., Katz Y., Cloetingh S., Kaban M. Giant quasi-ring mantle structure in the African-Arabian junction: Results derived from the geological-geophysical data integration. Geotectonics (Springer), Vol. 55, No. 1, 2021, pp. 67-93.

Eppelbaum L. and Katz Y. Tectonic-geophysical mapping of Israel and Eastern Mediterranean: implication for hydrocarbon prospecting. Positioning, Vol. 2, No. 1, 2011, pp. 36-54.

Eppelbaum L.V. and Katz Y.I. Mineral deposits in Israel: a contemporary view. In: Israel: Social, Economic and Political Developments (Ya'ari A., Zahavi E.D. eds.), Nova Science Publishers. N.Y., USA, 2012, pp. 1-41.

Eppelbaum L.V. and Katz Yu.I. Newly developed paleomagnetic map of the Easternmost Mediterranean Unmasks geodynamic history of this region. Central European Jour. of Geosciences (Open Geosciences), Vol. 7, No. 1, 2015a, pp. 95-117.

Eppelbaum L.V. and Katz Yu.I. Eastern Mediterranean: combined geological-geophysical zonation and paleogeodynamics of the Mesozoic and Cenozoic structural-sedimentation stages. Marine and Petroleum Geology, Vol. 65, 2015b, pp. 198-216.

Eppelbaum L.V. and Katz Yu.I. A New regard on the tectonic map of the Arabian-African Region inferred from the satellite gravity analysis. Acta Geophysica, Vol. 65, 2017, pp. 607-626.

Eppelbaum L. and Katz Yu. Significant tectonic-geophysical features of the African-Arabian tectonic region: An overview. Geotectonics (Springer), Vol. 54, No. 2, 2020, pp. 266-283.

Eppelbaum L. and KatzYu. Akchagylian hydrospheric phenomenon in aspects of deep geodynamics. Stratigraphy and Sedimentation of Oil-Gas Basins, No. 2, 2021a, pp. 8-26.

Eppelbaum L.V. and Katz Yu.I. Deep tectono-geodynamic aspects of development of the Nubian-Arabian Region. In: Dercourt J., Gaetani M., Vrielinck B., Barrier E., Biju-Duval B., Brunet V.F., Cadet J.P., Crasquin S., Sandylescu M. (eds). Peri-Tethys Paleogeographical Atlas. CCGM/CGMW, Paris, 2000.

Dibni I. and Middlemiss F.A. Pygopid brachiopods from the Venetian Alps. Boll. della Societa Paleontologica Italiana, Vol. 20, 1981, pp. 19-48.

Dixon J.E. and Robertson A.H.F. (eds.). The Geological evolution of the Eastern Mediterranean. Geol. Soc. Spec. Publ., No. 17, Bl. Publ. Oxford, UK, 1984, 832 p.

Eppelbaum L.V., Ben-Avraham Z., Katz Y., Cloetingh S., Kaban M. Giant quasi-ring mantle structure in the African-Arabian junction: Results derived from the geological-geophysical data integration. Geotectonics (Springer), Vol. 55, No. 1, 2021, pp. 67-93.

Eppelbaum L. and Katz Y. Tectonic-geophysical mapping of Israel and Eastern Mediterranean: implication for hydrocarbon prospecting. Positioning, Vol. 2, No. 1, 2011, pp. 36-54.

Eppelbaum L.V. and Katz Y.I. Mineral deposits in Israel: a contemporary view. In: Israel: Social, Economic and Political Developments (Ya'ari A., Zahavi E.D. eds.), Nova Science Publishers. N.Y., USA, 2012, pp. 1-41.

Eppelbaum L.V. and Katz Yu.I. Newly developed paleomagnetic map of the Easternmost Mediterranean Unmasks geodynamic history of this region. Central European Jour. of Geosciences (Open Geosciences), Vol. 7, No. 1, 2015a, pp. 95-117.

Eppelbaum L.V. and Katz Yu.I. Eastern Mediterranean: combined geological-geophysical zonation and paleogeodynamics of the Mesozoic and Cenozoic structural-sedimentation stages. Marine and Petroleum Geology, Vol. 65, 2015b, pp. 198-216.

Eppelbaum L.V. and Katz Yu.I. A New regard on the tectonic map of the Arabian-African Region inferred from the satellite gravity analysis. Acta Geophysica, Vol. 65, 2017, pp. 607-626.

Eppelbaum L. and Katz Yu. Significant tectonic-geophysical features of the African-Arabian tectonic region: An overview. Geotectonics (Springer), Vol. 54, No. 2, 2020, pp. 266-283.

Eppelbaum L. and KatzYu. Akchagylian hydrospheric phenomenon in aspects of deep geodynamics. Stratigraphy and Sedimentation of Oil-Gas Basins, No. 2, 2021a, pp. 8-26.

Eppelbaum L.V. and Katz Yu.I. Deep tectono-geodynamic aspects of development of the Nubian-Arabian Region. In: The Arabian Seas biodiversity, environment challenges and conservation measures (Jawad L., ed.), Springer. 2021b, pp. 199-237.

Eppelbaum L.V. and Katz Y.I. Paleomagnetic-geodynamic mapping of the transition zone from ocean to the continent: A review. Applied Sciences, Vol. 12, Spec. Issue: Advances in Applied Geophysics, 2022, pp. 1-20.

Eppelbaum L.V. and Katz Y.I. Where were the initial sources of the allochthonous oceanic crust of the southern Easternmost Mediterranean formed? Trans. of the Intern. Conf. "Mediterranean Geosciences Union 2023", Springer. Istanbul, Turkey, 2023, pp. 1-7.

Eppelbaum L.V. and Katz Yu.I. African-Levantine areal of ancient Hominin Dispersal: a new look, derived from comprehensive geological-geophysical integration. In: Emerging issues in environment, geography and earth science (Yousef A.F., ed.), Vol. 7, BP International, London, 2024, pp. 151-222.

Eppelbaum L.V., Katz Y.I., Ben-Avraham Z. Geodynamic aspects of magnetic data analysis and tectonic-paleomagnetic mapping in the Easternmost Mediterranean: A review. Applied Sciences, Spec. Issue "Ground-Based Geomagnetic Observations: Techniques, Instruments and Scientific Outcomes", 13, No. 18, 2023a, pp. 1-44.

The Arabian Seas biodiversity, environment challenges and conservation measures (Jawad L., ed.), Springer. 2021b, pp. 199-237.

Eppelbaum L.V. and Katz Y.I. Paleomagnetic-geodynamic mapping of the transition zone from ocean to the continent: A review. Applied Sciences, Vol. 12, Spec. Issue: Advances in Applied Geophysics, 2022, pp. 1-20.

Eppelbaum L.V. and Katz Y.I. Where were the initial sources of the allochthonous oceanic crust of the southern Easternmost Mediterranean formed? Trans. of the Intern. Conf. "Mediterranean Geosciences Union 2023", Springer. Istanbul, Turkey, 2023, pp. 1-7.

Eppelbaum L.V. and Katz Yu.I. African-Levantine areal of ancient Hominin Dispersal: a new look, derived from comprehensive geological-geophysical integration. In: Emerging issues in environment, geography and earth science (Yousef A.F., ed.), Vol. 7, BP International, London, 2024, pp. 151-222.

Eppelbaum L.V., Katz Y.I., Ben-Avraham Z. Geodynamic aspects of magnetic data analysis and tectonic-paleomagnetic mapping in the Easternmost Mediterranean: A review. Applied Sciences, Spec. Issue "Ground-Based Geomagnetic Observations: Techniques, Instruments and Scientific Outcomes", 13, No. 18, 2023a, pp. 1-44.

Eppelbaum L.V., Katz Y.I., Kadirov F.A., Ben-Avraham Z. The enormous Earth's crust tension and hydrocarbon pipeline exploration in the South Caucasus – Eastern Mediterranean. ANAS Transactions, Earth Sciences, No. 3, 2023b, pp. 80-85.

Eppelbaum L.V., Katz Y.I., Ben-Avraham Z. The reasons for enormous accumulation of the geodynamic tension in Eastern Turkey: a multidisciplinary study. Geology Geophysics and Earth Science, Vol. 2, No. 2, 2024, pp. 1-28.

Eppelbaum L., Katz Yu., Klokochnik J., Kosteletsky J., Zheludev V., Ben-Avraham Z. Tectonic insights into the Arabian-African Region inferred from a comprehensive examination of satellite gravity big data. Global and Planetary Change, Vol. 171, 2018, pp. 65-87.

Eppelbaum L.V. and Khesin B.E. Geophysical studies in the Caucasus. Springer. Heidelberg – N.Y., 2012, 411 p.

Eppelbaum L.V., Nikolaev A.V., Katz Y.I. Space location of the Kiama paleomagnetic hyperzone of inverse polarity 179 in the crust of the eastern Mediterranean. Doklady Earth Sciences (Springer), Vol. 457, No. 6, 2014, pp. 710-714.

Faccenna C., Becker T.W., Auer L., Billi A., Boschi L., Brun J.P., Capitanio F.A., Funiciello F., Horvàth F., Jolivet L., Piromallo C., Royden L., Rossetti F., Serpelloni E. Mantle dynamics in the Mediterranean. Review of Geophysics, Vol. 52, 2014, pp. 283-332.

Feldman H.R. A new species of the Jurassic (Callovian) Brachiopod Septirhynchia from the Northern Sinai. Journal of Paleontology, Vol. 61, No. 6, 1987, pp. 1156-1172.

Feldman H.R., Schemm-Gregory M., Ahmad F., Wilson M.A. A Jurassic (Bathonian-Callovian) *Daghanirhynchia* brachiopod fauna from Jordan. Geologica Acta, Vol.12, No. 1, 2014, pp.1-18.

Garfunkel Z. and Katz A. New magmatic features in Makhtesh Ramon, southern Israel. Geological Magazine, Vol. 104, No. 6, 1967, pp. 608-629.

Gamkrelidze I. Geodynamic evolution of the Caucasus and adjacent areas in Alpine time. Tectonophysics, Vol. 127, Nos. 3-4, 1986, pp. 261-277.

Gasanov T. The history of development of the Sevan-Akera ophiolite zone of the Lesser Caucasus. Geotectonics, No. 2, 1986, pp. 92-104 (in Russian).

Golonka J. Plate tectonic evolution of the southern margin of Eurasia in Mesozoic and Cenozoic. Tectonophysics, Vol. 381, 2004, pp. 233-273.

Eppelbaum L.V., Katz Y.I., Kadirov F.A., Ben-Avraham Z. The enormous Earth's crust tension and hydrocarbon pipeline exploration in the South Caucasus – Eastern Mediterranean. ANAS Transactions, Earth Sciences, No. 3, 2023b, pp. 80-85.

Eppelbaum L.V., Katz Y.I., Ben-Avraham Z. The reasons for enormous accumulation of the geodynamic tension in Eastern Turkey: a multidisciplinary study. Geology Geophysics and Earth Science, Vol. 2, No. 2, 2024, pp. 1-28.

Eppelbaum L., Katz Yu., Klokochnik J., Kosteletsky J., Zheludev V., Ben-Avraham Z. Tectonic insights into the Arabian-African Region inferred from a comprehensive examination of satellite gravity big data. Global and Planetary Change, Vol. 171, 2018, pp. 65-87.

Eppelbaum L.V. and Khesin B.E. Geophysical studies in the Caucasus. Springer. Heidelberg – N.Y., 2012, 411 p.

Eppelbaum L.V., Nikolaev A.V., Katz Y.I. Space location of the Kiama paleomagnetic hyperzone of inverse polarity 179 in the crust of the eastern Mediterranean. Doklady Earth Sciences (Springer), Vol. 457, No. 6, 2014, pp. 710-714.

Faccenna C., Becker T.W., Auer L., Billi A., Boschi L., Brun J.P., Capitanio F.A., Funiciello F., Horvàth F., Jolivet L., Piromallo C., Royden L., Rossetti F., Serpelloni E. Mantle dynamics in the Mediterranean. Review of Geophysics, Vol. 52, 2014, pp. 283-332.

Feldman H.R. A new species of the Jurassic (Callovian) Brachiopod Septirhynchia from the Northern Sinai. Journal of Paleontology, Vol. 61, No. 6, 1987, pp. 1156-1172.

Feldman H.R., Schemm-Gregory M., Ahmad F., Wilson M.A. A Jurassic (Bathonian-Callovian) *Daghanirhynchia* brachiopod fauna from Jordan. Geologica Acta, Vol.12, No. 1, 2014, pp.1-18.

Garfunkel Z. and Katz A. New magmatic features in Makhtesh Ramon, southern Israel. Geological Magazine, Vol. 104, No. 6, 1967, pp. 608-629.

Gamkrelidze I. Geodynamic evolution of the Caucasus and adjacent areas in Alpine time. Tectonophysics, Vol. 127, Nos. 3-4, 1986, pp. 261-277.

Golonka J. Plate tectonic evolution of the southern margin of Eurasia in Mesozoic and Cenozoic. Tectonophysics, Vol. 381, 2004, pp. 233-273.

Golonka J. and Ford D. Pangean (Late Carboniferous – Middle Jurassic) paleoenvironment and lithofacies. Palaeogeography, Paleoclimatology, Paleoecology, Vol. 161, 2000, pp. 1-34.

Gvirtzman G., Weissbrod T., Baer G., Brenner J. The age of Aptian stage and its magmatic events: New Ar-Ar ages and paleomagnetic data from the Negev, Israel. Cretaceous Research, Vol. 17, 1996, pp. 293-310.

Hall J.K., Krasheninnikov V.A., Hirsch F., Benjamini C., Flexer A. Geological Framework of the Levant, Vol. 2: The Levantine Basin and Israel. Historical Productions-Hall. Jerusalem, Israel, 2005, 828 p.

Hallam A. Jurassic Environments. Cambridge Univ. Press. Cambridge University, UK, 1975, 269 p.

Hepworth J., Morris A., Harris M., Brenner A., Fu R., Harrison R., Schwarzenbach E. Novel paleomagnetic insights into the timing of serpentinization of peridotites in the Troodos ophiolite. Proceed. of the EGU General Assembly, Vienna, Austria, 2024, EGU24-11793.

Hirsch F. Jurassic biofacies versus sea level changes in the Middle Eastern Levant (Ethiopian province). Trans. of the 2nd Intern. Symp. of Jurassic Stratigraphy, Lisbon, 1988, pp. 963-981.

Hirsch F. The Triassic Conodont zonation across the Dead Sea Rift. Geol. Survey of Israel, Current Research, Vol. 11, 1997, pp. 62-64.

Hirsch F. and Picard L. The Jurassic facies in the Levant. Jour. of Petroleum Geology, Vol. 11, No. 3, 1988, pp. 277-308.

Golonka J. and Ford D. Pangean (Late Carboniferous – Middle Jurassic) paleoenvironment and lithofacies. Palaeogeography, Paleoclimatology, Paleoecology, Vol. 161, 2000, pp. 1-34.

Gvirtzman G., Weissbrod T., Baer G., Brenner J. The age of Aptian stage and its magmatic events: New Ar-Ar ages and paleomagnetic data from the Negev, Israel. Cretaceous Research, Vol. 17, 1996, pp. 293-310.

Hall J.K., Krasheninnikov V.A., Hirsch F., Benjamini C., Flexer A. Geological Framework of the Levant, Vol. 2: The Levantine Basin and Israel. Historical Productions-Hall. Jerusalem, Israel, 2005, 828 p.

Hallam A. Jurassic Environments. Cambridge Univ. Press. Cambridge University, UK, 1975, 269 p.

Hepworth J., Morris A., Harris M., Brenner A., Fu R., Harrison R., Schwarzenbach E. Novel paleomagnetic insights into the timing of serpentinization of peridotites in the Troodos ophiolite. Proceed. of the EGU General Assembly, Vienna, Austria, 2024, EGU24-11793.

Hirsch F. Jurassic biofacies versus sea level changes in the Middle Eastern Levant (Ethiopian province). Trans. of the 2nd Intern. Symp. of Jurassic Stratigraphy, Lisbon, 1988, pp. 963-981.

Hirsch F. The Triassic Conodont zonation across the Dead Sea Rift. Geol. Survey of Israel, Current Research, Vol. 11, 1997, pp. 62-64.

Hirsch F. and Picard L. The Jurassic facies in the Levant. Jour. of Petroleum Geology, Vol. 11, No. 3, 1988, pp. 277-308.

Johnson P.R. and Kattan F.H. Lithostratigraphic revision in the Arabian shield: The impacts of geochronology and tectonic analysis. Arabian Jour. for Science and Engineer, Vol. 33(1C), 2008, pp. 3-16.

Kadirov F., Floyd M., Alizadeh A., Guliev I., Reilinger R., Kuleli S., King R., Toksoz M.N. Kinematics of the eastern Caucasus near Baku, Azerbaijan. Natural Hazards, Vol. 63, No. 2, 2012, pp. 997-1006.

Kadirov F.A. and Gadirov A.H., A gravity model of the deep structure of South Caspian Basin along submeridional profile Alborz-Absheron Sill. Global and Planetary Change, Vol. 114, 2014, pp. 66-74.

Kadirov F.A., Gadirov A.G., Babayev G.R., Agayeva S.T., Mammadov S.K., Garagezova N.R. Seismic zoning of the southern slope of Greater Caucasus from the fractal parameters of the earthquakes, stress state, and GPS velocities. Izvestiya, Physics of the Solid Earth, Vol. 49, No. 4, 2013, pp. 554-562.

Katz Y.I. New genera of Upper Cretaceous Articulate Brachiopoda of the Tadzhik depression and adjacent regions. Sci. Jour. of Kharkov Univ., Vol. CXXV, Geol. Dept., Vol. 15, Ser: Lithology and Stratigraphy, 1962, pp. 132-154 (in Russian).

Katz Y.I. Cretaceous thalassocratic maximum and planetary movements of the hydrosphere. In: Cretaceous period. Paleogeography and paleooceanology (Naidin D.P., ed.). Nauka. Moscow, 1986, pp. 191-237 (in Russian).

Kazmer M. Pygopid brachiopods and Tethyan margins. In: Mesozoic brachiopods of Alpine Europe (Palfy J., Voros A., eds.). Hungarian Geolog. Soc., Budapest, 1993, pp. 59-68.

Khaffou M., Raji M., El-Ayachi M. East African Rift dynamics. E3S Web of Conferences, Vol. 412, 01030, 2023, pp. 1-10.

Khain V.E. Main Problems of Modern Geology. Nauka. Moscow, 1994, 190 p. (in Russian).

Khain V.E. Tectonics of continents and oceans. Nauchnyi Mir. Moscow, 2000. 606 p. (in Russian).

Khalafly A.A. Paleomagnetism of the Lesser Caucasus. Takhsil. Baku, 2006,189 p. (in Russian).

Khramov A.N., Goncharov G.I., Komissarova R.A., Osipova E.P., Pogarskaya I.A., Rodionov V.P., Slautsitais I.P., Smirnov L.S., Forsh N.N. Paleomagnetism of the Paleozoic. Nedra. Leningrad, 1974, 276 p. (in Russian).

Johnson P.R. and Kattan F.H. Lithostratigraphic revision in the Arabian shield: The impacts of geochronology and tectonic analysis. Arabian Jour. for Science and Engineer, Vol. 33(1C), 2008, pp. 3-16.

Kadirov F., Floyd M., Alizadeh A., Guliev I., Reilinger R., Kuleli S., King R., Toksoz M.N. Kinematics of the eastern Caucasus near Baku, Azerbaijan. Natural Hazards, Vol. 63, No. 2, 2012, pp. 997-1006.

Kadirov F.A. and Gadirov A.H., A gravity model of the deep structure of South Caspian Basin along submeridional profile Alborz-Absheron Sill. Global and Planetary Change, Vol. 114, 2014, pp. 66-74.

Kadirov F.A., Gadirov A.G., Babayev G.R., Agayeva S.T., Mammadov S.K., Garagezova N.R. Seismic zoning of the southern slope of Greater Caucasus from the fractal parameters of the earthquakes, stress state, and GPS velocities. Izvestiya, Physics of the Solid Earth, Vol. 49, No. 4, 2013, pp. 554-562.

Kazmer M. Pygopid brachiopods and Tethyan margins. In: Mesozoic brachiopods of Alpine Europe (Palfy J., Voros A., eds.). Hungarian Geolog. Soc., Budapest, 1993, pp. 59-68.

Khaffou M., Raji M., El-Ayachi M. East African Rift dynamics. E3S Web of Conferences, Vol. 412, 01030, 2023, pp. 1-10.

Khramov A.N. and Iosifidi A.G. Asymmetry of geomagnetic polarity: Equatorial dipole, Pangaea, and the Earth's core. Izvestiya, Phys. Solid Earth, Vol. 48, 2012, pp. 28-41.

Krasheninnikov V.A., Hall J.K., Hirsch F., Benjamini H., Flexer A. Geological Framework of the Levant. Vol. 1: Cyprus and Syria, Jerusalem, 2005, 499 p.

Lang B., Steinitz G. K-Ar dating of Mesozoic magmatic rocks in Israel: A review. Israel Jour. of Earth Sci., Vol. 38, 1989, pp. 89-103.

Lapkin I.Y. and Katz Y.I. Geological events at the Carboniferous and Permian boundary. Izvestiya Acad. Sci. USSR, No. 8, 1990, pp. 45-58.

Le Nindre Y-M., Davies R.B., Issautier B., Krystyn L., Vaslet D., Vrielynck B., Memesh A. The Middle to Late Triassic of Central Saudi Arabia with emphasis on the Jilh Formation. Part II: Sequence stratigraphy, depositional and structural history, correlations and paleogeography. Comptes Rendus. Géoscience, Vol. 355, No. S2, 2023, pp. 99-135.

Le Pichon X. and Kreemer C. The Miocene-to-present kinematic evolution of the Eastern Mediterranean and Middle East and its implications for dynamics. Annu. Rev. Earth Planet. Sci., Vol. 38, 2010, pp. 323-351.

Le Pichon X., Şengör A.M.C., Jellinek M., Lenardic A., İmren C. Breakup of Pangea and the Cretaceous Revolution. Tectonics, Vol. 42, e2022TC007489, 2023, pp. 1-30.

Mahmoud S.M. Seismicity and GPS-derived crustal deformation in Egypt. Geodynamics, Vol. 35, 2003, pp. 333-352.

McElhinny M.W. and McFadden P.L. Paleomagnetism. Continents and Oceans. Academic Press. San Diego, California, USA, 2000, 407 p.

McKenzie D. Active tectonics of the Mediterranean region. Geoph. J. of the Royal Ast. Soc., Vol. 30, No. 2, 1972, pp. 109-185.

Muttoni G., Kent D.V., Garzanti E., Brack P., Abrahamsen N., Gaetani M., Early Permian Pangea 'B' to Late Permian Pangea 'A'. Earth Planet. Sci. Lett., Vol. 215, 2003, pp. 379-394.

Nur A., Ron H., Scott O. Mechanics of distributed fault and block rotation. In: Paleomagnetic rotations and continental deformation (Kissel C., Laj C., eds.), Kluwer Academic Publ. 1989, pp. 209-228.

Reilinger R.E., McClusky S., Vernant P., Lawrence S., Ergintav S., Cakmak R., Ozener H., Kadirov F., Guliyev I. et al. GPS constraints on continental deformation in the Africa-Arabia-Eurasia continental collision zone and implications for the dynamics of plate interactions. Jour. of Geophys. Research, BO5411, 2006, pp.1-26.

Khramov A.N. and Iosifidi A.G. Asymmetry of geomagnetic polarity: Equatorial dipole, Pangaea, and the Earth's core. Izvestiya, Phys. Solid Earth, Vol. 48, 2012, pp. 28-41.

Krasheninnikov V.A., Hall J.K., Hirsch F., Benjamini H., Flexer A. Geological Framework of the Levant. Vol. 1: Cyprus and Syria, Jerusalem, 2005, 499 p.

Lang B., Steinitz G. K-Ar dating of Mesozoic magmatic rocks in Israel: A review. Israel Jour. of Earth Sci., Vol. 38, 1989, pp. 89-103.

Lapkin I.Y. and Katz Y.I. Geological events at the Carboniferous and Permian boundary. Izvestiya Acad. Sci. USSR, No. 8, 1990, pp. 45-58, https://www.tandfonline.com/doi/pdf/10.1080/00206819009465817.

Le Nindre Y-M., Davies R.B., Issautier B., Krystyn L., Vaslet D., Vrielynck B., Memesh A. The Middle to Late Triassic of Central Saudi Arabia with emphasis on the Jilh Formation. Part II: Sequence stratigraphy, depositional and structural history, correlations and paleogeography. Comptes Rendus. Géoscience, Vol. 355, No. S2, 2023, pp. 99-135.

Le Pichon X. and Kreemer C. The Miocene-to-present kinematic evolution of the Eastern Mediterranean and Middle East and its implications for dynamics. Annu. Rev. Earth Planet. Sci., Vol. 38, 2010, pp. 323-351.

Le Pichon X., Şengör A.M.C., Jellinek M., Lenardic A., İmren C. Breakup of Pangea and the Cretaceous Revolution. Tectonics, Vol. 42, e2022TC007489, 2023, pp. 1-30.

Leonov Yu.G. (ed.). The Greater Caucasus. GEOS. Moscow, 2007, 368 p. (in Russian).

Mahmoud S.M. Seismicity and GPS-derived crustal deformation in Egypt. Geodynamics, Vol. 35, 2003, pp. 333-352.

Makridin V.P. and Katz Y.I., The problems of the methods of the paleobiogeographical investigations. In: Organism and Environment in Geological Past. Nauka. Moscow, 1966, pp. 98-115 (in Russian).

Makridin V.P., Katz Y.I., Kuzmicheva E.I. Principles, methodology, and significance of fauna of coral constructions for zoogeographic zonation of Jurassic and Cretaceous seas of Europe, Middle Asia, and adjacent countries. In: Fossil Organogenic Constructions and Methods of Their Studying (Smirnov G.A., Kluzhina M.L., eds.). Ural Branch of the USSR Acad. of Sci., 1968, pp. 184-195 (in Russian).

McElhinny M.W. and McFadden P.L. Paleomagnetism. Continents and Oceans. Academic Press. San Diego, California, USA, 2000, 407 p.

McKenzie D. Active tectonics of the Mediterranean region. Geoph. J. of the Royal Ast. Soc., Vol. 30, No. 2, 1972, pp. 109-185.

Muttoni G., Kent D.V., Garzanti E., Brack P., Abrahamsen N., Gaetani M., Early Permian Pangea 'B' to Late Permian Pangea 'A'. Earth Planet. Sci. Lett., Vol. 215, 2003, pp. 379-394.

Nur A., Ron H., Scott O. Mechanics of distributed fault and block rotation. In: Paleomagnetic rotations and continental deformation (Kissel C., Laj C., eds.), Kluwer Academic Publ. 1989, pp. 209-228.

Reilinger R.E., McClusky S., Vernant P., Lawrence S., Ergintav S., Cakmak R., Ozener H., Kadirov F., Guliyev I. et al. GPS constraints on continental deformation in the Africa-Arabia-Eurasia continental collision zone and implications for the dynamics of plate interactions. Jour. of Geophys. Research, BO5411, 2006, pp.1-26.

Ron H. and Baer G. Paleomagnetism of Early Cretaceous rocks from southern Israel. Israel Jour. of Earth Sci., Vol. 37, 1988, pp. 73-81.

Ron H., Freund R., Garfunkel Z., Nur A. Block rotation by strike-slip faulting: structural and paleomagnetic evidence. Jour. of Geophysical Research, Vol. 89P, 1984, pp. 6256-6270.

Said R. (ed.). The Geology of Egypt. Routledge. London, UK, 2017, 734 p.

Ron H. and Baer G. Paleomagnetism of Early Cretaceous rocks from southern Israel. Israel Jour. of Earth Sci., Vol. 37, 1988, pp. 73-81.

Ron H., Freund R., Garfunkel Z., Nur A. Block rotation by strike-slip faulting: structural and paleomagnetic evidence. Jour. of Geophysical Research, Vol. 89P, 1984, pp. 6256-6270.

Said R. (ed.). The Geology of Egypt. Routledge. London, UK, 2017, 734 p.

Sandy M.R. with a contribution by A V6R6S. Tithonian Brachiopoda. In: Evolution of the Northern Margin of Tethys (Rakus M., Dercourt J., Nairn A.E.M.,eds.). I. Memoires de Ia Societe Geol. de France, Nouvelle Serie, Vol. 154, 1988, pp. 71-74.

Sandy M.R. Aspects of Middle-Late Jurassic-Cretaceous Tethyan brachiopod biogeography in relation to tectonic and paleoceanographic developments. Palaeogeography, Palaeoclimatology, Palaeoecology, Vol. 87, 1991, pp. 137-154.

Scotese C.R. Jurassic and Cretaceous plate tectonic reconstructions. Palaeogeography, Palaeoclimatology, Palaeoecology, Vol. 87, 1991, pp. 493-501.

Segev A. Synchronous magmatic cycles during the fragmentation of Gondwana: Radiometric ages from the Levant and other provinces. Tectonophysics, Vol. 325(3-4), 2000, pp. 257-277.

Segev A., Weissbrod T., Lang B. $^{40}Ar/^{39}Ar$ dating of the Aptian-Albian igneous rocks in Makhtesh Ramon (Negev, Israel) and its stratigraphic implications. Cretaceous Research, Vol. 26, 2005, pp. 633-656.

Şengör A.M.C. Tectonic evolution of the Mediterranean: a dame with four husbands. Trabajos de Geología (Universidad de Oviedo), Vol. 29, 2009, pp. 45-50.

Sneh A., Bartov Y., Rozensaft M. Geological map of Israel, Scale 1:200,000. Geol. Surv. of Israel, Min. of Nation. Infrastructure, Jerusalem, 1998.

Stampfli G.M. Borel G.D. A plate tectonic model for the Paleozoic and Mesozoic constrained by dynamic plate boundaries and restored synthetic oceanic isochrons. Earth and Plan. Sci. Lett., Vol. 96, Nos. 1-2, 2002, pp. 17-33.

Stampfli G.M., Hochard C., Vérard C., Wilhem C., von Raumer J. The formation of Pangea. Tectonophysics, Vol. 593, 2013, pp.1-19.

Stampfli G.M. and Kozur H.W. Europe from the Variscan to the Alpine cycles. Geological Society, London, Memoirs, Vol. 32, No. 1, 2006, pp. 57-82.

Stern R.J. Arc assembly and continental collision in the Neoproterozoic East African orogen: Implications for the Consolidation of Gondwanaland. Annual Review of Earth and Plan. Sci., Vol. 22, No. 1, 1994, pp. 319-351.

Stern R.J. and Johnson P. Continental lithosphere of the Arabian Plate: A geologic, petrologic, and geophysical synthesis. Earth-Science Reviews, Vol. 101, 2010, pp. 29-67.

Stern R.J., Johnson P.R., Kröner A., Yibas B. Neoproterozoic ophiolites of the Arabian-Nubian Shield, In: Precambrian Ophiolites and Related Rocks (Kusky T.M., ed.), Vol. 13 of Dev. Precambrian Geol., 2004, pp. 95-128.

Tauxe L. Paleomagnetic principles and practice. Kluwer Acad. Publishers. N.Y. – Boston – Dordrecht, 2002, 299 p.

Tchoumatchenco P.V. Callovian-Tithonian Brachiopoda from the northern limb of the Belogradcik anticlinorium, northwest Bulgaria. Palaeontology, Stratigraphy, Lithology, Vol. 8, 1978, pp. 3-54.

Tye A.R., Niemi N.A., Cowgill E., Kadirov F.A., Babayev G.R. 2022. Diverse deformation mechanisms and lithologic controls in an active orogenic wedge: Structural geology and thermochronometry of the eastern Greater Caucasus. Tectonics, Vol. 41, No. 12, e2022TC007349, pp. 1-41.

Uzel B., Langereis C., Kaymakci N., Sozbilir H., Ozkaymak C. and Ozkaptan M., Paleomagnetic Evidence for an inverse ro-

Sandy M.R. with a contribution by A V6R6S. Tithonian Brachiopoda. In: Evolution of the Northern Margin of Tethys (Rakus M., Dercourt J., Nairn A.E.M.,eds.). I. Memoires de Ia Societe Geol. de France, Nouvelle Serie, Vol. 154, 1988, pp. 71-74.

Sandy M.R. Aspects of Middle-Late Jurassic-Cretaceous Tethyan brachiopod biogeography in relation to tectonic and paleoceanographic developments. Palaeogeography, Palaeoclimatology, Palaeoecology, Vol. 87, 1991, pp. 137-154.

Scotese C.R. Jurassic and Cretaceous plate tectonic reconstructions. Palaeogeography, Palaeoclimatology, Palaeoecology, Vol. 87, 1991, pp. 493-501.

Segev A. Synchronous magmatic cycles during the fragmentation of Gondwana: Radiometric ages from the Levant and other provinces. Tectonophysics, Vol. 325(3-4), 2000, pp. 257-277.

Segev A., Weissbrod T., Lang B. $^{40}Ar/^{39}Ar$ dating of the Aptian-Albian igneous rocks in Makhtesh Ramon (Negev, Israel) and its stratigraphic implications. Cretaceous Research, Vol. 26, 2005, pp. 633-656.

Şengör A.M.C. Tectonic evolution of the Mediterranean: a dame with four husbands. Trabajos de Geología (Universidad de Oviedo), Vol. 29, 2009, pp. 45-50.

Sneh A., Bartov Y., Rozensaft M. Geological map of Israel, Scale 1:200,000. Geol. Surv. of Israel, Min. of Nation. Infrastructure, Jerusalem, 1998.

Stampfli G.M. Borel G.D. A plate tectonic model for the Paleozoic and Mesozoic constrained by dynamic plate boundaries and restored synthetic oceanic isochrons. Earth and Plan. Sci. Lett., Vol. 96, Nos. 1-2, 2002, pp. 17-33.

Stampfli G.M., Hochard C., Vérard C., Wilhem C., von Raumer J. The formation of Pangea. Tectonophysics, Vol. 593, 2013, pp.1-19.

Stampfli G.M. and Kozur H.W. Europe from the Variscan to the Alpine cycles. Geological Society, London, Memoirs, Vol. 32, No. 1, 2006, pp. 57-82.

Stern R.J. Arc assembly and continental collision in the Neoproterozoic East African orogen: Implications for the Consolidation of Gondwanaland. Annual Review of Earth and Plan. Sci., Vol. 22, No. 1, 1994, pp. 319-351.

Stern R.J. and Johnson P. Continental lithosphere of the Arabian Plate: A geologic, petrologic, and geophysical synthesis. Earth-Science Reviews, Vol. 101, 2010, pp. 29-67.

Stern R.J., Johnson P.R., Kröner A., Yibas B. Neoproterozoic ophiolites of the Arabian-Nubian Shield, In: Precambrian Ophiolites and Related Rocks (Kusky T.M., ed.), Vol. 13 of Dev. Precambrian Geol., 2004, pp. 95-128.

Tauxe L. Paleomagnetic principles and practice. Kluwer Acad. Publishers. N.Y. – Boston – Dordrecht, 2002, 299 p.

Tchoumatchenco P.V. Callovian-Tithonian Brachiopoda from the northern limb of the Belogradcik anticlinorium, northwest Bulgaria. Palaeontology, Stratigraphy, Lithology, Vol. 8, 1978, pp. 3-54.

Tye A.R., Niemi N.A., Cowgill E., Kadirov F.A., Babayev G.R. 2022. Diverse deformation mechanisms and lithologic controls in an active orogenic wedge: Structural geology and thermochronometry of the eastern Greater Caucasus. Tectonics, Vol. 41, No. 12, e2022TC007349, pp. 1-41.

Tzankov V. Geology of the Shumen Plateau and its Nearby Surroundings. Bulgarian Geol. Society, year II, Vol. I, 1930 (in Bulgarian).

Uzel B., Langereis C., Kaymakci N., Sozbilir H., Ozkaymak C. and Ozkaptan M., Paleomagnetic Evidence for an inverse rotation history of Western Anatolia during the exhumation of Menderes Core Complex. Earth and Planet. Sci. Lett., Vol. 414, 2015, pp. 108-125.

Van der Voo R., Scotese C.R., Bonhommet N. (eds.). Plate reconstruction from Paleozoic paleomagnetism (Geodynamics Series). Amer. Geoph. Union, Vol. 12, 1991,136 p.

tation history of Western Anatolia during the exhumation of Menderes Core Complex. Earth and Planet. Sci. Lett., Vol. 414, 2015, pp. 108-125.

Van der Voo R., Scotese C.R., Bonhommet N. (eds.). Plate reconstruction from Paleozoic paleomagnetism (Geodynamics Series). Amer. Geoph. Union, Vol. 12, 1991,136 p.

Vapnik Y., Sharygin V., Samoilov V., Yudalevich Z. The petrogenesis of basic and ultrabasic alkaline rocks of Western Makhtesh Ramon, Israel: melt and fluid inclusion study. Int. Jour. Earth sci. (Geol. Rundsh.), Vol. 96, 2007, pp. 663-684.

Vörös A. Jurassic brachiopods of the Bakony Mts. (Hungary): Global and local effects on changing diversity. In: Mesozoic Brachiopods of Alpine Europe (Palfy J., Voros A., eds.), Hungarian Geological Soc. Budapest, 1993, pp. l79-187.

Yancey T.E., Wilson M.A., Mione A.C.S. The Ramonalinids: A new family of mound-building bivalves of the Early-Middle Triassic. Palaeontology, Vol. 52, Part 6, 2009, pp. 1349-1361.

Zak I. Geological Map of Israel (1:20,000). Makhtesh Ramon, Har Gevanim. Israel Geol. Survey, 1968.

Zakariadze G.S., Dilek Y., Adamia S.A., Oberhänsli R.E., Karpenko S.F., Bazylev B.A., Solov'eva N. Geochemistry and geochronology of the Neoproterozoic Pan-African Transcaucasian Massif (Republic of Georgia) and implications for island arc evolution of the Late Precambrian Arabian-Nubian Shield. Gondwana Research, Vol. 11, 2007, pp. 92-108.

Zilberman E. and Avni Y. The geological map of Israel, 1:50,000. Sheet 21-I, Har Hamran. Israel Geol. Survey, Jerusalem, 2004a.

Zilberman E. and Avni Y. The geological map of Israel, 1: 50,000. Sheet 21-II: Mizpe Ramon. Israel Geol. Surv., Jerusalem, 2004b.

Benzaggagh M. and Atrops F. Stratigraphie et association de faune d'ammonites des zones du Kimméridgien, Tithonien et Berriasien basal dans le Prérif interne (Rif, Maroc). Newsletters on Stratigraphy, Vol. 35(3), 1997, pp. 127-163

Énay R., Hantzpergue P., Soussi M., Mangold C. La limite Kimméridgien-Tithonien et l'âge des formations du Jurassique supérieur de la Dorsale tunisienne, comparaisons avec l'Algérie et Sicily. Géobios, Vol. 38, 2005, pp. 437-450.

Абдулкасумзаде М.П. Верхняя юра Малого Кавказа в пределах Азербайджанской ССР (стратиграфия и аммонитовая фауна). Елм. Баку, 1988,184 с.

Ализаде А.А. Меловые белемниты Азербайджана. Недра. Москва, 1972, 280с.

Ализаде А.А., Алиев С.А., Кац Ю.И., Гамзаев Г.А., Мамедзаде А.М. Новые данные о наличии данианского яруса между реками Хачинчай и Тертерчай (Малый Кавказ). Доклады Академии Наук Азерб.ССР, Том 39, No. 1, 1983, с. 49-51.

Аскеров Р.Б. Позднеюрские брахиоподы азербайджанской части Малого Кавказа и их стратиграфическое значение. Автореферат кандидатской диссертации. Институт геологии Академии наук Азербайджана. Баку, 1965, 18 с.

Гасанов Т. История развития Севано-Акеринской офиолитовой зоны Малого Кавказа. Геотектоника, No. 2, 1986, с. 92-104.

Зоненшайн Л.П. и Савостин Л.А. Введение в геодинамику. Недра. Москва, 1979, 311 с.

Кац Ю.И. Новые роды верхнемеловых Articulate Brachiopoda Таджикской впадины и прилегающих районов. Научный Журн. Харьковского унив., Том CXXV, Научн. Журн. Харьковского университета, Том CXXV, Геол. отдел, Том 15, Сер: Литология и стратиграфия, 1962, стр. 132-154.

Кац Ю.И. Меловой талассократический максимум и планетарные движения гидросферы. В кн.: Меловой период. Палеогеография и палеоокеанология (Найдин Д.П., ред.). Наука. Москва, 1986, с. 191-237.

Vapnik Y., Sharygin V., Samoilov V., Yudalevich Z. The petrogenesis of basic and ultrabasic alkaline rocks of Western Makhtesh Ramon, Israel: melt and fluid inclusion study. Int. Jour. Earth sci. (Geol. Rundsh.), Vol. 96, 2007, pp. 663-684.

Vörös A. Jurassic brachiopods of the Bakony Mts. (Hungary): Global and local effects on changing diversity. In: Mesozoic Brachiopods of Alpine Europe (Palfy J., Voros A., eds.), Hungarian Geological Soc. Budapest, 1993, pp. l79-187.

Yudalevich Z.A., Fershtater G.B., Eyal M. Magmatism of Makhtesh-Ramon: Geology, geochemistry, petrogenesis (Conservation area Har Ha-Negev, Israel). Lithosphere, No. 3, 2014, pp. 70-92 (in Russian).

Yudalevich Z. and Vapnik E. Xenocrysts and megacrysts of alkali-olivine-basalt-basanite-nephelinite association of Makhtesh Ramon (Israel): Interaction with transporting magmas and morphological adjustment. Lithosphere, 18, No. 5, 2018, pp. 718-742 (in Russian).

Yancey T.E., Wilson M.A., Mione A.C.S. The Ramonalinids: A new family of mound-building bivalves of the Early-Middle Triassic. Palaeontology, Vol. 52, Part 6, 2009, pp. 1349-1361.

Zak I. Geological Map of Israel (1:20,000). Makhtesh Ramon, Har Gevanim. Israel Geol. Survey, 1968.

Zakariadze G.S., Dilek Y., Adamia S.A., Oberhänsli R.E., Karpenko S.F., Bazylev B.A., Solov'eva N. Geochemistry and geochronology of the Neoproterozoic Pan-African Transcaucasian Massif (Republic of Georgia) and implications for island arc evolution of the Late Precambrian Arabian-Nubian Shield. Gondwana Research, Vol. 11, 2007, pp. 92-108.

Zilberman E. and Avni Y. The geological map of Israel, 1:50,000. Sheet 21-I, Har Hamran. Israel Geol. Survey, Jerusalem, 2004a.

Zilberman E. and Avni Y. The geological map of Israel, 1: 50,000. Sheet 21-II: Mizpe Ramon. Israel Geol. Surv., Jerusalem, 2004b.

Zonenshain L.P. and Savostin L.A. Introduction to Geodynamics. Nedra. Moscow, 1979, 311 p. (in Russian).

Леонов Ю.Г. (ред.). Большой Кавказ. ГЕОС. Москва, 2007, 368 с.

Макридин В.П. и Кац Ю.И. Некоторые вопросы методики палеобиогеографических исследований**.** В: Организм и окружающая среда в геологическом прошлом. Наука. Москва, 1966, с. 98-115.

Макридин В.П., Кац Ю.И., Кузьмичева Е.И. Принципы, методология и значение фауны коралловых сооружений для зоогеографического районирования юрских и меловых морей Европы, Средней Азии и сопредельных стран. В: Ископаемые органогенные постройки и методы их изучения (Смирнов Г.А., Клужина М.Л., ред.). Уральское отделение Академии наук СССР, 1968, с. 184-195.

Хаин В.Е. Основные проблемы современной геологии. Наука. Москва, 1994, 190 с.

Хаин В.Е. Тектоника континентов и океанов. Научный мир. Москва, 2000. 606 с.

Храмов А.Н., Гончаров Г.И., Комиссарова Р.А., Осипова Е.П., Погарская И.А., Родионов В.П., Слауцитаис И.П., Смирнов Л.С., Форш Н.Н. Палеомагнетизм палеозоя. Недра. Ленинград, 1974, 276 с.

Цанков В. Геология на Шуменското плоскогорие и близките му околности. Българско геологическо дружество, година II, том I, 1930 г.

Чумаков И.С. Плиоценовые и плейстоценовые отложения долины Нила и Нубии в. Верхнем Египте. Тр. Геол. ин-та АН СССР, вып. 170, Наука. Москва, 1967, 119 с.

Юдалевич З.А., Вапник Е. Ксенокристы и мегакристы щелочной оливин-базальт-базанит-нефелинитовой ассоциации Махтеш Рамона (Израиль), их петрохимические взаимодействия с выносящими расплавами и кристаллографические преобразования. Литосфера, No. 5, 2018, с. 718-742, https://doi.org/10.24930/1681-9004-2018-18-5-718-742.

Юдалевич З.А., Ферштатер Г.Б., Эйял М. Магматизм Махтеш Рамона: геология, геохимия, петрогенезис (природоохранная зона Хар Ха-Негев, Израиль). Литосфера, No. 3, 2014, с. 70-92.

СВЯЗЬ ПАЛЕОБИОГЕОГРАФИЧЕСКИХ ИНДИКАТОРОВ СЕВЕРНОГО И ЮЖНОГО БОРТОВ НЕОТЕТИС С ГЛУБИННЫМИ ГЕОДИНАМИЧЕСКИМИ ПРОЦЕССАМИ

Эппельбаум Л.[1,2], Кац Ю.[3], Кадиров Ф.[4]

[1]Кафедра наук о Земле, Факультет точных наук, Тель-Авивский университет, Израиль
Рамат Авив 6997801, Тель-Авив: levap@tauex.tau.ac.il
[2]Азербайджанский Государственный Университет Нефти и Промышленности, Азербайджан
AZ1010, Баку, просп. Азадлыг, 20
[3]Музей Естественной Истории им. Штейнгарда и Национальный Исследовательский Центр,
Факультет Наук о Жизни, Тель-Авивский Университет, Израиль
Тель-Авив 6997801
[4]Министерство науки и образования Азербайджанской Республики, Институт геологии и геофизики, Азербайджан
AZ1143, Баку, просп. Г.Джавида, 119

Резюме. В ряде наших предыдущих исследований (Eppelbaum et al., 2021, 2023b, 2024) было обосновано открытие феномена глубинной мантийной структуры, вращающейся против часовой стрелки, очевидно, влияющей на тектонику и различные геолого-экологические процессы на Южном Кавказе и в Восточном Средиземноморье. Данное исследование позволило оценить время начала влияния глубинной структуры и охарактеризовать структурно-тектонические изменения, произошедшие в разные геологические эпохи. Широкое использование палеонтологических данных дало возможность классифицировать миграцию организмов из отдалённых провинций и получить данные о формировании бассейнов, основанные на изучении геодинамики террейновых поясов, островных дуг, сдвиговых зон и глубинных подвижек, обусловленных характером мантийной конвекции и топологии глубокой мантии. Показана роль палеобиогеографии и конседиментационной тектоники и палеогеографии в оценке автохтонных и аллохтонных структур как необходимого дополнения в тектонике плит прошлых геологических эпох и современности. Исследована геодинамическая эволюция Мезозойского террейного пояса (МТБ), расположенного в южном регионе Неотетиса (северная часть Гондваны). Наши комплексные исследования показали аллохтонную природу МТБ и подтвердили ранее полученные данные о террейновой природе и мезозойском возрасте перемещенных тектонических блоков. На Малом Кавказе биогеографические и тектонофизические исследования резко отделили восточную (азербайджанскую) часть Малого Кавказа от офиолитового пояса в его юго-западном продолжении. Структурно-геодинамическое своеобразие смешанной позднемеловой фауны Гарабахского региона (Западный Азербайджан) получило

всестороннее обоснование. Наконец, была произведена оценка начала влияния мантийного структуры на приповерхностные тектоно-структурные элементы.

***Ключевые слова**: геодинамика, глубинная вращающаяся структура, палеобиогеографические карты, тектонофизическая интерпретация, океан Неотетис*

NEOTETİSİN ŞİMAL VƏ CƏNUB TƏRƏFLƏRİNİN PALEOBİOCOĞRAFİ İNDİKATORLARININ DƏRİNDƏ BAŞ VERƏN GEODİNAMİK PROSESLƏRLƏ ƏLAQƏSİ

Eppelbaum L.[1,2], Kats Yu.[3], Qədirov F.[4]

[1]Təl-Əviv Universiteti, Dəqiq Elmlər Fakültəsi, Yer Elmləri Departamenti, İsrail
6997801, Tel-Əviv, Ramat Əviv: levap@tauex.tau.ac.il
[2]Azərbaycan Dövlət Neft və Sənaye Universiteti, Azərbaycan
AZ1010, Bakı, Azadlıq prosp., 20
[3]Steinhardt adına Təbiət Tarixi Muzeyi və Milli Tədqiqat Mərkəzi, Həyat Elmləri Fakültəsi, Tel-Əviv Universiteti, İsrail
6997801, Tel-Əviv
[4]Azərbaycan Respublikasının Elm və Təhsil Nazirliyi, Geologiya və Geofizika İnstitutu, Azərbaycan
Az1143, Bakı, H.Cavid pr., 119

Xülasə. Bir sıra əvvəlki tədqiqatlarımızda Cənubi Qafqazda və Şərqi Aralıq dənizində aydın şəkildə tektonikaya və müxtəlif geoloji və ekoloji proseslərə təsir edən, saat əqrəbinin əksi istiqamətində fırlanan dərin mantiya strukturu fenomeninin kəşfi əsaslandırılmışdır (Eppelbaum et al., 2021, 2023b, 2024). Bu tədqiqat dərin strukturun təsirinin başlanğıcını qiymətləndirməyə və müxtəlif geoloji dövrlərdə baş verən struktur və tektonik dəyişiklikləri xarakterizə etməyə imkan verəcəkdir. Paleontoloji məlumatların geniş istifadəsi orqanizmlərin uzaq əyalətlərdən miqrasiyasını təsnif etməyə və müəyyən edilmiş ərazi qurşaqlarının, mantiya konveksiyasının təbiəti və dərin mantiyanın topologiyasına əsaslanan ada qövslərinin, sürüşmə zonalarının və dərin qatlarda hərəkətlərin geodinamikasının öyrənilməsi əsasında hövzələrin əmələ gəlməsinə dair məlumatlar əldə etməyə imkan vermişdir. Avtoxton və alloxton strukturların qiymətləndirilməsində paleobiocoğrafiya və konsedimentasiya tektonikasının və paleocoğrafiyanın rolu keçmiş geoloji dövrlərin və indiki dövrün plitə tektonikasına zəruri əlavə kimi göstərilir. Tədqiqatlarımızdan əvvəl, Şərqi Aralıq dənizində Qondvananın kənarlarının riftoqenezi və Ölü dəniz qırılması boyunca yeni transform yerdəyişmələri ilə əlaqəli avtoxton Kaynozoy Suriya Tağı müəyyən edilmişdi. Bizim hərtərəfli tədqiqatlarımız bu strukturun alloxton xarakterini göstərmış və yerdəyişmiş tektonik blokların terreyn xarakterini və mezozoy yaşı haqqında əvvəlki məlumatları təsdiqləmişdir. Eynilə, Kiçik Qafqazda biocoğrafi və tektonogeofiziki tədqiqatlar göstərmişdir ki, Kiçik Qafqazın şərq (Azərbaycan) hissəsi onun cənub-qərb sərhədindəki ofiolit qurşağından kəskin şəkildə ayrılmışdır. Azərbaycanın Qarabağ bölgəsinin qarışıq son təbaşir faunasının struktur və geodinamik unikallığı hərtərəfli əsaslandırılmış və təsdiqlənmişdir. Nəhayət, ilk dəfə olaraq mantiya strukturunun səthə yaxın tektono-struktur elementlərə təsirinin başlanğıcı ilə bağlı qiymətləndirmə aparılmışdır.

***Açar sözlər**: geodinamika, dərin fırlanan struktur, paleobiocoğrafi xəritələr, tektonofizik şərh, Neo-Tetis okeanı*

ANAS Transactions Earth Sciences 1 / 2024

http://www.journalesgia.com

ХАРАКТЕРИСТИКА НЕФТЕГАЗОМАТЕРИНСКИХ ТОЛЩ И ОСОБЕННОСТИ УГЛЕВОДОРОДНЫХ СИСТЕМ ЮЖНО-КАСПИЙСКОГО БАССЕЙНА

Керимов В.Ю.[1,3], Гулиев И.С.[2], Джавадова А.С.[1], Кадиров Ф.А.[1,4], Мустаев Р.Н.[3], Гурбанов В.Ш.[1], Гусейнова Ш.М.[1]

[1]Министерство науки и образования Азербайджанской Республики, Институт нефти и газа, Азербайджан
AZ1000, Баку, ул. Ф. Амирова, 9: huseynova_shalala@yahoo.com
[2]Президиум Национальной академии наук Азербайджана, Азербайджан
AZ1001 Баку, ул. Истиглалият, 30: i.s.guliyev@gmail.com
[3]Российский государственный геологоразведочный университет имени Серго Орджоникидзе, Российская Федерация
117997, Москва, ул. Миклухо-Маклая, 23: mustaevrn@mgri.ru
[4]Министерство науки и образования Азербайджанской Республики, Институт геологии и геофизики, Азербайджан
AZ1073, Баку, просп, Г. Джавида, 119: kadirovf@gmail.com

CHARACTERISTICS OF SOURCE ROCKS AND FEATURES OF PETROLEUM SYSTEMS OF THE SOUTH CASPIAN BASIN

Kerimov V.Yu.[1,3], Guliyev I.S.[2], Javadova A.S.[1], Kadirov F.A.[1,4], Mustaev R.N.[3], Gurbanov V.Sh.[1], Huseynova Sh.M.[1]
[1]Ministry of Science and Education of the Republic of Azerbaijan, Institute of Oil and Gas, Azerbaijan
9, F.Amirov str., Baku, AZ1000: huseynova_shalala@yahoo.com
[2]Presidium of the Azerbaijan National Academy of Sciences, Azerbaijan
30, Istiglaliyyat str., Baku, AZ1001: i.s.guliyev@gmail.com
[3]Sergo Ordzhonikidze Russian State University for Geological Prospecting, Russian Federation
23, Miklouho-Maclay str., Moscow, 117997: mustaevrn@mgri.ru
[4]Ministry of Science and Education of the Republic of Azerbaijan, Institute of Geology and Geophysics, Azerbaijan
119, H.Javid ave., Baku, AZ1073: kadirovf@gmail.com

Keywords: *South Caspian basin, petroleum system, shale petroleum system, source rocks, organic matter, pyrolysis*

Summary. To assess the generation potential of oil and gas source strata of the South Caspian Basin (SCB) of the Cenozoic age, pyrolytic studies were carried out using the Rock-Eval-6 pyrolysis method from VINCI Technologies. In the SCB with a complex geological structure and geodynamic development, there are very difficult conditions for the development and distribution of generation-accumulation hydrocarbon systems. During the evolution of the basin, unique conditions were created for the formation of hydrocarbon systems that differed significantly from the classical ones. The paper examines the rates of sedimentation and subsidence, as well as the regional geo-temperature background influencing the catagenetic evolution of organic matter. In the SCB there is a unique natural phenomenon – the Miocene-Pliocene generation-migration-accumulation hydrocarbon megasystem with a reservoir in the productive strata (PS), the oil and gas content of which is formed due to the migration of hydrocarbons from several oil and gas source strata – mainly from the Oligocene-Miocene (Maykop) and Miocene (Tarkhan Chokrakian and diatom) age, partly from the Eocene and the PS (Productive Series) itself, mainly its lower section, both according to classical migration patterns and according to systems of mud volcanoes, widespread in the SCB. Along with the above megasystem, shale hydrocarbon systems were formed within the SCB: diatomaceous shale hydrocarbon system, Oligocene-Miocene shale hydrocarbon system and Eocene shale hydrocarbon system, which are combined unconventional oil and gas systems with hydrocarbons, partially emigrated from oil and gas source strata and partially preserved (not displaced).

Введение

Южно-Каспийский бассейн (ЮКБ) является геологическим феноменом, не имеющим аналога в мире. Осадочное выполнение бассейна толщиной более 20 км представлено широким стратиграфическим диапазоном отложений от ааленского яруса средней юры до голоцена включительно. Уникальная 7-километровая терригенная продуктивная толща (ПТ) содержит более 95% всех известных запасов нефти и газа Азербайджана. В ЮКБ со сложным геологическим строением и геодинамическим развитием созданы весьма своеобразные условия для развития и распространения генерационно-аккумуляционных углеводородных систем (ГАУС), отличающихся от классических (Алиева и др., 2015; Багир-Заде и др., 1988).

В последнее время нефтегазоматеринские породы все чаще рассматриваются в качестве объекта непосредственной добычи углеводородов. На основании исследований последних лет можно сделать вывод, что нефтегазоматеринские толщи (НГМТ) являются не только источником генерации, но также и местом их скоплений (Глумов и др., 2004; Джафаров и др., 2005; Мехтиев, 1985; Керимов и др., 1990, 2014).

В статье приведена характеристика НГМТ и рассмотрены особенности углеводородных систем ЮКБ на основе результатов геохимических исследований преимущественно образцов пород из обнажений и кернового материала из скважин, выбросов грязевых вулканов (рис. 1) и нефти из месторождений ЮКБ, а также ранее проведенных исследований, изложенных в ряде публикаций (Дахнова и др., 2015;Лебедев и др., 2016; Inan et al, 1997; Katz et al., 2005; Керимов и др., 2017; Guliev et al., 2018; Dolson, 2016; Mustaev et al., 2023).

Методика исследований

Для оценки генерационного потенциала НГМТ кайнозойского возраста ЮКБ были проведены пиролитические исследования методом пиролиза Rock-Eval-6 компании VINCI Technologies. Данный метод прямого определения углеводородного потенциала пород и органического вещества (ОВ) позволяет выявить спектр параметров, отражающих качественные и количественные характеристики ОВ пород, в том числе: содержание органического углерода (TOC), реализованный S_1 и остаточный S_2 генерационный потенциал породы, кислородный (OI) и водородный (HI) индексы, температуру максимального выхода углеводородов при пиролизе керогена T_{max}, индекс продуктивности (PI) и др.

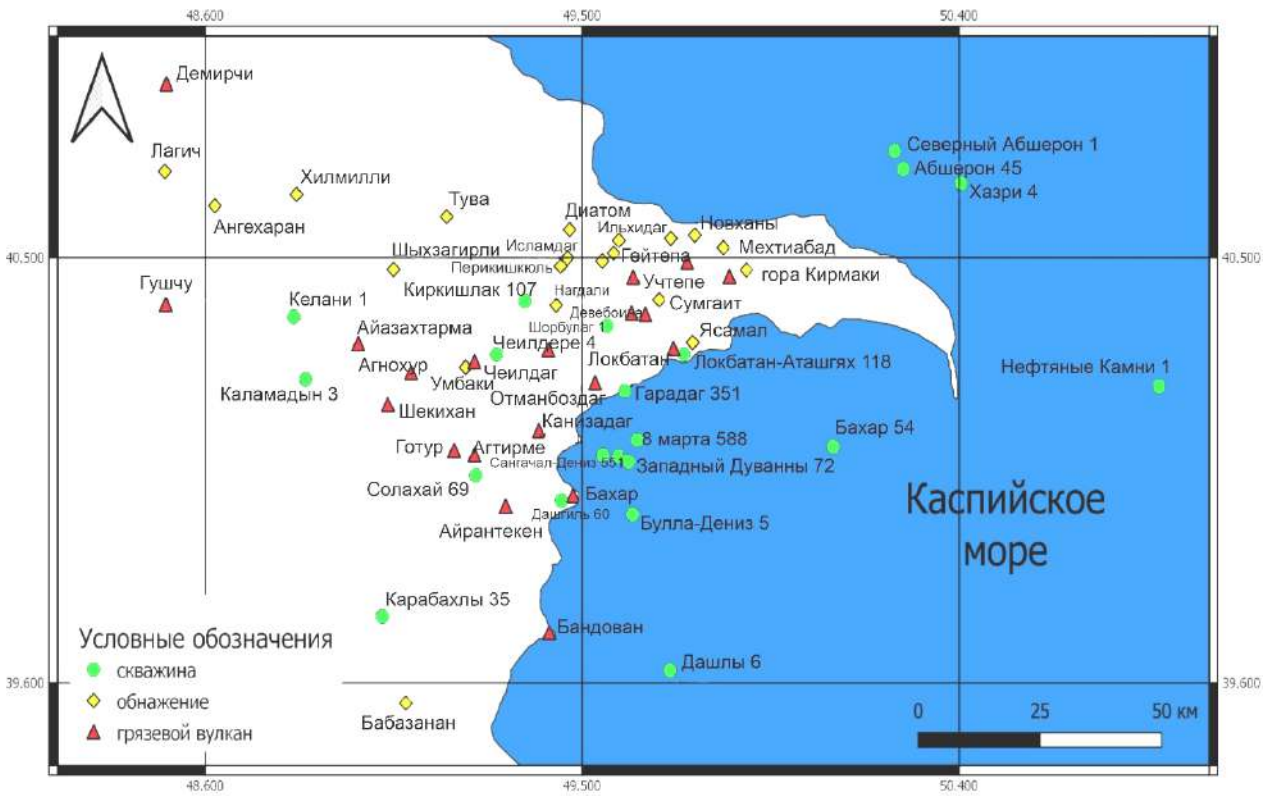

Рис. 1. Карта местоположения исследуемых грязевых вулканов и обнажений

Результаты исследований

Результаты пиролитических исследований интерпретировались по пяти комплексам отложений: продуктивной толще, диатомовой свите, тархан-чокракским отложениям, майкопской серии и палеоцен-эоценовому комплексу (рис. 2-4). Результаты проведенных исследований позволили дать характеристику нефтегазоматеринских осадочных комплексов кайнозойского возраста (таблица) и выявить их генерационные особенности.

Нижнеплиоценовые отложения (ПТ). В образцах пород из обнажений преобладает кероген II и III типов, а в образцах пород из скважин преобладает кероген III типа, которые обладают диапазоном значений по углеводородно-генерационному потенциалу от низкого до высокого. Отличительной чертой геотемпературного режима ЮКБ является весьма низкая прогре-тость плиоценовых и четвертичных отложений, в связи с чем степень катагенетической преобразованности ОВ в них достаточно низкая. Однако часть полученных значений T_{max} из подошвенных свит находится в пределах 420-437°С. По всему бассейну температура на срезе (–5 км) не превышает 110°С, что можно соотнести к началу углеводородообразования – градации катагенеза $ПК_3$ (75-90°С) – $МК_1$ (95-120°С). В целом на стадии $ПК_3$ кероген II типа еще не созрел для интенсивной генерации углеводородов, однако это еще не означает, что в зоне позднего протокатагенеза ($ПК_3$) не возникают условия для генерации так называемой незрелой нефти. На этой стадии начинается перестройка керогена, происходят процессы, такие как сокращение доли кислорода в керогене, удаление из него групп C=C, разрыв гетероатомных связей наиболее неустойчивых карбонильных и карбоксильных групп. Перестройка структуры керогена сопровождается образованием в небольших объемах низкотемпературного сухого биогенного метана (CH_4), CO_2, N_2.

Миоценовые отложения. Нефтематеринскими свойствами в этом интервале обладают диатомовая свита и тархан-чокракские отложения. Согласно модифицированной диаграмме Ван Кревелена, кероген в миоценовом комплексе – III типа и в меньшей степени – II типа. Как водородный, так и кислородный индексы демонстрируют широкую вариабельность. Рассматриваемые образцы обладают широким диапазоном значений по углеводородно-генерационному потенциалу от удовлетворительного до превосходного.

Диатомовая свита. Часть образцов попадает в раннюю стадию углеводородообразования – градации катагенеза $ПК_3$– $МК_1$. В свою очередь, T_{max} для некоторых образцов достигает 440-458°С и более. По расчетам авторов, в миоценовых отложениях наиболее глубокой центральной части бассейна рассчитанные значения температуры достигают 170°С, что соответствует градации $МК_1$–$МК_3$, в зоне которой интенсивно протекают термические и термокаталитические процессы преобразования и происходит принципиальная перестройка молекулярной структуры керогена, а также с максимальной активностью происходит генерация углеводородов, в том числе и легких (до 4%). В целом в диатомовых отложениях процесс генерации углеводородов продолжается и в настоящее время, однако в очагах нефтегазообразования степень генерации может достигать критического момента, о чем свидетельствуют повышенные содержания S_1 в определенной части образцов. Это также подтверждается результатами моделирования процесса генерации углеводородов (рис.5). В связи с этим диатомовая свита может рассматриваться в качестве одного из основных нефтегазогенерирующих комплексов в ЮКБ.

Тархан-чокракские отложения. В образцах пород преобладает кероген II и III типов. Кислородный индекс имеет широкую вариативность (от 20 до 200 мг CO_2/ г ТОС). Часть значений T_{max} находится в пределах 420-437°С, что традиционно соотносят с началом углеводородообразования – градации катагенеза $ПК_3$– $МК_1$, а низкие значения T_{max} подчеркивают миграционную природу битумоида.

Олигоцен – нижний миоцен (майкопская серия) характеризуется широким диапазоном значений по углеводородно-генерационному потенциалу от удовлетворительного до превосходного. В образцах выделяется равное количество значений керогена III и II типа. Часть полученных значений T_{max} лежит в пределах от 420-445°С, а рассчитанные значения температуры составляют 171-200°С и соответствуют градации катагенеза $МК_3$-$МК_4$. Следовательно, отложения майкопского возраста находятся в интервалах глубин, находящихся в зоне нефтяного окна (oil window), в которой происходит генерация углеводородов с максимальной активностью, в том числе и легких (до 4%). В групповом составе преобладают метановые углеводороды (приблизительно до 54%), среди которых порядка 30% нормального строения и около 24% – изостроения. Результаты исследований свидетельствуют о повышенном содержании S_1 (появление паравтохтонных битумоидов) в ряде образцов. С переходом в зону $МК_4$ майкопские отложения в главной зоне газообразования начинают генерировать газообразные углеводороды. Результаты моделирования процесса генерации углеводородов в отложениях майкопской серии показывают, что в большей части бассейна степень генерации может достигать пика и стадии завершения углеводородообразования (см. рис. 5).

Отложения майкопской серии отличаются высоким содержанием $C_{орг}$, достигающим 15.1% при среднем содержании 1.86%. Качество и содержание ОВ майкопских отложений улучшаются в восточном направлении в сторону Каспийского моря.

Палеоцен-эоценовый комплекс отложений. Эоценовые отложения характеризуются широким диапазоном значений по углеводородно-генерационному потенциалу от низкого до превосходного. В образцах преобладает кероген III типа. Результаты исследований показывают, что рассчитанные значения температуры составляют 210°C и более, а образцы эоценовых отложений соответствуют градации катагенеза $МК_4$ – $МК_5$ – $АК_1$ и входят в главную зону газообразования. Содержание углерода в керогене достигает 85-86%, что свидетельствует об «уплотнении» углеродной структуры, связанной с потерей гетероэлементов и в особенности – водорода, содержание которого менее 2%. Удаление водорода происходит за счет интенсивной генерации газообразных углеводородов. На этом этапе происходит резкое снижение объемов генерации углеводородов, в том числе и метана, что подтверждается также результатами моделирования процесса генерации углеводородов в эоценовых отложениях (см. рис. 5).

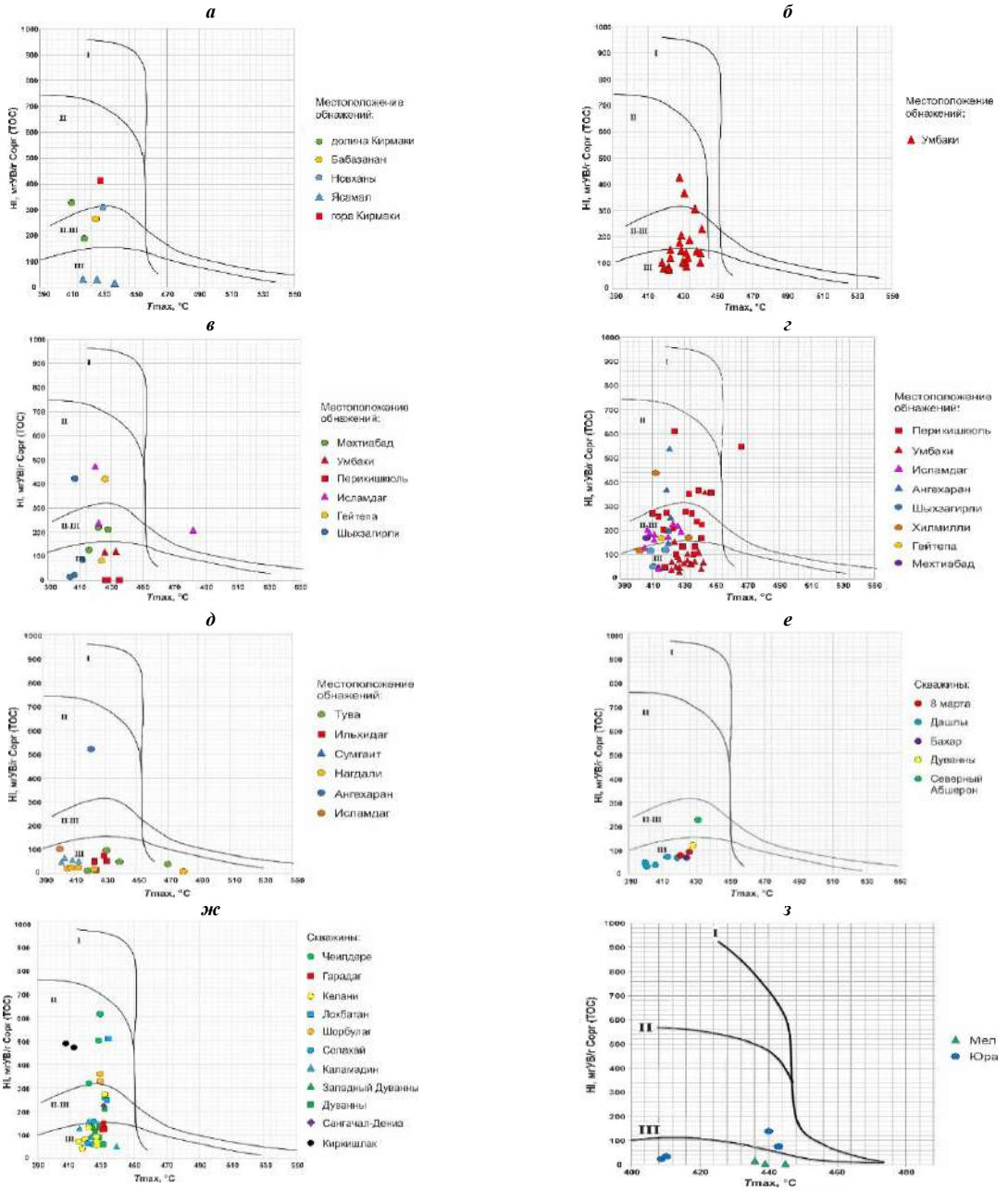

Рис. 2. Модифицированные диаграммы Ван Кревелена, отражающие зависимость водородного индекса HI от максимальной температуры пиролиза T_{max}: ***а*** – для образцов продуктивной толщи из обнажений; ***б*** – образцов диатомовой свиты; ***в*** – тархан-чокракских отложений; ***г*** – майкопских отложений; ***д*** – палеоцен-эоценовых отложений; ***е*** – образцов продуктивной толщи из скважин; ***ж*** – образцов миоценового комплекса из скважин; ***з*** – юрских и меловых образцов

а ***б***

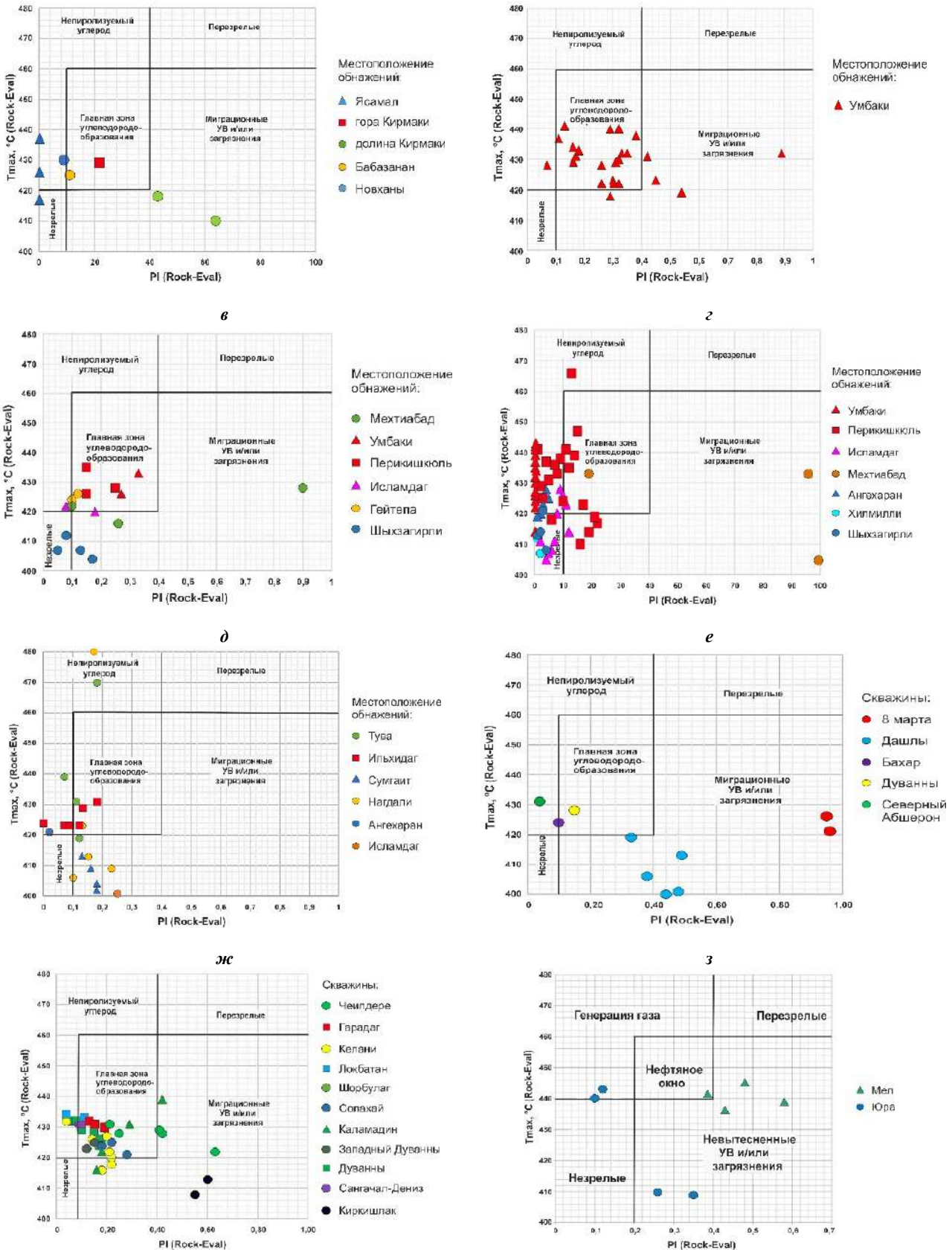

Рис. 3. Диаграммы соотношения максимальной температуры пиролиза T_{max} и индекса продуктивности PI: ***а*** – для образцов продуктивной толщи из обнажений; ***б*** – образцов диатомовой свиты; ***в*** – тархан-чокракских отложений; ***г*** – майкопских отложений; ***д*** – палеоцен-эоценовых отложений; ***е*** – образцов продуктивной толщи из скважин; ***ж*** – образцов миоценового комплекса из скважин; ***з*** – юрских и меловых образцов

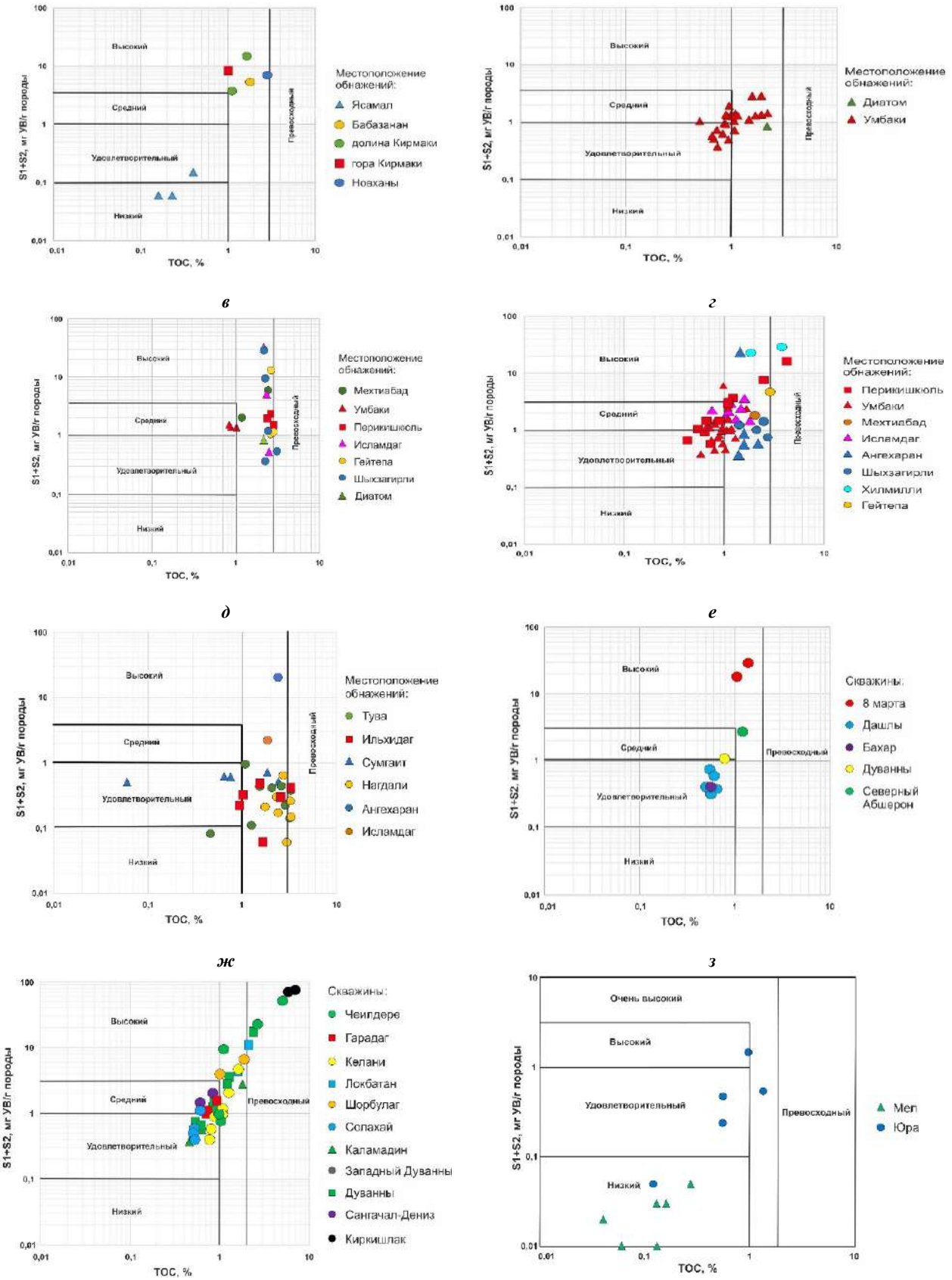

Рис. 4. Диаграммы соотношения генерационного потенциала материнской породы и общего содержания органического углерода $C_{орг}$: ***а*** – для образцов продуктивной толщи из обнажений; ***б*** – образцов диатомовой свиты; ***в*** – тархан-чокракских отложений; ***г*** – майкопских отложений; ***д*** – палеоцен-эоценовых отложений; ***е*** – образцов продуктивной толщи из скважин; ***ж*** – образцов миоценового комплекса из скважин; ***з*** – юрских и меловых образцов

К настоящему времени

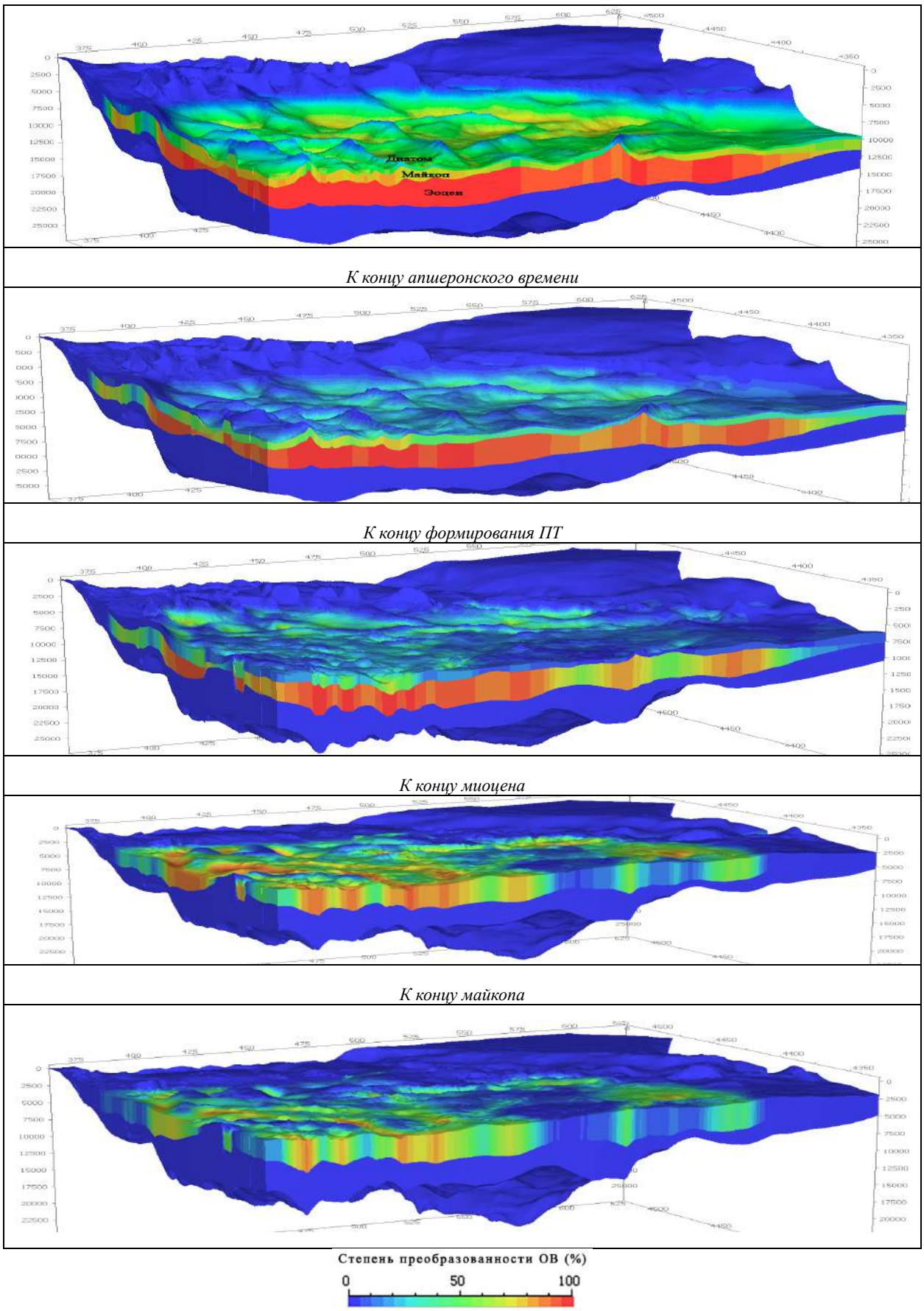

Рис. 5. Трехмерные модели генерации УВ (катагенетической эволюции) основных нефтегазоматеринских толщ кайнозойского комплекса - эоцена, майкопа и диатома ЮК

Таблица 1

Характеристика нефтегазоматеринских свойств осадочных комплексов кайнозойского возраста

Возраст пород	**Углеводородно-генерационный потенциал**	**Градация катагенеза**	**Температура (расчетная), °С**
Нижнеплиоценовые	От низкого до высокого	$ПК_3$ $МК_1$	75-90 95-120
Миоценовые Диатомовые	От удовлетворительного до превосходного	$ПК_3$ $МК_1$ $МК_2$ $МК_3$	75-90 95-120 120-160 160-170
Тархан-чокракские	От удовлетворительного до превосходного	$ПК_3$ $МК_1$ $МК_2$ $МК_3$	75-90 95-120 120-160 160-170
Олигоцен-миоценовые (майкопская серия)	От удовлетворительного до превосходного	$МК_3$ $МК_4$	171-190 190-200
Эоценовые	От низкого до превосходного	$МК_4$ $МК_5$ $АК_1$	190-200 200-215 Более 220

Обсуждение результатов

В ЮКБ со сложным геологическим строением и геодинамическим развитием создавались весьма сложные и уникальные условия для развития и распространения ГАУС. История геодинамического развития Каспийского региона характеризуется чередованием периодов преимущественного растяжения, сжатия и относительной тектонической стабилизации, которые нашли отражение в геофлюидодинамической эволюции ЮКБ и сопредельных осадочных бассейнов. В регионе широко развиты региональные и локальные линеаменты, хиатусы и размывы. Регион характеризуется доминированием мощных субвертикальных межформационных и межрезервуарных пульсационно-инъекционных флюидомассоперетоков, высокой сейсмичностью, активным грязевым вулканизмом и другими геофизическими аномалиями. В этих условиях в кайнозойском комплексе ЮКБ выделяются четыре углеводородные системы: *миоцен-плиоценовая генерационно-миграционно-аккумуляционная углеводородная мегасистема, диатомовая сланцевая углеводородная система, олигоцен-миоценовая сланцевая углеводородная система и эоценовая сланцевая углеводородная система,* которые подтверждаются геохимическими, геотермическими исследованиями и результатами моделирования углеводородных систем.

Важным фактором формирования углеводородных систем является скорость осадконакопления и прогибания в ЮКБ. Величина скорости седиментации, составляющая 1 мм/1000 лет, называется единицей Бубнова или Б – в честь известного немецкого геолога русского происхождения С.Н. Бубнова. Скорость осадконакопления изменяется от нулевой или минимальной до высокой или сверхвысокой. Высокие и сверхвысокие скорости осадконакопления, превышающие 100мм/1000 лет (100 Б) и 1000мм/1000 лет (1000 Б), соответственно, характеризуют лавинную седиментацию. Это понятие введено в научный обиход исследованиями А.П. Лисицына (Лисицын, 1988; 2009). Максимальные скорости осадконакопления, характерные для верхнего и среднего уровней лавинной седиментации, то есть для устьевых частей рек и прилегающих зон морей, согласно оценкам А.П. Лисицына (Лисицын, 2009), превышают 5000-6000 Б (устья рек Миссисипи, Ориноко, Нил, Рона и др.) и в ряде случаев могут достигать 18000–30000 Б и более (реки Потомак, Менам, Хуанхэ и др.).

Среди осадочных комплексов в ЮКБ наибольшей толщиной и ритмичным чередованием песчанистых и глинистых отложений выделяется нижнеплиоценовый. Он отделяется несогласием от нижележащего понтического яруса. Время формирования продуктивно-красноцветной толщи – около 2.2-2.5 млн. лет, что составляет 1.5% геологического времени от альпийского мегацикла. За это время накопилась огромная масса грубообломочного материала с максимальной толщиной 7.0-8.5 км, то есть около 25-30% от общей толщины осадочного чехла ЮКБ. Вычисление скорости осадконакопления даже без учета уплотнения пород и частых перерывов,

на которые приходится 40-60% геологического времени, дает 25-3.0 км/млн. лет, что само по себе на порядок выше лавинной скорости седиментации. В этом отношении раннеплиоценовый палеобассейн не имеет аналогов среди палео- и современных бассейнов Мирового океана. Такая высокая сверхлавинная скорость седиментации обусловлена транспортировкой грубообломочного материала в замкнутый плиоценовый бассейн многочисленными мелкими и крупными реками (Палео-Волгой, Палео-Курой и Палео-Узбоем). Однако такая лавинная скорость накопления осадков характерна для плиоценового периода, до которого скорости осадконакопления и прогибания в бассейне были низкими. Общее опускание бассейна за альпийский цикл (–180 млн. лет) составляет 25-30 км. Согласно проведенным расчетам (рис. 6), выявлено следующее:

– *в средне-позднеюрскую эпоху* на этапе расширения моря за счет термального погружения континентальная кора (КК) оседала на 1.2 км со скоростью 50-60 м/млн. лет;

– *к началу мелового периода* с учетом нагрузки осадочных вулканогенных толщ и водного слоя (высотой 2.5-3.5 км) общее тектоническое погружение КК доходило до 5-6 км. В меловом периоде КК погружалась с меньшей скоростью – 10-20 м/млн. лет – всего на 3 км (в общем 9 км);

– *в палеоцен-эоцене* бассейн оставался глубоководным. К началу олигоцена расширение моря практически приостановилось, резко замедлилось тектоническое погружение (5-8 м/млн. лет). К концу эоцена КК погружалась на 1 км за счет только нагрузки осадков. Общая амплитуда погружения достигала 10-5 км;

– *в олигоцен – раннем миоцене* кора ЮКБ тектонически погружалась очень медленно, в основном за счет увеличения нагрузки осадочной толщи, толщина которой достигала 14-16 км. Далее в среднем и позднем миоцене глубина бассейна постепенно уменьшилась от 4.5-4.0 км до 2.0 км из-за интенсивного заполнения осадками;

– *в плиоцене* скорость тектонического прогибания достигла 1000-2000 м/млн. лет. Расчет амплитуды погружения в районе Абшеронского порога в плиоцен-квартере с учетом поправок на нагрузку осадочной толщи и батиметрию дает величину 10-12 км. Скорость прогибания в плиоцене в северной части ЮКБ в 20-30 раз выше, чем на рифтогенном этапе раскрытия и на 2 порядка (100-200 раз) больше, чем в меловом и палеогеновом периодах. В этот период (и только в этот период) ЮКБ может быть отнесен к молодым активным («живым») бассейнам с лавинным седиментогенезом, для которых характерны устойчивое погружение, высокий темп и скорости седиментации.

Скорости прогибания до плиоценового времени были весьма умеренными, что благоприятно влияло на катагенетическую эволюцию ОВ. Такая ситуация не могла не повлиять на формирование углеводородных систем и ее элементов, а также на распределение палео- и современных температур, игравших важную роль в катагенетической зональности в ЮКБ. Согласно В.Ю. Керимову и М.З. Рачинскому (2011), в ЮКБ распределение по глубине фактических значений пластовых температур в интервале гипсометрических отметок (0)-(–6000) м аппроксимируется выражением $t = 13.7 + 0.196H^{0.725}$, удовлетворяющим функцию $t = a + bHn$, где t – температура, °С, на глубине H, м; a – среднегодовая температура местности; b и n – коэффициенты, определяющие особенности по отдельным районам в связи со спецификой их геологического развития, тектоники, литологии и другими влияющими факторами.

Региональный геотемпературный фон ЮКБ в общем виде характеризуется следующими основными чертами (Гулиев и др., 1992; Дахнова и др., 2015; Калмыков и др., 2019; Левин, Сенин, 2003; Левин, Федоров, 2001; Мехтиев, 1957, 1985; Lapidus et al., 2018):

– **в мезозойских отложениях** наиболее прогнутой части бассейна температура (t_{mz}) на подошве комплекса – поверхности фундамента – на гипсометрических срезах (–26) и (–28) км составляет соответственно 458–484 и 489–514°С при геотемпературных градиентах ($G^t=dt/dH$) –1.53–1.58 и 1.50–1.57°С/100 м; приведенная к тем же глубинам температура ($t^{пр.}{}_{mz}$.) составляет 17.6-18.6 и 17.5-18.4°С/км. На западном борту бассейна зависимость температура – глубина для мезозойского комплекса в интервале глубин 0.5-28 км имеет вид $t_{mz}=13.9+0.0635H^{0.871}$ при геотемпературных градиентах G^t_{mz}= 2.48-1.48°С/100 м;

– *в палеоген-миоценовых отложениях* наиболее глубокой центральной части бассейна на подошве комплекса – поверхности мезозоя – в интервале глубин 8.7-10.5 км рассчитанные значения $t_{pg\text{-}mi}$ составляют 171-231°С, величины $G^t_{pg\text{-}mi}$ соответственно – 2.17–2.27°С/100 м, $t^{пр.}{}_{pg\text{-}mi}$ – 19.7-22.0°С/км. На западном борту бассейна в интервале глубин 0.5-12.0 км $t_{pg\text{-}mi}=13.9+0.0544H^{0.898}$ и $G^t_{pg\text{-}mi}$= 2.59-1.87°С/100 м;

– *в плиоценовых отложениях* на гипсометрическом срезе (–1000 м) $t^{-1000}{}_{PS(RS)}$ варьирует в пределах 27-59.5°С; геотемпературные градиенты $G_{PS(RS)}$ в интервале 1-5 км составляют 1.19-2.30°С/100 м; в районах наиболее глубокого за-

легания комплекса на его подошве (поверхности подстилающего миоцен-палеогена) $t_{PS(RS)}$ в пределах глубин 6.25-8.30 км составляет 127-178°C; температура, приведенная к подошве ПТ-КТ ($t^{np}_{PS(RS)}$), – 18.1-23.5°C/км; для ПТ западного борта бассейна зависимость температура – глубина в интервале глубин 0.05-8.50 км имеет вид t_{PS}=13.7+0.149H$^{0.716}$ и G^t_{PS}= 3.51-0.82°C/100 м. Низкая прогретость плиоценовых и четвертичных отложений является особенностью геотемпературного режима ЮКБ. Во всех районах бассейна температура на срезе (–5 км) не превышает 110°C, а величины геотермического градиента составляют 0.80-1.05°C/100 м. Поэтому при вышеуказанных температурах весь мезо-кайнозойский осадочный комплекс ЮКБ относить к холодным бассейнам некорректно (Rachinsky, Kerimov, 2015).

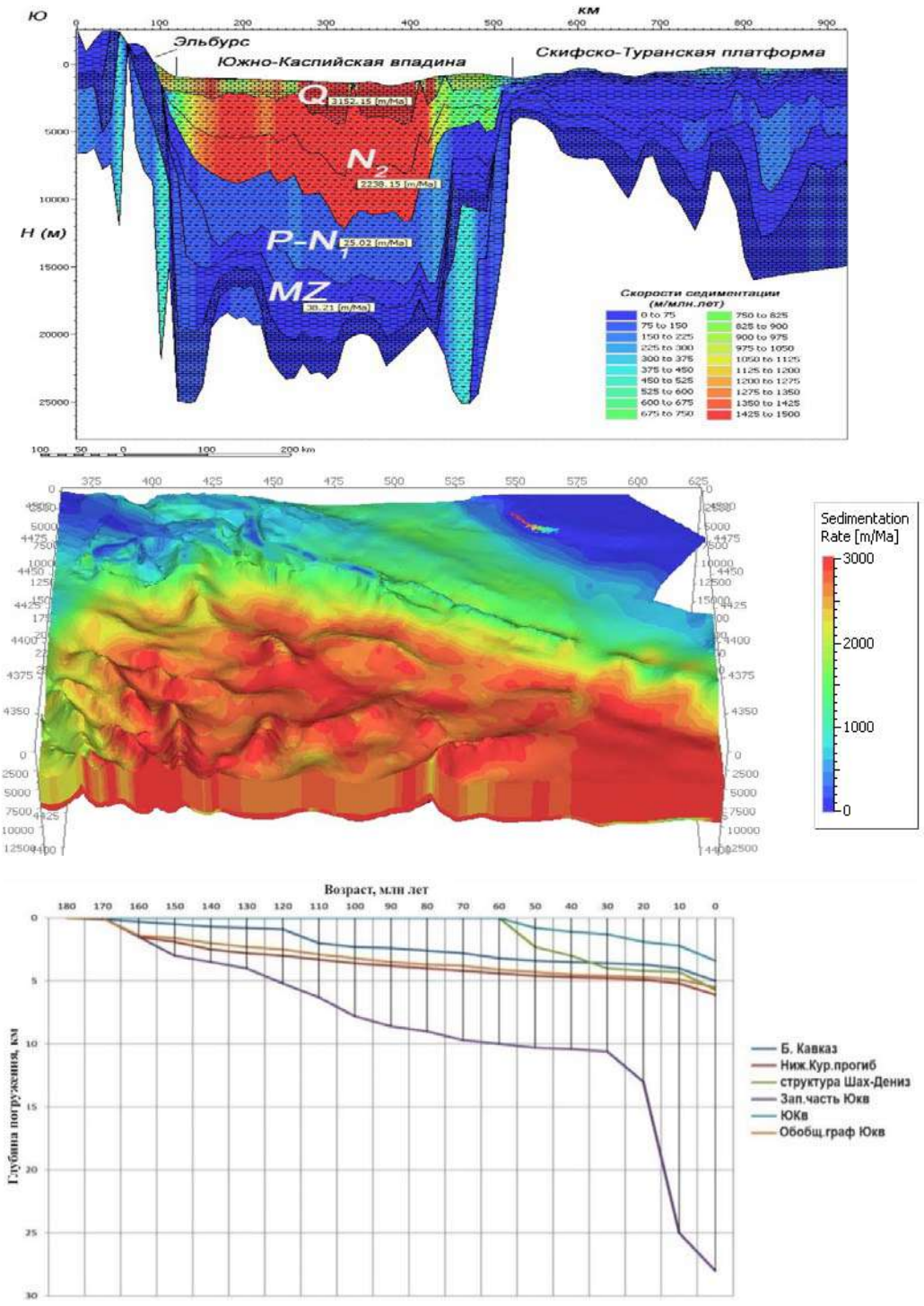

Рис. 6. Модель скоростей седиментации ЮКБ (а), трехмерная модель скоростей седиментации плиоценового комплекса ЮКБ (б) и графики тектонического погружения ЮКБ (в)

Региональное геотемпературное поле бассейна имеет явно выраженный мозаичный характер, соответствующий его ступенчато-блоковому строению и различиям литофациальной композиции разрезов отдельных районов. Этот фактор влияет на мозаичный характер пространственного распространения очагов генерации углеводородов в пределах углеводородных систем (Сенин и др., 2022; Kerimov et al., 2016, 2023).

В процессе формирования ЮКБ создавались уникальные ситуации, отличающиеся от классических условий формирования углеводородных систем. Так, НГМТ могли обеспечивать углеводородами несколько резервуаров, в том числе стратиграфически более молодые. Резервуары более молодых углеводородных систем могли насыщаться за счет эмиграции углеводородов из нескольких НГМТ. Таким образом, уникальный резервуар ПТ насыщается за счет миграции углеводородов из нескольких НГМТ – в основном миоценового (тархан-чокракского и диатомового) и майкопского возраста. Такого мнения придерживаются, наряду с авторами статьи, и предыдущие исследователи (Мехтиев, 1956, 1985; Гулиев, Фейзуллаев, 1996; Abrams, Narimanov, 1997; Feyzullayev и др., 2022; Керимов, Серикова, 2023).

Это подтверждается результатами исследований экстрактов битумоидов из кайнозойских отложений, которые выявили различие отдельных стратиграфических комплексов по изотопному составу углерода (ИСУ) (Ализаде и др., 2018; Фейзуллаев и др., 2022). В свою очередь, ИСУ был использован как важнейший диагностический признак для стратиграфической и генетической типизации нефти ЮКБ, с одной стороны, и корреляции порода – нефть и нефть – нефть, с другой. По характеру распределения $\delta^{13}C$ в керогене весь осадочный разрез кайнозоя четко разграничивается на палеоген-нижнемиоценовые и диатомовые отложения.

В керогене *палеоген-нижнемиоценовых отложений* содержания $\delta^{13}C$ изменяются от -28.24 до -24.15‰ (здесь и далее первая цифра соответствует $\delta^{13}C$ в алкановой фракции, а вторая – суммарному углероду нефти), а среднее равно -26.48‰.

В *диатомовых отложениях* наблюдается резкое утяжеление изотопного состава углерода, где среднее значение $\delta^{13}C$ составляет -23.33‰ при его вариациях от -25.25 до -21.53‰.

Значения изотопных отношений углерода $\delta^{13}C$ в нефти ЮКБ варьируют в широких пределах – от -28.00 до -24.34‰ для суммарного углерода и от -29.1 до -24.8‰ для алкановой фракции нефти.

Согласно значениям изотопных соотношений, нефти ЮКБ группируются в два класса:

1) *изотопно-легкие* со значениями $\delta^{13}C$ от -28.0 до -27.0‰ по суммарному углероду и от -29.1 до -27.0‰ по углероду алкановой фракции. Наиболее изотопно-легкие нефти в кайнозойском комплексе характерны для эоценовых отложений (-28.32‰; -27.86‰), далее для майкопского (-28.05‰; -27.64‰) и чокракского комплексов (-27.95‰; -27.5‰) (рис.7).

2) *изотопно-утяжеленные* со значениями $\delta^{13}C$ от -26.5 до -24.0‰ и от -26.5 до -24.5‰, соответственно.

Резкое изотопное утяжеление нефти происходит при переходе к нефти из диатомовой свиты (-26.45‰; -26.13‰). Наиболее тяжелые нефти приурочены к резервуарам нижне- и верхнеплиоценового возраста (-26.35‰; -25.75‰) (см. рис. 7).

Основную массу нефти ЮКБ составляет нефть второй группы, на долю которой приходится от 57.64 до 68.66% проанализированных проб, тогда как изотопно-легкие нефти составляют 31.35 – 42.35%.

При этом наблюдается отчетливая дифференциация нефтегазоносных районов по величинам $\delta^{13}C$ алкановой фракции нефти плиоценовых резервуаров. По средним значениям этого параметра нефтегазоносные районы располагаются в следующей последовательности: Нижнекуринский (-26.8‰) → Абшеронский (-26.29‰) → Шамаха-Гобустанский (26.1‰) → Бакинский архипелаг (-26.04‰) → Абшеронский архипелаг (-25.87‰) (рис.8). Как видно из приведенного графика, нефти плиоценового резервуара акваториальной части ЮКБ выделяются некоторым утяжелением изотопного состава.

Проведенные исследования показывают:

– Морские месторождения содержат в основном смесь палеоген-нижнемиоценовой и диатомовой нефти, с преимуществом диатомовых.

– На Абшеронском полуострове объем смешанной нефти уменьшается за счет обособления преимущественно палеоген-нижнемиоценовой, а объем нефти с диатомовой изотопной меткой остается примерно тем же.

– Общим для морской части ЮКБ и Абшеронского полуострова является примерно одинаковый объем модальных значений (от -26.5 до -26.0‰), составляющий 47.36 и 42.85%, соответственно.

– Плиоценовый резервуар Нижне-Куринского нефтегазоносного района по содержанию палеоген-нижнемиоценовой и диатомовой нефти кардинально отличается от вышеописанного зна-

чительного уменьшения диатомовой нефти, увеличением объема палеоген-нижнемиоценовой и резким смещением модальных значений $\delta^{13}C$ в области от -27.5 до -27.0‰ (изотопно-легких) объемом 30.77% и от -27.0 до -26.5‰ в объеме 26.92%, которые в сумме составляют 57.69%. Таким образом, в составе нефти плиоценового резервуара Нижне-Куринского нефтегазоносного района доля палеоген-нижнемиоценовой нефти заметно выше.

Как следует из вышеизложенного, нефть плиоценового резервуара представляет собой смесь нефти из различных нефтематеринских толщ эоценового, олигоцен-миоценового (майкопского), миоценового (тархан-чокракского и диатомового) возраста, роль которых в каждой конкретной геологической ситуации (как в масштабе региона в целом, так и в пределах отдельных нефтегазоносных районов) различна. Не исключено участие в нефтегенерации и самой ПТ, в частности, ее нижнего отдела.

В процессе формирования углеводородных систем, наряду с классическими схемами миграции углеводородов, большую роль играет система грязевых вулканов, широко распространенная в ЮКБ.

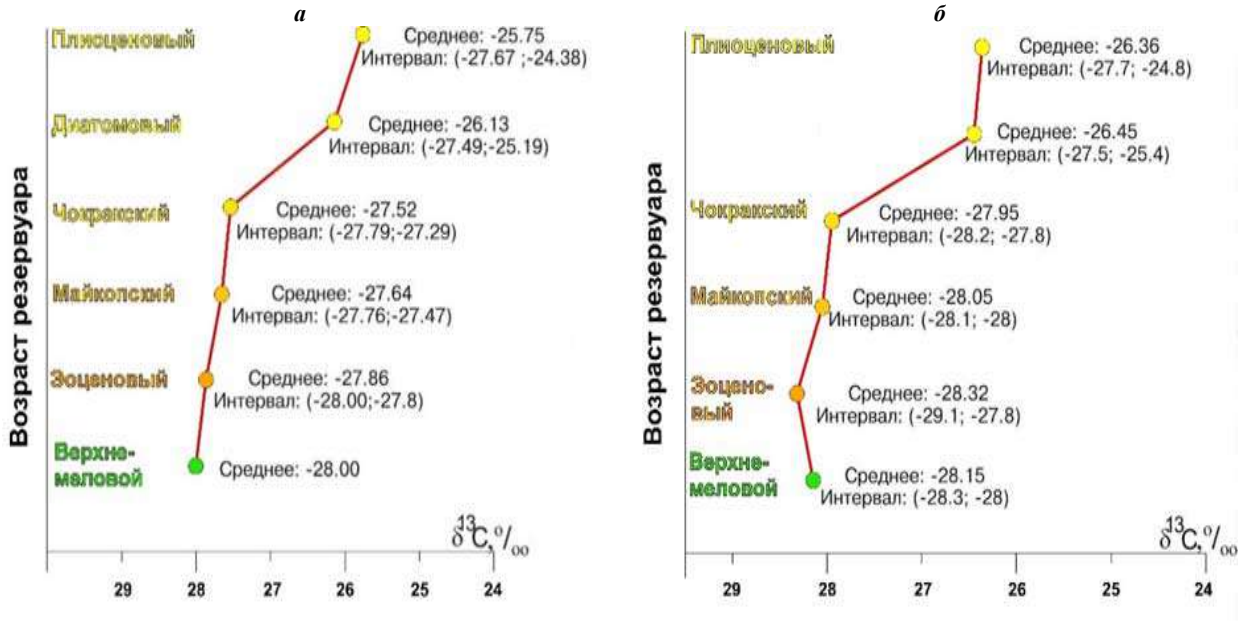

Рис. 7. Диаграммы вариаций величин изотопных отношений суммарного углерода (**а**) и углерода алкановой фракции (**б**) нефти разновозрастных резервуаров ЮКБ (Ализаде и др., 2018)

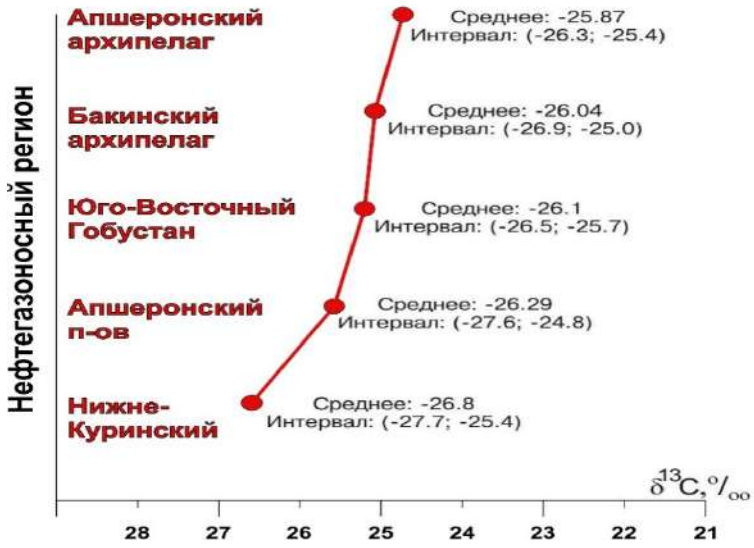

Рис. 8. Диаграммы вариаций величин изотопных отношений углерода алкановой фракции нефти плиоценового резервуара ЮКБ (Ализаде и др., 2018)

Заключение

В ЮКБ выделяется уникальный природный феномен – ***миоцен-плиоценовая генерационно-миграционно-аккумуляционная углеводородная мегасистема*** с резервуаром ПТ, нефтегазоносность которой формируется за счет миграции углеводородов из нескольких нефтегазоматеринских толщ – в основном из олигоцен-миоценового (майкопского) и миоценового (тарханчокракского и диатомового) возраста, частично из эоценового и самой ПТ, главным образом ее нижнего отдела, как по классическим схемам миграции, так и по системам грязевых вулканов, широко распространенных в ЮКБ.

Наряду с вышеуказанной мегасистемой в пределах ЮКБ сформировались сланцевые углеводородные системы: ***диатомовая сланцевая углеводородная система, олигоцен-миоценовая сланцевая углеводородная система*** и ***эоценовая сланцевая углеводородная система,*** которые являются комбинированными нетрадиционными нефтегазовыми системами с углеводородами, частично эмигрировавшими из НГМТ и частично сохраненными (не вытесненными).

Информация о сланцевых углеводородных системах будет полностью опубликована в следующей публикации.

This work was supported by the SOCAR Science Foundation (grant no. 20LR-EF/2024).

ЛИТЕРАТУРА

Алиева С.А., Авербух Б.М., Серикова У.С., Мустаев Р.Н. Геология и нефтегазоносность Каспийской впадины (под. ред. В.Ю. Керимова). ИНФРА-М. Москва, 2015, 486 с.

Ализаде А.А., Гулиев И.С., Мамедов П.З. и др. Продуктивная толща Азербайджана. Монография в 2-х томах. Том I. Недра. Москва, 2018, 305 с.

Ализаде А.А., Гулиев И.С., Мамедов П.З. Продуктивная толща Азербайджана. Монография в 2-х томах. Том II. Недра. Москва, 2018, 236 с.

Багир-Заде Ф.М., Нариманов А.А., Бабаев Ф.Р. Геолого-геохимические особенности месторождений Каспийского моря. Недра. Москва, 1988, 206 с.

Глумов И.Ф., Маловицкий Я.П., Новиков А.А., Сенин Б.В. Региональная геология и нефтегазоносность Каспийского моря. ООО «Недра-Бизнесцентр». Москва, 2004, 342 с.

Гулиев И.С., Кляцко Н.В., Мамедова С.А., Сулейманова С.Ф. Нефтегазопродуцирующие и коллекторские свойства отложений Южно-Каспийской впадины. Литология и полезные ископаемые, No. 2. 1992, с. 110-119.

Гулиев И.С., Фейзуллаев А.А. Зональность углеводородообразования и ресурсы нефти и газа в Южно-Каспийской впадине. Азерб.нефтяное хозяйство, No. 4, 1996, с. 6-8.

Дахнова М.В., Можегова С.В., Назарова Е.С., Пайзанская И.Л. Оценка запасов «сланцевой нефти» с использованием геохимических параметров. Геология нефти и газа, No. 4, 2015, с. 55-61.

Джафаров И.С., Керимов В.Ю., Шилов Г.Я. Шельф, его изучение и значение для поисков и разведки скоплений нефти и газа. Недра. Санкт-Петербург, 2005, 384 с.

Калмыков А.Г., Карпов Ю.А., Топчий М.С. и др. Влияние катагенетической зрелости на формирование коллекторов с органической пористостью в баженовской свите и особенности их распространения. Георесурсы, Том 21, No. 2, 2019, с. 159-171.

Керимов В.Ю., Авербух Б.М., Мильничук В.С. Тектоника северного Каспия и перспективы нефтегазоносности. Советская геология, No. 7, 1990, с. 23-29.

Керимов В.Ю., Бондарев А.В., Мустаев Р.Н., Хоштария В.Н. Оценка геологических рисков при поисках и разведке месторождений углеводородов. Нефтяное хозяйство, No. 8, 2017, с. 36-41.

Керимов В.Ю., Осипов А.В., Мустаев Р.Н., Монакова А.С. Моделирование углеводородных систем в регионах со сложным геологическим строением. 16th Science and Applied Research Conference on Oil and Gas Geological Exploration and Development, GEOMODEL 2014, DOI:10.3997/2214-4609.20142245.

REFERENCES

Abrams M.A., Narimanov A.A. Geochemical evaluation of hydrocarbons and their potential sources in the western South Caspian depression, Republic of Azerbaijan. Marine and Petroleum Geology, No. 14, 1997, pp. 451.

Alieva S.A., Averbukh B.M., Serikova U.S., Mustaev R.N. Geology and oil and gas potential of the Caspian Basin (edited by V.Yu. Kerimov). INFRA-M. Moscow, 2015, 486 p. (in Russian).

Alizadeh A.A., Guliev I.S., Mamedov P.Z. and others. Productive strata of Azerbaijan. Monograph in 2 volumes. Volume I. Nedra. Moscow, 2018, 305 p. (in Russian).

Alizadeh A.A., Guliev I.S., Mamedov P.Z. Productive strata of Azerbaijan. Monograph in 2 volumes. Volume II. Nedra. Moscow, 2018, 236 p. (in Russian).

Bagir-Zadeh F.M., Narimanov A.A., Babaev F.R. Geological and geochemical features of the fields of the Caspian Sea. Nedra. Moscow, 1988, 206 p. (in Russian).

Dakhnova M.V., Mozhegova S.V., Nazarova E.S., Paizanskaya I.L. Estimation of shale oil reserves using geochemical parameters. Geology of Oil and Gas, No. 4, 2015, pp. 55-61 (in Russian).

Dolson J. Understanding oil and gas shows and seals in the search for hydrocarbons. Springer International Publishing. Switzerland, 2016, 486 p.

Feyzullaev A.A., Guseinov D.A., Rashidov T.M. Isotopic composition of the products of mud volcanoes activity in the South Caspian Basin in connection with petroleum potential of the deeply barried sediments. ANAS Transactions, Earth Sciences, No. 1, 2022, pp. 68-80, DOI: 10.33677/ggianas20220100073 (in Russian).

Glumov I.F., Malovitsky Ya.P., Novikov A.A., Senin B.V. Regional geology and oil and gas potential of the Caspian Sea. Nedra-Business Center LLC. Moscow, 2004, 342 p. (in Russian).

Guliev I.S., Feizullaev A.A. Zoning of hydrocarbon formation and oil and gas resources in the South Caspian Basin. Azerbaijan Oil Industry, 1996, No. 4, pp. 6-8 (in Russian).

Guliev I.S., Klyatsko N.V., Mamedova S.A., Suleymanova S.F. Oil and gas producing and reservoir properties of sediments of the South Caspian Basin. Lithology and Minerals, 1992, No. 2, pp. 110-119 (in Russian).

Guliev I.S., Mustaev R.N., Kerimov V.Y., Yudin M.N. Degassing of the Earth: Scale and implications. Gornyi Zhurnal, No.11, 2018, pp. 38-42, DOI:10.17580/gzh.2018.11.06

Inan U.S., Barrington-Leigh C., Hansen S. et al. Rapid lateral expansion of optical luminosity in lightning-induced ionospheric flashes referred to as 'elves'. Geophys. Res. Lett., Vol. 24, No. 5, 1997, pp. 583-586.

Керимов В.Ю., Рачинский М.З. Геофлюидодинамика нефтегазоносности подвижных поясов. ООО «Издательский дом Недра». Москва, 2011, 599 с.

Керимов В.Ю., Серикова У.С. Основатель современного азербайджанского государства Гейдар Алиев – автор концепции о нефтяной стратегии Азербайджана. ANAS Transactions, Earth Sciences, Special Issue, 2023, pp. 18-21, DOI: 10.33677/ggianasconf20230300004.

Лебедев С.А., Костяной А.Г. и др. Система Каспийского моря. Российская академия наук, Институт океанологии им. П.П. Ширшова. Научный мир. Москва, Том 1, 2016, 479 с.

Левин Л.Э., Сенин Б.В. Глубинное строение и динамика осадочных бассейнов в Каспийском регионе. ДАН, Том 338, No. 2, 2003, с. 216-219.

Левин Л.Э., Федоров Д.Л. Среднекаспийский и Южно-Каспийский бассейны: геолого-геофизические параметры нефтегазоносных систем и распределение потенциальных ресурсов углеводородов. В: Современные проблемы геологии нефти и газа. Научный мир. Москва, 2001, с. 278-286.

Лисицын А.П. Закономерности осадкообразования в областях быстрого и сверхбыстрого осадконакопления (лавинной седиментации) в связи с образованием нефти и газа в Мировом океане. Геология и геофизика, Том 50, No. 4, 2009, с. 373-400.

Лисицын А.П. Лавинная седиментация и перерывы в осадкообразовании в морях и океанах. Наука. Москва, 1988, 310 с.

Мехтиев Ш.Ф. Вопросы происхождения нефти и формирования нефтяных залежей Азербайджана. Изд-во АН Аз. ССР. Баку, 1956, 319 с. [Рец.] Ахмедбейли Ф.С. Обсуждение книги Ш.Ф. Мехтиева… Изв. АН Аз. ССР, 1957, No. 6, с. 225-228.

Мехтиев Ш.Ф. Процессы формирования и преобразования состава нефти и газа в природе. Элм. Баку, 1985, 144 с.

Сенин Б.В., Керимов В.Ю., Мустаев Р.Н., Леончик М.И. Структурно-геодинамические системы фундамента Черноморско-Каспийского региона и их эволюция в позднем палеозое-кайнозое. Геотектоника, No. 1, 2022, с. 27-50.

Фейзуллаев А.А., Гусейнов Д.А., Рашидов Т.М. Изотопный состав продуктов деятельности грязевых вулканов Южно-Каспийского бассейна в связи с нефтегазоносностью глубокопогруженных отложений. ANAS Transactions, Earth Sciences, No.1, 2022, pp. 68-80, DOI: 10.33677/ggianas20220100073.

Abrams M.A., Narimanov A.A. Geochemical evaluation of hydrocarbons and their potential sources in the western South Caspian depression, Republic of Azerbaijan. Marine and Petroleum Geology, No. 14, 1997, pp. 451.

Dolson J. Understanding oil and gas shows and seals in the search for hydrocarbons. Springer International Publishing. Switzerland, 2016, 486 p.

Guliev I.S., Mustaev R.N., Kerimov V.Y., Yudin M.N. Degassing of the Earth: Scale and implications. Gornyi Zhurnal, No. 11, 2018, pp. 38-42, DOI:10.17580/gzh.2018.11.06

Inan U.S., Barrington-Leigh C., Hansen S. et al. Rapid lateral expansion of optical luminosity in lightning-induced ionospheric flashes referred to as ‘elves’. Geophys. Res. Lett., Vol. 24, No. 5, 1997, pp. 583-586.

Katz M.E., Wright J.D., Miller K.G. et al. Biological overprint of the geological carbon cycle. Marine Geology, No. 217, 2005, pp. 323-338.

Kerimov V.Yu., Senin B.V., Serikova U.S. et al. Assessment of the conditions of formation and distribution of structural, lithological, stratigraphic and combined traps in the Black Sea – Caspian region. ANAS Transactions, Earth Sciences, No. 1, 2023, pp. 81-99.

Jafarov I.S., Kerimov V.Yu., Shilov G.Ya. The shelf, its study and significance for the search and exploration of oil and gas accumulations. Nedra. St. Petersburg, 2005, 384 pp. (in Russian).

Kalmykov A.G., Karpov Yu.A., Topchiy M.S. and others. The effect of catagenetic maturity on the formation of reservoirs with organic porosity in the Bazhenov formation and peculiarities of their extension. Georesources, Vol. 21, No. 2, 2019, pp. 159-171 (in Russian).

Katz M.E., Wright J.D., Miller K.G. et al. Biological overprint of the geological carbon cycle. Marine Geology, No. 217, 2005, pp. 323-338.

Kerimov V.Yu., Averbukh B.M., Milnichuk V.S. Tectonics of the northern Caspian Sea and oil and gas prospects. Soviet Geology, No. 7, 1990, pp. 23-29 (in Russian).

Kerimov V.Yu., Bondarev A.V., Mustaev R.N., Khoshtaria V.N. Estimation of geological risks in searching and exploration of hydrocarbon deposits. Oil Industry Journal, No. 8, 2017, pp. 36-41 (in Russian).

Kerimov V.Yu., Osipov A.V., Mustaev R.N., Monakova A.S. Modeling of hydrocarbon systems in regions with complex geological structure. 16th Science and Applied Research Conference on Oil and Gas Geological Exploration and Development, GEOMODEL 2014. DOI:10.3997/2214-4609.20142245 (in Russian).

Kerimov V.Yu., Rachinsky M.Z. Geofluid dynamics of oil and gas content of moving belts. Nedra Publishing House LLC. Moscow, 2011, 599 p. (in Russian).

Kerimov V.Yu., Senin B.V., Serikova U.S. et al. Assessment of the conditions of formation and distribution of structural, lithological, stratigraphic and combined traps in the Black Sea – Caspian region. ANAS Transactions, Earth Sciences, No. 1, 2023, pp. 81-99.

Kerimov V.Yu., Serikova U.S. Founder of the modern Azerbaijani State Heydar Aliyev – author of the concept on the oil strategy of Azerbaijan. ANAS Transactions, Earth Sciences, Special Issue, 2023, pp. 18-21, DOI: 10.33677/ggianasconf20230300004 (in Russian).

Kerimov V.Yu., Shilov G.Ya., Mustayev R.N., Dmitrievskiy S.S. Thermobaric conditions of hydrocarbons accumulations formation in the low-permeability oil reservoirs of khadum suite of the Pre-Caucasus. Neftyanoe Khozyaystvo – Oil Industry, No 2, 2016, pp. 8-11.

Lapidus A.L., Kerimov V.Y., Mustaev R.N., Salikhova I.M., Zhagfarov F.G. Natural Bitumens: physicochemical properties and production technologies. Solid Fuel Chemistry, Vol. 52, No. 6, 2018, pp. 344-355.

Lebedev S.A., Kostyanoy A.G. et al. Caspian Sea system. Russian Academy of Sciences, Institute of Oceanology named after P.P.Shirshova. Scientific world. Moscow, Vol. 1, 2016, 479 p. (in Russian).

Levin L.E., Senin B.V. Deep structure and dynamics of sedimentary basins in the Caspian region. DAN, Vol. 338, No. 2, 2003, pp. 216-219 (in Russian).

Levin L.E., Fedorov D.L. Middle Caspian and South Caspian basins: geological and geophysical parameters of oil and gas bearing systems and distribution of potential hydrocarbon resources. In: Modern problems of oil and gas geology, Nauchniy mir. Moscow, 2001, p. 278-286 (in Russian).

Lisitsyn A.P. Patterns of rapid and extremely rapid (avalanche) sedimentation: implications for marine oil and gas generation. Geology and Geophysics, Vol. 50, No. 4, 2009, pp. 373-400 (in Russian).

Lisitsyn A.P. Avalanche sedimentation and breaks in sedimentation in the seas and oceans. Nauka. Moscow, 1988, 310 p. (in Russian).

Mehdiev Sh.F. Issues of the origin of oil and the formation of oil deposits in Azerbaijan. Publishing house of the Academy of Sciences of Az. SSR. Baku, 1956, 319 p. [Rec.] Akhmed-

Kerimov V.Yu., Shilov G.Ya., Mustayev R.N., Dmitrievskiy S.S. Thermobaric conditions of hydrocarbons accumulations formation in the low-permeability oil reservoirs of khadum suite of the Pre-Caucasus. Neftyanoe Khozyaystvo – Oil Industry, No. 2, 2016, pp. 8-11.

Lapidus A.L., Kerimov V.Y., Mustaev R.N., Salikhova I.M., Zhagfarov F.G. Natural Bitumens: physicochemical properties and production technologies. Solid Fuel Chemistry, Vol. 52, No. 6, 2018, pp. 344-355.

Mustaev R.N., Kerimov V.Yu., Senin B.V., Lavrenova E.A. Structural-geodynamic and hydrocarbon systems in the Black Sea-Caspian region. ANAS Transactions, Earth Sciences, Special Issue, 2023, pp. 41-45.

Rachinsky M.Z., Kerimov V.Y. Fluid dynamics of oil and gas reservoirs. Wiley & Sons Ltd**.** New Jersey, 2015, 617 p., DOI: 10.1002/9781118999004. – EDN XNGONX.

bayli F.S. Discussion of the book by Sh.F. Mehdiyev... Izv. AN Az. SSR, No. 6, 1957, pp. 225-228 (in Russian).

Mehdiev Sh.F. Processes of formation and transformation of the composition of oil and gas in nature. Elm. Baku, 1985, 144 p. (in Russian).

Mustaev R.N., Kerimov V.Yu., Senin B.V., Lavrenova E.A. Structural-geodynamic and hydrocarbon systems in the Black Sea-Caspian region. ANAS Transactions, Earth Sciences, Special Issue, 2023, pp. 41-45.

Rachinsky M.Z., Kerimov V.Y. Fluid dynamics of oil and gas reservoirs. Wiley & Sons Ltd**.** New Jersey, 2015, 617 p., DOI: 10.1002/9781118999004. – EDN XNGONX.

Senin B.V., Kerimov V.Yu., Mustaev R.N., Leonchik M.I. Structural-geodynamic systems of the basement of the Black Sea-Caspian region and their evolution in the late Paleozoic-Cenozoic. Geotectonics, No. 1, 2022, pp. 27-50 (in Russian).

ХАРАКТЕРИСТИКА НЕФТЕГАЗОМАТЕРИНСКИХ ТОЛЩ И ОСОБЕННОСТИ УГЛЕВОДОРОДНЫХ СИСТЕМ ЮЖНО-КАСПИЙСКОГО БАССЕЙНА

Керимов В.Ю.[1,3], Гулиев И.С.[2], Джавадова А.С.[1], Кадиров Ф.А.[1,4], Мустаев Р.Н.[3], Гурбанов В.Ш.[1], Гусейнова Ш.М.[1]

[1]Министерство науки и образования Азербайджанской Республики, Институт нефти и газа, Азербайджан
AZ1000, Баку, ул. Ф. Амирова, 9: huseynova_shalala@yahoo.com
[2]Президиум Национальной академии наук Азербайджана, Азербайджан
AZ1001 Баку, ул. Истиглалият, 30: i.s.guliyev@gmail.com
[3]Российский государственный геологоразведочный университет имени Серго Орджоникидзе, Российская Федерация
117997, Москва, ул. Миклухо-Маклая, 23: mustaevrn@mgri.ru
[4]Министерство науки и образования Азербайджанской Республики, Институт геологии и геофизики, Азербайджан
AZ1073, Баку, просп, Г. Джавида, 119: kadirovf@gmail.com

Резюме. В статье приведена характеристика нефтегазоматеринских толщ (НГМТ) Южно-Каспийского бассейна (ЮКБ) на основе результатов геохимических исследований и моделирования углеводородных систем. Для оценки генерационного потенциала НГМТ кайнозойского возраста ЮКБ были проведены пиролитические исследования методом пиролиза Rock-Eval-6 компании VINCI Technologies. В ЮКБ со сложным геологическим строением и геодинамическим развитием существуют весьма сложные условия для развития и распространения генерационно-аккумуляционных углеводородных систем. В процессе эволюции бассейна создавались уникальные условия для формирования углеводородных систем, существенно отличающихся от классических. В статье рассмотрены скорости осадконакопления и прогибания, а также региональный геотемпературный фон, влияющий на катагенетическую эволюцию органического вещества. Процессы генерации углеводородов в нефтегазоматеринских толщах кайнозойского возраста были исследованы на основе результатов моделирования углеводородных систем. В ЮКБ выделяется уникальный природный феномен – миоцен-плиоценовая генерационно-миграционно-аккумуляционная углеводородная мегасистема с резервуаром в продуктивной толще (ПТ), нефтегазоносность которой формируется за счет миграции углеводородов из нескольких нефтегазоматеринских толщ – в основном из олигоцен-миоценового (майкопского) и миоценового (тархан-чокракского и диатомового) возраста, частично из эоценового и самой ПТ, главным образом ее нижнего отдела, как по классическим схемам миграции, так и по системам грязевых вулканов, широко распространенных в ЮКБ. Наряду с вышеуказанной мегасистемой в пределах ЮКБ сформировались сланцевые углеводородные системы: диатомовая сланцевая углеводородная система, олигоцен-миоценовая сланцевая углеводородная система и эоценовая сланцевая углеводородная система, которые являются комбинированными нетрадиционными нефтегазовыми системами с углеводородами, частично эмигрировавшими из НГМТ и частично сохраненными (не вытесненными).

Ключевые слова: *Южно-Каспийский бассейн, углеводородная система, сланцевая углеводородная система, нефтегазоматеринская толща, органическое вещество, пиролиз*

CƏNUBİ XƏZƏR HÖVZƏSİNDƏ NEFT-QAZ ANA SÜXURLARININ SƏCİYYƏLƏNDİRİLMƏSİ VƏ KARBOHİDROGEN SİSTEMLƏRİNİN XÜSUSİYYƏTLƏRİ

Kərimov V.Yu.[1,3], Quliyev İ.S.[2], Cavadova A.S.[1], QədirovF.Ə.[1,4], Mustayev R.N.[3], Qurbanov V.Ş.[1], Hüseynova Ş.M.[1]

[1]Azərbaycan Respublikasının Elm və Təhsil Nazirliyi, Neft və Qaz İnstitutu, Azərbaycan
AZ1000, Bakı, F.Əmirov küç., 9: huseynova_shalala@yahoo.com
[2]Azərbaycan Milli Eəmlər Akademiyasının Rəyasət Heyəti, Azərbaycan
AZ1001, Bakı ş., İstiqlaliyyət küç., 30: i.s.guliyev@gmail.com
[3]Serqo Orconikidze adına Rusiya Dövlət Geoloji Kəşfiyyat Universiteti, Rusiya Federasiyası
117997, Moskva, Mikluxo-Maklay küç., 23: mustaevrn@mgri.ru
[4]Azərbaycan Respublikasının Elm və Təhsil Nazirliyi, Geologiya və Geofizika İnstitutu, Azərbaycan
AZ1073, Bakı, H.Cavid pr., 119, kadirovf@gmail.com

Xülasə. Məqalədə geokimyəvi tədqiqatların nəticələrinə və karbohidrogen sistemlərinin modelləşdirilməsinə əsasən Cənubi Xəzər hövzəsinin (CXH) neft-qaz ana süxurlarının (NQAS) xüsusiyyətləri təqdim olunur. CXH-nin Kaynozoy yaşlı NQAS-nın generasiya potensialını qiymətləndirmək üçün VINCI Technologies şirkətinin Rock-Eval-6 piroliz metodundan istifadə etməklə pirolitik tədqiqatlar aparılmışdır. Mürəkkəb geoloji quruluşa və geodinamik inkişafa malik CXH-də generasiya-akkumulyasiya karbohidrogen sistemlərinin inkişafı və yayılması üçün olduqca mürəkkəb şərait mövcuddur. Hövzənin təkamülü zamanı klassik sistemlərdən əhəmiyyətli dərəcədə fərqlənən karbohidrogen sistemlərinin formalaşması üçün unikal şərait yaranmışdır. Hövzənin çöküntütoplanma və çökmə sürətləri, həmçinin üzvi maddələrin katagenetik çevrilməsinə təsir edən regional geotemperatur fonu araşdırılır. Karbohidrogen sistemlərinin modelləşdirilməsinin nəticələri əsasında Kaynozoy yaşlı neft-qaz ana süxurları laylarında karbohidrogenlərin əmələ gəlməsi prosesləri tədqiq edilmişdir. Cənubi Xəzər hövzəsində unikal təbiət fenomeni olan Oliqosen-Miosen-Pliosen generasiya-miqrasiya-akkumulyasiya karbohidrogen meqasistemi müəyyən edilmişdir ki, həmin meqasistemin rezervuarı olan Alt Pliosen yaşlı Məhsuldar Qatın neft-qazlılığı bir neçə mənbədən, əsasən Oliqosen-Miosen (Maykop) və Miosen (Tarxan-Çokrak və Diatom) yaşlı neft-qaz ana süxurlarından, qismən Eosen və Məhsuldar qatın aşağı hissəsindən, həm klassik sxemlər üzrə həm də geniş yayılmış palçıq vulkanları sismeləri ilə miqrasiya edən karbohidrogenlərin hesabına formalaşır. Yuxarıda qeyd edilən meqasistemlə yanaşı, CXH daxilində şist karbohidrogen sistemləri də formalaşmışdır: Diatom şist karbohidrogen sistemi, Oliqosen-Miosen şist karbohidrogen sistemi və Eosen şist karbohidrogen sistemi. Həmin kombinə olunmuş qeyri-ənənəvi neft-qaz sistemlərindəki karbohidrogenlər qismən neft-qaz ana süxurlarından qismən emmiqrasiya etmiş və qismən saxlanılmışdır (emmiqrasiya etməmişdir).

Açar sözlər: *Cənubi Xəzər hövzəsi, karbohidrogen sistemi, şist karbohidrogen sistemi, neft-qaz ana süxurları, üzvi maddə, piroliz*

ANAS Transactions Earth Sciences 1 / 2024

http://www.journalesgia.com

TECTONICS AND MINERAGENY OF THE GARABAGH AND EAST ZANGAZUR (SOUTHEASTERN END OF THE LESSER CAUCASUS, AZERBAIJAN)

Kangarli T.N.

Ministry of Science and Education of the Republic of Azerbaijan,
Institute of Geology and Geophysics, Azerbaijan
119 H.Javid Ave., Baku, AZ1143: tkangarli@gmail.com

Keywords: *Lesser Caucasus, Garabagh and East Zangazur economic regions, tectonic zoning, minerageny, metallogenic zone, ore district, metallic (ore) and non-metallic (non-metalliferous) minerals*

Summary. The paper is devoted to tectonics, as well as formation and distribution regularities of various types of minerals within the Garabagh and East Zangazur economic regions (components of the Garabagh historical-geographical region of Azerbaijan), territorially confined to the southeastern margin of the Lesser Caucasus mountain-fold system. It is shown that tectonically the region belongs to the southeastern segment of the Artvin-Garabagh uplift (megazone), consisting of Lok-Garabagh, Goycha-Hakari and Gafan secondary structural zones and plunging northeast and southeastwards under recent continental molasses of the Middle Kur and Lower Araz superimposed depressions. It is noted that various types of metallic (ore) and non-metallic minerals are developed in the region. Minerageny of the metallic minerals characterizes geological regularities of the formation and distribution of various types of the ore minerals within the structure of metallogenic zones (corresponding to the same-named tectonic zones of the Artvin-Garabagh megazone) and ore districts of the region. Metallogenic zones were distinguished on the basis of tectonic-geodynamic zoning, geological evolution history and genetic types of the known ore deposits, and the ore bearing potential of separate geological formations within the Lesser Caucasus system. Minerageny of the non-metallic mineral deposits reflects the revealed placement and occurrence regularities of various non-metallic raw materials during the certain periods of geological evolution. The potential for increasing the list of industrially significant deposits is determined by numerous manifestations of ore and non-metallic mineral raw materials.

Introduction

The Garabagh and East Zangazur economic regions territorially related to the Garabagh historical-geographical region (Garabagh HGR) – one of the most resource-rich territories of Azerbaijan. The region covers the southeastern part of the Lesser Caucasus and the adjacent sloping plains of the Kura-Araz lowland south of the Tartar River. Territory of the region is part of the Pyrenean-Lesser Caucasus branch of the Alpine-Himalayan mobile-fold belt. Region covers the southeastern segment of the Artvin-Garabagh megazone of the Lesser Caucasus mountain-fold system, and the adjoining part of the Middle Kur depression (Геология Азербайджана. Том IV …, 2005; Azerbaycanın geologiyası. Cild I, 2015; Хаин, 1984, 2001). The border between these two systems is formed by the Pre-Lesser Caucasus deep fault which is buried under recent formations. The region is characterized by tectonic heterogeneity pronounced in complex correlation between its' structural units with different lithology-stratigraphic sections, diverse type of deformations and geological evolution background (Fig. 1).

Modern structure of the Lesser Caucasus was formed at the Alpine stage of tectogenesis within the spatial limits covering the northern edge of the South Azerbaijan segment of the Central Iranian microcontinent and the southern edge of the South Caucasus continental microplate (Геология Азербайджана. Том IV …, 2005; Azerbaycanın geologiyası. Cild I, 2015). The latter is a fragment of the Gondvana passive margin that was torn from the mainland during the Paleotethys opening and attached to Eurasia during movements of the tectogenesis of Hercynian cycle. In the tectogenesis of Alpine cycle the South Caucasus microplate looked like an island arc system (with a corresponding set of formations and mineragenic specialization), that separated the Greater Caucasus marginal sea from the Lesser Caucasus arm of the Mesotethys. In the contemporary structure, the plate central section corresponds to the Kur megadepression (intermountain

trough), where as its lateral sections, composed of volcanogenic and sedimentary complexes of the Jurassic, Cretaceous and Cenozoic rocks, participate in the generation of fold-mountain structures of the Greater (Kakheti-Vandam-Gobustan megazone) and the Lesser (Artvin-Garabagh megazone) Caucasus (Геология Азербайджана. Том IV, 2005; Azerbaycanın geologiyası. Cild I, 2015).

The main structural elements of the Artvin-Garabagh megazone are Lok-Qarabagh, Goycha-Hakari and Gafan secondary structural zones, built by the Mesozoic and partly Paleogene volcano-sedimentary and sedimentary rocks, and complicated by folding and rupture dislocations of the different shapes and genesis (Геология Азербайджана. Том IV, 2005; Azerbaycanın geologiyası. Cild I, 2015; Shikhalibeyli, 1966, 1994). On the southeastern immersion of the megazone, the Mesozoic structures plunge under the Eopleistocene-Holocene molasses of the Lower Araz superimposed depression. On the southwestern wing these structures are overlapped by the Eocene-Holocene volcanics of Kalbajar superimposed trough.

Complex and diverse geology-tectonic structure of the Earth's crust in the region preconditioned the formation of a wide range of both endogenous and exogenous mineral deposits (Геология Азербайджана. Том VI, 2005; Azerbaycanın geologiyası. Cild III, 2015; Минерально-сырьевые ресурсы Азербайджана, 2005; Мустафаев, 2002).

The study of the petrographic, mineralogical and geochemical features of the ore-bearing strata and the carried out tectonic-geodynamic reconstructions made it possible to carry out a structural-mineragenic zoning of the region with the identification of mineragenic taxa corresponding to the tectonic zones of the same name of various orders.

Tectonics

As stated above, the tectonic structure of the Garabagh HGR involves the Artvin-Garabagh and Middle Kur megazones (Геология Азербайджана. Том IV, 2005; Azerbaycanın geologiyası. Cild I, 2015).

The Artvin-Garabagh megazone represents a structural uplift on the natural eastern extension of the East Pontian (Artvin) uplift in Turkey. Within the boundaries of the region, the megazone is represented by its' southeastern termination covering the axial line, as well as the northeastern, southeastern and southwestern slopes of the Lesser Caucasus mountains. The northeastern wing of the megazone is separated from the Middle Kur megazone by the Pre-Lesser Caucasus deep fault buried under the Pliocene-Pleistocene molasses. The southwestern border is formed by the Girratagh deep fault, along which the Paleozoic complex of the Araz block within the Dinar-Zond branch of the Alpine-Himalayan belt is thrusted over the Upper Jurassic-Neocomian complex of the Artvin-Garabagh megazone.

Fig. 1. Tectonic zoning of the Garabagh HGR

The main structural elements of the megazone are the Lok-Garabagh, Goycha-Hakari and Gafan secondary structural zones, built by the Mesozoic and partly Paleogene volcano-sedimentary and sedimentary rocks, and complicated by folding and rupture dislocations of the different shapes and genesis. On the southeastern immersion of the megazone, the Mesozoic structures plunge under the Eopleistocene-Holocene molasses of the Lower Araz superimposed depression. On the southeastern wing these structures are overlapped by the Eocene-Holocene volcanics of the Kalbajar superimposed trough (Геология Азербайджана. Том IV, 2005; Azerbaycanın geologiyası. Cild I, 2015; Шихалибейли, 1966, 1994).

Therefore, modern geological structure of the megazone is represented by the following secondary structural zones, from the northeast to the southeast:

1. The Lok-Garabagh zone represents a complexly structured folded block system, composed of an echelon of anticlinal and synclinal structures. The composition of the zone includes the Mesozoic and partly Paleogene volcanic, volcano-sedimentary and sedimentary material complexes, as well as differently composed intrusive formations. The northeastern flank of the zone is concealed under the Pliocene-Holocene molasses of the Middle Kur depression. The southwestern flank is bordered by the Goycha-Hakari zone along the system of large upthrusts and overthrusts.

2. The Goycha-Hakari zone is built by the Jurassic, Cretaceous and Paleocene-Eocene sedimentary-volcanic series gathered in compressed folds. The structure of the zone covers the Toraghaychay and Saribaba troughs located en echelon and conjugated along a tectonic contact. The southwestern border of the zone is determined by the Lachin-Bashlibel deep fault. The zone includes the southeastern segment of Amasya-Goycha-Hakari allochthonous ophiolite belt represented by a pack of tectonic nappes and olistostromes. The nappes had been formed between the Late Cenomanian and the Eocene. Joint structural plan of autochthonous and allochthonous complexes is leveled by a neoautochthonous cover formed by the Upper Santonian-Eocene sedimentary-volcanogenic strata (Геология Азербайджана. Том IV, 2005; Azerbaycanın geologiyası. Cild I, 2015; Hasanov, 1985).

3. The Gafan zone is built by sedimentary-volcanic and volcanic complexes of the Jurassic, Cretaceous and Paleogene. The northeastern flank of the zone is complicated by the anticlinal highs of Lachin and Kohna Taghlar, separated from each other by Chaylaggala synclinal stripe. The central place in the zone is occupied by the Hochaz trough overlapped by the Eocene-Holocene complex of the Kalbajar superimposed trough in the northwest, and plunging under the Pleistocene continental molasses of the Lower Araz trough in the southeast. The southwestern flank of the zone is represented by Gafan-Basitchay dome elevation.

4. The Kalbajar zone covers the upper course basins of Tartar and Hakari rivers. It corresponds to the eastern segment of Goycha-Ordubad rift graben built by the Paleocene-Holocene volcano-sedimentary and volcanic complexes. The zone forms an Eocene-Pliocene superimposed depression that gently levels the structural plan of the western extension of the Gafan and Goycha-Hakari structural zones.

5. The Lower Araz zone represents a transverse superimposed trough extending along the riverbed of Araz, starting from the Mighri canyon till joining with the Pre-Lesser Caucasus trough. The sedimentary rocks of the zone are represented by the Eopleistocene-Quaternary molasses. The molasses overlap the Jurassic, Cretaceous and Paleogene-Eocene stratas of the first three structural zones, all plunging under the Lower Araz zone with azimuthal unconformity from the northwest.

The Middle Kur meqazone corresponds to an intermountain depression, occupies the central place in the structure of the Kur superimposed depression, being its' largest and the most complexly structured component. The megazone consists of secondary structural zones that are buried under gentle Pliocene-Holocene molasses, built by dislocated volcanic and sedimentary series of the Meso-Cenozoic (Геология Азербайджана. Том IV, 2005; Azerbaycanın geologiyası. Cild I, 2015).

1. The Pre-Lesser Caucasus zone corresponds to the northeastern flank of the Artvin-Garabagh megazone, downcast along the Pre-Lesser Caucasus fault that is buried under recent deposits, and built by the Mesozoic volcano-sedimentary and Paleogene-Quaternary mainly molasses formations. With gentle and smooth bedding of the Pliocene-Quaternary deposits observed, the underlying Paleogene-Mesozoic stratas are gathered in a system of brachiform folds.

2. The Yevlakh-Aghjabadi zone represents a deep trough formed over the formations of the Mesozoic, Paleogene and partly Miocene rocks complicated by local uplifts and gently overlapped by the Pliocene-Quaternary molasses. The Alpine cover thickness in the most immersed part of the zone reaches and sometimes even exceeds 16 km. The trough is bordered by the Imishli-Goychay buried deep fault from the northeast, and by the Southern Kur buried deep fault from the southwest. İn the northeast (outside Garabagh) the zone along the İmishli-Göychay deep fault is separated from the Kurdamir-Saatli zone (buried Mesozoic uplift), which an eroded cover of the Cretaceous series plunges under the series of the Upper Miocene

– Holocene (depth -3.0-3.5 km) and pre-Jurassic basement (depth -9-10 km).

Minerageny of metallic minerals

Metallic minerals of the zone are represented by deposits of chrome, copper, polymetals, gold, mercury and antimony. Along with basic metals, ore bodies of these deposits contain silver, molybdenum, nickel, bismuth, tellurium, and other valuable metals (Геология Азербайджана. Том VI, 2005; Azerbaycanın geologiyası. Cild III; Ismail-Zadeh, Kangarli, 2012; Минерально-сырьевые ресурсы Азербайджана, 2005; Мустафаев, 2002; Шихалибейли, 1994). The most significant reserves of the region are the gold bearing deposits.

Minerageny of metallic minerals characterizes geological regularities of the formation and distribution of various types of the ore minerals within the structure of metallogenic zones (corresponding to the same-named tectonic zones of the Artvin-Garabagh megazone) and ore districts of the region. Metallogenic zones were distinguished on the basis of tectonic-geodynamic zoning, geological evolution history and genetic types of the known ore deposits, and the ore bearing potential of separate geological formations within the Lesser Caucasus system (Fig. 2).

The Lok-Garabagh metallogenic zone is characterized by a mineralization associated with the Middle Jurassic quartz plagioporphyres, plagiogranites and andesites, as well as with the Upper Jurassic-Lower Cretaceous granitoids. The main mineralization types are distributed as follows: 1) plagioporphyres – pyrite, copper-pyrite and gold-copper-pyrite; 2) plagiogranite massifs – copper-porphyry, complicated by tectonic faults; 3) andesites – copper-pyrite; and 4) granitoids – magnetite, cobalt, alunite, vein-polymetallic, copper-porphyry. Mineralization is represented by the deposits and occurrences spread within the ore districts of Mehmana and partly South Garabagh.

The Mehmana ore district is located on the southeastern wing of the Tartar-Injachay faulting zone. It covers the interfluve of Tartar and Khachinchay rivers, where a number of deposits and occurrences of copper-porphyry, copper-pyrite, gold-copper-pyrite and polymetallic (lead-zinc) ore formations had been developed. Derivatives of the copper-porphyry ore formation are grouped within the Demirli and Khachinchay ore fields. The Demirli ore field consists of the Demirli deposit and the occurrences of Aghdara, Yukhari Janyatag, Ashagi Gulyatag, Boyahmadli, Khatinbeyli, etc. The Khachinchay ore field includes the Khachinchay, Galaychilar, Yeddigyrkhman and several other different-size occurrences. Both ore fields are located on the western endo- and exocontact strip of the Mehmana granitoid intrusive of the Upper Jurassic-Lower Cretaceous age.

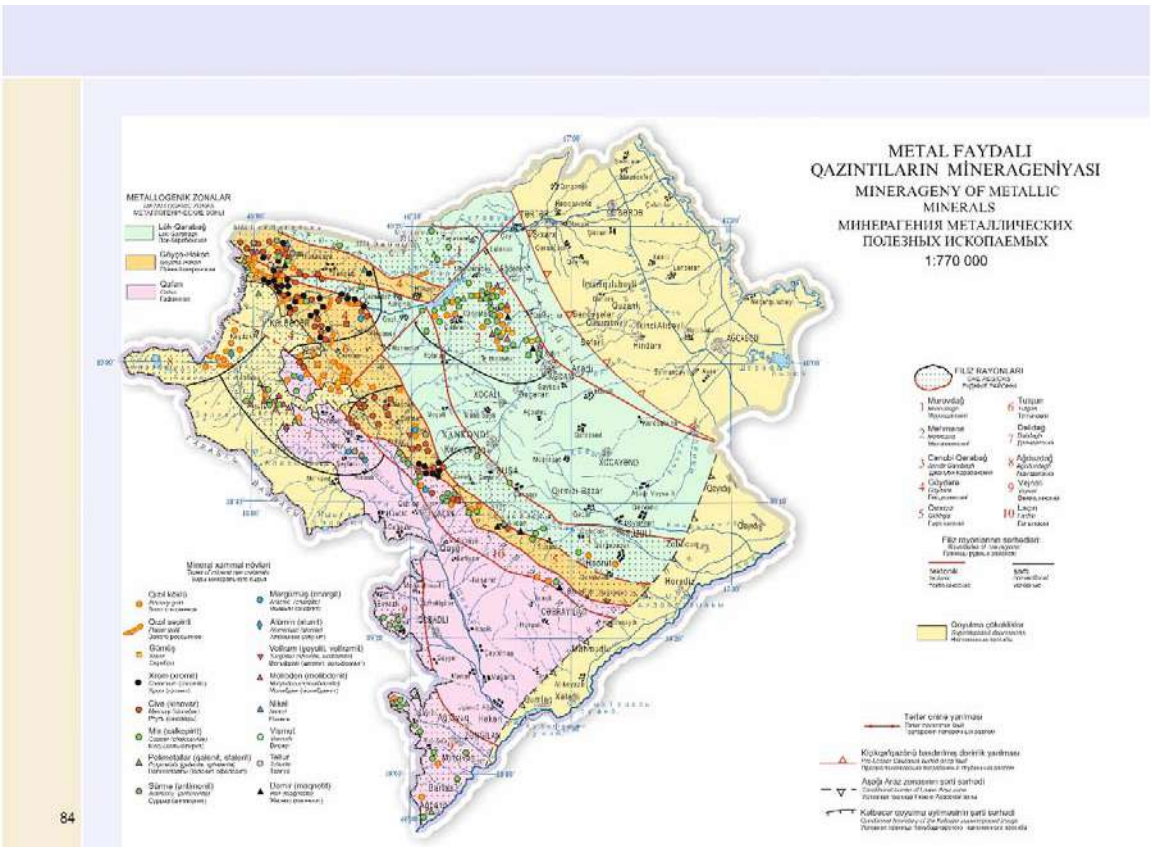

Fig. 2. Minerageny of metallic minerals of the Garabagh HGR

Additionally, there are several bodies of copper-pyrite ore formation observed at the same endo- and exocontact and at some distance from the intrusive among the Bathonian volcanics. Pyrite-chalcopyrite mineralization of the impregnated-veinlet type is represented by several occurrences, including Yukhari Gulyatag, Khazinadagh, Chullu, Demirli, Ashaghi Janyatag, Gazanchi and Vankli. The gold-copper-pyrite ore formation is represented by the Gizilbulag ore field corresponding to an ancient volcanic center located on the right shore of the Sarsang water reservoir. The ore field consists of Gizilbulag copper-gold deposit and a number of occurrences, including Heyvali, Almali, Anbarchay, Girmizitepe, Garbi Gizilbulag, etc. The polymetallic (lead-zinc) ore formation consists of Mehmana deposit and Chiragli occurrence localized within the structure of the Mehmana ore field in the interfluve of Tartar and Gabartichay.

The South Garabagh ore district is confined to the southeastern termination of the Lok-Garabagh metallogenic zone. Structurally it corresponds to the Garabagh uplift. In the district, there are several minor copper-pyrite deposits (Boyuk Taghlar, Argunesh, Bina, etc.) having no commercial value but important as ore prospecting criteria. The ore mineralization is usually confined to the zone of tectonic dislocations and dyke complexes and represented by native copper, chalcopyrite, chalcosine, cuprite, pyrite, sphalerite and galenite.

Mineralization of the **Goycha-Hakari metallogenic zone** is associated with ophiolite association, Upper Cretaceous limestones, Eocene granitoid intrusives and Miocene-Pliocene acidic volcanics. The ophiolite association is represented by chromite and scheelite mineralization, while the other complexes – by the occurrences of mercury, antimony, gold and arsenic. The part of the province that covers the territory of the Garabagh nature zone, is divided into Goydara, Girkhgiz and Tutgun ore districts.

The Goydara ore district is located in the middle course of Tartar, covering an area between Shargi Goycha range and the river valley of Tutgunchay. The district is represented by the deposits and occurrences of chromite, mercury (arsenic-antimony-mercury), gold (gold-polysulphide-quartz) and molybdenum-tungsten) ore formations. Genetically related to widely developed ultrabasites, the chromite ore formation forms Goydara and Kazimbina group of chromite deposits and occurrences. The mercury (arsenic-antimony-mercury) formation is represented by more than 40 mercury and sometimes complex mercury-antimony deposits, occurrences and mineralization fields. The ore manifestations are either grouped within the structure of Levchay, Guneypaya, Gamishli, Soyudlu, Gilinjli, Agyatag ore fields, or represented as separate objects. Commercially valuable manifestations identified by geological exploration reconnaissance activities are Agyatag, Eyvan, Levchay, Shorbulag, Aggaya, Arkhajdere, Gamishli and Zulfugarli mercury deposits, as well as multiple occurrences, including Garbi and Yeni Lev, Garagaya, Shirran, Yelizgol, Seyidler, Atdashi, Yalkend, Garbi Gamishli, Tal, Bashkend, Milli, Saridash, Arkhajdere, Goyukguney, Sarigilinj, Abdullaushaghi, Hajidere, Duzyurd, Gayali, Gushyuvasi, Kiliseli, Otaglar, Chapar, Bashlibel, etc. Gold (gold-polysulphide-quartz) ore formation is concentrated in the Soyudlu ore cluster detected on the northwestern flank of the ore district. The formation is represented by the Zod deposit and more than 20 occurrences, including Gonur, Goydara, Damirchidam, Istibulag, Alagollar, Nariman, Garbi Palidli, Soyudlu, etc. Quartz-scheelite subformation is observed in the quartzy veinlets of the listvenite zones, where it is detected together with pyrite, stibnite, bismuthinite and cinnabar. In the ore district there are several scheelite occurrences, including Goydara, Gonur, Saridash, etc.

The Girkhgiz ore district covers part of the Garabagh range between watershed peaks of Chilgaz and Saribaba. The district is characterized by chromite, mercury and partly arsenic mineralization. The chromite ore formation is represented by Ipak group of occurrences (Ashaghi Ipak, Orta Ipak I and II, Khalifali, Gozlu, etc.) confined to serpentized peridotites that are exposed in the southeastern part of the district in the upper courses of Khalifalichay and Ipakchay rivers. The mercury (arsenic-antimony-mercury) ore formation is represented by Chilgazchay and Narzanli deposits, as well as several occurrences (Nagdalichay, Shamkend, Erikli, Garaboylu, Garibli, Dumanli, Ipak, Bozguney, Shimshak, Elyeri, Gorchu, etc.) and mineralization fields. Forming part of the formation and confined to the rupture dislocation zones, arsenic mineralization is represented by Deveboynu and Goshasu occurrences detected in the upper course basin of Hakari River.

The Tutgun ore district is located on the southwestern wing of the Goycha-Hakari metallogenic province. Characterized by the gold-quartz mineralization, it covers the upper course basin of Tutgunchay River. Within the ore district boundaries, there are more than 100 hydrothermally altered zones with different gold content, all distributed over several gold-bearing areas in the following ratio: Giziliten – 40, Agzibir – 20, Gazikhanli – 30, Galaboynu – 11, etc.

The Gafan metallogenic zone is characterized by copper-molybdenum, copper-pyrite, gold-quartz and partly tungsten and alunite mineralization. In the territory of the Garabagh nature zone, the province is

divided into Dalidagh, Aghduzdagh and Vejnali ore districts, as well as Lachin perspective ore bearing zone.

The Dalidagh ore district covers the upper courses of the rivers of Tartar and partly Hochazsu (right-bank tributary of Hakari). The district is characterized by the development of secondary copper-molybdenum and polymetallic, and partly molybdenum-tungsten ore formations. Copper-molybdenum formation is represented by the ore containing quartz veins and hydrothermally altered rock zones located within an endocontact of the Dalidagh granitoid intrusive in the northwestern and partly southeastern parts of the district. There are Teymuruchandagh deposit and Baghirsag, Sultanheydar, Gatardash, Dalidagh-Aghchay occurrences of molybdenum-tungsten ores in this territory. The polymetallic ore formations are in most cases confined to the exocontact and apical parts of the Dalidagh interusive, where they are represented by Baghirsag, Dalidagh, Garanlig and several other occurrences localized among skarnified carbonate and volcano-sedimentary series. The molybdenum-tungsten ore formation is represented by scheelite-tungsten mineralization. In total within the ore district boundaries, there are 81 tungsten containing quartz veins, 37 of which have been thoroughly studied and assessed.

The Aghduzdagh ore district is situated in the northwestern limb of the Kalbajar superimposed trough, covering the slopes of Shargi Goycha range on the left riverbank of Tartar and represented by secondary gold-quartz and alunite ore formations. The gold-quartz formation is developed relative to Keytidagh caldera and a controlling submeridional fault zone. The structure of the formation contains the Aghduzdagh deposit as well as Shirvan, Keytidagh, Zaylik, Vagif, Sabir, Fuzuli and several other occurrences of gold bearing ores. Alunite ore formation is represented by non-commercial Zar-Zaylik occurrence situated in the northeastern vicinity of Keytidagh caldera.

The Vejnali ore district corresponds to the southern segment of the Gafan-Basitchay uplift which covers the interfluve of Bargushad and Araz rivers. The geological structure of the district is constituted by the Middle-Upper Jurassic and Lower Cretaceous volcanic and volcano-sedimentary rocks protruded by hypabyssal intrusive of granodiorites, gabbros, diorites and quartz diorites. Presence of the latter formations had preconditioned development of the gold-polysulphide-quartz and copper-pyrite ore formations. The gold-polysulphide-quartz formation is represented by the Vejnali deposit and several occurrences located on the southwestern wing of the district. The copper-pyrite formation includes Aghkend occurrence located in the north on the right riverbank of Bargushadchay, as well as Garadere-Aghband group of copper ore occurrences detected in the district's central segment.

The Lachin perspective ore district corresponds to the same-named structural high built by the Middle-Upper Jurassic and Lower Creetaceous volcanic and volcano-sedimentary rocks and protruded by granitoid intrusives. There are several mineralization spots and minor occurrences of sulphur-copper-pyrite, arsenic, gold and mercury mineralization within the district boundaries.

Minerageny of non-metallic minerals

Non-metallic mineral deposits of the Garabagh nature zone are represented by mining, chemical and refractory raw materials, semiprecious and ornamental stones, as well as construction materials, including saw, facing and rubble stones, lime and cement, binding brick production materials, as well as fillers for concrete and the road construction materials. Total reserves of these minerals amount to tens of millions of cubic meters (Геология Азербайджана. Том VI, 2005; Azerbaycanın geologiyası. Cild III, 2015; Минерально-сырьевые ресурсы Азербайджана, 2005; Shikhalibeyli, 1994).

Minerageny of the non-metallic mineral deposits reflects the revealed placement and occurrence regularities of various non-metallic raw materials during the certain periods of geological evolution (Figs. 3, 4). Within the region boundaries, there are two minerogenic taxons corresponding to the same-named tectonic zones in the mountainous (the Artvin-Garabagh tectonic megazone) and lowland (the Middle Kur tectonic megazone and the Lower Araz tectonic zone in the southeastern subsidence of the Lesser Caucasus system) parts of the area. The first taxon is placed in the structure of Lok-Garabagh, Goycha-Hakari, Gafan and Kalbajar zones, where it is built by the Jurassic, Cretaceous and Paleogene-Eocene rocks in magmatic, terrigenous and carbonate facies, as well as the Miocene-Pliocene-Holocene volcanics of Garabagh plateau. The second taxon is represented by the Oligocene-Holocene marine and continental deposits of the Middle Kur and Lower Araz zones.

The cited formations are connected to multiple deposits and occurrences of various nonmetallic minerals used in the following industry sectors: 1) mining and chemical (barite, pyrite, soda, Icelandic spar (optical calcite), piezoquartz, zeolites, lithographic stone); 2) mining and metallurgical (flux limestones, kaolinite, bentonite clays, serpentinites); 3) precious, semi-precious and ornamental stone production; and 4) construction (e.g. sawing, facing and building stones, cement raw materials (lime-

stone, loam, marl, volcanic ash, pumice), binders (gypsum, drywall), mineral paints, raw materials for brick production (clay and loam), fillers for concrete and road-building materials (sand-gravel and sand-boulder-gravel mixture, construction sand, perlite, vermiculite).

According to formation conditions, industrial mineral deposits may be of the endogenous (actually magmatic, hydrothermal and skarn deposits, pegmatites), exogenous (weathering (clastic, residual, infiltration and hypergene) and sedimentary (mechanical and chemogenic) deposits) or metamorphogenic (metasomatic) origin. In terms of tectonic and formational confinement, industrial mineral deposits of the Garabagh nature zone are distinguished within the structure of the following formations:

The Lok-Garabagh zone is represented by the Bajocian-Bathonian volcanic-terrigenous, Late Jurassic terrigenous-volcanic-carbonate, Early, Middle and Late Cretaceous volcanic-terrigenous-carbonate formations, as well as Paleogene terrigenous formation exposed in the zone's northeastern periphery. The first two formations of the zone are rich in various types of industrial mineral deposits.

The Middle Jurassic volcanic-terrigenous formation is represented by effusive and partly sedimentary rocks, and characterized by widely developed zones of hydrothermally altered series scattered along differently oriented fault dislocations. The structure of the formation is broken by multiple different-size Middle and Upper Jurassic acidic intrusives. The formation contains resources of hydrothermal barite, pyrite, mineral paints, secondary quartzites, pegmatite jewelry (agate, chalcedony) and ornamental (jasper) stones, magmatogenic ornamental (felsitic tuff) and facing (basalt, porphyrites) stones, metamorphogenic andalusite and hypergene malachite (a product of copper ores weathering), as well as fossilized remains of trees as ornamental stone.

Being in paragenesis with predominantly acidic (gabbro-tonalite formation) intrusions, *the Late Jurassic terrigenous-volcanic-carbonate formation* contains manifestations of hydrothermal Icelandic spar, mineral paints, jewelery stones (opal), pegmatite jewelry and ornamental stones (agate, carnelian), biogenic and chemogenic limestones and corals, magmatogenic facing and building stones (volcanic tuffs, gabbros, gabbroids, gabbro-diabases, diorites, granodiorites), metamorphogenic andalusite and marbled limestones, as well as chemogenic and hydrothermal gypsum. Additionally, there are the deposits and occurrences of coal used as fuel and energy raw material.

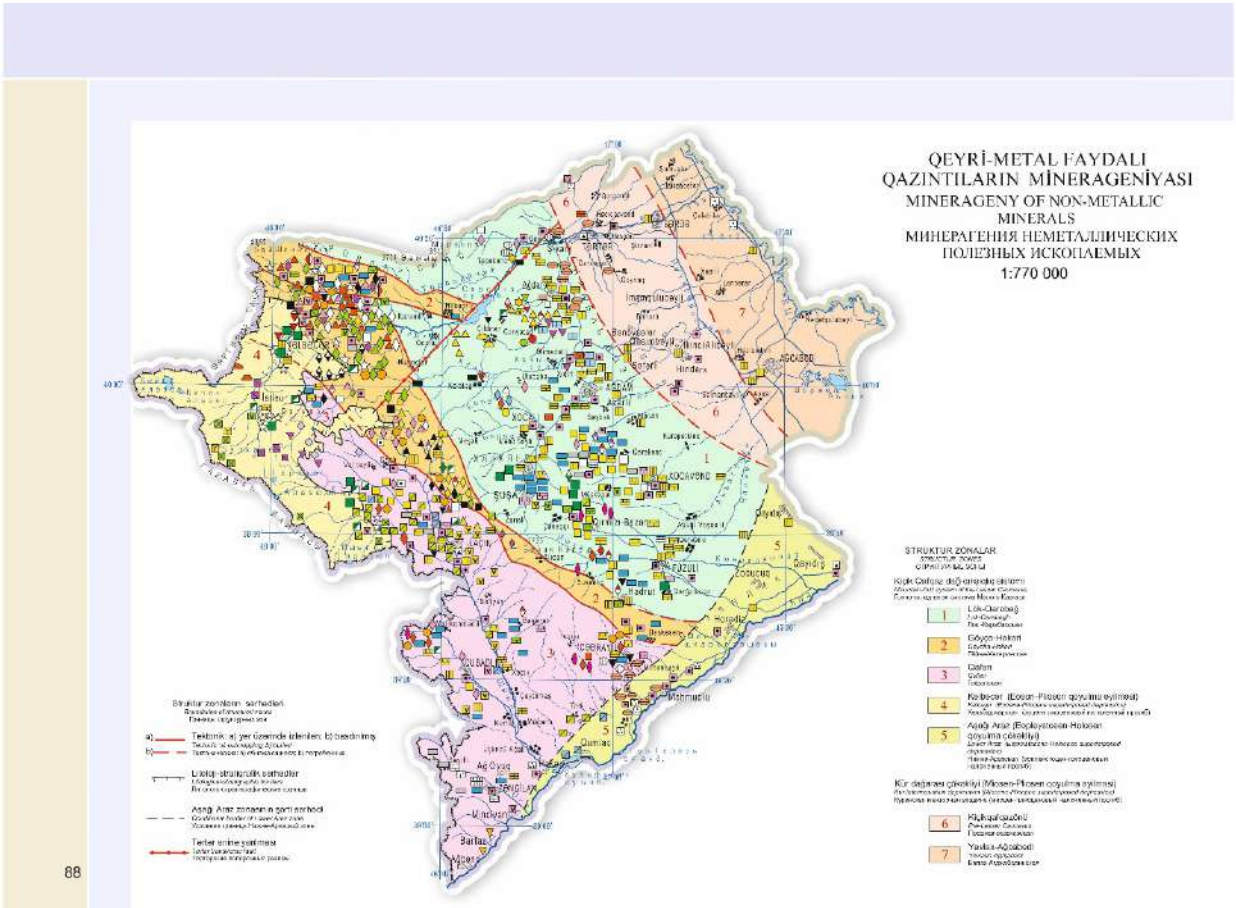

Fig. 3. Minerageny of non-metallic minerals of the Garabagh HGR

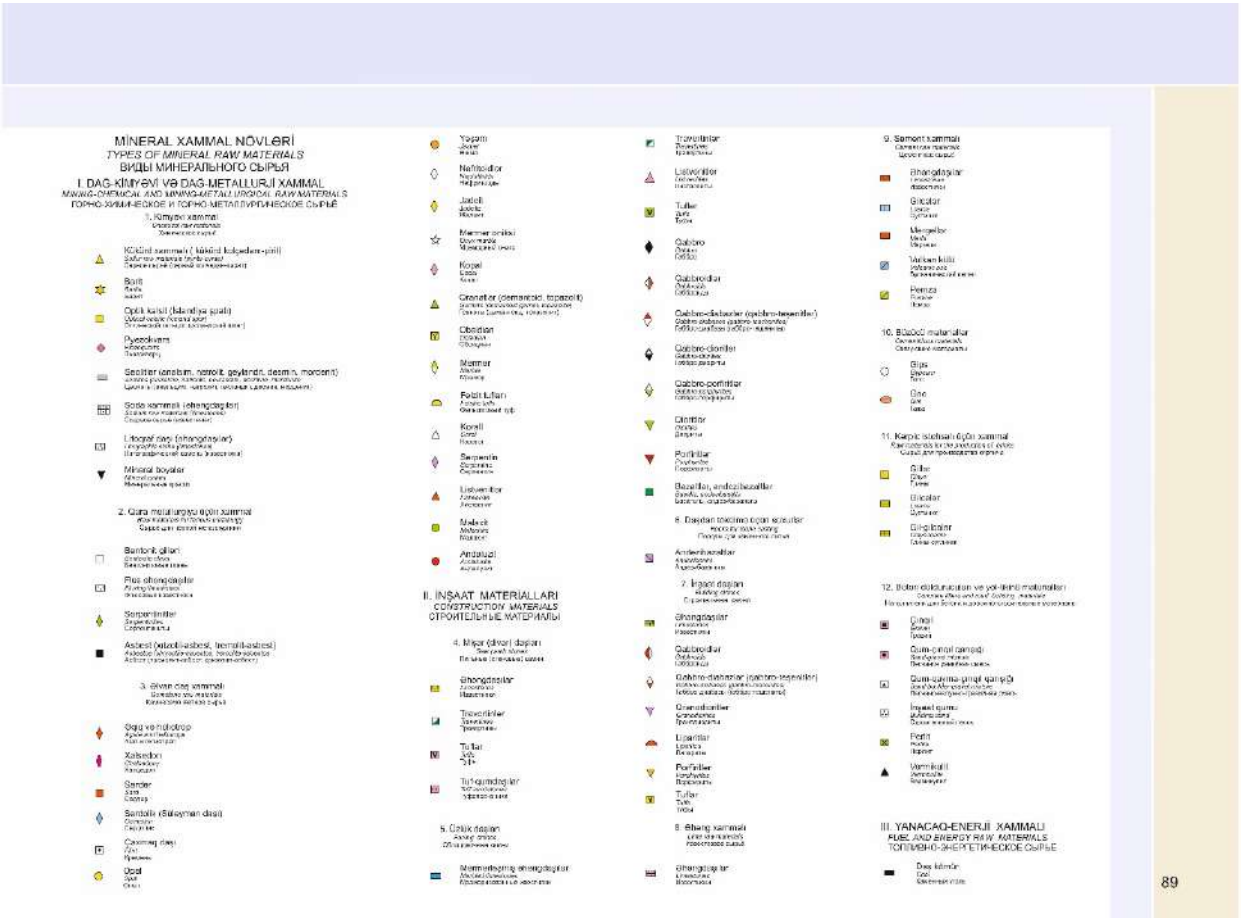

Fig. 4. Legend to the map of minerageny of non-metallic minerals

The volcanic-terrigenous-carbonate formation of the Early-Middle Cretaceous deposits is in paragenesis with mainly acidic (gabbro-tonalite formation) intrusives. There are the deposits and occurrences of such nonmetallic minerals as biogenic and chemogenic limestones (fluxing, building) and biogenic precious stones (copal), pegmatite precious (agate) and ornamental (jasper) stones, magmatogenic facing (gabbro-diabases, gabbro-porphyrites) and building (porphyrites, tuffs) stones, metamorphic marbled limestones, etc. in the formation.

Being similar to the previous complex in terms of formation, the Late Cretaceous complex is in paragenetical relation with intrusions of basic composition (formation of subalkaline gabbroids). The formation is characterized by the presence of deposits and occurrences of hydrothermal Icelandic spar, zeolites, kaolinite and mineral paints, residual bentonites, chemogene lithographic stone, pegmatite precious (agate, chalcedony) and ornamental (jasper) stones, magmatogenic building (tuff) and facing (gabbro-diabase) stones, biogenic and chemogenic saw and building limestones, chemogenic marls (cement raw material), mechanical sludge (clays), metamorphic marbled limestones and volcanic pumice (cement raw material).

In addition to the listed mineral raw material types, there are young occurrences of chemogenic travertine, as well as deposits of different building materials, including sandstone, gaja, clay, loam, mason's sand, gravel and sand-gravel deposits. These manifestations are detected in the formation of the Pleistocene-Holocene continental molasses. This formation is superposed on the more ancient complexes of the northeastern wing of the zone.

The Goycha-Hakari zone is mainly represented by the *Upper Cretaceous ophiolite formation* which overlies the Lower Cretaceous volcanic-terrigenous-carbonate series and partly underlies the terrigenous-volcanic rocks of Eocene. The formation is associated with manifestations of hydrothermal zeolites, Icelandic spar, secondary quartzites, pyrites, mineral paints, hydrothermal-metamorphic serpentinites, listvenites, asbestos, marbles, pegmatite precious (carnelian, sarder, cream) and ornamental (jasper) stones, biogenic precious stones (copal), hydrothermal precious (nephrites, jadeite, garnets) and ornamental (listvenite, serpentine) stones, magmatogenic facing (gabbros, gabbroids, gabbro-diabases, gabbro-diorites, diorites, basalts, basaltic andesites), facade (tuffs) and construction (granodiorites, gabbroids, tuffs) stones, as well as hypergene

vermiculite, volcanic pumice, residual bentonite clays, biogenic and chemogenic limestones as cement raw materials, wall stones, rubble stones, and marbled limestones.

Within the zone's boundaries, there are also ornamental (marble onyx) and facing (travertine) stone occurrences confined to *the chemogenic formation of the Late Pliocene-Holocene* – products of chemical precipitation of a calc-spar from hot mineral springs. In addition, one deposit of the Lower Pleistocene clays and several gravel and sand-gravel deposits were established in the alluvium of the mountain rivers.

The Gafan zone has its' northeastern wing built by the Bajocian-Bathonian volcanic-terrigenous formation. In its' southeastern plunge, the formation is superstructed by the Late Jurassic terrigenous-volcanic-carbonate formation. The southeastern wing of the zone is represented by volcanic-terrigenous-carbonate formation of the Early and Middle Cretaceous series, and the central segment – by the similarly composed Late Cretaceous formation, southwestern segment of which is overlapped by the Late Pliocene-Holocene formation of secondary trachybasalts and trachyandesites.

The Middle Jurassic formation is composed similarly to the same-age complex of the Lok-Garabagh zone. The formation is breached by different-age acidic intrusives, and characterized by the occurrences of hydrothermal mineral paints, pyrite and listvenite, magmatic building (tuff) and facing (gabbro) stones, pegmatite ornamental stones (jasper) and residual bentonite clays.

Composition of the *Upper Jurassic terrigenous-volcanic-carbonate formation* includes marbled limestones and limestones that are used as the wall stones.

The Early-Middle Jurassic formation is in paragenetic relations with acidic (gabbro-tonalite formation) intrusives. The composition of the formation includes biogenic and chemogenic limestones (fluxing, wall and soda raw materials), metamorphic marbled limestones, hydrothermal zeolites, biogenic precious stones (copal), pegmatite precious (agate) and ornamental (jasper) stones, magmatogenic facing (gabbro-diabase), walling (tuff) and building (porphyrites, tuff) stones.

The Late Cretaceous volcanic-terrigenous formation contains deposits and occurrences of hydrothermal Icelandic spar, piezoquartz, zeolites, mineral paints, sulfur pyrite, pegmatite precious (agate, chalcedony, sardius, flintstone) and ornamental (jasper) stones, biogenic, chemogenic (walling stones and raw materials for the production lime) and marbled limestones, magmatic facing (basalts, gabbro), walling (tuffs) and building (granodiorites, tuffs) stones, volcanic ash and pumice, as well as volcano-sedimentary tuffaceous sandstones.

The Late Pliocene-Holocene chemogenic formation is represented by travertines, suitable for walling and facing works. In the section of the same-aged trachybasalt-trachyandesite formation, there are deposits of magmatic volcanic ashes and pumice (raw materials for the production of cement). The deluvial deposits of the same age include manifestations of clays and loams, and the river alluvium contains occurrences of sand-gravel and sand-boulder-gravel mixtures. Finally, there are deposits of chemogenic gypsum and drywall detected in the section of continental molasses, confined to the southeastern immersion of the Gafan zone.

The Kalbajar zone (Garabagh plateau). The surface structure of the zone is constituted by magmatic formations of the Eocene-Holocene. The Eocene terrigenous-volcanic formation is in paragenesis with mainly acidic intrusives (granosyenite-granite formation). Within the formation structure, there are deposits of magmatic facing (basalts, porphyrites, andesibasalts, gabbro-diorites) and construction (liparites) stones. Also being in paragenesis with mainly acidic intrusives (granosyenite-granite formation), the Miocene andesite-dacite-rhyolite formation is represented by the building stone deposits of hydrothermal-vein piezoquarts and granodiorites. The Late Pliocene rhyolite formation contains deposits of iridescent obsidian. In the trachybasalt-trachyandesite formation of the Late Pliocene-Holocene, there are the deposits of cast stone materials (basaltic andesites), volcanic tuffs and ash, as well as pumice and perlite used for the production of cement and other building materials. In turn, the same-aged chemogenic formation is represented by the deposits of ornamental (marble onyx) and facing (travertine) stones, both products of chemical precipitation of calc-spar from the thermal mineral springs.

The Middle Kur zone. On the erosional truncation, the zone is built by Late Pliocene marine terrigenous formation containing sedimentary sandstones, and Pleistocene-Holocene continental molasse formation, containing chemogenic gaja and mechanical sediments (clay, loam, sandy loam, masonry sand, gravel, sand-gravel and sand-boulder-gravel mixtures) used as construction materials.

The **Lower Araz zone** is represented by two continental formations. Late Pliocene-Early Pleistocene terrigenous-volcanic formation contains the horizons of volcanic ash, vitric tuff and pumice (raw material for the production of cement and other construction materials) enclosed in the alluvial-proluvial continental molasses. Pleistocene-Holocene continental molasse formation has a nonmetallic mineral content similar to its' analogue within the structure of the Middle Kur zone.

Conclusions

The minerageny of the southeastern end of the Lesser Caucasus is determined by the geodynamic setting of the formation of structural zones, the geochemical characteristics of structural-material complexes, and their age evolution. The established geological patterns of the formation and spatial distribution of various types of mineral raw materials make it possible to predict the discovery of new industrially significant deposits, both due to the known numerous manifestations, and new promising areas. Provision with mineral resources is a factor of economic security and a guarantor of the social stability of the region in the medium and long term.

REFERENCES

Geology of Azerbaijan (chief ed. Ak.A.Ali-zadeh). Volume VI. Economic minerals. Nafta-Press. Baku, 2005, 578 p. (in Russian).

Geology of Azerbaijan (chief ed. Ak.A.Ali-zadeh). Volume IV. Tectonics. Nafta-Press. Baku, 2005, 506 p. (in Russian).

Geology of Azerbaijan (chief ed. Ak.A.Ali-zadeh). Volume I. Stratigraphy, lithology, tectonics. Nafta-Press. Baku, 2015, 532 p. (in Azerbaijani).

Geology of Azerbaijan (chief ed. Ak.A.Ali-zadeh). Volume III. Magmatism, solid minerals, hydrogeology, geological engineering. Nafta-Press. Baku, 2015, 382 p. (in Azerbaijani).

Hasanov T.Ab. Ophiolites of Lesser Caucasus. Nedra. Moscow, 1985, 240 p. (in Russian).

Ismail-Zadeh A.J., Kangarli T.N. Geodynamic environment of the formation of ore complexes and metallogenic epochs of the Eastern Caucasus. In the book: The modern problems of geology and geophysics of Eastern Caucasus and the South Caspian depression. Nafta-Press. Baku, 2012, pp. 132-145.

Khain V.Ye. Regional geology. Alpine-Himalayan belt. Nedra. Moscow, 1984, 344 p. (in Russian).

Khain V.Ye. Tectonics of continent and oceans. Nauchni Mir. Moscow, 2001, 606 p. (in Russian).

Mineral-products resources of Azerbaijan (chief ed. V.M.Baba-zadeh). Ozan. Baku, 2005, 808 p. (in Russian).

Mustafayev G.V. Main features of Azerbaijan's metallogeny. Nafta-Press. Baku, 2002, 231p. (in Russian).

Shikhalibeyli E.Sh. Geological structure and history of tectonic development of the eastern part of the Lesser Caucasus (tectonic structure and magmatism). Publishing house of the Academy of Sciences of the Azerbaijan SSR. Baku, 1966, 263 p. (in Russian).

Shikhalibeyli E.Sh. Geology and mineral resources of Nagorno-Karabakh of Azerbaijan. Elm. Baku, 1994, 284 p. (in Russian).

ЛИТЕРАТУРА

Ismail-Zadeh A.J., Kangarli T.N. Geodynamic environment of the formation of ore complexes and metallogenic epochs of the Eastern Caucasus. In the book: The modern problems of geology and geophysics of Eastern Caucasus and the South Caspian depression. Nafta-Press. Baku, 2012, pp. 132-145.

Геология Азербайджана (гл.ред. Ак.А.Ализаде). Том VI. Полезные ископаемые. Nafta-Press. Баку, 2005, 578 с.

Геология Азербайджана. (гл.ред. Ак.А.Ализаде). Том IV. Тектоника. Nafta-Press. Баку, 2005, 506 с.

Гасанов Т.А. Офиолиты Малого Кавказа. Недра. Москва, 1985, 240 с.

Хаин В.Е. Региональная геология. Альпийско-Гималайский пояс. Недра. Москва, 1984, 344 с.

Хаин В.Е. Тектоника континентов и океанов. Научный Мир. Москва, 2001, 606 с.

Минерально-сырьевые ресурсы Азербайджана (гл.ред. В.М.Баба-заде). Озан. Баку, 2005, 808 с.

Мустафаев Г.В. Основные черты металлогении Азербайджана. Nafta-Press. Баку, 2002, 231 с.

Шихалибейли Э.Ш. Геологическое строение и история тектонического развития восточной части Малого Кавказas (тектоническая структура и магматизм). Изд-во АН Азербайджанской ССР. Баку, 1966, 263 с.

Шихалибейли Э.Ш. Геология и минеральные ресурсы Нагорного Карабаха Азербайджана. Элм. Баку, 1994, 284 с.

Azerbaycanın geologiyası (baş red. Ak.A.Əli-zadə). Cild I. Stratigrafiya, litologiya, tektonika. Nafta-Press. Bakı, 2015, 532 s.

Azerbaycanın geologiyası (baş red. Ak.A.Əli-zadə). Cild III. Maqmatizm, bərk faydalı qazıntılar, hidrogeologiya, mühəndisi geologiya. Nafta-Press. Bakı, 2015, 382 s.

ТЕКТОНИКА И МИНЕРАГЕНИЯ ГАРАБАГА И ВОСТОЧНОГО ЗАНГЕЗУРА (ЮГО-ВОСТОЧНОЕ ОКОНЧАНИЕ МАЛОГО КАВКАЗА, АЗЕРБАЙДЖАН)

Кенгерли Т.Н.

Министерство науки и образования Азербайджанской Республики, Институт геологии и геофизики AZ1143, г.Баку, просп. Г.Джавида, 119: tkangarli@gmail.com

Резюме. Статья посвящена тектонике и закономерностям формирования и распространения различных видов полезных ископаемых в пределах Гарабагского и Восточно-Зангезурского экономических районов Азербайджанской Республики, территориально связанных с юго-восточным окончанием горно-складчатой системы Малого Кавказа. В ней показано, что регион тектонически относится к юго-восточному сегменту Артвин-Гарабагского поднятия (мегазоны), состоящего из структурных зон второго порядка (Лок-Гарабагской, Гейча-Хакаринской и Гафанской) и погружающегося на северо-востоке и юго-востоке под современные континентальные молассы Средне-Куринской и Нижне-Аразской наложенных впадин. Отмечается, что в регионе распространены различные виды металлических (рудных) и неметаллических полезных ископаемых. Приведены сведения об их минерагении и промышленно значимых залежах. Минерагения металлических полезных ископаемых характеризует геологические закономерности формирования и размещения различных видов рудного минерального сырья в металлогенических зонах (отвечают одноименным тектоническим зонам Артвин-Гарабагской мегазоны) и рудных районах, которые выделяются исходя из тектоно-геодинамического районирования, истории геологического развития, генетических типов известных рудных месторождений и потенциальной рудоносности геологических формаций Малого Кавказа. Минерагения неметаллических полезных ископаемых отражает выявленные закономерности размещения объектов различного нерудного сырья в пространстве и их возникновения в определенные периоды геологи-

ческого развития. Потенциал увеличения перечня промышленно значимых месторождений определяется многочисленными проявлениями рудного и нерудного минерального сырья.

Ключевые слова: *Малый Кавказ, Гарабагский и Восточно-Зангезурский экономические районы, тектоническое районирование, минерагения, металлогеническая зона, рудный район, металлические (рудные) и неметаллические (нерудные) полезные ископаемые*

QARABAĞ VƏ ŞƏRQİ ZƏNGƏZURUN TEKTONİKASI VƏ MİNERAGENİYASI (KİÇİK QAFQAZIN CƏNUB-ŞƏRQ QURTARACAĞI, AZƏRBAYCAN)

Kəngərli T.N.
Azərbaycan Respublikasının Elm və Təhsil Nazirliyi, Geologiya və Geofizika İnstitutu
AZ1143, Bakı şəh., H.Cavid prosp., 119: tkangarli@gmail.com

Xülasə: Məqalə ərazi baxımından Kiçik Qafqaz dağ-qırışıqlıq sisteminin cənub-şərq qurtaracağı ilə bağlı Azərbaycan Respublikası Qarabağ və Şərqi Zəngəzur iqtisadi rayonlarının tektonikası və müxtəlif faydalı qazıntıların formalaşma və yayılma qanunauyğunluqlarına həsr edilmişdir. Göstərilmişdir ki, region tektonik cəhətdən ikincidərəcəli struktur zonalardan (Lök-Qarabağ, Göyçə-Xəkara və Qafan) ibarət olan və şimal-şərq və cənub-şərqdə Orta Kür və Aşağı Araz qoyulma çökəkliklərinin müasir qitə molassları altına gömülən Artvin-Qarabağ qalxmasının (meqazonanın) cənub-şərq seqmentinə aiddir. Qeyd olunur ki, regionda müxtəlif növ metal (filiz) və qeyri-metal faydalı qazıntılar yayılmışdır. Onların minerageniyası və sənaye əhəmiyyətli yataqları haqqında məlumat verilmişdir. Metal faydalı qazıntıların minerageniyası Artvin-Qarabağ meqazonunun eyniadlı tektonik zonalarına uyğun gələn metallogenik zonalarda və filiz sahələrində müxtəlif növ filiz mineral xammalının əmələ gəlməsinin və yerləşdirilməsinin geoloji qanunauyğunluqlarını xarakterizə edir. Bu zona və sahələr Kiçik Qafqazın tektono-geodinamik rayonlaşdırma, geoloji inkişaf tarixi, məlum filiz yataqlarının genetik tipləri və geoloji formasiyalarının potensial filizliliyi nəzərə alınmaqla ayrılır. Qeyri-metal faydalı qazıntıların minerageniyası müxtəlif qeyri-metal xammal obyektlərinin məkan yerləşdirilməsinin və geoloji inkişafın müəyyən dövrlərində onların yaranmasının aşkar edilmiş qanunauyğunluqlarını əks etdirir. Sənaye əhəmiyyətli yataqların siyahısını artırmaq potensialı çöxsaylı filiz və qeyri-filiz mineral xammal təzahürlərinin mövcudluğu ilə müəyyən edilir.

Açar sözlər: *Kiçik Qafqaz, Qarabağ və Şərqi Zəngəzur iqtisadi rayonları, tektonik rayonlaşdırma, minerageniya, metallogenik zona, filiz rayonu, metal (filiz) və qeyri-metal (qeyri-filiz) faydalı qazıntılar*

ANAS Transactions **Earth Sciences** **1 / 2024**

http://www.journalesgia.com

STRUCTURAL CONDITIONS FOR THE LOCALIZATION OF GOLD MINERALIZATION WITHIN THE TUTKHUN ORE FIELD (THE CENTRAL PART OF THE LESSER CAUCASUS)

Baba-zadeh V.M., Abdullayeva Sh.F., Novruzova S.R.

Baku State University, Azerbaijan

33, acad. Zahid Khalilov str., Baku, AZ 1148: vasifbabazadeh1938@bsu.edu.az; shakhla.a@gmail.com; samiranovruzova001@gmail.com

Keywords: *the central part of the Lesser Caucasus, field, area, structure, epithermal, gold, silver, secondary quartzites, genetic features, mineralization, gold-quartz ore zones*

Summary. The gold-bearing areas of the ore field, the similarities and differences of the structural conditions of their formation, the elemental and mineral composition of the ores, various metasomatictes-propylites, beresites and, especially, secondary quartzites were studied.

Gold ore mineralization can be considered in terms of some regional features of the geological development of the Lesser Caucasus. The Upper Eocene intrusive and subvolcanic rocks represent a single complex that forms the Gazikhanli-Zargulu massif in the region, approaching the subvolcanic facies of magmatic rocks. The field of development of gold ore formations mainly covers outcrops of granitoid rocks of the massif and its exocontact aureoles, into which abundant dikes, the latest members of the Upper Eocene complex of intrusive formations, penetrate. The particularly close positional connection of gold ore mineralization with vein rocks cutting through all the massive and porphyry rocks of the massif indicates the control of this mineralization by the latest structural elements of the area, which occurred in the final period of the evolution of the Gazikhanli-Zargulu complex.

As can be seen, gold-bearing zones are paragenetically associated with dikes that complete the development of granitoid intrusive complexes. Both of them, which are closest in time to the development of magmatic and post-magmatic processes, use uniform structures of an earlier period of development in their localization.

Introduction

The epithermal Tutkhun ore field is located in the Kalbajar region and occupies part of the northern slope of the Mykhtokyan ridge in the upper reaches of the Tutkhun River (right large tributary of the Terter River). The tectonic structure of the ore field is determined by its location in the southwestern wing of the Saribaba trough within the Goycha-Akera structural-formational zone, which is associated with the development of the northeastern branch of the transregional Mesozoic Anatolian fault. Geological prospecting and exploration work in this area was carried out in the 60-70s of the last century and was accompanied by scientific research by researchers of the Institute of Geology and Geophysics of the National Academy of Sciences of Azerbaijan, Baku State University, CRGPI (Moscow), etc. A scientific database was formed in the course of the work, including numerous published works and production reports, the generalization and analysis of which made it possible to identify the main geological and genetic features of the ore field (Кашкай и др., 1967; Сулейманов, 1982 and etc.). This paper continues a series of publications concerning the structural features of ore localization and the structure of the ore field, ranging from the regional position to the characteristics of ore-bearing areas with different gold mineralization and resource potential (Баба-заде и др., 2003, 2023). The relevance of this paper is quite obvious, as since the publication of the monograph “Gold of Azerbaijan” in 2023 (Baba-zadeh V.M. and others), which collected materials of Azerbaijan researchers, a series of precision analytical studies that were previously inaccessible have been carried out. Despite the wide coverage of geological material and the novelty of the obtained data, while interpreting them, the abovementioned researchers did not take into account a number of works that could have resolved some controversial issues of the geological and genetic order. We will try to clarify these and other questions in this work that led to the formation of the Tutkhun field, and a large group of orogenic gold fields in the central part of the Lesser Caucasus.

Geological structure

The ore field, with an area of about 20 km^2, is composed of sedimentary and volcanogenic-sedimentary formations from the lower (Albian) and the upper structural stages (Cenomanian, Santonian, Campanian-Maastrichtian) of the Cretaceous to modern ones with numerous breaks, distinguished by the facies variation of the lithological composition of the rocks and the scale of effusive and intrusive magmatism (Fig.1). These rock complexes are accumulated in the linearly elongated Gazikhanli anticline in the northwestern direction, which is complicated by smaller faults that feather them and is accompanied by differently oriented zones of fracture intensity. Volcanogenic and sedimentary deposits of the Upper Cretaceous and individual bodies of syncollisional granitoids of the Tertiary intrusive complex breaking through them are exposed in the central part of the structure, beyond which the gold mineralization does not extend practically.

The duration of the geotectonic development of the Gazikhanli structure is evidenced by the occurrence of a thick series of intraformational conglomerates of the Cenomanian Age, which developed near this structure and extended along it. The abovementioned conglomerates contain gabbroids, granitoids, quartzites, jaspers, etc.

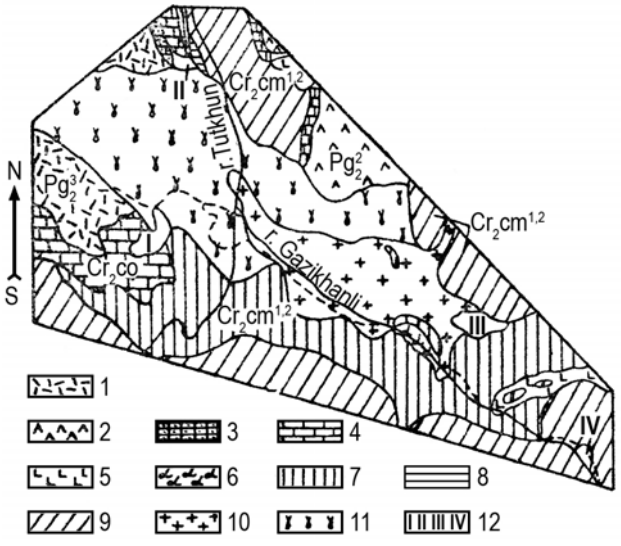

Fig. 1. Schematic geological map of the Tutkhun river basin (Compiled by A.I. Mammadov). 1 – The Upper Eocene-hydrothermally altered andesites and tuff breccias; 2 – the Middle Eocene tuffs and tuff sandstones; 3 – nummulitic limestones of the Middle Eocene; 4 – the Campanian-Maastrichtian stage-marly limestones; 5 – the Post-Santonian gabbroids; 6 – the Post-Santonian amphibolites; 7 – the Cenomanian stage-hornfels; 8 – epidosites; 9 – the Cenomanian stage-conglomerates, argillites, sandstones, lenses of limestones, tuff sandstones and gravelites; 10 – quartz diorite porphyry, adamellite porphyry and granodiorite porphyry (phase III); 11 – quartz and quartz-free diorites, tonalites, granodiorites (phase II); 12 – skarn areas: I – South Turkuchevan; II – North Turkuchevan; III – Gizilitan; IV – along the path from Turkuchevan village to Gazikhanli village

The Gazikhanli zone is limited by the Galaboynu from the southwest, and by the Boyukboz synclinal folds from the northeast, which also played a fairly active role in the formation of the Tutkhun gold ore field.

There are intrusive analogues of younger terrestrial formations within the anticline that are similar in age and petrographic composition, represented by a diverse series of igneous rocks. All of them are the Post-Cenomanian and, mainly the Post-Campanian (Кашкай и др., 1967).

The most ancient intrusive rocks are serpentinized and talcose ultrabasic rocks, confined to local anticlinal structures and intruded by small intrusive bodies of basic, intermediate and felsic composition.

The main mass of intrusive formations within the Tutkhun ore field consists of the Post-Upper Eocene subvolcanic and hypabyssal granitoid bodies of the Gazikhanli-Zargulu intrusive complex (Геология Азербайджана, 2005). Rocks of two intrusion phases take part in its structure (Баба-заде и др., 2003; Волков и др., 2021). Earlier gabbroids, gabbro-diorites, diorites and quartz diorites are developed along the periphery of the complex. There are several stocks of granodiorites and granites in the central part of the complex. All these formations break through the Albian-Cenomanian and Middle Eocene deposits, having a contact impact on them, transforming them metasomatically into sericite-hydromicaceous-quartz rocks. According to its shape, the intrusion refers to a large fractured pluton, elongated in the northwest direction (300-310º), along the Tutkhun River valley for 10 km with a width of 0.2-2 km. The massif has a laccolith-like shape and a thickness of 300-500 m in cross section (Баба-заде и др., 2003; Волков и др., 2021).

The latter is represented by bodies of different morphology and size. Different parts of the intrusive were formed at different stratigraphic levels. The largest Gazikhanli massif of granitoids breaks through terrigenous deposits of the Cenomanian and Early Senonian (the main part of the intrusion), the marginal parts – the Upper Senonian-Lower Paleogene carbonate-tuffaceous rocks. The central, most deeply eroded part of the Gazikhanli intrusion, was formed at a depth of about 750-800 m, and the peripheral parts, breaking through the deposits of the Upper Senonian and Lower Paleogene were formed at a depth of 350-400 m. The same formation depth is observed on the Zargulu intrusion. In addition to paleogological data (Баба-заде и др., 2003), the near-surface conditions for the formation of the marginal parts of the considered intrusion are confirmed by the presence of low-temperature contact minerals (epidote, zoisite, albite, actinolite, chlorite, etc.) and the predominant porphyry structure of the

intrusive rocks. The second intrusive massif is located in the northwest of the previous one in Aghzibir. It breaks through the Cenomanian deposits and gabbroids of the first phase. Numerous apophyses in the form of dikes extend from the intrusion into the host rocks, as in the Gazikhanli massif. The main occurrences of gold mineralization (the Agzibir and Malinovaya Balka areas) are associated with the rocks of the intrusive massif.

The next outcrop of the granitoid intrusion in the Turkuchevan area in the lower course of the Gazikhanli River is hypsometrically located slightly below, due to which the erosion cutting into the granitoid body turned out to be deeper. Naturally, the occurrence of deep facies in the intrusive massif is holocrystalline syenite-diorites, quartz diorites, etc. Porphyritic varieties occur in the elevated areas of the relief, and the marginal facies of the massif are characterized by effusive rocks.

There is a thick zone of clarified, silicified and kaolinized rocks in the contact zone of the intrusion with the host rocks. According to E.S.Suleymanov (Сулейманов, 1982), the content of combined water is 0.7-1.0% in 53 analyzes taken from quartz diorites and granodiorites, the Gazikhanli-Zargulu igneous complex, which is characteristic of intrusive massifs that crystallized at a depth of about 1 km (Баба-заде и др., 2003). Most likely, the massif records one of the large early Tertiary faults, accompanied by regional structures of the area, in particular, with the axis of the abovementioned anticlinal fold, composed of chalk volcanic-sedimentary formations. Holocrystalline rocks, which are structurally homogeneous, mainly hornblende-biotite quartz diorites are found along the tectonic faults. Plutonic rocks of the intrusion are accompanied by their subvolcanic analogues (stocks of quartz-diorite porphyrites and quartz-monzonite porphyrites predominate) along the contacts with the host rocks and, probably, in the roof.

Later, steeply dipping dikes were formed, concentrated in the apical and marginal parts of the intrusive massifs, often in the host rocks, as well as subvolcanic rocks of the same complex, at the final stage of which gold-bearing areas of the Tutkhun ore field were formed. The dikes are close to plutonic and subvolcanic rocks in terms of mineral composition, emphasizing the comagmatic nature of all igneous formations of the complex, but they are close to rocks of the effusive facies in formation and structure. Most of them can be called intrusive andesites and trachyandesites. A structural connection has been shown between dikes that complete the development of granitoid intrusive complexes and gold veins (Абдуллаева, 2023; Абдуллаева, Новрузова, 2023; Баба-заде, Новрузова, 2023). Both use the same structures from an earlier period of development in their location.

Most of the dikes are pre-ore, oriented to northwest and host ore bodies or are intersected by them. Dikes become denser and structurally isolated dike fields occur near granitoid massifs or in the contours of the latter. The largest and longest dikes represent a system of predominant northeastern swarms (formations), traced at a distance of 1-2 km or more.

All intrusive rocks of the Tertiary age represent a single complex of comagmatic formations, also related apparently to the strata of the Eocene andesites and their tuffs, developed within adjacent synclinal structures.

The boundaries of the Tutkhun ore field are limited by the contours of a tectonic block, within which a system of intersecting sublatitudinal (northwestern), near-meridional and diagonal faults of a lower order is developed (Минерально-сырьевые ресурсы Азербайджана, 2005). The latter led to the occurrence of a series of elevated and downthrown blocks, causing the stepped-block structure of the considered area. Gold-bearing stockworks and compound veins are controlled by this fault system and consist of en echelon zones of veinlet-impregnated ores (Баба-заде и др., 2003). The largest is the regional ore-controlling Gazikhanli fault of the northwestern orientation, which represents a system of steeply dipping faults within which ore-bearing zones are located (Fig. 2).

The tectonic zone is accompanied by numerous intersecting faults of a lower order, bearing traces of active hydrothermal alteration in the body of the intrusion and in the host volcanic-sedimentary rocks (including ultrabasites and gabbroids).

According to geophysical data, the Tutkhun ore field is localized in the superintrusive zone of the Gazikhanli-Zargulu intrusive complex, which creates a dome structure and is characterized by an alternating, rugged magnetic field (Баба-заде и др., 2003; Волков и др., 2021).

Metasomatic alteration in host rocks

Hydrothermal and metasomatic alterations in the host rocks were widely occurred with the development of albite, epidote, biotite, actinolite, sericite, chlorite, carbonates, kaolinite, argillite, sulfides, etc. in the Tutkhun ore field. More intense hydrothermal and metasomatic alterations occurred in the footwall of gold-bearing zones, where the host rocks were completely replaced by the secondary minerals, i.e. converted into metasomatic rocks (Баба-заде и др., 2003; Абдуллаева, Новрузова, 2023; Баба-заде и др., 2020; Баба-заде и др., 2023; Кашкай и др., 1967; Минерально-сырьевые ресурсы Азербайджана, 2005; Li, Yang, 2022).

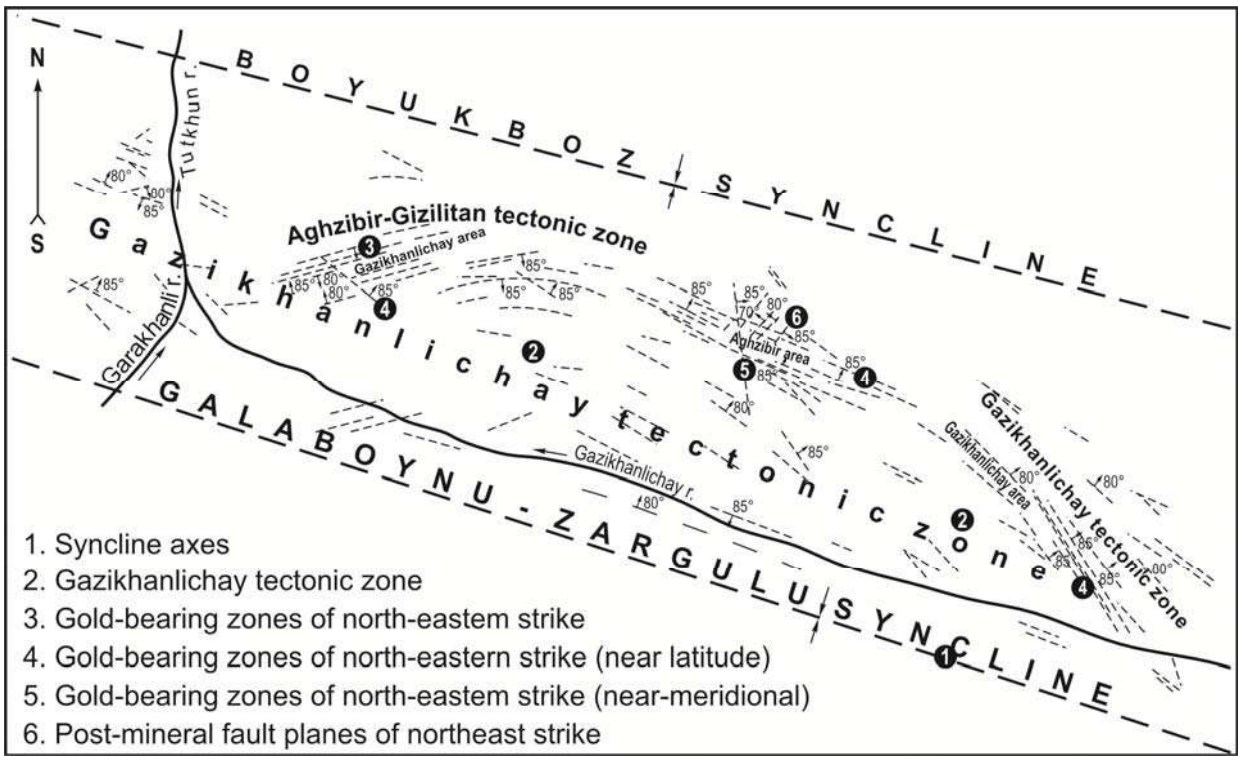

Fig. 2. Structural scheme of the Tutkhun ore field

Metasomatites in the direction from bottom to top and from the center of the field to its periphery are replaced by partially altered rocks. The outer zones correspond to higher temperature facies of propylites – albite-actinolite, albite-epidote-actinolite and biotite (weakly developed) developed mainly in the body of granitoids; the area of medium-temperature propylitization, reminiscent of listvenites (zones closest to the fracture cavity) with abundant pyrite, often with late quartz segregations, including hydromicas and adularia, is composed of mica-carbonate metasomatites – epidote-chlorite, kaolinite-sericite-quartz and sericite-chlorite-quartz varieties; the area of low-temperature propylitization facies consists of quartz-hydromica-kaolinite-carbonate formations with ferruginous carbonates, sulfides and subordinate alunite-group minerals, usually with veinlets and lenses of chalcedonic quartz and kaolinite. These new formations are observed at significantly lower hypsometric levels along fractures and zones of increased porosity and fracturing associated with faults, dike contacts, etc.

So, the structure of the altered rocks shows clearly vertical zoning, which allows them being considered in many ways similar to epithermal gold ore fields of the Tertiary formation.

Gold-bearing vein bodies occupy a definite position in this zonation, located on the border between metasomatites and partially altered rocks, i.e. zones, which are composed of sulfides, are mineral facies of the general aureole of hydrothermal and metasomatic alterations (Баба-заде и др., 2023; Абдуллаева, Новрузова, 2023; Баба-заде и др., 2003). The structure and composition of such zones correspond to areas of the ore field determined by the depth of development and does not occur together in all cases. The lowest temperature associations are better expressed at lower section levels and penetrate to a significant depth only along well-developed fracture zones. According to their composition, they show a noticeable difference in rocks of different initial compositions, approaching listvenites in rocks of a more basic composition, or kaolinite-hydromica beresites in rocks of a more acidic composition.

The formation of these halos covers predominantly the pre-ore (pre-productive) period of the formation of ore zones, but they are closely associated with the latest minerals of the early ore stage in their composition – nest-like and veinlet accumulations of coarse-grained quartz and scattered impregnations of coarse-crystalline pyrite, which experience distinct breaking and recrystallization in subsequent late stages.

Secondary quartzites occupy higher hypsometric elevations, developing due to granitoid intrusions (partially located in the endocontact zone) and effusive-pyroclastic rocks far from the intrusive outcrops (Баба-заде и др., 2023; Кашкай и др., 1967). Areal secondary quartzites are widely developed with numerous quartz, less quartz-carbonate vein-veinlet zones of northwestern strike, coinciding with the deep fault of the Gazikhanlichay tectonic zone.

Peculiarities of the Tutkhun ore field are the occurrence of pre-ore argillizated rocks, the presence of which allows us considering the field to be slightly eroded. Argillicites replace completely low-temperature propylites and hydromica alterations in the supra-ore gold-bearing zone, which are of a near-fracture nature.

Mineral composition of ores

According to the mineral composition, the fields of the ore field belong to the class of sulfide epithermal gold ores (Волков и др., 2018; 2021; Гордиенко и др., 2019; Кашкай и др., 1967; Некрасов, Дорожкина, 2020; Cong et al., 2023; Hlaing et al., 2021; Groves et al., 2020; Sillitoe et al., 2020). More than 50 minerals have been observed in the ores. At the same time, they are relatively simple in terms of the set of main minerals. The main ore minerals are pyrite (dominates sharply), chalcopyrite, sphalerite, galena, native gold, fahlores, and non-metallic are quartz, calcite, ankerite (Figs. 3-5). The ores contain small quantities of magnetite, molybdenite, tetrahedrite, boulangerite, jamesonite, bournonite, antimonite, orpiment, etc. The quantitative relationships between the main sulfide minerals remain quite stable, pyrite (more than 90%), chalcopyrite (5-8%) always predominant, and only in some cases chalcopyrite is inferior to sphalerite (2-5%). Galena (1-2%) is found in subordinate quantities in relation to sphalerite and pyrite, but almost always predominates over fahlores. Pyrite ores are characterized by an inequigranular texture, massive and brecciated textures.

Pyrites of gold ores in general, depending on the predominant development of faces in combinations, are classified into more than ten habitus. The highest frequency of occurrence is characterized by crystals of cubic, pentagonal dodecahedral and cube-pentagonal dodecahedral habitus (Коробейников и др., 1993). Research has shown (Кашкай и др., 1967) that the pyrites of the Tutkhun field have a zonal structure and emphasize the variability of crystal habitus during the growth process: early – pentagon-dodecahedral, late – cubic. Similar cases are observed in the Burgali epithermal gold field in Northeast Russia (Волков и др., 2021). Accumulation of aggregates of pyrite grains often have a round or oval shape with a concentrically zonal internal structure. Microthermometric studies of fluid inclusions in samples show that primary, primary-secondary and secondary inclusions are distinguished among them. A wide range of ore formation temperatures from 190°C to 240°C has been established (Баба-заде и др., 2003; Сулейманов, 1982). The highest temperature regime is characteristic of the initial (230ºC-240ºC), and the lowest (180ºC-200ºC) final stages of ore formation. These temperatures are close to the conditions for the formation of epithermal fields.

The available factual material allows assuming the occurrence of hydrothermal and metasomatic ore deposition, which is confirmed by clearly defined supra-ore hydrothermal halos, synchronous with ore formation.

The field has two productive stages of mineralization and mineral associations typical for them, separated by tectonic movements: I. Quartz-pyrite with a small amount of magnetite and molybdenite and milky white quartz. II. Main ore stage. The main ore stage is divided into 2 substages: 1) quartz-carbonate sulfide – quartz, carbonates (insignificantly), late pyrite, sulfides of lead, copper and zinc, tetrahedrite, silver, native gold were released in this substage; 2) quartz-carbonate-sulfoantimony substage, consisting mainly of fine-grained chalcedonic quartz and sulfides, sulfoantimonites, native gold, silver, which intersect the early generation quartz of the first stage in the form of small veinlets.

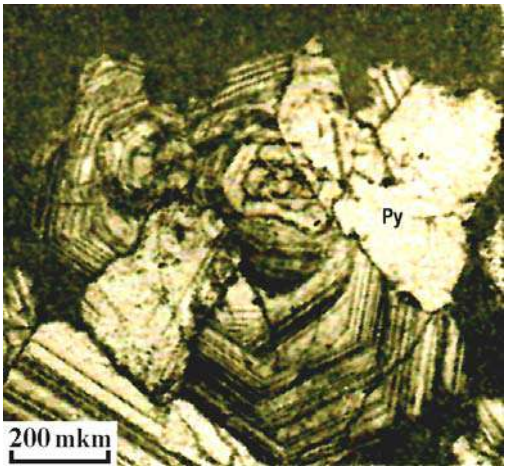

Fig. 3. Pyrite grains showing zonal structure after etching HCl+Zn dust. Etching revealed a small cataclasis in the pyrite grains. Gizilitan area

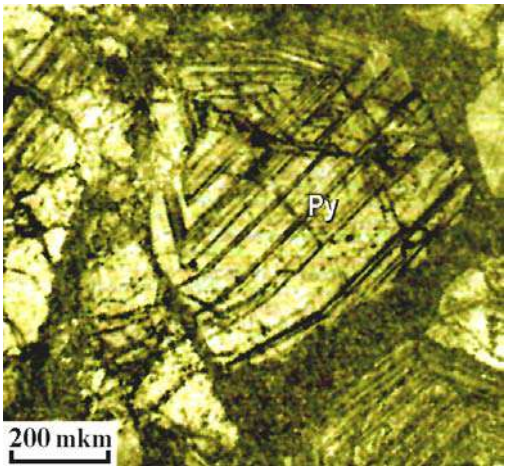

Fig. 4. Large zoned pyrite crystal. The pyrite grain (Py) of late generation grown on it. Etched with HCl+Zn dust. Gizilitan area

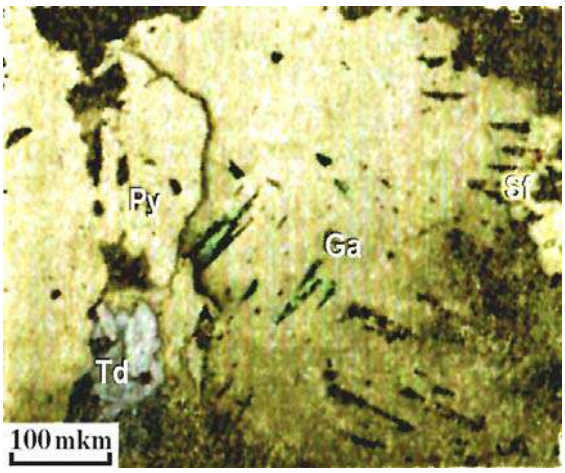

Fig. 5. Structural relationships of galena (Ga), pyrite (Py), white relief, sphalerite (Sf), dark gray and fahlore (Td). You can see how fahlore cements pyrite segregations in the lower left part of the figure. Ore vein on the Galaboynusu river

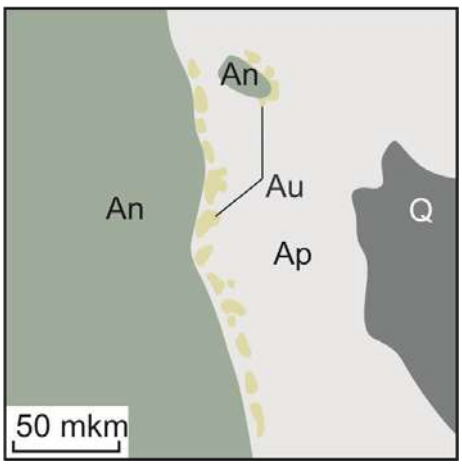

Fig. 6. Overgrowths and curved segregations of gold (Au) in association with orpiment (Ap) and antimonite (An) and quartz (Q). Aghzibir area

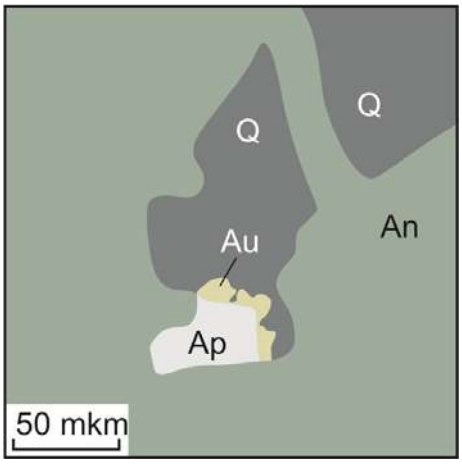

Fig. 7. Chain segregations of gold (Au) at the junctions of orpiment (Ap) and antimonite (An). The inclusion of quartz on the right (<3). Aghzibir area

Most of the gold of the first substage is dispersed in quartz, developing along the boundaries of euhedral crystals of the latter. Native gold of various gold fineness is found mainly in samples of quartz veins and zones, where sulfides and sulfosalts of copper and lead are visually observed, and microscopy also shows the occurrence of realgar and orpiment (Кашкай и др., 1967).

Besides native and finely dispersed gold, there is coarse dust-like gold, the occurrence of which is confirmed by spectral and chemical analysis data. Au is observed intergrown with antimonite, realgar and orpiment, and the largest number of grains of this metal is confined to areas of the zone where antimonite is in association with orpiment and realgar (Кашкай и др., 1967) (Figs. 6, 7). Sometimes, there are tiny inclusions of low-grade gold (300-350‰) with the addition of a small amount of Ag from fahlores, hessite in quartz (Баба-заде и др., 2003; Волков и др., 2018; 2021) which is rare (fine to dust-like 5-50 μm). Au grain sizes vary between 0.018-0.08 mm.

The relationship between Au and accompanying minerals shows the proximity in time of their precipitation from solutions, with some delay of gold, which allows placing them in the following series: antimonite → realgar → orpiment → gold (Кашкай и др., 1967). Silver, like gold, is characterized by uneven distribution. It is found in the form of its own minerals (native silver, hessite) and in the form of impurities. It was observed (V.Ramazanov, E.Suleymanov) in three minerals out of five subjected to local X-ray spectral analysis in the composition of freibergite, tetrahedrite and galena. The highest concentration corresponds to freibergite (16.18 wt.%). Silver follows generally gold in a multistage hydrothermal process, and forms higher concentrations in the middle and late stages of mineralization.

The quartz-carbonate ore-free third stage of mineralization is represented by quartz, calcite, and ankerite. Mineral associations of the third stage of the ore process in most cases are also clearly telescoped, forming independent systems of thin, almost irregular quartz-carbonate veinlets and veins, which cut the veinlets of ores of early stages clearly in all possible directions.

This alteration in mineral parageneses is also reflected in other epithermal gold ore fields of the Tertiary formation. At the same time, autonomous features are observed in the Tutkhun field that distinguish it from other epithermal gold ore fields of the Tertiary formation, in particular the Zod field, with which it is located in a single tectonic zone and, apparently, coincides in the time of formation. The most significant difference of the Zod field is the much clearer isolation of mineral associations of different stages. According to S.O.Amiryan (Амирян, 1984), mineral associations of different stages

of the ore process of the Zod field form clearly independent veinlets, deposited in different conditions and differing in the textures and structures of the ores, which indicates very active intra-mineralization tectonic movements and heterogeneous changes in the regimes of the hydrothermal process (for example, the formation of independent stages of productive mineral associations – carbonate veinlets with native gold and cobalt and nickel diarsenides, or later native gold with silver and gold tellurides in the environment of little altered rocks, which are rich in bases – gabbro-peridotites). At the same time, mineral associations of different stages of the ore process are weakly telescoped and spatially closely combined in the gold ore zones of the Tutkhun field. Here, minerals such as pyrite, magnetite, chalcopyrite and sphalerite are observed in the parageneses of the early stages, which are also characteristic of the composition of the ores of the early stages of the Zod field. Typical minerals are sulfoantimonites (boulangerite, jamesonite, bournonite and antimonite in association with calcite and ankerite) in both fields in the associations of the latest stages. Besides low-grade native gold, there are chalcopyrite, fahlores-tetrahedrite in productive gold ore stages, however, they are accompanied by diarsenides of nickel, cobalt and tellurides of gold and silver at the Zod field, while these elements (Ag, Ni, Co, Te) have so far been observed only in a dispersed state in the ores of the Tutkhun field.

All mineral associations in the ores of the Tutkhun field, although with variable gold concentrations, are located in highly altered rocks of the most recent stages of acidic near-fracture metasomatism. Highly productive mineral associations with native gold and tellurides are usually localized in slightly altered bedrocks at the Zod field.

The field includes more than ten gold-bearing areas, 5 of which are of practical interest: Gazikhanli, Aghzibir, Gizil-Itan, Zargulu and Galaboynu. All of them are characterized by similar features of the geological structure, so below we will limit ourselves to a very brief description of *the Gazikhanli area*. The latter is located between the third and fourth tributaries of the Gazikhanli River on the northwestern flank of the eastern outlet of the Gazikhanli-Zargulu massif, which adjoins a steeply dipping ore-control fault here. There are frequent cases of alterations of its direction along strike and dip (Баба-заде и др., 2003; Геология Азербайджана, 2005; Минерально-сырьевые ресурсы Азербайджана, 2005; Сулейманов, 1984). The long-term development of the fault is determined by the position of the rocks of the main facies of the intrusion. It is also recorded by later dikes of several age series and even later gold-bearing zones of hydrothermally altered rocks, studied mainly from the surface and from drill-hole cores to depth. All these elements of the structure of the Gazikhanli area, including propylitized gold-bearing zones (more than 15), are dissected by quartz veinlets and veins of varying thickness (from 3-10 to 25-30 cm in places of swelling) and are developed along the pleural sutures of the fault with a predominant northwestern orientation and steep dip angles (Figs. 8-10). They are subparallel to the fault and the contacts (extensions) of the intrusive outcrop.

Hydrothematically altered gold-bearing zones are the main morphological type. Many of them have a sharply varying thickness from 10-20 cm to 1.5-2 m (average 0.4-0.5 m) along their strike and therefore have winding outlines. The length of zones is up to 500 m and more. The distance between zones is 10-50 m. Gold-bearing quartz veins are less common and are confined to shear fractures in the bodies of granitoid massifs. Their length is 100-200 m, only in some cases their length reaches 400-500 m. Veins with a thickness of 15-20 cm predominate. Most of them have a simple structure, but there are complex bodies of filling, caused by the extension of veins in their thickness, extent and dip, due to repeated reopening of fractures and filling them with new portions of hydrothermal vents.

Stockworks of variable thickness, which are represented by veins and veinlets, are associated with fracture zones and are being developed in the Gazikhanli and Aghzibir areas. The fractures are conducted with quartz-carbonate material and are accompanied by pyrite, chalcopyrite, galena, sphalerite, antimonite, realgar, fahlores, molybdenite and native gold. There are rich accumulations of pyrite, molybdenite, fahlores, etc. in individual quartz veins (Gizil-Itan area). Veins with a quartz-carbonate aggregate are occasionally found in the gold-bearing belt, where there is approximately the same amount of carbonates (calcite, dolomite) as quartz. Mineralization is characterized by a rich content of sulfides (10-15 %), oxides, hydroxides, etc.

The distribution of gold and silver in gold-bearing zones and veins is extremely uneven.

Genetically, the zones are younger than the dikes and cut them. Their thickness often decreases to 0.1 m and the quartz disappears in dikes. According to exploration data, the length of the zones is up to 800 m, their thickness varies from several tens of cm to 3 m or more in the central part. The vertical range of mineralization is up to 300 m. The gold-bearing zones of the Gazikhanli area, like other areas, are characterized by branching along strike. Au content from “mark” up to 5.2 g/t, with the maximum gold content concentrated in selvages.

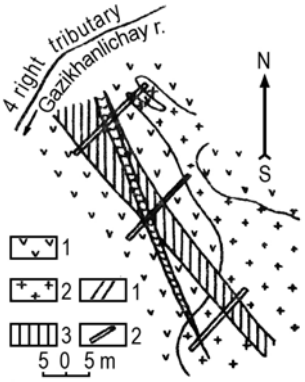

Fig. 8. Relationship between porphyrites (1), granitoids (2), hornblende diorite porphyrite dike (3) and the gold-bearing zone in the northwestern direction (4). The left slope of the fourth right tributary of the Gazikhanli river

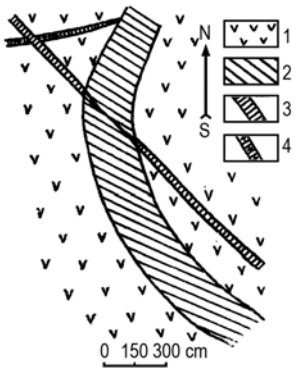

Fig. 9. Age relationship between a diorite porphyrite dike and two mineralized fractures of different directions. Gazikhanli area. 1 – porphyrites; 2 – dike; 3 – gold-bearing zone in NW direction; 4 – galenite-bearing zone in NE direction

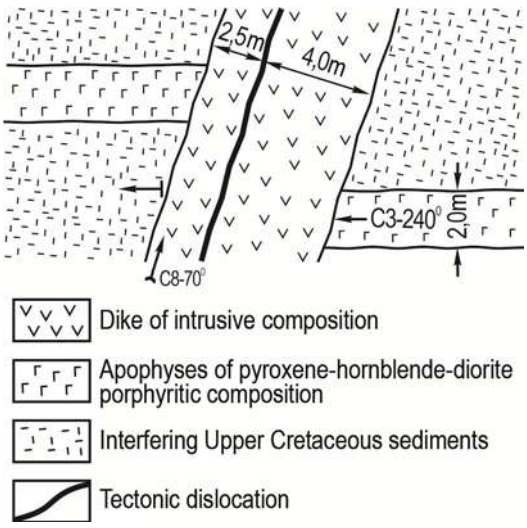

Fig. 10. Displacement by a dike of intrusive andesites of a vein apophyses of pyroxene-hornblende-diorite of porphyritic composition (sketch of an outcrop at the junction of the Gazikhanli and Tutkhun rivers)

Sulfides form abundant impregnation in quartz. They are represented by pyrite, less chalcopyrite, sphalerite and galena. Sulfoantimonites, fahlores and other minerals are observed in a number of zones. Magnetite, molybdenite, hematite, arsenopyrite, scheelite, chalcopyrite and malachite were observed in the crushed sample.

Physical and mechanical properties of rocks

The study of the physical and mechanical properties of rocks shows that the intensity of deformation of rocks, besides their chemical composition, was of decisive importance for the course of hydrothermal processes and the spatial distribution of their occurrences, including occurrences of gold mineralization, causing its predominant concentration in individual rocks. In this aspect, the interaction zone of the Gazikhanli-Zargulu intrusive complex, which is saturated with the latest dikes and sills, was a particularly permeable and favorable environment for ore deposition. Earlier generations of pyroxene-hornblende porphyrite dikes in each area, as well as massive granitoid rocks and host porphyrites are intersected by ore zones in the same direction in which later generations of dikes intersect them.

So, the later generations of dikes (intrusive andesites, intrusive dacites, granodiorite porphyries) created the mechanical heterogeneity (anisotropy) of the environment, thereby predetermining the main direction of the ore zones. The influence of such dikes on the formation of ore zones was associated not only with their position in the structure, but also with their physical and mechanical properties. As the most recent formations, they experienced the least deformation relative to all host rocks, including dikes of earlier generations.

Thus representing a rigid framework in the structures of gold-bearing areas, late dikes determined the greatest possibility of fracture opening, which are parallel to them along the strike. Ore solutions were used by these fractures at all subsequent stages of the ore process. The movement of solutions along such fractures and the widespread metasomatism of rocks along them were facilitated by the higher porosity (and correspondingly less volume and weight) of all rocks of the host dyke of the latest generation.

The results presented in Table 1 and Fig. 11 do not take into account or take into account very insufficiently the dependence of the strength properties of various types of rocks on confining pressure, temperature, the degree of previous deformation, on the duration of stress and other factors that determine one or another deformation mechanism. However, even in approximate form, these data illustrate the conclusions on the predominant localization of gold mineralization in certain zones and the dependence of the nature of deformation and its intensity on the primary petrographic features of certain formations.

The mineralized zones develop well in tuffaceous rocks, which are characterized by intense dislocation, fragility and significant porosity. The thickness of the zones decreases sharply with the transition to denser rocks (granitoids), and they branch into a number of small, rapidly cropping out veins and veinlets.

The presence of tectonic structures, hypabyssal and subvolcanic bodies and contacts between lithologically contrasting formations is also of great importance for increasing the deformation of certain parts of the ore field.

All these features determined the physical and mechanical heterogeneity of the environment subjected to deformation and the maximum concentration of tectonic fractures in certain areas and rocks. The intensity of rock deformation, besides their chemical composition, was of decisive importance for the course of hydrothermal processes and the spatial distribution of their occurrence, including occurrences of gold mineralization, determining its predominant concentration in certain zones occupying a certain stratigraphic position in the section of the ore field (Groves et al., 2020, Li, Yang, 2022).

Table 1

Table to determine the effective porosity of rock samples taken from the Tutkhun ore field (laboratory of IGEM RAS, analyst B.P.Belikov)

Rock names	Volume weight	Effective porosity, %
Hornfelsed rock	2.95	0.35
Dyke of intrusive dacite	2.95	0.68
Dyke of intrusive dacite	2.64	1.21
Dyke of plagioclase-quartz porphyrite	2.65	1.27
Dyke of intrusive dacite	2.67	1.34
Dyke of plagioclase-quartz porphyrite	2.69	1.40
Dyke of intrusive andesite	2.61	1.59
Hornblende quartz diorite-banatite (massif)	2.68	2.17
Altered porphyrite (host rock)	2.69	2.58
Quartz diorite-banatite	2.66	2.95
Andesite-dacite lavas	2.61	3.00
Quartz monzonite porphyry	2.56	3.53
Quartz monzonite porphyry	2.63	4.08

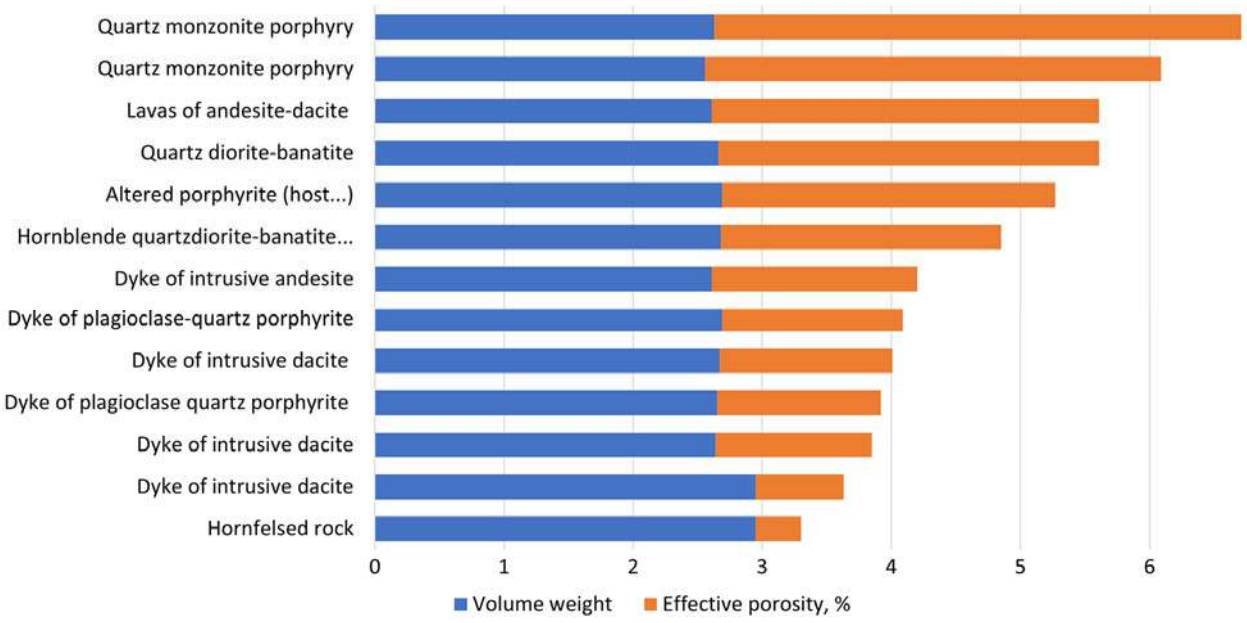

Fig. 11. Petrographic composition of the studied rock samples taken from the Tutkhun ore field

Petrochemical characteristics of rocks of the Tertiary intrusive complex

Analysis of the petrographic features, which are developed in the Tutkhun ore field of igneous complexes and the conditions of their spatial distribution allow drawing a number of conclusions on the evolution of magmatism in Tertiary times, on the relationships between the types of igneous rocks, which is important for elucidating the patterns of distribution of gold mineralization in space. Igneous rocks are distinguished by certain petrochemical characteristics. Tables 2, 3 and Figure 12 give every reason to consider all the characterized rocks of the Tertiary intrusive complex as a single family of rocks associated with the differentiation of the original diorite (andesite) magma. According to the data in the diagram, some phases of this intrusive complex differ little in their petrochemical features. At the same time, the rocks of the complex with a similar bulk composition differ significantly due to the different facial position of the rocks.

So, the above-mentioned rocks, although they represent independent intrusive facies, belong undoubtedly to a single comagmatic series with similar typomorphic features of the rock-forming minerals and are associated with general chemical features. The compiled diagram allows combining them into a single complex corresponding to a series of calc-sodium rocks, which are saturated moderately with silica.

The following facts, which have obviously important petrological significance, attract attention with all the diversity of igneous rocks of the Tertiary intrusive complex.

1. The intrusive rocks of the massif are distinguished by a slight excess of alumina, of which the early phase of subvolcanic rocks such as quartz diorites and monzonite porphyrites are characterized by slightly increased alkalinity. Subsequent phases of vein rocks are distinguished by an excess of lime, not counting extremely propylitized rock varieties, in which a relative excess of alumina is associated with superimposed processes.

2. The earlier series of porphyrite dikes are enriched in bases, and the latest series of quartz plagioporphyrite dikes (porphyry granodiorite) is significantly more acidic than all the preceding rocks of the intrusive complex. This course of melt differentiation explains easily the accumulation in residual melts, together with volatile bases, which are associated with subsequent magmatic carbonatization, chloritization and epidotization of all members of the intrusive series, as well as the host strata of Cretaceous porphyrites where these rocks were subjected to tectonic disturbances.

3. Rocks of the subvolcanic facies and the earliest dykes of pyroxene-hornblende diorite porphyrites, which are closely related to them, belong to the group of moderately saturated silica and alkalis, with a significant predominance of sodium, as well as mesocratic types. They are closest to the average type of quartz monzonite. Data from recalculation of chemical analyzes of rocks of the plutonic facies of the intrusion, as well as their structures and mineral composition, indicate that they belong to the soda-calcareous series of rocks of the diorite family, which somewhat oversaturated with silica and relatively poor in alkalis, very close to the average composition of quartz diorites.

4. The alkali content is relatively low and moderate with a sharp predominance of sodium. Unlike plutonic analogues (quartz diorites), the vein series of the first three generations show some deficiency of alumina, despite clear signs of secondary alteration, usually leading to a relative accumulation of alumina. Such accumulation is observed only for extremely propylitized varieties.

5. Finally, the most significant feature of the chemistry of the latest series of vein rocks is the sharply increased amount of silica and alkalis, with a simultaneous increase in the role of potassium, although still with a relative predominance of sodium. The numerical characteristics of rocks of this type are closest to the average type of dacite.

Conclusion

The Tutkhun gold epithermal ore field is a fairly large object in the central part of the Lesser Caucasus (Баба-заде и др., 2020; Минерально-сырьевые ресурсы Азербайджана, 2005). Analysis of the geological and structural features of the ore field showed that the presence of a regional steeply dipping fault of the northwestern strike, which are accompanied by numerous parallel and feathering fractures, can serve as an important predictive and prospecting criterion, indicating the possibility of discovering a similar type of epithermal gold ore fields, including those not exposed to the surface. It has been established that the Tutkhun field is very similar to other epithermal gold fields in the region, in particular Zod (Амирян, 1984). Two successively formed gold-bearing mineral associations have been observed: quartz-carbonate sulfide and quartz-carbonate-sulfoantimonite, separated by tectonic movements. It should be noted that the ores of the Tutkhun and Zod fields are similar in the occurrence in productive associations of late stages of sulfoantimonites (boulangerite, jamesonite, bournonite and antimonite), the occurrence of chalcopyrite, fahlores, similar temperature conditions of ore formation, etc. The studies made it possible to establish that dikes and ore-bearing zones often fill the same tectonic fractures.

Table 2

Chemical composition of igneous rocks of the Tertiary intrusive complex of the Tutkhun ore field

№	1	8	26	39	2	506	558	227	552	557	6	7	13	14	32
SiO_2	60.01	57.29	59.28	63.84	61.11	64.01	62.27	53.89	51.86	57.15	55.67	56.78	53.78	59.23	66.03
TiO_2	0.02	0.04	0.05	0.05	0.01	0.07	0.05	0.60	0.12	0.07	0.01	0.01	0.02	0.02	0.03
Fe_2O_3	6.14	5.63	5.22	4.48	4.60	6.32	5.18	6.16	5.84	6.12	5.79	5.36	5.80	7.10	4.02
Al_2O_3	19.84	20.76	18.13	18.39	16.99	16.11	17.17	19.36	20.90	18.75	18.77	18.17	20.26	17.28	17.03
Na_2O	5.28	5.46	4.14	3.28	5.56	5.13	4.62	4.39	6.59	4.74	4.64	4.74	3.74	4.57	3.77
K_2O	0.45	0.44	0.36	0.17	0.57	1.32	0.13	1.04	1.33	1.33			0.30	0.21	1.96
MnO		0.03	0.16	0.04								0.17	0.17	0.01	
CaO	7.06	5.04	6.08	6.14	2.0	3.02	2.86	6.06	4.86	5.74	6.70	7.00	6.82	5.63	5.10
MgO	0.20	3.28	2.10	2.12	3.06	2.50	0.62	4.58	3.02	3.38	4.10	3.06	3.16	1.82	0.39
SO_3				0.20	2.06	0.58	3.92	0.36		1.30		0.78			
H_2O	0.19	0.29	0.36	0.30	0.35		0.39	0.39	0.39	0.46	0.59	0.10	0.88	0.38	0.49
LOI	1.35	1.67	3.28	1.00	3.94	1.28	3.27	4.01	5.40	1.47	3.65	3.76	5.28	4.65	1.54
∑	100.54	99.98	94.75	99.36	100.2	100.34	100.48	100.34	100.31	100.39	99.91	100.48	100.17	100.43	100.36
		Hornblende-biotite quartz diorites, banatites (plutonic facies of the massif)		Dikes of pyroxene-hornblende-diorite porphyrite		Quartz-diorite (monzonite) porphyrites, subvolcanic facies of the massif		Dikes of pyroxene hornblende (diabase) porphyrite		Plagioclase hornblende porphyrites (intrusive andesites and trachyandesites)		Plagioclase quartz porphyrites		Quartz plagioporphyries (intrusive dacites and granodiorite porphyries)	

Table 3

Numerical characteristics of rocks of the Tertiary intrusive complex of the Tutkhun ore field

№	1	8	26	39	2	506	558	227	552	557	6	7	13	14	32
a	15.1	13.6	10.4	7.6	13.6	13.1	10.6	12	18.6	12.8	10.9	10.9	9.7	9.3	11.6
c	8.9	2.4	7.9	7.7	2.4	3.6	3.7	7.9	6.3	6.3	7.9	7.3	9.1	6.9	6
b	8.9	12.7	9.8	9.9	12.7	10.6	11.7	14.1	11.1	12.1	13.4	14.2	13.6	16.1	4.7
s	67.1	71.3	71.9	74.8	71.3	78.7	74	66	64	68.8	67.8	67.6	67.4	67.4	77.7
c'	22.1	–	1.6	–	–	–	–	0	1.4	4.3	6	11.2	–	–	9.1
d'	–	26.4	–	22.7	26.4	10.3	50.9	–	–	–	–	–	15.9	0.9	–
f'	73.1	31.8	55	39.7	31.8	50	40	40.6	48.5	45.2	39.6	34.7	39.8	18.4	74.8
m'	4.8	41.8	43.4	37.6	41.8	39.7	9.1	59.4	50.1	50.5	54.4	53.6	44.8	80.7	16.1
n'	94.4	92.5	94.5	96.6	92.5	85.5	96.9	86.5	88.3	84.4	100	100	95.3	96	74.4
afc	1.7	5.8	1.3	1	5.8	3.6	2.9	1.6	3	8.1	1.4	1.4	1.1	1.3	2
Q	4.9	1.3	15.1	26.7	13	15.6	23.1	0.4	15.5	55	4.1	6.1	6.5	9.6	26.2
	Hornblende-biotite quartz diorites, banatites (plutonic facies of the massif)				Dikes of pyroxene-hornblende diorite porphyrite	Quartz-diorite (monzonite) porphyrites, sub-volcanic facies of the massif		Dikes of pyroxene hornblende (diabase) porphyrite	Plagioclase hornblende porphyrites (intrusive andesites and trachyandesites)		Plagioclase quartz porphyrites				Quartz plagioporphyries (intrusive dacites and granodiorite porphyries)

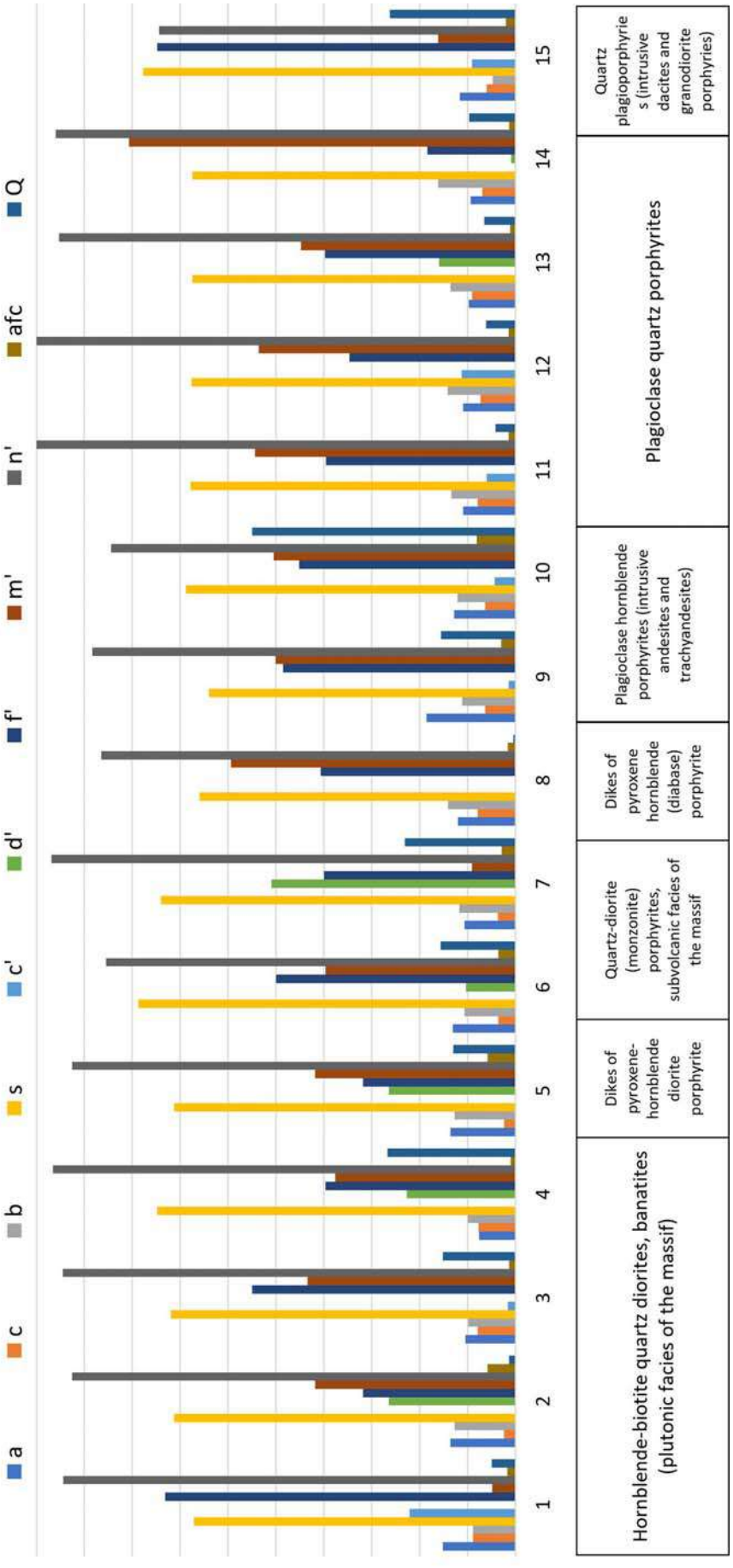

Fig. 12. Petrochemical diagram of rocks of the Tertiary intrusive complex of the Tutkhun ore field

At the same time, the mineralized zones clearly intersect and often displace the most ancient, and in some places, young dikes. So, late dikes created the mechanical heterogeneity of the environment, which predetermined the main directions of ore-bearing zones. At the same time, the dikes experienced the greatest hydrothermal alteration and contain a large amount of epigenetic minerals (carbonate, sericite, sulfides, kaolinite, chlorite, dispersed gold), similar to minerals of ore-bearing zones.

Elements of the internal structure of the mineralized zones, their morphology, thickness and ultimately, their gold mineralization are determined by the following structural and lithological features: impermeable barriers, boundaries of lithological strata, bends of ore-bearing zones, intense fracturing of ore-bearing rocks, especially between adjacent and parallel dikes, and others.

Ore-bearing zones of hydrothermally altered rocks are placed on all members of the intrusive complex, including the latest dykes. At the same time, comparative data on the content of dispersed gold in rocks of the Gazikhanli-Zargulu granitoid massif and its vein rocks that differ in the time of formation show that gold accumulates in the rocks of more and more recent intrusive members along with an increase in the content of volatile components in the same rocks (sulfuric anhydride, carbon dioxide and water).

REFERENCES

Abdullayeva Sh.F. The triune ore-concentrating structure – the junctions of large deep faults that control the placement of gold ore fields in the central part of the Lesser Caucasus. Materials of the Republican Scientific Conference. Baku, May 2-3, 2023 (in Russian).

Abdullayeva Sh.F., Novruzova S.R. Gold ore epithermal Tutkhun ore field (the central part of the Lesser Caucasus): geological aspects, structure, mineralogical and geochemical features, conditions of ore formation. Materials of the Republican Scientific Conference. Baku, 2023, pp.23-24 (in Russian).

Amiryan S.O. Gold formations of the Armenian SSR. Publishing House of the Academy of Sciences of the Armenian SSR. Yerevan, 1984, 303 p. (in Russian).

Baba-zadeh V.M., Kekelia S.A., Abdullayeva Sh.F., Kekelia M.A. Main features of the metallogeny of the Caucasus. Nedra. Moscow, 2020, 187 p. (in Russian).

Baba-zadeh V.M., Musayev Sh.D., Nasibov T.N., Ramazanov V.G. Gold of Azerbaijan. Azerbaijan National Encyclopedia. Baku, 2003, 424 p. (in Russian).

Baba-zadeh V.M., Novruzova S.R. On the relationship between hydrothermally altered rocks and mineralization at the main gold fields of Azerbaijan (Tutkhun ore field). News of Baku University (Series of natural sciences). 2023, No. 1, pp. 42-57 (in Russian).

Cong D., Yuan F., Pan T. et al. Genesis of the Heihaibei gold deposit in the East Kunlun Orogenic Belt, China: Evidence from in situ trace elements of gold-bearing sulfides and stable isotopes. Ore Geology Reviews, Jun., Vol. 157, 2023, pp. 105431-1-16.

Geology of Azerbaijan (ed. Ali-Zadeh Ak.A.). Vol. III. Magmatism. Nafta-Press. Baku, 2005, 434 p. (in Russian).

Geology of Azerbaijan (ed. Ali-Zadeh Ak.A.). Vol. IV. Tectonics (Goycha-Akera zone). Baku, Nafta-Press. 2005, pp. 262-317 (in Russian).

Geology of Azerbaijan (ed. Ali-Zadeh Ak.A.). Vol. VI. Minerals (Gold fields of the NE and central part of the Lesser Caucasus. Nafta-Press. Baku, 2005, pp. 236-272 (in Russian).

Gordienko I.V., Badmatsirenova R.A., Lantseva V.S., etc. Selenga ore region of Western Transbaikalia: structural and mineragenic zoning, genetic types of fields and geodynamic conditions of their formation. Geology of ore deposits, 2019, V. 61, No 5. pp. 3-36 (in Russian).

Groves D.I., Santosh M., Zhang L. A scale-integrated exploration model for orogenic gold deposits based on a mineral system approach. Geoscience Frontiers, Vol. 11, No. 3, 2020, pp. 719-738, DOI:10.1016/j.gsf.2019.12.007.

ЛИТЕРАТУРА

Абдуллаева Ш.Ф. Триединая рудоконцентрирующая структура – узлы сопряжения крупных глубинных разломов, контролирующих размещение золоторудных месторождений центральной части Малого Кавказа. Материалы республиканской научной конференции. Баку, 2-3 мая 2023.

Абдуллаева Ш.Ф., Новрузова С.Р. Золоторудное эпитермальное Тутхунское рудное поле (центральная часть Малого Кавказа): геологическое строение, структура, минералого-геохимические особенности, условия рудообразования. Материалы республиканской научной конференции. Баку, 2023, с.23-24.

Амирян Ш.О. Золоторудные формации Армянской ССР. Изд-во АН Арм.ССР. Ереван, 1984, 303 с.

Баба-заде В.М., Мусаев Ш.Д., Насибов Т.Н., Рамазанов В.Г. Золото Азербайджана. Азербайджан Милли Энсиклопедиясы. Баку, 2003. 424 с.

Баба-заде В.М., Кекелия С.А., Абдуллаева Ш.Ф., Кекелия М.А. Основные черты металлогении Кавказа. Недра. Москва, 2020, 187 с.

Баба-заде В.М., Новрузова С.Р. О соотношении гидротермально измененных пород и оруденения на главнейших золоторудных месторождениях Азербайджана (Тутхунское рудное поле). Вестник Бакинского Университета (серия естественных наук), No. 1, 2023, с. 42-57.

Волков А.В., Савва Н.Е., Колова Е.Е. и др. Au-Ag эпитермальное месторождение Двойное (п-ов Чукотка, Россия). Геология рудных месторождений, Т.60, No. 6, 2018, с. 590-609.

Волков А.В., Савва Н.Е., Ишков Б.И. и др. Эпитермальное Au-Ag месторождение Бургали в палеозойском Кедонском вулканическом поясе (Северо-Восток России). Геология рудных месторождений, Т. 63, No. 1, 2021, с. 40-61.

Геология Азербайджана (под ред. Али-Заде Ак.А.). Т.III. Магматизм. Nafta-Press. Баку, 2005, 434 с.

Геология Азербайджана (под ред. Али-Заде Ак.А.). Т.IV. Тектоника (Гейча-Акеринская зона). Nafta-Press. Баку, 2005, с. 262-317.

Геология Азербайджана (под ред. Али-Заде Ак.А.). Т.VI. Полезные ископаемые (Золоторудные месторождения СВ и центральной части Малого Кавказа). Nafta-Press. Баку, 2005, с. 236-272.

Гордиенко И.В., Бадмацыренова Р.А., Ланцева В.С. и др. Селенгинский рудный район Западного Забайкалья: структурно-минерагеническое районирование, генетические типы месторождений и геодинамические условия их образования. Геология рудных месторождений, 2019, Т. 61, No. 5, с. 3-36.

Hlaing M.K., Yonezu K., Zaw Kh. et al. Origin and characteristics of the Shwetagun Deposit, Modi Taung-Nankwe Gold District and the Kunzeik and Zibyaung Deposits, Kyaikhto Gold District in Mergui Belt, Myanmar: Implications for fluid source and orogenic gold mineralization. Frontiers in Earth Science, Vol. 9, 2021, pp. 772083-1-24, https://doi.org/10.3389/feart.2021.772083.

Kashkai M.A., Aliyev V.I., Mammamdov A.I., etc. Petrology and metallogeny of igneous rocks of the Tutkhun River basin. Publishing House of the Academy of Sciences of the Azerbaijan SSR. Baku, 1967, 207 p. (in Russian).

Korobeinikov A.F., Narseyev V.A., Pshenichkin A.Ya. et al. Pyrites of gold ore fields (properties, zoning, practical use). TsNIGRI. Moskva, 1993, 213 p. (in Russian).

Li H., Yang L. Alteration and mineralization patterns in orogenic gold deposits: Constraints from deposit observation and thermodynamic modeling. Chemical Geology, Vol. 607, No. 4, 2022 Sep., p. 121012.

Mineral resources of Azerbaijan (chief editor: V.M. Babazadeh). Azerbaijan National Encyclopedia. Baku, 2005, 808 p. (in Russian).

Nekrasov E.M., Dorozhkina L.A. Sukholozhskoe gold ore field and possible searches for ores on its flanks. Proceedings of higher educational institutions. Geology and exploration. Vol. 63(2), 2020, p. 21-34 (in Russian), https://doi.org/10.32454/0016-7762-2020-63-2-21-34.

Sillitoe R.H., Goldfarb R.J., Robert. F. et al. Geology of the world's major gold deposits and provinces [Special publications of the society of economic geologists]. Vol. 23, 2020, 845 p., https://doi.org/10.5382/SP.23.

Suleymanov E.S. Gold ore formations of the Lesser Caucasus. Elm. Baku, 1982, 280 p. (in Russian).

Volkov A.V., Savva N.E., Ishkov B.I. et al. Burgali epithermal Au-Ag field in the Paleozoic Kedon volcanic belt (North-East Russia). Geology of ore deposits, V. 63, No. 1, 2021, pp. 40-61 (in Russian).

Volkov A.V., Savva N.E., Kolova E.E. et al. Dvoinoye Au-Ag epithermal field (Chukotka Peninsula, Russia). Geology of ore fields, 2018, V.60, No. 6. pp. 590-609 (in Russian).

Коробейников А.Ф., Нарсеев В.А., Пшеничкин А.Я. и др. Пириты золоторудных месторождений (свойства, зональность, практическое применение). ЦНИГРИ. Москва, 1993, 213 с.

Кашкай М.А., Алиев В.И., Мамедов А.И. и др. Петрология и металлогения магматических пород бассейна реки Тутхун. Изд-во АН Азерб.ССР. Баку, 1967, 207 с.

Минерально-сырьевые ресурсы Азербайджана (под ред. В.М. Баба-заде). Азербайджан Милли Энсиклопедиясы. Баку, 2005, 808 с.

Некрасов Е.М., Дорожкина Л.А. Сухоложское золоторудное месторождение и возможные поиски руд на его флангах. Известия высших учебных заведений. Геология и разведка, Том 63(2), 2020, с. 21-34, https://doi.org/10.32454/0016-7762-2020-63-2-21-34.

Сулейманов Э.С. Золоторудные формации Малого Кавказа. Элм. Баку, 1982, 280 с.

Cong D., Yuan F., Pan T. et al. Genesis of the Heihaibei gold deposit in the East Kunlun Orogenic Belt, China: Evidence from in situ trace elements of gold-bearing sulfides and stable isotopes. Ore Geology Reviews, Jun., Vol. 157, 2023, pp. 105431-1-16.

Hlaing M.K., Yonezu K., Zaw Kh. et al. Origin and characteristics of the Shwetagun Deposit, Modi Taung-Nankwe Gold District and the Kunzeik and Zibyaung Deposits, Kyaikhto Gold District in Mergui Belt, Myanmar: Implications for fluid source and orogenic gold mineralization. Frontiers in Earth Science, Vol. 9, 2021, pp. 772083-1-24, https://doi.org/10.3389/feart.2021.772083.

Groves D.I., Santosh M., Zhang L. A scale-integrated exploration model for orogenic gold deposits based on a mineral system approach. Geoscience Frontiers, Vol. 11, No. 3, 2020, pp. 719-738, DOI:10.1016/j.gsf.2019.12.007.

Li H., Yang L. Alteration and mineralization patterns in orogenic gold deposits: Constraints from deposit observation and thermodynamic modeling. Chemical Geology, Vol. 607, No. 4, 2022 Sep., p. 121012.

Sillitoe R.H., Goldfarb R.J., Robert. F. et al. Geology of the world's major gold deposits and provinces [Special publications of the society of economic geologists]. Vol. 23, 2020, 845 p., https://doi.org/10.5382/SP.23.

СТРУКТУРНЫЕ УСЛОВИЯ ЛОКАЛИЗАЦИИ ЗОЛОТОГО ОРУДЕНЕНИЯ В ПРЕДЕЛАХ ТУТХУНСКОГО РУДНОГО ПОЛЯ (ЦЕНТРАЛЬНАЯ ЧАСТЬ МАЛОГО КАВКАЗА)

Баба-заде В.М., Абдуллаева Ш.Ф., Новрузова С.Р.

Бакинский государственный университет, Азербайджан

г. Баку, ул. академика Захид Халилова, 33, AZ 1148: vasifbabazadeh1938@bsu.edu.az; shakhla.a@gmail.com; samiranovruzova001@gmail.com

Резюме. Исследованы золотоносные участки рудного поля, сходства и различия структурных условий их образования, элементный и минеральный состав руд, различные метасоматиты-пропилиты, березиты и особенно вторичные кварциты. Определены основные закономерности размещения оруденения в плане, на флангах и на глубину.

Золоторудная минерализация может быть рассмотрена в плане некоторых региональных особенностей геологического развития Малого Кавказа, определивших благоприятное сочетание в этом районе геологических условий и тем самым намечающих естественные границы рудного поля, а также в плане частных элементов структуры, определяющих структурное положение и строение золоторудных образований. Интрузивные и субвулканические породы верхнеэоценового возраста представляют единый комплекс, формируют в районе Казыханлы-Заргулинский массив, приближающийся к субвулканической фации магматических образований. Поле развития золоторудных образований охватывает преимущественно выходы гранитоидных пород массива и его экзоконтактовые ореолы, куда проникают обильные дайки, наиболее поздние члены верхнеэоценового комплекса интрузивных образований. На этой площади золоторудная минерализация локализуется в узких и протяженных зонах сильно измененных пропилитизированных пород массива и его ближних ореолов. Распределение их в пределах рудного поля весьма неравномерное. Местами такие зоны образуют сближенные свиты, в большинстве случаев совпадающие с полями наиболее обильного развития дайковых пород.

Как видно, золотоносные зоны парагенетически связаны с дайками, завершающими развитие гранитоидных интрузивных комплексов. Те и другие, наиболее близкие по времени развития магматического и послемагматических процессов, используют в своем размещении единые структуры более раннего периода развития.

Ключевые слова: *центральная часть Малого Кавказа, месторождение, участок, структура, эпитермальное, золото, серебро, вторичные кварциты, генетические особенности, рудообразование, золото-кварцевые рудные зоны*

TUTQUN FİLİZ SAHƏSİ DAXİLİNDƏ QIZIL FİLİZLƏŞMƏSİ LOKALLAŞMASININ STRUKTUR ŞƏRAİTİ (KİÇİK QAFQAZIN MƏRKƏZİ HİSSƏSİ)

Baba-zadə V.M., Abdullayeva Ş.F., Novruzova S.R.
Bakı Dövlət Universiteti, Azərbaycan
Bakı şəh., akademik Zahid Xəlilov küç., 33, AZ 1148: vasifbabazadeh1938@bsu.edu.az; shakhla.a@gmail.com; samiranovruzova001@gmail.com

Xülasə. Filiz sahəsinin qızıl daşıyan sahələrinin əmələgəlmələrinin oxşar və fərqli struktur şəraitləri, filizlərin element və mineral tərkibi, müxtəlif metasomatitlər-propillitlər berizitlər və xüsusən törəmə kvarsitlər tətqiq edilmişdir. Filizləşmənin planda, cinahlarda və dərinlikdə əsas yerləşmə qanunauyğunluğu müəyyən edilmişdir. Planda qızıl minerallaşmasına Kiçik Qafqazın geoloji inkişafının, o cümlədən rayonda əlverişli geoloji şəraitin birləşmələrini, filiz sahəsinin sərhədlərini, həmçinin planda qızıl filizi əmələgəlməsinin quruluşunu və struktur vəziyyətini müəyyən edən bir sıra regional xüsusiyyətləri kimi baxmaq olar. Gec eosen yaşlı intruziv və subvulkanik süxurları rayonda Qazıxanlı-Zərqulu massivi əmələ gətirərək vahid massivi əks etdirir. Qızıl filizi əmələgəlmələrinin inkişaf sahəsinin çıxışını və onun ekzotəmas oreolunu əhatə edir. Burada gec eosen intruziv kompleksinin daha gec üzvləri və daykalar təzahür edir.

Bu sahədə qızıl filizi minerallaşması massivin güclü dəyişilmiş propillitləşmiş süxurların ensiz və uzanmış zonalarında və onun yaxın oreollarında lokallaşırlar. Bəzi yerlərdə belə zonalar, əksər hallarda dayka süxurlarının daha geniş inkişaf tapdığı sahələrdə yaxınlaşmış yaruslar əmələ gətirir. Ən çox rast gəlinən sahə və yaxınlaşmış filiz zonası filiz sahəsi kimi ayrılır.

Göründüyü kimi, qızıl filizi daşıyan zonalar qranitoid intruziv kompleksinin yekun inkişafının daykaları ilə əlaqədardır. Zamanca inkişafı üzrə daha yaxın maqmatik və postmaqmatik proseslər onların yerləşməsində əvvəlki inkişaf dövrünün vahid strukturlarından istifadə edir. Bu zaman filiz damarları ilə tamamlanmış çat strukturlarının vəziyyəti tamamilə ətraf süxurların mexaniki xüsusiyyətlərini təyin edir.

Açar sözlər: *Kiçik Qafqazın mərkəzi hissəsi, yataq, sahə, struktur, epitermal, qızıl, gümüş, törəmə kvarsitlər, genetik xüsusiyyətlər, filiz əmələgəlmə, qızıl-kvarslı filiz zonaları*

ANAS Transactions Earth Sciences 1 / 2024

http://www.journalesgia.com

BIOMARKERS OF NAFTALAN OIL

Guliyev I.S.[1], Huseynov D.A.[2], Martynova G.S.[2], Maksakova O.P.[2], Zeinalov S.G.[2]

[1]Presidium of the Azerbaijan National Academy of Sciences, Azerbaijan
30, Istiglaliyyat str., Baku, AZ1001
[2]Ministry of Science and Education of the Republic of Azerbaijan,
Institute of Geology and Geophysics
119, H. Javid Ave., Baku, Azerbaijan, AZ1143: martgs@rambler.ru

Keywords: *Naftalan oil, geochemistry, hydrocarbon composition, biomarkers, gas chromatography-mass spectrometry*

Summary. The results of a study using chromatography-mass spectrometry of Naftalan oil: medicinal (I-II horizon), fuel (III-IV horizon) and used for medicinal purposes during a year in the Naftalan health center in order to determine hydrocarbon and biomarker compositions are presented. Terpanes (191), steranes (m/z 217), hopanes (m/z 191) and adamantanoids (m/z 135, 136, 149, 163) were identified for the first time in Naftalan oil. It was noted that medicinal oil contains approximately 4 times more biomarkers than fuel oil (7.6%; 1.6%, respectively). As a result of a comparative analysis of biomarker indicators of medicinal and fuel Naftalan oil, carried out on a biodegradation scale, it was shown that medicinal Naftalan oil belongs to the biodegraded oil type B-1, stage I-II, with a moderate degree of biodegradation, and fuel Naftalan oil belongs to the chemical type A2, which is typical for oils with a low degree of biodegradation – stage I. Based on the decrease of biomarkers in the composition of Naftalan oil, used throughout the year for treatment, a conclusion was made about their possible participation in the balneological process. Judging by the geochemical parameters, medicinal and fuel oil has the same genesis.

Introduction

Studying biomarkers in oils is very important for understanding their genesis and geochemical history, for increasing reliability of prognosis of oil-and-gas bearing capacity because the complex structures of biomarkers give the detailed information concerning their origin. There is practically no information about biomarkers in Naftalan oil.

Individuality and uniqueness of the Naftalan oil field are explained (Мехтиев и Ахмедбейли, 1969; Шихмамедова и др., 2014) by its confinement to the deep fracture zone. The Naftalan structure is situated within the Arpa-Samur fracture zone, which at all times from Paleozoic till now, was the zone of active display of tectonic movements, conductor of magmatic melts, ore bearing solutions and seismicity. In the formation of the specific shape of oil the participation of the underlying fluids is possible, both as a result of interaction with the organic matter during its fossilization or at the stage of its transformation into the oil, and at the interaction of the mantle emanations with the already formed oil. At the same time, emanation of fluids into the paleobasin and formation of specific conditions of fermentation of initial organic matter at certain stages of sedimentogenesis, which in principle can explain the presence of different-type oils within the same field, seem to be quite probable.

Numerous studies of Naftalan oil have been conducted for many years, but there are still no clear understandings about the difference in composition and properties of naphthenic oil and medicinal Naftalan oil, and moreover, there is no difference in composition and properties of Naftalan oil from different horizons: medicinal heavy oil – in upper horizons of the Upper Maykop and fuel light oil – in lower horizons of the Upper and Lower Maykop.

Objects and methods of research

The aim of this work was to study the biomarker composition of Naftalan oil:

1. Medicinal Naftalan oil from oil base I-II horizon, filter 151-586 m;
2. Fuel Naftalan oil from petroleum base III-IV horizon 1 well;
3. A year used medicinal oil from petroleum base of Naftalan city;

HC composition and biomarkers investigations were made by chromatography-mass spectrometry (GC-MS) on Perkin-Elmer Clarus 680 instrument having interface with high-efficiency mass-selective detector Clarus SQ8T. Hydrocarbon chromatograms were obtained using total ion current (TIC). The chromatograph was equipped with a quartz capillary column of 100 m length, 0.25 mm diameter and impregnated with ZB-1 phase. The carrier gas is helium, with a flow rate of 1ml/min. Evaporator temperature 300°C; programmed temperature ramp from 80 to 290°C at a rate of 4°C/min followed by an isotherm for 70 min. Ionizing source voltage – 70 eV, source temperature – 250°C. Methylene chloride was used as a solvent.

Discussion of results

Hydrocarbon composition of samples of Naftalan oil was determined by the method of chromatography-mass spectrometry (Бабаев и др., 2017; Бабаев и др., 2015; Бабаев и др., 2018a). As we can see (Fig.1, Table 1), medical and fuel naphthalene have essential differences in hydrocarbon composition, namely ∑amount of alkane HC in fuel oil is 23%, whereas in medicinalutic oil their amount is only 3.5%; amount of naphthenic HC in fuel oil is ~59.4%, whereas in medicinal oil it is 83.69%.

Values of Pr=4.94; Ph=2.11; Pr/Ph=2.34 have been calculated for the sample of Naftalan fuel oil (2). According to the literature data, if Pr/Ph = 1.08 - 2.3, it corresponds to sapropel-humus genesis, i.e. mixed genesis.

As for Naftalan oil used for medicinal purposes, its content of alkane HC according to GC-MS data is ~9.1%, naphthenic HC – ~76.79% and aromatic HC – ~14.11 %.

Terpanes, steranes, hopanes and adamantanes were identified in all oil samples. Here are given mass spectra plots for calculation of terpanes, hopanes (m/z 191), steranes (m/z 217) and adamantoids (m/z 135, 136, 149, 163) in the samples of Naftalan oil (Fig. 2-4).

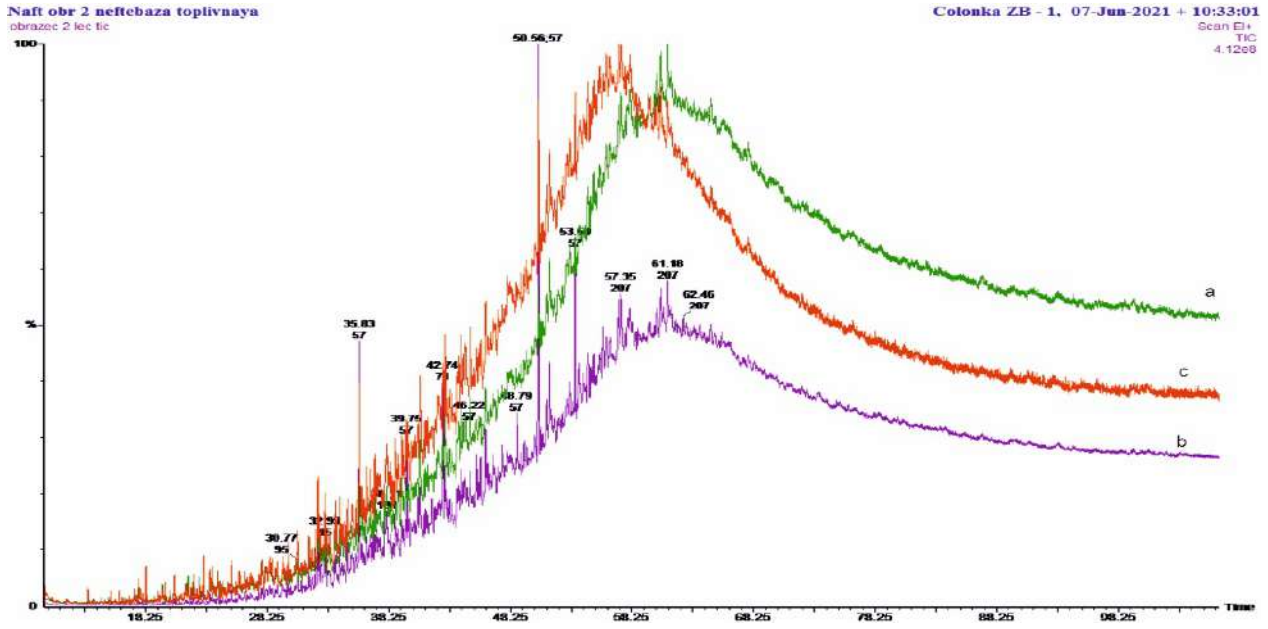

Fig. 1. Mass chromatogram of medicinal (a), fuel (b) and Naftalan oil used during the year for medical purposes (c)

Table 1

Hydrocarbon composition of medicinal and fuel Naftalan oil

Naftalan	n-alk %	i-alk %	isoprenoid %	∑ alkanes	Naphtenes					∑ naphten	Arenes			∑ aren
					mono	bi	tri	tetra	penta		mono	bi	tri	
1) medicinal *	-	3.53	-	3.53	44.08	35.3	4.31	-	-	83.69	2.33	4.67	5.11	12.11
2) fuel **	6,81	16,12	7.05	22.93	41.7	17.14	-	0.53	-	59.37	3.7	1.76	12.02	17.48
3) used 1 year	-	9.1	-	9.1	49.91	26.57	0.12	0.19	-	76.79	4.13	3.45	6.53	14.11

*Dif – 0.67; **Dif- 0.22

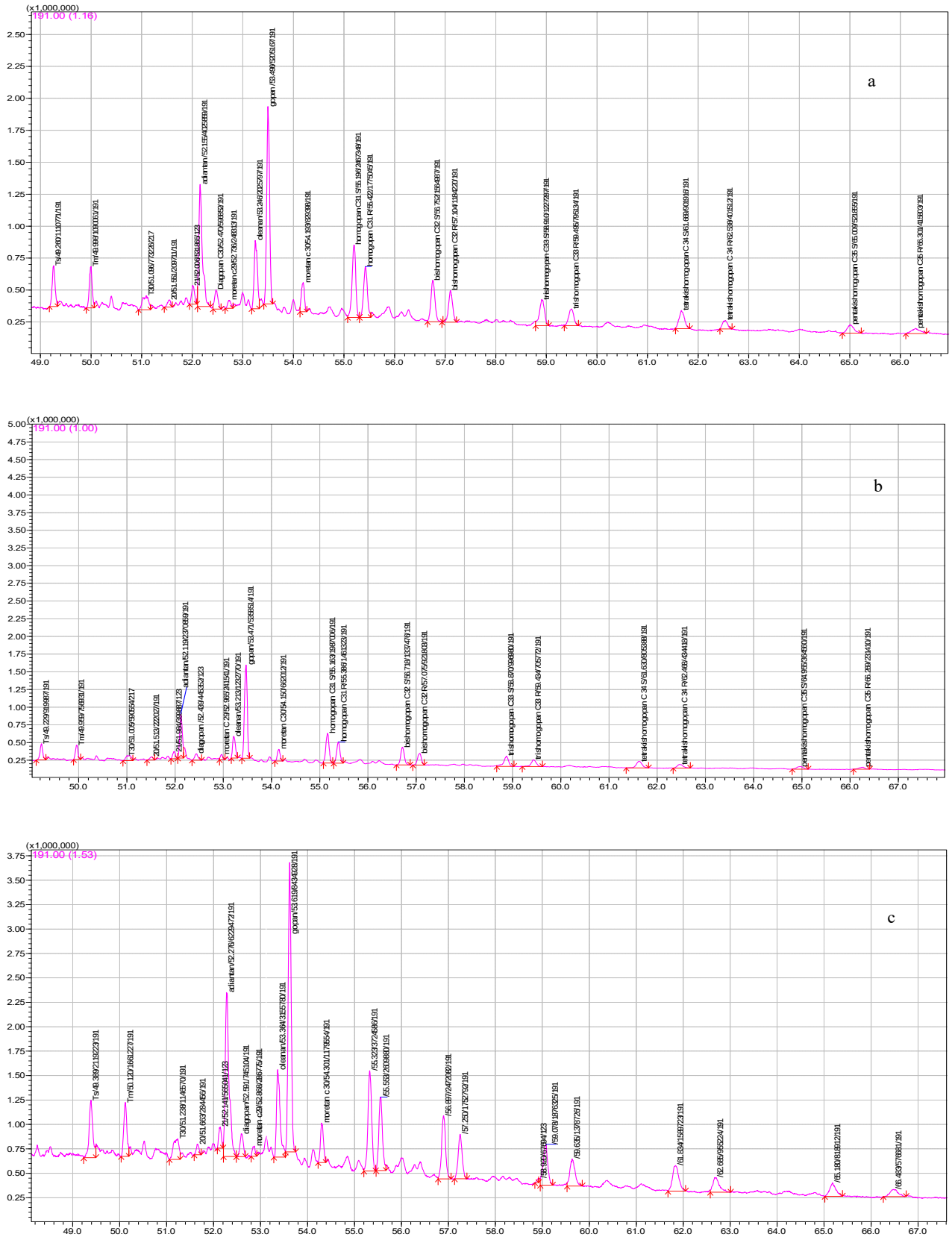

Fig. 2. Chromatography-mass spectrum section of hopanes (m/z 191) in Naftalan medicinal (a), fuel (b) and 1 year used (c) oil

Table 2

Hopane content (m/z 191) in Naftalan oil

Sample / Hopanes	1 - medicinal, %	2 - fuel, %	3- used,%
Ts	4.09	4.21	5.00
Tm	4.02	3.46	3.92
H_{28}17αH, 18αH,21βH bisnorhopane	0.77	1.02	0.67
H_{29} Nor- 25- hopane	1.96	1.83	1.33
Adiantane	14.84	10.85	14.69
Diahopane H_{30}	2.2	2.04	1.76
Moretane H_{29}	0.92	1.11	0.68
Oleanane	7.47	5.64	7.44
Hopane H_{30}	19.19	24.52	19.89
Moretane H_{30}	3.06	3.03	2.78
Homohopane Hh_{31}	15.63	15.78	14.93
Bis homohopane H_{32}	10.14	10.34	9.96
Tris homohopane Hh_{33}	9.45	7.79	7.67
Tetrakis homohopane Hh_{34}	4.8	5.67	6.00
Pentakis homohopane Hh_{35}	3.35	2.73	3.29
Geochemical indicators			
Ts / Tm	1.01	1.22	1.28
$Hh_{35}/(Hh_{31}$-$Hh_{35})$ Homohopane index	0.08	0.06	0.08
Hh_{34}/Hh_{35}	1.43	2.08	1.82
H_{29}/H_{30}	0.77	0.44	0.74
17β,21α-moretanes C_{29} +C_{30} /17α,21β-hopanes C_{29} +C_{30}	0.12	0.12	0.1

To estimate the degree of catagenetic transformation of oils a number of ratios is used: Ts/Tm; 17β, 21α-moretanes H_{29} +H_{30} /17α,21β-hopanes H_{29} +H_{30}. The Ts/Tm ratio increases with increasing maturity and is 1 in the main oil formation zone and ~ 5-10 – in the later stages of catagenesis. It is advisable to use this indicator to assess the degree of maturity of oils for oils with approximately the same level of biodegradation. So, for 1 – Ts/Tm = 1.01, for 2 – Ts/Tm = 1.22.

The hopanes consist of three stereoisomeric series, viz: 17α (H),21β(H), 17β(H),21α(H), 17β(H), 21β(H)-hopanes. The compounds in the βα series are called moretanes. The designations alpha (α) and beta (β) indicate that the hydrogen atoms are below or above the ring plane. The ratio of 17β,21α-moretanes C_{29} +C30 / 17α,21β-hopanes H_{29} +H_{30} decreases with increasing thermal maturity and reaches 0,05 (equilibrium level) in heavily transformed oils. For Naftalan oil sample 1 this coefficient is 0.16 whereas for sample 2 – 0.09 (Table 2) (Ten Haven et al., 1992).

It should be noted that due to the high degree of biodegradation of the studied oils, the calculated maturity parameters probably do not correspond to real values.

To determine the genotype of OM it is necessary to use the obtained indices and relations in combination with other geological indices and geology of the region. The relative distribution of Hh_{31}-Hh_{35} homohopanes is used as an indicator of the oxidation-reduction environment in sedimentogenesis and diagenesis. The ratio of Hh_{35} / (Hh_{31} - Hh_{35}) homohopanes is called the homohopane index. The index describes the aeration of the sedimentation basin, like Pr/Ph, but of a different chemical nature.

Relatively high concentrations of homohopane Hh_{35} indicate marine conditions of sedimentogenesis and reductive conditions of diagenesis (Nazir, Fazeelat, 2014). Relatively low concentrations of Hh_{35} indicate suboxidative or weakly reducing conditions. In our case, homohopane index for Naftalan medicinal oil is 0.08 and 0.06 – for fuel oil. As a result of secondary alteration (oxidation-biodegradation) the

homohopane index of Naftalan oils should differ from actual values and probably increase.

The ratio of C_{29} normethylhopane (adianthane) to hopane is used to establish the facial-geochemical conditions for the accumulation of organic matter. It is believed that in oils formed in terrigenous-carbonate deposits the adiantane/hopane ratio is lower than in oils from halogen-carbonate deposits. In marine anaerobic environments, the ratio of the concentrations of hopanes H_{29} and H_{30} is, as a rule, below 0.5, and in non-marine organic matter last ones are greater than 0.8. In oil from OM-rich carbonate-evaporite rocks H_{29}/H_{30} is close to 1 (Clark, Philip, 1989). In medicinal oil from the Naftalan field (sample 1), H_{29}/H_{30} is 0.77, and in fuel oil (sample 2) it is 0.44 (Table 2), which at first glance indicates a non-marine source of OM for oil sample 1 and marine anaerobic conditions for the accumulation of OM for sample 2. However, the secondary processes that altered the primary composition of Naftalan oils do not allow us to come to an **unambiguous conclusion** about the sources of their OM.

The distribution of C_{27}, C_{28}, and C_{29} sterane hydrocarbons is considered as an indicator of the type of organic matter (OM). The predominance of the C_{29} homologue indicates a large contribution of terrestrial vegetation to the original organic matter, whereas the dominance of C_{27} steranes indicates a significant contribution of zooplankton and algal (Clark, Philip, 1989). In the studied samples of Naftalan oils slightly prevail of C_{27} steranes (Fig. 3, Table 3). This is not consistent with the H_{29}/H_{30} hopane and Hh_{35} / (Hh_{31} - Hh_{35}) neohopane indices due to an imbalance in the biomarkers of biodegraded oils.

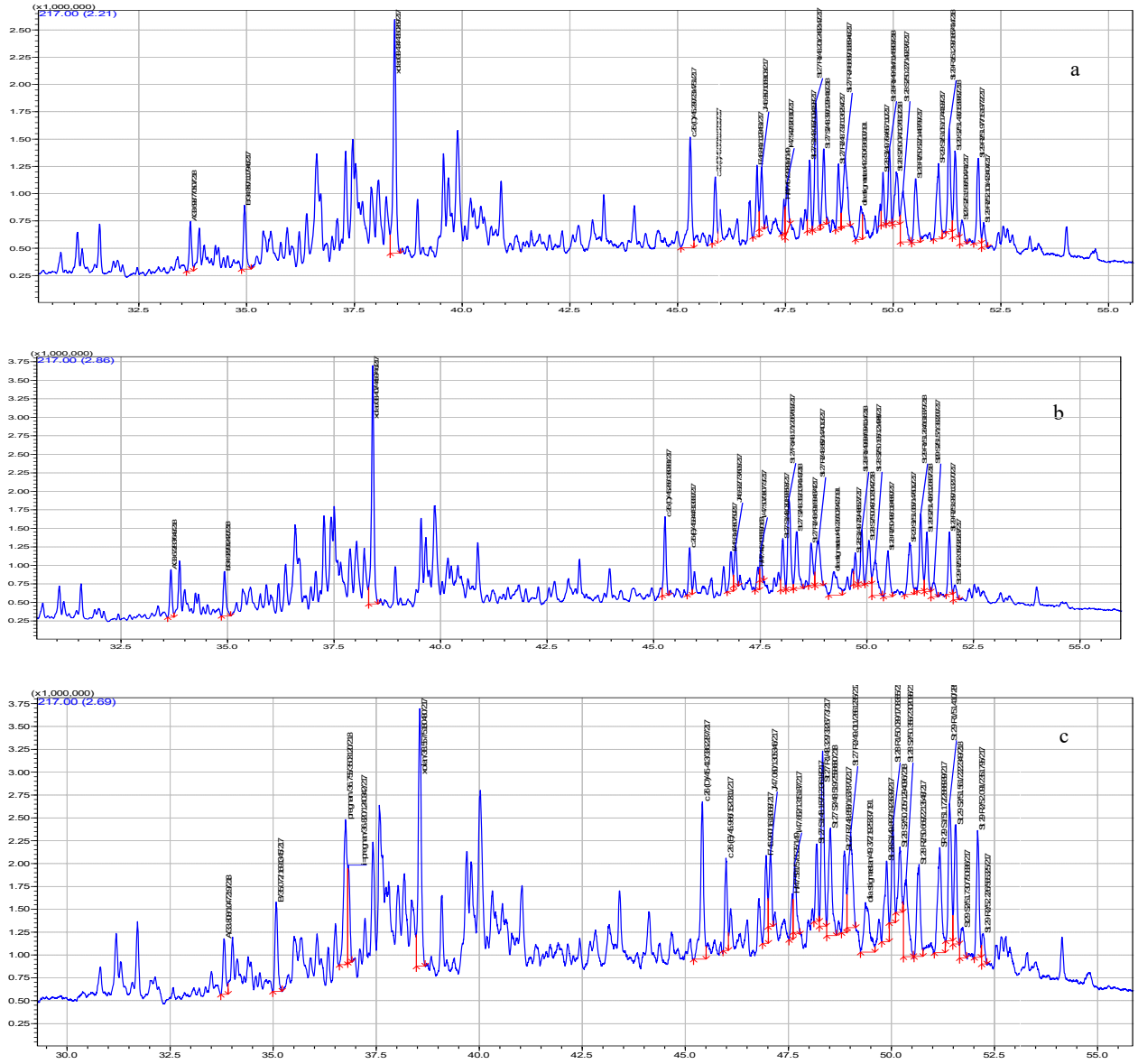

Fig 3. Plot of the chromatography-mass spectrum of steranes (m/z 217) in Naftalan medicinal (a), fuel (b) and a year used (c) oil

Table 3

Stearanes content (m/z 217) in Naftalan oil

Steranes % \ Sample	1. Medicinal	2. Fuel
Diasterane	19.41	15.47
Sterane $_{27}$	22.31	22.79
Sterane $_{28}$	17.14	16.63
Sterane $_{29}$	21.6	20.55
Sterane $_{21+22}$	5.37	5.94
St_{27} : St_{28} : St_{29}	22:17:22	23:17:21

Table 4

Sterols in sample 3 of Naftalan oil used during the year

Steranes % \ Sample	Naftalan oil 3
Diasterane	18.64
Sterane 27	21.92
Sterane 28	18.16
Sterane 29	22.36
Diasterane/reg.sterane 29	0.83

Comparison of the steranes distribution in original medicinal oil and in a year used for treatment medicinal oil shows that after medical treatment content of steranes in the oil almost unchanged (Tables 3 and 4).

Terpanes in Naftalan oils are represented mainly by tricyclic C_{19}-C_{20} (from 20.81 to 28.52) and pentacyclic triternenoids (18α (H) oleanane (5-7% RH). This indicates the presence of continental and higher vegetation in the initial OM. The 18α (H) oleanane in the oil clearly indicates the Cenozoic age of the source rocks.

Judging by the comparative star diagrams of the geochemical parameters of medicinal and fuel Naftalan (Fig.4), both samples generally have the same biomarker-geochemical features.

When considering the ratio of steranes C_{27}:C_{28}:C_{29} for medicinal and fuel Naftalan oil (Table 3), almost equal values of steranes C_{27} and C_{29} (phytoplankton and terrestrial plants) were noted with a lower value of sterane C_{28} (zooplankton), which allows us to judge that we are dealing with genetically similar oils generated by OM of identical rocks.

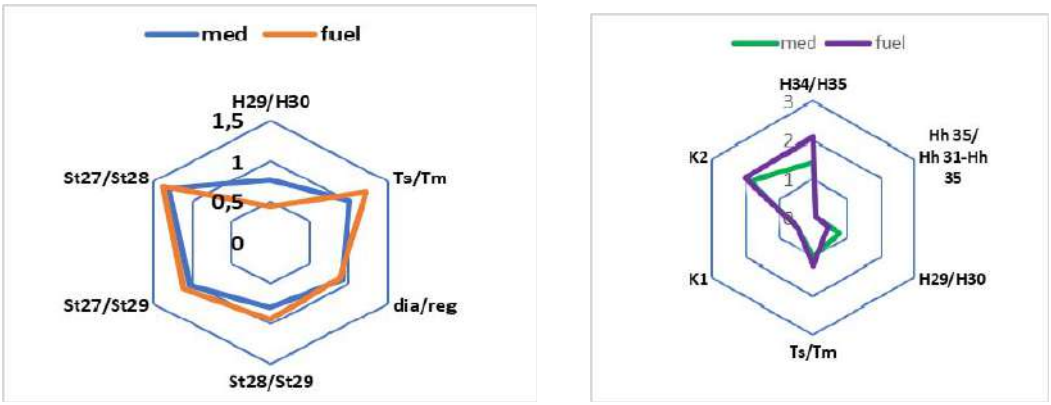

Fig. 4. Comparative diagram of medicinal and fuel Naftalan according to biomarker-geochemical parameters

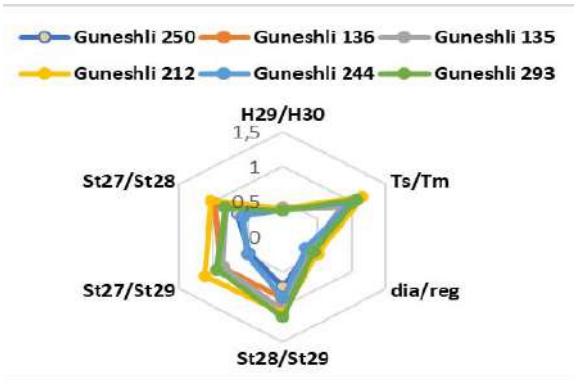

Fig. 5. Comparative diagram of different wells of the Guneshli field according to biomarker-geochemical parameters

For samples from the Guneshli deposit, all sterane ratios decrease sequentially from horizon samples: IX → X → hiatus suite. As can be seen (Fig. 5), the greatest difference in the diagram is observed in the ratios of C_{27}/C_{29} steranes. When considering the ratio of steranes C_{27}:C_{28}:C_{29}, it was noted that the IX horizon is characterized by a predominance of C_{27}, C_{28} steranes, and the X horizon and hiatus formation are characterized by a predominance of C_{29}. The presence of C_{27} sterane indicates the predominance of: phytoplankton, C_{28} – zooplankton, C_{29} – terrestrial plants – in the genesis of oil. It can be assumed that all oil samples from the Gunashli field are genetically of the same type, formed mainly in marine-type sediments, in which sedimentation and diagenesis occurred in a reducing environment (Бабаев и др., 2018b).

Identification of adamantoids in samples of Naftalan oil was carried out by chromatography-mass spectrometry by m/z 135 – alkyladamantanes, m/z 149 – dialkyladamantanes and m/z 163 – trimethyladamantanes according to NIST.

Fig. 6 (a,b,c) shows sections of chromatography-mass spectrum of alkyladamantanes for medicinal, fuel and used during the year Naftalan oil.

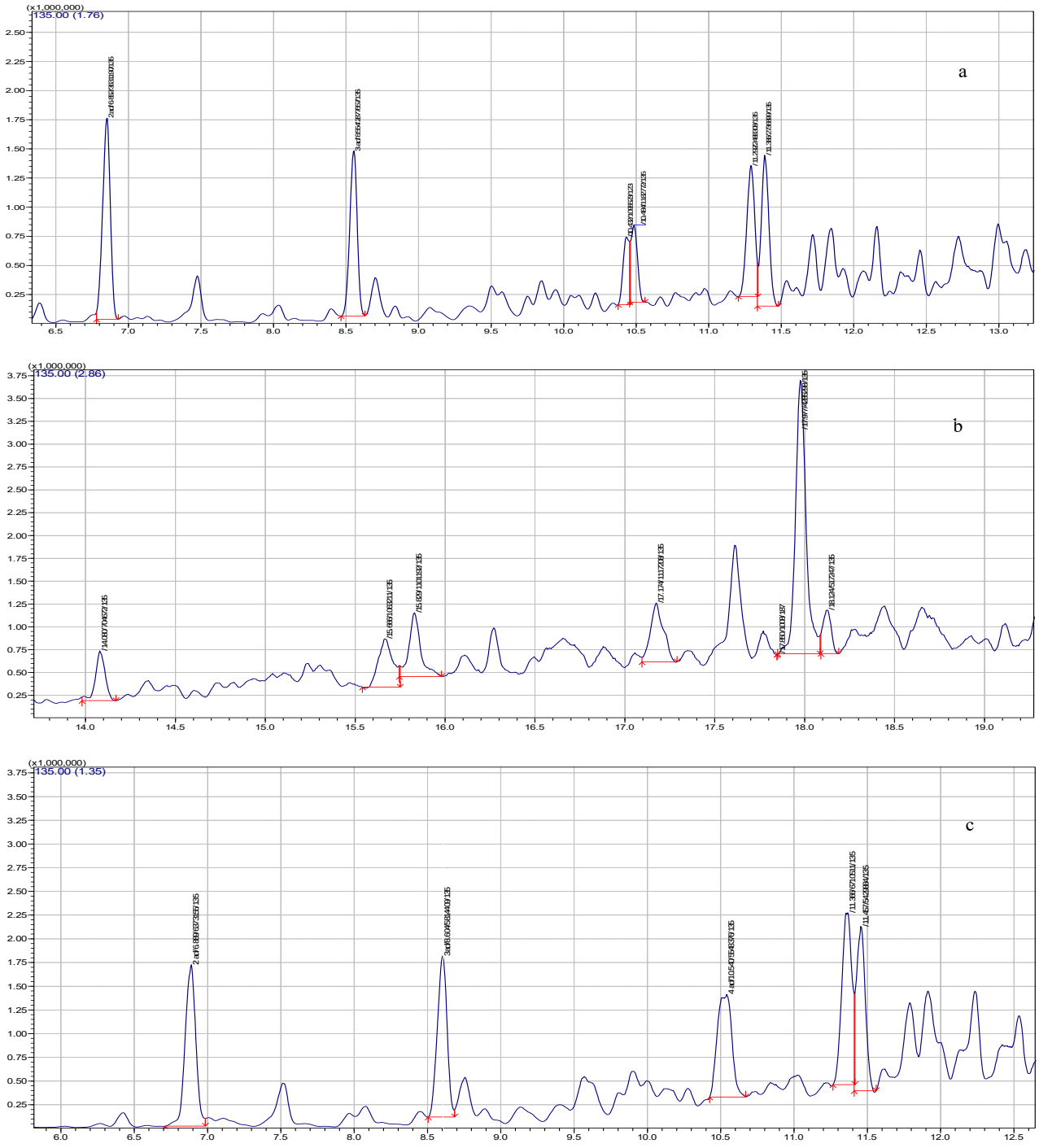

Fig. 6. Chromato-mass spectrum section of alkyladamantanes (m/z 135) in Naftalan medicinal (a), fuel (b) and a year used (c) oil

Table 5 shows the total adamantoid content in % in samples of Naftalan oil. GC/MS data show that dimethyl-substituted homologues (C_{12} dialkyladamantane) have the highest content among alkyladamantanes, and the relative concentration of unsubstituted adamantane is the lowest.

Based on the data in Tables 4-5 for the content of adamantantoids in medicinal oil and oil used during a year, it is shown that the content of dialkyl adamantane decreases by 7% during treatment. This suggests that the effect of medicinal Naftalan oil, along with hopanes and tricyclic terpanes, is also associated with dialkyladamantane.

In Table 6 total quantitative content of biomarkers (%) in samples of medicinal (sample 1), fuel (sample 2) and used (sample 3) Naftalan oil is presented. As it can be seen, the content of hopanes has changed to the greater extent after treatment procedures, namely in sample 3 there are no oleanane, diahopane H_{31}, moretane H_{30}, and the quantity of hopane H_{30} has decreased in 3 times (Table 2). At the same time, the amount of adiantane, diahopane H_{30} and moretane H_{29} increased in sample 3.

In our earlier work, we established that one of the distinctive features of medicinal Naftalan oil is the presence of a significant amount of hydrosaturated cyclic hydrocarbons with decahydronaphthalenes in their composition (m/z–95) ~59.68...60.12%, in contrast to fuel oil, where the amount of hydrosaturated cyclic hydrocarbons is ~ 5.82...11.21% (Бабаев и др., 2017; Бабаев и др., 2015).

ICP / MS method for trace metals and noble metals content in Naftalan have shown that, in quantitative terms, their content exceeds their amount in naphtenic oils of Absheron (Нанаджанова и др., 2016). The natural nanodispersed Naftalan oil was studied (Гулиев и др., 2017). According to dynamic light scattering data, the intensity of particles with a diameter in the range from 100 to 1000 nm was revealed in medicinal Naftalan oil. The fuel oil sample contained particles with a diameter of 50 nm and below. The diffusion coefficients for medicinal oil samples were calculated to be greater than for fuel oil, which obviously also contributes to the balneological effect. As for the used Naftalan oil, its tendency to aggregate particles with a diameter from 100 to 8000 nm was noted, and particles above 1000 nm are stable up to 50^0C (Martynova et al., 2022). Comparative studies of Naftalan oil samples have shown that dynamic light scattering data can provide a distinctive fingerprint of the used medicinal oil.

By serial dilutions of Naftalan followed by inoculation onto a culture of buccal epithelial cells using a micronucleus test, the toxicity dose of native Naftalan was established and its non-toxicity was shown in decimal dilutions (10^{-2}, 10^{-5}, 10^{-8}) of physiological solution (Гулиев и др., 2022).

Judging by the data obtained, we can conclude that in the process of Naftalan treatment the amount of all biomarkers is significantly reduced, but to a greater extent – triterpanes, hopanes and adamantanes, which makes it possible to assume their participation in the healing process.

Table 5

Content of adamantoids in Naftalan oil

Sample / Naftalan oil / Adamantanes, %	1. Medicinal oil, %	2. Fuel oil, %	3.Used a year oil, %
C_{11} (alkyladamantanes)	12.9	15.01	16.41
C_{12} (dialkyladamantane)	65.29	72.04	58.23
C_{13} (trialkyladamantane)	10.82	11.8	17.95

Table 6

The comparative content of biomarkers in Naftalan oil

Naftalan oils	Triterpanes	Hopanes	Steranes	Adamantanes	Σ% in oil
sample 1	1.280	0.470	0.160	5.70	7.60
sample 2	0.250	0.040	1.07	0.020	1.60
sample 3	0.057	0.026	0.200	0.140	0.423

Judging by the data obtained, we can conclude that in the process of Naftalan treatment the amount of all biomarkers is significantly reduced, but to a greater extent – triterpanes, hopanes and adamantanes, which makes it possible to assume their participation in the healing process.

Conclusion

For the first time identification of terpanes (191), steranes (m/z 217), hopanes (m/z 191) and adamantanoids (m/z 135, 136, 149, 163) in Naftalan oil was carried out.

Medicinal and fuel oils from the Naftalan field are biodegraded to varying degrees. This greatly complicates their reliable facial-geochemical conditions of OM accumulation, correlation, genetic typing and assessment of oils maturity based on the content and ratio of terpanes, steranes, and hopanes. At the same time, it can be confidently stated that, along with marine zoo- and phytoplankton, a significant amount of terrestrial plants accumulated in the paleobasin. This is confirmed by the high contents of oleanane in oils. In both fuel and medicinal oils, oleanane is detected in high concentration (5% and 7% respectively). At the same time, this biomarker proves the Paleogene–Lower Miocene age of the studied oils.

Steranes C_{27} dominate among steranes both in fuel and in medicinal oil. The content of adamantoids in both oils (medicinal and fuel oils) is approximately the same, the prevailing content of dialkyladamantanes – C_{12} is the same as in the naphthenic oils of Absheron.

Consideration of the ratio of steranes in medicinal and fuel oil allows us to judge that we are dealing with genetically related oils formed by the organic matter of identical rocks.

Judging by the data obtained, we can conclude that during the treatment process the amount of all biomarkers, but to a greater extent – triterpanes, hopanes and adamantanes, significantly decreases in Naftalan oil, which makes it possible to assume their healing effect.

REFERENCES

Babaev F.R., Martynova G.S., Maksakova O.P. et al. Spesific properties of oil from the Naftalan field. Oil and Gas Geologyç No. 2, 2017, pp. 71-75 (in Russian).

Babaev F.R., Martynova G.S., Maksakova O.P., Nanadzhanova R.G. Guneshli oil. Collection of scientific works "Bakirov Readings" Oil and gas. Moscow, 2018b, p. 28-33 (in Russian).

Babaev F.R., Martynova G.S., Maksakova O.P., Nanajanova R.G. Naftalan field oil. Russian oil and gas Geology, No. 5, 2018a, pp. 87-94 (in Russian).

Babaev F.R., Martynova G.S., Mamedova S.G. et al. On the composition of unique oil of Naftalan field. Geology, Geophysics and Development of Oil and Gas Fields, No. 3, 2015, pp. 36-42 (in Russian).

Clark J.P., Philip R.P. Geochemical characterization of evaporite and carbonate depositional environments and correlation of associated crude oils in the Black Creek Basin, Alberta. Canadian Petroleum Geologist Bulletin, Vol. 37, 1989, pp. 401-416.

Guliev I.S., Huseynov D.A., Martynova G.S., Babaev F.R., Maksakova O.P., Alizadeh A.E., Nanajanova R.G. Study of Naftalan oil nanodispersity. East European Scientific Journal, Vol. 3(19), part 2, 2017, pp. 90-98 (in Russian).

Guliyev I.S., Sadikhova F.E., Martynova G.S., Taghi-zadeh R.K., Ahmedova L.M., Zeynalov S.G., Salmanova S.E. To the problem of naphthalan therapy: about toxicity of native naphthalan. Modern Achievements of Azerbaijani Medicine, No. 4, 2022, p. 53-62 (in Russian).

Martynova G.S., Nanajanova R.G., Velimetova N.I., Zeinalov S.G., Babayeva N.I., Muradkhanova L.R. On some aspects of Naftalan oil properties. Chemical Problems, No. 2, 2022, pp. 122-132.

Mehtiev Sh.F., Akhmedbeyli F.S. Naftalan. Aznefteizdat. Baku, 1969, 129 p. (in Russian).

Nanajanova R.G., Velimetova N.I., Mamedbeyli S.F. Microelements of oil: non-ferrous and noble metals. In: Problems of geology and subsoil development: Proc. Twentieth International Symp. named after Acad. M.A.Usov, dedicated to the 120th anniversary of Tomsk Polytechnic. 120th anniversary of Tomsk Polytechnic University, April 4-8, 2016, TPU

ЛИТЕРАТУРА

Clark J.P., Philp R.P. Geochemical characterization of evaporite and carbonate depositional environments and correlation of associated crude oils in the Black Creek Basin, Alberta. Canadian Petroleum Geologist Bulletin, Vol. 37, 1989, pp. 401-416.

Martynova G.S., Nanajanova R.G., Velimetova N.I., Zeinalov S.G., Babayeva N.I., Muradkhanova L.R. On some aspects of Naftalan oil properties. Chemical Problems, No. 2, 2022, pp. 122-132.

Nazir A., Fazeelat T. Petroleum geochemistry of Lower Indus Basin, Pakistan: I. Geochemical interpretation and origin of crude oils. Journal of Petroleum Science and Engineering, Vol. 122, 2014, pp. 173-179.

Ten Haven H.L., Littke R., Rullkotter J. Hydrocarbon biological markers in Carboniferous coals of different maturities. In: Biological Markers in Sediments and Petroleum (Moldowan J.M., Albrecht P., Philp R.P., eds.). Prentice Hall. Englewood Cliffs, 1992, pp. 142-155.

Бабаев Ф.Р., Мартынова Г.С., Максакова О.П. и др. Особенности нефти месторождения Нафталан. Геология нефти и газа, No. 2, 2017, с. 71- 75.

Бабаев Ф.Р., Мартынова Г.С., Максакова О.П., Нанаджанова Р.Г. Нефть месторождения Нафталан. Геология нефти и газа, No. 5, 2018a, с. 87-94.

Бабаев Ф.Р., Мартынова Г.С., Максакова О.П., Нанаджанова Р.Г. Нефть месторождения Гюнешли. Сборник научных трудов «Бакировские чтения» Нефть и газ. Москва, 2018b, с. 28-33.

Бабаев Ф.Р., Мартынова Г.С., Мамедова С.Г. и др. О составе уникальной нефти месторождения Нафталан. Геология, геофизика и разработка нефтяных и газовых месторождений, No. 3, 2015, с. 36-42.

Гулиев И.С., Гусейнов Д.А., Мартынова Г.С., Бабаев Ф.Р., Максакова О.П., Ализаде А.Э., Нанаджанова Р.Г. Исследование нанодисперсности Нафталанской нефти. East European Scientific Journal, Vol. 3(19), part 2, 2017, pp. 90-98.

Гулиев И.С., Садыхова Ф.Э., Мартынова Г.С., Таги-заде Р.К., Ахмедова Л.М., Зейналов С.Г., Салманова С.Э. К проблеме нафталанотерапии: о токсичности нативного

Publishing House. Tomsk, pp. 365-366 (in Russian).
Nazir A., Fazeelat T. Petroleum geochemistry of Lower Indus Basin, Pakistan: I. Geochemical interpretation and origin of crude oils. Journal of Petroleum Science and Engineering, Vol. 122, 2014, pp. 173-179.
Shikhmamedova T.N., Allahverdiev E.G., Abasova P.D. Clarification of the geological structure of the Maikop Formation in the Naftalan area based on the interpretation of 3D seismic data and the results of modeling together with GIS data. Azerb.Neft.Khozyavstvo, No. 11, 2014, pp. 3-7 (in Russian).
Ten Haven H.L., Littke R., Rullkotter J. Hydrocarbon biological markers in Carboniferous coals of different maturities. In: Biological Markers in Sediments and Petroleum (Moldowan J.M., Albrecht P., Philp R.P., eds.). Prentice Hall. Englewood Cliffs, 1992, pp. 142-155.
нафталана. Современные достижения азербайджанской медицины, No. 4, 2022, с. 53-62.
Мехтиев Ш.Ф., Ахмедбейли Ф.С. Нафталан. Азнефтеиздат. Баку, 1969, 129 с.
Нанаджанова Р.Г., Велиметова Н.И., Мамедбейли С.Ф. Микроэлементы нефти: цветные и благородные металлы. В кн.: Проблемы геологии и освоения недр: Тр. XX Межд. Симп. им. акад. М.А.Усова, посв. 120-летию Томского политехн. университета, 4-8 апреля 2016, Изд-во ТПУ. Томск, с. 365-366.
Шихмамедова Т.Н., Аллахвердиев Э.Г., Абасова П.Д. Уточнение геологического строения майкопской свиты на площади Нафталан на основе интерпретации 3D сейсморазведочных данных и результаты моделирования совместно с данными ГИС. Азерб.Нефт.Хозяйство, No. 11, 2014, с. 3-7.

БИОМАРКЕРЫ НАФТАЛАНСКОЙ НЕФТИ

Гулиев И.С.[1], Гусейнов Д.А.[2], Мартынова Г.С.[2], Максакова О.П.[2], Зейналов С.Г.[2]
[1]Президиум национальной академии наук Азербайджана
AZ1001 Баку, ул. Истиглалият, 30
[2]Министерство науки и образования Азербайджанской Республики, Институт геологии и геофизики
AZ1143, Баку, просп. Г. Джавида, 119: martgs@rambler.ru

Резюме. Представлены результаты исследования нафталанской нефти: лечебной (I-II горизонт), топливной (III-IV горизонт) и использованной в лечебных целях в течение года в оздоровительном центре Нафталана методом хромато-масс-спектрометрии с целью определения углеводородного и биомаркерного составов. Впервые в нафталанской нефти была проведена идентификация терпанов (191), стеранов (m/z 217), гопанов (m/z 191) и адамантаноидов (m/z 135, 136, 149, 163). Отмечено, что в лечебной нефти примерно в 4 раза больше биомаркеров, чем в топливной нефти (7.6%; 1.6% соответственно). В результате сравнительного анализа биомаркерных показателей лечебной и топливной нафталанской нефти, проведенного по шкале биодеградации, было показано, что лечебная нефть Нафталана относится к биодеградированной нефти типа Б-1, стадия I-II, с умеренной степенью биодеградации, а топливная нафталанская нефть относится к химическому типу А-2, который характерен для нефтей слабой степени биодеградации – стадии I. На это указывает отсутствие н-алканов и изопреноидов, пристана, фитана, а также завышенные значения многих геохимических параметров. Согласно проведенным расчетам, соотношение Олеанан/Гопан(30) и Моретан/Гопан(30) для лечебной нафталанской нефти, соответствует биодеградированной нефти типа Б-1. В нефтях, находящихся на этой стадии, стераны не изменены. Что касается топливной нефти, то на ее биодеградацию указывает отсутствие в составе н-алканов C_{17}, C_{18}. Содержание изопреноидов (Pr, Ph) превосходит значение н-алканов, что свойственно для нефтей типа А-2. Соотношения Олеанан/Гопан(30) и Моретан/Гопан(30) для топливной нефти также имеют такие же значения, как и для биодеградированной нефти типа А-2. Показано, что в процессе лечения углеводородный состав нефти не претерпел существенных изменений, зато уменьшилось суммарное количество биомаркеров, что дает возможность предположить их участие в бальнеологическом процессе. Судя по геохимическим параметрам, лечебная и топливная нефть имеют единый генезис.

Ключевые слова*: нафталанская нефть, геохимия, углеводородный состав, биомаркеры, хромато-масс-спектрометрия*

NAFTALAN NEFTİNDƏ BİOMARKERLƏR

Quliyev İ.S.[1], Hüseynov D.A.[2], Martınova Q.S.[2], Maksakova O.P.[2], Zeynalov S.Q.[2]
[1]Azərbaycan Milli Elmlər Akademiyasının Rəyasət Heyəti
AZ1001, Bakı ş., İstiqlaliyyət küç., 30
[2]Azərbaycan Respublikası Elm və Təhsil Nazirliyi, Geologiya və Geofizika İnstitutu
AZ1143, Bakı, H. Cavid pr.119: martgs@rambler.ru

Xülasə. Karbohidrogen və biomarker tərkibinin müəyyən edilməsi üçün xromatoqrafiya-mass spektrometriyasından istifadə etməklə müalicəvi (I-II horizont), yanacaq (III-IV horizont) və Naftalan sağlamlıq mərkəzində 1 il ərzində müalicəvi məqsədlər üçün istifadə olunan Naftalan neftinin tədqiqatının nəticələri təqdim olunur. Naftalan neftində ilk dəfə olaraq terpanlar (191), steranlar (m/z 217), hopanlar (m/z 191) və adamantanoidlər (m/z 135, 136, 149, 163) müəyyən edilmişdir. Qeyd edilib ki, dərman neftinin tərkibində yanacaqdan təxminən 4 dəfə çox biomarker var (müvafiq olaraq 7.6%; 1.6%). Biodeqradasiya miqyasında aparılan müalicəvi və yanacaq Naftalan neftinin biomarker göstəricilərinin müqayisəli təhlili nəticəsində məlum olmuşdur ki, müalicəvi Naftalan nefti B-1 tipli, I-II mərhələli biodeqradasiyaya uğramış neftə aiddir. Yanacaq Naftalan nefti isə biodeqradasiya dərəcəsinə əsasən A-2 kimyəvi növünə aiddir ki, bu da zəif biodeqradasiyaya məruz qalmış olan neftlər üçün xarakterikdir - I mərhələ. Bu, n-alkanların və izoprenoidlərin, pristan, fitanın olmaması, həmçinin bir çox geokimyəvi parametrlərin həddindən artıq yüksək qiymətləri ilə göstərilir. Hesablamalara görə, müalicəvi Naftalan nefti üçün oleanane/hopane(30) və moretane/hopane(30) nisbəti B-1 tipli biodeqradasiya olunmuş neftə uyğundur. Bu mərhələdə neftlərdə steranlar dəyişmir. Yanacaq neftinin biodeqradasiyası onun tərkibində C_{17} və C_{18} n-alkanların olmaması ilə göstərilir. İzoprenoidlərin (Pr, Ph) tərkibi A2 tipli neftlər üçün xarakterik olan n-alkanların dəyərini üstələyir. Yanacaq neftinin oleanane/hopane(30) və moretane/hopane(30) nisbətləri də A-2 tipli biodeqradasiyaya uğramış neftlərə uyğundur. Göstərilmişdir ki, interpretasiya zamanı neftin karbohidrogen tərkibi əhəmiyyətli dəyişikliklərə məruz qalmamış, lakin biomarkerlərin ümumi sayı azalmışdır ki, bu da onların balneoloji prosesdə iştirakını güman etməyə imkan verir. Geokimyəvi parametrlərə görə müalicəvi və yanacaq neftləri eyni mənşəyə malikdir.

Açar sözlər*: Naftalan nefti, geokimya, karbohidrogen tərkibi, biomarkerlər, xromato-mass spektrometriya*

ANAS Transactions Earth Sciences 1 / 2024

http://www.journalesgia.com

MAGNETO-BASED EARTHQUAKE HAZARD MODELS FOR ABSHERON PENINSULA

Babayev G.R.[1,2], Aliyev Z.V.[1]

[1]Ministry of Science and Education of the Republic of Azerbaijan, Institute of Geology and Geophysics, Azerbaijan
119, H.Javid ave., Baku, AZ1143
[2]Azerbaijan State Oil and Industry University, Azerbaijan
20, Azadlig Ave., Baku, AZ1010

Keywords: *Azerbaijan, Absheron peninsula, earthquake hazard, peak ground acceleration, intensity, magnetic susceptibility, simulation*

Summary. An earthquake hazard model based on the variations of magnetic susceptibility of rocks integrating with macroseismic parameters of a credible earthquake, considering dynamics of the site effects was developed and applied to the Absheron peninsula (Azerbaijan). Magnetic well logging data, lithological and geological maps of the Absheron peninsula, seismic catalogues were also utilized. The maximum expected ground motion for Absheron is estimated for shallow Baku-Caspian 25.11.2000 earthquake near the site, which is noted as a scenario "near-event earthquake" and considered as credible earthquake with moment magnitudes Mw=6.18 and Mw=6.08. The moment magnitude is accepted as Mw=6.8. Local site effect assessment was carried out by detailed geotechnical investigation of soil from bedrock to surface using one-dimensional (1-D) ground response analysis with SHAKE2000. We estimated the response of soil layers under earthquake effect by computing soil amplification and the variation of ground motion characteristics on the surface. Based on the scenario earthquake parameters, the surface peak ground acceleration is computed, correlated with the MSK-64 intensity, and mapped. We simulated ground acceleration, seismic intensity and magnetic susceptibility. The northeast and southeast parts of the peninsula are characterized by surface peak ground acceleration of 165-250 gal and intensity VIII-IX, which is 31% and 49% higher than the seismic hazard in the same values compared to other parts. For the eastern part, magnetic susceptibility varies between 0.5-1.0. The values indicate the distinct relationship of variations in the magnetic field with the seismic effect of earthquakes. Our approach makes a significant contribution to improving existing methods for seismic hazard assessment.

Introduction

Magnetic properties of rocks in the fault zones are natural archives of the fault associated processes in tectonically active regions. It generates rock magnetism, which is the study of the magnetic properties of rocks, sediments, soils, and even fossils, a promising tool to unravel faulting processes (Yang et al., 2020). The rock's magnetic features are sensitive to both chemical and physical changes occurring in rocks during the faulting. For example, variations in physical grain size are often reflected in magnetic granulometry, which is the (inferred) grain-size distribution of magnetic particles in a sample, usually expressed through the magnetic domain structure (Yang et al., 2020).

The magnetic properties of fault rocks can be used as tracers for physical and chemical alterations caused by frictional heating during earthquakes (Pei et al., 2014). Magnetic susceptibility and rock magnetism have commonly been used to understand fault slip zones' physical characteristics and chemical processes (Enomoto and Zheng, 1998; Nakamura and Nagahama, 2001; Ferré et al., 2005, 2012).

Recently, a few studies (Wenchuan Earthquake with Mw=7.9, 2008) of high magnetic susceptibility within fault gouges have been described from several faults related to large earthquakes (Enomoto and Zheng, 1998; Nakamura and Nagahama, 2001; Fukuchi et al., 2005; Hirono et al., 2006; Mishima et al., 2006, 2009). It permits the utilization of magnetic properties of rocks in terms of magnetic susceptibility to integrate with seismic effect parameters of credible earthquakes to assess seismic hazard for the area of the study.

In this paper we model earthquake hazard assessment with consideration of the rocks' magnetic

susceptibility variations integrating with a credible earthquake's macroseismic parameters (magnitude, depth, location, epicentral distance) and site effects applied to the Absheron peninsula in Azerbaijan.

The Absheron peninsula is situated in the central part of the Alpine-Himalayan seismic belt and is involved in the dynamics of lithospheric structural units of the Arabian and Eurasian plates (Jackson et al., 2002). This lithosphere dynamics results in stress-strain localization and release in earthquakes, magmatic and mud volcanism, landslides, and other active geological and geophysical processes (Panahi, 2003). Absheron peninsula, together with the part of the adjacent basin of the Caspian Sea (Azerbaijan), is located on the south-eastern border of the Greater Caucasus.

Earthquakes in the region migrate along the Alpine-Himalayan seismic belt (Ismail-Zadeh et al., 1996) and are associated with the fault zones located either in the peninsula itself, in the Azerbaijan sector of the Caspian Sea, or in the adjacent folding structures of the Greater Caucasus and Kopet-Dag (Jackson et al., 2002).

Seismically, there are two main active zones affecting the Absheron peninsula. The northern zone is a part of the North Caucasus thrust belt that continues to the east along the Absheron Sill, which is interpreted to be a zone of active subduction (Jackson et al., 2002). Earthquakes occurring in the northern zone are mainly deep reverse or shallow normal focal mechanisms (Jackson et al., 2002). The southern zone is interpreted to be a continuation of the Greater Caucasus thrust. Earthquakes in this area are mainly reverse or right-lateral strike-slip focal mechanisms (Babayev et al., 2010). The peninsula was shaken because of earthquakes from adjacent focal zones (Shamakhi-Ismayilli and the Caspian Sea), including several large and destructive events (Babayev et al., 2010). More recently, in 2000, two consequent earthquakes with moment magnitudes Mw=6.18 and Mw=6.08 struck the peninsula with some human losses and slight damages to buildings, felt by citizens of an area with a large radius (Babayev et al., 2020). The mentioned earthquake occurred in the southern zone of the Absheron peninsula.

Geologically, the Absheron peninsula is represented by a Quaternary system (Holocene and Pleistocene period) in the northeastern and southeastern parts of the peninsula, a Neocene and Quaternary system (Upper Pliocene and Pleistocene period) in the middle part of the peninsula, and a Neogene (Upper Miocene and Lower Pliocene period) in the southwestern part of the peninsula (Alizadeh, 2008).

Lithologically, the study area is composed mainly of clay, sand, sandstone, and limestone of solid and semi-solid configuration. Clay and sand layers are observed more than solid and semi-solid rocks, such as limestone and sandstone, in the different parts of the peninsula (Table 1). Consideration of the lithological factor is one of the important steps in seismic hazard assessment research and is an essential parameter in seismic hazard analysis (Babayev et al., 2010; Babayev and Telesca, 2016; Murphy and O˙brien, 1977; Panza et al., 2011).

In this study, the maximum expected ground motion for the Absheron peninsula is estimated based on the shallow Baku-Caspian earthquake that occurred on November 25, 2000, with moment magnitudes Mw=6.18 and Mw=6.08, which is accepted as scenario "near-event earthquake" and considered as a credible one. Consequently, the relationship between seismic effect parameters and magnetic susceptibility values was analyzed to advance earthquake hazard assessment with application for the Absheron peninsula.

In this study, we applied the macroseismic parameters (magnitude, depth, hypocentral and epicentral distance) of the near-event earthquake and researched the magnetic susceptibility of grounds and soils. Our main objective was to identify a potential relation between the seismic effect and the magnetic properties of rocks in terms of peak ground acceleration (PGA), intensity of shaking, and magnetic susceptibility distributions.

Methodological approach

Choosing the right method (or number of methods) can be based on a qualitative-quantitative estimate. For this purpose, reliable informational and statistical criteria are needed to apply firstly these criteria to geology and geophysics (Eppelbaum, 2014).

For this current research, first and foremost, it was necessary to select scenario earthquakes in order to conduct a correlation between seismic effect parameters of earthquakes and the magnetic susceptibility of rocks. Thus, the 25.11.2000 Baku-Caspian "near-event earthquake" was employed as a scenario earthquake. Magnitude, location of the earthquake epicenter to the investigated site, location on the fault zones, effects on the area, and depth of earthquake (h=35 km) are important criteria in choosing this seismic event as a scenario. Macroseismic parameters (magnitude, depth, hypocentral and epicentral distance) of the scenario earthquake were taken from local and international catalogues. Based on the method of seismic hazard assessment (Babayev et al., 2024), it was considered effective to take the magnitude of the near-event earthquake for this study at 6.8. Thus, the seismic effect from the near-event earthquake parameters with hypothetic moment magnitude Mw=6.8 and 35 km focal depth (h) was assessed.

We integrated analysis of geology in terms of the ages of the rocks, lithology of rock layers, macro-

seismic values of scenario earthquake (Mw=6.8), and magnetic properties of rocks with each other. Identification of the sediment types, thickness of layers, and magnetic susceptibility of rocks were determined by using the respective published papers (Исрафилбеков и др., 1983; Babayev et al., 2020; Hrouda et al., 2009). We attempted to find any relation between parameters of seismic effects and magnetic properties of rocks through analysis of surface peak ground acceleration (PGA), intensity of shaking, soil amplification factor, and rocks' magnetic susceptibility.

Google Earth system was utilized to define the basemap for this research which consequently was meshed into 39 cells with a step 5km×5km grid (Fig. 1) (Google maps, 2024).

Fig. 1. The map of Azerbaijan with the rectangle showing the study area

Macroseismic parameters (magnitude, focal depth) of the Caspian earthquake 25.11.2000, which is accepted in this study as a scenario, near-event earthquake, were used to calculate epicentral/hypocentral distances to each cell of the study area from epicenter of the scenario earthquake (Fig. 2) and consequently to compute bedrock peak ground acceleration (PGA) under each cell and consequently, at the surface of those cells.

Table 1 demonstrates rocks' magnetic susceptibility values. Those values were analyzed and estimated from magnetic well logging data, the wellbores of which are illustrated in Fig. 3.

Consequently, magnetic susceptibility values of rocks were utilized to map the study area in terms of their distribution (Fig. 4).

Peak ground acceleration (PGA) was computed to evaluate the anticipated ground motion at both bedrock and surface level with 1D site effects of lithological layers. The expected bedrock PGA was estimated considering near-event earthquake parameters (magnitude, focal depth) by ground motion prediction equation (GMPE) (1).

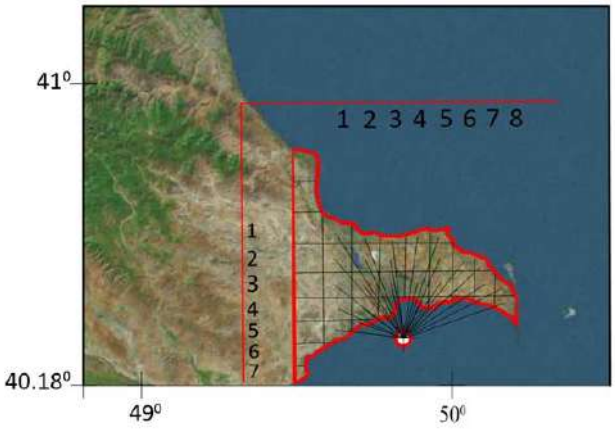

Fig. 2. Meshing of the study area.
Near-event scenario earthquake (accepted as Mw=6.8, focal depth h=35 km) is demonstrated by a circle. Numbers beyond the meshing area were used to enumerate cells

Table 1

Magnetic susceptibility values
in Absheron peninsula for each layer

Cell number	Area	Magnetic susceptibility	Rock type
4.4	Zigh	0.5-1.0	shale
		0.3-0.5	sandstone
		0.1-0.3	limestone
		0.01-0.1	marl
4.7	Zire	0.5-1.0	shale
		0.3-0.5	sandstone
		0.1-0.3	limestone
		0.01-0.1	marl
3.5	Surakhani	0.01 - 0.1	shale
		0.01 - 0.1	marl
		0.01 - 0.1	sandstone
		0.001 - 0.01	limestone
		0.001 - 0.01	granite
2.4	Ramani	0.01 - 0.1	sandstone
		0.01 - 0.1	shale
		0.01 - 0.1	marl
		0.001 - 0.01	limestone
5.2	Bibiheybat	0.01 - 0.1	sandstone
		0.01 - 0.1	shale
		0.01 - 0.1	marl
		0.001 - 0.01	limestone
3.4	Ahmadli	0.01 - 0.1	shale
		0.01 - 0.1	marl
		0.01 - 0.1	sandstone
		0.001 - 0.01	limestone
4.2	Lokbatan	0.5 - 1.0	marl
		0.07 - 0.5	shale
		0.03 - 0.1	sandstone
		0.02 - 0.05	limestone
4.5	Hovsan	0.02 - 0.05	limestone
		0.03 - 0.1	sandstone
		0.07 - 0.5	shale
		0.5 - 1.0	marl

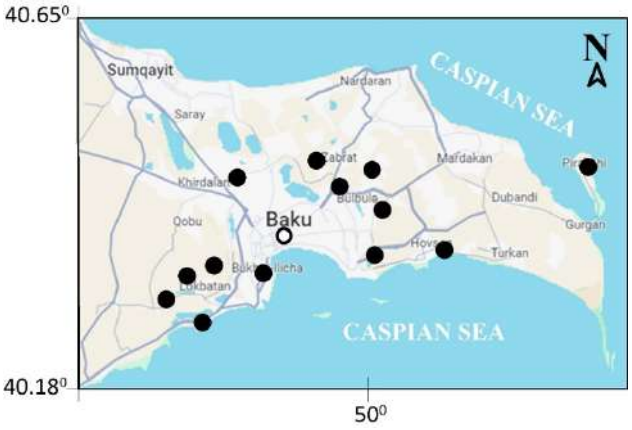

Fig. 3. Dots of magnetic well logging data across Absheron peninsula

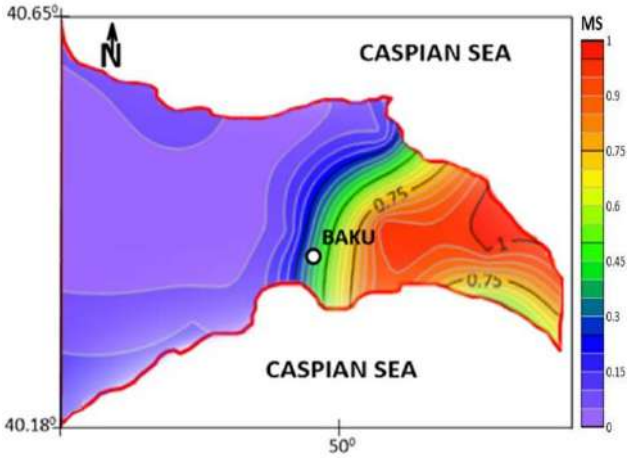

Fig. 4. Distribution of magnetic susceptibility of rocks in Absheron peninsula.
Note: MS indicates magnetic susceptibility

In (1) A is peak ground acceleration (in Gal = 10^{-2} m/s^{-2}), M is the magnitude and R is the hypocentral distance (in km):

$$lg\, A = 0.28M - 0.8\, lg\, R + 1.7 \qquad (1)$$

The Equation (1), an empirical function to compute PGA (Аптикаев и Копничев, 1979), the amplitude of ground motion, is the best-fitting empirically-derived equated function for predicting ground motion for Azerbaijan and, therefore, for the study region (Babayev et al., 2020).

Several studies concluded that shear wave velocity was an important parameter for evaluating the dynamic behavior of soil in the subsurface depth (Kanli et. al., 2006, 2008; Panza et al., 2011). Subsurface shear wave velocity values are significant in calculating seismic hazards (Kanlı et al., 2010; Panza et al., 2011).

The estimation of shear wave velocity (V_s) was derived from an empirical relation (2) with the P-wave velocity (V_p value). V_p value was measured for the specific soils by experimental method (Seed et al., 1969).

$$V_s = V_p/(4.34 - 0.49V_p) \qquad (2)$$

Furthermore, the amplification factor of soil for soft rocks in a subsurface layer was estimated from shear-wave velocities, density, and thickness of the layer using the SHAKE software (Ordonez, 2000) and for hard sedimentary rocks, the amplification factor within a layer has been calculated by using the Eq. (3) using shear-wave velocity (Midorikawa et al., 1992):

$$lg\, A_{AMP} = 1.11 - 0.42\, lg\, V_s \qquad (3)$$

The geological analysis in terms of rock ages and lithology of rock layers was generalized in the subsurface models used in our study in the calculation of the amplification factor of each layer (Table 2). We have calculated time domain peak ground acceleration based on the synthetic accelerograms obtained from the hypothetic earthquake data and respective parameters for all subsurface models. Fig. 5 shows the time domain parameters for eight different subsurface models.

Knowing amplification factor of layers from bedrock up to the surface soil of the Absheron peninsula through subsurface ground thus, the amplification factor for the whole cross-section, the peak ground acceleration (PGA) at surface and the intensity of shaking were computed, providing a comprehensive assessment of seismic effect of the earthquake. The peak ground acceleration (PGA) at the surface was computed through the following equation:

$$A_{SR} = A_{BR} * A_{AMP} \qquad (4)$$

where, A_{SR} is the surface PGA (in gal =10^{-2} m/s^{-2}), A_{BR} is the peak ground acceleration at bedrock (in Gal = 10^{-2} m/s^{-2}), A_{AMP} is the amplification factor.

The surface peak ground acceleration was compared with the intensity values using the correlation scale (Table 3) (Murphy and O'brien, 1977; Trifunac and Brady, 1975).

Table 4 demonstrates the seismic effect values computed from the near-event scenario earthquake parameters. The computation utilized the surface peak ground acceleration (PGA) (Table 4, (10)) and the predicted earthquake intensity (Table 4, (11)) as finals to simulate the peninsula.

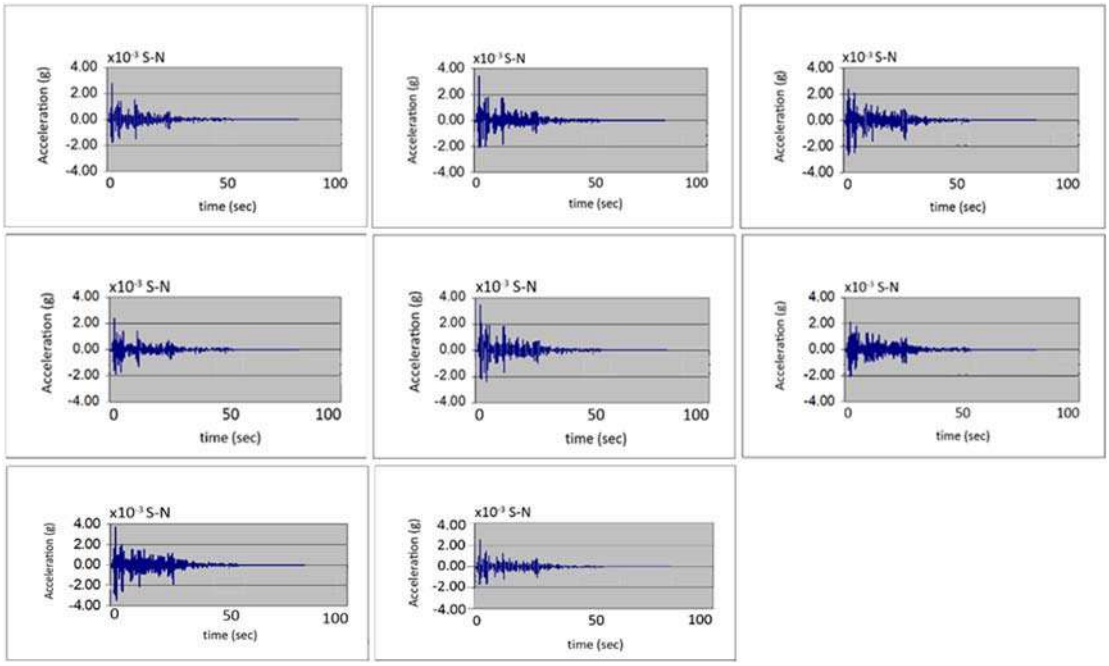

Fig. 5. Simulated time domain PGA based on best-fitted scenario for subsurface models (from above left to the left below: B5, C1, C3, C4, C6, E2, E5, E6)
Note: see Table 2 for the subsurface model description

Table 2

Subsurface lithological-geological models for the Absheron peninsula

Model	Thickness of sediments (m)	Age	Lithology
B5	20	Q	sands, clay, limestone
	110	Q	clays
	1960	N	sands, sandstone, carbonated clays
C1	4	Q	sand, gravel-pebble
	5	Q	clay, argillaceous sand
	20	Q	clay
	3800	N	clay, sand, argillaceous sandstone and limestone
C3	12	Q	limestone
	20	Q	clay, sand, limestone
	1500	N	argillaceous limestone and sandstone
C4	5	Q	sand with sandstone
	5	Q	sand, clay, sandstone
	20	Q	sand, clay, sandstone
	1910	N	sand, sandstone, organic clay
C6	160	Q	sands, clay, limestone
	120	Q	clays
	1960	N	sands, sandstone, carbonated clays
E2	60	Q	sands, sandstone
	290	Q	sands, clay, limestone
	1960	N	sands, sandstone, carbonated clays
E5	5	Q	sands
	150	Q	sands, clay, limestone
	120	Q	clays
	1960	N	sands, sandstone, carbonated clays
E6	5	Q	limestone
	10	Q	sands
	270	Q	sands, clays, limestone
	1960	N	sands, sandstone, carbonated clays

Note: Q – Quaternary; and N – Neogene

Table 3

Conversion between PGA (gal) and intensity (MSK-64) (Murphy and O'brien, 1977; Trifunac and Brady, 1975)

PGA gal	5–12	12–25	25–50	50–100	100–200	200–400
MSK-64	4	5	6	7	8	9

Table 4

Parameters of seismic effect for the near-event earthquake with macroseismic values of the event used for simulation of the surface peak ground acceleration and intensity

N (1)	Cell (2)	M (3)	H(km) (4)	The epicentral distance (km) (5)	R(km) (6)	PGA bedrock (Gal) (7)	Average ground type (8)	Amplification Factor (9)	PGA surface (Gal) (10)	MSK-64 (11)
1	1.1	6.8	35	43	55.44	161.78	clay	1.10	177.96	8
2	1.2	6.8	35	36	50.20	175.13	sand	1.10	192.65	8
3	1.3	6.8	35	34	48.79	179.18	sand	1.10	197.10	8
4	1.4	6.8	35	35	49.49	177.15	sand	1.10	194.86	8
5	1.5	6.8	35	37	50.93	173.15	solid and semi-solid rocks	0.57	98.69	7
6	2.1	6.8	35	39	52.40	169.25	clay	1.10	186.17	8
7	2.2	6.8	35	31	46.75	185.41	clay	0.76	140.91	8
8	2.3	6.8	35	27	44.20	193.92	clay	0.76	147.38	8
9	2.4	6.8	35	26	43.60	196.07	clay	0.95	186.26	8
10	2.5	6.8	35	28	44.82	191.78	solid and semi-solid rocks	0.53	101.64	8
11	2.6	6.8	35	32	47.42	183.32	solid and semi-solid rocks	0.53	97.16	7
12	2.7	6.8	35	37	50.93	173.15	sand	0.53	91.77	7
13	3.1	6.8	35	36	50.20	175.13	clay	1.10	192.65	8
14	3.2	6.8	35	25	43.01	198.21	clay	0.76	150.64	8
15	3.3	6.8	35	19	39.82	210.80	clay	0.53	111.73	8
16	3.4	6.8	35	18	39.35	212.80	clay	0.53	112.79	8
17	3.5	6.8	35	23	41.88	202.48	clay	0.53	107.32	8
18	3.6	6.8	35	28	44.82	191.78	solid and semi-solid rocks	0.53	101.64	8
19	3.7	6.8	35	32	47.42	183.32	solid and semi-solid rocks	0.53	97.16	7
20	3.8	6.8	35	38	51.66	171.18	sand	0.57	97.57	7
21	4.1	6.8	35	31	46.75	185.41	clay	1.10	203.95	9
22	4.2	6.8	35	22	41.34	204.60	clay	1.10	225.06	9
23	4.3	6.8	35	13	37.33	221.97	solid and semi-solid rocks	0.57	126.52	8
24	4.4	6.8	35	14	37.69	220.27	clay	1.10	242.30	9
25	4.5	6.8	35	15	38.07	218.50	sand	0.53	115.81	8
26	4.6	6.8	35	23	41.88	202.48	sand	1.10	222.73	9
27	4.7	6.8	35	30	46.09	187.52	clay	1.10	206.28	9
28	4.8	6.8	35	38	51.66	171.18	sand	1.10	188.30	8
29	5.1	6.8	35	21	40.81	206.70	clay	1.10	227.36	9
30	5.2	6.8	35	31	46.75	185.41	sand	1.10	203.95	9

The investigated parameters (Table 4, (10), (11)) were plotted for the study area, and their distribution patterns are illustrated in Fig. 6 and 7, respectively.

As a part of the comprehensive analysis, magnetic susceptibility, surface peak ground acceleration (PGA), and intensity maps were simulated (Fig. 8, 9). These models allowed us to correlate magnetic susceptibility, surface peak ground acceleration (PGA), and intensity values.

Results and discussions

The simulation of magnetic susceptibility distribution across the study area and the predicted intensity map of the scenario earthquake with hypothetic magnitude 6.8 allowed conducting a correlation between high-intensity zones of VIII-IX and high magnetic susceptibility values of 0.5-1.0 observed in the eastern part, extensively in the northeastern, southeastern parts of the Absheron peninsula, especially in the populated areas of Mardakan, Bulbule, and Dubandi.

Furthermore, the simulation of magnetic susceptibility and surface peak ground acceleration (PGA) distribution maps allowed conducting a correlation between high surface PGA and high magnetic susceptibility of rocks observed specifically in the populated settlements of Turkan, Bulbule, Hovsan, Dubandi in the eastern, southeastern, northeastern parts of the Absheron peninsula where 200-250 Gal surface PGA coincided with 0.5-1.0 magnetic susceptibility values.

Based on this current study, the eastern, southeastern, and northeastern parts of the Absheron peninsula are prone to high intensity of shaking (VIII-IX) and extensively surface peak ground acceleration (200-250 Gal). The magnetic susceptibility of rocks exhibits high values of 0.5-1.0.

The magnetic susceptibility of a rock depends on the type and abundance of magnetic minerals it contains (Awad et al., 2023). The high value of magnetic susceptibility indicates a high abundance of magnetic minerals, while a low magnetic susceptibility value indicates a low abundance of magnetic minerals in rock samples (Siregar et al., 2022).

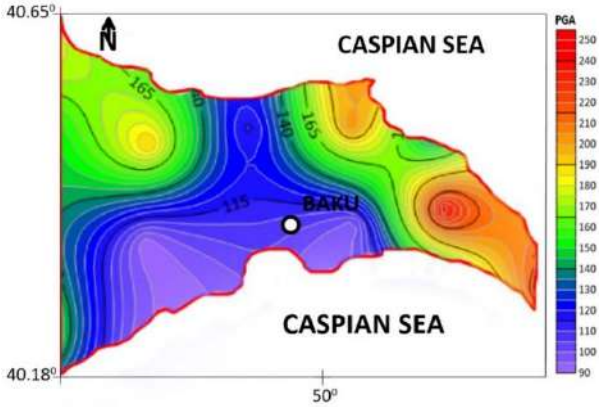

Fig. 6. Distribution of the surface peak ground acceleration (PGA) for a near-event earthquake scenario

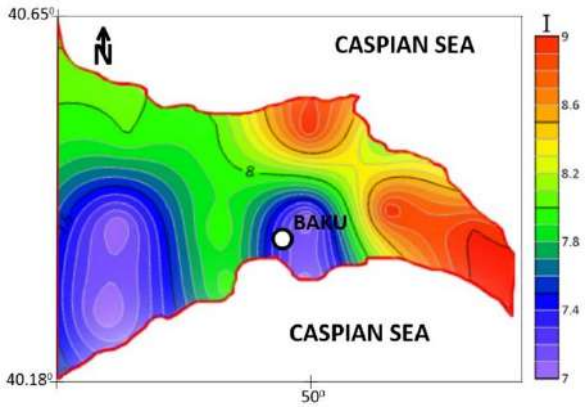

Fig. 7. Intensity (I) distribution for a near-event earthquake scenario

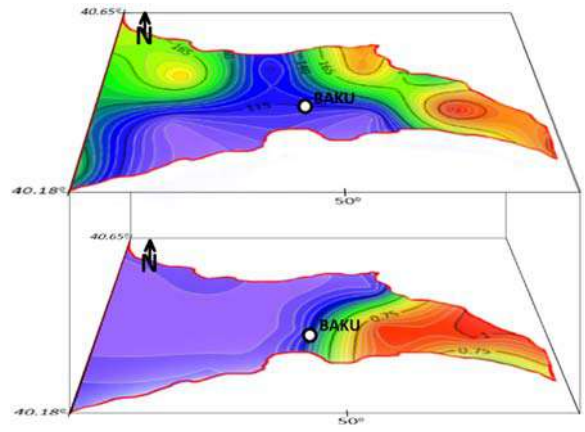

Fig. 8. Simulation of surface peak ground acceleration (PGA) and magnetic susceptibility of the study area (upper one is the distribution of surface peak ground acceleration (PGA) for the near-event earthquake scenario, lower one is the distribution of magnetic susceptibility of rocks)

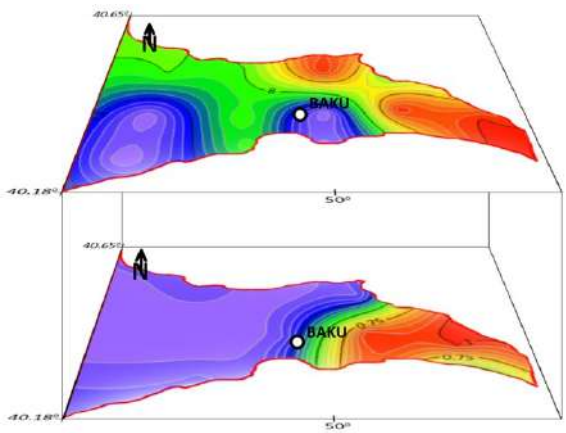

Fig. 9. Simulation of intensity and magnetic susceptibility of the study area (the upper one is intensity distribution for the near-event earthquake scenarios, lower one is a distribution of magnetic susceptibility of rocks)

Theoretically, the high magnetic susceptibility values in the eastern, southeastern, and northeastern parts of the peninsula might indicate the abundance of the sporadic existence of magnetic minerals in the sandstone, limestone, marl, and shale rock formations.

Rocks can also be categorized on their magnetic susceptibility values: any mineral with a positive magnetic susceptibility value is paramagnetic, while a negative magnetic susceptibility value corresponds to a diamagnetic mineral (Elsayed et al., 2021). Among the most common minerals that pose paramagnetism in rocks are illite, pyrite, chamosite, chlorite, and celadonite, which are usually found in sandstone and shale formations (Elsayed et al., 2021). Shales, a mixture of clay and carbonate minerals, represent 2/3 of the sedimentary rocks on Earth with a magnetic mineral group which, at first order, appears simple with ferrimagnetic iron oxides as the main magnetic mineral group present (Kars et al., 2023). Based on the findings they presented, we assume that these mineral compositions of the rock layers might amplify shear wave velocity in the eastern part, extensively in the northeastern and southeastern parts of the Absheron peninsula.

For this study, the amplification factor of soil for soft rocks in a subsurface layer was computed through shear-wave velocities, density, and thickness of the layers. It is assumed that this rock formation with high magnetic susceptibility values affect the amplification factor of soil, specifically in the eastern part, southeastern, and northeastern parts of the Absheron peninsula. Thus, it causes high surface peak ground acceleration values, consequently, compared intensity of shaking.

As a consequence, this current study permits to claim that there is an existing direct, physical relation between surface peak ground acceleration, the intensity of shaking of the earthquake, and magnetic susceptibility of rocks. High surface peak ground acceleration (PGA) and magnetic susceptibility values coincided and demonstrated convergence in the eastern, southeastern, and northeastern parts of the peninsula including areas of Hovsan, Turkan, Bulbule, Mardakan, and Dubandi. The same convergence was demonstrated in the eastern, southeastern, and northeastern parts of the peninsula between the magnetic susceptibility values and predicted seismic intensity of shaking.

As a result, rocks with high magnetic susceptibility values will be characterized by a high trend of earthquakes' seismic effect parameters in terms of peak ground acceleration and intensity of shaking.

Conclusions

This research aimed to model earthquake hazard assessment for the Absheron peninsula by integrating magnetic properties of rocks regarding magnetic susceptibility with seismic effect parameters: computed surface peak ground acceleration (PGA) and intensity of shaking from a credible earthquake. The Baku-Caspian earthquake of 25.11.2000 with accepted moment magnitude Mw=6.8 was taken as a scenario earthquake near the investigated site and considered as a "near-event earthquake." The study analyzed the local site effects and computed soil amplification factors, revealing the variation of ground motion characteristics on the surface. The simulated models allowed revealing convergent correlations between values of magnetic susceptibility and seismic intensity of shaking in the eastern, southeastern, and northeastern parts of the peninsula. Specifically, areas with high seismic intensity of shaking (VIII-IX) coincided with high magnetic susceptibility values (0.5-1.0) in the eastern, southeastern, and northeastern areas. This technique permits disclosing convergence of investigated parameters in terms of magnetic susceptibility of rocks, surface peak ground acceleration (PGA), and seismic intensity of shaking computed by the scenario earthquake.

Consequently, we can conclude that rocks with high magnetic susceptibility values are interlinked with the seismic effect that an earthquake can produce depending on the shallow depth and high magnitude. We interpret this approach as an additional input towards improving seismic hazard assessment methods. This successful integration between seismic hazard and magnetic properties of rocks demonstrates productivity of interdisciplinary researches and indicates the need for integration of geophysical methods for future studies. The results can be served as an additional input in the studies of magnetic influence on the earthquakes and the researches of the relationship between the magnetic perturbations and seismic responses.

REFERENCES

Alizadeh A.A. (Ed.) Geological map of Azerbaijan Republic, Scale 1:500,000, with Explanatory Notes. Baki Kartoqrafiya Fabriki. Baku, 2008.

Aptikayev F. and Kopnichev Y. Considering focal earthquake mechanism at the prediction of strong motion parameters. Dokl. Akad. Nauk SSSR, Vol. 247, 1979, pp. 822-825 (in Russian).

Awad A., Elnaggar O.M., Mohamed Sh.F. Magnetic susceptibility as an indication of reservoir properties of the Nubia

ЛИТЕРАТУРА

Alizadeh A.A. (Ed.) Geological map of Azerbaijan Republic, Scale 1:500,000, with Explanatory Notes. Baki Kartoqrafiya Fabriki. Baku, 2008.

Awad A., Elnaggar O.M., Mohamed Sh.F. Magnetic susceptibility as an indication of reservoir properties of the Nubia Group in Aswan-Komombo, Southern Egypt. Egyptian Journal of Petroleum, Vol. 32, No. 3, 2023, pp. 31-41, https://doi.org/ 10.1016/j.ejpe.2023.08.002.

Group in Aswan-Komombo, Southern Egypt. Egyptian Journal of Petroleum, Vol. 32, No. 3, 2023, pp. 31-41, https://doi.org/ 10.1016/j.ejpe.2023.08.002.

Babayev G., Telesca L, Agayeva S., Ismail-zade T., Muradi I., Aliyev Y., Aliyev M. Seismic hazard analysis for southern slope of the Greater Caucasus (Azerbaijan). Pure and Appl. Geophys. Vol. 177, No 8, 2020, pp. 3747-3760, https://doi.org/ 10.1007/s00024-020-02478-0.

Babayev G.R., Babayev T., Telesca L. Deterministic ground motion modeling with target earthquakes and site effects in eastern Azerbaijan. Arab J. Geoscience, Vol. 17, article number 61, 2024, https://doi.org/10.1007/s12517-024-11866-y.

Babayev G.R., Ismail-Zadeh A., Le Mouël J.-L. Scenario-based earthquake hazard and risk assessment for Baku (Azerbaijan). Natural Hazards Earth System Science, Vol. 10, No. 12, 2010, pp. 2697-2712, https://doi.org/10.5194/nhess-10-2697.

Babayev G.R., Telesca L. Site specific ground motion modeling and seismic response analysis for microzonation of Baku, Azerbaijan. Acta Geophysica, Vol. 64, No. 6, Dec. 2016, pp. 2151-2170, DOI: 10.1515/acgeo-2016-0105.

Elsayed M., El-Husseiny A., Kadafur I., Mahmoud M., Aljawad M.S., Alqubalee A. An experimental study on the effect of magnetic field strength and internal gradient on NMR-Derived petrophysical properties of sandstones. Journal of Petroleum Science and Engineering, Vol. 205, 108811, 2021, https://doi.org/10.1016/j.petrol.2021.108811.

Enomoto Y., Zheng Z. Possible evidences of earthquake lightning accompanying the 1995 Kobe earthquake inferred from the Nojima fault gouge. Geophys. Res. Lett., Vol. 25, No. 14, 1998, pp. 2721-2724.

Eppelbaum L.V. Estimating informational content in geophysical observations on an example of searching economic minerals in Azerbaijan. Proceed. Azerb. National Acad. Sci. The Sciences of Earth, No. 3-4, 2014, pp. 31-40.

Ferré E. C., Zechmeister M.W., Geissman J., Mathana Sekaran N., Kocak K. The origin of high magnetic remanence in fault pseudotachylytes: theoretical considerations and implications for co-seismic electrical currents. Tectonophysics, Vol. 402(1), 2005, pp.125-139, DOI:10.1016/j.tecto.2005.01.008.

Ferré E.C., Geissman J.W., Zechmeister M.S. Magnetic properties of fault pseudotachylytes in granites. J. Geophysics Res. Solid Earth, Vol. 117, No. B1, B01106, 2012, DOI: 10.1029/ 2011JB008762.

Fukuchi T., Mizoguchi K., Shimamoto T. Ferrimagnetic resonance signal produced by frictional heating: a new indicator of paleoseismicity. J. Geophysics Res., Vol. 110, No. B12, 2005, CiteID B12404, DOI:10.1029/2004JB003485.

Google Maps. "Azerbaijan," Satellite image, 2024.

Hirono T., Ikehara M., Otsuki K., Mishima T., Sakaguchi M., Soh W., Omori M., Lin WR., Yeh EC., Tanikawa W., Wang C. Evidence of frictional melting from diskshaped black material, discovered within the Taiwan Chelungpu fault system. Geophys. Res. Lett., Vol. 33, L19311, 2006, DOI:10.1029/ 2006GL027329.

Hrouda F., Chlupacova M., Chadima M. The use of magnetic susceptibility of rocks in geological exploration. Terraplus. Brno, 2009.

Ismail-Zadeh A. Migration of seismic activity in the Caspian Sea. In: Computational seismology and geodynamics (Chowdhury D.K., ed.), Vol. 3, American Geophysical Union, Washington D.C. 1996, pp. 125-129.

Israfilbekov I.A., Listengarten V.A., Shakhsuvarov A.S. Album of hydrogeological and engineering-geological maps of the Absheron Peninsula. Scale 1:50000. Ministry of Geology of Azerbaijan SSR, Azerbaijan. Hydrogeol. Expedition, Moscow, 1983, 70 p. (in Russian).

Jackson J., Priestley K., Allen M., Berberian M. Active tectonics of the South Caspian Basin. Geophys. J. Int., Vol. 148, 2002, pp. 214-245.

Babayev G., Telesca L, Agayeva S., Ismail-zade T., Muradi I., Aliyev Y., Aliyev M. Seismic hazard analysis for southern slope of the Greater Caucasus (Azerbaijan). Pure and Appl. Geophys. Vol. 177, No 8, 2020, pp. 3747-3760, https://doi.org/ 10.1007/s00024-020-02478-0.

Babayev G.R., Babayev T., Telesca L. Deterministic ground motion modeling with target earthquakes and site effects in eastern Azerbaijan. Arab J. Geoscience, Vol. 17, article number 61, 2024, https://doi.org/10.1007/s12517-024-11866-y.

Babayev G.R., Ismail-Zadeh A., Le Mouël J.-L. Scenario-based earthquake hazard and risk assessment for Baku (Azerbaijan). Natural Hazards Earth System Science, Vol. 10, No. 12, 2010, pp. 2697-2712, https://doi.org/10.5194/nhess-10-2697.

Babayev G.R., Telesca L. Site specific ground motion modeling and seismic response analysis for microzonation of Baku, Azerbaijan. Acta Geophysica, Vol. 64, No. 6, Dec. 2016, pp. 2151-2170, DOI: 10.1515/acgeo-2016-0105.

Elsayed M., El-Husseiny A., Kadafur I., Mahmoud M., Aljawad M.S., Alqubalee A.. An experimental study on the effect of magnetic field strength and internal gradient on NMR-Derived petrophysical properties of sandstones. Journal of Petroleum Science and Engineering, Vol. 205, 108811, 2021, https://doi.org/10.1016/j.petrol.2021.108811.

Enomoto Y., Zheng Z. Possible evidences of earthquake lightning accompanying the 1995 Kobe earthquake inferred from the Nojima fault gouge. Geophys. Res. Lett., Vol. 25, No. 14, 1998, pp. 2721-2724.

Eppelbaum L.V. Estimating informational content in geophysical observations on an example of searching economic minerals in Azerbaijan. Proceed. Azerb. National Acad. Sci. The Sciences of Earth, No. 3-4, 2014, pp. 31-40.

Ferré E. C., Zechmeister M.W., Geissman J., Mathana Sekaran N., Kocak K. The origin of high magnetic remanence in fault pseudotachylytes: theoretical considerations and implications for co-seismic electrical currents. Tectonophysics, Vol. 402(1), 2005, pp. 125-139, DOI:10.1016/j.tecto. 2005.01.008.

Ferré E.C., Geissman J.W., Zechmeister M.S. Magnetic properties of fault pseudotachylytes in granites. J. Geophysics Res. Solid Earth, Vol. 117, No. B1, B01106, 2012, DOI:10.1029/2011JB008762.

Fukuchi T., Mizoguchi K., Shimamoto T. Ferrimagnetic resonance signal produced by frictional heating: a new indicator of paleoseismicity. J. Geophysics Res., Vol. 110, No. B12, 2005, CiteID B12404, DOI:10.1029/2004JB003485.

Google Maps. "Azerbaijan," Satellite image, 2024.

Hirono T., Ikehara M., Otsuki K., Mishima T., Sakaguchi M., Soh W., Omori M., Lin WR., Yeh EC., Tanikawa W., Wang C. Evidence of frictional melting from diskshaped black material, discovered within the Taiwan Chelungpu fault system. Geophys. Res. Lett., Vol. 33, L19311, 2006, DOI:10.1029/ 2006GL027329.

Hrouda F., Chlupacova M., Chadima M. The use of magnetic susceptibility of rocks in geological exploration. Terraplus. Brno, 2009.

Ismail-Zadeh A. Migration of seismic activity in the Caspian Sea. In: Computational seismology and geodynamics (Chowdhury D.K., ed.), Vol. 3, American Geophysical Union, Washington D.C. 1996, pp. 125-129.

Israfilbekov I.A., Listengarten V.A., Shakhsuvarov A.S. Album of hydrogeological and engineering-geological maps of the Absheron Peninsula. Scale 1:50000. Ministry of Geology of Azerbaijan SSR, Azerbaijan. Hydrogeol. Expedition, Moscow, 1983, 70 p. (in Russian).

Jackson J., Priestley K., Allen M., Berberian M. Active tectonics of the South Caspian Basin. Geophys. J. Int., Vol. 148, 2002, pp. 214-245.

Kanlı A.I. Integrated approach for surface wave analysis from near-surface to bedrock. In: Advances in near-surface seismology and ground-penetrating radar (Miler R.D., Bradford J.D., Holiger K., ed.), Society of exploration geophysics, Tulsa, 2010, pp. 461-475.

Kanlı A.I. Integrated approach for surface wave analysis from near-surface to bedrock. In: Advances in near-surface seismology and ground-penetrating radar (Miler R.D., Bradford J.D., Holiger K., ed.), Society of exploration geophysics, Tulsa, 2010, pp. 461-475.

Kanli A.I., Kang T.S., Pınar A., Tildy P., Pronay Z. A systematic geophysical approach for site response of the Dinar Region, South Western Turkey. Journal of Earthquake Engineering, Vol. 12(1), 2008, pp. 165-174.

Kanli A.I., Tildy P., Pronay Z., Pınar A., Hermann L. V-S(30) mapping and soil classification for seismic site effect evaluation in Dinar region, SW Turkey. Geophysical Journal International, Vol. 165, No.1, 2006, pp. 223-235.

Kars M., Aubourg Ch., Pozzi J.-P. Impact of temperature increase on the formation of magnetic minerals in shales. The example of Tournemire, France. Physics of the Earth and Planetary Interiors, Vol. 338(1-2), 107021, 2023, https://doi.org/ 10.1016/ j.pepi.2023.107021.

Midorikawa S., Matsuoka M., Sakugawa K. Evaluation of site effects on peak ground acceleration and velocity observed during the 1987 Chiba-ken-toho-oki earthquake. Journal of Structural and Construction Engineering Architectural Institute of Japan, Vol. 442, 1992, pp. 71-78 (In Japanese with English abstract).

Mishima T., Hirono T., Nakamura N., Tanikawa W., Soh W., Song S.R. Changes to magnetic minerals caused by frictional heating during the 1999 Taiwan Chi-Chi earthquake. Earth Planets Space, Vol. 61, 2009, pp. 797-801.

Mishima T., Hirono T., Soh W., Song S.R. Thermal history estimation of the Taiwan Chelungpu fault using rock-magnetic methods. Geophys. Res. Lett., Vol. 33, No. 23, 2006, DOI:10.1029/2006GL028088.

Murphy J. and O'brien L. The correlation of peak ground acceleration amplitude with seismic intensity and other physical parameters. Bull. Seismol. Soc., Vol. 67 (3), 1977, pp. 877-915.

Nakamura N. and Nagahama H. Changes in magnetic and fractal properties of fractured granites near the Nojima Fault, Japan. Island Arc, Vol. 10, No 3-4, 2001, pp. 486-494.

Ordonez G.A. SHAKE2000: A computer program for the 1-D analysis of the geotechnical earthquake engineering problem, 2000.

Panahi B.M. Estimation of geological hazards and risk in Azerbaijan. In: Shamakha Earthquake 1902 (Kheyrullaoglu G.,ed.). Nafta-Press. Baku, 2003, pp. 37-63 (in Russian).

Panza G., Irikura K., Kouteva M., Peresan A., Wang Z., Saragoni R. Advanced seismic hazard assessment. Vol. 168, 2011, pp. 1-9. Springer, Basel AG, DOI:10.1007/s00024-010-0179-9

Pei J., Li H., Wang H., Si J., Sun Z., Zhou Z. Magnetic properties of the Wenchuan Earthquake Fault Scientific Drilling Project Hole-1 (WFSD-1), Sichuan Province, China. Earth, Planets and Space, Vol. 66, Article number 23, 2014.

Seed H.B., Idriss J.M., Kiefer F.M. Characteristics of rock motions during earthquakes. ASCE Journal of the Soil Mechanics and Foundations Division, Vol. 95, No SM5, proc. paper 6783, 1969, pp. 1199-1218.

Siregar N.D., Syafriani H.R., Fauzi A., Mufit F. Magnetic susceptibility of volcanic rocks from Pahae Julu Region, North Sumatera Province. Journal of Physics and Its Applications, Vol. 4, No. 2, 2022, pp. 42-46, DOI: https://doi.org/10.14710/ jpa. v4i2.13597.

Trifunac M. and Brady A. On the correlation of seismic intensity scales with the peaks of recorded strong ground motion. Bulletin of the Seismological Society of America, Vol. 65 (1), 1975, pp. 139-162.

Yang T., Chou Y.-M., Ferré E.C., Dekkers M. J., Chen J., Yeh E.-C., Tanikawa W. Faulting processes unveiled by magnetic properties of fault rocks. Reviews of Geophysics, Vol. 58, No. 4, 2020, https://doi.org/10.1029/2019RG000690.

Kanli A.I., Kang T.S., Pınar A., Tildy P., Pronay Z. A systematic geophysical approach for site response of the Dinar Region, South Western Turkey. Journal of Earthquake Engineering, Vol. 12(1), 2008, pp. 165-174.

Kanli A.I., Tildy P., Pronay Z., Pınar A., Hermann L. V-S(30) mapping and soil classification for seismic site effect evaluation in Dinar region, SW Turkey. Geophysical Journal International, Vol. 165, No.1, 2006, pp. 223-235.

Kars M., Aubourg Ch., Pozzi J.-P. Impact of temperature increase on the formation of magnetic minerals in shales. The example of Tournemire, France. Physics of the Earth and Planetary Interiors, Vol. 338(1-2), 107021, 2023, https://doi.org/10.1016/ j.pepi.2023.107021.

Midorikawa S., Matsuoka M., Sakugawa K. Evaluation of site effects on peak ground acceleration and velocity observed during the 1987 Chiba-ken-toho-oki earthquake. Journal of Structural and Construction Engineering Architectural Institute of Japan, Vol. 442, 1992, pp. 71-78 (In Japanese with English abstract).

Mishima T., Hirono T., Nakamura N., Tanikawa W., Soh W., Song S.R. Changes to magnetic minerals caused by frictional heating during the 1999 Taiwan Chi-Chi earthquake. Earth Planets Space, Vol. 61, 2009, pp. 797-801.

Mishima T., Hirono T., Soh W., Song S.R. Thermal history estimation of the Taiwan Chelungpu fault using rock-magnetic methods. Geophys. Res. Lett., Vol. 33, No. 23, 2006, DOI:10.1029/2006GL028088.

Murphy J. and O'brien L. The correlation of peak ground acceleration amplitude with seismic intensity and other physical parameters. Bull. Seismol. Soc., Vol. 67 (3), 1977, pp. 877-915.

Nakamura N. and Nagahama H. Changes in magnetic and fractal properties of fractured granites near the Nojima Fault, Japan. Island Arc, Vol. 10, No 3-4, 2001, pp. 486-494.

Ordonez G.A. SHAKE2000: A computer program for the 1-D analysis of the geotechnical earthquake engineering problem, 2000.

Panza G., Irikura K., Kouteva M., Peresan A., Wang Z., Saragoni R. Advanced seismic hazard assessment. Vol. 168, 2011, pp. 1-9. Springer, Basel AG, DOI:10.1007/s00024-010-0179-9

Pei J., Li H., Wang H., Si J., Sun Z., Zhou Z. Magnetic properties of the Wenchuan Earthquake Fault Scientific Drilling Project Hole-1 (WFSD-1), Sichuan Province, China. Earth, Planets and Space, Vol. 66, Article number 23, 2014.

Seed H.B., Idriss J.M., Kiefer F.M. Characteristics of rock motions during earthquakes. ASCE Journal of the Soil Mechanics and Foundations Division, Vol. 95, No SM5, proc. paper 6783, 1969, pp. 1199-1218.

Siregar N.D., Syafriani H.R., Fauzi A., Mufit F. Magnetic susceptibility of volcanic rocks from Pahae Julu Region, North Sumatera Province. Journal of Physics and Its Applications, Vol. 4, No. 2, 2022, pp. 42-46, DOI: https://doi.org/10.14710/ jpa.v4i2.13597.

Trifunac M. and Brady A. On the correlation of seismic intensity scales with the peaks of recorded strong ground motion. Bulletin of the Seismological Society of America, Vol. 65 (1), 1975, pp. 139-162.

Yang T., Chou Y.-M., Ferré E.C., Dekkers M. J., Chen J., Yeh E.-C., Tanikawa W. Faulting processes unveiled by magnetic properties of fault rocks. Reviews of Geophysics, Vol. 58, No. 4, 2020, https://doi.org/10.1029/2019RG000690.

Аптикаев Ф.Ф. и Копничев Ю.Ф. Учет механизма очага землетрясения при прогнозе параметров сильных движений. Докл. АН СССР, Т. 247, No. 4, 1979, с. 822-825.

Исрафилбеков И.А., Листенгартен В.А., Шахсуваров А.С. Альбом гидрогеологических и инженерно-геологических карт Апшеронского полуострова. Масштаб 1:50000. М-во геологии СССР, Управление геологии Азерб.ССР, Азерб. гидрогеологическая экспедиция. Москва, 1983, 70 с.

Панахи Б.М. Оценка геологических опасностей и риска в Азербайджане. В кн.: Шемахинское землетрясение 1902 (Хейруллаоглу Г., ред.). Nafta-Press. Баку, 2003, с. 37-63.

МОДЕЛИ СЕЙСМИЧЕСКОЙ ОПАСНОСТИ АБШЕРОНСКОГО ПОЛУОСТРОВА С УЧЁТОМ МАГНИТНЫХ СВОЙСТВ ГОРНЫХ ПОРОД

Бабаев Г.Р.[1,2], Алиев З.В.[1]
[1]Министерство науки и образования Азербайджанской Республики, Институт геологии и геофизики, Азербайджан
AZ1143, Баку, просп. Г. Джавида, 119
[2]Азербайджанский Государственный Университет нефти и промышленности, Азербайджан
AZ1010, Баку, просп. Азадлыг, 20

Резюме. Разработана модель опасности землетрясений по вариациям магнитной восприимчивости горных пород, интегрирующим с макросейсмическими параметрами достоверного землетрясения, с учетом динамики площадных эффектов, примененная для Абшеронского полуострова (Азербайджан). Также были использованы данные магнитного каротажа, литологические и геологические карты Абшеронского полуострова, сейсмические каталоги. Максимально ожидаемое движение грунта на Абшероне рассчитано для неглубокого Баку-Каспийского землетрясения 25.11.2000 г. вблизи зоны исследования, которое отмечено как сценарий «близкого землетрясения» и рассматривается как достоверное землетрясение с моментными магнитудами Mw=6.18 и Mw=6.08. В данном исследовании моментная магнитуда принята равной Mw=6.8. Оценка воздействия на территорию проводилась путем детальной геотехнической обработки грунтовых условий от нижележащих слоев до земной поверхности с использованием одномерного (1-D) анализа отклика грунта с помощью SHAKE2000. Мы оценили реакцию слоев грунта на землетрясение, рассчитав усиление амплитуды сейсмической волны и изменение характеристик колебания земной поверхности. На основе параметров сценария землетрясения рассчитано пиковое ускорение земной поверхности, скоррелировано с интенсивностью MSK-64. Проведено моделирование параметров ускорения грунта, сейсмической интенсивности и магнитной восприимчивости. Северо-восточная и юго-восточная части полуострова характеризуются пиковым ускорением грунта 165-250 гал и интенсивностью VIII-IX, что на 31% и 49% выше сейсмической опасности в тех же значениях по сравнению с другими частями. Для восточной части магнитная восприимчивость изменяется в пределах 0.5-1.0. Эти значения указывают на отчетливую связь вариаций магнитного поля с сейсмическим эффектом землетрясений. Наш подход вносит существенный вклад в совершенствование существующих методов оценки сейсмической опасности.

Ключевые слова: *Азербайджан, Абшеронский полуостров, сейсмическая опасность, пиковое ускорение грунта, интенсивность, магнитная восприимчивость, моделирование*

ABŞERON YARIMADASI ÜÇÜN SÜXURLARIN MAQNİT XASSƏLƏR İLƏ ƏLAQƏDAR OLAN ZƏLZƏLƏ TƏHLÜKƏSİ MODELLƏRİ

Babayev Q.R.[1,2], Əliyev Z.V.[1]
[1]Azərbaycan Respublikasının Elm və Təhsil Nazirliyi, Geologiya və Geofizika İnstitutu, Azərbaycan
AZ1143, Bakı, H. Cavid prosp., 119
[2]Azərbaycan Dövlət Neft və Sənaye Universiteti, Azərbaycan
AZ1010, Bakı, Azadlıq prosp., 20

Xülasə. Abşeron yarımadası timsalında (Azərbaycan) qrunt təsirinin dinamikası nəzərə alınmaqla, baş vermiş zəlzələnin makroseysmik parametrləri (maqnituda, dərinlik, coğrafi yerləşmə, episentral məsafə) ilə süxurların maqnit həssaslığının qiymətlərini inteqrasiya edilərək zəlzələ təhlükəsinin qiymətləndirilməsi üçün modellər qurulmuşdur. Quyuların maqnit karotaj məlumatlarından, ərazinin litoloji və geoloji xəritələrindən, yerli və beynəlxalq seysmik kataloqlardan istifadə edilmişdir. Abşeron üçün qruntun gözlənilən maksimal hərəkəti, 25.11.2000-ci ildə baş vermiş ərazinin yaxınlığındakı dayaz Bakı-Xəzər zəlzələsi üçün hesablanmışdır ki, bu da tədqiqatda ssenar "yaxın zəlzələ" kimi qəbul olunur və Mw=6.18 və 6.08 maqnitudalı mümkün olan zəlzələ kimi sayılır. Tədqiqatda moment maqnitudası Mw=6.8 qiymətində istifadə olunub. Qrunt təsirinin qiymətləndirilməsi SHAKE 2000 proqram təminatı ilə birölçülü (1-D) qruntun effekt analizindən istifadə etməklə ana süxurdan səthə qədər ətraflı geotexniki cəhətdən xarakterizə olunaraq həyata keçirilmişdir. Beləliklə, seçilmiş zəlzələlərin süxur laylarına təsiri təyin edilmiş, qruntun seysmik dalğa amplitudasının güclənmə əmsalı hesablanmış və səthdə yerin hərəkət xüsusiyyətlərinin dəyişməsi müəyyənləşdirilmişdir. Ssenar zəlzələnin parametrlərinə əsasən, yer səthində qruntun maksimal təcili (QMT) vahidləri hesablanmış, MSK-64 intensivlik şkalası üzrə korrelyasiya olunmuşdur və nəticə olaraq, tədqiqat ərazisi üçün qruntun təsiri ilə səthdə qruntun maksimal təcili (QMT), intensivlik və maqnit həssaslığının qiymətləri modelləşdirilmişdir.

Nəticələr göstərir ki, Abşeronun şimal-şərq və cənub-şərq hissələrində qruntun maksimal təcili 165-250 qal və VIII-IX intensivlikdə təyin edilmişdir ki, bu da yarımadanın qərb hissələri ilə müqayisədə həmin qiymətlərdəki seysmik təhlükədən 31% və 49% yüksəkdir. Yarımadanın şərq hissəsi üçün maqnit həssaslığı 0.5-1.0 arasında dəyişir. Bu qiymətlər, maqnit sahəsindəki dəyişikliklərin zəlzələlərin seysmik təsiri ilə mövcud fərqli əlaqəsini göstərməyə imkan verir. Təklif etdiyimiz yanaşma seysmik təhlükənin qiymətləndirilməsində mövcud metodların təkmilləşdirilməsinə mühüm töhfə verir.

Açar sözlər: *Azərbaycan, Abşeron yarımadası, zəlzələ təhlükəsi, qruntun maksimal təcili, intensivlik, maqnit həssaslığı, simulyasiya*

ANAS Transactions Earth Sciences 1 / 2024

http://www.journalesgia.com

POSSIBLE POSITIVE EFFECTS OF CHRONIC LOW-DOSE IONIZING RADIATION ON HUMAN LIFE-SPAN IN TALYSH, AZERBAIJAN

Aliyev Ch.S.[1], Kamilova N.M.[2], Mahmudova F.F.[1], Baghirli R.J.[1], AliyevaA.R.[1]

[1]Ministry of Science and Education of the Republic of Azerbaijan,
Institute of Geology and Geophysics, Azerbaijan
119, H.Javid ave., Baku, AZ1143: aliyev.chingiz47@gmail.com
[2]Azerbaijan Medical University, Ministry of Health of the Republic of Azerbaijan, Azerbaijan
100, Mardanov Qardashlar str., Baku, AZ1078

Keywords: *radiation hormesis, Talysh, radon volume activity, life expectancy, human health*

Summary. Radiation hormesis is the hypothesis that low doses of ionizing radiation (within the region of and just above natural background levels) are beneficial, stimulating the activation of repairing mechanisms that protect against disease, that are not activated in absence of ionizing radiation. The paper describes research results supporting hormesis through exposure to low-dose ionizing radiation conducted in the Talysh region of Azerbaijan. According to the International Committee on Radiation Protection, 40-75% of total human exposure to natural radioactive sources comes from radon and its decay products. Radiometric studies covered five districts of the Talysh region: Masalli, Lankaran, Astara, Yardimli and Lerik. The volume activity of radon in residential areas was measured with radon Scout and radon Scout Plus radiometers from SARAD. Based on the obtained results, maps of the distribution of radon volume activity are constructed separately for each region. According to this map, the Lerik district, known for its long-lived inhabitants, is characterized by a relatively high level of radon. The ECG (electrocardiograph) of cardiac activity is written in the modern cardiograph Cardi Max Fx 8222 produced by the Japanese company Denshi Fukuda. The results of the research showed that there is a certain correlation between the level of radon in homes and life expectancy. According to the current regulatory document, the indoor radon volume activity should not exceed 200 Bq/m³. Based on research results, in villages where centenarians are living, the level of indoor radon varies between 100-200 Bq/m^3, averaging 150 Bq/m^3.

Introduction

The exposure of humans to radiation from natural sources is unavoidable. Radiation exposure from natural sources varies globally and within a country depending on the geology and altitude where people live. Studies of the health of populations living in areas with high levels of background radiation conducted during the past 25 years are a potential source of information on the effects of low-dose protracted exposures. Radiation hormesis is the hypothesis that low doses of ionizing radiation (within the region of and just above natural background levels) are beneficial, stimulating the activation of repair mechanisms that protect against disease, that are not activated in absence of ionizing radiation. The reserve repair mechanisms are hypothesized to be sufficiently effective when stimulated as to not only cancel the detrimental effects of ionizing radiation but also inhibit disease not related to radiation exposure. The International Commission on Radiological Protection (ICRP 2007), National Academy of Sciences Biologic Effects of Ionizing Radiation (National Research…, 2006), the United Nations Scientific Committee on the Effects of Atomic Radiation and the National Council on Radiation Protection and Measurement (NCRP) have adopted 100 mSv or less as low dose (UNSCEAR, 2010; Boice, 2017). Previously, the UNSCEAR Scientific Report (UNSCEAR, 2011) had defined low doses as those of ≤200 mGy, and low-dose-rate 0.1 mGy per minute (averaged over one hour or less) for external X-and γ-rays. Recently, Multidisciplinary European Low Dose Initiative (MELODI), a European radiation protection research platform, have defined low doses as those between 10 and <100 mGy and moderate doses from 100 mGy to 1 Gy and >1 Gy as high doses (Seibold, 2020; Kreuzer, 2018).

According to the International Committee on Radiation Protection, 40-75% of total human exposure to natural radioactive sources comes from radon

and its decay products. In 1987 radon and its decay products were classified by the International Agency for Research on Cancer as being carcinogenic to humans. Investigations conducted in Europe and USA showed that radon is the second cause after smoking providing lung cancer diseases (Cohen, 1993). Radon is the main factor of lung cancer among non-smokers. A study of the radon problem in Azerbaijan shows that its distribution in space is uneven and mosaic in nature. The regions with the highest concentrations are confined to the mountainous folded massifs of the G.Caucasus and Talysh, while those with the lowest concentrations are confined to the lowlands (Aliyev et al., 2017). In this regard, it is interesting to note that the longest duration of life in Azerbaijan is also noted among the people living in mountainous regions (in the Caucasus, especially in Talysh). According to the official statistics, the duration of life of women in Azerbaijan is higher than men. So, currently there are 838 people (814 women and 24 men) in Azerbaijan who have reached a hundred and more years. In this connection, it is very interesting that statistical analysis and experimental studies on the effect of radon exposure on human health have established that men are more susceptible to irradiation as compared with women.

The main objective of the study was to assess the results of the current monitoring of the radiation situation in the Talysh region and the correlation analysis between the life expectancy and quality of the population and radon levels in their places of residence.

Materials and methods

Radiometric works of the studied region included measurements of the radon volume activity in residential premises and in water of mineral springs, the water of which is used by local residents, and measurements of radiation levels in the environment. Radon volume activity in residential premises was measured with Radon Scout and Radon Scout Plus radiometers from SARAD. They were installed in residential premises for several days. Radon volumetric activity in soil and water was measured by using RAD7 radiometers (DURRIDGE). The radiation level was measured by using dosimeter radiometer МКС-АТ1125. Based on the averaged values of the obtained data, the maps of the distribution of the radon volume activity in areas of the studied region have been constructed. Maps were constructed by using the Surfer program (production of Golden Software).

For medical studies 3 types of questionnaires were developed, differing from each other in questions. This was due to the fact that the studies were conducted with different age groups. Also among the surveyed citizens, psychophysical tests adapted to local conditions were conducted. The ECG of cardiac activity is written in the modern cardiograph Cardi Max Fx 8222 produced by the Japanese company Denshi Fukuda. Participation in the studies was voluntary. The study participants were fully acquainted with the aspects of participation in the study, which fully complied with the requirements of the Helsinki Declaration.

Results and discussion

Radiometric studies had covered five districts of the Talysh region: Masalli, Lankaran, Astara, Yardimli and Lerik. As mentioned above, measurements of volumetric radon activity in residential buildings were carried out in the populated areas of the studied region. Indoor radon concentrations are measured in the living rooms of houses at ground level. Regarding the recruited of participants, the priority was given to the older houses by selecting 3-5 dwellings from each district randomly. The majority of the houses examined were built 30 to 50 years ago using bricks composed of sand and cement along with cemented floors. In the Masalli district, studies were carried out in 17 settlements. The radon concentration here varied within 20-170 Bq/m^3. In 38 surveyed settlements of the Lankaran region radon concentration varied within 20-600 Bq/m^3. In the Astara region, studies were conducted in 23 localities. The radon concentration here varied within 50-190 Bq/m^3. In Yardimli region 19 settlements were surveyed. The radon volume activity here varied within 50-730 Bq/m^3. In Lerik region, studies were conducted in 32 localities. The radon concentration here varied within 89-215 Bq/m^3. On the basis of the obtained data the map of distribution of radon volume activity for the Talysh region has been constructed. According to this map, the Lerik region, known for its long-livers, is characterized by a relatively high level of radon (Feyzullayev et al., 2021). According to the current regulatory document, the indoor radon volume activity should not exceed 200 Bq/m^3. In villages where centenarians are living, the level of indoor radon varies between 100-200 Bq/m^3, averaging about 150 Bq/m^3.

During the study, 24 long-livers, 30 their close relatives and 30 members of the control group have been investigated. Among the studied centenarians, the number of women (14 people) exceeds men. It should be noted that the genetic factors are an important component of longevity.

Analysis of electrocardiographic indicators of centenarians showed that the pathological changes noted in cardiac activity do not exceed the age-related changes (Fig.). Thus, in 35% of the studied centenarians, deep hypoxia in the heart muscle, T-negative

(disorders of blood circulation in the heart), ecstrocystolias, ischemic changes, bundle branch block, rupture of the heart vessels (acute disorders of nutrition of the heart muscle, T - negative), cardiosclerosis changes were recorded. In 25% of studied centenarians a normal ECG was observed. Also in ECG of 45% of the studied centenarians age-related changes were observed. At this time, all teeth and complexes of the ECG had a small amplitude. Despite severe pathological changes on the ECG (damage of the myocardium, hypertrophy of the left ventricle, complete or partial blockade of the bundle branch block), the average indicator of arterial pressure among centenarians is 145-85 mmHg, the average indicator of heart rate was 75-78 beats per minute. In only one of the studied centenarians, the amount of sugar in the blood was slightly higher than the norm.

The analysis of the ECG of close relatives of centenarians showed that deep pathological changes in this group are much less common than the control group. From the 24 studied relatives, the ECG was normal only in 14 people. Pathological changes were noted in 4 people (T-negative, blockade of the bundle branch block). In 6 people were observed age-related changes (hypoxia, disorders of the nutrition of the heart muscle). In this group, hypoxic and neurotic (T- vagus) changes in ECG were most common.

Among the group at age 100, there were not noted cardiovascular pathologies. Heart rate and blood pressure were in full compliance with the norm.

In the process of aging, the cardiovascular system undergoes involution changes which lead to the development of cardiac dysfunctions. The hormetic effect of low-dose ionizing radiation has been reported to promote growth and development, also to suppress the ageing process, enhancing immune functions, and delaying cancer progression (Cui, 2017). The obtained results showed that due to the strong adaptive compensatory and genetic factors pathological changes among centenarians do not lead to lethal outcome. This fact shows the presence of strong mechanisms and a strong vitauct system of the organism against various external stress factors.

Conclusion

The results of the conducted studies have shown that radon volume activity between 100-200 Bq/m^3 can have a beneficial effect on people's health and their life expectancy. However, this does not mean that radon can definitely be considered the main factor of longevity. Thus, further studies are required to rigorously determine the circumstances of how the chronic low-dose ionizing radiation can affect cellular senescence and aging. To demonstrate the effect of chronic low-dose ionizing radiation on human health more robust evidence is required and there are several unanswered questions that require further investigation.

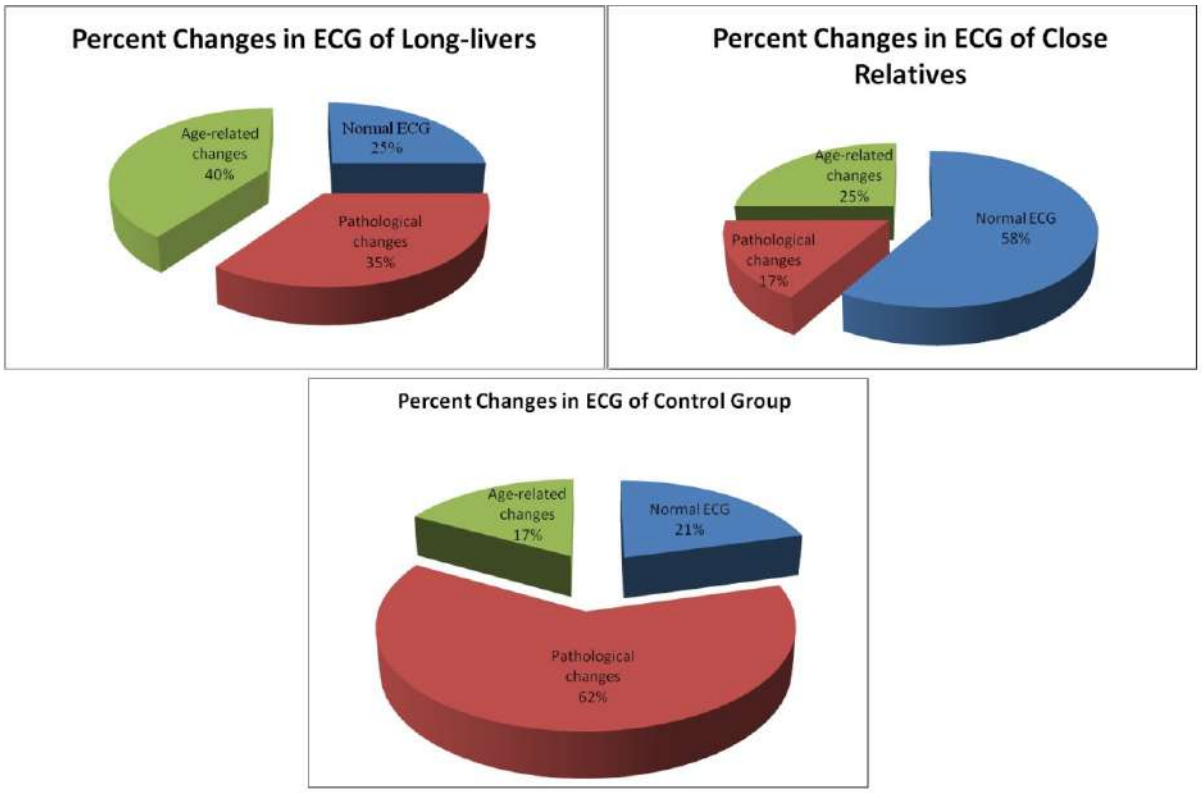

Percent changes in ECG of long-livers, close relatives and control group

REFERENCES

Boice J.D.Jr. The linear nonthreshold (LNT) model as used in radiation protection: An NCRP update. International Journal of Radiation Biology, Vol. 93, No.10, 2017, pp. 1079-1092, https://doi.org/10.1080/09553002.2017.1328750.

Cohen B. Relationship between exposure to radon and various types of cancer. Health Physics, Vol. 65, No. 5, 1993, pp. 529-531.

Cui J., Yang G., Pan Z., Zhao Y., Liang X., Li W., Cai L. Hormetic focus on the immune system and its clinical implications. International Journal of Molecular Sciences, Vol. 18, No.2, 2017, pp. 1-12.

Feyzullayev A.A., Aliyev Ch.S., Baghirli R.J., Mahmudova F.F. Assessment of indoor and outdoor radon concentrations in Talysh, Azerbaijan. ANAS Transactions, Earth Sciences, No. 1, 2021, pp. 43-46, DOI:10.33677/ggianas20210100053.

ICRP Publication. The 2007 Recommendations of the International Commission on radiological protection. Vol. 37, No. 2-4, 2007, 1-332 p., DOI: 10.1016/j.icrp.2007.10.003.

Kreuzer M., Auvinen A., Cardis E., Durante M., Harm-Ringdahl M., Jourdain J.R., Madas B.G., Ottolenghi A., Pazzaglia S., Prise K.M., Quintens R, Sabatier L, Bouffler S. Multidisciplinary European Low Dose Initiative (MELODI): Strategic research agenda for low dose radiation risk research. Radiation and Environmental Biophysics, Vol. 57, No. 1, 2018, pp. 5-15, DOI: 10.1007/s00411-017-0726-1.

National Research Council of the National Academies. Health risks from exposure to low levels of ionizing radiation: BEIR VII Phase 2, 2006, 442 p.

Seibold P., Auvinen A., Averbeck, D., Bourguignon M., Hartikainen J.M., Hoeschen C., Laurent O., Noel, G., Sabatier L., Salomaa S., Blettner M. Clinical and epidemiological observations on individual radiation sensitivity and susceptibility. International Journal of Radiation Biology, Vol. 96, No. 3, 2020, pp. 324-339.

UNSCEAR. Sources and Effects of Ionizing Radiation. UNSCEAR 2008 Report to the General Assembly with Scientific Annexes, 2010, 683 p.

UNSCEAR. Scientific Report on the Effects of Atomic Radiation. United Nations Scientific Committee on the Effects of Atomic Radiation 2010, United Nations. New York, 2011, 106 p.

Aliyev Ch.S., Feyzullaev A.A., Baghirli R.J, Mahmudova F.F. Regularities of radon distribution on the territory of Azerbaijan and controlling factors. Scientific and technical journal. Euro-Asia Geophysical Society. Geophysics, No. 1, 2017, pp. 72-77 (in Russian).

ЛИТЕРАТУРА

Boice J.D.Jr. The linear nonthreshold (LNT) model as used in radiation protection: An NCRP update. International Journal of Radiation Biology, Vol. 93, No. 10, pp. 1079-1092, https://Doi.org/10.1080/09553002.2017.1328750.

Cohen B. Relationship between exposure to radon and various types of cancer. Health Physics, Vol. 65, No. 5, 1993, pp. 529-531.

Cui J., Yang G., Pan Z., Zhao Y., Liang X., Li W., Cai L. Hormetic response to low-dose radiation: focus on the immune system and its clinical implications. International Journal of Molecular Sciences, Vol. 18, No. 2, 2017, pp. 1-12.

Feyzullayev A.A., Aliyev Ch.S., Baghirli R.J., Mahmudova F.F. Assessment of indoor and outdoor radon concentrations in Talysh, Azerbaijan. ANAS Transactions, Earth Sciences, No 1, 2021, pp. 43-46, DOI:10.33677/ggianas20210100053.

ICRP Publication. The 2007 Recommendations of the International Commission on radiological protection. Vol. 37, No. 2-4, 2007, pp. 1-332.

Kreuzer M., Auvinen A., Cardis E., Durante M., Harm-Ringdahl M., Jourdain J.R., Madas B.G., Ottolenghi A., Pazzaglia S., Prise K.M., Quintens R, Sabatier L, Bouffler S.. Multidisciplinary European Low Dose Initiative (MELODI): Strategic research agenda for low dose radiation risk research. Radiation and Environmental Biophysics, Vol. 57, No. 1, 2018, pp. 5-15, DOI: 10.1007/s00411-017-0726-1.

National Research Council of the National Academies. Health risks from exposure to low levels of ionizing radiation: BEIR VII Phase 2, 2006, 442 p.

Seibold P., Auvinen A., Averbeck, D., Bourguignon M., Hartikainen J.M., Hoeschen C., Laurent O., Noel, G., Sabatier L., Salomaa S., Blettner M. Clinical and epidemiological observations on individual radiation sensitivity and susceptibility. International Journal of Radiation Biology, Vol. 96, No. 3, 2020, pp. 324-339.

UNSCEAR. Sources and Effects of Ionizing Radiation. UNSCEAR 2008 Report to the General Assembly with Scientific Annexes, 2010, 683 p.

UNSCEAR. Scientific Report on the Effects of Atomic Radiation. United Nations Scientific Committee on the Effects of Atomic Radiation 2010, United Nations. New York, 2011, 106 p.

Алиев Ч.С., Фейзуллаев А.А., Багирли Р.Дж., Махмудова Ф.Ф. Закономерности распределения радона в Азербайджане и контролирующие их факторы. Научно-технический журнал. Евро-Азийское геофизическое общество. Геофизика, No. 1, 2017, с. 72-77.

ВОЗМОЖНОЕ ПОЛОЖИТЕЛЬНОЕ ВЛИЯНИЕ ХРОНИЧЕСКОГО ИОНИЗИРУЮЩЕГО ИЗЛУЧЕНИЯ В МАЛЫХ ДОЗАХ НА ПРОДОЛЖИТЕЛЬНОСТЬ ЖИЗНИ НАСЕЛЕНИЯ В ТАЛЫШЕ, АЗЕРБАЙДЖАН

Алиев Ч.С.[1], Камилова Н.М.[2], Махмудова Ф.Ф.[1], Багирли Р.Дж.[1], АлиеваА.Р.[1]

[1]Министерство науки и образования Азербайджанской Республики, Институт геологии и геофизики, Азербайджан AZ1143, Баку, просп. Г.Джавида, 119: aliyev.chingiz47@gmail.com

[2]Министерство науки и образования Азербайджанской Республики, Азербайджанский Медицинский Университет, Азербайджан AZ1078, Баку, ул.братьев Мардановых,100

Резюме. Понятие «радиационный гормезис» предполагает, что ионизирующее облучение, являясь при больших дозах губительным для живых организмов, в малых дозах может индуцировать положительные биологические процессы и оказывать стимулирующее благоприятное действие на организм, которое регистрируется как повышение плодовитости, роста, деления клеток и увеличение продолжительности жизни различных биологических объектов. В статье описаны результаты исследований, подтверждающих радиационный гормезис от воздействия низких доз ионизирующего излучения, проведенных в Талышском районе Азербайджана. По данным Международного Комитета по Радиационной защите на радон и дочерние продукты его распада приходится 40-75% от суммарной дозы облучения, получаемого от природных источников. Радиометрические исследования охватили пять районов Талышской области: Масаллинский, Лянкяранский, Астаринский,

Ярдымлинский и Лерикский. При радиометрических исследованиях проведены мониторинги уровня концентрации радона в жилых помещениях. Измерения объемной активности радона в жилых домах проводились в населенных пунктах исследуемого региона. Объемную активность радона в жилых помещениях измеряли радиометрами Radon Scout и Radon Scout Plus от SARAD. На основе полученных данных построена карта распределения объемной активности радона для Талышского региона. Согласно этой карте Лерикский район, известный своими долгожителями, характеризуется относительно высоким уровнем радона. Функциональное состояние сердечной деятельности регистрировалось с помощью современного кардиографа Cardi Max FX 8222 производства японской компании Denshi Fukuda. Результаты исследования показали, что существует определенная корреляция между уровнем радона в домах и продолжительностью жизни. Согласно действующим нормативным документам объемная активность радона в жилых помещениях не должна превышать 200 Бк/м³. По результатам исследования установлено, что категория населения старше 90 лет проживает в основном в районах с умеренным радиационным фоном.

Ключевые слова: *радиационный гормезис, Талыш, объемная активность радона, продолжительность жизни, здоровье населения*

AZƏRBAYCANIN TALIŞ BÖLGƏSİNDƏ XRONİKİ KİÇİK DOZADA İONLAŞDIRICI ŞÜALANMANIN UZUNMÜDDƏTLİ TƏSİRİNƏ MƏRUZ QALMANIN ƏHALİNİN UZUNÖMÜRLÜLÜYÜNƏ MÜMKÜN MÜSBƏT TƏSİRLƏRİ

Əliyev Ç.S.[1], Kamilova N.M.[2], MahmudovaF.F.[1], Bağırlı R.J.[1], Əliyeva Ə.R.[1]
[1] Azərbaycan Respublikasının Elm və Təhsil Nazirliyi, Geologiya və Geofizika İnstitutu, Azərbaycan
AZ1143, Bakı, H. Cavid pr., 119: *aliyev.chingiz47@gmail.com*
[2]Azərbaycan Respublikası Səhiyyə Nazirliyi, Azərbaycan Tibb Universiteti, Azərbaycan
AZ1078, Bakı, Mərdanov qardaşları küç., 100

Xülasə. Radiasion hormezis fenomeni radiasiyanın zəif və orta dozalarının hüceyrə, toxumaların və ümumilikdə insan orqanizminin həyat fəaliyyətinə stimullaşdırıcı, bərpaedici və dəstəkləyici təsir etməsidir. Aparılmış tədqiqatlar zamanı radiasiyanın kiçik dozalarının mezenximal sütun hüceyrələrində orqanizmdə gedən apoptoz prosesinin yavaşıdılmasına yönəlmiş siqnal mexanizmini aktivləşdirdiyi təsdiq edilmişdir. Beynəlxalq Radiasiyadan Müdafiə Təşkilatının məlumatlarına əsasən əhalinin təbii mənbələrdən şüalanmasının ümumi miqdarının 40-75 %-i radon və onun parçalanma məhsullarının payına düşür. Bütün bunlar nəzərə alınaraq məqalədə uzunömürlülərin daha çox məskunlaşdığı Talış regionunda aparılmış ətraflı radiometrik, tibbi-bioloji və tibbi-sosioloji tədqiqatların, həmçinin region üçün xarakterik olan yaş xüsusiyyətləri analiz edilmiş, uzunömürlülərin qan-damar sisteminin funksional vəziyyətinin qiymətləndirilməsinin nəticələri təsvir edilmişdir. Talış vilayətinin beş rayonunda radiometrik tədqiqatlar aparılmışdır: Masallı, Lənkəran, Astara, Yardımlı və Lerik. Yaşayış yerlərində radonun həcmli aktivliyi Radon Scout və Radon Scout Plus radiometrləri vasitəsilə ölçülmüşdür. Ürək fəaliyyətinin funksional vəziyyəti Yaponiyanın Denshi Fukuda şirkəti tərəfindən istehsal olunan Cardi Max Fx 8222 müasir kardioqrafı vasitəsilə qeydə alınmışdır. Aparılmış tədqiqatlar nəticəsində yaşayış yerlərində radon qazının həcmi aktivliyi və əhalinin ömür uzunömürlulüyü arasında müsbət korrelyasiya aşkar edilmişdir. Mövcud normativ sənədlərə əsasən yaşayış yerlərində radonun həcmi aktivliyi 200 Bq/m^3-dən çox olmamalıdır. Tədqiqat nəticələrinə əsasən, uzunömürlülərin məskunlaşdığı kəndlərdə radonun həcmi aktivliyii 100-200 Bq/m^3 arasında dəyişir və orta hesabla 150 Bq/m^3 təşkil edir. Tədqiqatın nəticələrinə əsasən 90 yaşdan yuxarı əhali kateqoriyasının əsasən zəif və orta radiasiya fonlu ərazilərdə yaşadığı müəyyən edilmişdir.

Açar sözlər: *radonun həcmi aktivliyi, Talış, uzunömürlülük, radiasion hormezis, insan sağlamlığı*

ANAS Transactions Earth Sciences 1 / 2024

http://www.journalesgia.com

НОВЫЕ НАХОДКИ ФРАГМЕНТОВ АРТРОПОД (ARACHNIDA, INSECTA) ИЗ ПОЗДНЕПЛЕЙСТОЦЕНОВЫХ БИТУМНЫХ ОТЛОЖЕНИЙ АБШЕРОНА (АЗЕРБАЙДЖАН)

Новрузов Н.Э.[1], **Таптыгова К.А.**[1], **Эйбатов Т.М.**[2]

[1]*Министерство науки и образования Азербайджанской Республики, Институт зоологии, Азербайджан*
AZ1073, Баку, проезд 1128, квартал 504: niznovzoo@mail.ru
[2]*Музей естественной истории Азербайджана, Азербайджан*
AZ1006, Баку, ул. Лермонтова, 3: t_eybatov@mail.ru

NEW RECORDS OF ARTHROPOD FRAGMENTS (ARACHNIDA, INSECTA) FROM LATE PLEISTOCENE BITUMEN DEPOSITS OF THE ABSHERON (AZERBAIJAN)

Novruzov N.E.[1], Taptygova K.A.[1], Eybatov T.M.[2]
[1] *Ministry of Science and Education of the Republic of Azerbaijan, Institute of Zoology, Azerbaijan block 504, Passage 1128, Baku, AZ1073: t_eybatov@mail.ru*
[2] *Museum of Natural History of Azerbaijan, Azerbaijan 3, Lermontov, Baku, AZ1006: t_eybatov@mail.ru*

Keywords: *bitumen deposit, chitin fragments, insects, arachnids*

Summary. During planned paleontological excavations in the Binagadi bitumen deposit (Absheron Peninsula), famous as one of the large burials of samples of fauna and flora of the Quaternary period, a large number of remains of fossil fauna and flora were recovered from a depth of about 1.8 m. Among them, well-preserved fragments of arthropods were identified: insects of four orders (Lepidoptera, Mantodea, Coleoptera, Odonata) and arachnids of two orders (Scorpiones, Solifugae). In the scope of the work done to identify the material, the taxonomic affiliation of the discovered chitinous fragments of arthropods was established with certainty to the genus. In total, 3 genera from the order Lepidoptera (*Aporia*, *Vanessa*, *Thiotricha*), 8 genera from the order Coleoptera (*Hydrophilus*, *Cybister*, *Blaps*, *Tenebrio*, *Scarabaeus*, *Carabus*, *Zabrus*, *Nebria*), one genus each from the order Mantodea (*Mantis*), the order Odonata (*Anax*), the order Scorpiones (*Mesobuthus*) and the order Solifugae (*Galeodes*) were identified. Fragments of the pedipalp (thigh, claw), segments of the metasoma and telson of scorpions (Scorpiones), chelicerae of solpugids (Solifugae), wings of butterflies (Lepidoptera) and dragonflies (Odonata), elytrae, thoracic and abdominal parts, legs of beetles (Coleoptera), anterior grasping legs (femur, tibia, tarsus) of a praying mantis (Mantodea). During the entire period of study of the world's bituminous burial flora and fauna (including Binagadi deposit), fragments of Lepidoptera, Mantodea, Odonata, Socriones and Solifugae were recorded for the first time. The collected material is stored in the Natural History Museum of Baku and in the paleozoology laboratory of the Institute of Zoology of Azerbaijan.

Введение

Битумные месторождения с древними остатками флоры и фауны отмечаются в тех участках нефтеносной местности, где наблюдаются естественные выходы нефти на земную поверхность. В подобных месторождениях органические остатки, как правило, накапливаются на протяжении длительного периода времени, образуя достаточно разнообразный видовой состав, сохранность таких остатков для дальнейших морфологических исследований чаще бывает вполне удовлетворительна. Месторождения природных битумов в Азербайджане сосредоточены в основном в Абшеронском, Шамаха-Гобустанском, Нижне-Куринском, Габалинском и Губинском районах (Эфендиева, 2021). На Абшеронском полуострове известны 5 битумных месторождений с присутствием остатков фауны: Гырмакинское, Бинагадинское, Хырдаланское, Бабазананское и Пиралахинское (на одноименном острове Абшеронского архипелага) в Каспийском море. Но удовлетворительно исследованы на предмет обнаруже-

ния палеофауны только два из них – Гырмакинское и Бинагадинское (Халилов, 2003). Бинагадинское битумное месторождение, открытое в феврале 1938 г., является уникальным и крупнейшим верхнеплейстоценовым кладбищем фауны и флоры. С тех пор до настоящего времени там проводятся раскопки и изучение ископаемых остатков фауны и флоры. Большой вклад в изучение фауны Бинагадинского битумного месторождения внесли А.В.Богачев, В.В.Богачев, П.В.Серебровский, Н.И.Бурчак-Абрамович, Р.Д.Джафаров, Д.В.Гаджиев, Т.М.Эйбатов и др. За весь период сбора и изучения ископаемых остатков Бинагадинской фауны здесь было выделено более 400 видов животных и растений. Из них около 140 видов составляют беспозвоночные. В настоящее время весь собранный ископаемый материал хранится в музее Естественной истории Азербайджана (г. Баку). В настоящей статье приводятся данные последних находок фрагментов артроподофауны, обнаруженных во время раскопок в Бинагадинском битумном месторождении за период с 2019 по 2023 гг.

Материал и методы

Сбор ископаемого материала осуществлялся в центральной части Абшеронского полуострова в юго-восточной части поселка Бинагады (40.06°с.ш.; 47.45°в.д.), где расположено Бинагадинское захоронение четвертичной фауны и флоры. Битумный материал, добытый с глубины разреза 1.60-1.80 м, при первичной обработке был разложен по лоткам и маркирован в соответствии со стратиграфическим горизонтом. При вторичной обработке, которая заключалась в препарировании органического материала, механическом и химическом очищении его от битума и доведения до состояния пригодности для дальнейшей таксономической идентификации, было выявлено большое количество хитиновых фрагментов членистоногих. Из них наиболее пригодными для идентификации были фрагменты насекомых (жуков, бабочек, стрекоз и богомола) и фрагменты паукообразных (скорпионов и сольпуг). Окраска фрагментов была незначительно изменена битумом, поэтому при их очистке ограничились применением этилового спирта. Найденные хитиновые фрагменты после очистки от битума фотографировали с наложением масштабной линейки. Морфометрические измерения проведены с помощью цифрового штангенциркуля и окуляр-микрометра микроскопа МБС-1 с точностью до 0.01 мм. При определении материала в качестве сравнительных (эталонных) образцов были использованы арахнологические и энтомологические коллекции Института зоологии Азербайджана. Дополнительно использовалась справочная литература (Богачев, 1934; Яхонтов, 1935; Бялыницкий-Бируля, 1938; Богачев, 1939a; 1939b; Богачев, Аргиропуло, 1939; Рихтер, 1947; Богачев, 1948; Бурчак-Абрамович, Джафаров, 1955; Кириченко,1956; Мамаев и др., 1976; Белышов, Харитонов, 1977; Алиев, 1984; Miller, Brown, 1989; Brezina, 1999; Иванов, 2006; Абдурахманов, Набоженко, 2011; Bird et al., 2015; Zinovyev et al., 2016; Артохин и др., 2016; Aliev et al., 2018; Kovařík et al., 2022; Novruzov et al., 2022) и интернет ресурсы (ICS, 2017; WSC, 2023; Иллюстрированный атлас жуков).

Фрагменты хелицер сольпуг измеряли по 10 размерным особенностям зубных рядов хелицер: (дорсальный палец) FT-FD – длина между концевыми и дистальными зубами; FT-FM – длина между концевыми и медиальными зубами; FT-FP – длина между концевыми и проксимальными зубами; FD-FM – длина между дистальными и медиальными зубами; FM-FP – длина между медиальными и проксимальными зубами; RFM-RFSP – длина между ретрофондально-медиальными и ретрофондально-супрапроксимальными зубами; (подвижный палец) MT-MM – длина между концевыми и медиальными зубами; MT-MP – длина между маргинальными и проксимальными зубами; MM-MSM – длина между медиальными и субмедиальными зубами; MM-MP – длина между медиальными и проксимальными зубами (Bird et al., 2015).

Геологический возраст Бинагадинского битумного месторождения определен как широкий временной интервал от позднего плейстоцена до голоцена (Геология Азербайджана, 1997). По обновленной международной стратиграфической шкале исследуемые горизонты соответствовали верхнему плейстоцену (0.126-0.0117 млн. лет) (Гиббард, 2015; ICS, 2017).

Результаты

В битумном материале, извлеченном с глубины разреза около 1.8 м, были выявлены хитиновые фрагменты членистоногих: насекомых (жуков, бабочек, стрекоз и богомола) и паукообразных (скорпионов и сольпуг) (рис. 1).

Аннотированный таксономический список членистоногих, фрагменты которых были обнаружены в бинагадинских битумных отложениях Абшеронского полуострова.

Тип: Artropoda Gravenhorst, 1843
Подтип: Hexapoda Latreille, 1825
Класс: Insecta Linnaeus, 1758
Отряд: Lepidoptera Linnaeus, 1758
Надсемейство: Papilionoidea Latreille, 1802

Семейство: Pieridae Duponchel, 1835
Подсемейство: Pierinae Swainson, 1820
Род: *Aporia* Hübner, 1819
Aporia sp.
(Рис. 2)

Рис. 1. Фрагменты членистоногих, обнаруженных в бинагадинских битумных отложениях: (1-4) – Lepidoptera; (5,6) – Odonata; (7-12) – Coleoptera; (13) – Mantodea; (14) – Scorpiones; (15) – Solifugae

Материал. Правая и левая (передние и задние) пары крыльев.

Описание. Крылья белые, почти прозрачные. Жилкование темное. Переднее крыло имеет форму прямоугольного треугольника с округлыми краями. Заднее крыло округло-овальное, с двумя анальными жилками. Центральная ячейка на обоих крыльях замкнута и занимает чуть больше половины длины крыла. Жилкование как у большинства современных представителей рода *Aporia*.
Размеры. Длина переднего крыла 34.5 мм, заднего крыла 22.5 мм.
Замечания. Материал морфологически сравнивался с 8 современными видами рода *Aporia* коллекции Института зоологии Азербайджана. Морфологически присутствующие в материале фрагменты были идентифицированы как *Aporia* sp.

Семейство: Nymphalidae Rafinesque, 1815
Подсемейство: Nymphalinae Swainson, 1827
Триба: Nymphalini Rafinesque, 1815
Род: *Vanessa* Fabricius, 1807
Vanessa sp.
(Рис. 3)

Материал. Целое левое переднее крыло, поврежденное правое переднее крыло.
Описание. Общая окраска бледная буро-кирпичная. Цвет изменен от пребывания в битуме. Темные пятна и глазки сохранены.
Размеры. Длина цельного левого переднего крыла 29.3 мм.
Замечания. Материал морфологически сравнивался с современными видами рода *Vanessa* коллекций Естественно-исторического музея и Института зоологии Азербайджана. Морфологически присутствующие в материале фрагменты предположительно можно отнести к виду *Vanessa cardui*.

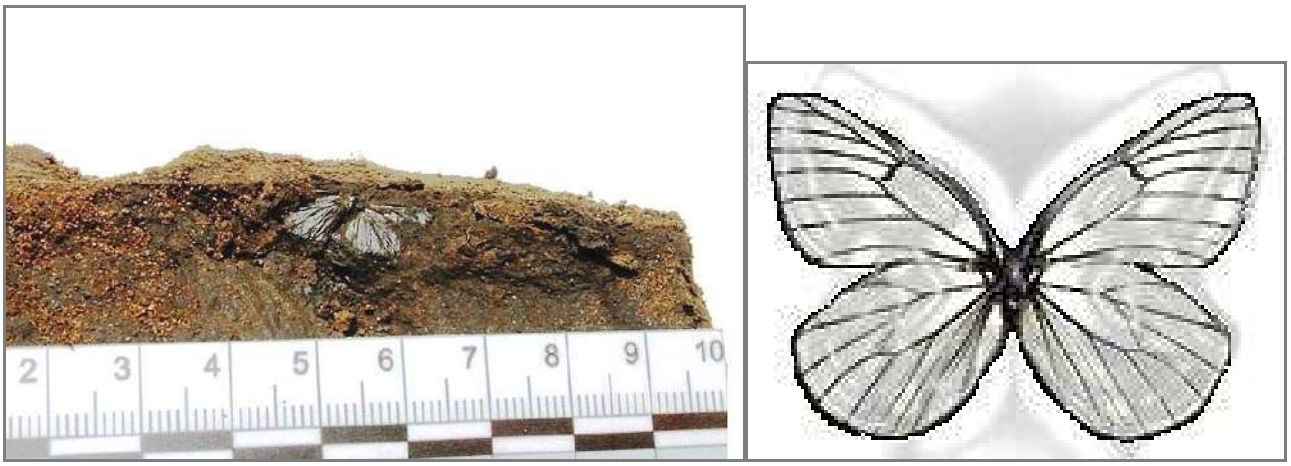

Рис. 2. Фрагменты Lepidoptera рода *Aporia* (Pieridae) (передние, задние крылья и брюшко). Справа: изображение бабочки, реконструированное в графическом редакторе

Рис. 3. Фрагменты Lepidoptera (*Vanessa* sp.), обнаруженные в бинагадинских битумных отложениях

Надсемейство: Gelechioidea Fracker, 1915
Семейство: Gelechiidae Stainton, 1854
Подсемейство: Thriotrichinae Karsholt, Mutanen, Lee & Kaila, 2013
Род *Thiotricha* Meyrick, 1886 (?)
(Рис. 4)

Материал. Два экземпляра бабочек молей рода *Thiotricha* (?).
Описание. Цвет коричневато-бурый с 3 темно-бурыми пятнами на каждом из передних крыльев.
Измерения. Общая длина тела – 8.5-8.7 мм.

Примечание. Оба экземпляра бабочек были обнаружены в битуме среди растительных остатков (между волокнами древесины). Определение до рода и вида затруднительно ввиду разноречивых данных по систематике этой группы чешуекрылых.

Отряд: Odonata Fabricius, 1793
Подотряд: Anisoptera Selys, 1854
Надсемейство: Aeshnoidea Leach, 1815
Семейство: Aeshnidae Rambur, 1842
Род: *Anax* Leach, 1815
Anax sp.
(Рис. 5-8)

Материал. Три передних и два задних крыльев стрекоз.
Описание. На крыльях стрекоз (использовали упрощенную схему обозначения) жилкование состояло из основных продольных жилок (костальная, субкостальная, радиальная, медиальная, кубитальная, анальная с ветвями и интеркалярными секторами), основных поперечных жилок (антенодальная, постнодальная, супранодальная), отдельных полей и ячеек (рис. 7, 8). Жилкование передних и задних крыльев стрекоз густое, но общий облик крыльев и тип их жилкования довольно однообразные. Обращает на себя внимание некоторая вытянутость и узкость основного и внутреннего треугольников (t) вдоль крыловой пластинки. Жилки R_4 и M идут почти параллельно друг другу до заднего края крыла, затем немного расходятся; жилка R_3 не делает изгиба в направлении птеростигмы (Pt); область самой птеростигмы достаточно длинная, соответствующая на передних крыльях 2.5-3.5 ячейкам.
Размеры (мм). Промеры крыльев стрекоз выполнены ограниченно (так как для идентификации материала они значения не имели): общая длина (L) (от основания до вершины); максимальная ширина (S) (самое широкое место крыловой пластинки); индекс ширины (S/L) (отношение ширины к длине) (табл. 1).

Рис. 4. Почти идеально сохранившиеся бабочки-моли рода *Thiotricha* (*Gelechiidae*)

Таблица 1

Метрические данные крыльев стрекоз (мм)

№	Общая длина (L)	Наибольшая ширина (S)	Индекс ширины (S/L)
1	45.0	9.0	0.200
2	42.0	8.5	0.202
3	43.0	8.0	0.186
4	18.0	7.0	0.388
5	30.0	7.5	0.250

Замечания. Материал морфологически сравнивался с современными видами рода *Anax* коллекции Института зоологии Азербайджана. Морфологически присутствующие в материале фрагменты отличались от всех имеющихся в наличии видов.

5

6

Рис. 5, 6. Крылья стрекоз рода *Anax* из битумных отложений (n=5)

Отряд: Coleoptera Linnaeus, 1758
Надсемейство: Hydrophiloidea Latreille, 1802
Семейство: Hydrophilidae Latreille, 1802
Подсемейство: Hydrophilinae Latreille, 1802
Триба: Hydrophilini Bertrand, 1954
Род: *Hydrophilus* Geoffroy, 1762
Hydrophilus sp.
(Рис. 9, 10)

Материал. Правые и левые надкрылья (элитры) (n=12).
Описание. Элитры интенсивно черного цвета, умеренно узкие и длинные по конфигурации. Хорошо различимы все морфологические структуры: 1) сочленовный участок (место крепления надкрыльев к среднеспинке насекомого); 2) основание (базальный край); 3) боковой (наружный) край; 4) плечо (плечевой угол на границе основания и бокового края); 5) вершина (задний конец); 6) эпиплевра (подогнутый вниз наружный край надкрылья); 7) шовный выступ (слева); 8) шовный паз (справа).
Размеры (мм). Длина элитры 43-47 мм, наибольшая ширина 16-19 мм.
Замечания. Материал сравнивался с современными представителями рода *Hydrophilus* коллекций Естественно-исторического музея и Института зоологии Азербайджана. Морфологически присутствующие в материале фрагменты отличались от всех имеющихся в наличии видов.

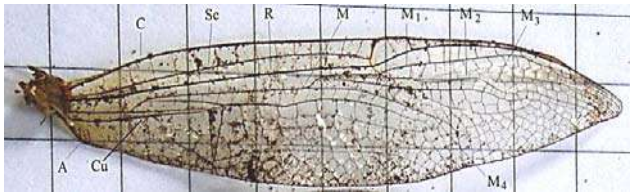

7

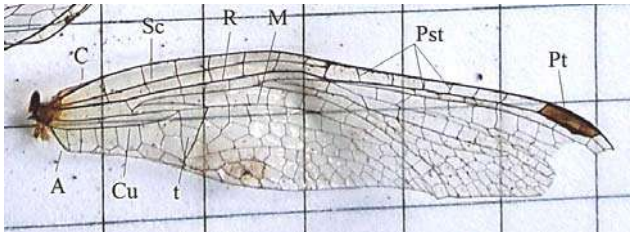

8

Рис. 7, 8. Жилкование крыльев стрекоз, использованное для идентификации: *C – costale; Sc – subcostale; R – radiale; M – mediale; M₁-M₄ – rami mediale; Cu – cubitale; A – anale; t – trigonum; Pt – pterostigmate; Pst – postnodale*

Подотряд: Adephaga Schellenberg, 1806
Семейство: Dytiscidae Latreille, 1802
Подсемейство: Dytiscinae Leach, 1815
Род: *Cybister* Curtis, 1827
Подрод: *Cybister* Curtis, 1827 (?)
(рис. 11, 12)

Материал. Надкрылья, брюшко и переднеспинка 2 экз. жуков плавунцов.
Описание. Надкрылья гладкие, темно-бурого цвета, при естественном освещении с легким темно-охровым отливом, по наружному краю проходит едва заметная светлая кайма.

Дифференциальный диагноз. Проводился на уровне родов: *Cybister* Curtis, 1827; *Dytiscus* Linnaeus, 1758; *Megadytes* Sharp, 1882; Rhantus Dejean, 1833.
Измерения. Длина – 25.3-25.7 мм, наибольшая ширина – 16.7-17.3 мм, высота – 10.1 мм.

9

10

Рис. 9, 10. Фрагменты жесткокрылых рода *Hydrophilus* (элитры)

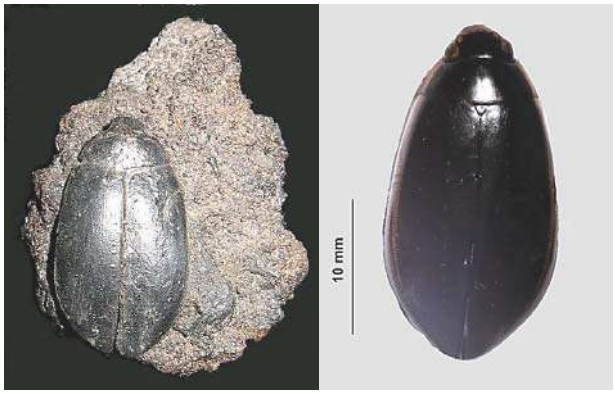

Рис. 11, 12. Экземпляры жесткокрылых рода *Cybister*

Семейство: Tenebrionidae Latreille, 1802
Подсемейство: Blaptinae Leach, 1815
Триба: Blaptini Leach, 1815
Подтриба: Blaptina Latreille, 1802
Род: *Blaps* Fabricius 1775
Blaps sp.
(Рис. 13)

Материал. Элитры и брюшко 6 экз. жуков.
Описание. Переднеспинка поперечная (ширина больше длины), трапециевидная, с наибольшей шириной посередине. Отношение ширины переднеспинки у переднего края к наибольшей ширине и ширине в основании соответственно равно 5:7:6.

Боковые стороны переднеспинки умеренно закругленные, широко слабовыемчатые в базальной четверти. Передний край переднеспинки широко выемчатый. Основание переднеспинки двухвыемчатое. Передние углы переднеспинки острые, задние слабо тупоугольные, почти прямые, на вершине закругленные. Плечевой зубец выше основания элитр; диск умеренно выпуклый; шовный край прямой, пришовный промежуток слегка закруглен; бороздки отчетливые на всем протяжении; вершины не выступают за край брюшка. Надкрылья слабо выпуклые, вдоль шва широко вдавленные, со сглаженными спинными и боковыми ребрами. Надкрылья с грубой умеренно частой пунктировкой вдоль основания переднеспинки, остальная поверхность надкрылий с едва заметной поперечной морщинистостью. Надкрылья умеренно удлиненные (длина надкрылий больше ширины), с наибольшей шириной в средней части.
Дифференциальный диагноз. Материал сравнивался с 5 современными представителями рода *Blaps*: *Blaps brachyura* Kuester, 1848; 2 – *Blaps pterotapha* Menetries, 1832; 3 – *Blaps lethifera* (Marsham, 1802); 4 – *Blaps lustanica* Herbst, 1799; 5 – *Blaps alternans* Brulle, 1838).
Измерения. Длина элитры – 12.9-13.0 мм и 16.6-22.5 мм, наибольшая ширина – 7.0-12.3 мм, высота – 4.8-7.7 мм.

Рис. 13. Фрагменты жесткокрылых рода *Blaps* (элитры и брюшные части)

Подсемейство: Tenebrioninae Latreille, 1802
Триба: Tenebrionini Latreille, 1802
Род: *Tenebrio* Linnaeus, 1758
Tenebrio sp.
(Рис. 14)

Материал. Переднеспинка, элитры, дорсальная и вентральная брюшная часть тела.
Описание. Цвет коричневый, черно-бурый, красновато-коричневый, матово черный. Переднеспинка пунктированная. Элитры продольно пунктированы, образуя 8-9 промежутков между пунктирными линиями. Длина каждой элитры 8-10 мм, ширина 3-4 мм. Общая длина жука предположительно 12-14 мм.

Рис. 14. Фрагменты жесткокрылых рода *Tenebrio* (переднеспинка, элитры и брюшко)

Семейство: Scarabeidae Latreille, 1802
Подсемейство: Scarabaeinae, Latreille, 1802
Триба: Scarabaeini Latreille, 1802
Род *Scarabaeus* Linnaeus, 1758
Scarabaeus sp.
(рис. 15)

Материал. Голова, переднеспинка, надкрылья, брюшная часть тела и две передние лапки.
Описание. Окрас матово-черный. Голова спереди имеет наличник в виде гребешка с 5-6 зубцами. Голени передних ног снаружи с 4-5 зубцами. Тело широкое, овально-субквадратное, слабо выпуклое. Переднеспинка эллиптической формы, сильно поперечно вытянутая, с боков и на основании обычно мелко зазубрена. Надкрылья длиннее переднеспинки в 1.5 раза, их основание не окаймлено, дорсальная поверхность с 5-6 продольными сплошными бороздками и дырчатыми бороздками, 7-я и 8-я бороздки заменены сближенными боковыми килями. Брюшко из 6 стернитов.
Измерения. Длина – 19.4-21.7 мм, ширина – 19.2-19.4 мм.

Рис. 15. Фрагменты жесткокрылых рода *Scarabaeus*

Семейство: Carabidae Latreille, 1802
Подсемейство: Carabinae Latreille, 1802
Триба: Carabini Linnaeus, 1802
Род: *Carabus* Linnaeus, 1758
Carabus sp.
(рис. 16)

Материал. Переднеспинка, надкрылья, брюшная часть и передние ноги.
Описание. Окраска черноватая с металлическим оттенком. Переднеспинка четырехугольной формы, у основания она чуть сужена. Щиток хорошо развит. Надкрылья из плотного хитина, твёрдые, почти целиком покрывают брюшко, лишь на вершине срезаны. Скульптура надкрылий сложная. Поверхность с продольными бороздками и слабо пунктирована. Количество бороздок – 6-9, некоторые бороздки раздвоенные или частично редуцированные.
Измерения. Длина элитр – 12.9 мм, ширина – 7.0 мм, высота – 4.8 мм.

Рис. 16. Фрагменты жесткокрылых рода *Carabus* (Carabidae) (брюшная часть и элитры)

Подсемейство: Pterostichinae Bonelli, 1810
Триба: Zabrini Bonelli, 1810
Подтриба: Zabrina Bonelli, 1810
Род: *Zabrus* Clairville, 1806
Подрод: *Zabrus* (*Zabrus*) Clairville, 1806
Zabrus sp.
(Рис. 17)

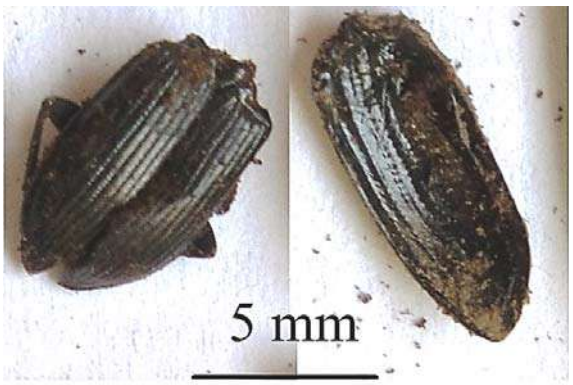

Рис. 17. Фрагменты жесткокрылых рода *Zabrus* (Carabidae) (брюшная часть, задние ноги и элитры)

Материал. Брюшная часть и надкрылья (элитры).
Описание. Окраска смолисто-черная с металлическим блеском и едва заметным при естественном освещении коричневатым отливом. Элитры с глубокими бороздками.
Измерения. Длина элитр – 8.6-8.9 мм, ширина – 4-5 мм.

Подсемейство: Nebriinae Laporte, 1834
Триба: Nebriini Laporte, 1834
Род: *Nebria* Latreille, 1802
Подрод: *Nebria* (*Nebria*) Fabricius, 1892
Nebria sp.
(Рис. 18)

Материал. Переднеспинка и брюшная часть.
Описание. Окраска переднеспинки и элитр темно-коричневая, вентральная поверхность брюшка почти черная. Элитры с продольными бороздками в количестве 7 или 8. Бороздки элитр неоднородно пунктированы.
Размеры. Общая длина сохранившегося тела 14 мм, переднеспинка – 3.7 мм, брюшная часть – 10.3 мм.

Рис. 18. Переднеспинка и брюшная часть жужелицы *Nebria* sp.

Отряд: Mantodea Burmeister, 1838
Семейство: Mantidae Burmeister, 1838
Подсемейство: Mantinae Burmeister, 1838
Триба: Mantini Burmeister, 1838
Род: *Mantis* sp. (?)
(Рис. 19)

Материал. Фрагменты правой и левой передних хватательных конечностей (вертел, бедро, голень, плюсна и лапка).
Описание. Бедро по нижнему краю усажено 3 рядами сильных шипов. Голень по нижнему краю тоже усажена острыми шипами; плюсна одночлениковая, лапка тонкая, 4х-члениковая. Окраска фрагментов изменена битумом. Использована классическая схема морфологических признаков (Brannoch et al., 2017).

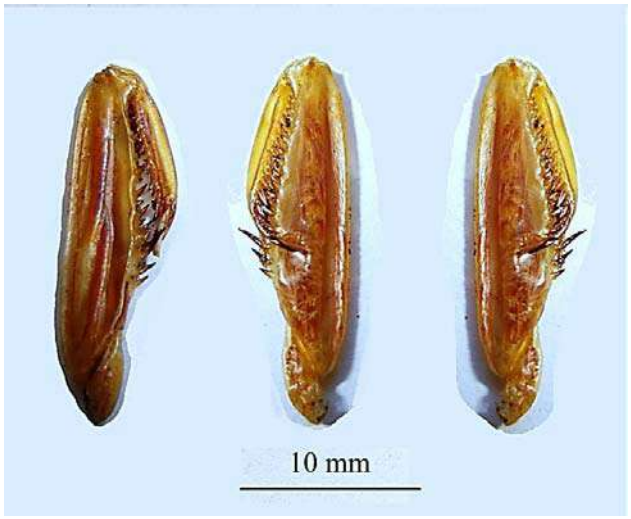

Рис. 19. Передние хватательные конечности богомола рода *Mantis* (Mantidae)

Дифференциальный диагноз. Материал морфологически сравнивался с современными видами коллекции Института зоологии Азербайджана рода *Mantis* Linnaeus, 1758 – *Mantis religiosa* (Linnaeus, 1758), *Mantis religiosa caucasica* (Lindt, 1974), рода *Hierodula* Burmeister, 1838 – *Hierodula transcaucasica* Brunner von Wattenwyl, 1878, рода *Iris* Saussure, 1869 – Iris polystictica (Fischer-Waldheim, 1846).
Измерения. Coxa – 15.1 мм, trochanter – 3.2 мм, femur – 21.0 мм, tibia – 10.9 мм, tarsus – 11.4 мм.
Примечание. Морфологически присутствующие в материале фрагменты не были близки ни к одному из сравниваемых видов. Установленная принадлежность фрагментов к роду *Mantis* – всего лишь предположение, требующее уточнения. Не исключено что найденные фрагменты принадлежат к вымершему виду.

Класс: Arachnida Lamarck, 1801
Отряд: Scorpiones C. L. Koch, 1837
Семейство: Buthidae C.L. Koch, 1837
Род: *Mesobuthus* Vachon, 1950
Mesobuthus sp.
(Рис. 20)

Материал. Правая педипальпа: бедро, пателла, клешня (рис. 1a). Левая педипальпа (пателла и клешня) (рис. 1b). Сегменты метасомы (I-V), тельсон (рис. 1c). Вся метасома (сегменты I-V) и тельсон (рис. 1d).

Описание. Правая педипальпа. Бедро педипальпы с 4 гранулированными килями. Пателла имеет 8 слабо гранулированных килей. Клешня килей не имеет. Острый край подвижного пальца клешни с отчетливыми зубцами, разделенными на 12 линейных рядов. Левая педипальпа. Пателла имет 8 слабо гранулированных килей. Клешня килей не имеет. Острый край подвижного пальца клешни с отчетливыми зубцами, разделенными на 12 линейных рядов. Сегменты метасомы. I сегмент метасомы – с 10 килями; сегменты II, III, IV – с 8 килями; V сегмент – с 5 килями. Тельсон слегка вытянутой формы. Анальная лопасть разделена на три части. Вся метасома. Сегмент I метасомы – с 10 килями; сегменты со II по IV – с 8 килями, два киля на II и III сегментах метасомы с неполным рядом зубцов; сегмент V – с 5 килями. Все кили метасомы гранулированные. Интеркаринальные поверхности на I сегменте метасомы латерально гладкие.

Размеры (мм). Правая педипальпа: бедро (длина 4.35; ширина 1.72; высота 1.33); пателла (длина 6.01; ширина 2.46; высота 2.05); клешня (длина 10.83, ширина 3.09); неподвижный палец (длина 5.76); подвижный палец (длина 6.48); соотношение длины клешни к ширине – 3.50. Левая педипальпа: пателла (длина 5.03; ширина 2.09; высота 1.64); клешня (длина 8.59, ширина 2.34); неподвижный палец (длина 4.67); подвижный палец (длина 5.88); соотношение длины клешни к ширине – 3.67. Метасомальные сегменты: I (длина 4.82, ширина 3.22, глубина 3.07); сегмент II (длина 4.30, ширина 3.26, глубина 3.0); сегмент III (длина 3.87, ширина 3.42, глубина 2.33); сегмент IV (длина 4.21, ширина 3.18, глубина 2.32); сегмент V (длина 5.56, ширина 2.83, глубина 2.31); тельсон (длина без акулюса 3.20, с акулюсом 5.60); соотношение длины III сегмента метасомы к глубине – 1.66; соотношение длины IV сегмента метасомы к глубине – 1.81. Цельная метасома. Длина метасомы без тельсона 21.31; сегмент I (длина 2.99, ширина 3.24, глубина 2.55); сегмент II (длина 4.03, ширина 2.87, глубина 2.94); сегмент III (длина 4.12, ширина 3.15, глубина 3.0); сегмент IV (длина 4.81, ширина 3.14, глубина 2.73); сегмент V (длина 5.36, ширина 2.63, глубина 1.96); тельсон (длина без акулюса 3.01, с акулюсом 5.16).

Замечания. Видовая идентификация не проводилась ввиду отсутствия многих диагностически важных фрагментов тела.

Рис. 20. Фрагменты скорпионов рода *Mesobuthus* (Buthidae) (педипальпы и метасома)

Отряд: Solifugae Sundevall, 1833
Семейство: Galeodidae Sundevall, 1833
Род: *Galeodes* Olivier, 1791
Galeodes sp.
(Рис. 21)

Материал. Фрагменты правой и левой хелицер: челюсти дорсальных (неподвижных) и вентральных (подвижных) пальцев.

Описание. Правая хелицера. На челюсти дорсального (неподвижного) пальца 9 зубцов, из которых 2 крупные; во втором ряду 4 зубца. На вентральном (подвижном) пальце 3 зубца, из которых один крупный и один среднего размера. Левая хелицера. На дорсальном (неподвижном) пальце 8 зубцов, из которых 2 крупные; во втором ряду 3 зубца. На вентральном (подвижном) пальце 3 зубца, из которых один крупный и один среднего размера. Форма верхних челюстей – овальная, нижних – эллипсовидная.

Размеры. FT-FD – 1.15; FT-FM – 1.82; FT-FP – 3.54; FD-FM – 0.70; FM-FP – 1.39; RFM-RFSP – 0.83; MT-MM – 1.60; MT-MP – 3.25; MM-MSM – 0.51; MM-MP – 1.06.

Замечания. Материал морфологически сравнивался с современными видами рода *Galeodes* Olivier 1791 и *Paragaleodes* Kraepelin 1899 фауны Азербайджана (Aliev et al., 2018). Ввиду отсутствия среди фрагментов некоторых диагностически важных частей тела и конечностей видовую идентификацию провести не удалось.

Рис. 21. Фрагменты хелицер сольпуг рода *Galeodes* (Galeodidae) (жвалы дорсальных и вентральных пальцев хелицер) (масштабная линейка 5 мм)

Сводный таксономический список членистоногих, обнаруженных в бинагадинском битумном материале, представлен в таблице (табл. 2).

Таблица 2

Сводный таксономический список членистоногих, обнаруженных в бинагадинских битумных отложениях

Класс / Отряд / Семейство / Род	
Класс: Arachnida	Триба: Blaptini Leach, 1815
Отряд: Scorpiones	Подтриба Blaptina Latreille, 1802
Семейство: Buthidae C.L. Koch, 1837	Род: *Blaps* Fabricius 1775
Род: *Mesobuthus* Vachon, 1950	Подсемейство: Tenebrioninae Latreille, 1802
Отряд: Solifugae	Триба Tenebrionini Latreille, 1802
Семейство: Galeodidae Sundevall, 1833	Род *Tenebrio* Linnaeus, 1758
Род: *Galeodes* Olivier 1791	Семейство: Scarabeidae Latreille, 1802
Класс: Insecta	Подсемейство: Scarabaeinae Latreille, 1802
Семейство: Pieridae Duponchel, 1835	Триба Scarabaeini Latreille, 1802
Подсемейство: Pierinae Swainson, 1820	Род: *Scarabaeus* Linnaeus, 1758
Род: *Aporia* Hübner, 1819	Семейство: Carabidae Latreille, 1802
Семейство: Nymphalidae Rafinesque, 1815	Подсемейство: Carabinae Latreille, 1802
Подсемейство: Nymphalinae Swainson, 1827	Триба Carabini Linnaeus, 1802
Триба: Nymphalini Rafinesque, 1815	Род: *Carabus* Linnaeus, 1758
Род: *Vanessa* Fabricius, 1807	Подсемейство: Pterostichinae Bonelli, 1810
Надсемейство: Gelechioidea Fracker, 1915	Триба: Zabrini Bonelli, 1810
Семейство: Gelechiidae Stainton, 1854	Подтриба: Zabrina Bonelli, 1810
Подсемейство: Thriotrichinae Karsholt, Mutanen, Lee & Kaila, 2013	Род: *Zabrus* Clairville, 1806
Род: *Thiotricha* Meyrick, 1886 (?)	Подсемейство: Nebriinae Laporte, 1834
Отряд: Coleoptera	Триба: Nebriini Laporte, 1834
Надсемейство: Hydrophiloidea Latreille, 1802	Род: *Nebria* Latreille, 1802
Семейство: Hydrophilidae Latreille, 1802	Подрод: *Nebria* (*Nebria*) Fabricius, 1892
Подсемейство: Hydrophilinae Latreille, 1802	Отряд: Mantodea
Триба Hydrophilini Bertrand, 1954	Семейство: Mantidae Burmeister, 1838
Род: *Hydrophilus* Geoffroy, 1762	Подсемейство: Mantinae Burmeister, 1838
Подотряд: Adephaga Schellenberg, 1806	Триба Mantini Burmeister, 1838
Семейство: Dytiscidae Latreille, 1802	Род: *Mantis* Linnaeus, 1758
Подсемейство: Dytiscinae Latreille, 1802	Отряд: Odonata
Род: *Cybister* Curtis, 1827	Подотряд: Anisoptera Selys, 1854
Подрод: *Cybister* Curtis, 1827 (?)	Надсемейство: Aeshnoidea Leach, 1815
Семейство: Tenebrionidae Latreille, 1802	Семейство: Aeshnidae Rambur, 1842
Подсемейство: Blaptinae Leach, 1815	Род: *Anax* Leach, 1815

Заключение

В материале, извлеченном из разрезов почвы в местах раскопок бинагадинского битумного захоронения четвертичной фауны и флоры, расположенного в поселке Бинагады в центральной части Абшеронского полуострова, было выявлено большое количество хитиновых фрагментов членистоногих (насекомых и паукообразных), среди которых впервые выделены фрагменты бабочек и стрекоз (крылья), богомола (передние хватательные лапки), скорпионов (педипальпа и метасома) и сольпуги (жвалы дорсальных и вентральных пальцев хелицер). Идентификация членистоногих достоверно проведена до рода.

ЛИТЕРАТУРА

Абдурахманов Г.М., Набоженко М.В. Определитель и каталог жуков-чернотелок (Coleoptera, Tenebrionidae) Кавказа и Юга Европейской части России. Товарищество научных изданий КМК. Москва, 2011, 382 с.

Алиев Ш.И. Сольпуги (Arachnida, Solifugae) Азербайджана. Автореферат кандидатской диссертации, Киев, 1984, 24 с.

Артохин К.С., Арзанов Ю.Г., Негробов О.П., Полтавский А.Н. Определитель насекомых юга России. Ростов-на-Дону, 2016, 1036 с.

Белышов Б.Ф., Харитонов А.Ю. Определитель стрекоз по крыльям. Наука. Новосибирск, 1977, 398 с.

Богачев А.В. Бинагады, кладбище четвертичной фауны на Апшеронском полуострове. Издательство АзФАН СССР. Баку, 1939б, 83 с.

Богачев А.В. Материалы к познанию фауны жуков Апшеронского полуострова. Труды Азербайджанского отделения Закавказского филиала АН СССР, Т. 7, 1934, с. 14-71.

Богачев А.В. Фауна бинагадинских кировых пластов Coleoptera. Известия АзФАН, Т. 1-2, Баку, 1939а, с. 135-141.

Богачев А.В. Фауна бинагадинских кировых пластов. Жуки – Coleoptera. Труды естественно-исторического музея им. Зардаби, Вып. 1 и 2, Издательство АН Азерб. ССР. Баку, 1948, с. 137-160.

Богачев А.В., Аргиропуло А.И. Четвертичная фауна апшеронских отложений битума (кира). Природа, No. 6, 1939, с. 76-78.

Бурчак-Абрамович Н.И., Джафаров Р.Д. Бинагадинское местонахождение верхнечетвертичной фауны и флоры на Апшеронском полуострове. Труды естественно-исторического музея им. Г. Зардаби, Вып. X, часть IV. Издательство АН Азерб. ССР. Баку, 1955, с. 89-145.

Бялыницкий-Бируля А.А. Фауна СССР. Паукообразные. Том 1, No. 3 – Фаланги (Solifuga). Издательство АН СССР. Москва-Ленинград, Новая сер.17, 1938, 188 с.

Геология Азербайджана. Т.1 – Стратиграфия. Ч. 2. Мезозой и кайнозой. Nafta-Press. Баку, 1997, 636 с.

Гиббард Ф.Л. Четвертичная система (период) и ее основные подразделения. Геология и геофизика, Т. 56, No. 4, 2015, с. 873-875, DOI: 10.15372/GiG20150415.

Иванов А.В. Морфология рисунка элитр жесткокрылых, на примере представителей рода Aphodius Ill. (Coleoptera: Scarabaeidae: Aphodini) фауны России и сопредельных территорий. Автореф. дис... канд. биол. наук, Томск, 2006, 22 с.

Иллюстрированный атлас жуков. http.//www.zin.ru/animalia/coleoptera.

Кириченко А.Н. Фауна бинагадинских кировых пластов. Доклады АН Азерб. ССР, Т. 12, No. 8, 1956, с. 563-564.

Мамаев Б., Медведев Л., Правдин Ф. Определитель насекомых европейской части СССР. Просвещение. Москва, 1976, 304 с.

Рихтер А.А. Ископаемые златки из бинагадинских кировых слоев (Coleoptera, Buprestidae). Доклады АН Арм. ССР, Т. 6, No. 5, 1947, с. 147-150.

Халилов Н.Ю. Путешествие в Кирмакинскую долину. Газета: Вышка от 15, 18 апреля 2003.

REFERENCES

Abdurakhmanov G.M., Nabozhenko M.V. Determinant and catalog of dark beetles (Coleoptera, Tenebrionidae) of the Caucasus and the South of the European part of Russia. Partnership of scientific publications KMK. Moscow, 2011, 382 p. (in Russian).

Aliev Kh.A., Novruzov N.E., Nabieva Kh.A. et al. Review of the species from the order Solifugae (Arachnida) in the collection of the Institute of Zoology of the Azerbaijan National Academy of Sciences, Baku Arthropoda Selecta, Vol. 27, No. 3, 2018, pp. 257-259, DOI:10.15298/arthsel.27.3.10.

Aliyev Sh.I. Solpugi (Arachnida, Solifugae) of Azerbaijan. Abstract of a Ph.D. thesis, Kyiv, 1984, 24 p. (in Russian).

Artokhin K.S., Arzanov Yu.G., Negrobov O.P., Poltavsky A.N. The determinant of insects of the South of Russia. Rostov-on-Don, 2016, 1036 p. (in Russian).

Belyshov B.F., Kharitonov A.Yu. Determinant of dragonflies by wings. Nauka. Novosibirsk, 1977, 398 p. (in Russian).

Bialynitsky-Birulya A.A. Fauna of the USSR. Spiders. Vol. 1, No. 3 – Phalanges (Solifuga). Publishing House of the Academy of Sciences of the USSR. Moscow-Leningrad, Novaya ser. 17, 1938, 188 p. (in Russian).

Bird T.L., Wharton R.A., Prendini L. Cheliceral morphology in Solifugae (Arachnida): primary homology, terminology, and character survey. Bulletin of the American Museum of Natural History, Vol. 394, 2015, 355 p.

Bogachev A.V. Binagadi, a cemetery of Quaternary fauna on the Apsheron Peninsula. Publishing house of the AzFAN of the USSR. Baku, 1939b, 83 p. (in Russian).

Bogachev A.V. Fauna of Binagadi bitumen strata Coleoptera. Izvestia AzFAN, T. 1-2, Baku, 1939a, pp. 135-141 (in Russian).

Bogachev A.V. Fauna of the Binagadi bitumen strata. Beetles – Coleoptera. Proceedings of the Natural History Museum named after Zardabi. No. 1 and 2, Publishing House of the Academy of Sciences of the Azerbaijan SSR. Baku, 1948, pp. 137-160 (in Russian).

Bogachev A.V. Materials for the knowledge of the fauna of beetles of the Absheron Peninsula. Proceedings of the Azerbaijan branch of the Transcaucasian department of the USSR Academy of Sciences, Vol. 7, 1934, p. 14-71 (in Russian).

Bogachev A.V., Argiropulo A.I. Quaternary fauna of the Apsheron deposits of bitumen (kir). Nature, No. 6, 1939, pp. 76-78 (in Russian).

Brannoch S.K., Wieland F., Rivera J., Klass K.D., Béthoux O., Svenson G.J. Manual of praying mantis morphology, nomenclature, and practices (Insecta, Mantodea). ZooKeys, Vol. 696, 2017, pp. 1-100, https://doi.org/10.3897/zookeys.696.12542.

Brezina B. World catalogue of the genus Carabus (Coleoptera, Carabidae). Pensoft Series Faunistica. Vol. 15, Pensoft Publishers. Sofia, 1999,170 p.

Burchak-Abramovich N.I., Jafarov R.D. Binagadi location of the Upper Quaternary fauna and flora on the Apsheron Peninsula. Proceedings of the Natural History Museum named after G. Zardabi, No. 10, part 4. Publishing house of the Academy of Sciences of the Azerbaijan SSR. Baku, 1955, pp. 89-145 (in Russian).

Efendiyeva Z.J. Bitumen deposits of Azerbaijan. Gorny jurnal, No. 10, 2021, pp. 110-114 (in Russian).

Эфендиева З.Дж. Битумные месторождения Азербайджана. Горный журнал, No. 10, 2021, с. 110-114.
Яхонтов А.А. Наши дневные бабочки (определитель). Государственное учебно-педагогическое издательство. Москва, 1935, 161 с.
Aliev Kh.A., Novruzov N.E., Nabieva Kh.A. et al. Review of the species from the order Solifugae (Arachnida) in the collection of the Institute of Zoology of the Azerbaijan National Academy of Sciences, Baku Arthropoda Selecta, Vol. 27, No. 3, 2018, pp. 257-259, DOI:10.15298/arthsel.27.3.10.
Bird T.L., Wharton R.A., Prendini L. Cheliceral morphology in Solifugae (Arachnida): primary homology, terminology, and character survey. Bulletin of the American Museum of Natural History, Vol. 394, 2015, 355 p.
Brannoch S.K., Wieland F., Rivera J., Klass K.D., Béthoux O., Svenson G.J. Manual of praying mantis morphology, nomenclature, and practices (Insecta, Mantodea). ZooKeys, Vol. 696, 2017, pp. 1-100, https://doi.org/10.3897/zookeys.696.12542.
Brezina B. World catalogue of the genus Carabus (Coleoptera, Carabidae). Pensoft Series Faunistica. Vol. 15, Pensoft Publishers. Sofia, 1999,170 p.
ICS (International Chronostratigraphic Chart), 2017, www. stratigraphy.org.
Kovařík F., Fet V., Gantenbein B., Graham M.R., Yağmur E.A., Št'áhlavský F., Poverennyi N.M., Novruzov N.E. A revision of the genus *Mesobuthus* Vachon, 1950, with a description of 14 new species (Scorpiones: Buthidae). Euscorpius, No. 348, 2022, pp. 1-189.
Miller J.Y., Brown F.M. A new Oligocene fossil butterfly, Vanessa amerindica (Lepidoptera: Nymphalidae), from the Florissant Formation, Colorado. Bulletin of the Allyn Museum, No. 126, 1989, pp. 1-9.
Novruzov N.E., Kovařík F., Fet V. *Mesobuthus zarudnyi* sp. n. from Azerbaijan (Scorpiones: Buthidae) Euscorpius, No. 347, 2022, pp. 1-9.
Zinovyev E.V., Dudko R.Yu., Gurina A.A., Prokin A.A., Mikhailov Yu.E., Tsepelev K.A., Tshernyshev S.E., Kireev M.S., Kostyunin A.E., Legalov A.A. First records of subfossil insects from Quaternary deposits in the southeastern part of West Siberia, Russia. Quaternary International, Vol. 420, 2016, pp. 221-232.
WSC – World Solifugae Catalog. Natural History Museum Bern, 2023, online at *http://wac.nmbe.ch.*
Geology of Azerbaijan. Vol. 1 – Stratigraphy. Part 2: Mesozoic and Cenozoic. Nafta-Press. Baku, 1997, 636 p. (in Russian).
Gibbard F.L. Quaternary system (period) and its main divisions. Geology and Geophysics, Vol. 56, No. 4, 2015, p. 873-875, DOI: 10.15372/GiG20150415 (in Russian).
ICS (International Chronostratigraphic Chart), 2017, www. stratigraphy.org.
Illustrated beetle atlas. http.//www.zin.ru/animalia/coleoptera.
Ivanov A.V. Morphology of the of the Coleoptera Elytra pattern, on the example of representatives of the genus Aphodius Ill. (Coleoptera: Scarabaeidae: Aphodini) of the fauna of Russia and adjacent territories. Thesis of Cand. of Biological Sciences, Tomsk, 2006, 22 p. (in Russian).
Khalilov N.Yu. Journey to the Kirmaki Valley. Newspaper: Vyshka, dated April 15, 18, 2003 (in Russian).
Kirichenko A.N. Fauna of Binagadi bitumen strata. Reports of AS Azerb. SSR, Vol. 12, No. 8, 1956, pp. 563-564 (in Russian).
Kovařík F., Fet V., Gantenbein B., Graham M.R., Yağmur E.A., Št'áhlavský F., Poverennyi N.M., Novruzov N.E. A revision of the genus *Mesobuthus* Vachon, 1950, with a description of 14 new species (Scorpiones: Buthidae). Euscorpius, No. 348, 2022, pp. 1-189.
Mamaev B., Medvedev L., Pravdin F. The determinant of insects in the European part of the USSR. Prosveshenie. Moscow, 1976, 304 p. (in Russian).
Miller J.Y., Brown F.M. A new Oligocene fossil butterfly, Vanessa amerindica (Lepidoptera: Nymphalidae), from the Florissant Formation, Colorado. Bulletin of the Allyn Museum, No. 126, 1989, pp. 1-9.
Novruzov N.E., Kovařík F., Fet V. *Mesobuthus zarudnyi* sp. n. from Azerbaijan (Scorpiones: Buthidae) Euscorpius, No. 347, 2022, pp. 1-9.
Richter A.A. Fossil goldfish from Binagadi bitumen layers (Coleoptera, Buprestidae). Reports of the Academy of Sciences Arm. SSR, Vol. 6, No. 5, 1947, pp. 147-150 (in Russian).
Yakhontov A.A. Our day butterflies (determinant). Gosudarstvennoe uchebnoe i pedagogicheskoe izdatelstvo. Moscow, 1935, 161 p. (in Russian).
Zinovyev E.V., Dudko R.Yu., Gurina A.A., Prokin A.A., Mikhailov Yu.E., Tsepelev K.A., Tshernyshev S.E., Kireev M.S., Kostyunin A.E., Legalov A.A. First records of sub-fossil insects from Quaternary deposits in the southeastern part of West Siberia, Russia. Quaternary International, Vol. 420, 2016, pp. 221-232.
WSC – World Solifugae Catalog. Natural History Museum Bern, 2023, online at *http://wac.nmbe.ch.*

НОВЫЕ НАХОДКИ ФРАГМЕНТОВ АРТРОПОД (ARACHNIDA, INSECTA) ИЗ ПОЗДНЕПЛЕЙСТОЦЕНОВЫХ БИТУМНЫХ ОТЛОЖЕНИЙ АБШЕРОНА (АЗЕРБАЙДЖАН)

Новрузов Н.Э.[1], **Таптыгова К.А.**[1], **Эйбатов Т.М.**[2]
[1]*Министерство науки и образования Азербайджанской Республики, Институт зоологии, Азербайджан AZ1073, Баку, проезд 1128, квартал 504: niznovzoo@mail.ru*
[2] *Музей естественной истории Азербайджана, Азербайджан E- AZ1006, Баку, ул. Лермонтова, 3: t_eybatov@mail.ru*

Резюме. При проведении плановых палеонтологических раскопок на Бинагадинском битумном месторождении (Абшеронский полуостров), знаменитом как одно из крупных захоронений образцов фауны и флоры четвертичного периода, с глубины около 1.8 м извлечено большое количество останков ископаемой фауны и флоры. Среди них были выявлены хорошо сохранившиеся фрагменты членистоногих: насекомых 4 отрядов (Lepidoptera, Mantodea, Coleoptera, Odonata) и паукообразных 2 отрядов (Scorpiones, Solifugae). При определении материала в качестве сравнительных (эталонных) образцов были использованы арахнологические и энтомологические коллекции Института зоологии Азербайджана, справочная литература и онлайн каталоги. В объеме проделанной работы по идентификации материала установлена таксономическая принадлежность обнаруженных хитиновых фрагментов членистоногих с достоверностью до рода. Всего выявлено 3 рода из отряда Lepidoptera (*Aporia*, *Vanessa*, *Thiotricha*), 8 родов из отряда Coleoptera (*Hydrophilus*, *Cybister*, *Blaps*, *Tenebrio*, *Scarabaeus*, *Carabus*, *Zabrus*, *Nebria*), по одному роду из отряда Mantodea (*Mantis*), отряда Odonata (*Anax*), отряда Scorpiones (*Mesobuthus*) и отряда Solifugae (*Galeodes*). Выявлены фрагменты педипальпы (бедро, клешня), сегменты метасомы и тельсон скорпионов (Scorpiones), хелицеры сольпуги (Solifugae), крылья бабочек (Lepidoptera) и стрекоз (Odonata), элитры,

грудные и брюшные части, конечности жуков (Coleoptera), передние хватательные конечности (бедро, голень, лапка) богомола (Mantodea). За весь период изучения мировых битумных захоронений флоры и фауны (в том числе бинагадинского) фрагменты Lepidoptera, Mantodea, Odonata, Scorpiones и Solifugae были обнаружены впервые. Собранный материал хранится в музее Естественной истории города Баку и в лаборатории палеозоологии Института зоологии.

Ключевые слова: *битумное месторождение, хитиновые фрагменты, насекомые, паукообразные*

ABŞERONUN (AZƏRBAYCAN) SON PLEİSTOSEN BİTUM YATAQLARINDAN ARTROPOD (ARACHNİDA, INSECTA) PARÇALARININ YENİ TAPINTILARI

Novruzov N.Ə.[1], Taptıqova K.A.[1], Eybatov T.M.[2]
[1]Azərbaycan Respublikasının Elm və Təhsil Nazirliyi, Zoologiya İnstitutu, Azərbaycan
AZ1073, Bakı şəhəri, 1128, məhəllə 504: niznovzoo@mail.ru
[2]Azərbaycan Təbiət Tarixi Muzeyi, Azərbaycan
E-AZ1006, Bakı, Lermontov küç., 3: t_eybatov@mail.ru

Xülasə. Binəqədi dördüncü dövr flora və fauna tapıntı yerində, binəqədi qəbiristanlığı kimi tanınan bitum yatağında (Abşeron yarımadası) planlı paleontoloji qazıntılar zamanı təxminən 1.8 m dərinlikdən çoxlu sayda fosil Fauna və Flora qalıqları çıxarılıb. Bunların arasında artropodların yaxşı vəziyyətdə saxlanılmış çoxsaylı fraqmentləri aşkar edilmişdir: həşəratlardan 4 dəstə (Lepidoptera, Mantodea, Coleoptera, Odonata) və hörümcəkkimilərdən 2 dəstə (Scorpiones, Solifugae). Material müəyyən edilərkən Azərbaycan Zoologiya İnstitutunun araxnoloji və entomoloji kolleksiyaları, istinad ədəbiyyatı və onlayn kataloqlar müqayisəli (istinad) nümunələri kimi istifadə edilmişdir. Materialın identifikasiyası üzrə görülən işlərin həcmində, cinsə etibarlılığı olan artropodların aşkar edilmiş xitin fraqmentlərinin taksonomik mənsubiyyəti müəyyən edilmişdir. Təxminən Lepidoptera dəstəsindən 3 cins (*Aporia, Vanessa, Thiotricha*), Coleoptera dəstəsindən 8 cins (*Hydrophilus, Cybister, Blaps, Tenebrio, Scarabaeus, Carabus, Zabrus, Nebria*), Mantodea dəstəsindən (*Mantis*), Odonata dəstəsindən (*Anax*), Scorpiones dəstəsindən (*Mesobuthus*), Solifugae dəstəsindən (*Galeodes*) müəyyən edilmişdir. Əqrəblərin (Scorpiones) pedipalp parçaları (bud, qısqac), metasoma seqmentləri və telson (əqrəblər), bövlərin (Solifugae) xeliserləri, kəpənəklərin (Lepidoptera) və iynəcələrin (Odonata) qanadları, böcəklərin (Coleoptera) üst qanadları (elitalar), torakal və qarın hissələri, dəvədəlləyinin (Mantodea) ön tutucu ətrafları (bud, baldır, pəncə) aşkar edilmişdir. Qeyd etmək istəyirik ki dünyada aşkar edilmiş çox saylı bitumlu faunaların tərkibində Lepidoptera, Mantodea, Odonata, əqrəblər və bövlər fraqmentləri ilk dəfə aşkar edilmişdir. Toplanılmış material Bakı şəhərinin Təbiət Tarixi Muzeyində və Zoologiya İnstitutunun paleozoologiya laboratoriyasında saxlanılır.

Açar sözlər*: bitum yatağı, xitin fraqmentləri, həşəratlar, araxnidlər*

ANAS Transactions Earth Sciences 1 / 2024

http://www.journalesgia.com

ARTIFICIAL INTELLIGENCE (AI) EVALUATION OF CURRENT RESERVOIR PRESSURE DISTRIBUTION BASED ON OIL PRODUCTION DATA

Suleimanov B.A., Huseynova N.I.

OilGasScientificResearchProject Institute, SOCAR, Azerbaijan

AZ1012, Baku, Zardabi ave., 88A

Keywords: *reservoir, reservoir pressure, reservoir enhanced oil recovery, zonal impact, productive horizon, well productivity, diagnostics, filtration, monitoring, streamlines*

Summary. The paper investigates a quick-look approach for the assessment of the distribution of current reservoir pressure based on production data. The method is based on an algorithm that includes calculation of the current distribution of values of stream functions, potentials and flow velocity in a selected area. The method allows monitoring the factual distribution of the current reservoir pressure of the producing horizon in the area under consideration, as well as evaluating the effectiveness of the impact on the reservoir in order to maintain reservoir pressure.

Based on the proposed method, it is possible to create Artificial Intelligence (AI) technologies for analyzing operational data, machine learning to predict changes in reservoir pressure. The use of neural networks in the integration of geological, geophysical and operational data, operational risk management allows to create automatic expert systems to optimize the process of development and operation of oil and gas fields in conditions of insufficient information.

The accomplishment of the investigated approach carried out applying data samples from Oil Rocks field (Horizon X, Block V) provided high accuracy for values obtained by calculations. The average relative error rate of the calculated values of reservoir pressure to the actual values of bottomhole pressure measurements in wells is no more than 1%, and the average calculated value of reservoir pressure in the productive strata in the study area is in conformity with its actual reduced value.

Introduction

At any stage of field development, the distribution of reservoir pressure in productive formations is an important energy characteristic of the reservoir, both as a whole and in its individual sections. Reservoir pressure in the productive horizon for a certain period of time, taking into account the well interventions, is called current or dynamic formation pressure. Typically, the distribution of current reservoir pressure is determined by constructing isobar maps at the current time based on data from almost simultaneous (as soon as possible) systematic selective pressure measurements on the maximum possible number of idled (nonoperating) or specially shut-in wells for measurements using deep pressure gauges, which requires significant amount of money and time. If it is impossible to use deep pressure gauges (compressor or flowing wells operation), the pressure at the wells is estimated by calculation. The choice of the most correct calculation method depends on many factors – the well design, the distribution of flow properties of the formation and the geological and field conditions of reservoir development (Сулейманов, Гусейнова, 2023a; Suleimanov et al., 2022; Rasulov, Jalalov, 2023; Ибрагимов и др., 2021; Jamalbayov, Ibrahimov, 2023; Choubey, Karmakar, 2021; Khan et al., 2020; Li et al., 2021; Gupta, Shah, 2022; Koroteeva, Tekic, 2021; Weiss et al., 2002; Дмитриевский и др., 2020; Сулейманов, Гусейнова, 2023б; Hung et al., 2023; Шиланбаев и др., 2023; Велиев и др., 2022; Дмитриевский и др., 2022; Велиев и др., 2021; Велиев, 2021; Джамалбеков и др., 2023).

This paper sets forth an AI approach which provides a means for the calculation and visualization of the current distribution of reservoir pressure in a selected section of a productive formation based on the results of calculating the distribution of such hydrodynamic parameters as flow functions, potentials, and the modulus of the formation fluid velocity at a certain point in time, which, in turn, are determined from conventionally measured current well productivity data. At the same time, systematic automated control over the distribution of current reservoir pressure in the field offers the prospect of rational use of reservoir energy during the development and operation of the field.

Statement of the Problem

In order to determine the pressure distribution in the porous medium of a productive formation containing a moving fluid, it is proposed to consider the formation as a set of small elements (cells), for each of which the corresponding values of mass, pore volume, force, pressure and other indicators that determine the movement of the fluid are recorded, which, due to the comparative smallness of the volumes and edges of the elements, within the framework of the element under consideration can be considered uniformly and equally distributed at the moment within the period of review. In an effort to determine the above fixed values, it is put forward to use the results of calculating the distribution of hydrodynamic indicators by solving a plane filtration problem applying the methods of functions of complex variable theory (Suleimanov et al., 2022). It should also be noted that during the development of oil and gas fields, the fluid filtration communications in the horizon occurs due to the pressure difference that exists between the formation elements interacting with each other in the course of flow of the fluid and having different potentials. In those formation elements in which wells are located, the pressure drop between the formation and the well arises due to the difference between the pressures in a given cell and the neighboring ones that make up the external boundary of the well.

Assuming that a certain number of production and injection wells were operated in the area of the reservoir under consideration. As is known, the distribution of such hydrodynamic parameters as flow functions, potentials, complex potential, and the modulus of the velocity of formation fluid at a certain point in time characterizes the corresponding filtration state of the formation system (Сулейманов, Гусейнова, 2023a). Supposing that the distribution of the corresponding hydrodynamic parameters over the area be calculated for two certain successive periods of time Δt_1 and Δt_2, (respectively, for oil $F^{t_1}{}_{1_o}$, $F^{t_2}{}_{1_o}$, $F^{t_1}{}_{2_o}$, $F^{t_2}{}_{2_o}$, ${F_o}^{t_1}$, ${F_o}^{t_2}$, ${W_o}^{t_1}$, ${W_o}^{t_2}$, $grad\left({F_o}^{t_1}\right)$, $grad({F_o}^{t_2})$ for water $F^{t_1}{}_{1_w}$, $F^{t_2}{}_{1_w}$, $F^{t_1}{}_{2_w}$, $F^{t_2}{}_{2_w}$, ${F_w}^{t_1}$, ${F_w}^{t_2}$, ${W_w}^{t_1}$, ${W_w}^{t_2}$, $grad\left({F_w}^{t_1}\right)$, $grad({F_w}^{t_2})$ and for the reservoir fluid as a whole $F^{t_1}{}_{1_f}$, $F^{t_2}{}_{1_f}$, $F^{t_1}{}_{2_f}$, $F^{t_2}{}_{2_f}$, ${F_f}^{t_1}$, ${F_f}^{t_2}$, ${W_f}^{t_1}$, ${W_f}^{t_2}$, $grad({F_f}^{t_1}), grad({F_f}^{t_2})$ with subsequent representation in the form tensors of dimension $n \times m$, where $n \times m$ is the number of grid cells, n is the number of partition nodes in the grid along the OX axis, m is the number of partition nodes along the OY, axis $j=1, \ldots, n \times m$ is the serial number of the cell. The elements of each of the tensors are the total for all wells corresponding values of the stream function and potentials in each j -th grid cell theory (Suleimanov et al,, 2022), depending on the flow rate of each i -th well, the distance r_{ij} from the i -th well to an arbitrary point of the reservoir with coordinates (x_j, y_j), where $i=1, \ldots \kappa$ is the number of operating wells in the field area allocated for research:

As per oil, in the period of time Δt_1:

$$F^{t_1}{}_{1_o} = \begin{bmatrix} (F^{t_1}{}_{1_o})_{1,1} & \ldots & (F^{t_1}{}_{1_o})_{1,n} \\ \ldots & \ldots & \ldots \\ (F^{t_1}{}_{1_o})_{m,1} & \ldots & (F^{t_1}{}_{1_o})_{m,n} \end{bmatrix};$$

$$F_{2_o}{}^{t_1} = \begin{bmatrix} (F_{2_o}{}^{t_1})_{1,1} & \ldots & (F_{2_o}{}^{t_1})_{1,n} \\ \ldots & \ldots & \ldots \\ (F_{2_o}{}^{t_1})_{m,1} & \ldots & (F_{2_o}{}^{t_1})_{m,n} \end{bmatrix};$$

$$F_o{}^{t_1} = \begin{bmatrix} (F_o{}^{t_1})_{1,1} & \ldots & (F_o{}^{t_1})_{1,n} \\ \ldots & \ldots & \ldots \\ (F_o{}^{t_1})_{m,1} & \ldots & (F_o{}^{t_1})_{m,n} \end{bmatrix};$$

$$W_o{}^{t_1} = \begin{bmatrix} (W_o{}^{t_1})_{1,1} & \ldots & (W_o{}^{t_1})_{1,n} \\ \ldots & \ldots & \ldots \\ (W_o{}^{t_1})_{m,1} & \ldots & (W_o{}^{t_1})_{m,n} \end{bmatrix};$$

$$grad(F_o{}^{t_1}) = \begin{bmatrix} (grad(F_o{}^{t_1}))_{1,1} & \ldots & (grad(F_o{}^{t_1}))_{1,n} \\ \ldots & \ldots & \ldots \\ (grad(F_o{}^{t_1}))_{m,1} & \ldots & (grad(F_o{}^{t_1}))_{m,n} \end{bmatrix} \quad (1)$$

As per water, in the period of time Δt_1:

$$F^{t_1}{}_{1_w} = \begin{bmatrix} (F^{t_1}{}_{1_w})_{1,1} & \ldots & (F^{t_1}{}_{1_w})_{1,n} \\ \ldots & \ldots & \ldots \\ (F^{t_1}{}_{1_w})_{m,1} & \ldots & (F^{t_1}{}_{1_w})_{m,n} \end{bmatrix};$$

$$F_{2_w}{}^{t_1} = \begin{bmatrix} (F_{2_w}{}^{t_1})_{1,1} & \ldots & (F_{2_w}{}^{t_1})_{1,n} \\ \ldots & \ldots & \ldots \\ (F_{2_w}{}^{t_1})_{m,1} & \ldots & (F_{2_w}{}^{t_1})_{m,n} \end{bmatrix};$$

$$F_w{}^{t_1} = \begin{bmatrix} (F_w{}^{t_1})_{1,1} & \ldots & (F_w{}^{t_1})_{1,n} \\ \ldots & \ldots & \ldots \\ (F_w{}^{t_1})_{m,1} & \ldots & (F_w{}^{t_1})_{m,n} \end{bmatrix};$$

$$W_w{}^{t_1} = \begin{bmatrix} (W_w{}^{t_1})_{1,1} & \ldots & (W_w{}^{t_1})_{1,n} \\ \ldots & \ldots & \ldots \\ (W_w{}^{t_1})_{m,1} & \ldots & (W_w{}^{t_1})_{m,n} \end{bmatrix};$$

$$grad(F_w{}^{t_1}) = \begin{bmatrix} (grad(F_w{}^{t_1}))_{1,1} & \ldots & (grad(F_w{}^{t_1}))_{1,n} \\ \ldots & \ldots & \ldots \\ (grad(F_w{}^{t_1}))_{m,1} & \ldots & (grad(F_w{}^{t_1}))_{m,n} \end{bmatrix} \quad (2)$$

As per fluid, in the period of time Δt_1:

$$F^{t_1}{}_{1_f} = \begin{bmatrix} (F^{t_1}{}_{1_f})_{1,1} & \ldots & (F^{t_1}{}_{1_f})_{1,n} \\ \ldots & \ldots & \ldots \\ (F^{t_1}{}_{1_f})_{m,1} & \ldots & (F^{t_1}{}_{1_f})_{m,n} \end{bmatrix};$$

$$F_{2_f}{}^{t_1} = \begin{bmatrix} (F_{2_f}{}^{t_1})_{1,1} & \dots & (F_{2_f}{}^{t_1})_{1,n} \\ \dots & \dots & \dots \\ (F_{2_f}{}^{t_1})_{m,1} & \dots & (F_{2_f}{}^{t_1})_{m,n} \end{bmatrix};$$

$$F_f{}^{t_1} = \begin{bmatrix} (F_f{}^{t_1})_{1,1} & \dots & (F_f{}^{t_1})_{1,n} \\ \dots & \dots & \dots \\ (F_f{}^{t_1})_{m,1} & \dots & (F_f{}^{t_1})_{m,n} \end{bmatrix};$$

$$W_f{}^{t_1} = \begin{bmatrix} (W_f{}^{t_1})_{1,1} & \dots & (W_f{}^{t_1})_{1,n} \\ \dots & \dots & \dots \\ (W_f{}^{t_1})_{m,1} & \dots & (W_f{}^{t_1})_{m,n} \end{bmatrix};$$

$$grad(F_f{}^{t_1}) = \begin{bmatrix} (grad(F_f{}^{t_1}))_{1,1} & \dots & (grad(F_f{}^{t_1}))_{1,n} \\ \dots & \dots & \dots \\ (grad(F_f{}^{t_1}))_{m,1} & \dots & (grad(F_f{}^{t_1}))_{m,n} \end{bmatrix} \quad (3)$$

And

As per oil, in the period of time Δt_2:

$$F^{t_2}{}_{1_o} = \begin{bmatrix} (F^{t_2}{}_{1_o})_{1,1} & \dots & (F^{t_2}{}_{1_o})_{1,n} \\ \dots & \dots & \dots \\ (F^{t_2}{}_{1_o})_{m,1} & \dots & (F^{t_2}{}_{1_o})_{m,n} \end{bmatrix};$$

$$F_{2_o}{}^{t_1} = \begin{bmatrix} (F_{2_o}{}^{t_1})_{1,1} & \dots & (F_{2_o}{}^{t_1})_{1,n} \\ \dots & \dots & \dots \\ (F_{2_o}{}^{t_1})_{m,1} & \dots & (F_{2_o}{}^{t_1})_{m,n} \end{bmatrix};$$

$$F_o{}^{t_1} = \begin{bmatrix} (F_o{}^{t_1})_{1,1} & \dots & (F_o{}^{t_1})_{1,n} \\ \dots & \dots & \dots \\ (F_o{}^{t_1})_{m,1} & \dots & (F_o{}^{t_1})_{m,n} \end{bmatrix};$$

$$W_o{}^{t_2} = \begin{bmatrix} (W_o{}^{t_2})_{1,1} & \dots & (W_o{}^{t_2})_{1,n} \\ \dots & \dots & \dots \\ (W_o{}^{t_2})_{m,1} & \dots & (W_o{}^{t_2})_{m,n} \end{bmatrix};$$

$$grad(F_o{}^{t_2}) = \begin{bmatrix} (grad(F_o{}^{t_2}))_{1,1} & \dots & (grad(F_o{}^{t_2}))_{1,n} \\ \dots & \dots & \dots \\ (grad(F_o{}^{t_2}))_{m,1} & \dots & (grad(F_o{}^{t_2}))_{m,n} \end{bmatrix} \quad (4)$$

As per water, in the period of time Δt_2:

$$F^{t_2}{}_{1_w} = \begin{bmatrix} (F^{t_2}{}_{1_w})_{1,1} & \dots & (F^{t_2}{}_{1_w})_{1,n} \\ \dots & \dots & \dots \\ (F^{t_2}{}_{1_w})_{m,1} & \dots & (F^{t_2}{}_{1_w})_{m,n} \end{bmatrix};$$

$$F_{2_w}{}^{t_2} = \begin{bmatrix} (F_{2_w}{}^{t_2})_{1,1} & \dots & (F_{2_w}{}^{t_2})_{1,n} \\ \dots & \dots & \dots \\ (F_{2_w}{}^{t_2})_{m,1} & \dots & (F_{2_w}{}^{t_2})_{m,n} \end{bmatrix};$$

$$F_w{}^{t_2} = \begin{bmatrix} (F_w{}^{t_2})_{1,1} & \dots & (F_w{}^{t_2})_{1,n} \\ \dots & \dots & \dots \\ (F_w{}^{t_2})_{m,1} & \dots & (F_w{}^{t_2})_{m,n} \end{bmatrix};$$

$$W_w{}^{t_2} = \begin{bmatrix} (W_w{}^{t_2})_{1,1} & \dots & (W_w{}^{t_2})_{1,n} \\ \dots & \dots & \dots \\ (W_w{}^{t_2})_{m,1} & \dots & (W_w{}^{t_2})_{m,n} \end{bmatrix};$$

$$grad(F_w{}^{t_2}) = \begin{bmatrix} (grad(F_w{}^{t_2}))_{1,1} & \dots & (grad(F_w{}^{t_2}))_{1,n} \\ \dots & \dots & \dots \\ (grad(F_w{}^{t_2}))_{m,1} & \dots & (grad(F_w{}^{t_2}))_{m,n} \end{bmatrix} \quad (5)$$

As per fluid, in the period of time Δt_2:

$$F^{t_2}{}_{1_f} = \begin{bmatrix} (F^{t_2}{}_{1_f})_{1,1} & \dots & (F^{t_2}{}_{1_f})_{1,n} \\ \dots & \dots & \dots \\ (F^{t_2}{}_{1_f})_{m,1} & \dots & (F^{t_2}{}_{1_f})_{m,n} \end{bmatrix};$$

$$F_{2_f}{}^{t_2} = \begin{bmatrix} (F_{2_f}{}^{t_2})_{1,1} & \dots & (F_{2_f}{}^{t_2})_{1,n} \\ \dots & \dots & \dots \\ (F_{2_f}{}^{t_2})_{m,1} & \dots & (F_{2_f}{}^{t_2})_{m,n} \end{bmatrix}$$

$$F_f{}^{t_2} = \begin{bmatrix} (F_f{}^{t_2})_{1,1} & \dots & (F_f{}^{t_2})_{1,n} \\ \dots & \dots & \dots \\ (F_f{}^{t_2})_{m,1} & \dots & (F_f{}^{t_2})_{m,n} \end{bmatrix};$$

$$W_f{}^{t_2} = \begin{bmatrix} (W_f{}^{t_2})_{1,1} & \dots & (W_f{}^{t_2})_{1,n} \\ \dots & \dots & \dots \\ (W_f{}^{t_2})_{m,1} & \dots & (W_f{}^{t_2})_{m,n} \end{bmatrix};$$

$$grad(F_f{}^{t_2}) = \begin{bmatrix} (grad(F_f{}^{t_2}))_{1,1} & \dots & (grad(F_f{}^{t_2}))_{1,n} \\ \dots & \dots & \dots \\ (grad(F_f{}^{t_2}))_{m,1} & \dots & (grad(F_f{}^{t_2}))_{m,n} \end{bmatrix} \quad (6)$$

Applying the algorithm provided in (Сулейманов, Гусейнова, 2023а,), tensors (1) - (6) are calculated, characterizing the distribution of the above filtration characteristics in the field area allocated for study within the period of time under study. As initial data, the results of measurements at wells operating from the studied productive horizon on the current date are used, namely: the flow rate of production wells (the volume of oil and water produced per unit of time), the injectivity of injection wells (the volume of injection per layer of working agent per unit time), filter length values, conditional coordinates of the location of the corresponding wells in the studied area of the productive formation.

As is known, the distribution of acceleration values of a fluid flow $\vec{a}$ over a certain period of time $\Delta t=t_1-t_2$ in a selected area is defined as the ratio of the change in the true speed of the flow to the time interval:

$$\vec{a} = \frac{v^{t_2} - v^{t_1}}{t_2 - t_1} \quad (7)$$

The rate of percolation is expressed through the actual flow velocity and rock porosity K as follows (Rasulov, Jalalov, 2023):

$$W = v \cdot K \quad (8)$$

The volume of fluid located at this moment in time in the porous medium of the formation, limited by each of the grid cells superimposed on the area under consideration, is determined by the value of the stream function in each grid cell, that is, the volumetric distribution of fluid in the area at the current time is determined by the tensor $F^{t_1}{}_{1_f}$. Knowing that the volume of the cell under consideration consists of rock and the liquid saturating it, we can determine the volume occupied by the rock as the difference between the volume of a parallelepiped 1m high and a rectangular surface, the dimensions of which are determined by the choice of grid scale.

Using these data, it is also possible to estimate the distribution of effective porosity during the period of time under consideration in the studied area of the productive formation. As is known, the current effective porosity K means the ratio of the volume of interconnected voids V_l filled with fluid to the total volume V. The total volume of the cell in which the effective porosity $V_я$ is determined is known, since it is determined by the scale of the grid superimposed on the area. The change in the volume of pore space filled with formation fluid over a period of time Δt is determined by the difference in the tensor elements $F^{t_1}{}_{1_f}$ and $F^{t_1}{}_{1_f}$ in the time period under consideration:

$$dV_f = (F_1{}^{t_2}{}_f - F_1{}^{t_1}{}_f) \cdot dt = K \cdot a \cdot b \cdot h$$

From here the value of the current effective porosity K^{t_2} is determined:

$$K^{t_2} = \frac{\left(F_1{}^{t_2}{}_f - F_1{}^{t_1}{}_f\right) \times dt}{a \times b \times h}$$

$$= \frac{(F_1{}^{t_2}{}_f - F_1{}^{t_1}{}_f) \times (t_2 - t_1)}{a \times b \times h} \quad (9)$$

Where:
$h = 1м$ – height of the cell, presented in the form of a rectangular parallelepiped, a and b- sides, depending on the choice of the scale of the grid superimposed on the area under study.

Then formula (7) can be rewritten as:

$$\vec{a} = \frac{W^{t_2}/K^{t_2} - W^{t_1}/K^{t_1}}{t_2 - t_1} \quad (10)$$

It is impossible to determine the mass of liquid distributed over the area based on the values $F^{t_1}{}_{1_f}$, since the liquid is two-phase and consists of oil and water distributed in the pore space of the formation, conventionally divided into cells. Knowing that $m = \rho \cdot V$, where m is mass, ρ is density, V is volume, to determine the mass of liquid contained in each fixed cell, based on the values of $F^{t_1}{}_{1_o}$,$F^{t_1}{}_{1_w}$ and $F^{t_2}{}_{1_o}$,$F^{t_2}{}_{1_w}$, we separately determine the volume of oil and the volume of water contained in each of these moments in time in each of the grid cells superimposed on the site. Next, based on the data obtained for each of the considered moments of time, we determine the tensor characterizing the distribution of liquid mass in the area:

$$m^{t_1}{}_f = \mathrm{m}^{t_1}{}_o + \mathrm{m}^{t_1}{}_w = \rho_o \cdot \mathrm{V}^{t_1}{}_o + \rho_w \cdot \mathrm{V}^{t_1}{}_w = (\rho_o \cdot \mathrm{F}^{t_1}{}_{\mathrm{o1}} + \rho_w \cdot \mathrm{F}^{t_1}{}_{\mathrm{1w}}) \cdot dt \quad (11)$$

$$m^{t_2}{}_f = \mathrm{m}^{t_2}{}_o + \mathrm{m}^{t_2}{}_w = \rho_o \cdot V^{t_2}{}_o + \rho_w \cdot V^{t_2}{}_w = (\rho_o \cdot \mathrm{F}^{t_2}{}_{\mathrm{o1}} + \rho_w \cdot \mathrm{F}^{t_2}{}_{\mathrm{1w}}) \cdot dt$$

With a knowledge of the density of oil and water, as well as the volume of each phase located at this moment in time in each of the grid cells superimposed on the area, it is possible to determine the distribution of the mass of liquid saturating the pore space of the productive formation in this area.

Next, in accordance with Newton's law, the distribution of the force exerted on the surface of the pore space is determined:

$$F = m^{t_2}{}_f \cdot \vec{a} \quad (12)$$

Knowing the area of the gaps whereby the liquid to which the force is applied enters the cell, we can determine the pressure that the liquid exerts on the cell during its movement:

$$P = F / S_n \quad (13)$$

The area of the gaps S_n on the lateral surface of a cell with area S at time t is determined as follows (Rasulov, Jalalov, 2023):

$$S_n = S \cdot K^t \quad (14)$$

Determining the lateral surface area of a cell S is not difficult:

$$S = 2 \cdot h \cdot (a + b) \quad (15)$$

Taking into account correlations (10)-(12) in (13), we obtain:

$$P^{t_2} = \frac{F}{S_{\text{п}}} = \left(m^{t_2}{}_f \cdot \vec{a}\right) \cdot \frac{1}{S \cdot \mathrm{K}^{t_2}}$$

$$= (\rho_o \cdot F^{t_2}{}_{o1} + \rho_w \cdot F^{t_2}{}_{1w}) \cdot (t_2 - t_1) \cdot \frac{1}{t_2 - t_1} \cdot \left(\frac{W^{t_2}}{K^{t_2}} - \frac{W^{t_1}}{K^{t_1}}\right) \cdot \frac{1}{S \cdot K^{t_2}}$$

$$= (\rho_o \cdot F^{t_2}{}_{o1} + \rho_w \cdot F^{t_2}{}_{1w}) \cdot \frac{1}{K^{t_2} \cdot K^{t_1}} \cdot (W^{t_2} \cdot K^{t_1} - W^{t_1} \cdot K^{t_2}) \cdot \frac{1}{2 \cdot h \cdot (a+b) \cdot K^{t_2}}$$

$$= (\rho_o \cdot F^{t_2}{}_{o1} + \rho_w \cdot F^{t_2}{}_{1w}) \cdot \frac{h^2 \cdot a^2 \cdot b^2}{\left(F^{t_2}{}_f - F^{t_1}{}_f\right) \cdot (t_2 - t_1) \cdot \left(F^{t_1}{}_f - F^{t_0}{}_f\right) \cdot (t_1 - t_0)}$$

$$\cdot \frac{\left(W^{t_2} \cdot \left(F^{t_1}{}_f - F^{t_0}{}_f\right) \cdot (t_1 - t_0) - W^{t_1} \cdot \left(F^{t_2}{}_f - F^{t_1}{}_f\right) \cdot (t_2 - t_1)\right)}{h \cdot a \cdot b}$$

$$\cdot \frac{h \cdot a \cdot b}{2 \cdot h \cdot (a+b) \cdot \left(F^{t_2}{}_f - F^{t_1}{}_f\right) \cdot (t_2 - t_1)}$$

$$= \frac{(\rho_o \cdot F^{t_2}{}_{o1} + \rho_w \cdot F^{t_2}{}_{1w}) \cdot (W^{t_2} \cdot (F^{t_1}{}_f - F^{t_0}{}_f) \cdot (t_1 - t_0) - W^{t_1} \cdot (F^{t_2}{}_f - F^{t_1}{}_f) \cdot (t_2 - t_1)) \cdot h \cdot a^2 \cdot b^2}{2 \cdot (a+b) \cdot (t_2 - t_1)^2 \cdot (t_1 - t_0) \cdot (F^{t_2}{}_f - F^{t_1}{}_f)^2 \cdot (F^{t_1}{}_f - F^{t_0}{}_f)} \quad (16)$$

where:

$$K^{t_2} = \frac{(F^{t_2}{}_f - F^{t_1}{}_f) \cdot (t_2 - t_1)}{a \cdot b \cdot h}$$

$$K^{t_1} = \frac{(F^{t_1}{}_f - F^{t_0}{}_f) \cdot (t_1 - t_0)}{a \cdot b \cdot h}.$$

$F^{t_2}{}_{o1}, F^{t_2}{}_{1w}$ – distribution of current function over oil and water, m^3/day;

W^{t_1}, W^{t_2} – distribution of flow velocity by liquid, m^3/day;

$F^{t_1}{}_{1f}, F^{t_0}{}_{1f} F^{t_2}{}_{1f}$ – distribution of current function over liquid, m^3/day;

ρ_o, ρ_w – density of oil and water, kg/m^3

$\Delta t_1 = t_1 - t_0$, day

$\Delta t_2 = t_2 - t_1$, day

h, a, b – respectively, the height and length of the sides of a scale grid cell superimposed on the study area, m.

Field Application

In order to automate the calculations and visualize the results obtained, a special software module has been developed on the basis of the "Matlab" engineering and scientific calculation system package, which makes it possible to calculate and visualize the pressure distribution in the area under study at the current time in accordance with the algorithm proposed above. In an effort to demonstrate the calculation results, data from the "Oil Rocks" field (horizon X, block V), which has been under development from 1957 to the present, were used (Fig. 1). The initial reservoir pressure at the horizon X was 21 MPa. During the period of formation stimulation, the average reduced pressure in block V was about 12 MPa. In individual wells of the experimental area, the bottomhole pressure varied in the range of 2.7-8.5 MPa, respectively, the reduced reservoir pressure had values in the range of 2.9 - 8.9 MPa (Table). The average actual reduced pressure at the study site was 4.5 MPa. For many wells in the stimulation area, bottomhole pressure measurements have not been made at the current date. However, the proposed method offers the prospect of estimating both bottomhole and reduced reservoir pressure in the vicinity of these wells, knowing the productivity of the wells. The following information was used as initial data for carrying out calculations for the current date:

1. Consumption of production wells (volume of production recovered from the reservoir per unit of time);
2. Injectivity of injection wells (volume of injection of working agent into the formation);
3. Values of the length of well filters;
4. Conditional coordinates of the corresponding wells.

The collection of necessary data was carried out during the planning period for reservoir stimulation in order to ramp up oil recovery (August 2015). The calculation used field data for the periods before and after the stimulation (08.2015-10.2015). The obtained calculated values were compared with the values of measurements of bottomhole and reduced reservoir pressure in the wells of the experimental area for the period after the stimulation of the reservoir (11.2015-02.2016).

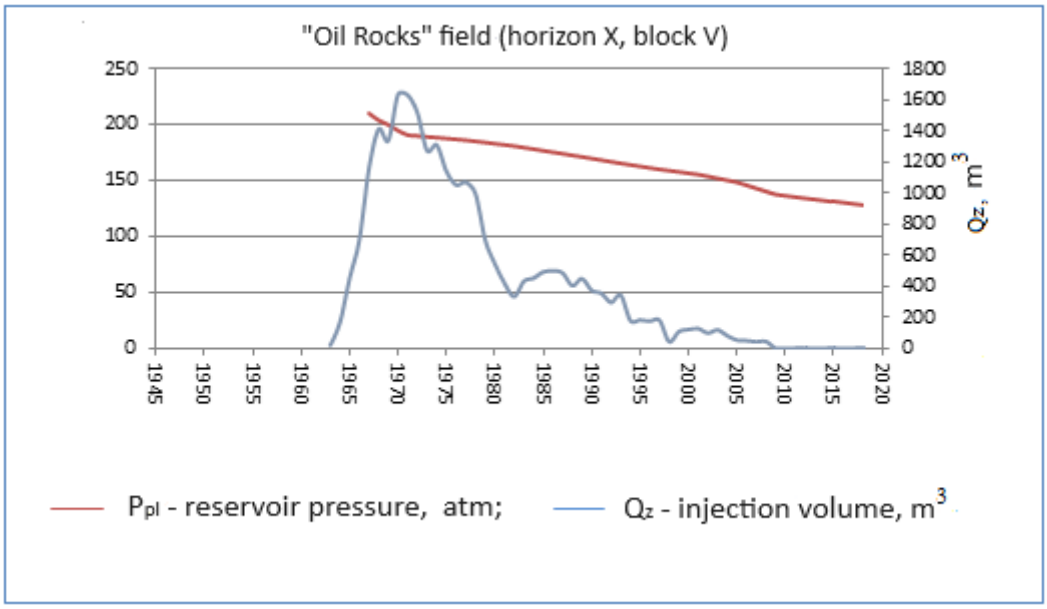

Fig. 1. Dynamics of the values of the reduced reservoir pressure and the volume of water injected into the reservoir along the horizon X on block V of "Oil Rocks" field.

Initial data and results of comparative analysis of calculated and actual values of reservoir pressure at the test site

№	Production for the period under review		Provisional coordinates		Filter	$P_{расч}$	$P_{заб}$	$P_{пл}$
	Oil $Q_н$, т	Water $Q_в$, м^3	*X*, м	*Y*, м	F, м	atm		
2361	5.0	0	156.19	107.12	8	**48.3**	40.5	42.7
2429	18.8	0	189.00	65.07	5	**50.8**	53.98	63.1
2423	22.0	0	191.86	78.52	10	**70.4**	70.14	76.2
2422	18.0	0	200.94	88.78	36	**53.1**	54.75	58.1
2444	23.0	0	194.55	97.53	14	**58.4**	56.67	61.7
2421	23.0	0	196.90	113.17	20	**51.7**	58.74	67.6
2414	2.0	0	152.82	86.77	8	**27.0**	27.12	29.5
2383	7.1	0	140.54	93.83	10	**34.6**	36.21	39.7

In line with the method of calculation and visualization of the distribution of filtration characteristics of formation fluid (Сулейманов и др., 2017; Лятифов 2021), the matrixes of distribution of hydrodynamic parameters were calculated and visualized at the time points of August-October 2015 (Fig. 2-8). Next, using the data obtained, the distribution of current reservoir pressure for December 2015 was calculated and visualized (Fig. 9). Digital visualization of isobar lines characterizing the current pressure distribution was obtained in the following way. The maximum and minimum values of the elements that make up the tensor of pressure values are highlighted. The resulting range of values is divided into equal intervals, each of which is assigned a specific color. Each color of the scale is associated with a specific pressure value. Cells with equal values are connected by a line. In accordance with the results obtained, a pressure distribution map is constructed in the area allocated for research (Fig. 9).

The results of a comparative analysis of calculated data with actual data from bottomhole pressure measurements at wells are given in the table. At the same time, the average value of the relative error of the calculated values to the actual values is no more than 1%. The average calculated reservoir pressure for the area was 4.5 MPa, that is, the average calculated value of the reservoir pressure coincides with its actual reduced value.

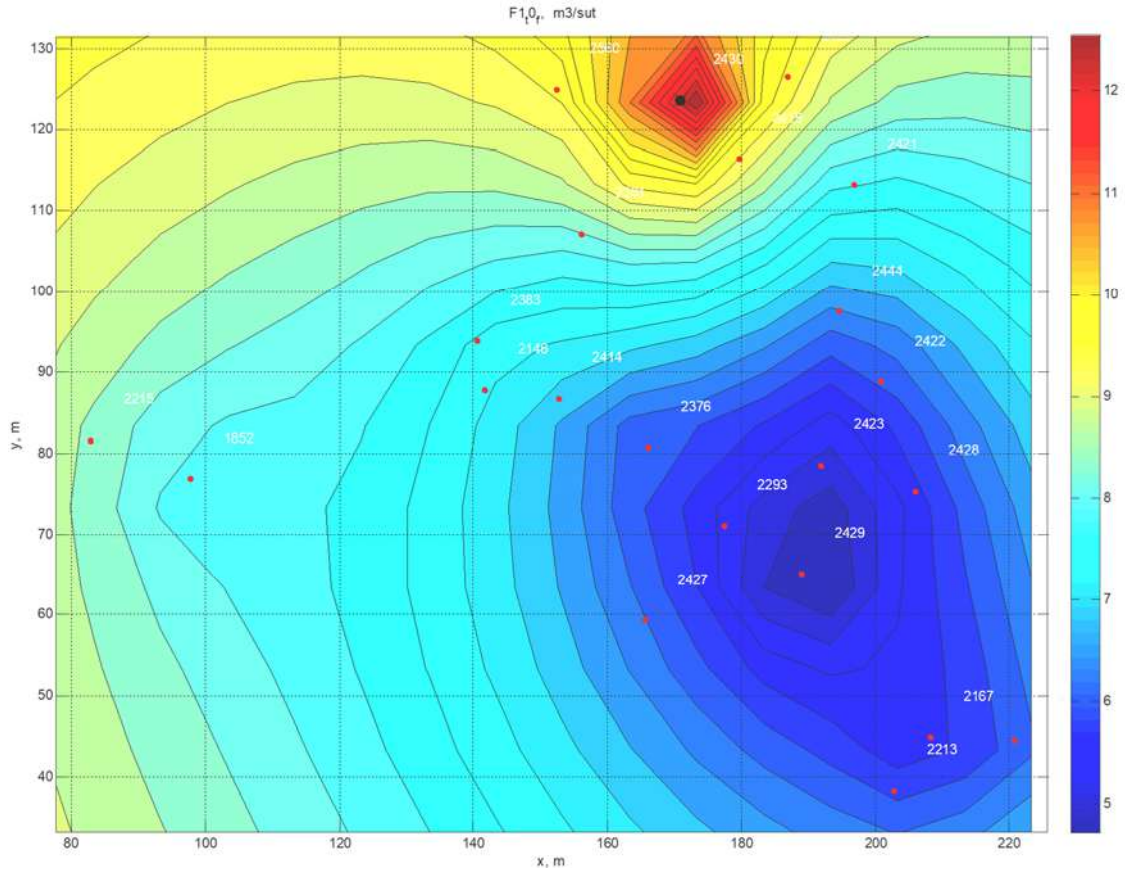

Fig. 2. Distribution of streamlines in the liquid $F_{1n}{}^{t}{}_{0}$ at time t_0

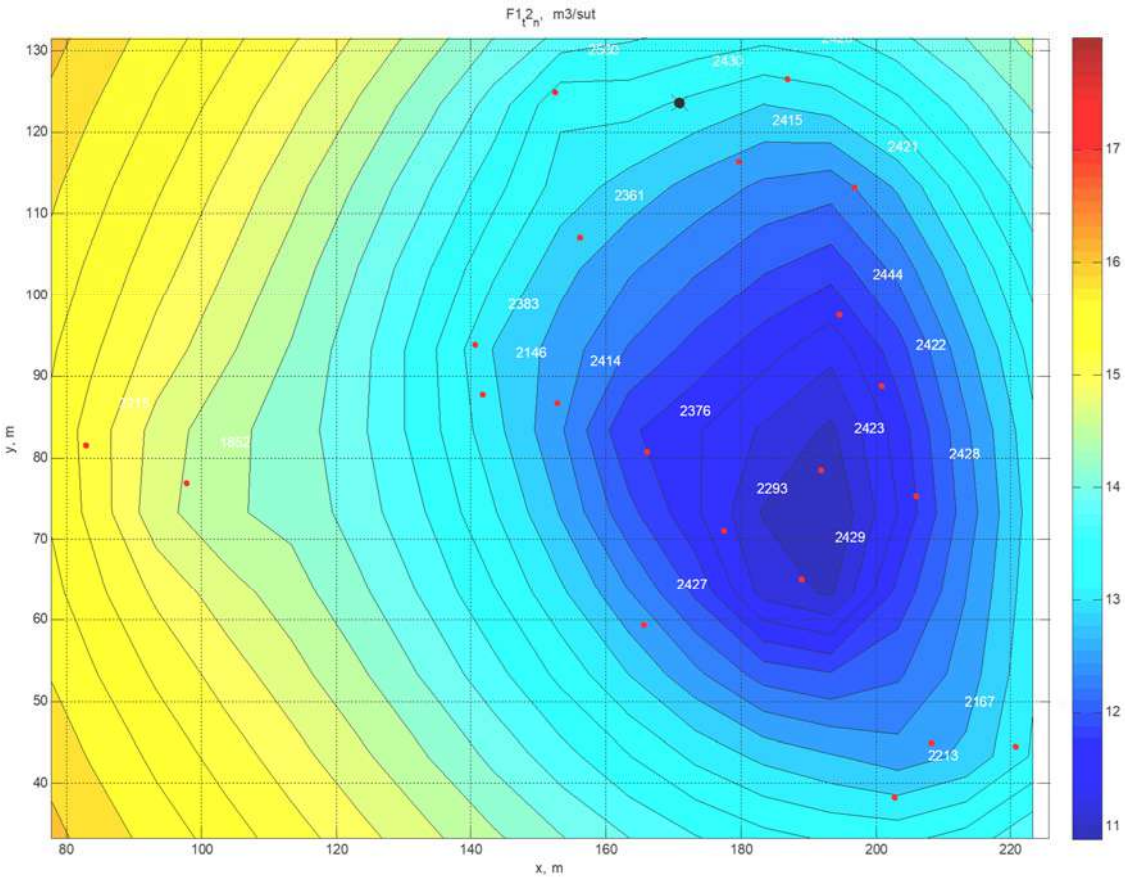

Fig. 3. Distribution of streamlines in oil $F_{1n}{}^{t}{}_{2}$ at time t_2.

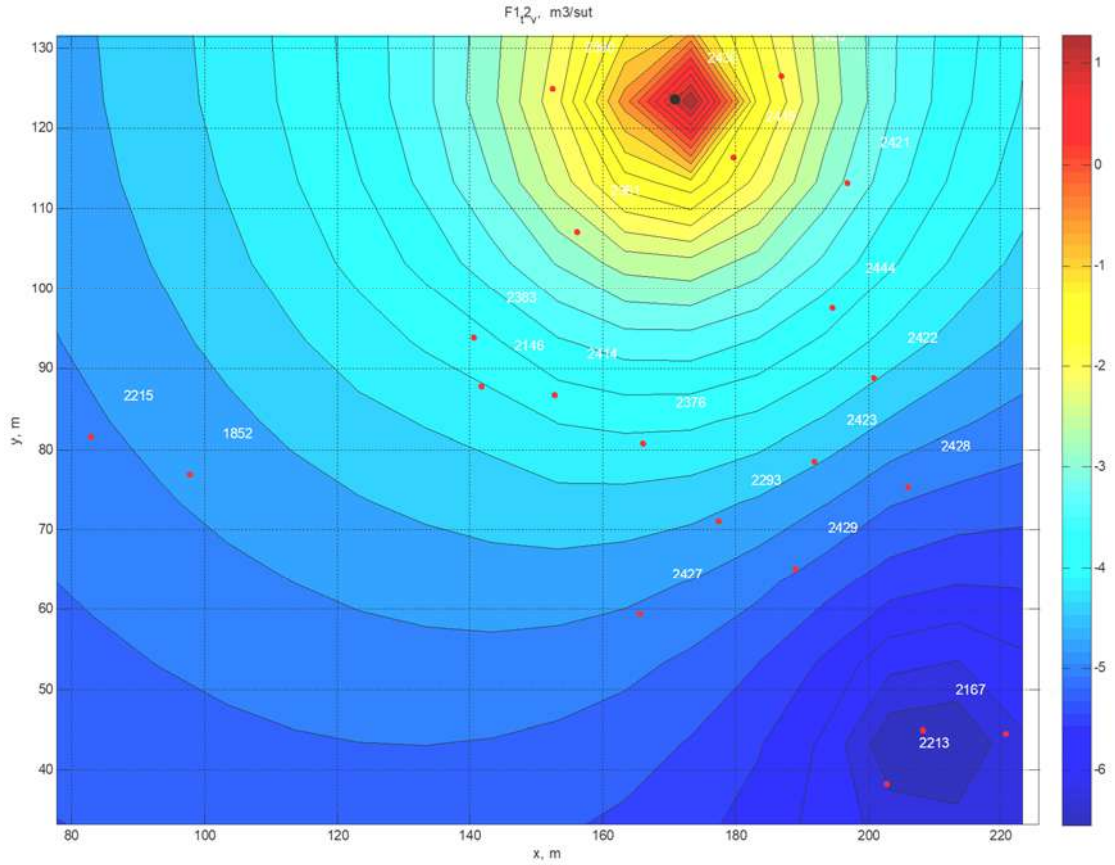

Fig. 4. Distribution of streamlines in water $F_{1v}{}^{t}{}_{2}$ at time t_2

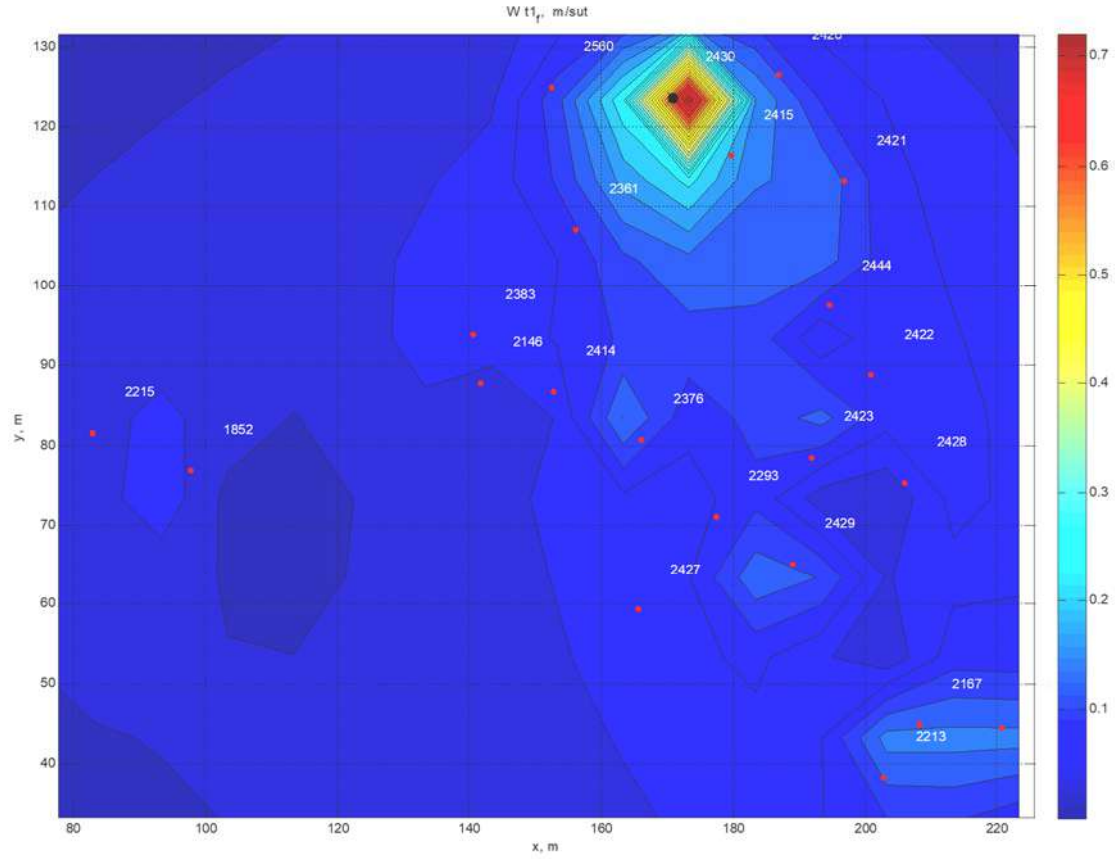

Fig. 5. Distribution of flow velocity $W_f{}^{t}{}_{1}$ of formation fluid at time t_1

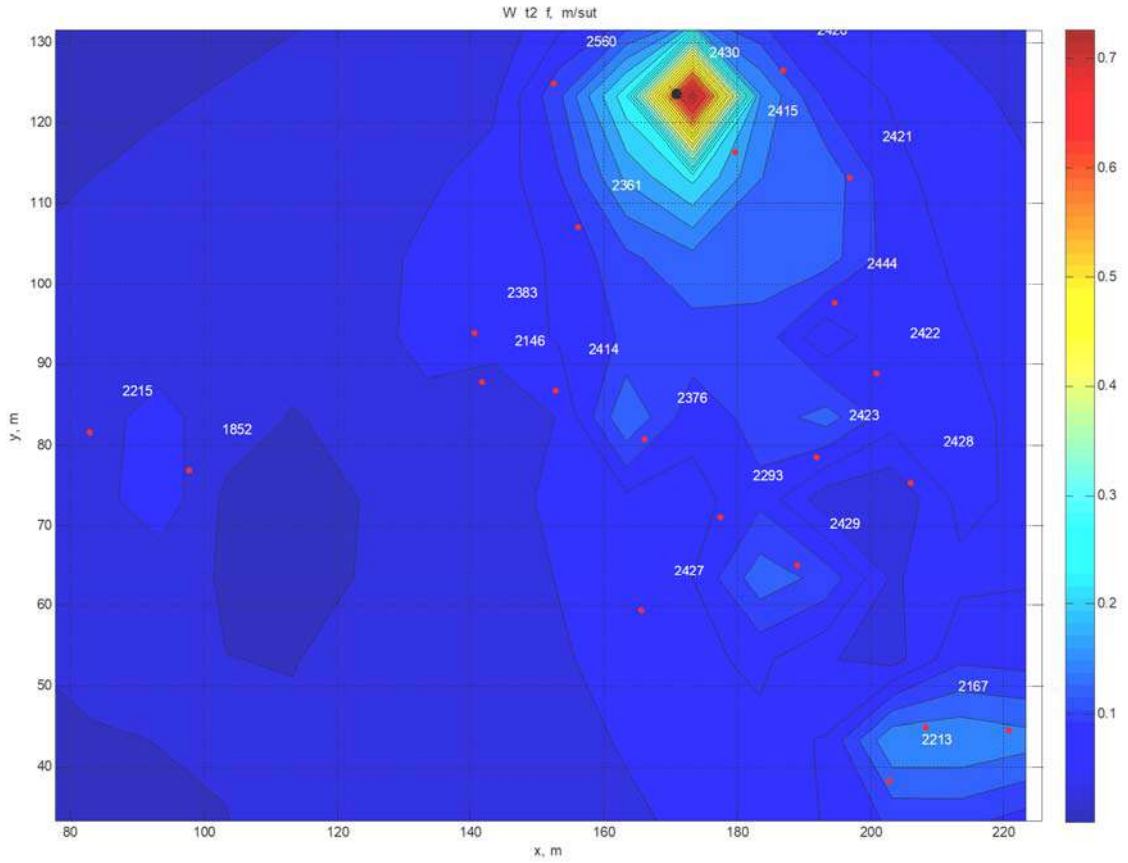

Fig. 6. Distribution of formation fluid flow velocity W^{n}_{2} at time t_2

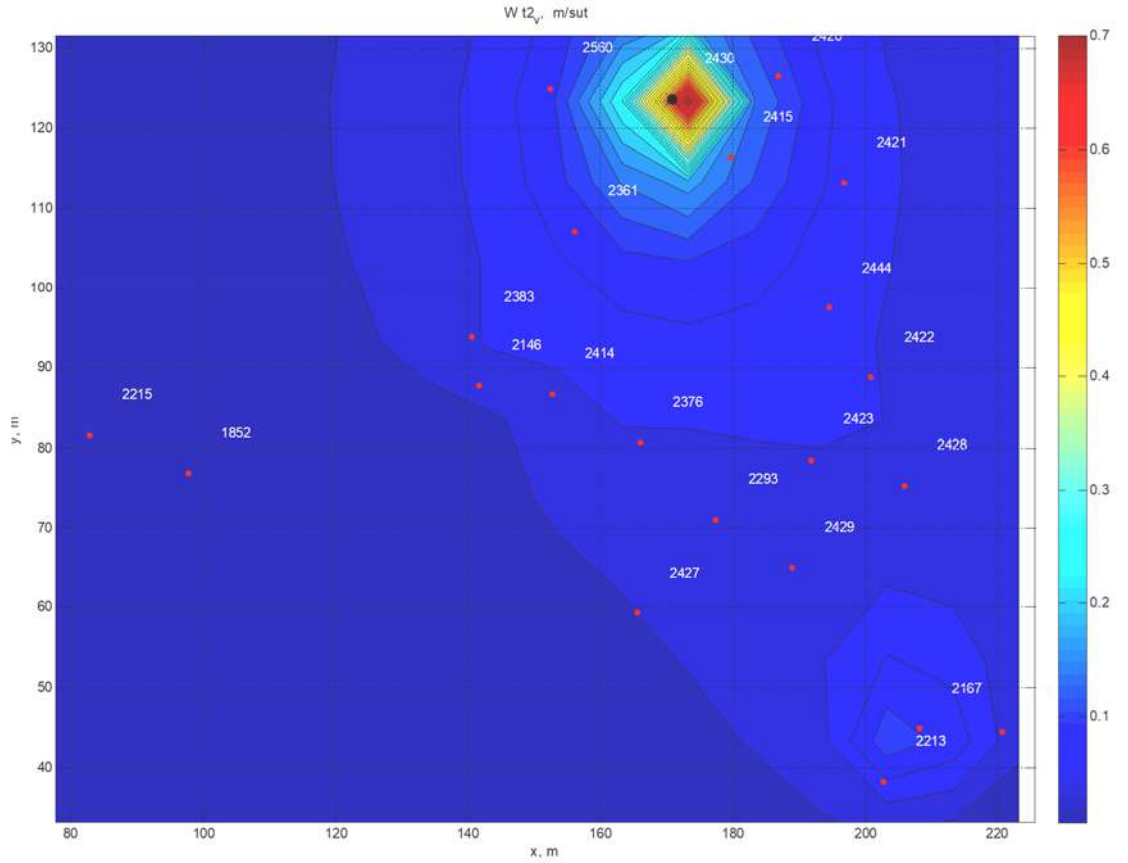

Fig. 7. Distribution of water flow velocity W^{n}_{2} at time t_2

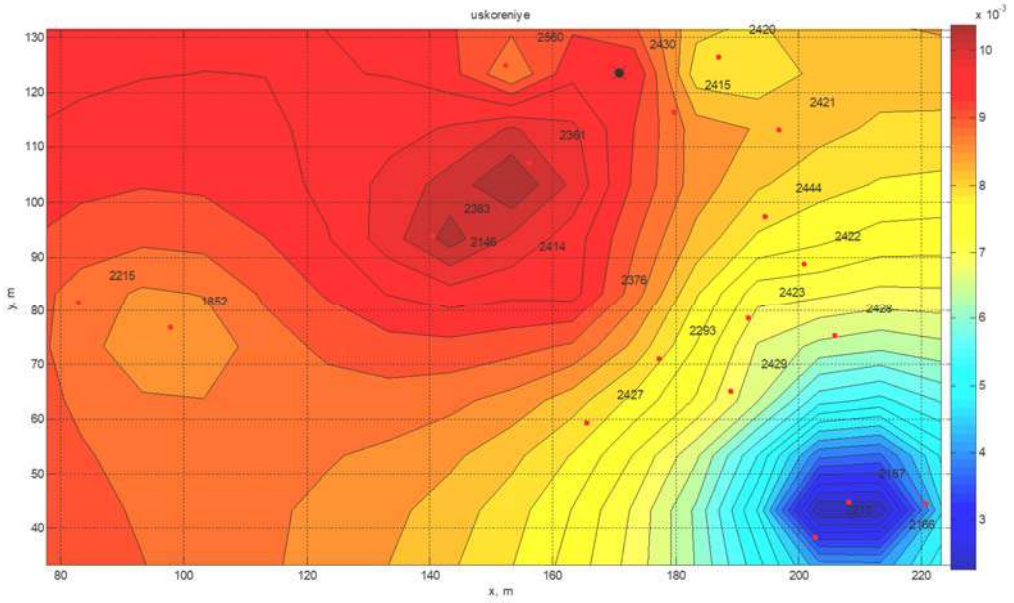

Fig. 8. Distribution of acceleration ***a*** in the reservoir fluid at time t_1

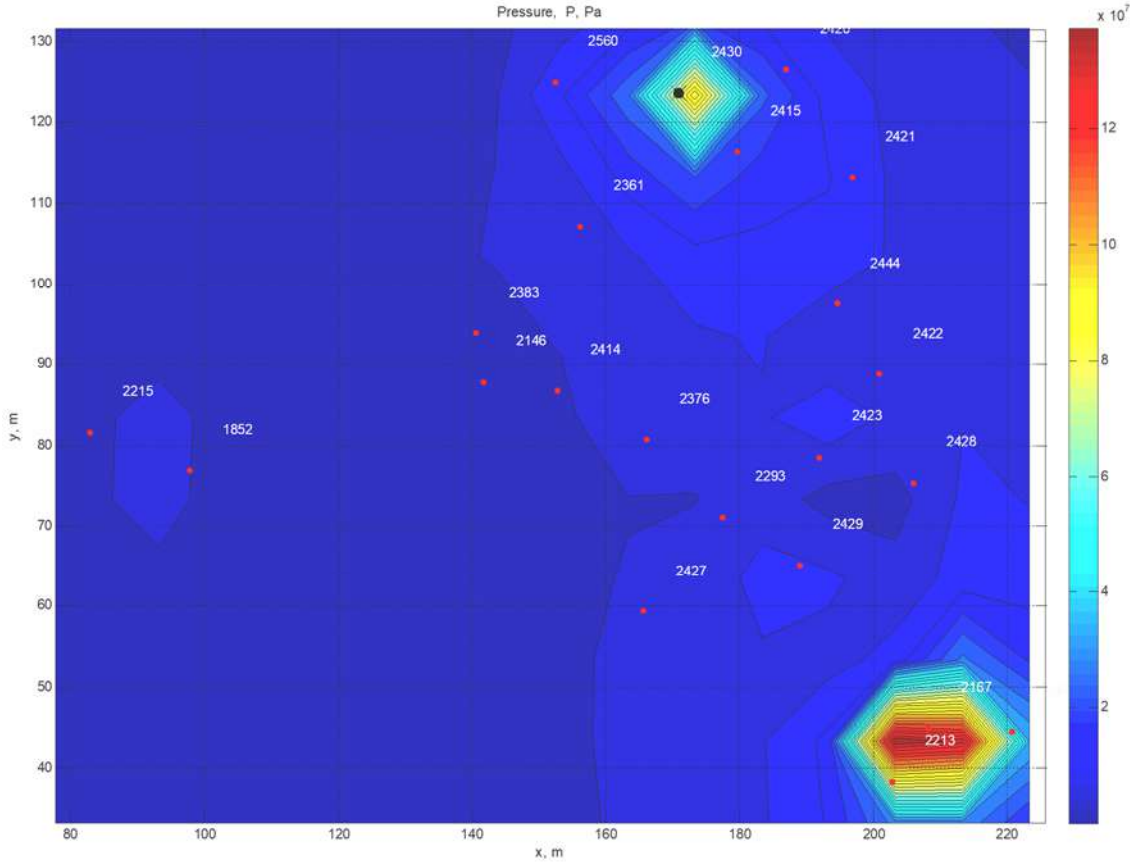

Fig. 9. Distribution of current reservoir pressure P at time t_2

Conclusion

1. An AI approach for rapid assessment of the distribution of current reservoir pressure based on oil production data is presented. The method is based on an algorithm that includes calculation of the current distribution of values of current functions, potentials, and flow velocity in a selected area;

2. In order to automate the calculations and visualize the obtained results, a special software module has been created on the basis of the "Matlab" engineering and scientific computing system package, which provides the facilities to calculate and visualize the pressure distribution in the area under study at the current time in accordance with the proposed algorithm;

3. The approach allows to monitor the current distribution of the current reservoir pressure of the productive reservoir in the area under consideration, as well as to evaluate the effectiveness of the impact on the reservoir to maintain the reservoir pressure;

4. The application of the proposed method to the data of the "Oil Rocks" field (horizon X, block V) as an example showed the high accuracy of the calculations. The average relative error of the calculated values of the reservoir pressure to the actual values of the bottomhole pressure measurements in the wells is not more than 1%, and the average calculated value of the reservoir pressure in the productive formation in the study area coincides with its actual reduced value.

REFERENCES

Choubey S., Karmakar G.P. Artifcial intelligence techniques and their application in oil and gas industry. Artifcial Intelligence Review, No. 54, 2021, pp. 3665-3683, https://link.springer.com/article/10.1007/s10462-020-09935-1.

Dmitrievsky A.N., Eremin N.A., Safarova E.A., Filippova D.S., Borozdin S.O. Qualitative analysis of time series GeoData to prevent complications and emergencies during drilling of oil and gas wells. SOCAR Proceedings, No. 3, 2020, pp. 31-37, http: //dx.doi.org/10.5510/OGP20200300442 (in Russian).

Dmitrievsky A.N., Eremin N.A., Safarova E.A., Stolyarov V.E. Implementation of complex scientific and technical programs at the late stages of operation of oil and gas fields. SOCAR Proceedings, SI2, 2022, pp. 1-8, DOI: 10.5510/OGP2022SI200728 (in Russian).

Gupta D., Shah M. A comprehensive study on artificial intelligence in oil and gas sector. Environ. Sci. Pollut. Res., Vol. 29(34), 2022, pp. 50984-50997, DOI: 10.1007/s11356-021-15379-z.

Hung N.T., Hoa N.M., Duong V.H. Predicting production flow rates using artificial neural network – HST field case. SOCAR Proceedings, No. 4, 2023, pp. 65-71, https://proceedings. socar.az/ru/journal/98#:~:text=DOI%3A%2010.5510/OGP20230400916.

Ibrahimov Kh.M., Huseynova N.I., Hajiyev A.A. Development of new controlling methods for the impact on the productive formation for «Neft Dashlary» oilfield. Scientific Petroleum, No. 1, 2021, pp. 37-42, DOI:10.53404/Sci.Petro.20210100005 (in Russian).

Jamalbayov M.A., Ibrahimov Kh. M. New waterflooding efficiency evaluation method (on the example of 9th horizon of the Guneshli field). Scientific Petroleum, No. 1, 2023, pp. 43-47, DOI:10.53404/Sci. Petro.20230100039.

Jamalbayov M.A., Ibrahimov Kh.M., Alizadeh N.A. Mathematical model of the hydrocarbon displacement process by water in zonally heterogeneous deformable reservoirs. Scientific Petroleum, No. 2, 2023, pp. 48-56.

Khan M.R., Tariq Z., Abdulraheem A. Application of artificial intelligence to estimate oil flow rate in gas-lift wells. Nat .Resour. Res., 29, 2020, pp. 4017-4029, DOI:10.1007/s11053-020-09675-7.

Koroteeva D., Tekic Z. Artificial intelligence in oil and gas upstream: Trends, challenges, and scenarios for the future. Energy and AI, Vol. 3, 2021, p. 100041, DOI:10.1016/j.egyai. 2020.100041.

Latifov Y.A. Non-stationary effect of thermoactive polymer composition for deep leveling of filtration profile. Scientific Petroleum, No. 1, 2021, pp. 25-30, https://doi.org/10.53404/Sci. Petro.20210100003 (in Russian).

Li H., Yu H., Cao N. et al. Applications of artificial intelligence in oil and gas development. Arch. Computat. Methods Eng., Vol. 28(1), 2021, pp. 937-949, https://doi.org/10.1007/s11831-020-09402-8.

Rasulov M.A., Jalalov G.I. Numerical method for studying the process of mass - heat transfer in deformable layers in a class of discontinuous functions. SOCAR Proceedings, No. 4, 2023, pp. 72-75.

Shilanbayev B.A., Ishangaliyev S.V., Zhetruov Zh.T., Shayakhmet K.N., Koldei M. Development of intelligent system

ЛИТЕРАТУРА

Choubey S., Karmakar G.P. Artifcial intelligence techniques and their application in oil and gas industry. Artifcial Intelligence Review, No. 54, 2021, pp. 3665-3683, https://link.springer.com/article/10.1007/s10462-020-09935-1.

Gupta D., Shah M. A comprehensive study on artificial intelligence in oil and gas sector. Environ. Sci. Pollut. Res., Vol. 29(34), 2022, pp. 50984-50997, DOI: 10.1007/s11356-021-15379-z.

Hung N.T., Hoa N.M., Duong V.H. Predicting production flow rates using artificial neural network – HST field case. SOCAR Proceedings, No. 4, 2023, pp. 65-71, https://proceedings. socar.az/ru/journal/98#:~:text=DOI%3A%2010.5510/OGP20230400916.

Jamalbayov M.A., Ibrahimov Kh. M. New waterflooding efficiency evaluation method (on the example of 9th horizon of the Guneshli field). Scientific Petroleum, No. 1, 2023, pp. 43-47, DOI:10.53404/Sci. Petro.20230100039.

Khan M.R., Tariq Z., Abdulraheem A. Application of artificial intelligence to estimate oil flow rate in gas-lift wells. Nat .Resour. Res., 29, 2020, pp. 4017-4029, DOI:10.1007/s11053-020-09675-7.

Koroteeva D., Tekic Z. Artificial intelligence in oil and gas upstream: Trends, challenges, and scenarios for the future. Energy and AI, Vol. 3, 2021, p. 100041, DOI:10.1016/j.egyai. 2020.100041.

Li H., Yu H., Cao N. et al. Applications of artificial intelligence in oil and gas development. Arch. Computat. Methods Eng., Vol. 28(1), 2021, pp. 937-949, https://doi.org/10.1007/s11831-020-09402-8.

Rasulov M.A., Jalalov G.I. Numerical method for studying the process of mass - heat transfer in deformable layers in a class of discontinuous functions. SOCAR Proceedings, No. 4, 2023, pp. 72-75.

Suleimanov B.A., Veliyev E., Vishnyakov V. Nanocolloids for petroleum engineering: Fundamentals and practices. John Wiley & Sons. 2022, 288 p., DOI:10.1002/9781119889762.

Weiss W.W., Balch R.S., Stubbs B.A. How artificial intelligence methods can forecast oil production. Paper presented at the SPE/DOE Improved Oil Recovery Symposium, Tulsa, Oklahoma, April 2002, https:|//doi.org/10.2118/75143-MS.

Велиев Э.Ф. Применение смягченной воды для улучшения эффективности мицеллярного заводнения. Scientific Petroleum, No. 2, 2021, с. 52-56, DOI:10.53404/Sci.Petro.0210200016.

Велиев Э.Ф., Алиев А.А., Маммедбейли Т.Е. Применение машинного обучения для прогнозирования эффективности внедрения технологий борьбы с конусообразованием. SOCAR Proceedings, No. 1, 2021, с. 104-113, DOI: 10.5510/OGP20210100487.

Велиев Э.Ф., Ширинов Ш.В., Маммедбейли Т.М. Интеллектуальное нефтегазовое месторождение на основе технологий искусственного интеллекта. SOCAR Proceedings, No. 4, 2022, с. 70-75, DOI: 10.5510/OGP20220400785.

Джамалбеков М.А., Ибрагимов Х.М., Ализаде Н.А. Математическая модель процесса вытеснения углеводородных смесей водой в зонально-неоднородных деформируемых пластах. Scientific Petroleum, No. 2, 2023, pp. 48-56, https://doi.org/10.53404/Sci.Petro.20230200048.

operational maintenance of the level of oil and gas production and waterflooding management. SOCAR Proceedings, SI1, 2023, pp. 6-18, DOI: 10.5510/OGP2023SI100824 (in Russian).

Suleimanov B.A., Guseinova N.I. Visualization of reservoir fluid filtration characteristics distribution, as a method of oil field development management. SOCAR Proceedings, SI1, 2023a, pp. 35-45, http://dx.doi.org/10.5510/OGP2023SI100821 (in Russian).

Suleimanov B.A., Huseynova N.I. Method for operative estimation of current reservoir pressure distribution based on the wells normal production data. SOCAR Proceedings, SI2, 2023б, pp. 12-19, 12-19, http://dx.doi.org/10.5510/OGP2023SI200876 (in Russian).

Suleimanov B.A., Latifov Ya.A., Ibrahimov Kh.M., Guseinova N.I. Field testing results of enhanced oil recovery technologies using thermoactive polymer compositions. SOCAR Proceedings, No. 3, 2017, pp. 17-31, DOI: 10.5510/OGP20170300320 (in Russian).

Suleimanov B.A., Veliyev E., Vishnyakov V. Nanocolloids for petroleum engineering: Fundamentals and practices. John Wiley & Sons. 2022, 288 p. DOI:10.1002/9781119889762.

Veliyev E.F. Softened water application to improve micellar flooding performance. Scientific Petroleum, No. 2, 2021, pp. 52-56, DOI:10.53404/Sci.Petro.0210200016 (in Russian).

Veliyev E.F., Aliyev A.A., Mammadbayli T.E. Machine learning application to predict the efficiency of water coning prevention techniques implementation. SOCAR Proceedings, No. 1, 2021, pp. 104-113, DOI: 10.5510/OGP20210100487 (in Russian).

Veliyev E.F., Shirinov S.V., Mammedbeyli T.E. Intelligent oil and gas field based on artificial intelligence technology. SOCAR Proceedings, No. 4, 2022, pp. 70-75, DOI: 10.5510/OGP20220400785 (in Russian).

Weiss W.W., Balch R.S., Stubbs B.A. How artificial intelligence methods can forecast oil production. Paper presented at the SPE/DOE Improved Oil Recovery Symposium, Tulsa, Oklahoma, April 2002, https:|//doi.org/10.2118/75143-MS.

Дмитриевский А.Н., Еремин Н.А., Сафарова Е.А., Столяров В. Е. Внедрение комплексных научно-технических программ на поздних стадиях эксплуатации нефтегазовых месторождений. SOCAR Proceedings, Спец. вып. 2, 2022, с. 1-8, DOI: 10.5510/OGP2022SI200728.

Дмитриевский А.Н., Еремин Н.А., Сафарова Е.А., Филиппова Д.С., Бороздин С.О. Качественный анализ геоданных временного ряда для предупреждения осложнений и аварийных ситуаций при бурении нефтяных и газовых скважин. SOCAR Proceedings, No. 3, 2020, с. 31-37 http: //dx.doi.org/10.5510/OGP20200300442.

Ибрагимов Х.М., Гусейнова Н.И., Гаджиев А.А. Разработка новых методов контроля над воздействием на продуктивные пласты на примере месторождения "Нефт Дашлары." Scientific Petroleum, No. 1, 2021, с. 37-42, DOI:10.53404/Sci.Petro.20210100005.

Лятифов Я.А. Нестационарное воздействие термоактивной полимерной композицией для глубинного выравнивания профиля фильтрации. Scientific Petroleum, No. 1, 2021, с. 25-30, https://doi.org/10.53404/Sci.Petro.20210100003.

Сулейманов Б.А., Гусейнова Н.И. Визуализация распределения фильтрационных характеристик пластовой жидкости как способ контроля разработки нефтяных залежей. SOCAR Proceedings, спец. выпуск 1, 2023а, с. 27-37, http://dx.doi.org/10.5510/OGP2023SI100821.

Сулейманов Б.А., Лятифов Я.А., Ибрагимов Х.М., Гусейнова Н.И. О результатах промысловых испытаний технологии повышения нефтеотдачи пласта на основе применения термоактивной полимерной композиции. SOCAR Proceedings, No. 3, 2017, с. 17-31, DOI: 10.5510/OGP20170300320.

Сулейманов Б.А.,. Гусейнова Н.И. Метод оперативной оценки распределения текущего пластового давления по данным нормальной эксплуатации. SOCAR Proceedings, спец. вып. No. 2, 2023б, с. 12-19, http://dx.doi.org/10.5510/OGP2023SI200876.

Шиланбаев Б.А., Ишангалиев С.В., Жетруов Ж.Т., Шаяхмет К.Н., Колдей М. Разработка интеллектуальной системы оперативного поддержания уровня добычи нефти и газа и управление заводнением. SOCAR Proceedings, спец. номер 1, 2023, с. 6-18. DOI: 10.5510/OGP2023SI100824.

ОЦЕНКА РАСПРЕДЕЛЕНИЯ ТЕКУЩЕГО ПЛАСТОВОГО ДАВЛЕНИЯ ПО ДАННЫМ ДОБЫЧИ НЕФТИ С ПОМОЩЬЮ ИСКУССТВЕННОГО ИНТЕЛЛЕКТА (ИИ)

Сулейманов Б.А., Гусейнова Н.И.

Научно-исследовательский проектный институт ГНКАР НИПИ "Нефтегаз", Азербайджан

AZ1012, г. Баку, просп. Зардаби, 88А

Резюме. На любом этапе разработки месторождений нефти и газа распределение пластового давления в продуктивных пластах является важной энергетической характеристикой пласта как в целом, так и на отдельных его участках. В данной статье рассматривается экспресс-метод оценки распределения текущего пластового давления на основе данных, полученных при разработке и эксплуатации нефтяных месторождений. Предлагаемая методика основана на алгоритме, включающем последовательный расчет и визуализацию текущего распределения значений таких гидродинамических показателей как функции тока, потенциалов, скорость потока, а также их градиентов на выделенном участке месторождения. Метод позволяет отслеживать фактическое распределение текущего пластового давления в продуктивном горизонте на рассматриваемой территории и оценивать эффективность воздействия на пласт, направленное на поддержание давления.

Разработанный подход также открывает широкие возможности для создания технологий искусственного интеллекта, для использования при анализе данных добычи нефти и газа, а также для машинного обучения при прогнозировании изменения пластового давления. Использование нейронных сетей при интеграции различных данных геологического, геофизического эксплуатационного характера и управлении операционными рисками позволяет создавать автоматические экспертные системы для оптимизации процессов разработки и эксплуатации месторождений нефти и газа.

Реализация предлагаемого подхода, проведенная на примере данных месторождения «Нефтяные Камни» (Горизонт X, Блок V), показала высокую точность расчетных значений пластового давления. Сравнительный анализ средней относительной погрешности расчетных значений пластового давления с фактическими значениями замеров забойного давления в скважинах составляет не более 1%, а среднее расчетное значение пластового давления в продуктивных пластах на исследуемой площади соответствует его фактическому значению.

Ключевые слова: *месторождение, пластовое давление, повышение нефтеотдачи пластов, зональное воздействие, продуктивный горизонт, продуктивность скважины, диагностика, фильтрация, мониторинг, линии тока*

SÜNİ İNTELLEKT VASİTƏSİLƏ NEFTİN ÇIXARILMASI MƏLUMATLARI ƏSASINDA CARİ LAY TƏZYİQİNİN PAYLANMASININ QİYMƏTLƏNDİRİLMƏSİ

Süleymanov B.A., Hüseynova N.İ.
Neft Qaz Elmi-Tədqiqat Layihə İnstitutu, SOCAR, Azərbaycan
AZ1012, Bakı, Həsən Bəy Zərdabi prosp., 88A

Xülasə. Neft və qaz yataqlarının işlənməsinin istismar mərhələsində məhsuldar layda və onun müəyyən hissəsində lay təzyiqinin paylanması neftvermənin artırılması məsələlərin həllində mühüm xarakteristikaların biridir. Bu məqalədə neft yataqlarının işlənməsi və istismarı zamanı əldə edilmiş məlumatlar əsasında layda cari təzyiqin paylanmasının qiymətləndirilməsinin ekspress metodu təklif edilir. İşlənmiş metodologiya, məhsuldar layın seçilmiş sahəsində axın və potensial funksiyaları, axın sürəti və onların qradiyentləri kimi hidrodinamik göstəricilərin lay üzrə cari paylanmasının hesablanması və vizuallaşdırılmasını aparmaq üçün işlənmiş alqoritmə əsaslanır. Metod cari lay təzyiqinin faktiki paylanmasını izləməyə və lay təzyiqin müəyyən səviyyədə saxlamaq üçün lazımı təsir tətbirlərin seçilməsi və bu təsirin effektivliyini qiymətləndirməyə imkan verir.

Təklif edilmiş yanaşma həmçinin neft və qaz hasilatı məlumatlarının təhlilində istifadə üçün, eləcə də lay təzyiqində dəyişikliklərin proqnozlaşdırılmasında, süni intellekt texnologiyalarının yaradılması üçün geniş imkanlar açır. Müxtəlif geoloji və geofiziki əməliyyat məlumatlarının inteqrasiyasında və əməliyyat risklərinin idarə edilməsində neyroşəbəkələrdən istifadə, neft və qaz yataqlarının işlənməsi və istismarı proseslərinin optimallaşdırılması üçün avtomatik ekspert sistemlərinin yaradılmasına imkan verir. Nümunə kimi, "Neft Daşları" yatağından (horizon X, blok V) məlumatlardan istifadə etməklə təklif olunan yanaşmanın həyata keçirilməsi lay təzyiqinin hesablanmış qiymətlərinin yüksək dəqiqliyini göstərdi. Quyularda lay təzyiqinin hesablanmış qiymətlərinin orta nisbi səhvinin quyudibi təzyiqinin ölçülmələrinin faktiki qiymətləri ilə müqayisəli təhlili 1%-dən çox deyil. Məhsuldar laylarda lay təzyiqinin orta hesablanmış qiyməti onun faktiki qiyməti ilə üst-üstə düşür.

Açar sözlər: *yataq, lay təzyiqi, neft veriminin artırılması, zonal təsir, məhsuldar lay, quyu məhsuldarlığı, diaqnostika, süzülmə, monitorinq, axin xətləri*

ANAS Transactions **Earth Sciences** **1 / 2024**

http://www.journalesgia.com

РАЗРАБОТКА ПЕТРОФИЗИЧЕСКОГО МОДЕЛИРОВАНИЯ НА ОСНОВЕ ЭФФЕКТИВНОЙ ПОРИСТОСТИ И ФАЗОВЫХ ПРОНИЦАЕМОСТЕЙ КОЛЛЕКТОРОВ (НА ПРИМЕРЕ БИНАГАДИНСКОГО МЕСТОРОЖДЕНИЯ)

Пашаев Н.В.

Азербайджанский Государственный Университет Нефти и Промышленности, Азербайджан

AZ1010, Баку, просп. Азадлыг, 34: namat.pashayev@mail.ru

DEVELOPMENT OF PETROPHYSICAL MODELING BASED ON EFFECTIVE POROSITY AND PHASE PERMEABILITIES OF RESERVOIRS (BINAGADI OIL FIELD AS A CASE STUDY)

Pashayev N.V.

Azerbaijan State Oil and Industry University, Azerbaijan

34, Azadlig ave., Baku, AZ1010: namat.pashayev@mail.ru

Keywords: *logging, well, porosity, permeability, electrical resistivity*

Summary. The paper presents the results of studying the change in the oil saturation and porosity coefficients of the productive strata of the Underkirmaki suite (UKS) of the Binagadi field one hundred and ten years after the start of its development. Considering that practical methods for quantifying the current oil saturation factor in cased wells have not yet been developed, in the determinations, logging data and core data were mainly used for wells during their operation. Based on new data from correlated well sections the dependence of K_{per} on K_p was plotted for all reservoir intervals identified in the well sections. It has been established that there are no initial contours of oil content in the study area. To assess the influence of lithological features on the porosity and permeability properties of reservoirs, paired dependencies between K_{per} and K_p for the studied horizon were established. The resulting dependence is characterized by a high closeness of the relationship (R=0.85). In order to study the spatial distribution of reservoirs over the area (wells), as well as porosity, permeability and oil saturation, three-dimensional grids of the geomodel were created. As a result, a practical use of a petrophysical model is shown, the effectiveness of which lies in the fact that it is comparable with well log data, which makes it possible to dissect intervals where there are no well logs with great certainty.

Введение

Актуальность проблемы. Перспективы увеличения нефтедобычи в Республике связаны с разработкой залежей в море и суше, а также с повышением эффективности доразработки эксплуатируемых в настоящее время месторождений нефти и газа, находящихся в различной стадии их освоения. Характерный особенностью разработки нефтяных месторождений является то, что этот процесс происходит в большинстве случаев в условиях некомпенсированного отбора углеводородов. Важно учитывать указанный процесс при оценке начальных и текущих запасов нефти и газа, геомоделировании разрабатываемого объекта и анализа разработки на различных ее этапах.

Изучению этого вопроса посвящены многочисленные исследования, из которых можно отметить работы М.Т.Абасова (2007), Л.А.Буряковского (1990), Р.Ю.Алиярова (2010), Р.А.Рамазанова (2011) и др.

Это задача имеет особое значение для отложений продуктивный толщи (ПТ) месторождения Бинагади. Месторождение Бинагади как уникальная нефтеносная залежь расположено на Абшеронском полуострове и более 110 лет находится в эксплуатации. Углеводороды (УВ) добывают из отложений ПТ. Основным объектом разработки в разрезе ПТ является подкирмакинская свита (ПК), содержащая более 34% геологического балансового запаса УВ.

Литологическая характеристика месторождения довольно разнообразна. Пласты песчаников средних, мелко и тонкозернистых, иногда слабоцементированных, мощностью в основном 5-8 м переслаиваются с глинами темно-серыми,

плотными, а также песчанистыми, карбонатными. Пачки часто чередующихся пластов песчаников и глин расчленены мощными глинистыми разделами (Пашаев и др., 2017).

Методика и результаты

С целью уточнения процесса разработки в свете новых геолого-промысловых и геофизических данных для определения характера насыщения коллекторов и остаточной нефтенасыщенности в стволе действующих и нагнетательных скважин проводился определенный объем исследований петрофизическими, промыслово-геофизическими и гидродинамическими методами. Во время изучения данного вопроса были использованы материалы геофизических исследований скважин (ГИС), геолого-промысловая информация по скважинам, накопленная в период эксплуатации, а также керновые данные, охватывающие все отложения свиты ПК.

Корреляция разрезов скважин по данным ГИС

Изучение геологического строения залежей начинается с корреляции разрезов скважин.

Детальная корреляция необходима для выделения одноименных пластов или пачек внутри зоны или свиты, что имеет первостепенное значение при рациональной разработке месторождений. Продуктивные зоны месторождения Бинагади сложены пропластками, весьма изменчивыми по разрезу и площади месторождения. Это достаточно наглядно подтверждается керновыми, геофизическими и гидродинамическими данными. Такая сложная картина строения продуктивных пластов сильно затрудняет корреляцию разрезов скважин. Фациальная неоднородность зон по разрезу и площади, являющаяся, вероятно, следствием локальных геологических причин, настолько сильна, что в значительной мере затушевывает существенные черты геологического строения, обусловленные явлениями региональными, более высокого порядка и, в первую очередь, ритмичностью процесса осадконакопления.

Таким образом, продуктивные отложения подкирмакинской свиты обычно четких и выдержанных реперов по площади не имеют. В разрезе продуктивных отложений на каротажных диаграммах можно выделить так называемые реперы местного значения, которые прослеживаются лишь по группам скважин (рис. 1).

На рис. 1а,б,с показаны схемы корреляции разрезов скважин по линии скв. 2812-2727-2841-2843-2840-2772-2854-2852. Корреляция проведена с использованием методов Гамма каротажа (ГК) и Индукционного каротажа (ИК). Линией выравнивания при корреляции разрезов скважин являлась кровля отложений свиты ПК (максимальное значение ГК). Представлены результаты интерпретации геофизических исследований этих скважин (коллектор-неколлектор).

Зеленым цветом отмечены интервалы разреза с коллекторами, серым – неколлекторами.

При этом предполагается, что один и тот же интервал в разрезах разных скважин примерно одинаково отражается на каротажных диаграммах, поскольку его состав и мощность остаются мало измененными.

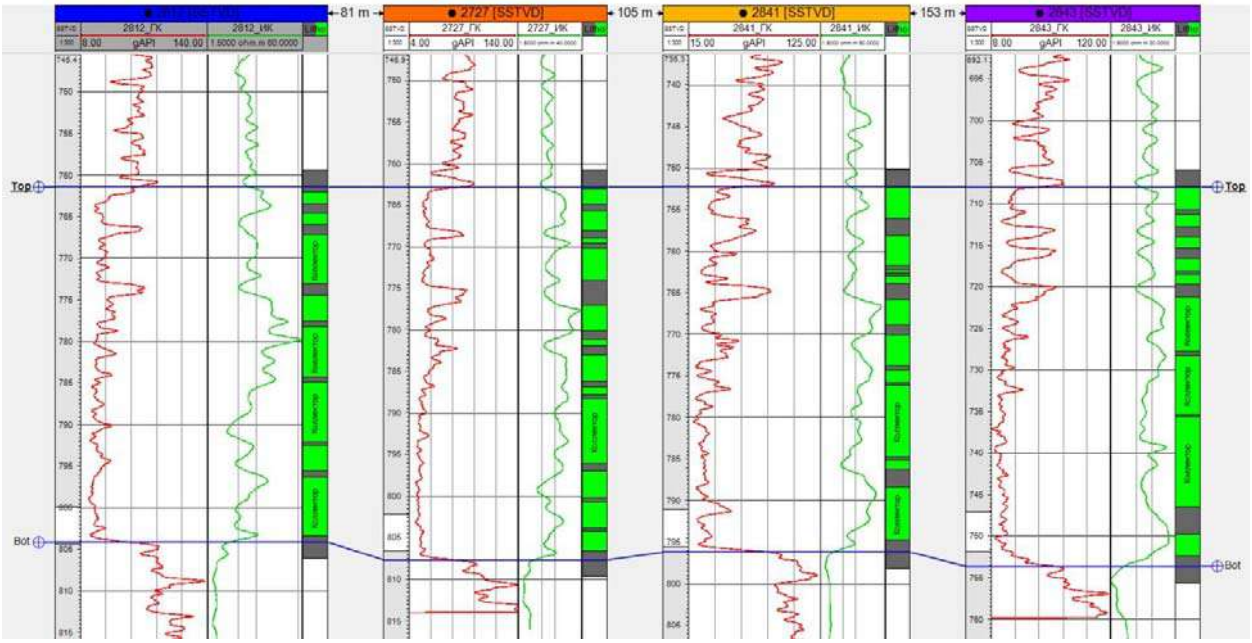

Рис. 1а. Схема корреляции скв. 2812-2727-2841-2843

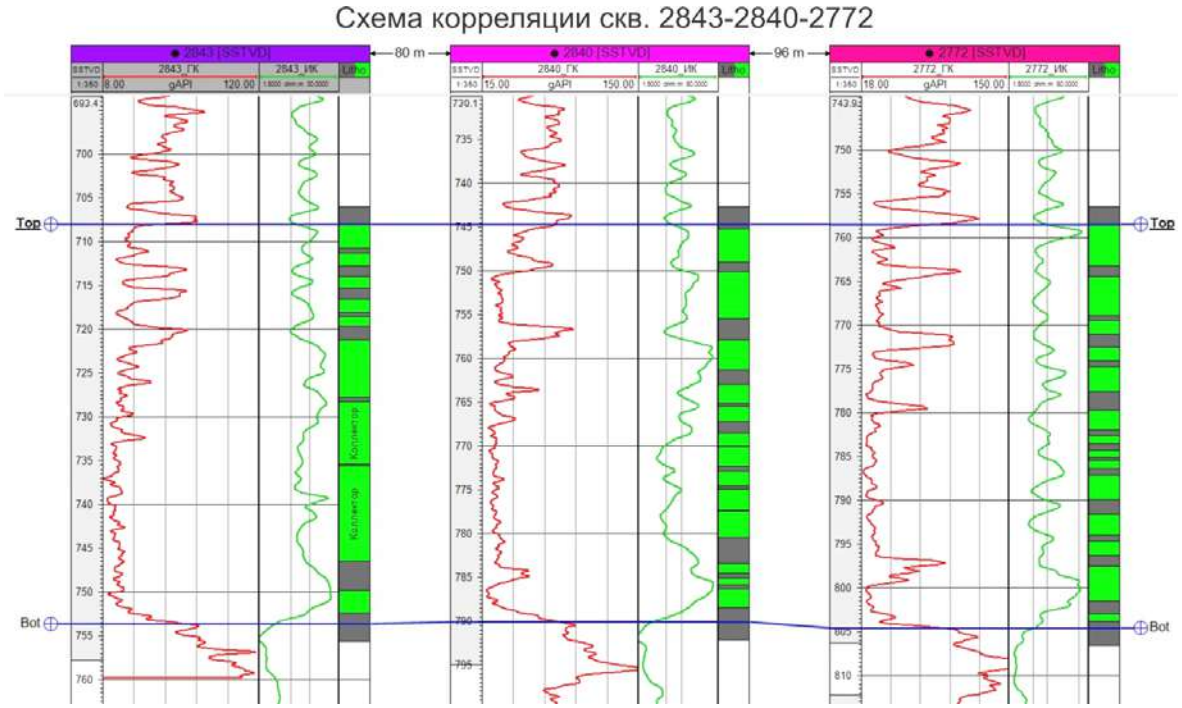

Рис. 1б. Схема корреляции скв. 2843-2840-2772

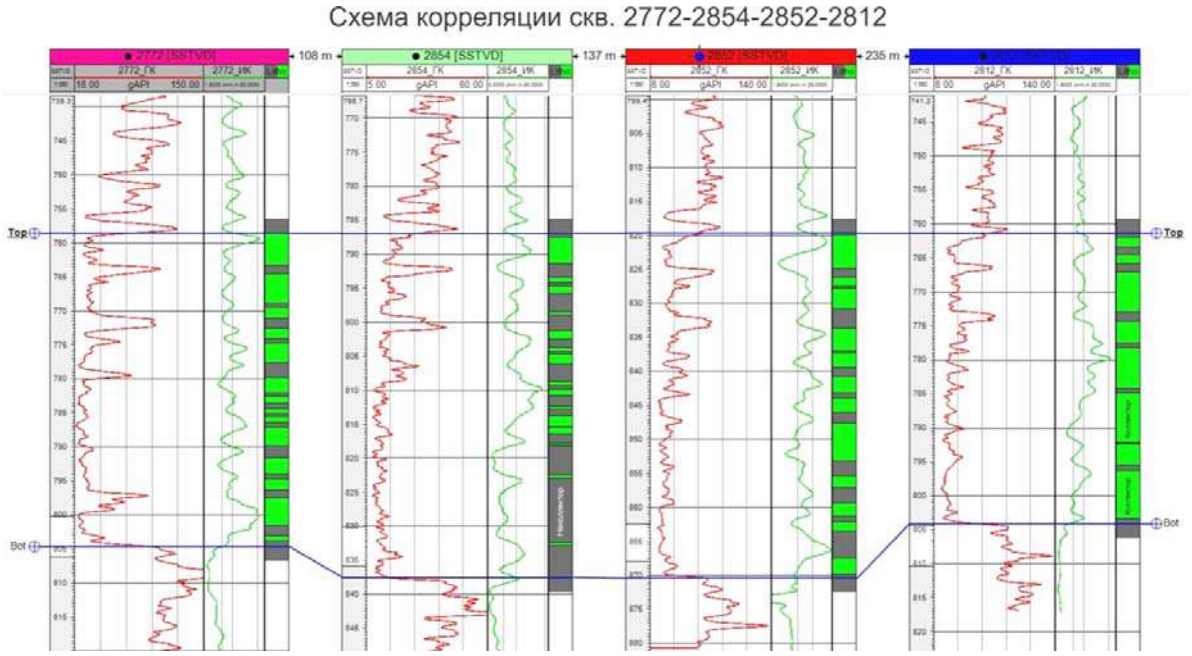

Рис. 1с. Схема корреляции скв. 2843-2840-2772

Рассматриваемые скважины пробурены в период 2008-2019 гг. К этому времени в отложения свиты ПК был закачен большой объем воды для поддержания пластового давления, что привело к значительному обводнению продукции.

Используя данные рис. 2, вычислены текущие нефтенасыщенности всех интервалов коллекторов, выделенных в разрезах исследуемых скважин.

Для определения текущих запасов нефти в отложениях свиты ПК в зоне исследований для необводненных интервалов разреза выявлена петрофизическая зависимость между пористостью и текущей нефтенасыщенностью (рис. 2).

Для оценки влияния литологических особенностей на основные параметры коллекторов – проницаемость и пористость установлены парные зависимости между коллекторскими свойствами пород свиты ПК Бинагадинского месторождения (рис. 3).

Корреляционные зависимости между проницаемостью ($К_{пр}$) и пористостью ($К_{п}$) были вве-

дены на основе комплексного исследования керна скважин данного месторождения.

Сопоставление величин $К_{пр}$ и $К_{п}$, приведенное на рис.3, показывает, что систематические расхождения в сопоставляемых параметрах отсутствуют, случайные же расхождения можно объяснить изменчивостью свойств пород по разрезу и залежи, а также различными выборками образцов. Распределение точек на корреляционном поле свидетельствует о том, что в пределах Бинагадинского нефтеносного района имеется единая закономерность в изменении фильтрационно-емкостных свойств пород.

Данные зависимости были использованы для изучения фильтрационно-емкостных свойств отложений свиты ПК (Зинченко, 2005; Mohammad, 2019).

Обоснование положения водонефтяного контакта (ВНК)

Зона исследований находится на площади блока 5b. Этот блок на месторождении Бинагади является изолированным и не имеет первоначального водонефтяного контакта. Поэтому все коллекторы, вскрытые пробуренными скважинами, первоначально были нефтенасыщенными.

На исследуемой площади нет начальных контуров нефтеносности.

Построение трехмерной сетки модели и контроль качества

После выполнения структурного моделирования создается трехмерная сетка модели, на которую переносятся данные каротажа скважин и построенные поверхности.

Эта сетка необходима для пространственного распределения коллекторов, а также таких параметров, как пористость и нефтенасыщенность.

Исходя из размеров изучаемой структуры, размер ячеек сетки (по горизонтали) составляет 50x50 м.

Вся мощность пласта разбивается на 3 зоны:

- зона 1 – кровля пласта - кровля коллекторов;
- зона 2 – кровля коллекторов - подошва коллекторов;
- зона 3 – подошва коллекторов - подошва пласта.

В зонах 1 и 3 выделен 1 слой (в каждой зоне), так как в этих зонах отсутствует коллекторы, и модель в этих зонах будет состоять из неколлекторов.

Разрез зоны 2 разделен на несколько слоев. Количество слоев выбиралось, исходя из минимальной толщины пропластка коллектора. В нашем случае это составляет 0.3 м. На основании схем корреляции разрезов скважин (рис. 1а,б,с) нарезка слоев производилась параллельно поверхности кровли свиты ПК с толщиной слоя, равной 0.2 м.

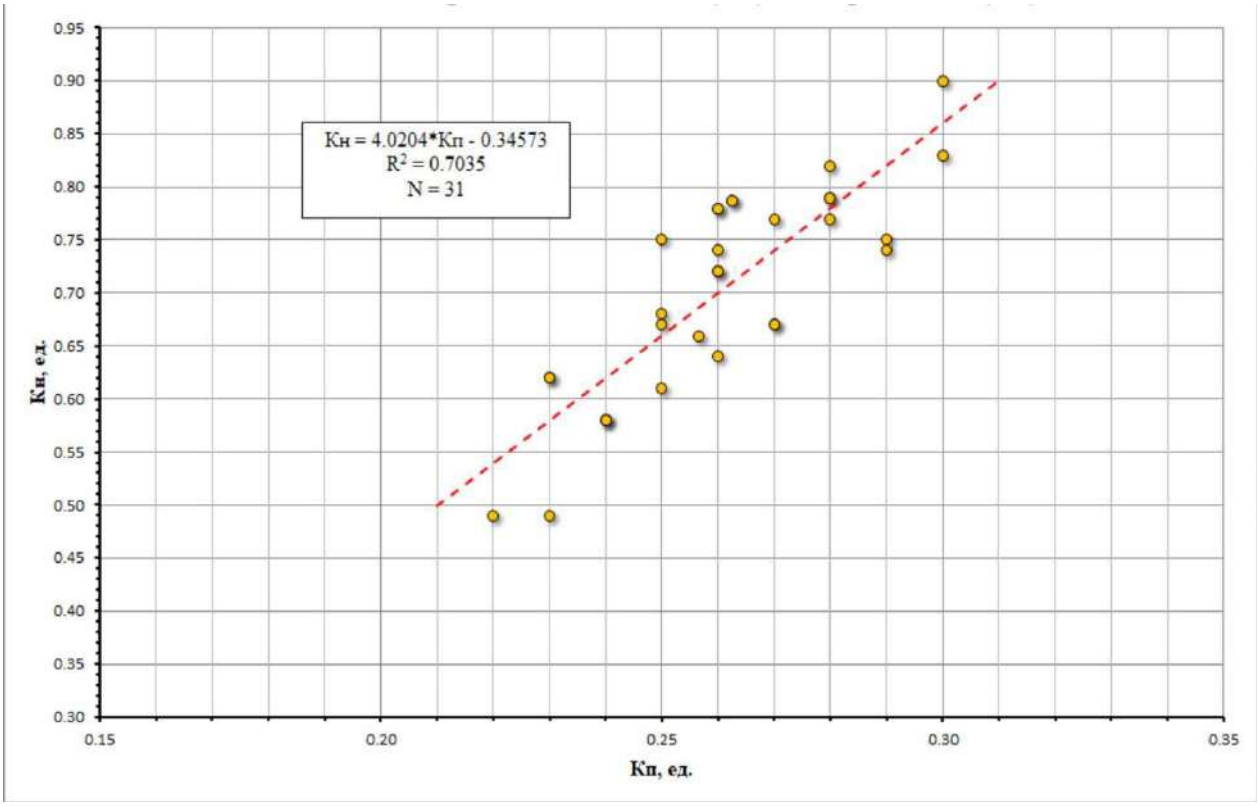

Рис. 2. Зависимость текущей нефтенасыщенности ($К_{н}$) от пористости ($К_{п}$)

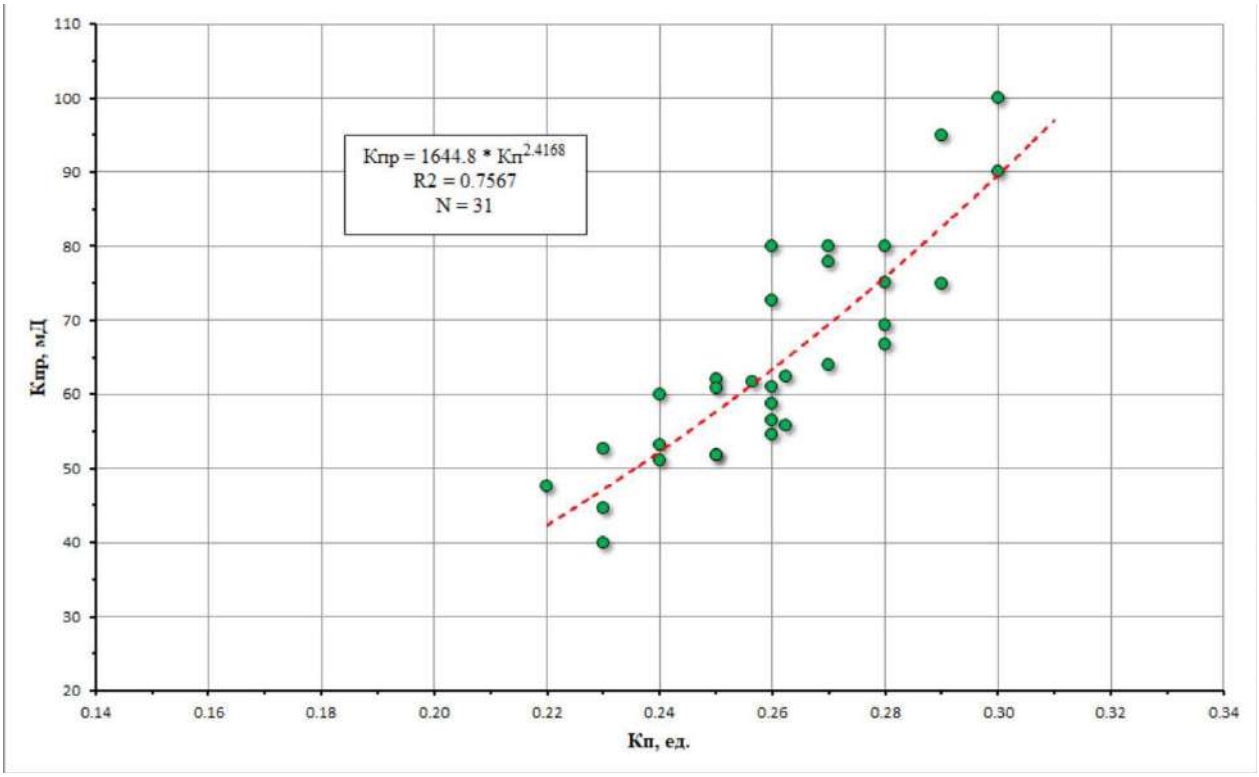

Рис. 3. Зависимость проницаемости ($К_{пр}$) от пористости ($К_{п}$)

Такой подход гарантирует, что вся информация по данным ГИС будет учтена в трехмерной модели.

На рис. 4 показано сопоставление данных ГИС и перемасштабированного каротажа на сетке модели. Видно, что каждый пропласток, выделенный по каротажу в разрезе скважин (левый столбец), отражен на перемасштабированном каротаже на сетке модели (правый столбец).

Параметры трехмерной сетки представлены в таблице.

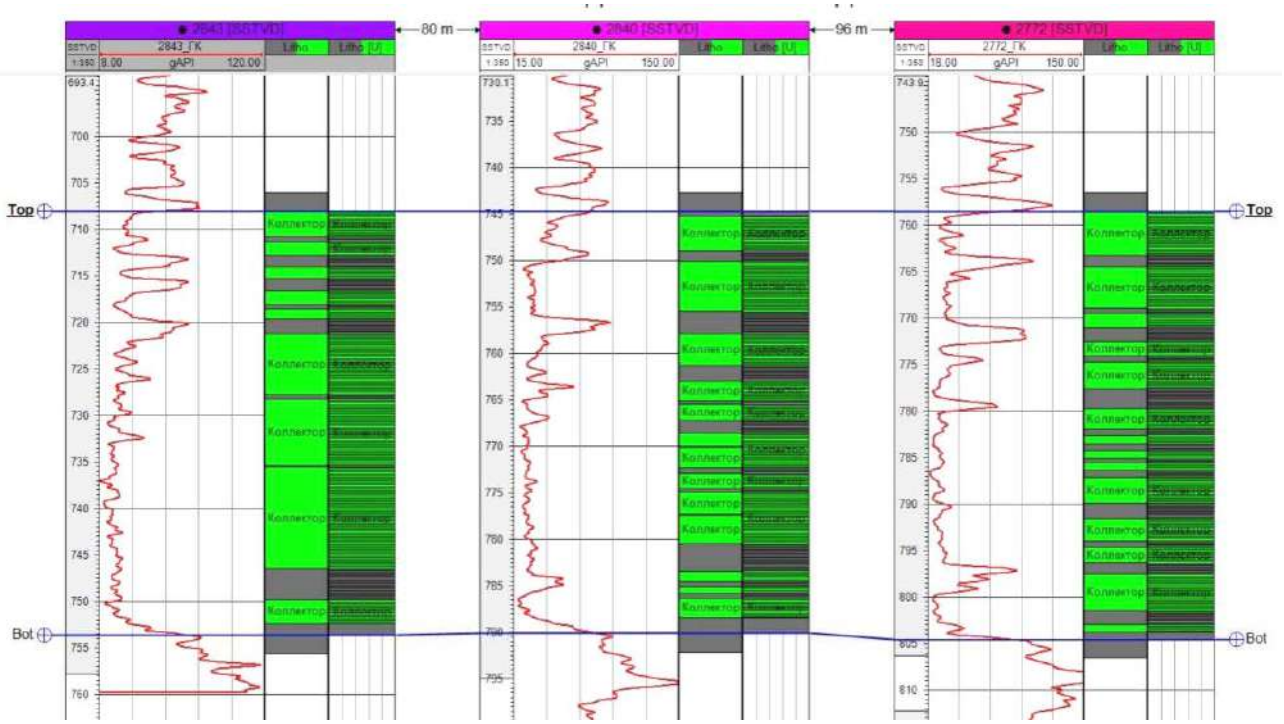

Рис. 4. Сопоставление данных ГИС и модели

Параметры трехмерной сетки

Количество зон	3
Количество ячеек	11568840
Количество слоев (Z)	255
Параметры 3D сетки (ячейки сетки)	214x212x255 (nIxnJxnGridLaers)
Размер ячейки (мм)	2x2

Петрофизическое моделирование

При использовании стохастического метода можно добиться, чтобы распространяемый параметр (в нашем случае "Литология") имел в объеме модели такое же распределение, как и в скважине. В связи с этим на рис. 5 представлен геологический профиль, построенный с использованием стохастического распределения (SIS - Sequential Indicator Simulation), а на рис. 6 – гистограмма сопоставления свойства "Литология" для данных ГИС в скважине, перемасштабированного каротажа и для модели (Гасанов и др., 2008).

Из рис. 6 видно, что у модели доли коллекторов (66.8%) и неколлекторов (33.2%) примерно соответствуют соотношениям по данным ГИС (67.0% и 33.0%).

Петрофизическое моделирование происходит посредством переноса данных ГИС, таких как пористость и нефтенасыщенность, с разрезов скважин на сетку модели и распространение этих данных по площади и по объему (Абасов и др., 2007; Гутман, 2017; Коваленко, 2015).

Петрофизическое моделирование проводилось стохастическим методом Sequential Gaussian Simulation (SGS) с учетом свойства "Литология".

Распределение свойства "Пористость" представлено на рис. 7.

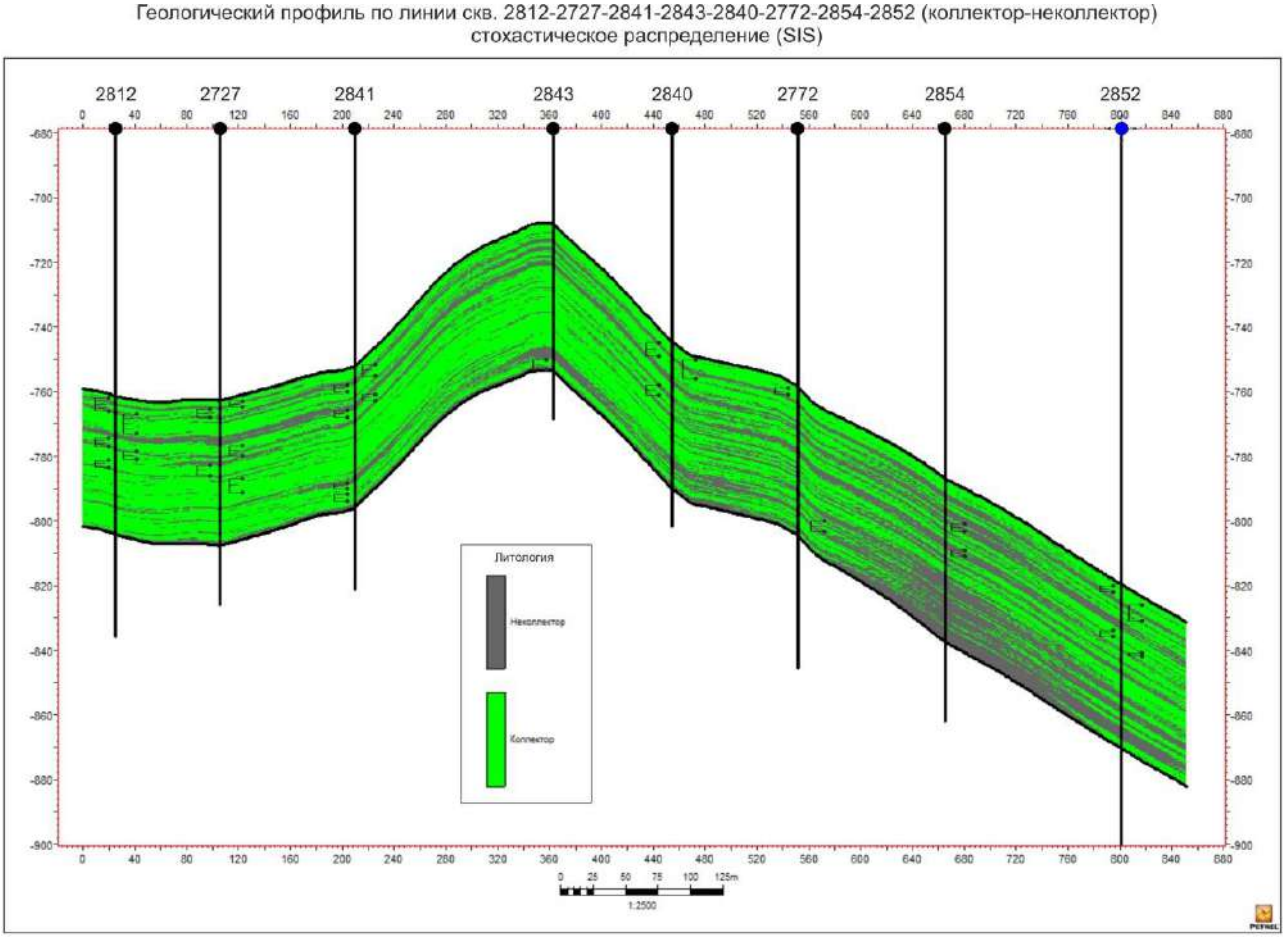

Рис. 5. Геологический профиль по линии скважин 2812-2843-2852 (литология)

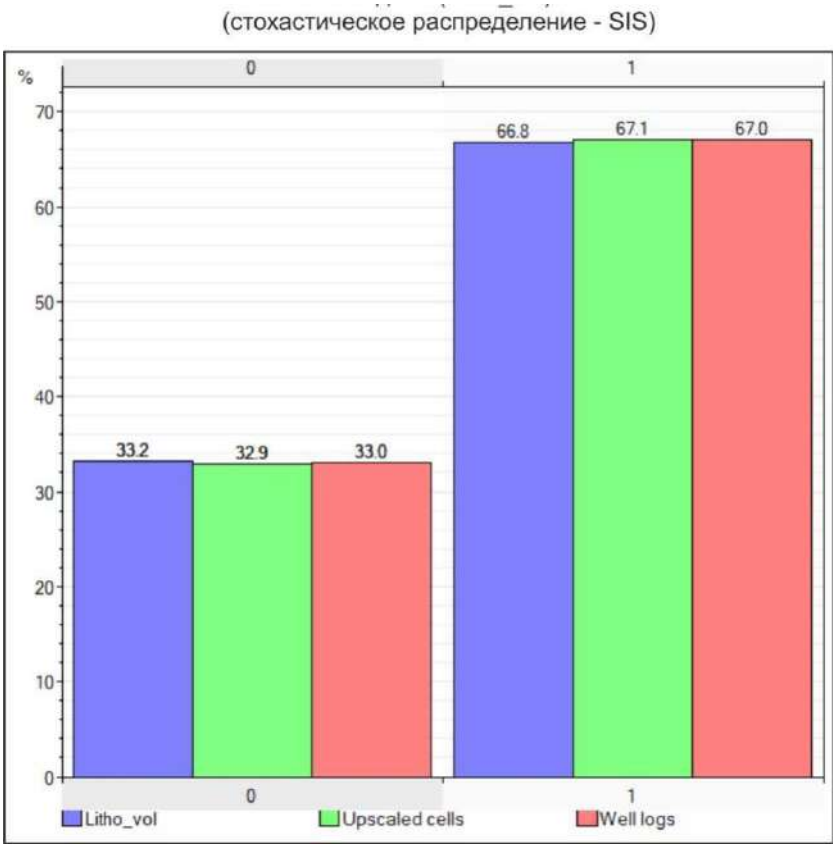

Рис. 6. Гистограмма сопоставления данных ГИС (Well logs), перемасштабированного каротажа (Upscaled cells) и модели (Litho_vol)

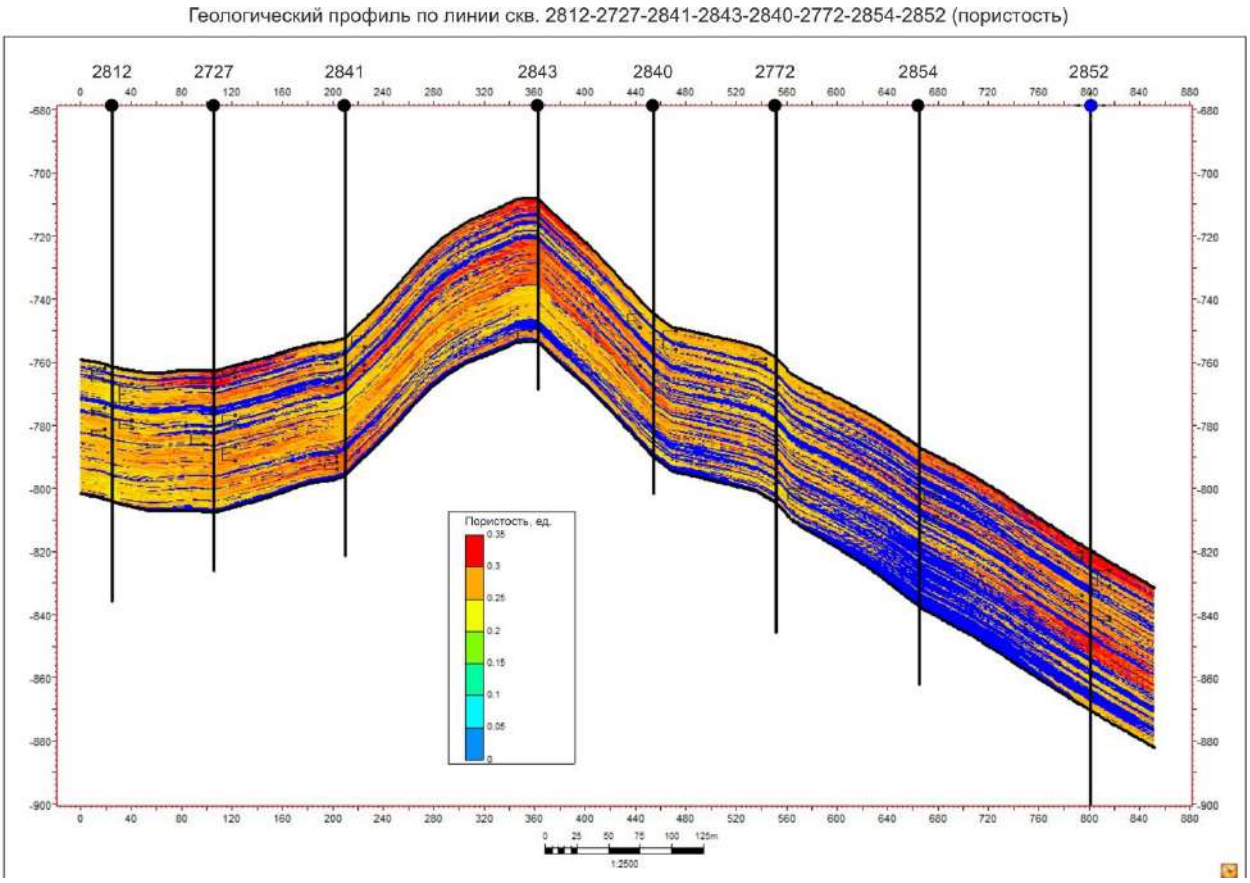

Рис. 7. Геологический профиль по линии скважин 2812-2843-2852 (пористость)

Выводы

Выполненные оценки и множество практических примеров интерпретации позволяют сделать следующие выводы и рекомендации:

– впервые по горизонту ПК построена трехмерная геомодель для пространственного распределения коллекторов подкирмакинской свиты ПТ нефтеносного месторождения Бинагади;

– эта модель также позволяет более правильно подбирать методы по доизвлечению остаточных запасов. В перспективе эти сведения могут быть использованы при прогнозировании нефтеотдачи и при составлении рекомендаций по управлению технологическими процессами разработки месторождений;

– распределение точек на корреляционном поле свидетельствует о том, что в пределах Бинагадинского нефтеносного района имеется единая закономерность изменения фильтрационно-емкостных свойств пород;

– несмотря на более чем сто десятилетнюю разработку объекта, еще не достигнуто значение конечного коэффициента нефтеотдачи. На сегодняшний день по ПК она составляет ≈0.7.

– построенная петрофизическая модель позволяет с большой достоверностью расчленить интервалы, где отсутствуют каротажные материалы.

ЛИТЕРАТУРА

Абасов М.Т., Кондрушкин Ю.М., Алияров Р.Ю., Крутых Л.Г. Изучение и прогнозирование параметров сложных природных резервуаров нефти и газа Южно-Каспийской впадины. Нафта-Пресс. Баку, 2007, 217 с.

Абасов М.Т., Алияров Р.Ю., Джалалов Г.И., Рамазанов Р.А. О методе оценки изменения относительной фазовой проницаемости пород-коллекторов в процессе разработки. ВНИИОЭНГ. Москва, Геология, геофизика и разработка нефтяных и газовых месторождений, No. 4, 2010, с. 51-57.

Буряковский Л.А., Джафаров И.С., Джеваншир Р.Д. Моделирование систем нефтегазовой геологии. Недра. Москва, 1990, 295 с.

Гасанов А.Б., Меликов Х.Ф., Сеидов В.М. Оценка распределения коллекторов в пространстве по комплексу геофизических и петрофизических данных. НТВ "Каротажник", Тверь, No. 7(172), 2008, с. 50-57.

Гутман И.С. Методы подсчета запасов и оценки ресурсов нефти и газа. Издательский дом Недра. Москва, 2017, 363 с.

Зинченко В.С. Петрофизические основы гидрогеологической и инженерно-геологической интерпретации геофизических данных. Издательство АИС. Москва, 2005, 387 с.

Коваленко К.В. Система петрофизического обеспечения моделирования залежей нефти и газа на основе эффективной пористости гранулярных коллекторов. Москва, 2015, 49 с.

Пашаев Н.В., Халилова Л.Н., Пашаева Ш.В. Геологическая оценка кирмакинской и подкирмакинской свит месторождения Бинагади по данным ГИС и петрофизики. Геофизические новости в Азербайджане, No. 1-2, Баку, 2017, с. 22-26.

Nooraiepour M., Mondol N.H., Hellevang H. Permeability and physical properties of semi-compacted fine-grained sediments – A laboratory study to constrain mudstone compaction trends. Marine and Petroleum Geology, Vol. 102, No. B12, 2019, pp. 590-603.

REFERENCES

Abasov M.T., Kondrushkin Yu.M., Aliyarov R.Yu., Krutix L.G. Study and forecasting of the parameters of complex natural oil and gas reservoirs in the South Caspian depression. Baku, "Nafta-Press", 2007, 217 p.

Abasov M.T Aliyarov R.Yu., Jalalov G.I., Ramazanov R.A. Method of evaluation of relative phase permeability change of rocks-collectors during their development. Moscow, Geology, geophysics and development of oil and gas fields, No. 4, 2010, pp. 51-57.

Buryakovski L.A., Jafarov I.S., Janavanshir R.D. Modeling of petroleum geology systems. Nedra. Moscow, 1990, 295 p.

Hasanov A.B., Melikov Kh.F., Seyidov V.M. Estimation of distribution in space by a complex of geophysical and petrophysical data. Karotajnik, Tver, No. 7(172), 2008, pp. 50-57.

Gutman I.S. Methods for calculating reserves and estimating oil and gas resources. Nedra. Moscow, 2017, 363 p.

Zinchenko V.S. Petrophysical foundations of hydrogeological and engineering-geological interpretation of geophysical data. AIS. Moscow, 2005, 387 p.

Kovalenko K.V. Petrophysical support system for modeling oil and gas deposits based on the effective porosity of granular reservoirs. Moscow, 2015, 49 p.

Pashayev N.V., Khalilova L.N., Pashayeva Sh.V. Geological assessment of the Kirmaki and Underkirmaki suites of the Binagadi field according to well logging and petrophysical data. Geophysical news in Azerbaijan, No. 1-2, 2017, Baku, pp. 22-26.

Nooraiepour M., Mondol N.H., Hellevang H. Permeability and physical properties of semi-compacted fine-grained sediments – A laboratory study to constrain mudstone compaction trends. Marine and Petroleum Geology, Vol. 102, No. B12, 2019, pp. 590-603.

РАЗРАБОТКА ПЕТРОФИЗИЧЕСКОГО МОДЕЛИРОВАНИЯ НА ОСНОВЕ ЭФФЕКТИВНОЙ ПОРИСТОСТИ И ФАЗОВЫХ ПРОНИЦАЕМОСТЕЙ КОЛЛЕКТОРОВ (НА ПРИМЕРЕ БИНАГАДИНСКОГО МЕСТОРОЖДЕНИЯ)

Пашаев Н.В.

Азербайджанский Государственный Университет Нефти и Промышленности, Азербайджан
AZ1010, Баку, просп. Азадлыг, 34: namat.pashayev@mail.ru

Резюме. В статье приводятся результаты изучения изменения коэффициентов нефтенасыщенности и пористости продуктивных пластов подкирмакинской свиты (ПК) Бинагадинского месторождения спустя сто десять лет после начала его разработки.

Учитывая что, в настоящее время еще не разработаны практические методы количественной оценки текущего коэффициента нефтенасыщенности в обсаженных скважинах, при определениях были использованы в основном материалы ГИС и керновые данные – по скважинам в период их эксплуатации. В результате лучшего разделения коллекторов на продуктив-

ные и водоносные пласты, на основании корреляции разрезов скважин выделены одноименные продуктивные пласты внутри ПК, имеющие первостепенное значение при рациональной разработке месторождений. На основе новых данных построена зависимость $К_{пр}$ от $К_{п}$ для всех интервалов коллекторов, выделенных в разрезах скважин. Установлено, что на исследуемой площади нет начальных контуров нефтеносности. Кроме того, в целях оценки влияния литологических особенностей на фильтрационно-емкостные свойства коллекторов, установлены парные зависимости между $К_{пр}$ и $К_{п}$ по исследуемому горизонту. Полученная зависимость характеризуется высокой теснотой связи (R=0.85). В перспективе эти сведения могут быть использованы при прогнозировании нефтеотдачи и при составлении рекомендаций по управлению технологическими процессами разработки месторождений. С целью изучения пространственного распределения коллекторов по площади (скважинам), а также пористости, проницаемости и нефтенасыщенности созданы трехмерные сетки геомодели. В результате, показана практическая возможность использования петрофизической модели, построенной с помощью стохастического метода, для изучения литологии разреза. Эффективность модели заключается в том, что она сравнима с каротажными данными, позволяющими с большой достоверностью расчленить интервалы, где отсутствуют каротажные материалы.

Ключевые слова: *каротаж, скважина, пористость, проницаемость, электрическое сопротивление*

KOLLEKTORLARIN EFFEKTİV MƏSAMƏLİLİYİ VƏ FAZA KEÇİRİCİLİYİ ƏSASINDA PETROFİZİKİ MODELLƏŞDİRMƏNİN İŞLƏNİLMƏSİ (BİNƏQƏDİ YATAĞININ TİMSALINDA)

Paşayev N.V.
Azərbaycan Dövlət Neft və Sənaye Universiteti
AZ1010, Bakı, Azadlıq prosp., 34: namat.pashayev@mail.ru

Xülasə. Məqalədə yüz on ildən çox müddətdə işlənmədə olan Binəqədi yatağının Məhsuldar Qatın (MQ) Qırməkialtı lay dəstəsinin (QAD) məhsuldar kollektorlarının və neftdoyumluluğunun dəyişməsinin tədqiqi nəticələri verilir.

Hazırda istismar quyularında qalıq neftdoyumluluğunun praktik cəhətdən kəmiyyətcə qiymətləndirilmə metodikası işlənilmədiyindən təyinetmədə əsasən quyuların istismar müddətində əldə edilmiş QGT materiallarından və kern məlumatlarından istifadə edilmişdir.

Kollektorların məhsuldar və sulu kimi sinifləşdirilməsində daha önəmli yanaşmalardan sayılan quyu kəsilişlərinin korrelyasiyası əsasında yatağın rasional işlənməsində son dərəcə əhəmiyyət kəsb edən QAD-ın eyniadlı məhsuldar layları seçilmişdir.

Korrelyasiya ilə seçilmiş bütün kollektorlar üçün yeni məlumatlar bazasında kollektorların cari neftdoyumluluğu ilə məsaməliliyi arasında asılılıq qurulmuşdur. Tədqiqat obyektində olan neft konturunun mövcudluğu təsdiq edilməmişdir.

Əlavə olaraq, kəsilişin litoloji xüsusiyyətlərinin məhsuldar kollektorların filtrasiya-tutma xassələrinə təsirinin qiymətləndirilməsi üçün tədqiqat horizontu üzrə qurulmuş $K_{keç}=f(K_m)$ asılılığı yüksək əlaqəliliklə səciyyələnir (R=0.85).

Bu məlumatlar gələcək perspektivlikdə neftvermənin proqnozlaşdırılmasında, eləcə də yatağın işlənmə prosesinin texnoloji idarəedilməsinə təkliflərin verilməsində istifadə edilə bilər.

Kollektorların sahə üzrə paylanma məkanının öyrənilməsi üçün eləcə də məsaməliliyin, keçiriciliyin, neftdoyumluluğun dəyişmə xüsusiyyətlərini özündə ehtiva edən üçölçülü geomodel şəbəkəsi qurulmuşdur.

Nəhayət, kəsilişin litologiyasını öyrənmək məqsədi ilə stoxastik üsuldan istifadə etməklə petrofiziki model qurulmuşdur. Modelin əhəmiyyəti karotaj aparılmayan intervallarda litologiyanın səhih təyinindən ibarətdir.

Açar sözlər: *karotaj, quyu, qışqırıq, keçiricilik, elektrik müqaviməti*

ANAS Transactions **Earth Sciences** **1 / 2024**

http://www.journalesgia.com

INTEGRATED 2D GEOELECTRIC PROSPECTING FOR GOLD MINERALIZATION POTENTIAL WITHIN SOUTHERN PART OF KEBBI NW NIGERIA

Augie A.I.[1,2], Salako K.A.[2], Rafiu A.A.[2], Jimoh M.O.[3]

[1]Department of Applied Geophysics, Federal University Birnin Kebbi, Nigeria: ai.augie@fubk.edu.ng

[2]Department of Geophysics, Federal University of Technology Minna, Nigeria

[3]Department of Geology, Federal University of Technology Minna, Nigeria

Keywords: *2D Modelling, Electrical Resistivity Tomography, Induced Polarization, Self-Potential, gold mineralization*

Summary. This is a detailed geophysical research into the anomalous zones identified by previous aeromagnetic studies in the area. Integrated 2D geoelectric prospecting methods involving ERT, IP and SP techniques were used to delineate subsurface structure suitable for gold mineralization potential in parts of the Yauri, Shanga, and Magama areas of the states of Kebbi and Niger in the northwest Nigeria. The ERT, IP and SP measurements were carried out with a dipole-dipole configuration and the SuperSting resistivity meter. The research results revealed regions with low/high resistivity, high chargeability, and high SP values, which were identified as mineral potential zones. The ERT technique has helped to delineate regions with low resistivity anomalous which correspond to oxidized rocks associated with granite/quartzite veins. High resistivity range could exist over dyke structures associated with partially decomposed granite and quartzite, as indicated by the geological setting and borehole log of the area. The IP technique revealed a high chargeability (≥ 20 milliseconds) in the study area, possibly due to the accumulation of metallic minerals in host rocks, such as gold. The SP technique has also helped to identify regions with high SP anomalies (≥20 mV), which are characterized by vein-bearing ore minerals. The integration of ERT, IP, and SP results revealed oxidized rock zones, dyke subsurface structures of decomposed quartzite, granite, gneiss, and ore mineral veins. These zones are located in the northwest Mararraba, the southwest Jinsani, and the southern Sabon Gari in Niger and Kebbi states. The areas could be considered a potential pathway for gold exploration and exploitation.

1. Introduction

There are many areas of gold occurrence in Nigeria mainly associated with the schist belts which are composed of rocks like gneisses, schists, quartzites, amphibolites and granitoids (Olalekan et al., 2016; Ejepu et al., 2018). Gold mines are very important economic assets for many countries in the world including Nigeria in particular, therefore these activities require a geophysical approach that will delineate possible pathways for gold exploration and exploitation (Augie and Ridwan, 2021; Augie et al., 2021a). Two-dimensional electrical resistivity tomography (ERT), induced polarization (IP) and self-potential (SP) are some of the geophysical methods used for mapping the potential zones, especially those of gold (Bagare et al., 2018). Oduduru and Mamah (2014) revealed that the integration of electrical resistivity tomography and IP methods can be powerful and effective diagnostic tools to delineate geologic structures and for the identification of strata. The IP technique has been used over the past 30 years with proven potential in providing in-situ information about rock mineralogy, particularly in the search for disseminated minerals with electronic conductivity (Unuevho et al., 2016; Amoah et al., 2018).

Various field mapping exercises were conducted in the southern part of Kebbi NW Nigeria with the view of assessing the mineralization potential using aeromagnetic data alone. Consequently, mineralization potentials have been reported in the area by these studies (e.g. Ramadan and Abdel-Fattah, 2010; Bonde et al., 2019; Lawali et al., 2020; Lawal et al., 2021; Augie et al., 2021a, 2022b and 2022c). Results from these studies reveal major structural trends in the area oriented along ENE-WSW, NE-SW and E-W directions while minor trends were along NW-SE, NNE-SSW, NNW-SSE and N-S directions of the area. These results are generally concordant with the main regional structural trend dipping to the NW. The results also revealed that the southern part of the Kebbi,

NW Nigeria is dominantly a basement complex, which may play host to economic minerals. Augie et al. (2021b, 2022b, 2022c) further revealed that the structures delineated within the area when compared with the geological setting, correspond to quartz-mica schist, granite, biotite, gneiss, diorite, medium coarse-grained and biotite hornblende granite. The regions correspond to SE parts of Yauri and Shanga, Fakai, Ngaski, Zuru, Magama, Rijau, and the eastern part of Wasagu/Danko and Bukkuyum.

However, previous studies have only used aeromagnetic data and the anomalous zones detected from the aeromagnetic studies were not followed up by detailed work. A combined 2D ERT, IP and SP geophysical methods for gold prospects and their associated mineralization have not been conducted in the area. The 2D ERT would be used to unveil lithological boundaries and geologic structures such as faults, dykes, veins and other mineral trapping structures associated with gold-bearing alteration zones (Loke and Barker, 1996; Loke, 2004). Likewise, IP and SP methods are particularly useful for detecting disseminated minerals that are difficult to detect using resistivity alone (Unuevho et al., 2016). This integrated method would be employed to delineate gold mineral-bearing zones and lithological boundaries. The IP, SP and Resistivity are some of the geophysical methods used for mapping the gold minerals as they contribute to better-fined targets. The inversion of resistivity, IP and SP data could throw light into the subsurface by tomographic and other pattern analyses associated with gold mineralization (Shao et al., 2021).

This paper used data from 2D electrical resistivity tomography, induced polarization and self-potential data with the view to delineate the gold-bearing alteration zones and other subsurface striations as a potential host for other mineralization. The results from these techniques were used to map probable gold anomalous zones within the study area where detailed exploration for the gold can be concentrated. The dipole-dipole array was adopted because of its low EM (electromagnetic) coupling between the current and potential circuits, very sensitive to horizontal and vertical changes in resistivity. It is good for mapping vertical structures, such as dykes and cavities. It has a better resolution than both Wenner and Schlumberger configurations (Loke and Barker, 1996; Loke, 2004).

2. Theoretical Framework and Field Procedures

In geoelectrical methods, the current is driven through one pair of current-electrodes (A and B) and the potential differences are measured with the aid of pair of potential-electrodes (M and N) connected to a sensitive voltmeter called a Resistivity meter (Telford et al., 1990; Augie et al., 2022a). This will possibly determine an effective or apparent resistivity of the subsurface as shown in Fig. 1:

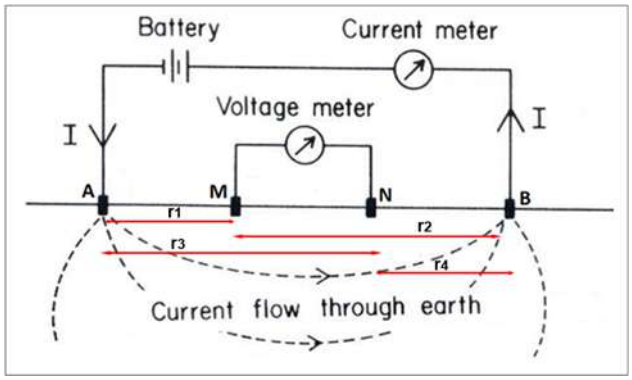

Fig. 1. Diagram used to determine the potential difference between two points

Ohm's law described that resistance (R) which is usually measured in ohm of a rock or particular sample is directly proportional to the length (L) of the resistive material (i.e., earth materials) and inversely proportional to its cross-sectional area (A) as given in equation (1):

$$\mathrm{R}\,\alpha\,\frac{L}{A} \tag{1}$$

$$\mathrm{R} = \rho\frac{L}{A} \tag{2}$$

where

ρ, the constant of proportionality called electrical resistivity. Electrical Resistivity is independent of the shape or size of the material but there are factors which affect the electrical resistivity such as moisture content, composition of strata, temperature and electrolytes. It is the true resistivity, and the resistivity values of rocks and minerals can be classified as good conductors, bad conductors, or isolators (Dahlin and Zhou, 2004).

According to Ohm's law:

$$\mathrm{R} = \frac{\Delta V}{I} \tag{3}$$

and

$$\Delta V = V_2 - V_1 \tag{4}$$

where; ΔV is the potential difference between the earth materials, I is the electric current through it and R is the resistance of the earth materials.

Substituting equation (3) into (2):

$$\frac{\Delta V}{I} = \rho\frac{L}{A} \tag{5}$$

This implies:

$$\rho = \frac{\Delta V}{I}\left(\frac{A}{L}\right) \tag{6}$$

where
$A = 2\pi r^2$ (hemispherical area under the earth) and $r = L$ (distance away from the source).

The potential difference (ΔV):

$$\Delta V = \frac{I\rho}{2\pi r} \tag{7}$$

$$\Delta V = \frac{I\rho}{2\pi}\left(\frac{1}{r}\right) \tag{8}$$

r is the distance between the current electrode point and the point where potential is measured.

Total potential at M due to current electrodes A and B (see Fig. 1);

$$V_{M\,(A,B)} = \frac{I\rho}{2\pi}\left(\frac{1}{r1} - \frac{1}{r2}\right) \tag{9}$$

Total potential at N due to current electrodes A and B;

$$V_{N\,(A,B)} = \frac{I\rho}{2\pi}\left(\frac{1}{r3} - \frac{1}{r4}\right) \tag{10}$$

The net potential difference is:

$$\Delta V_{MN\,(A,B)} = V_{M\,(A,B)} - V_{N\,(A,B)} \tag{11}$$

$$\Delta V_{MN\,(A,B)} = \frac{I\rho}{2\pi}\left(\frac{1}{r1} - \frac{1}{r2} - \frac{1}{r3} + \frac{1}{r4}\right) \tag{12}$$

$$\rho = \frac{\Delta V}{I} 2\pi \left(\frac{1}{\frac{1}{r1} - \frac{1}{r2} - \frac{1}{r3} + \frac{1}{r4}}\right) \tag{13}$$

and

$$K = 2\pi \left(\frac{1}{\frac{1}{r1} - \frac{1}{r2} - \frac{1}{r3} + \frac{1}{r4}}\right),\ R = \frac{\Delta V}{I} \tag{14}$$

Therefore

$$\rho = \mathrm{KR} \tag{15}$$

where; K is the geometrical factor of the electrode arrangement.

Time-domain IP estimations include observing the decaying voltage after the current is turned off. The most ordinarily measured parameter is the chargeability M, defined as the area A beneath the decay curve over a certain time interval standardized by the consistent state potential difference ΔVc (Bagare et al., 2018).

$$\mathrm{M} = \frac{\mathrm{A}}{\Delta \mathrm{V_c}} = \frac{1}{\Delta \mathrm{V_c}} \int_{t_1}^{t_2} \mathrm{v(t)\,dt} \tag{16}$$

Chargeability is measured over a specific time stretch not long after the polarizing current is cut off. Area A is determined within the measuring apparatus by analogue integration. Different minerals are distinguished by characteristic chargeabilities, for example, pyrite has M = 13.4 ms over an interval of 1 s, and magnetite 2.2 ms over the same interval (Bagare et al., 2018).

The total SP anomaly can be defined as (Fedi and Abbas, 2013)

$$S(P) = \int_V^0 \nabla \cdot \frac{\boldsymbol{K}}{r}\, dr \tag{17}$$

where, K is the electric dipole moment due to charge accumulation, either primary or induced, and r is the distance from the observation point P.

The streaming potential E_k which η is observed when a solution of electrical resistivity ρ and viscosity ρ is forced through the capillary of the porous medium. The resultant potential difference between the ends of the passage is: (Telford et al., 1990; Jamaluddeen et al., 2014; Augie et al., 2022a)

$$E_k = -\frac{\xi \Delta P K_p}{4\pi\eta} \tag{18}$$

where ξ is the adsorption potential, ΔP is the pressure difference and Kp is the solution dielectric constant.

2.1 Location and Geological Setting of the Study Area

The fieldwork was conducted in some selected areas of the Kebbi and Niger States. These areas are Shanga (Sabon Gari) and Yauri/Ngaski boundaries (Mararraba) of Kebbi state, and also Magama (Irana) of Niger State NW Nigeria (see Fig. 3). The study areas lie between latitudes 11°5′10″N to 11°5′40″N and longitudes 4°43′0″E to 4°43′25″E (Sabon Gari), latitudes 10°47′55″N to 10°48′20″N and longitudes 4°42′0″E to 4°54′0″E (Mararraba), and latitudes 10°31′40″N to 10°32′20″N and longitudes 4°55′59″E to 4°56′15″E (Irana).

Geologically, the study area falls under the basement complex rocks associated with: granite, rhyolite, biotite-granite, meta-conglomerate, quartz-mica schist, migmatite, undifferentiated schist including gneiss, biotite gneiss, medium coarse-grained and biotite-hornblende granite (Fig. 2). The southern part of Kebbi of the basement complex/schist belt is called Zuru-Yauri Schist Belts (Danjumma et al., 2019; Olugbenga and Augie, 2020), consist of an assemblage of muscovite-biotite banded gneisses, porphyroblastic gneisses, migmatites, schists, quartzites, metavolcanics (amphibolites), quartzites, mica schists, granulites, calc-silicates older granites and minor rocks such as gabbro, andesite, granulites and calc-silicates.

The structural elements in Zuru Schist Belt are the major NNE-SSW to NE-SW trending B/Yauri, Yauri and Ribah dextral faults, an NW-SE trending Gunu sinistral fault and a major N-S trending anticlinorium called the Zuru anticlinorium (Sani et al., 2019; Danbatta, 2005). These schists are lithologically different from the other schists belt in northwestern Nigeria and it is predominantly composed of quartzites with very subordinate schists and amphibolites (Danjumma et al., 2019; Danbatta, 2008).

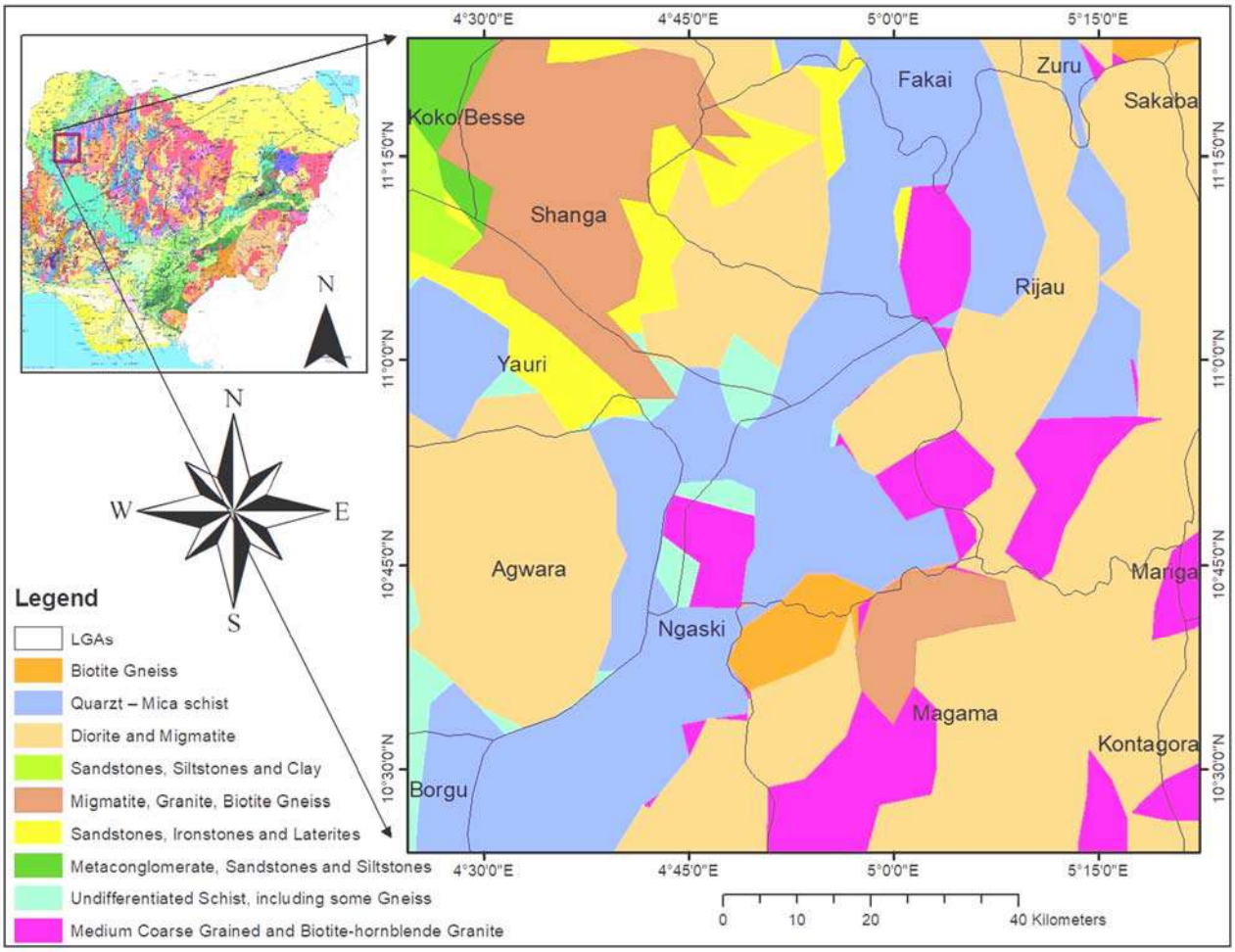

Fig. 2. Location and geological map of the study area

3. Methodology

In this study, a 2D geoelectrical survey was carried out at Yauri/Ngaski boundaries (Mararraba), Shanga (Sabon Gari) of Kebbi state, and also Magama (Irana) of Niger State NW Nigeria. An area of 490 m^2, 640 m^2, and 490 m^2 fields were investigated using a dipole-dipole configuration with minimum electrode spacing (a) of 10.00 m. A total of 7 profiles were designed for each 300 m distance along the profile, oriented NW-SE (Fig. 3). Profiles 1 and 2 were conducted at Magama (Irana), profiles 3 and 4 – at Shanga (Sabon Gari), and profiles 5, 6, and 7 – at Yauri/Ngaski boundaries (Jinsani and Mararraba).

The data was taken with the aid of Super Sting (resistivity meter) coupled with an electrode selector and powered by a 12 V battery. This instrument has the capability of measuring apparent resistivity, IP, and SP data. It has a transmitter with automatic/or user selectable currents in milliamps as; 1, 2, 5, 10, 20, 50, 100, 200, 500 and 1000 mA. The distance, between the two current electrodes (C1 and C2), is the same as that between the potential electrodes (P1 and P2). Distance between the current electrode C1 and the potential electrode P1 (dipole separation factor) was made in multiple of an integer n of the distance between the current and potential electrode pair (Fig. 4).

Initially, the dipole separation factor n was set to be 1, then it is increased to 2, 3, and so on until a maximum value of 8. Thus, both the dipole separation factor (n) and the spacing between the current electrode pair (a) were recorded. Measurements were done at an electrode spacing of 10 m and n was set at 1, 2, 3, up to 8 (Fig. 4). The more the increase in n which would equally increase the electrode spacing, the more the injected current flows to greater depths (Loke and Barker, 1996).

For the first measurement, electrodes number 1, 2, 3, and 4 were used. Electrode 1 was used as the second current electrode (C2) at 0 m, electrode 2 as the first current electrode (C1) at 10 m, electrode 3 as the first potential electrode (P1) at 20 m, and electrode 4 as the second potential electrode (C2) at 30 m.

Likewise, in the second measurement, electrodes number 1, 2, 3, and 4 were used for C2 at 10 m, C1 at 20 m, P1 at 30 m, and P2 at 40 m respectively. These procedures were repeated down the profile line using 1a 2a, 3a, 4a, 5a, 6a, 7a, and 8a spacing between C1 and P1 where a is 10 m.

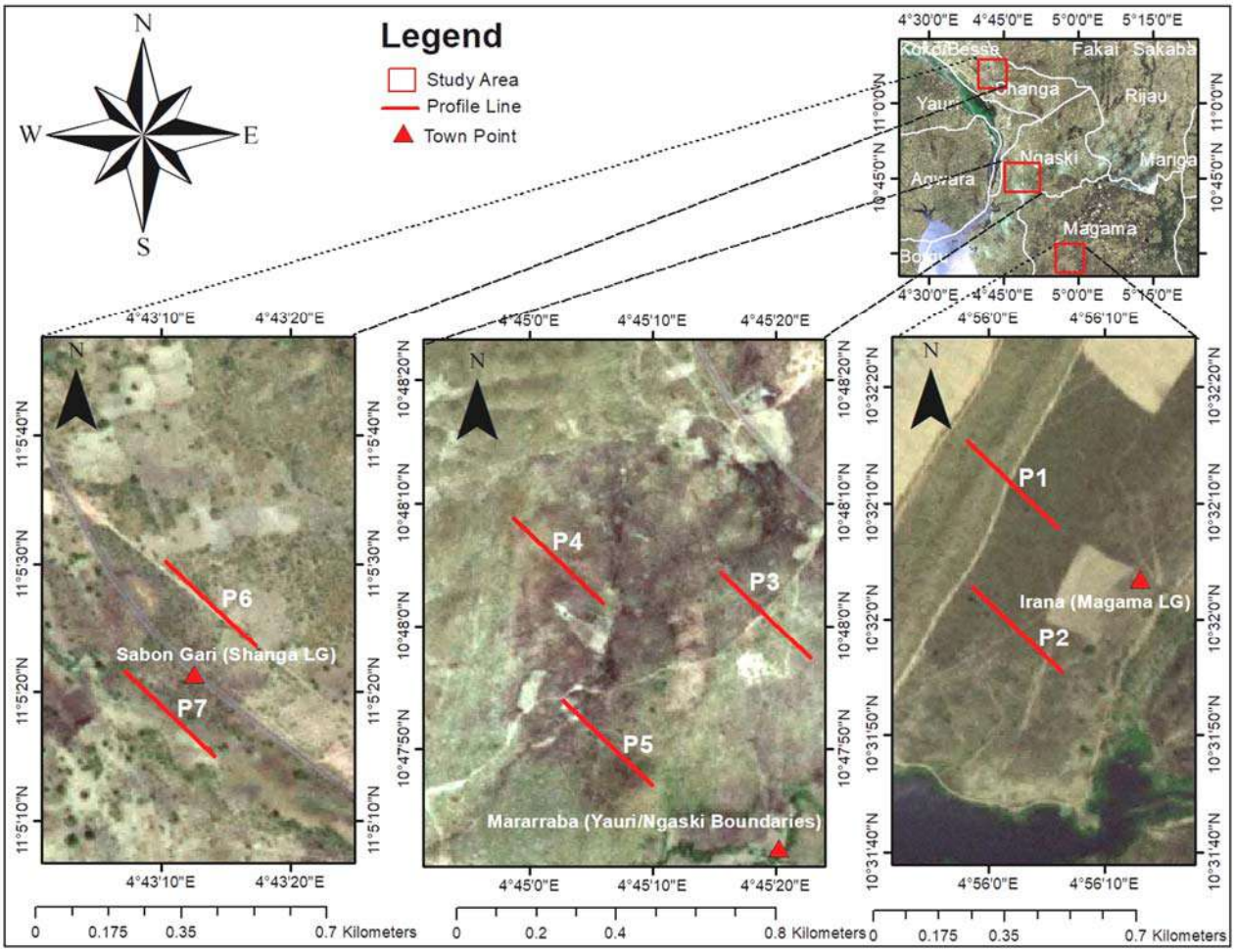

Fig. 3. Field survey layout using the dipole-dipole electrode configuration

At each measurement, the measured ground apparent resistivity, IP, and SP data were obtained. The acquired data were processed with the RES2DINV program developed by Loke (2004), which automatically determines a 2D resistivity and IP models for the subsurface. SP data were also analyzed and processed using surfer software version 13.

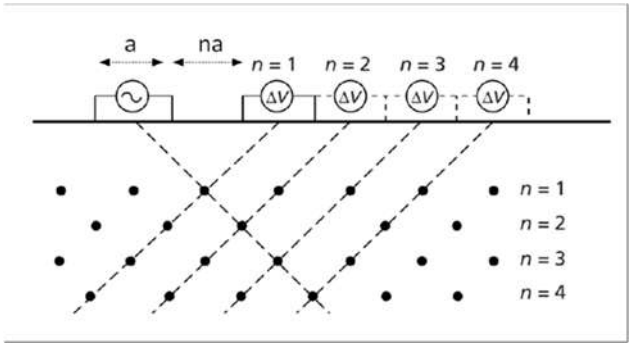

Fig. 4. Illustration of dipole-dipole array and pseudosection for putting the measured apparent resistivity and IP (Wahyu et al., 2016)

4. Result

In this study, the interpretation of the 2D geoelectric modeled sections is associated with the geological setting of the area. These include the borehole lithology of the southern part of Kebbi obtained from RUWASA (Rural Water Supply and Sanitation Agency) as shown in Table 1 and resistivity values obtained from previous works in the same basement complex which were used to correlate the results of the present survey (Osazuwa and Chii, 2010).

The sections have a vertical axis (y-axis) corresponding to the depth of investigation and a horizontal distance axis (x-axis) representing distance along the profile. The inverse section of each profile was interpreted in terms of geology (Fig. 2) and related information. The summary of results obtained from the integrated methods is given in Table 2.

Table 1

A borehole/lithology log of southern part of Kebbi areas (SARDA, 1988; Osazuwa and Chii, 2010)

Lithology	Depth(m)	Thickness(m)	Resistivity range (Ωm)
Lateritic Sand	0-2	2	60-1000
Highly Decomposed Schist	2-10	8	10-500
Partially Decomposed Granite	10-15	12	100-1000
Quartzite's and Gneiss	15-21	16	200-100000

4.1 Resistivity Model Section for Profile 1 (P1)

Profile 1 covers a lateral extent of 300 m (Fig. 5a). It is oriented in the NW-SE direction and lies between latitudes 10°32′13.2″N to 10°32′6″N and longitudes 4°56′6″E to 4°55′58″E (Fig. 3). The subsurface features from Fig. 5(a) could be sectionalized into four: **A**, **B**, **C**, and **D** zones. Zone **A** is characterized by low resistivity values ranging from 117 Ωm to 944 Ωm. It has a lateral length of 5-45 m, 55-102 m, 145-165 m, and 241-285 m at a depth/thickness of 19 m, 19-24.9 m, 19 m, and 17-24.9 m. Zone **B** has resistivity values of 945 Ωm to 7638 Ωm. This zone occupied a length of 50-90 m and 60-105 m, at a depth/thickness of 13 m and 18.5-20 m respectively. **C** is characterized by resistivity values ranging from 7639 Ωm to 21728 Ωm and it occupied the distance along the profile from 90-165 m at a depth/thickness of 18.5 m. However, zone **D** is characterized by the resistivity of 61815 Ωm to 175857 Ωm, it has a length of 90-140 m and 160-250 m with a corresponding depth/thickness of 7.5-24.9 m and 24.9 m.

The suggested subsurface lithology for features **A**, **B**, **C**, and **D** from Table 1, could be lateritic soil, highly decomposed schist, partially decomposed granite and quartzite, and quartzite/gneiss. However, low resistivity regions of **A** could be a result of water content and weathering in the oxidized rock. Some minerals, particularly gold, could be hosted mostly in a rock corroded by water called oxidized rocks, mainly of granite or rhyolite origin. Zone **C** of partially decomposed granite and quartzite has formed the dyke structures. Dyke subsurface structures of decomposed granite and quartzite usually play a pivotal role in determining the gold mineral. Zone **D** is the region with the highest resistivity. When compared to the borehole log and geological setting of the area, the region is underlain by quartzite and gneiss. These highest resistivity regions could be caused by the inclusion of impurity ions into particular minerals, which has a significant effect on resistivity of the zone. The results of the inverse model section (Fig. 5a) were indicated in the geologic section as given in Fig. 5(b).

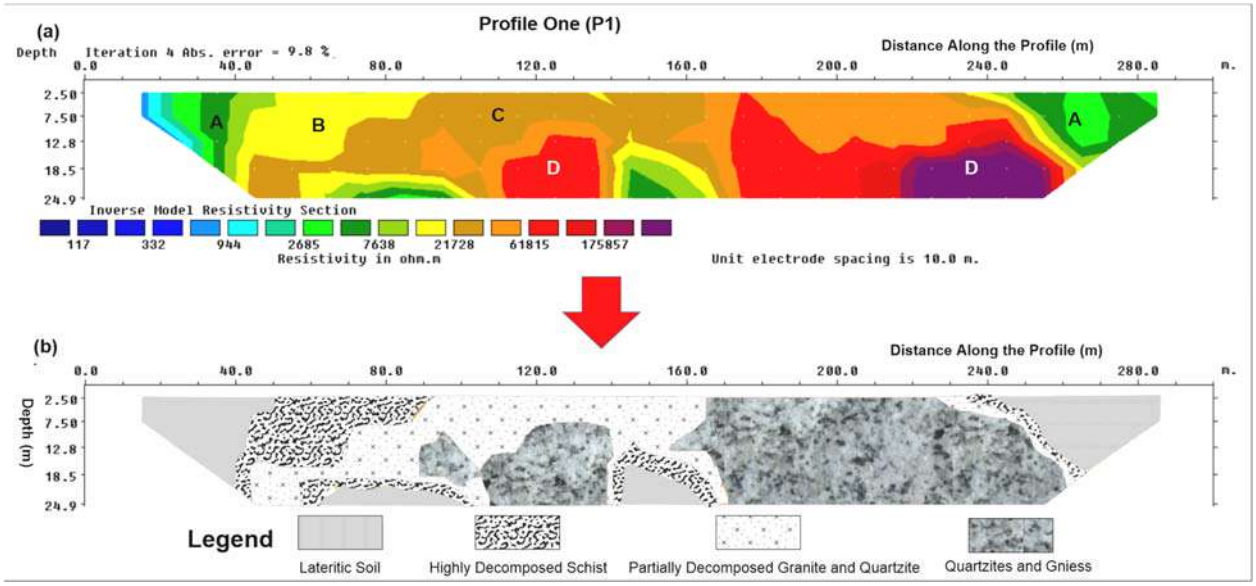

Fig. 5. (a) Inverse Model Resistivity Section and (b) Geologic Section for the Dataset Along Profile One (P1)

4.2 IP Model Section for Profile 1 (IP1)

Fig. 6 shows the inverse model chargeability section of profile one (IP1) which revealed the signatures of minerals. The model shows zones (**A1**) with the highest chargeability values ranging from 38.4 to 290 msec along the profile. It occupied the x-position of 120-140 m and 170-190 m and appeared at a depth/thickness of 18.5-24 m and 12.8 m. These regions with higher chargeability were further extended to 230-260 m and 205-290 m along the profile at a depth of 18.5 m and 24.9 m respectively. Higher chargeability usually occurs as a result of an accumulation of metallic minerals in host rocks such as gold minerals. These regions could be considered as a potential target for exploration particularly metallic minerals, particularly gold mineralization.

4.3 SP Section for Profile 1 (S1)

Fig. 7 gives the results of the SP section along profile one (S1). The sections revealed the high SP values ranged from 20 mV and above. They occupied the x-positions of 0-10 m, 55-75 m, and 120-140 m at a depth/thickness of 50 m, 80 m, and 40 m. These regions were labeled as zone **A2**. High SP values could occur as a result of either the reduction-oxidation effect associated with ore bodies and organic matter-rich-contaminants, or the streaming potential which is related to water flow (Lobo-Guerrero, 2004). For this, the regions with high SP values were characterized by vein (i.e quartz vein as compared with Fig. 2) bearing ore minerals. The veins could be associated with gold mineralization as compared with the geological setting coupled with the borehole log of the area (Table 1).

4.4 Resistivity Model Section for Profile 2 (P2)

The 2D inverse section for P2 situated in the NW-SE direction was given in Fig. 8(a). It covers a length of 300 m and lies between latitudes 10°32′2.4″N to 10°31′55.2″N and longitudes 4°55′56.6″E to 4°58′8″E (see Fig. 3). The subsurface section in Fig. 8(a) was categorized into four zones: **A**, **B**, **C**, and **D**. Zone **A** is described by low resistivity values ranging from 113 Ωm to 594 Ωm, it has a sidelong length of 10-30 m, 160-165 m, and 202-222 m at a depth/thickness of 12 m, 24.9, and 2.5 m respectively. Zone **B** has resistivity values of 1359 Ωm to 3112 Ωm, it has occupied a lateral distance of 12-41 m, 50-80 m, 110-160 m, 169-230 m, 231-249 m, and 270-285 m, and a corresponding depth/thickness of 24.9 m, 24.9 m, 12.8, 18.5 m, 24.9 m, and 18.5 m, respectively. **C** is portrayed by resistivity values going from 3113 Ωm to 7123 Ωm, it covers the distance along the profile from 41-50 m and 81-120 m and a depth/thickness of each 18.5 m. Nonetheless, zone **D** is portrayed by the resistivity of 7124 Ωm to 37331 Ωm, it has occupied a length of 41-70 m, 50-80 m, 110-160 m, 169-230 m, 170-220 m, 231-249 m, and 270-285 m at a corresponding depth/thickness of 12-24.9 m, 7.5-12 m, 12-24.9 m, 13.0-24.9 m and 250-270 m respectively.

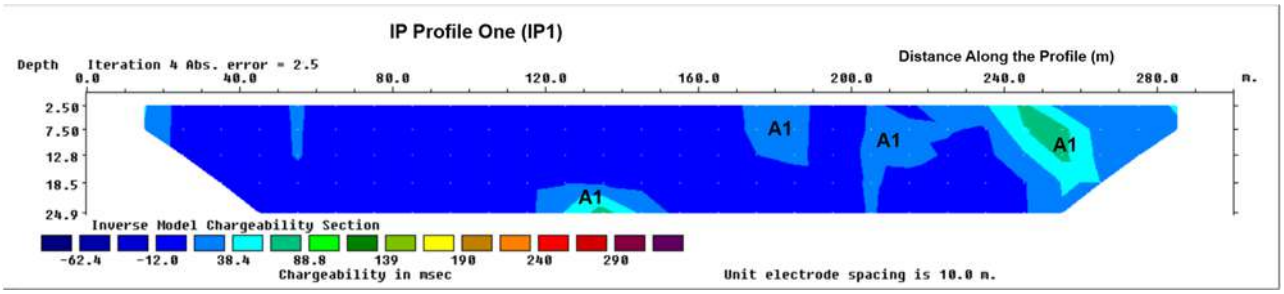

Fig. 6. Inverse Model Chargeability Section for Profile One (IP1)

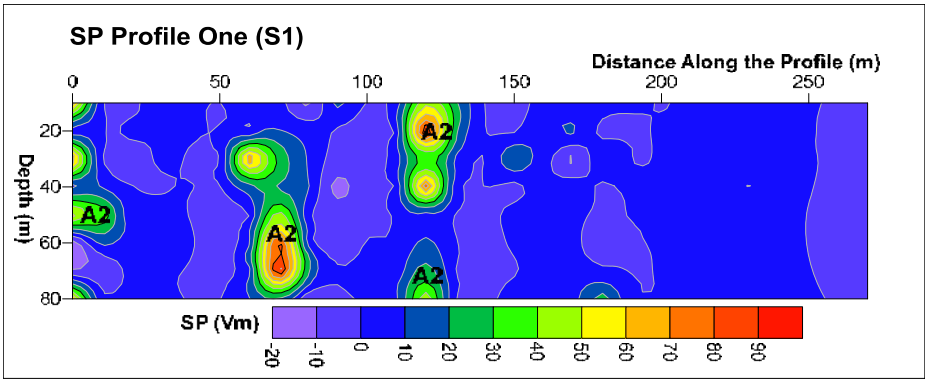

Fig.7. SP 2D Section for Profile One (S1)

The subsurface lithology for highlights **A**, **B**, **C**, and **D** from Table 1 could be lateritic soil, highly decomposed schist, partially decomposed granite and quartzite, and quartzite/gneiss. However, the low resistivity signature (zone **A**) in these regions could be a result of water content and weathering in the oxidized rock. This type of rock is mainly of granite or rhyolite origin. It could host some metallic minerals, particularly gold. Zone **C** has formed the dyke subsurface structures of decomposed granite and quartzite. These structures could play a pivotal role in determining the gold minerals. The results of the inverse model section given in Fig. 8(a), were transformed into a geologic section as shown in Fig. 8(b).

4.5 IP Model Section for Profile 2 (IP2)

The 2D inverse model chargeability section for profile two (IP2) was given in Fig. 9. The section has revealed the signature of minerals namely zones **A1**. These zones have the highest chargeability values ranging from 35 msec and above, which are located on along the x-positions of 35-60 m, 50-85 m, 140-175 m, 110-195 m, 198-220 m and 230-250 m at a depth/thickness of 12.8-24.9 m, 12.8 m, 12.8-24.9 m 12.8 m, 7.5 m and 18.5 m respectively. Higher chargeability of zones **A1** could occur as a result of an accumulation of metallic minerals in host rocks. These regions with high chargeability could be considered as a potential target for the exploration of metallic minerals such as gold mineralization.

4.6 SP Section for Profile 2 (S2)

The results of the SP section along with profile one (S1) were given in Fig. 10. The sections under the x-position of 0-54 m, 50-60 m, 61-100 m, 145-155 m, 160-210 m and 115-140 m at corresponding depth/thicknesses of 80 m, 80 m, 20-65 m, 40 m, 60 m, and 80 m have high SP values ranging from 20 mV and above. These areas were named zone **A2.** High SP values could happen because of either reduction-oxidation impact related to mineral bodies and natural matter-rich-pollutants, or the streaming potential which is connected with fluid flow. The zones with high SP signatures were described by vein-bearing metallic minerals. These veins could be related to gold mineralization as compared with the geological setting combined with the borehole log of the area.

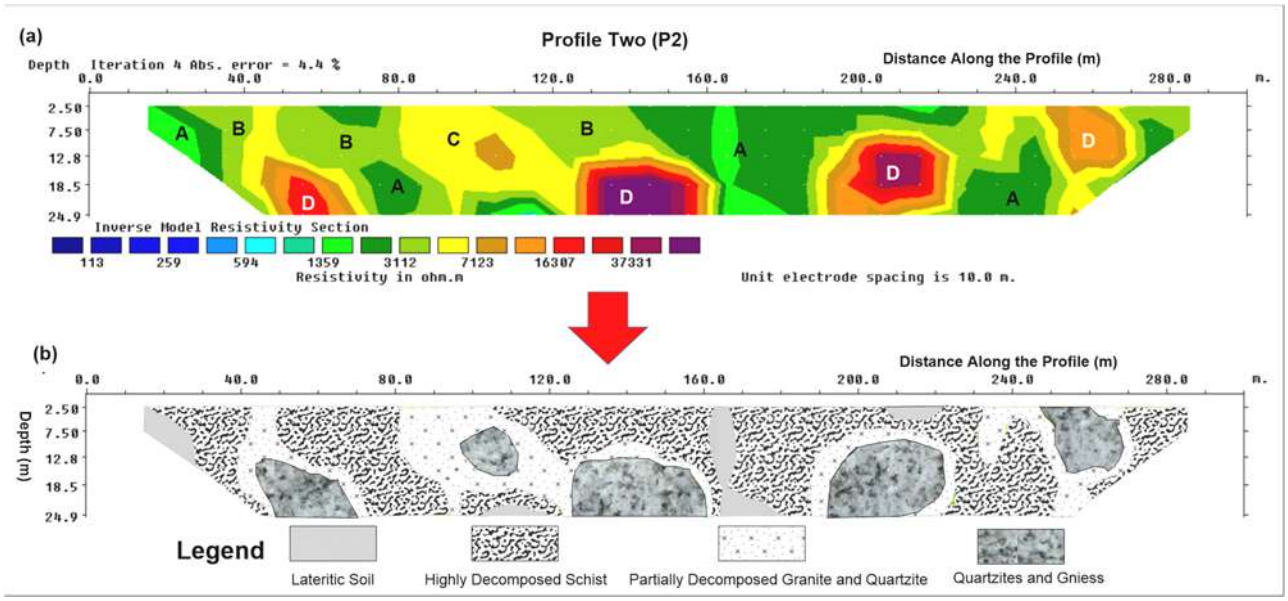

Fig. 8. (a) Inverse Model Resistivity Section and (b) Geologic Section for the Dataset along Profile Two (P2)

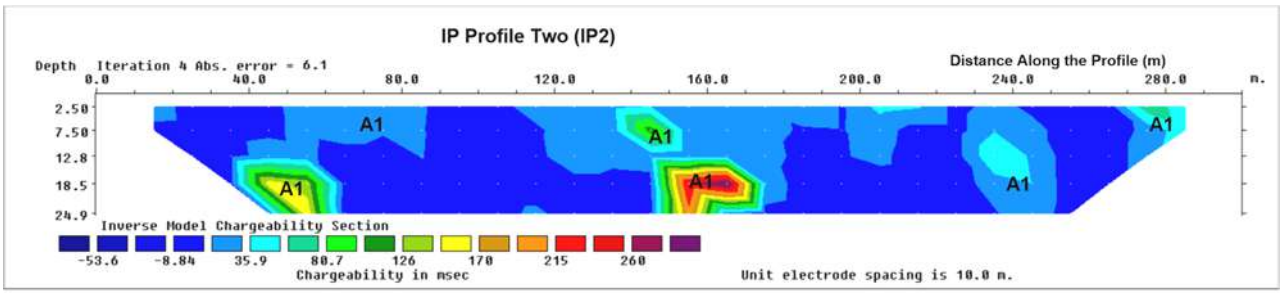

Fig. 9. Inverse Model Chargeability Section for Profile Two (IP2)

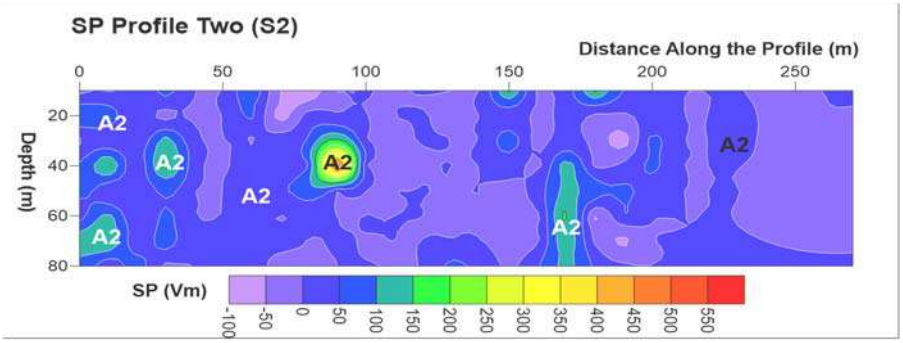

Fig. 10. SP 2D Section for Profile Two (S2)

4.2.7 Resistivity Model Section for Profile 3 (P3)

Fig. 11(a) is the 2D inverse model section for profile 3. It is oriented in the NW-SE direction and has a lateral distance of 300 m. The profile lies between latitudes 10°47′56.4″N to 10°48′3.6″N and longitudes 4°45′7.2″E to 4°45′18″E (see Fig. 3.). The subsurface feature was sectionalized into four different zones namely: **A**, **B**, **C**, and **D**. Zone **A** is characterized by resistivity values ranging from 1.6 Ωm to 459 Ωm, and are located on 10-80 m, 190-200 m, 250-265 m along the profile and a depth/thickness of 12.0 m, 18.5-24.9 m and 7.5-18.5 m respectively. **B** has resistivity values of 460 Ωm to 1888 Ωm, it covers a length of 30-110 m, 130-149 m, 190-200 m and 245-265 m at a corresponding depth/thickness of 2.5-18.5 m, 24.9 m, 18.5 m and 2.5-18.5 m. **C** is characterized by resistivity values going from 1889 Ωm to 7773 Ωm, it covers the distance along the profile of 35-55 m, 70-92 m, 105-130 m, 145-180 m, 200-210 m and 220-270 m and a depth/thickness of 8-24.9 m, 3-24.9 m, 24.9 m, 24.8 m, 24.9 m and 7.5 m. Likewise, zone **D** is portrayed by the resistivity of 7774 Ωm to 32002 Ωm, it has occupied a length of 100-125 m, 175-190 m, 200-250 m and 265-290 m at a corresponding depth/thickness of 7.5-24.9 m, 12-24.9 m, 2.5-24.9 m and 18.5 m respectively.

The subsurface lithology for features **A**, **B**, **C**, and **D** as compared with Table 1 could be lateritic soil, highly decomposed schist, partially decomposed granite and quartzite, and quartzite/gneiss. However, zone **A** of low resistivity areas could result from water content and enduring in the oxidized rock. Some minerals, especially gold, could be facilitated by this kind of oxidized rock that originates from granite or rhyolite. Zone **C** is associated with partially decomposed granite and quartzite which form dykes. Dyke subsurface structures of the aforementioned rock formation could play a pivotal role in determining the gold mineral. The results of the inverse model section given in Fig. 11(a) were further transformed into a geologic section as shown in Fig. 11(b).

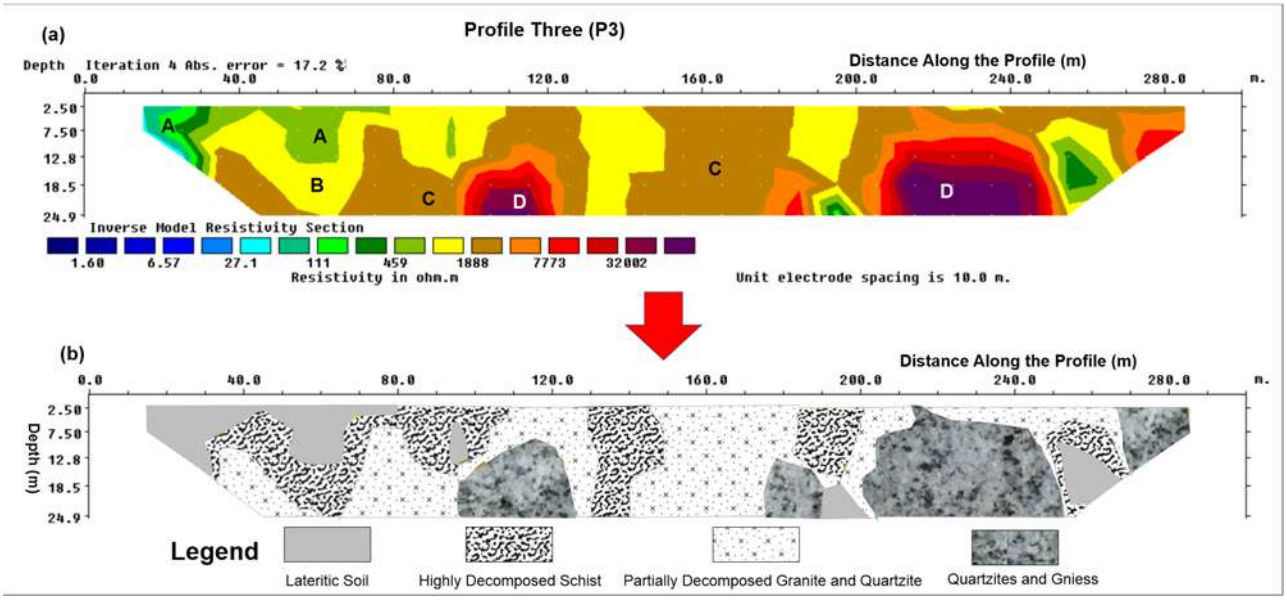

Fig. 11. (a) Inverse Model Resistivity Section and (b) Geologic Section for the Dataset along Profile Three (P3)

4.8 IP Model Section for Profile 3 (IP3)

The results of 2D inverse model chargeability sections along profile three (IP3) were given in Fig. 12. The sections revealed clearly the regions where exhibit metallic minerals, namely zone **A1**. These regions have the most noteworthy chargeability values ≥ 20 msec. The zone covers an x-position of 45-60 m, 190-202 m and 202-255 m at a corresponding depth/thickness of 7.5-18.5 m, 7.5 m and 12.8-24.9 m. The higher chargeability of zone **A1** generally happens because of the collection of metallic minerals in host rocks. These locales could be considered as a possible objective for the investigation of specific metallic minerals, particularly gold mineralization.

4.9 SP Section for Profile 3 (S3)

The results of the 2D SP section along profile one (S1) were given in Fig. 13. The regions with high SP (≥ 40 mV) signatures were labeled as zone **A2**. It has a lateral distance of 0-40 m, 50-60 m, 70-100 m, 120-200 m, 140-135, 190-240 m and a depth/thickness of 70 m, 21 m, 21-41 m, 15 m, 80 m and 21-80 m respectively. These regions with high SP signatures were depicted by veins, bearing metallic minerals. And these veins could be connected with gold mineralization as compared with the geological setting coupled with the borehole log of the area.

4.10 Resistivity Model Section for Profile 4 (P4)

Profile 4 covers a lateral extent of 300 m (Fig. 14a). It is oriented in the NW-SE direction and lies between latitudes 10°48′0″N to 10°48′7.2″N and longitudes 4°44′52.8″E to 4°45′0″E (see Fig. 3). The subsurface variations of resistivity were categorized into zone **A**, **B**, **C** and **D**. **A** is characterized by resistivity values ranging from 4.6 Ωm to 601 Ωm, it covers a lateral distance of 5-40 m, 165-185 m, 245-260 m, and a depth/thickness of 7.5 m, 18.5-24.9 m and 18.5-24.9 m respectively. **B** has resistivity values of 602 Ωm to 2033 Ωm, it covers a length of 40-90 m, 120-150 m, and 155-190 m at a corresponding depth/thickness of 12 m, 7.5 m and 18.5-24.9 m. **C** is characterized by resistivity values going from 2034 Ωm to 6873 Ωm, it covers the distance along the profile of 10-90 m, 95-120 m, 140-170 m, 180-205 m, 240-270 m, and a depth/thickness of 2.5-12.8 m, 24.9 m, 12.8 m, 12.8 m and 18.5 m. However, zone **D** is portrayed by the resistivity of 6874 Ωm to 23241 Ωm, it located on 10-105 m, 115-155 m, 170-180 m, 200-245 m, and 270-290 m along the profile at a corresponding depth/thickness of 7.5-24.9 m, 7.5-24.9 m, 12.8 m, 24.9 m and 18.5 m respectively.

The subsurface variations for zones **A**, **B**, **C** and **D** in relation to Table 1, could be lateritic soil, highly decomposed schist, partially decomposed granite and quartzite, and quartzite/gneiss. However, low resistivity (zone **A**) in these regions could be because of water content as well as weathering in an oxidized rock. These rock types are basically of granite or rhyolite origin. As such, it could be associated with some minerals, especially gold. Zone **C** formed the dyke structures associated with partially decomposed granite and quartzite. These structures could play a pivotal role in determining the minerals, particularly gold mineralization. These results led to the development of the geologic section as given in Fig. 14(b).

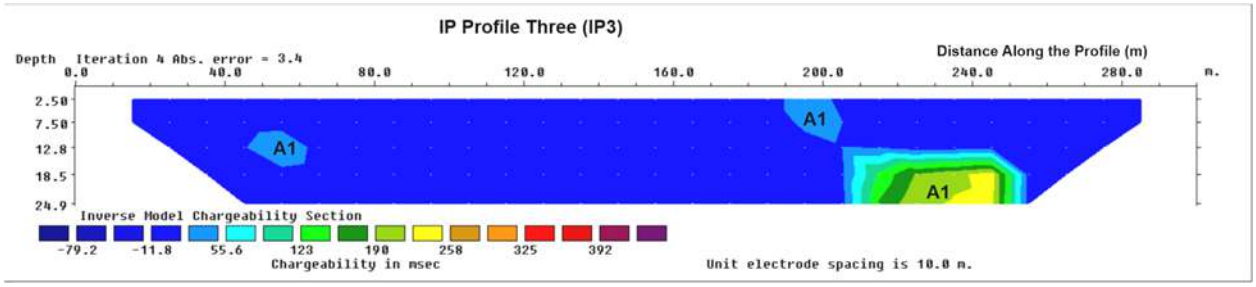

Fig 12. Inverse Model Chargeability Section for Profile Three (IP3)

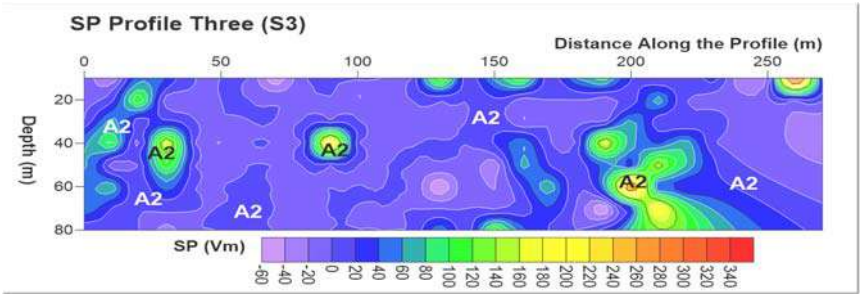

Fig. 13. SP 2D Section for Profile Three (S3)

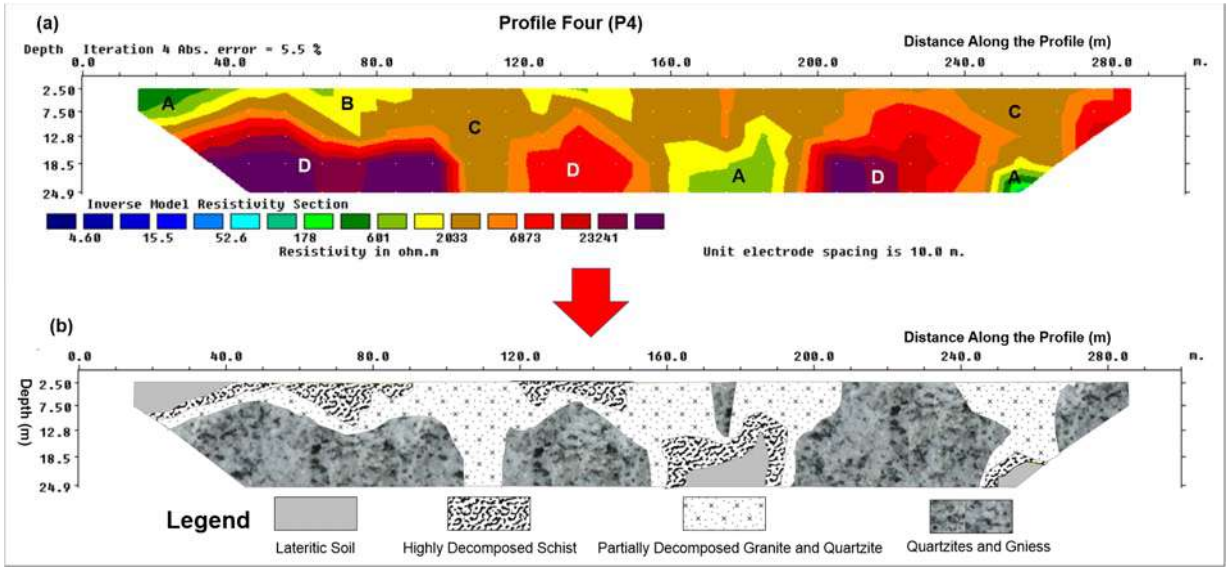

Fig. 14. (a) Inverse Model Resistivity Section and (b) Geologic Section for the Dataset along Profile Four (P4)

4.11 IP Model Section for Profile 4 (IP4)

Fig. 15 gives the results of the 2D inverse model chargeability section for profile four (IP4). The section uncovered some attributes of minerals, particularly within zone **A1**. The zones of **A1's** have the most imperative chargeability values ranging from 20 msec and above. It covers the lateral distance of 35-65 m, 55-80 m, 145-160 m, 200-220 m and 221-250 m at the corresponding depths of 12.8-24.9 m, 12.8 m, 18.5 m, 7.5 m and 7.5-24.9 m. Higher chargeability in zone **A1** is for the most part happening given an assortment of metallic minerals in host rocks. These areas could be considered as a potential target for the examination of explicit metallic minerals, particularly gold mineralization.

4.12 SP Section for Profile 4 (S4)

Fig. 16 gives the results of 2D SP sections along profile four (S4). The layer with high SP values (≥ 50 mV) was labeled as zone **A2.** It covers the lateral length of 1-40 m, 85-100 m, 145-200 m and 190-250 m, and a depth/thickness of 80 m, 22-60 m, 40 m and 80 m respectively. These regions with high SP values could occur due to either reduction-oxidation influence related to mineral bodies. These areas with high SP values were portrayed by vein-bearing metallic minerals. As such, the veins could be associated with gold mineralization in relation to the geological setting together with the borehole log of the area.

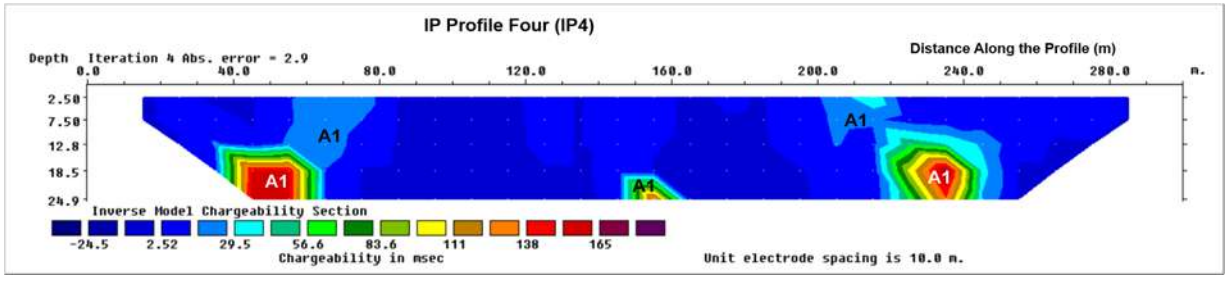

Fig. 15. Inverse Model Chargeability Section for Profile Four (IP4)

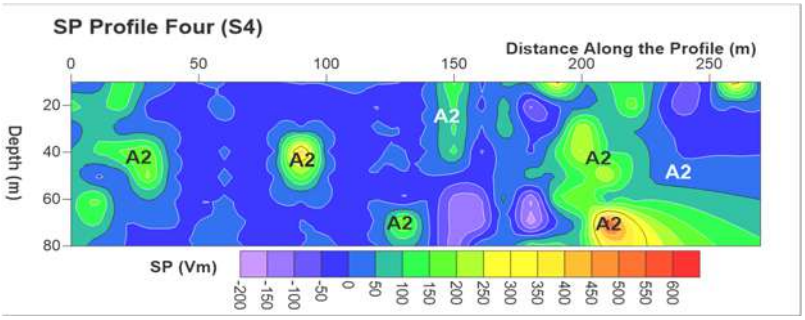

Fig. 16. SP 2D Section for Profile Four (S4)

4.13 Resistivity Model Section for Profile 5 (P5)

The 2D resistivity model section along profile five was given in Fig. 17(a). It covers a lateral distance of 300 m and lies between latitudes 10°47′42″N to 10°47′49.2″N and longitudes 4°44′56.4″E to 4°45′7.2″E (see Fig. 3). The subsurface resistivity signature was categorized as zones **A**, **B**, **C** and **D**. **A** is characterized by resistivity values ranging from 2.99 Ωm to 966 Ωm, it has occupied a length of 5-80 m, 90-105 m, 135-160 m, 170-190 m, 235-50 m and 270-290 m, and a depth/thickness of 7.5 m, 18.5-24.9 m, 7.5-18.5 m, 24.9 m, 18.5-24.9 m and 7.5 m respectively. **B** has resistivity values of 967 Ωm to 4095 Ωm, it covers a length of 10-90 m, 91-120 m, 145-180 m, 190-220 m and 240-270 m at a corresponding depth/thickness of 3-7.5 m, 18.5 m, 12.8 m, 24.9. m, and 18.5 m. **C** is characterized by resistivity values going from 4096 Ωm to 17353 Ωm, it covers the distance along the profile of 120-150 m, 160-175 m, 195-210 m, 220-240 m and 250-270 m, and a depth/thickness of 12.8 m, 18.5-24.9 m, 12.8-18.5 m, 19 m and 7.5-24.9 m respectively. However, zone **D** is portrayed by the resistivity of 17354 Ωm to 73547 Ωm, it has a length of 10-90 m, 110-170 m and 220-235 m at a corresponding depth/thickness of 7.5-24.9 m, 12.8-24.9 m and 12.8-18.5 m, respectively.

The suggested subsurface lithology for features **A**, **B**, **C**, and **D** from Table 1 could be lateritic soil, highly decomposed schist, partially decomposed granite and quartzite, and quartzite/gneiss. Zone **A** is associated with oxidized granite/quartzite and gneiss, and it could ordinarily be related to certain minerals, particularly gold. Zone **C** is also a potential zone for metallic minerals as it formed the dyke structures associated with partially decomposed granite and quartzite. These structures could play a pivotal role in determining the minerals, particularly gold mineralization. These results led to the development of the geologic section as given in Fig. 17(b).

4.14 IP Model Section for Profile 5 (IP5)

Fig. 18 revealed chargeability sections along profile five (IP5). The sections with high chargeability were labeled as zone **A1**. The zones cover a length of 30-45 m, 135-150 m, 140-170 m and 210-240 m and a depth/thickness of 7.5-18.5 m, 18.5-24.9 m, 2.5-18.5 m and 18.5 m respectively. Higher chargeability regions, **A1** (70 msec and above) could occur as a result of the existence of metallic minerals. These regions could be considered as an expected objective for the assessment unequivocal of gold mineralization.

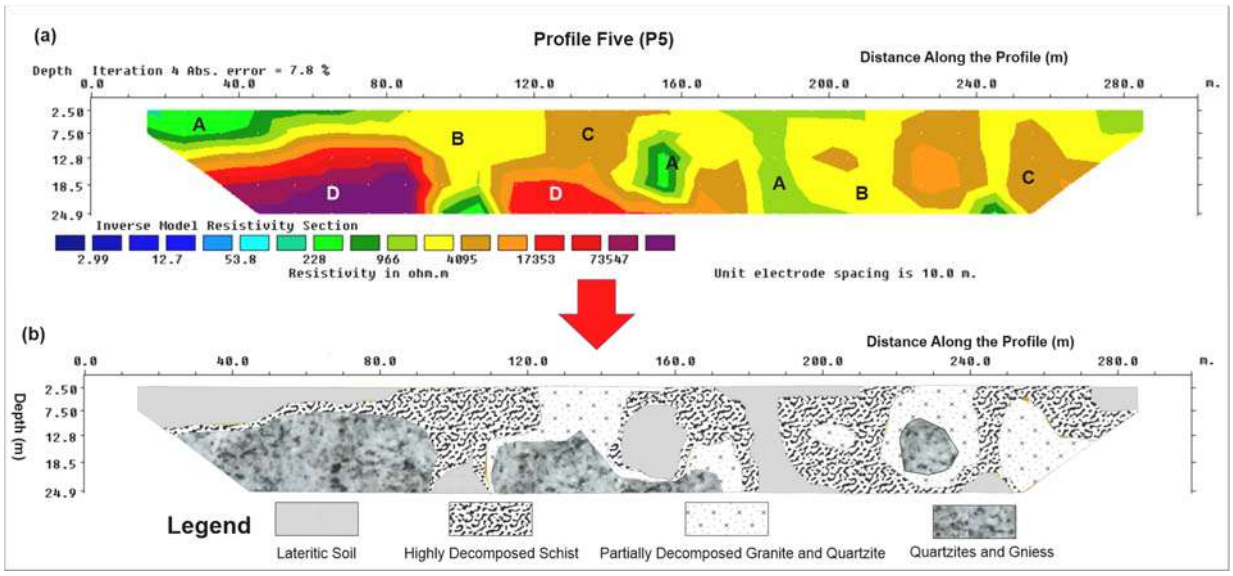

Fig. 17. (a) Inverse Model Resistivity Section and (b) Geologic Section for the Dataset along Profile Five (P5)

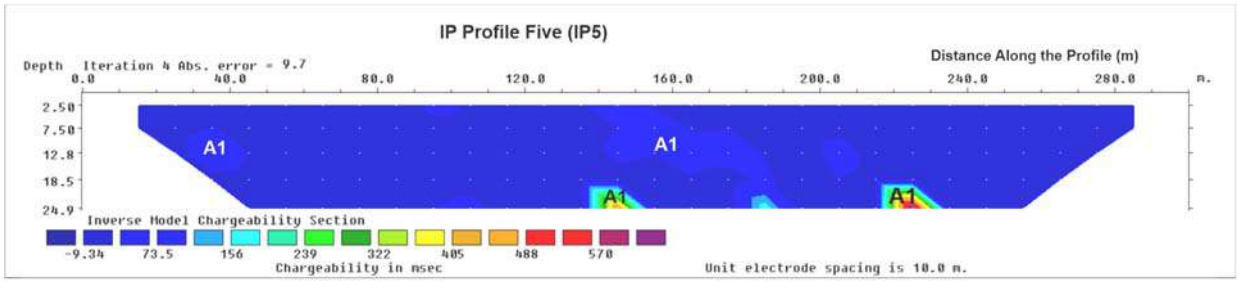

Fig. 18. Inverse Model Chargeability Section for Profile Five (IP5)

4.15 SP Section for Profile 5 (S5)

The results of 2D SP sections along profile five (S5) were given in Fig. 19. The section with high SP values (20 mV and above) was labeled as zone **A2**. These regions occupied a length of 60-80 m, 81-100 m and 140-180 m and a depth of 20-30 m, 45-64 m and 80 m respectively. These areas with high SP values were portrayed by vein-bearing metallic minerals. For that, the veins could be associated with gold mineralization related to the geological setting together with the borehole log of the area.

4.16 Resistivity Model Section for Profile 6 (P6)

Fig. 20(a) shows the 2D resistivity model section along profile six (P6). It is oriented in the NW-SE direction and covers a lateral extent of 300 m. The profile lies between latitudes 11°5′24″N to 11°5′34.8″N and longitudes 4°43′8.4″E to 4°43′19.2″E (see Fig. 3). The subsurface feature was sectionalized into zones **A**, **B**, **C** and **D**. Zone **A** is characterized by resistivity values ranging from 3.86 Ωm to 373 Ωm, it located on 5-45 m and 130-165 m, along the profile and a depth/thickness of 24.9 m and 18.5-24.9 m respectively. **B** has resistivity values of 374 Ωm to 1168 Ωm, it covers a length of 40-45 m, 130-165 m and 240-250 m at a corresponding depth/thickness of 24.9 m, 7.5-18.5 m and 12.8-18.5 m. **C** is characterized by resistivity values going from 41169 Ωm to 3664 Ωm, it covers the distance along the profile of 50-80 m, 120-150 m, 190-210 m and 230-270 m, and a depth/thickness of 24.9 m, 12.8 m, 18.5-24.9 m and 2.5-18.5 m. However, zone **D** is portrayed by the resistivity of 3665 Ωm to 11488 Ωm, it has a length of 50-60 m, 61-72 m, 80-130 m and 132-290 m at a corresponding depth/thickness of 12.8-24.9 m, 2.5-12.8 m, 24.9 m and 24.9 m.

The recommended subsurface lithology for highlights **A**, **B**, **C**, and **D** from Table 1 could be lateritic soil, highly decomposed schist, partially decomposed granite and quartzite, and quartzite/gneiss. Zone **A** is associated with oxidized granite/quartzite and gneiss, and it could ordinarily be related to certain minerals, particularly gold. **C** is also an expected zone for metallic minerals as it formed the dyke structures associated with partially decomposed granite and quartzite. These structures could play a pivotal role in determining the minerals, particularly gold mineralization. The result of the inverse model section given in Fig. 20(a) was further transformed into a geologic section as shown in Fig. 20(b).

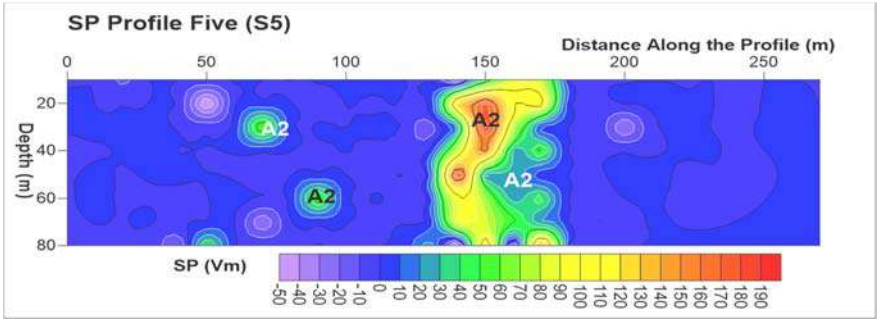

Fig. 19. SP 2D Section for Profile Five (S5)

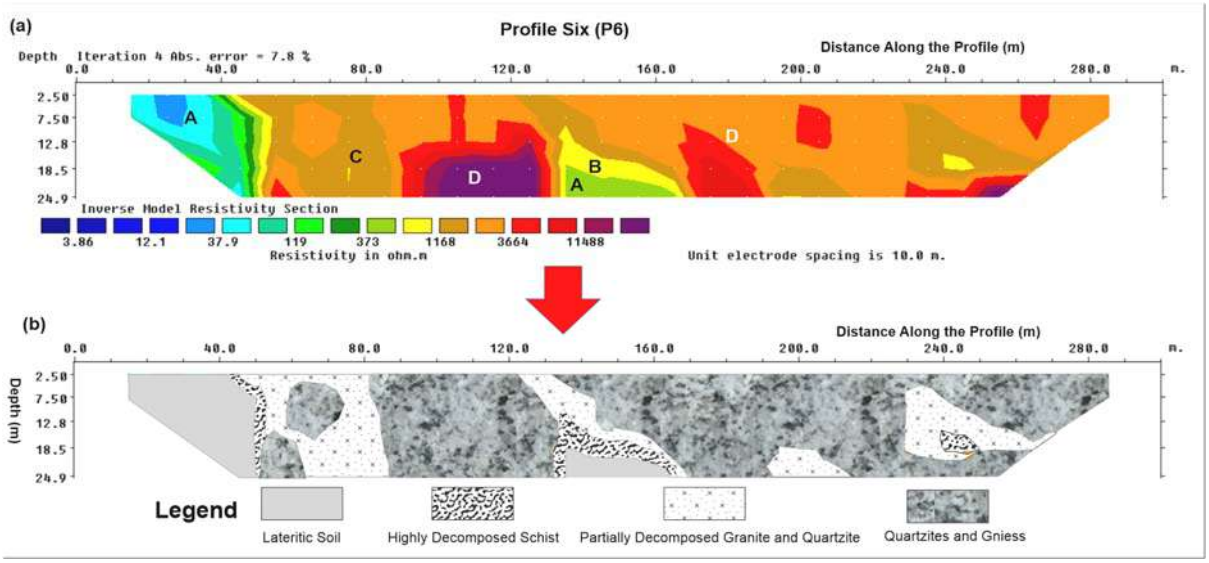

Fig. 20. (a) Inverse Model Resistivity Section and (b) Geologic Section for the Dataset along Profile Six (P6)

4.17 IP Model Section for Profile 6 (IP6)

2D chargeability section along profile six (IP6) was given in Fig. 21. The sections with high chargeability (≥ 20 msec) were labeled as zone **A1**. The zones occupied a length of 40-60 m, 75.5-120 m, 155-180 m and 200-220 m, and a depth/thickness of 12.8 m, 24.9 m, 24.9 m and 12.8 m respectively. Higher chargeability (zones **A1**) could occur as a result of the existence of metallic minerals. These regions could be considered as some of the expected areas for the exploration of gold mineralization.

4.18 SP Section for Profile 6 (S6)

The results of the 2D SP section along profile six (S6) were given in Fig. 22. The section with high SP values (≥20 mV) was labeled as zone **A2**. The zones A2's have a length of 0-50 m, 60-95 m, 110-140 m, 100-134 m, 150-190 m and 191-145 m and a depth/thickness of 80 m, 80 m, 44 m, 60-80 m, 80 m and 20-80 m respectively. The regions of high SP values were portrayed by vein-bearing metallic minerals. These veins could be associated with gold mineralization as compared with the geological setting coupled with the borehole log of the area.

4.2.19 Resistivity Model Section for Profile 7 (P7)

Profile 7 covers a lateral extent of 300 m (Fig. 23a). It is oriented in the NW-SE direction and lies between latitudes 11°5′16.8″N to 11°5′24″N and longitudes 4°43′15.6″E to 4°43′4.8″E (see Figure 3). The subsurface features from Fig. 23(a) could be sectionalized into four: **A**, **B**, **C**, and **D**. Zone **A** is characterized by low resistivity values ranging from 17.5 Ωm to 376 Ωm, it is located on 10-30 m, 45-70 m, 90-120 m, 160-200 m and 250-270 m distance along the profile at a corresponding depth/thickness of 2.5-18.5 m, 7.5-18.5 m, 7.5-18.5 m, 12.8-24.9 m and 7.5-18.5 m respectively. Zone **B** has resistivity features of 377 Ωm to 2912 Ωm, it has a length of 50-90 m and 60-105 m, and a depth/thickness of 12.8 m, 18.5 m and 12.8 m respectively. **C** is characterized by resistivity values ranging from 2913 Ωm to 8099 Ωm, it covers the distance along the profile from 10-40 m, 150-160 m, 190-235 m and 250-290 m and a depth/thickness of 12.8 m, 2.5 m, 12.8 m and 7.5 m respectively. However, zone **D** is characterized by the resistivity of 8100 Ωm to 22527 Ωm, it has a length of 45-90 m, 80-125 m, 00-150 m, and 200-240 m and a depth/thickness of 12.8-24.9 m, 7.5 m, 12.8-24.9 m, and 12.8-24.9 m respectively.

The suggested subsurface lithology for features **A**, **B**, **C**, and **D** from Table 1 could be lateritic soil, highly decomposed schist, partially decomposed granite and quartzite, and quartzite/gneiss. However, low resistivity regions of zone **A** could be a result of water content and weathering in the oxidized rock. Some minerals, particularly gold, could be hosted mostly in a rock corroded by water called oxidized rocks, mainly of granite or rhyolite origin. Zone **C** of partially decomposed granite and quartzite has formed the dyke structures. Dyke subsurface structures of decomposed granite and quartzite usually play a pivotal role in determining the gold mineral. The results of the inverse model section (Fig. 23a) were indicated in the geologic section as given in Fig. 23(b).

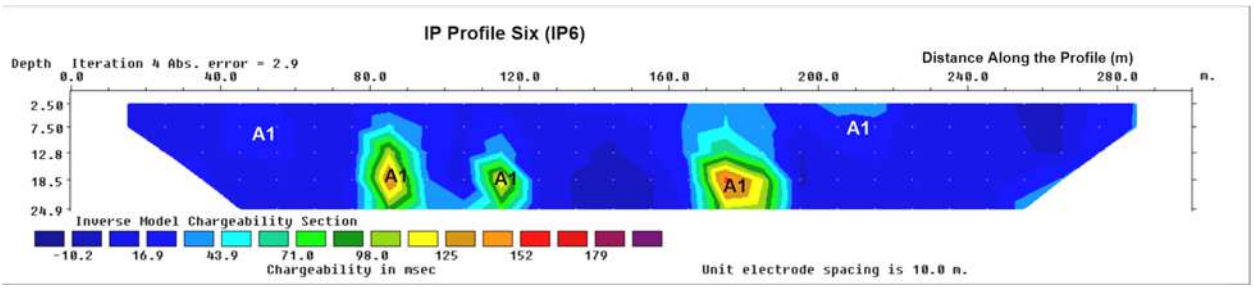

Fig. 21. Inverse Model Chargeability Section for Profile Six (IP6)

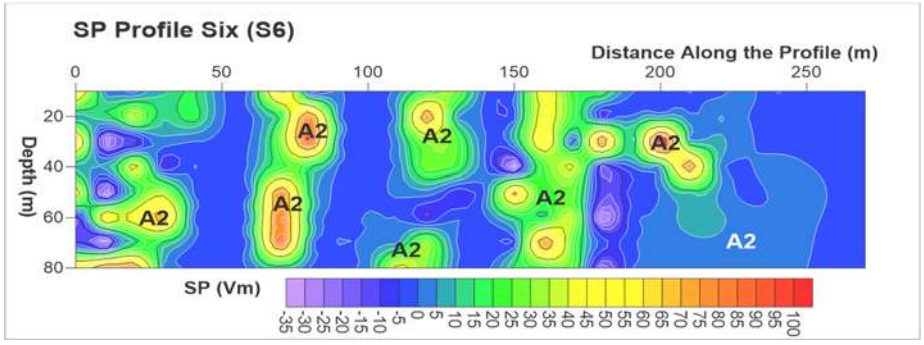

Fig. 22. SP 2D Section for Profile Six (S6)

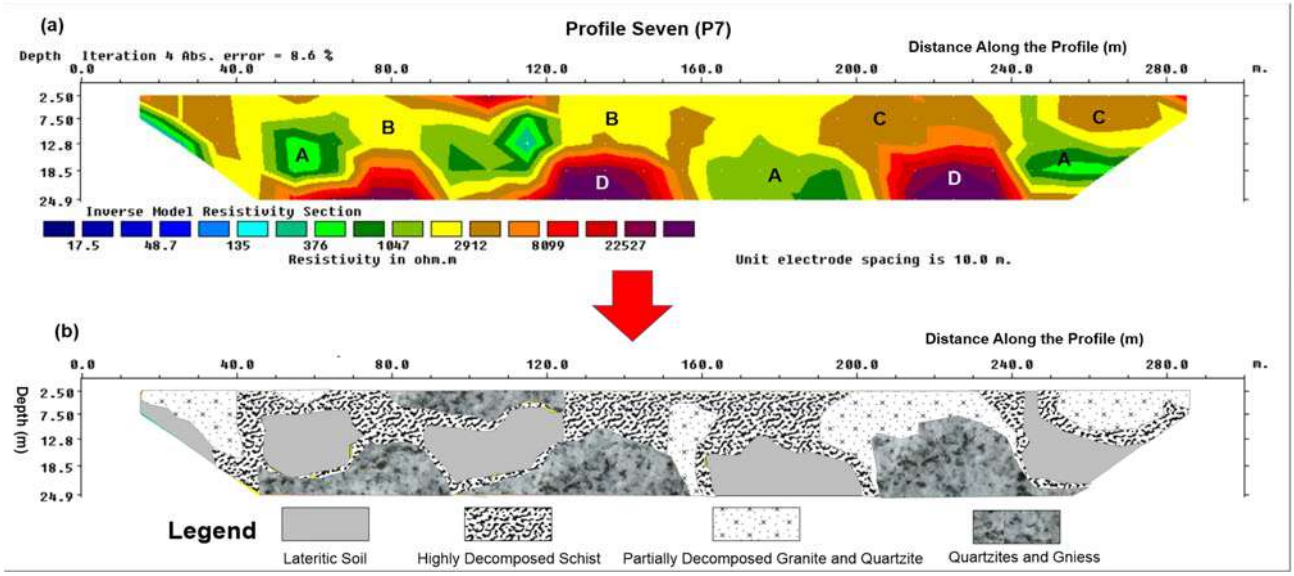

Fig. 23. (a) Inverse Model Resistivity Section and (b) Geologic Section for the Dataset along Profile Seven (P7)

4.2.20 IP Model Section for Profile 7 (IP7)

The 2D chargeability section along profile seven (IP7) was given in Fig. 24. It revealed the zone of high SP values (≥ 61 msec), was labeled as zone **A1.** The zones **A1** cover the lateral extent of 1-60 m, 62-80 m, 70-130 m, 150-190 m, 192-260 m and 265-300 m and a depth/thickness of 24.9 m, 18.5-24.9 m, 24.9 m, 24.9 m,18.5 m and 18.5 m respectively. Higher chargeability regions (zones **A1)** could be considered as an assortment of metallic minerals that could usually occur in a host rock. These areas could be considered potential zones of metallic minerals, particularly gold mineralization.

4.2.21 SP Section for Profile 7 (S7)

Fig. 25 gives the results of 2D SP segments along profile seven (S7). The section with high SP values (≥ 20 mV) was labeled as zone **A2**. It has a length of 1-48 m, 60-125 m, 130-175 m and 200-300 m, and a depth/thickness of 60 m, 80 m, 80 m and 60 m respectively. These regions could be considered as the areas depicted by vein-bearing metallic minerals, such as gold minerals.

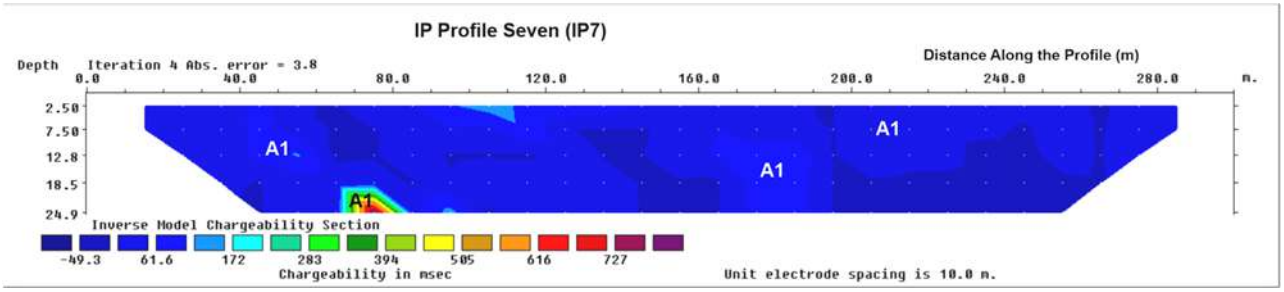

Fig. 24. Inverse Model Chargeability Section for Profile Seven (IP7)

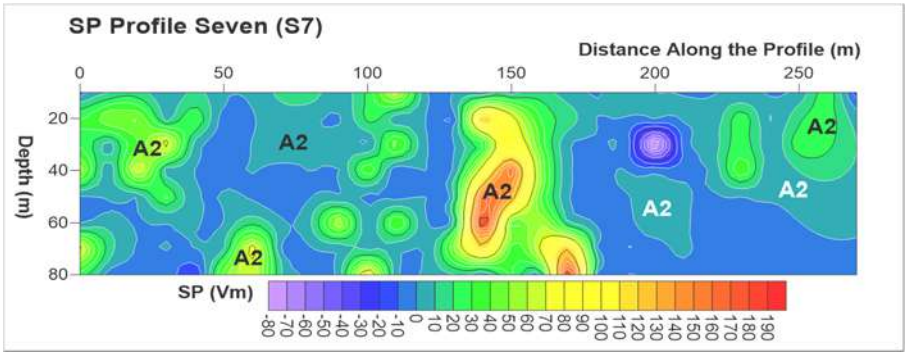

Fig. 25. SP 2D Section for Profile Seven (S7)

Table 2

Summary of results obtained from the integrated methods

Profile	Resistivity Results				Induced polarization Results				Self-Potential Results				Probable gold mineralization potential remarks
	Zone	Resistivity ranges (Ωm)	Lateral lengths (m)	Depth/ Thickness (m)	Zone	Chargeability ranges (msec)	Lateral lengths (m)	Depth/ Thickness (m)	Zone	SP ranges (mV)	Lateral lengths (m)	Depth/ Thickness (m)	
P1	A	117 to 944	5-45, 55-102, 145-165, and 241-285	19, 19-24.9, 19 and 17-24.9	A1	38.4 to 290	120-140, 170-190, 230-260 and 205-290	18.5-24, 12.8, 18.5 and 24.9	A2	20 and above	0-10 55-75 and 120-140	50, 80, and 40	Yes
	B	945 to 7638	50-90 and 60-105	13 and 18.5-20	-	-	-	-	-	-	-	-	No
	C	7639 to 21728	90-165	18.5	-	-	-	-	-	-	-	-	Yes
	D	61815 to 175857	90-140 and 160-250	7.5-24.9 and 24.9	-	-	-	-	-	-	-	-	No
P2	A	113 to 594	10-30, 160-165 and 202-222	12, 24.9 and 2.5	A1	35 and above	35-60, 50-85, 140-175, 110-195, 198-220 and 230-250	12.8-24.9, 12.8, 12.8-24.9, 12.8, 7.5 and 18.5	A2	20 and above	0-54, 50-60, 61-100, 145-155, 160-210 and 115-140	80, 80, 20-65, 40 m, 60, and 80	Yes
	B	1359 to 3112	12-41, 50-80, 110-160, 169-230. 231-249 and 270-285	24.9, 24.9, 12.8, 18.5, 24.9, and 18.5	-	-	-	-	-	-	-	-	No
	C	3113 to 7123	41-50 and 81-120	each 18.5	-	-	-	-	-	-	-	-	Yes
	D	7124 to 37331	41-70, 50-80, 110-160, 169-230, 170-220, 231-249, and 270-285	12-24.9, 7.5-12, 12-24.9, 13.0-24.9 and 250-270	-	-	-	-	-	-	-	-	No
P3	A	1.6 to 459	10-80, 190-200 and 250-265.	12.0, 18.5-24.9 and 7.5-18.5	A1	≥ 20	45-60, 190-202 and 202-255	7.5-18.5, 7.5 and 12.8-24.9	A2	≥ 40	0-40, 50-60, 70-100, 120-200, 140-135, 190-240	70, 21, 21-41, 15, 80 and 21-80	Yes
	B	460 to 1888	30-110, 130-149, 190-200 and 245-265	2.5-18.5, 24.9, 18.5 and 2.5-18.5	-	-	-	-	-	-	-	-	No
	C	1889 to 7773	35-55, 70-92, 105-130, 145-180, 200-210 and 220-270	8-24.9, 3-24.9, 24.9, 24.8, 24.9 and 7.5	-	-	-	-	-	-	-	-	Yes
	D	7774 to 32002	100-125, 175-190, 200-250 and 265-290	7.5-24.9, 12-24.9, 2.5-24.9 and 18.5	-	-	-	-	-	-	-	-	No
P4	A	4.6 to 601	5-40, 165-185, 245-260	7.5, 18.5-24.9 and 18.5-24.9	A1	20 and above	35-65, 55-80, 145-160, 200-220 and 221-250	12.8-24.9, 12.8, 18.5, 7.5 and 7.5-24.9	A2	≥50	1-40, 85-100, 145-200 and 190-250	80, 22-60, 40 and 80	Yes

Profile	Resistivity Results				Induced polarization Results				Self-Potential Results				Probable gold mineralization potential remarks
	Zone	Resistivity ranges (Ωm)	Lateral lengths (m)	Depth/ Thickness (m)	Zone	Chargeability ranges (msec)	Lateral lengths (m)	Depth/ Thickness (m)	Zone	SP ranges (mV)	Lateral lengths (m)	Depth/ Thickness (m)	
	B	602 to 2033	40-90, 120-150, and 155-190	12, 7.5 and 18.5-24.9	-	-	-	-	-	-	-	-	No
	C	2034 to 6873	10-90, 95-120, 140-170, 180-205, 240-270	2.5-12.8, 24.9, 12.8, 12.8 and 18.5	-	-	-	-	-	-	-	-	Yes
	D	6874 to 23241	10-105, 115-155, 170-180, 200-245, and 270-290	7.5-24.9, 7.5-24.9, 12.8, 24.9 and 18.5	-	-	-	-	-	-	-	-	No
P5	A	2.99 to 966	5-80, 90-105, 135-160, 170-190, 235-50 and 270-290	7.5, 18.5-24.9, 7.5-18.5, 24.9, 18.5-24.9 and 7.5	A1	70 and above	30-45, 135-150, 140-170 and 210-240	7.5-18.5, 18.5-24.9, 2.5-18.5 and 18.5	A2	20 and above	60-80, 81-100 and 140-180	20-30, 45-64 and 80	Yes
	B	967 to 4095	10-90, 91-120, 145-180, 190-220 and 240-270	3-7.5, 18.5, 12.8, 24.9, and 18.5	-	-	-	-	-	-	-	-	No
	C	4096 to 17353	120-150, 160-175, 195-210, 220-240 and 250-270	12.8, 18.5-24.9, 12.8-18.5, 19 and 7.5-24.9	-	-	-	-	-	-	-	-	Yes
	D	17354 to 73547	10-90, 110-170 and 220-235	7.5-24.9, 12.8-24.9 and 12.8-18.5	-	-	-	-	-	-	-	-	No
P6	A	3.86 to 373	5-45 and 130-165	24.9 and 18.5-24.9	A1	≥ 20	40-60, 75.5-120, 155-180 and 200-220	12.8, 24.9, 24.9 and 12.8	A2	≥20	0-50, 60-95, 110-140, 100-134, 150-190 and 191-145	80, 80, 44, 60-80, 80 and 20-80	Yes
	B	374 to 1168	40-45, 130-165 and 240-250	24.9, 7.5-18.5 and 12.8-18.5	-	-	-	-	-	-	-	-	No
	C	41169 to 3664	50-80, 120-150, 190-210 and 230-270	24.9, 12.8, 18.5-24.9 and 2.5-18.5	-	-	-	-	-	-	-	-	Yes
	D	3665 to 11488	50-60, 61-72, 80-130 and 132-290	12.8-24.9, 2.5-12.8, 24.9, 24.9	-	-	-	-	-	-	-	-	No
P7	A	17.5 to 376	10-30, 45-70, 90-120, 160-200 and 250-270	2.5-18.5, 7.5-18.5, 7.5-18.5, 12.8-24.9 and 7.5-18.5	A1	≥ 61	1-60, 62-80, 70-130, 150-190, 192-260 and 265-300	24.9, 18.5-24.9, 24.9, 24.9, 18.5 and 18.5	A2	≥ 20	1-48, 60-125, 130-175 and 200-300	60, 80, 80 and 60	Yes
	B	377 to 2912	50-90 and 60-105	12.8, 18.5 and 12.8	-	-	-	-	-	-	-	-	No
	C	2913 to 8099	10-40, 150-160, 190-235 and 250-290	12.8, 2.5, 12.8 and 7.5	-	-	-	-	-	-	-	-	Yes
	D	8100 to 22527	45-90, 80-125, 00-150, and 200-240	12.8-24.9, 7.5, 12.8-24.9, 12.8-24.9	-	-	-	-	-	-	-	-	No

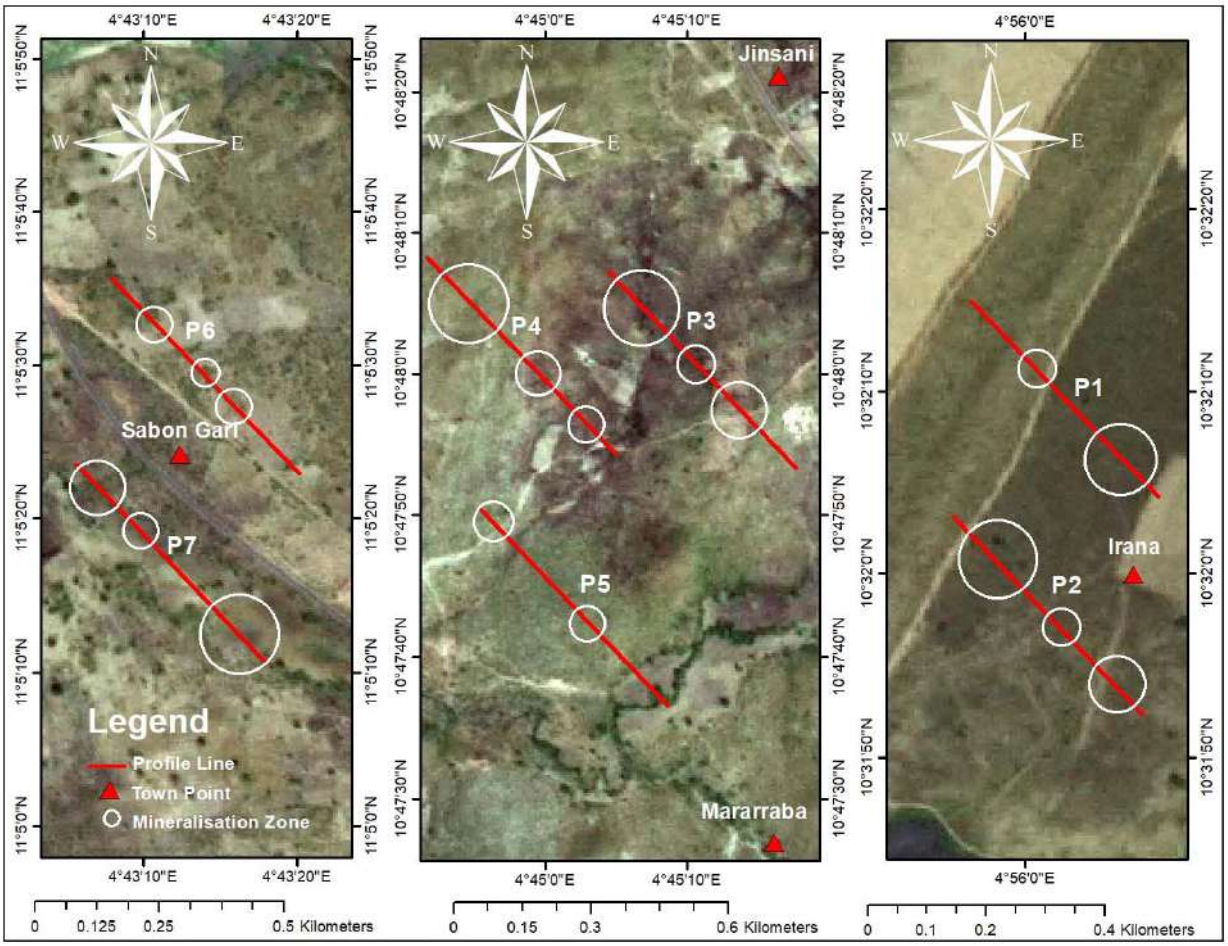

Fig. 26. Potential mineralization zones of the study areas

5. Discussion

5.1 Integrated results for profile one

The zones of potential mineralization were revealed within the regions of low (117 Ωm to 944 Ωm) and high (61815 Ωm to 175857 Ωm) resistivity in the resistivity cross sections along profile one (Fig. 5). Low resistivity anomalous areas (zones **A**) were corresponding to oxidized rock. These rock types are corroded by water and were mainly of granite or rhyolite origin. These regions could generally be associated with explicit minerals, particularly gold, while the regions with high resistivity signatures (zone **C**) formed dyke structures. These structures were associated with partially decomposed granite and quartzite as compared with the geological setting/borehole log of the area.

However, these zones for potential mineralization occurred within the zones of high chargeability of ≥ 20 msec in the IP cross sections (see Fig. 6), as well as occurred in the regions of high SP anomalies of 20 mV and above (Fig. 7). These areas revealed the presence of sulphide-containing gold.

The major zones of mineral potentials are located between 120-140 m and 230-290 m with a corresponding depth of 24.9 m each. These regions are **A** and **C** (Fig. 5), **A1** (Fig. 6) and **A2** (Fig. 7) of the low/or high resistivity, high chargeability and high SP values. The zones could be inferred to contain traces of minerals in their respective host rocks. These regions could be considered as a potential target for the exploration of metallic minerals such as gold mineralization. These areas corresponded to the northern part of Irana of Niger state (see Fig. 26).

5.2 Integrated results for profile two

Profile two shows the suggested zones of mineralization potential to occur at zones **A** and **C**, **A1** and **A2**. These zones were the areas of low/or high resistivity (zones **A** and **C**), high chargeability **A1**), and high SP (**A2**) anomalous as shown in Fig's 8, 9 and 10. The major zones of mineral potentials are suggested to be between 35-62 m, 41-120 m, 145-165 m and 202-240 m with a corresponding depth of 24.9 m, 18.5 m, 24.9 m and 18.5 m. The zones could be inferred to contain traces of minerals in their respective host rocks. These areas could be considered as a possible target for the exploration of metallic minerals, particularly, gold minerals. These regions corresponded to the SW part of Irana of Niger state (Fig. 26).

5.3 Integrated results for profile three

The suggested zones of mineralization potential along profile three are zone **A** and **C**, **A1** and **A2**. These regions are characterized by low/high resistivity, high chargeability and high SP anomalous (Fig's 11, 12 and 14). The major zones of mineral potentials are suggested to be between 10-80 m, 190-200 m and 202-255 m with a corresponding depth of 18.5 m, 24.9 m and 24.9 m. The zones could be inferred as a potential target for the exploration of metallic minerals, particularly gold mineralization. These areas corresponded to the northern part of Mararraba and SW of Jinsani areas of Kebbi state (Fig. 26).

5.4 Integrated results for profile four

Profile four shows the suggested zones of mineralization potential to occur at zone **A** and **C**, **A1** and **A2**. These zones were the areas of low/or high resistivity (zones **A** and **C**), high chargeability **A1**), and high SP (**A2**) anomalous as shown in Fig's 14, 15 and 16. The major zones of mineral potentials are suggested to be between 35-100 m, 145-200 m and 220-250 m with a corresponding depth of 12.8 m, 18.5 m and 24.9 m. The zones could be inferred to contain traces of minerals in their respective host rocks. These areas could be considered as a possible target for the exploration of metallic minerals, particularly gold minerals. These regions corresponded to the NW part of Mararraba and SW of Jinsani areas of Kebbi state (Fig. 26).

5.5 Integrated results for profile five

The suggested zones of mineral potential occurred at zones **A** and **C** (Fig. 17), **A1** (Fig. 18) and **A2** (Fig. 19). The zones were characterized by low/high resistivity, high chargeability and high SP anomalous. The integrated zones of mineral potentials are suggested to be between 0-45 m and 140-180 m with a corresponding depth of 18.5 m and 28.5 m. The zones could be inferred as a potential target for the exploration of metallic minerals, particularly gold mineralization. These regions corresponded to the NW part of the Mararraba area of Kebbi state (Fig. 26).

5.6 Integrated results for profile six

For profile six, the suggested zone for mineral trapping structure/ or mineralization potential was named zone **A&C**, **A1** and **A2** (Fig's 20, 21&22). The critical zones for mineralization prospects were found to be between 60-95 m, 110-140 m and 150-190 m at a corresponding depth of 7.5-60 m, 18.5-40 m and 2.5-80 m. These regions could be considered a potential target area for assessing metallic minerals, particularly gold mineralization. These zones corresponded to the northern part of the Sabon Gari area of Kebbi state (Fig. 26).

5.7 Integrated results for profile seven

The suggested zones of mineral potential occurred at zones **A&C** (Fig. 23), **A1** (Fig. 24) and **A2** (Fig. 25). The zones were characterized by low/high resistivity, high chargeability and high SP anomalous. The integrated zones of mineral potentials are suggested to be between 1-60 m, 130-170 m and 200-300 m with a corresponding depth of 45 m, 2.5-7.5 m and 18.5 m. The zones could be inferred as a potential target for the exploration of metallic minerals, particularly gold mineralization. These regions corresponded to the southern part of the Sabon Gari area of Kebbi state (Fig. 26).

6. Conclusions

Integrated 2D geoelectric prospecting methods involves of ERT, IP and SP techniques were employed as a follow-up details geophysical survey tools on the anomalous zones detected from the aeromagnetic studied by Authors: Augie et al. (2021b), (2022b) and (2022c). The anomalous detected by earlier studies conducted by the aforementioned Author revealed the major structures (lineament) associated with mineralization potential which could play an important role in gold exploration and exploitation in the area. These areas were found to be SE parts of Yauri and Shanga, Fakai, Ngaski, Zuru, Magama, Rijau, Eastern part of Wasagu/Danko and Bukkuyum. However, this study details a geophysical survey conducted at Yauri (Jinsani and Mararraba), Shanga (Sabon Gari) and Magama (Irana). A total of 7 profiles were designed using a dipole-pole configuration with each 300 m distance along the profile. Profiles 1 and 2 were conducted at Magama (Irana), profiles 3 and 4 at Shanga (Sabon Gari) and profiles 5, 6 and 7 at Yauri (Jinsani and Mararraba).

The results of profiles 1, 2, 3, 4, 5, 6 and 7 revealed the region's low/or high resistivity, high chargeability and high SP values that were inferred as zones for mineral potential. Low resistivity anomalous (zones **A**) corresponds to oxidised rocks associated with granite/quartzite veins. The regions with high resistivity signatures (zones **C**) formed dyke structures associated with partially decomposed granite and quartzite as compared with the geological setting and the borehole log of the area. These zones for potential mineralization coincided with the zones of high chargeability (≥ 20 msec) in the IP cross sections as well as the regions of high SP anomalies (20 mV and above).

The major zones of mineral potentials found in this study along the integrated profile one P1 are to be 35-62 m, 41-120 m, 145-165 m and 202-240 m at a corresponding depth/thickness of 24.9 m, 18.5 m, 24.9 m and 18.5 m. Potential mineralized zone for profile two P2 lies between 35-62 m, 41-120 m, 145-

165 m and 202-240 m at a corresponding depth of 24.9 m, 18.5 m, 24.9 m and 18.5 m. Likewise, P3 has a length of 10-80 m, 190-200 m and 202-255 m, and a depth/thickness of 18.5 m, 24.9 m and 24.9 m. Integrated profile four also revealed the lateral extent of 35-100 m, 145-200 m and 220-250 m at a corresponding depth/thickness of 12.8 m, 18.5 m and 24.9 m. P5 also is between 0-45 m and 140-180 m at a corresponding depth/thickness of 18.5 m and 28.5 m. P6 has a length of 60-95 m, 110-140 m and 150-190 m and it has a depth/thickness of 7.5-60 m, 18.5-40 m and 2.5-80 m respectively. And P4 reveals the lateral extent of 1-60 m, 130-170 m and 200-300 m with a corresponding depth of 45 m, 2.5-7.5 m and 18.5 m. These regions could be considered as a possible pathway for gold exploration and exploitation. These areas corresponded to the northern part of Irana, the SW part of Irana, the northern part of Mararraba, the NW part of Marrarba, the SW part of Jinsani, and the northern part of Sabon Gari and the southern part of Sabon Gari areas of Niger and Kebbi state.

Acknowledgements

The authors are grateful to the Tertiary Education Fund (Tetfund) for funding this research.

Thanks to the district heads of Mararraba, Sabon Gari and Irana of Kebbi and Niger states for approval and for facilitating geophysical data collection. Their appreciation also goes to the department of Physics, Bayero University Kano and the department of Geophysics, Federal University of Technology Minna for providing the instruments.

REFERENCES

Amoah B.K., Dadzie I., Takyi-kyeremeh K. Integrating gravity and magnetic field data to delineate structurally controlled gold mineralization in the Sefwi Belt of Ghana. Journal of Geophysics and Engineering, Vol. 15, No. 4, 2018, pp. 1197-1203, https://doi.org/10.1088/1742-2140/aaa7b2.

Augie A.I. and Ridwan M.M. Delineation of potential mineral zones from aeromagnetic data over eastern part of Zamfara. Savanna Journal of Basic and Applied Sciences, Vol. 3, No.1, 2021, pp. 60-66.

Augie A.I. and Sani A.A. Interpretation of aeromagnetic data for gold mineralization potential over Kabo and its environs NW Nigeria. Savanna Journal of Basic and Applied Sciences, Vol. 2, No. 2, 2020, pp. 116-123.

Augie A.I., Adamu A., Salako K.A., Alkali A., Narimi A.M., Yahaya M.N., Sani A.A. Assessment for gold mineralization potential over Anka schist belts NW Nigeria using aeromagnetic data. FUDMA Journal of Sciences (FJS), Vol. 5, No. 4, 2021a, pp. 235-242.

Augie A.I., Salako K.A., Rafiu A.A., Jimoh M.O. Estimation of depth to structures associated with gold mineralization potential over southern part of Kebbi state using aeromagnetic data. 3rd School of Physical Sciences Biennial International Conference Futminna 2021, Federal University of Technology Minna, 2021b, pp. 290-297.

Augie A.I., Salako K.A., Rafiu A.A., Jimoh M.O. Geophysical assessment for gold mineralization potential over the southern part of Kebbi state using aeromagnetic data. Geology, Geophysics and Environment, Vol. 48, No. 2, 2022b, pp. 177-193, https://doi.org/10.7494/geol.2022.48.2.177.

Augie A.I., Salako K.A., Rafiu A.A., Jimoh M.O. Geophysical magnetic data analyses of the geological structures with mineralization potentials over the southern part of Kebbi, NW Nigeria. Mining Science, Vol. 29, 2022c, pp. 179-203, https://doi.org/10.37190/msc222911.

Augie A.I., Saleh M., Ologe O., Salako K.A., Rafiu A.A., Yahaya M.N. Correlation of 2D electrical resistivity and self-potential methods for the assessment of the integrity of Goronyo dam NW Nigeria. Chiang Mai University Journal of Natural Sciences, Vol. 21, No. 3, 2022a, e2022043, https://doi.org/ 10.12982/CMUJNS.2022.043.

Bagare A.A., Saleh M., Aku M.O., Abdullahi Y.M. 2D electrical study to delineate subsurface structures and potential mineral zones at Alajawa artisanal mining site Kano state Nigeria. Journal of the Nigerian Geophysical Society, Vol. 1, No. 1, 2018, pp. 24-32.

ЛИТЕРАТУРА

Amoah B.K., Dadzie I., Takyi-kyeremeh K. Integrating gravity and magnetic field data to delineate structurally controlled gold mineralization in the Sefwi Belt of Ghana. Journal of Geophysics and Engineering, Vol. 15, No. 4, 2018, pp. 1197-1203, https://doi.org/10.1088/1742-2140/aaa7b2.

Augie A.I. and Ridwan M.M. Delineation of potential mineral zones from aeromagnetic data over eastern part of Zamfara. Savanna Journal of Basic and Applied Sciences, Vol. 3, No.1, 2021, pp. 60-66.

Augie A.I. and Sani A.A. Interpretation of aeromagnetic data for gold mineralization potential over Kabo and its environs NW Nigeria. Savanna Journal of Basic and Applied Sciences, Vol. 2, No. 2, 2020, pp. 116-123.

Augie A.I., Adamu A., Salako K.A., Alkali A., Narimi A.M., Yahaya M.N., Sani A.A. Assessment for gold mineralization potential over Anka schist belts NW Nigeria using aeromagnetic data. FUDMA Journal of Sciences (FJS), Vol. 5, No. 4, 2021a, pp. 235-242.

Augie A.I., Salako K.A., Rafiu A.A., Jimoh M.O. Estimation of depth to structures associated with gold mineralization potential over southern part of Kebbi state using aeromagnetic data. 3rd School of Physical Sciences Biennial International Conference Futminna 2021, Federal University of Technology Minna, 2021b, pp. 290-297.

Augie A.I., Salako K.A., Rafiu A.A., Jimoh M.O. Geophysical assessment for gold mineralization potential over the southern part of Kebbi state using aeromagnetic data. Geology, Geophysics and Environment, Vol. 48, No. 2, 2022b, pp. 177-193, https://doi.org/10.7494/geol.2022.48.2.177.

Augie A.I., Salako K.A., Rafiu A.A., Jimoh M.O. Geophysical magnetic data analyses of the geological structures with mineralization potentials over the southern part of Kebbi, NW Nigeria. Mining Science, Vol. 29, 2022c, pp. 179-203, https://doi.org/10.37190/msc222911.

Augie A.I., Saleh M., Ologe O., Salako K.A., Rafiu A.A., Yahaya M.N. Correlation of 2D electrical resistivity and self-potential methods for the assessment of the integrity of Goronyo dam NW Nigeria. Chiang Mai University Journal of Natural Sciences, Vol. 21, No. 3, 2022a, e2022043, https://doi.org/ 10.12982/CMUJNS.2022.043.

Bagare A.A., Saleh M., Aku M.O., Abdullahi Y.M. 2D electrical study to delineate subsurface structures and potential mineral zones at Alajawa artisanal mining site Kano state Nigeria. Journal of the Nigerian Geophysical Society, Vol. 1, No. 1, 2018, pp. 24-32.

Bonde D.S., Lawali S., Salako K.A. Structural mapping of solid mineral potential zones over southern part of Kebbi state, northwestern Nigeria. Journal of Scientific and Engineering Research, Vol. 6, No. 7, 2019, pp. 229-240.

Dahlin T., Zhou B. A numerical comparison of 2D resistivity imaging with 10 electrode arrays. Geophysical Prospecting, Vol. 52, 2004, pp. 379-398.

Danbatta U.A. Precambrian crustal development in the northwestern part of Zuru schist belt, northwestern Nigeria. Journal of Mining and Geology, Vol. 44, No. 1, 2008, pp. 43-56.

Danbatta U.A. Precambrian crustal development of the northwestern part of Zuru schist belt, NW Nigeria. A paper presented at the 41st annual conference of Nigerian mining, and geosciences society (NMGS), 2005, Abstr., p. 13.

Danjumma S.G., Bonde D.S., Mohammed A., Lawali S., Birnin Tudu A.M. Identification of mineral deposits in Garin Awwal mining site, Kebbi state, north-western Nigeria. Journal of Multidisciplinary Engineering Science and Technology (JMEST), Vol. 6, No. 6, 2019, pp. 10276-10280.

Ejepu J.S., Unuevho C.I., Agbor A.T., Abdullahi S. Integrated geosciences prospecting for gold mineralization in Kwakuti north-central Nigeria. Journal of Geology and Mining, Vol. 10, No. 7, 2018, pp. 81-94, https://doi.org/10.5897/JGMR 2018.0296.

Fedi M. and Abbas M.A. A fast interpretation of self-potential data using the depth from extreme points method. Geophysics, Vol. 78, No. 2, 2012, pp. 107-116.

Jamaluddeen S.S., Bunawa A.A., Saleh M. An assessment of the groundwater potential of Bayero University Kano Permanent Site using induced polarization and self-potential methods. Journal of Earth science and Engineering, Vol. 4, 2014, pp. 587-596.

Lawal M.M., Salako K.A., Abbas M., Adewumi T., Augie A.I., Khita M. Geophysical investigation of possible gold mineralization potential zones using a combined airborne magnetic data of lower Sokoto basin and its environs northwestern Nigeria. International Journal of Progressive Sciences and Technologies (IJPSAT), Vol. 30, No. 1, 2021, pp. 01-16.

Lawali S., Salako K.A., Bonde D.S. Delineation of mineral potential zones over lower part of Sokoto basin, northwestern Nigeria using aeromagnetic data. Academic Research International, Vol. 11, No. 2, 2020, pp. 19-29.

Lobo-Guerrero A. Application of spontaneous potential profiles for exploration of gold-rich epithermal low sulphidation veins in a humid region. Geoscience Africa 2004, Conference organized by the Geological Society of South Africa in Johannesburg, University of the Witwatersrand, Johannesburg, 2004.

Loke H.M. and Barker R.D. Rapid least-square inversion of apparent resistivity pseudosections. Geophysical Prospecting, Vol. 44(1), 1996, pp. 131-152**,** DOI:10.1111/j.1365-2478. 1996.tb00142.x.

Loke H.M. Tutorial: 2-D and 3-D electrical imaging surveys. Revised edition; 26th July 2004, 128 p.

Oduduru P.I. and Mamah L.I. Integration of electrical resistivity and induced polarization for subsurface imaging around Ihe pond, Nsukka, Anambra basin, Nigeria. Pacific Journal of Science and Technology, Vol. 15, No. 1, 2014, pp. 306-317.

Olalekan O., Afees O., Ayodele S. An Empirical analysis of the contribution of mining sector to economic development in Nigeria. Khazar Journal of Humanities and Social Sciences, Vol. 19, No. 1, 2016, pp. 88-106.

Olugbenga T.T. and Augie A.I. Estimation of crustal thickness within the Sokoto basin north-western Nigeria using Bouguer gravity anomaly data. WASET, International Journal of Geological and Environmental Engineering, Vol. 14, No. 9, 2020, 247–252.

Osazuwa I.B. and Chii E.C. Two-dimensional electrical resistivity survey around the periphery of an artificial lake in

Bonde D.S., Lawali S., Salako K.A. Structural mapping of solid mineral potential zones over southern part of Kebbi state, northwestern Nigeria. Journal of Scientific and Engineering Research, Vol. 6, No. 7, 2019, pp. 229-240.

Dahlin T., Zhou B. A numerical comparison of 2D resistivity imaging with 10 electrode arrays. Geophysical Prospecting, Vol. 52, 2004, pp. 379-398.

Danbatta U.A. Precambrian crustal development in the northwestern part of Zuru schist belt, northwestern Nigeria. Journal of Mining and Geology, Vol. 44, No. 1, 2008, pp. 43-56.

Danbatta U.A. Precambrian crustal development of the northwestern part of Zuru schist belt, NW Nigeria. A paper presented at the 41st annual conference of Nigerian mining, and geosciences society (NMGS), 2005, Abstr., p. 13.

Danjumma S.G., Bonde D.S., Mohammed A., Lawali S., Birnin Tudu A.M. Identification of mineral deposits in Garin Awwal mining site, Kebbi state, north-western Nigeria. Journal of Multidisciplinary Engineering Science and Technology (JMEST), Vol. 6, No. 6, 2019, pp. 10276-10280.

Ejepu J.S., Unuevho C.I., Agbor A.T., Abdullahi S. Integrated geosciences prospecting for gold mineralization in Kwakuti north-central Nigeria. Journal of Geology and Mining, Vol. 10, No. 7, 2018, pp. 81-94, https://doi.org/10.5897/JGMR 2018.0296.

Fedi M. and Abbas M.A. A fast interpretation of self-potential data using the depth from extreme points method. Geophysics, Vol. 78, No. 2, 2012, pp. 107-116.

Jamaluddeen S.S., Bunawa A.A., Saleh M. An assessment of the groundwater potential of Bayero University Kano Permanent Site using induced polarization and self-potential methods. Journal of Earth science and Engineering, Vol. 4, 2014, pp. 587-596.

Lawal M.M., Salako K.A., Abbas M., Adewumi T., Augie A.I., Khita M. Geophysical investigation of possible gold mineralization potential zones using a combined airborne magnetic data of lower Sokoto basin and its environs northwestern Nigeria. International Journal of Progressive Sciences and Technologies (IJPSAT), Vol. 30, No. 1, 2021, pp. 01-16.

Lawali S., Salako K.A., Bonde D.S. Delineation of mineral potential zones over lower part of Sokoto basin, northwestern Nigeria using aeromagnetic data. Academic Research International, Vol. 11, No. 2, 2020, pp. 19-29.

Lobo-Guerrero A. Application of spontaneous potential profiles for exploration of gold-rich epithermal low sulphidation veins in a humid region. Geoscience Africa 2004, Conference organized by the Geological Society of South Africa in Johannesburg, University of the Witwatersrand, Johannesburg, 2004.

Loke H.M. and Barker R.D. Rapid least-square inversion of apparent resistivity pseudosections. Geophysical Prospecting, Vol. 44(1), 1996, pp. 131-152**,** DOI:10.1111/j.1365-2478. 1996.tb00142.x.

Loke H.M. Tutorial: 2-D and 3-D electrical imaging surveys. Revised edition; 26th July 2004, 128 p.

Oduduru P.I. and Mamah L.I. Integration of electrical resistivity and induced polarization for subsurface imaging around Ihe pond, Nsukka, Anambra basin, Nigeria. Pacific Journal of Science and Technology, Vol. 15, No. 1, 2014, pp. 306-317.

Olalekan O., Afees O., Ayodele S. An Empirical analysis of the contribution of mining sector to economic development in Nigeria. Khazar Journal of Humanities and Social Sciences, Vol. 19, No. 1, 2016, pp. 88-106.

Olugbenga T.T. and Augie A.I. Estimation of crustal thickness within the Sokoto basin north-western Nigeria using Bouguer gravity anomaly data. WASET, International Journal of Geological and Environmental Engineering, Vol. 14, No. 9, 2020, 247–252.

Osazuwa I.B. and Chii E.C. Two-dimensional electrical resistivity survey around the periphery of an artificial lake in

the Precambrian basement complex of northern Nigeria. International Journal of Physical Science, Vol. 5, No. 3, 2010, pp. 238-245.

Ramadan T.M. and Abdel-Fattah M.F. Characterization of gold mineralization in Garin Hawal area, Kebbi state, NW Nigeria using remote sensing. Egyptian Journal of Remote Sensing and Space Science, Vol. 13, No. 2, 2010, pp. 153-163, https://doi.org/10.1016/j.ejrs.2009.08.001.

Sani A.A., Augie A.I., Aku M.O. Analysis of gold mineral potentials in Anka schist belt north western Nigeria using aeromagnetic data interpretation. Journal of the Nigerian Association of Mathematical Physics, Vol. 52, 2019, pp. 291-298.

SARDA – Sokoto agricultural and rural development authority: Sokoto Fadama. Ministry of Solid Minerals Kebbi State, book, 1988.

Shao P., Shang Y., Hasan M., Yi X., Meng H. Integration of ERT, IP and SP methods in hard rock engineering. Applied Sciences, Vol. 11, 2021, 10752. https://doi.org/10.3390/app1122 10752.

Srigutomo W., Trimadona P., Pratomo M. 2D resistivity and induced polarization measurement for manganese ore exploration. Journal of Physics: Conference Series 739, 2016, 012138, https://doi.org/10.1088/1742-6596/739/1/012138.

Telford W.M., Geldart L.P., Sheriff R.E. Applied Geophysics second edition. Cambridge university press. Cambridge, 1990, 744 p.

Unuevho C.I., Amadi A.N., Saidu S., Udensi E.E., Onuoha K.M., Ogunbajo M.I. Geo-electrical prospecting for ore minerals in Kundu western part of Zungeru sheet 163 NW Nigeria. Nigerian Mining Journal, Vol. 14, No. 2, 2016, pp. 73-82.

the Precambrian basement complex of northern Nigeria. International Journal of Physical Science, Vol. 5, No. 3, 2010, pp. 238-245.

Ramadan T.M. and Abdel-Fattah M.F. Characterization of gold mineralization in Garin Hawal area, Kebbi state, NW Nigeria using remote sensing. Egyptian Journal of Remote Sensing and Space Science, Vol. 13, No. 2, 2010, pp. 153-163, https://doi.org/10.1016/j.ejrs.2009.08.001.

Sani A.A., Augie A.I., Aku M.O. Analysis of gold mineral potentials in Anka schist belt north western Nigeria using aeromagnetic data interpretation. Journal of the Nigerian Association of Mathematical Physics, Vol. 52, 2019, pp. 291-298.

SARDA – Sokoto agricultural and rural development authority: Sokoto Fadama. Ministry of Solid Minerals Kebbi State, book, 1988.

Shao P., Shang Y., Hasan M., Yi X., Meng H. Integration of ERT, IP and SP methods in hard rock engineering. Applied Sciences, Vol. 11, 2021, 10752. https://doi.org/10.3390/app1122 10752.

Srigutomo W., Trimadona P., Pratomo M. 2D resistivity and induced polarization measurement for manganese ore exploration. Journal of Physics: Conference Series 739, 2016, 012138, https://doi.org/10.1088/1742-6596/739/1/012138.

Telford W.M., Geldart L.P., Sheriff R.E. Applied Geophysics second edition. Cambridge university press. Cambridge, 1990, 744 p.

Unuevho C.I., Amadi A.N., Saidu S., Udensi E.E., Onuoha K.M., Ogunbajo M.I. Geo-electrical prospecting for ore minerals in Kundu western part of Zungeru sheet 163 NW Nigeria. Nigerian Mining Journal, Vol. 14, No. 2, 2016, pp. 73-82.

КОМПЛЕКСНАЯ 2D ГЕОЭЛЕКТРИЧЕСКАЯ РАЗВЕДКА ДЛЯ ПОИСКА ПОТЕНЦИАЛЬНО ЗОЛОТОНОСНОЙ МИНЕРАЛИЗАЦИИ В ЮЖНОЙ ЧАСТИ КЕББИ, СЕВЕРО-ЗАПАД НИГЕРИИ

Оги А.[1,2], Салако К.А.[2], Рафиу А.А.[2], Химо М.О.[3]

[1]*Факультет прикладной геофизики, Федеральный университет Бирнин Кебби, Нигерия: ai.augie@fubk.edu.ng*

[2]*Факультет геофизики, Федеральный технологический университет Минны, Нигерия*

[3]*Факультет геологии, Федеральный технологический университет Минны, Нигерия*

Резюме. В статье дается детальное геофизическое исследование аномальных зон, выявленных предыдущими аэромагнитными исследованиями в южной части Кебби, северо-запад Нигерии. Комплексные 2D геоэлектроразведочные методы, включающие томографию электрического удельного сопротивления, индукционную поляризацию и собственный электрический потенциал, были использованы для оконтуривания подповерхностной структуры, пригодной для потенциально золотоносной минерализации в частях районов Yauri, Shanga и Magama в штатах Kebbi и Niger на северо-западе Нигерии.

Эти измерения проводились с помощью диполь-дипольной конфигурации и измерителя удельного сопротивления SuperSting. Результаты исследований выявили регионы с низким/высоким удельным сопротивлением, высокой поляризуемостью и высокими значениями собственного электрического потенциала, которые были определены как зоны минерального потенциала. Томография электрического удельного сопротивления помогла очертить области с аномально-низким удельным сопротивлением, которые соответствуют окисленным породам, связанным с прожилками гранита/кварцита. Высокий диапазон удельного сопротивления может существовать на дайковых структурах, связанных с частично разложившимся гранитом и кварцитом, о чем свидетельствуют геологические условия и каротажная диаграмма участка. Метод наведенной поляризации выявил высокую поляризуемость (≥ 20 миллисекунд) в исследуемом районе, возможно, из-за накопления во вмещающих породах рудных минералов, таких как золото. Этот метод также помог выявить регионы с высокими аномалиями индукционной поляризации (≥20 мВ), которые характеризуются жильными минералами руд. Интеграция результатов всех этих методов выявила зоны окисленных пород, дайковые подповерхностные структуры из распавшихся кварцитов, гранитов, гнейсов и жилы рудных минералов. Эти зоны расположены на северо-западе Мараррабы, юго-западе Джинсани и юге Сабон Гари в штатах Нигер и Кебби и их можно рассматривать как потенциал для разведки и добычи золота.

Ключевые слова: *2D-моделирование, томография электрического удельного сопротивления, индукционная поляризация, собственный электрический потенциал, золотое оруденение*

ŞİMALI-QƏRBİ NİGERİYA, KEBBİNİN CƏNUB HİSSƏSİNDƏ POTENSİAL QIZILDAŞIYAN MİNERALİZASİYANIN AXTARIŞI ÜÇÜN KOMPLEKS 2D GEOELEKTRİK KƏŞFİYYATI

Augie A.I.[1,2], Salako K.A.[2], Rafiu A.A.[2], Jimoh M.O.[3]
[1]Tətbiqi geofizika fakültəsi, Birnin Kebbi federal universiteti,Nigeriya: ai.augie@fubk.edu.ng
[2]Geofizika fakültəsi, Minnı Federal texnoloji universiteti, Nigeriya
[3]Geologiya fakültəsi, Minnı Federal texnoloji universiteti, Nigeriya

Xülasə. Əvvəllər bu rayonda aeromagnit tədqiqatlarla aşkar edilmiş anomal zonaların dəqiq geofiziki tədqiqatları aparılmışdır. Tomoqrafik elektrik xüsusi müqavimət, induksiya polyarizasiyası və məxsusi elektrik potensialı ehtiva edən, kompleks 2D geo-elektrokəşfiyyat metodları Şimali-Qərbi Nigeriyanın Kebbi və Niger ştatlarının Yauri, Shanga həmçinin Magama rayonlarında potensial qızıldaşıyan mineralizasiyanın səthaltı strukturun konturlaşdırılması üçün istifadə edilmişdir.

Bu ölçülmələr dipol-dipol konfigurasiyası və SuperSting xüsusi müqavimətin ölçülməsi üsulu ilə aparılmışdır. Tədqiqatların nəticələri əsasında aşağı/yüksək xüsusi müqavimət, yüksək polyarlaşma, məxsusi elektrik potensiallı regionlar aşkar edilmişdir ki, onlar mineral potensiallı obyektlər kimi təyin edilmişdir. Xüsusi müqavimətin elektrik tomoqrafiyası, qranat/kvarsit damarcıqları ilə əlaqədar oksidləşmiş süxürlara müvafiq anomal aşağı xüsusi müqavimətə malik, sahələri cizgiləməyə imkan verdi.

Xüsusi müqavimətin yüksək diapazonu qismən dağılmış qranit və kvarsla əlaqədar dayka strukturlarında mövcud ola bilər ki, bunu geoloji şəraitlər və sahənin karotaj diaqramı əks etdirir. Yönəldilmiş polyarizasiya metodu tədqiq olunan rayonda yüksək polyarlaşma (≥ 20 millisaniyə) fiksasiya etmişdir. Bu çox güman ki, filiz minerallarının (qızıl) yerləşdirici süxürlarında toplanması ilə əlaqədardır. Bu metod həmçinin filizlərin damar mineralları ilə səciyyələnən yüksək anomal induksiyon polyarizasiyasına malik (≥20 мВ) regionları aşkar etməyə imkan yaratmışdır. Bütün bu metodların nəticələrinin inteqrasiyası oksidləşmiş süxurların zonalarını, dağılmış kvarsitlərin, qranitlərin, qneyslərin və filiz minerallarının nüvələrinin dayk yeraltı quruluşlarını aşkar etmişdir.

Bu zonalar şimal-qərbi Mararabı, cənub-qərbi Cinsani və Sabon Garinin cənubunda, Niger, Kabbi ştatlarında yerləşir. Onlar qızıl kəşfiyyatı və hasilatı üçün potensial kimi qəbul edilə bilər.

Açar sözlər: *2D-modelləşdirmə, elektrik xüsusi müqavimət tomoqrafiyası, induksiya polyarlaşması, məxsusi elektrik potensialı, qızıl filizləşməsi*

ANAS Transactions Earth Sciences 1 / 2024

http://www.journalesgia.com

ELABORATION ON A NEW RGB-SPLIT METHOD TO ENHANCE BUILDING EXTRACTION IN SATELLITE IMAGES

Benali A.

Automatic Department, University of Sciences and Technology of Oran Mohamed Boudiaf, Algeria UstombBp 1505 El M'naouer Oran: benabdel0305@gmail.com ORCID: 0000-0002-8989-755X

Keywords: *image processing, mathematical morphology, RGB image, classification*

Summary. Image processing became necessary in various scientific applications and different research fields, especially satellite imaging. In the field of remote sensing, which is our area of interest, several researchers have developed classification and segmentation methods that are very useful. However, those applications are limited regarding the complexity and diversity of satellite images.

In this paper, we propose an original method for detecting buildings in RGB satellite images. The idea is to treat the three RGB matrices separately to accurately detect the pixel intensity variations, which provides better detection of building contours. Our method is mainly based on mathematical morphology operators. The method is a hybridization of two methods based on mathematical morphology which are the Hit or Miss Transform and the Top Hat, the Hit or Miss Transform detects all buildings because of its robust precision in detecting segments, after applying the HMT we apply the Top Hat to refine the segmentation result and finally detect clearly all building in the satellite image. We applied our method on several images from many datasets mainly Ikonos images, and Sentinel-2, the results of our method application gave great results with a Precision that exceeds 95%, Recall across 89%.

I. Introduction

Computer vision is used in various domains as it facilitates the digital data acquisition and classification. The challenge for researchers in this field lies in choosing suitable segmentation and classification methods, particularly the thresholding method. The thresholding phase is crucial in all research domains using image processing.

In their study, Praveena and Kasmewara (2022) used image processing techniques to detect brain tumors. One of the challenges they faced was the unstructured shape of tumors. The authors employed integrated learning-based training for shape detection.

Khan et al. (2023) used image processing techniques for person identification through iris recognition. Despite the difficulty in achieving accurate contour detection, the authors employed three contour detection methods in their study.

Hedhli et al. (2018) used image processing for multi-resolution, multi-date, and potentially multi-sensor classification. The proposed method integrates pixel-level information at the same resolution to achieve their classification goals.

Babaali et al. (2022) used image processing techniques to extract roads. However, the accuracy of road extraction remains limited. To address this, the authors proposed an approach based on semantic segmentation and neural networks to improve the accuracy of road extraction.

Dal Poz (2014) combined LIDAR and photogrammetric images to effectively detect building roofs. However, the challenge of complex building shapes still persists in their study.

Dikmen and Halici (2014) usedshadows properties. They first detected shadow areas and then attempted to merge shadow parts belonging to the same building that were affected by over-segmentation. Based on the detected shadow zone, they reconstructed the building. This approach allowed them to effectively utilize shadow information for building reconstruction.

In their study, Liu et al. (2005) performed roof extraction of buildings using a multi-scale object-oriented classification approach. They then proceeded with shape reconstruction using probabilistic Hough transform.

On the other hand, Sellaouti et al. (2013) adopted an object-oriented approach for building extrac-

tion. They applied a watershed algorithm to divide the image into regions, which caused over-segmentation. In the second step, they applied fusion techniques to reconstruct the over-segmented buildings.

Other researchers have also focursed on mathematical morphology, such as (Sheeren et al., 2007; Benediktsson et al., 2001; Peraresi and Benediktsson, 2001; Weber et al., 2006; Benblidia et al., 2006; Bres et al., 2003).

Previously, in our works (Benali et al., 2014a; 2014b; 2017), we used mathematical morphology to extract buildings from very high-resolution satellite images. We achieved satisfactory results; however, there is still room for improvement in these outcomes.

In this study, we once again employed mathematical morphology because this tool is well-suited for extracting geometric and spatial information from images. Additionally, its application is simple and fruitful.

II. Principle of developed method for the urban area detection RGB-split

The originality of our work lies in the separation of the three spectral components of the satellite image and the individual processing of each R, G, B component. Subsequently, we merge the final results from the three components to reconstruct a multispectral image that contains the extracted building information.

Our proposed method consists on the application of 8 steps as mentioned in the Fig. 1.

1. To begin, we apply a Top-Hat transform (TH) as follows:

a. Morphological closing on the original image.

b. Subtraction between the initial image and the result of the first phase.

$$\mathrm{I_f} = \mathrm{I} \bullet \mathrm{E} = (\mathrm{I} \oplus \mathrm{E}) \ominus \mathrm{E} \tag{1}$$

$$\mathrm{I_{chf}} = \mathrm{I} - \mathrm{I_f} \tag{2}$$

With:

$\mathrm{I_f}$: Resulting image from the morphological closing applied to the initial image (I).

$\oplus$: The dilation operator.

$\ominus$: Erosion operator.

I: The initial image.

E : The structuring element.

2. To eliminate non-important structures, we apply hysteresis thresholding.

$$\mathrm{I_{low}} = \begin{cases} 1 & \text{pour I} \geq \text{Slow} \\ 0 & \text{pour I} < Slow \end{cases} \tag{3}$$

$$\mathrm{I_{high}} = \begin{cases} 1 & \text{pour I} \leq \text{Shigh} \\ 0 & \text{pour I} > Shigh \end{cases} \tag{4}$$

$$\mathrm{It} = \mathrm{Ilow} * \mathrm{Ihigh} \tag{5}$$

With:

I_low: The resulting image from the low threshold.

I_high: The resulting image from the high threshold.

It: The resulting image from the hysteresis thresholding.

3. For denoising and road removal, we used a sequential alternating filter.

Alternating filters are obtained by combinations of closing (•) and openings (∘):

$$\varphi_{\mathrm{k}}(\mathrm{It}) = (\mathrm{It} \bullet \mathrm{B_k}) \circ \mathrm{B_k} \tag{6}$$

$$I_{f_K}(It) = \varphi_{\mathrm{k}}\varphi_{\mathrm{k-1}} \dots \varphi_1(It) \tag{7}$$

With:

B: Structuring element.

K: Filter size.

If: The resulting image of the sequential alternating median filtering.

4. The hole filling process consists of four steps

- Complementing the initial binary image.
- Labeling connected components to distinguish the objects of interest.
- Setting the pixel values of these regions to zero.
- Complementing to retrieve the refined result.

5. To finish the pre-processing we applied dilation, this step is applied to correct the gaps generated by the differents morphological operators that can distort the buildings or cause the loss of some useful information.

$$\mathrm{I_d} = \mathrm{I} \oplus \mathrm{E} \tag{8}$$

With:

Id: The resulting image from the dilation.

$\oplus$: The dilation operator.

6. The extraction was carried out by the Hit or Miss Transform (HMT):

$$\mathrm{A} \otimes (\mathrm{E}, \mathrm{F}) = (\mathrm{A} \ominus \mathrm{E}) \cap (\mathrm{A^c} \ominus \mathrm{F}) \tag{9}$$

With:

$\otimes$: The Hit or Miss transform operator.

$\ominus$: The erosion operator.

E, F: Structuring element.

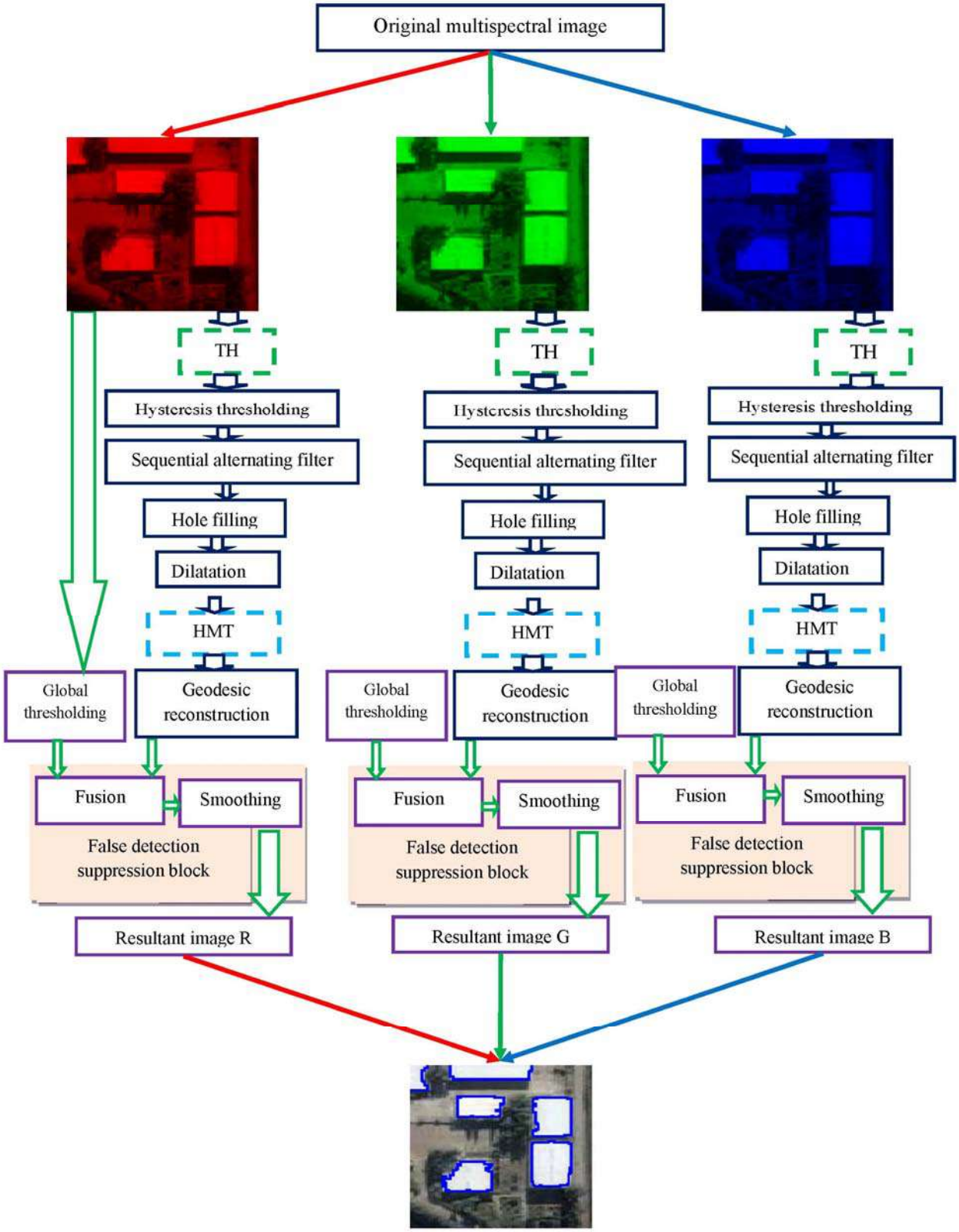

Fig. 1. Flowchart of the proposed RGB-SPLIT method

The transform consists in extracting all the objects with a size which is between the size of the structuring element E and that of F.

7. Restoration of the buildings shape by a geodesic reconstruction:

The buildings shapes deformation is clear after the application of HMT, which obliges us to apply a reconstruction step to restore the original buildings shapes.

The method requires a marker image which corresponds to the obtained HMT result, we apply a

succession of dilation to this latter, the obtained result will be conditioned by a mask image resulting from the 4th phases because this one contains all the non-deformed objects of interest.

$$I_{rec} = (I_{hmt} \oplus_{I_{smo}} C_i)^{\infty} \quad (10)$$

With an application of the conditional dilation until invariance of the transformation defined by:

$$I_{hmt} \oplus_{I_{smo}} C_i = (I_{hmt} \oplus C_i) \cap I_{smo} \quad (11)$$

With :

I_rec : The reconstructed image.

I_hmt : The resulting image of the hit or miss transforms.

C_i: The structuring elements ($1 \leq i \leq 3$)

I_smo : The smoothed image.

8. False detection suppression block.

• Since we are using an unsupervised approach, we need to construct a reference image using global thresholding. Sheeren et al. (2007) The result of our approach will be conditioned by the reference image in order to reduce false detections.

After the conditioning phase, we apply morphological smoothing to remove any remaining false detections.

$$I_{fus} = I_{rec} \cap I_{seg} \quad (12)$$

With:

I_fus: Resulting image from fusion.

I_seg: Resulting image from global thresholding.

• Morphological smoothing

$$I\_smo = I\_fus \circ N = (I\_fus \ominus N) \oplus N \quad (13)$$

With :

I_{smo}: The result of applying smoothing to the conditioned image.

N: The structuring element.

III. Experimental results

To validate our method, we tested it on a dataset of images with varying complexity and variability in terms of color, size, and shapes

We will illustrate the results for three different images to demonstrate the advantages and limitations of our approach.

We present the results of applying our methods to the images we have chosen. Images A and I contain homogeneous rectangular buildings with areas of vegetation and shaded regions. Image E contains buildings with more complex structures, more roof details, vegetation, some areas affected by shadows, and relatively similar colors.

Since our method is unsupervised, it is important to visually inspect the images used in order to choose structuring elements of appropriate size, especially relative to the smallest building in the scene.

IV. Results evaluation

In Figures 2, 3 and 4 we can clearly observe an improvement in the results obtained with our method (RGB-SPLIT) compared to the other methods studied.

1. The first evaluation criterion is the Quantitative evaluation. It involves to calculating the number of buildings detected. To consider a building as correctly detected, at least 60% of its size must be detected.

Table 1

Quantitative evaluation

	Image 1	**Image 2**	**Image 3**
Original Image	5	16	7
HMT	5	13	8
TH	6	11	9
Hybridation method of Benali et al. (2017)	5	13	8
RGB SPLIT	5	14	8

The first image (1) (Table 1) contains 5 built-up areas with trees. The application of the TTR (Thresholding and Region Growing) algorithm allowed the extraction of all the buildings with some deformations caused by the morphological operators.

The application of the second method, CHF (High Hat Filtering), also resulted in the same number of buildings with an additional area. This is because the pixel intensities in this area are quite similar to those of the buildings.

The third method Hybridation of Benali et al. (2017) has helped correct some deformations compared to the first two methods.

Our approach has allowed for well-defined building boundaries and improved detection quality.

The image (2) contains more complex structures and heterogeneous building shapes, as well as more information compared to the previous image. This has resulted in the loss of several buildings after applying the TTR method.

The application of the CHF method also resulted in the loss of several buildings due to the complexity of the image and the operators used in the method, which are not well-suited to the shapes of the building areas in the image.

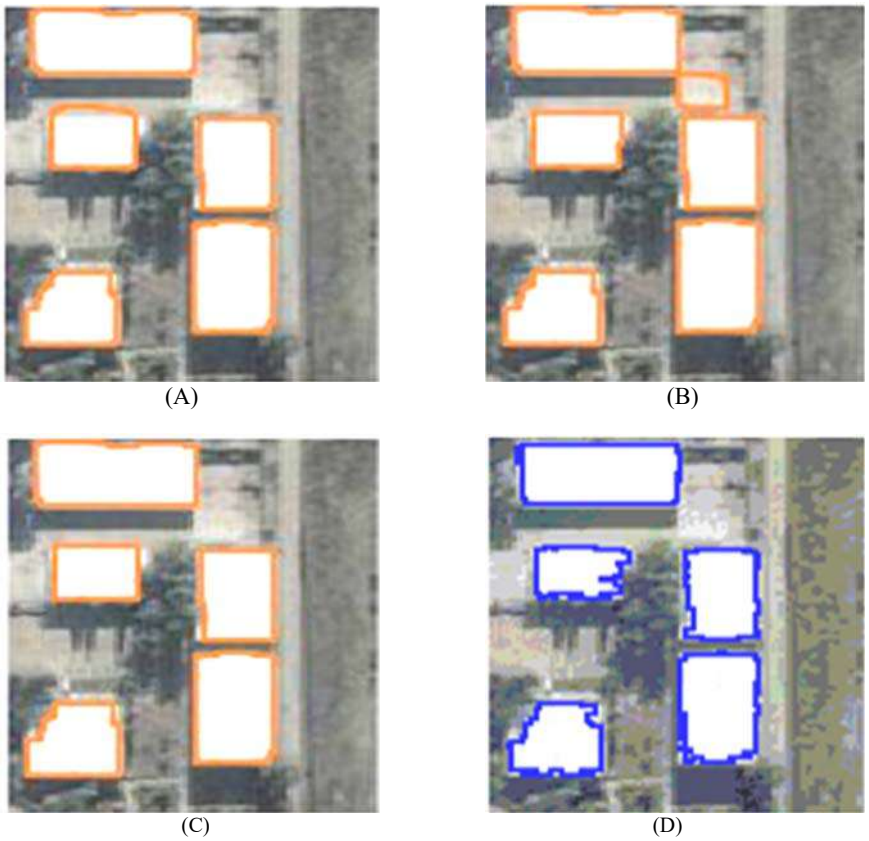

(A) (B)

(C) (D)

Fig. 2. (A). Resulting image of HMT, (B). Resulting image of TH, (C). Resulting image from hybridation method of Benali et al. (2017), (D). Proposed RGB-SPLIT

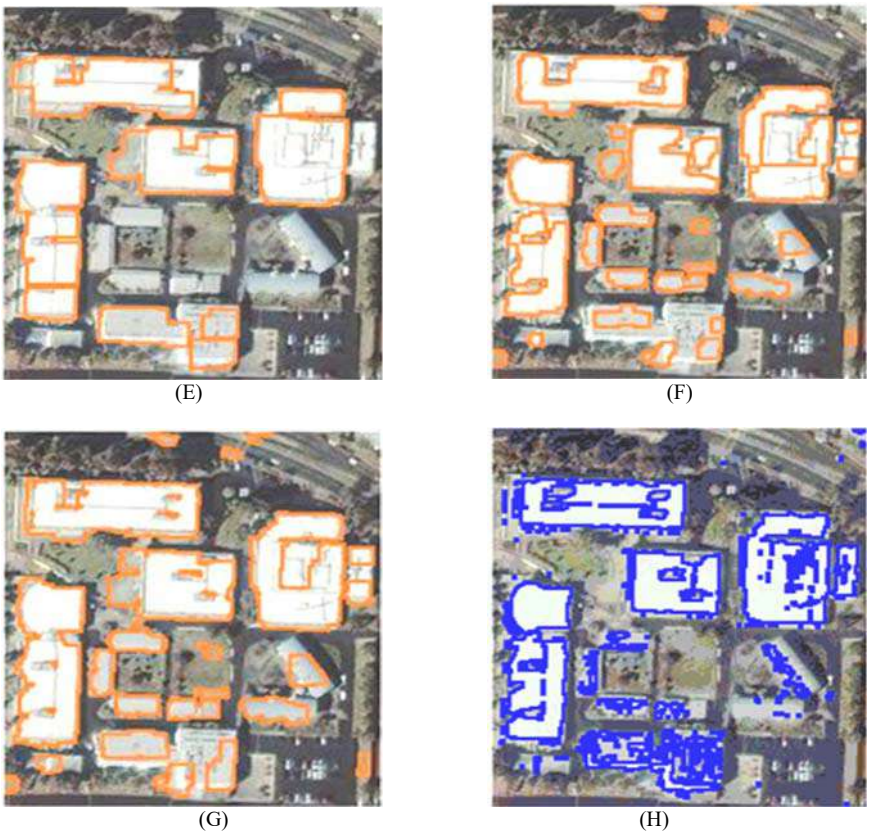

(E) (F)

(G) (H)

Fig. 3. (E). Resulting image of HMT, (F). Resulting image of TH, (G). Resulting image from hybridation method of Benali et al. (2017), (H). Proposed RGB-SPLIT

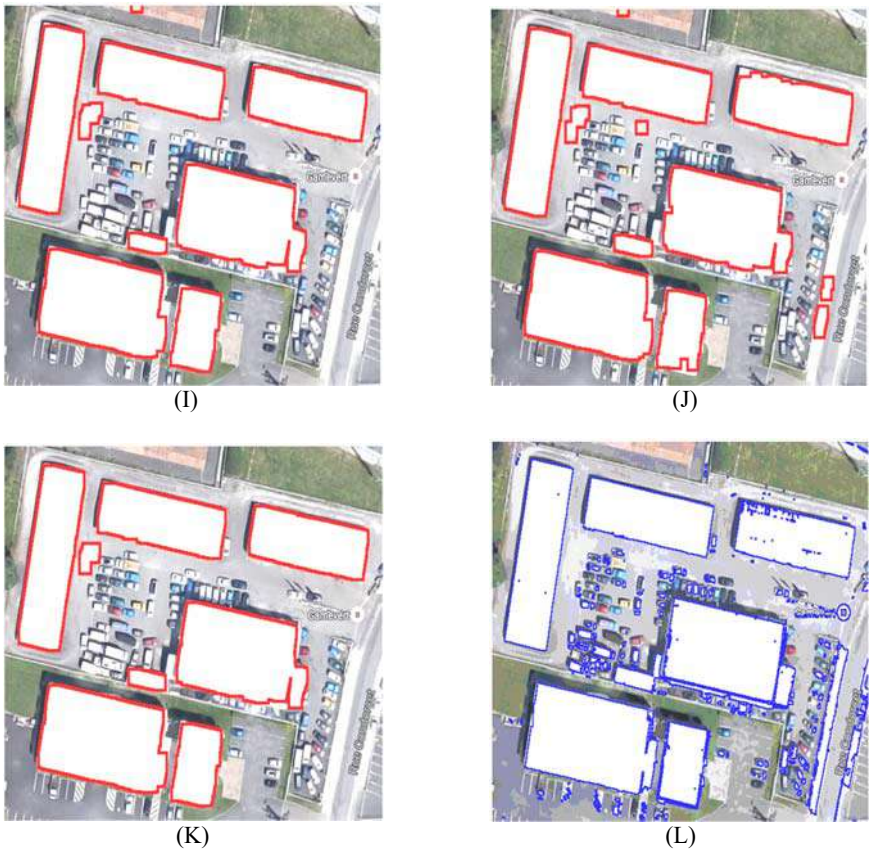

Fig. 4. (I). Resulting image of HMT, (J). Resulting image of TH, (K). Resulting image from the hybridation method of Benali et al. (2017), (L). Proposed RGB-SPLIT

The application of the Hybridation method of Benali et al. (2017) allowed us to reduce the number of false detections.

Our approach further allowed for a successful reconstruction of buildings and improved the detection quality.

The image (3) contains more buildings compared to the first image, along with a parking area with multiple cars of different shapes and colors. The high brightness of this image led to the detection of two additional areas, in addition to the existing buildings, after applying the TTR method.

An over-segmentation occurred after applying the CHF method, leading to an increase in false detections.

The application of the Hybridation method of Benali et al. (2017) did not allow for the suppression of false detections.

Our method allowed for the suppression of false detections, but it caused the detection of small vehicles as our method is sensitive to variations in pixel intensity.

To demonstrate the effectiveness of our approach, we applied our method to a carefully selected satellite image dataset, considering the complexity of structures and different shapes to distinguish the advantages and disadvantages of our approach. In the following, we present comparison graphs with multiple criteria for the four methods applied to our image dataset.

We observe (Fig. 5) that the result of applying our method is consistently closest to the number of buildings present in the original image.

2. The second evaluation criterion is the false rejection rate and the false acceptance rate.

The first image (1) (Table 2) contains very simple structures, which resulted in a similar false acceptance rate of around 2% after applying the four extraction methods.

The application of TTR resulted a false rejection rate of 1.7%, which is considered to be a very good detection rate. This rate increased to 2.42% after the application of CHF due to its complexity, causing deformation of the structures. The application of the third method reduced this rate to 0.5%, and finally, our contribution further reduced it to 0.28%, which is considered to be very good.

Image (E) contains more complex structures and condensed information, which increases the complexity and difficulty of extracting building zones.

The application of TTR resulted in a false acceptance rate of 13.18%, which is normal and acceptable for a complex image. This rate increased to 16.3% for CHF. The third method reduced this factor to 8.53%, and the RGB-SPLIT further reduced it to 5.8% because our method allows us distinguishing variations in each color spectrum separately.

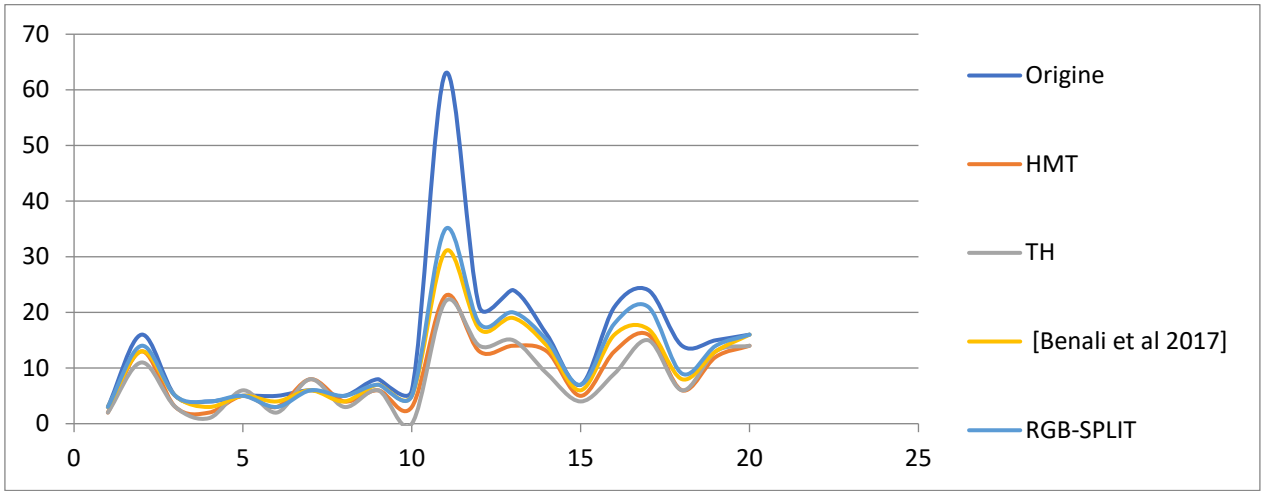

Fig. 5. Number of detected buildings

Table 2

Qualitative Evaluation TFA&TFR

		Image 1	Image 2	Image 3
HMT	TFA	2.47%	13.18%	2.62%
	TFR	1.7%	2.3%	11.23%
TH	TFA	2.6%	16.3%	3%
	TFR	2.42%	3.2%	9.93%
Hybridation of Benali et al. (2017)	TFA	2.7%	8.53%	2.87%
	TFR	0.5%	7.92%	9.65%
RGB SPLIT	TFA	1.64%	5.8%	3.41%
	TFR	0.28%	0.46%	0.32%

The false rejection rate obtained with TTR on image (2) is 2.3%, which is considered good. CHF still causes more deformations, resulting in an increase in this rate to 3.2%. The third method increased this rate to 7.92%, which is considered the detection limit for complex building areas. Our method was able to correct these deformations and reduce the rate to 0.46%, which demonstrates the robustness of our approach and its effectiveness in extracting the most complex zones.

For image (3), we have a nearly similar false acceptance rate after applying all four methods.

The false rejection rate is also nearly similar for the first three methods. However, the application of our proposed approach has significantly reduced this rate to 0.32%, demonstrating the effectiveness of our method.

3. To effectively demonstrate the efficiency of our approach, we have used a third evaluation criterion, which is the detection accuracy rate:

$$\mathrm{GDR} = 1 - \frac{(\mathrm{FRA} + \mathrm{FRR})}{2} \qquad (14)$$

We can clearly state (Table 3) that our method allows for the correction of detection errors and improves the detection accuracy rate.

Table 3

Good detection rate

	HMT	TH	Hybridation of Benali et al. (2017)	RGB-SPLIT
Image (1)	96.84%	97.11%	97.34%	99.04%
Image (2)	91.27%	95.36%	95.36%	96.87%
Image (3)	91.12%	94.09%	94.32%	98.14%

In the following, we present the results of applying the four methods to a dataset of 20 different images carefully chosen to study the advantages and disadvantages of our approach.

Regarding the false acceptance rate (Fig. 6), we can clearly see that the two methods that yield the best results are CHF and our method. Therefore, we can conclude that our approach effectively distinguishes non-relevant areas.

Regarding the false rejection rate (Fig. 7), we observe that the two methods that yield the best results are the third method and our method (RGB-SPLIT). Therefore, our method preserves the different shapes of building areas and effectively eliminates non-building structures.

In Fig. 8, we can observe that the rate of good detection obtained with our method is significantly better than that obtained with the other methods.

4. We will present a comparison of our results with previous works using the evaluation criterion called Precision and Recall.

$$\mathrm{P} = \frac{TP}{TP+FP} \qquad \mathrm{R} = \frac{TP}{TP+FN} \qquad (15)$$

TP: True Positive
FP: False Positive
FN: False Negative

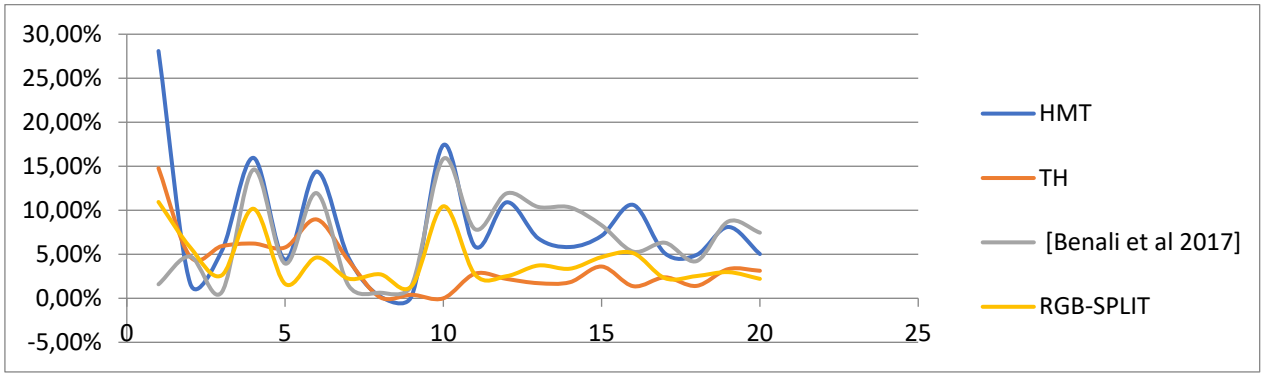

Fig. 6. False acceptation rate for database satellite images

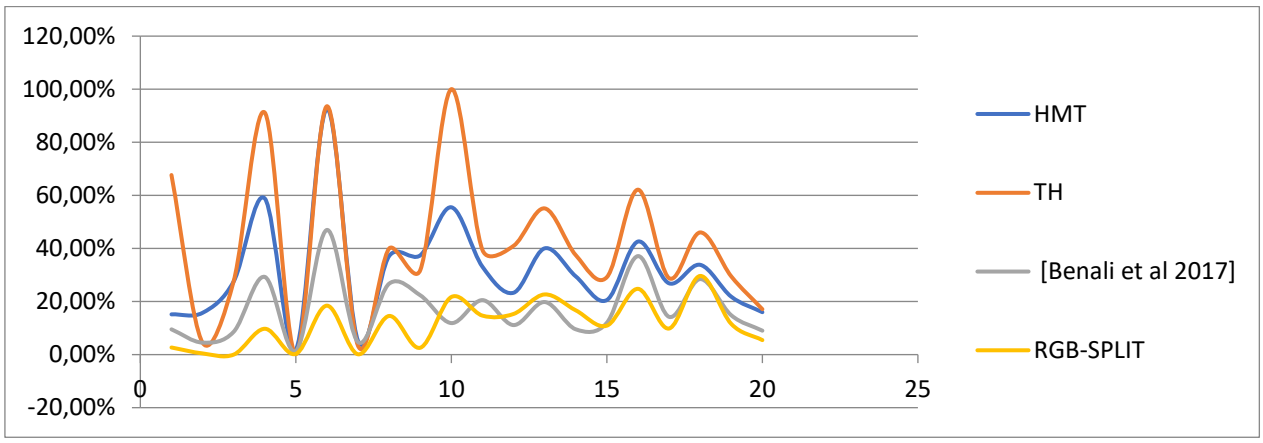

Fig. 7. False rejection rate for datasetsatellite images

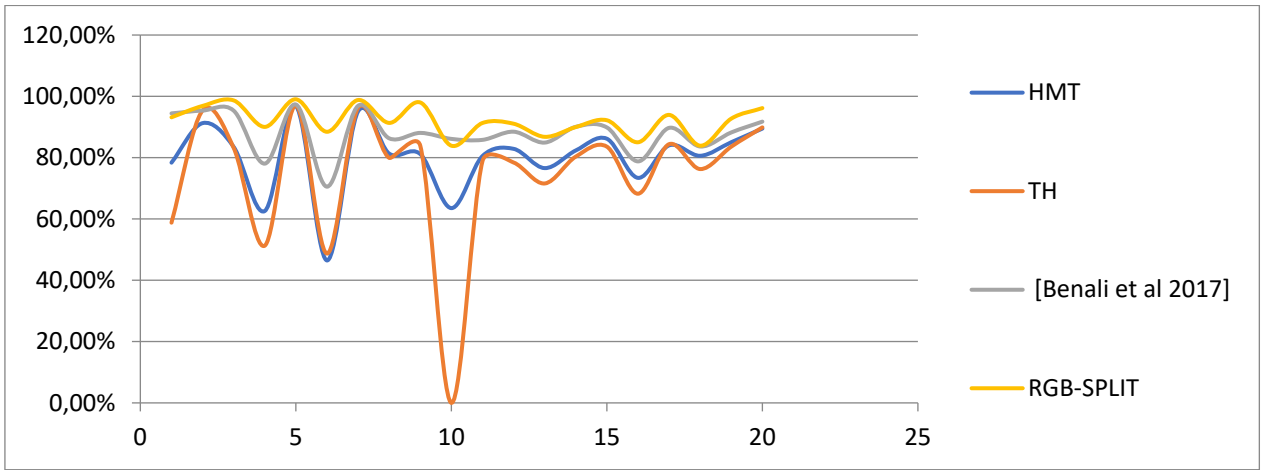

Fig. 8. The good detection rate for dataSET satellite images

Table 4

Comparative table illustrating Precision for different methods of detecting buildings

P									
HMT (Sheeren et al., 2007)	HMT (Benali et al., 2014)	HMT (Chandana et al., 2015)	TH (Benblidia et al., 2006)	TH (Benali et al., 2014)	(Hao et al., 2015)	(Qian et al., 2016)	(Dikmen and Halici, 2014)	(Benali et al., 2017)	RGB-SPLIT
91.00	91.86	94.46	92.00	93.25	92.76	93.00	65.94	93.1095	95,7625

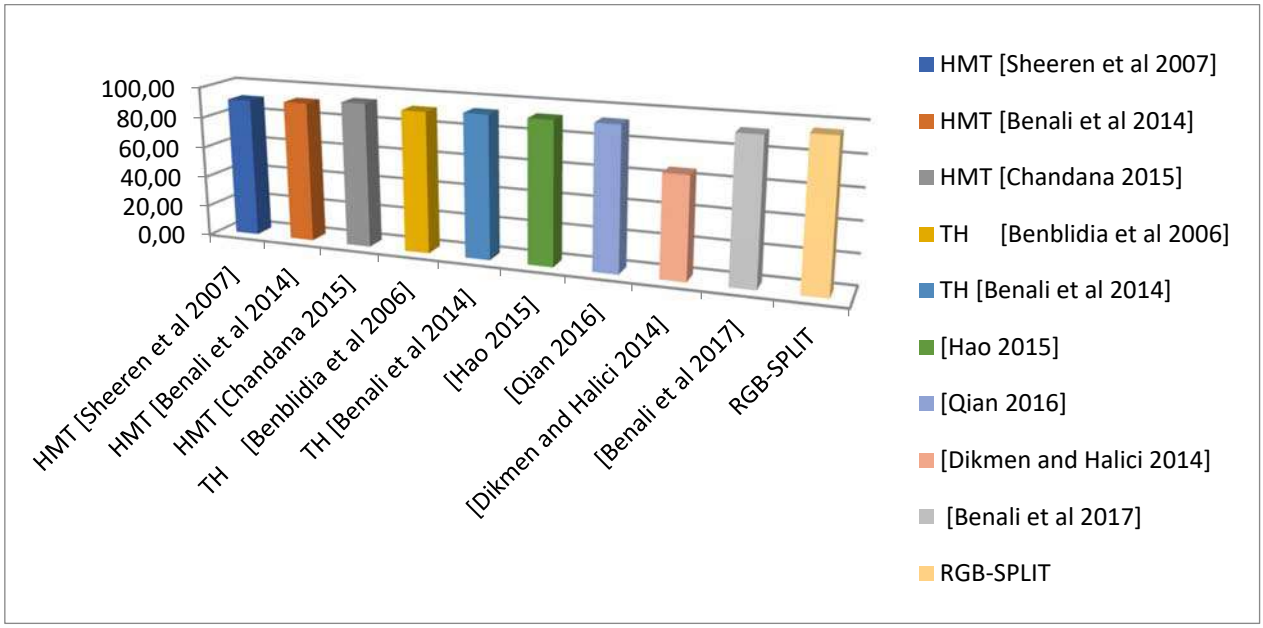

Fig. 9. Qualitative evaluation with: Précision

Table 5

Comparative table illustrating Recall for differents methods of detecting buildings

R									
HMT (Sheeren et al., 2007)	HMT (Benali et al., 2014)	HMT (Chandana et al., 2015)	TH (Benblidia et al., 2006)	TH (Benali et al., 2014)	(Hao et al., 2015)	(Qian et al.,, 2016)	(Dikmen and Halici., 2014)	(Benali et al., 2017)	RGB-SPLIT
71.50	74.33	81.22	89.00	86.56	92.79	85.00	79.15	84.46187	89.18883678

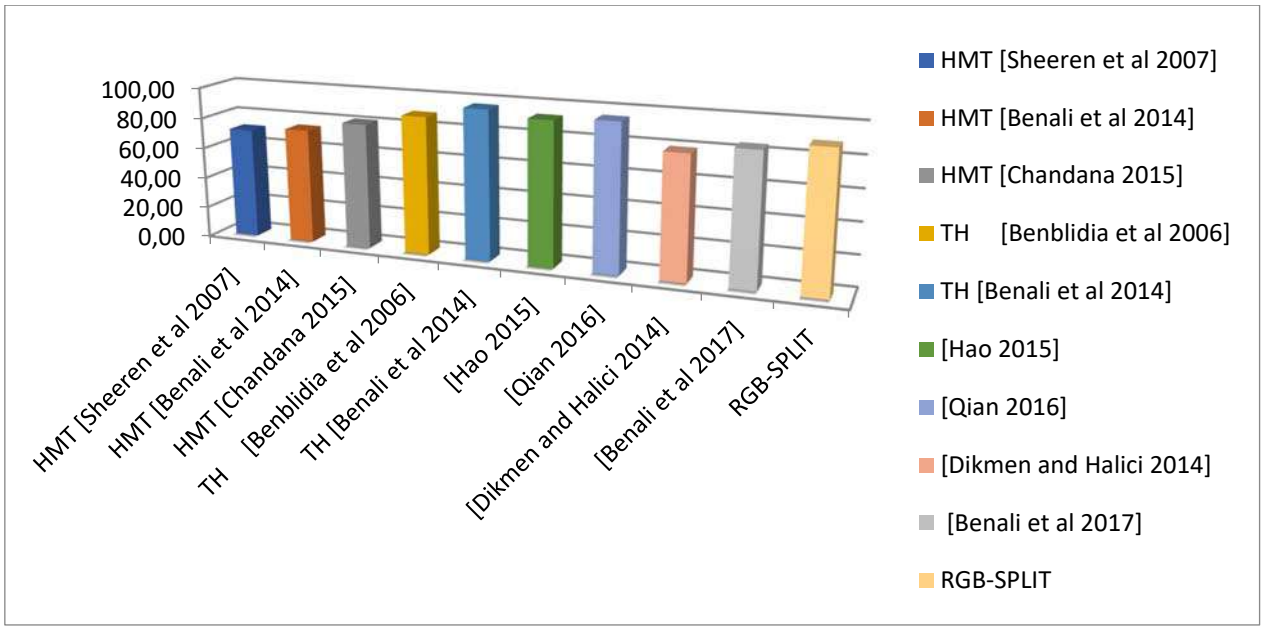

Fig. 10. Qualitative evaluation with: Recall

From (Table 4) we can confidently affirm the effectiveness of our approach, which has provided us with superior precision compared to other methods.

The two methods from (Table 5) that show a higher recall are the method of Hao et al. (2015) and our proposed method, which further demonstrates the effectiveness of our contribution.

VI. Conclusion

In this paper we have adopted a different approach which consists in separating the spectral components of an image then applying the hybridation method proposed in our previous paper (Benali et al., 2017) that we already developed to improve the efficiency of buildings detection.

The separation of the three spectral components allowed us clearly distinguishing the intensity variations of the pixels for each of the three components, which allowed us clearly delimiting the contours of the structures to be detected and to preserve the different shapes.

Our approach allowed reducing the deformations caused by the morphology operators, and the rejection rate.

The detection accuracy is well over 90%, which is very promising to our field which is the built-up areas extraction.

As perspectives, we can apply our method to other types of image to take advantage of it, such as medical or other images.

REFERENCES

Babaali K.O., Zigh E., Djebbouri M., Chergui Ou. A new approach for road extraction using data augmentation and semantic segmentation. Indonesian Journal of Electrical Engineering and Computer Science, Vol. 28, No. 3, 2022, pp. 1493-1501.

Benali A. et al. Buildings extraction of very high spatial resolution satellite images. International Conference on multimedia computing and systems, Vol. 14, Marrakech, Morocco, 2014, DOI:10.1109/ICMCS.2014.6911229.

Benali A. et al. Elaboration of a hybrid method for the enhancement of buildings reconstruction in multispectral images. International Journal of Imaging and Robotics, Vol. 17, No. 4, 2017, pp. 25-37.

Benali A. et al. Improvement of the Top Hat for the Buildings Extraction in the very High Spatial Resolution Satellite Images. International Journal of Emerging Sciences, Vol.4, No. 3, 2014, pp. 121-131.

Benblidia N., Abdellaoui A., GuessoumA., Bensaid A. Analysis of land occupation in urban and suburban presaharan areas: the case ofLaghouat (Algeria).Télédétection, Vol. 6, No. 2, 2006, pp. 177-190 (in French).

Benediktsson A., Arnason K., Peraresi M. The use of morphological profiles in classification of data from urban areas. IEEE/ISPRS Joint Workshop on Remote Sensing and Data Fusion over Urban Areas, 2001, pp. 30-34.

Bres S., Jolion J.M., Lebourgeois F. Digital image processing and analysis. Lavoisier. Hermès, 2003, 410 p. (in French).

Chandana D. et al. Optimization of structure elements for morphological Hit-Or-Miss transform for building extraction from VHR airborne imagery in natural hazard areas. International Journal of Machine Learning and Cybernetics, Vol. 6, 2015, pp. 641-650.

Dal Poz A.P. Synergy between Lidar and Image data in context of building extraction. The International Archives of the Photogrammetry, Remote Sensing and Spatial Information Sciences, Vol. XL-1, 2014, ISPRS Technical Commission I Symposium, 17-20 November 2014, Denver, Colorado, USA, pp. 89-93.

Dikmen M. and Halici U. A learning-based resegmentation method for extraction of buildings in satellite images. IEEE Geoscience and Remote Sensing Letters, Vol. 11, No. 12, 2014, pp. 2150-2153.

Hao S. et al. Accurate urban area detection in remote sensing images. IEEE Geoscience And Remote Sensing Letters, Vol. 12, No. 9, 2015, pp. 1948-1952.

Hedhli I., Moser G., Zerubia J. New cascade method for multitemporal hierarchical or multi-sensor classification of high resolution satellite images. Revue Française de Photogrammétrie et de Télédétection, Vol. 216, 2018, pp. 3-17 (in French).

Khan S.N., Urooj Khan S., Nwobodo O.J., Cyran K.A. Iris recognition through edge detection methods: application in flight simulator user identification. International Jour-

ЛИТЕРАТУРА

Benali A. et al. Buildings extraction of very high spatial resolution satellite images. International Conference on multimedia computing and systems, Vol. 14, Marrakech, Morocco, 2014, DOI:10.1109/ICMCS.2014.6911229.

Benali A. et al. Elaboration of a hybrid method for the enhancement of buildings reconstruction in multispectral images. International Journal of Imaging and Robotics, Vol. 17, No. 4, 2017, pp. 25-37.

Benali A. et al. Improvement of the Top Hat for the Buildings Extraction in the very High Spatial Resolution Satellite Images. International Journal of Emerging Sciences, Vol. 4, No. 3, 2014, pp. 177-190.

Benediktsson A., Arnason K., Peraresi M. The use of morphological profiles in classification of data from urban areas. IEEE/ISPRS Joint Workshop on Remote Sensing and Data Fusion over Urban Areas, 2001, pp. 30-34.

Chandana D. et al. Optimization of structure elements for morphological Hit-Or-Miss transform for building extraction from VHR airborne imagery in natural hazard areas. International Journal of Machine Learning and Cybernetics, Vol. 6, 2015, pp. 641-650.

Dal Poz A.P. Synergy between Lidar and Image data in context of building extraction. The International Archives of the Photogrammetry, Remote Sensing and Spatial Information Sciences, Vol. XL-1, 2014, ISPRS Technical Commission I Symposium, 17-20 November 2014, Denver, Colorado, USA, pp. 89-93.

Dikmen M. and Halici U. A learning-based resegmentation method for extraction of buildings in satellite images. IEEE Geoscience and Remote Sensing Letters, Vol. 11, No. 12, 2014, pp. 2150-2153.

Hao S. et al. Accurate urban area detection in remote sensing images. IEEE Geoscience And Remote Sensing Letters, Vol. 12, No. 9, 2015, pp. 1948-1952.

Babaali K.O., Zigh E., Djebbouri M., Chergui Ou. A new approach for road extraction using data augmentation and semantic segmentation. Indonesian Journal of Electrical Engineering and Computer Science, Vol. 28, No. 3, 2022, pp. 1493-1501.

Liu Z.J. et al. Building extraction from high resolution imagery based on multi-scale object oriented classification and probabilistic Hough transform. Geoscience and Remote Sensing Symposium, 2005, IGARSS '05. Proceedings. 2005 IEEE International, Vol. 4, http://dx.doi.org/10.1109/IGARSS.2005.1525421.

Peraresi M. and Benediktsson A. A new approach for the morphological segmentation of high-resolution satellite imagery. IEEE Transactions on Geoscience and Remote Sensing, Vol. 39, No. 2, 2001, pp. 309-320.

Praveena M., Kameswara Rao M. Brain tumor detection using Integrated Learning Process Detection (ILPD). International Journal of Advanced Computer Science and Applications, Vol. 13, No. 10, 2022, DOI:10.14569/IJACSA.2022.0131018.

nal of Advanced Computer Science and Applications, Vol. 14, No. 4, 2023.
Liu Z.J. et al. Building extraction from high resolution imagery based on multi-scale object oriented classification and probabilistic Hough transform. Geoscience and Remote Sensing Symposium, 2005, IGARSS '05. Proceedings. 2005 IEEE International, Vol. 4, http://dx.doi.org/10.1109/IGARSS.2005.1525421.
Peraresi M. and Benediktsson A. A new approach for the morphological segmentation of high-resolution satellite imagery. IEEE Transactions on Geoscience and Remote Sensing, Vol. 39, No. 2, 2001, pp. 309-320.
Praveena M., Kameswara Rao M. Brain tumor detection using Integrated Learning Process Detection (ILPD). International Journal of Advanced Computer Science and Applications, Vol. 13, No. 10, 2022, DOI:10.14569/IJACSA.2022.0131018.
Qian Z. et al. A morphological building detection framework for high-resolution optical imagery over urban areas. IEEE Geoscience And Remote Sensing Letters, Vol. 13, No. 9, 2016, pp. 1-5.
Sellaouti A. et al. Template-based hierarchical building extraction. IEEE geoscience and remote sensing letters, Vol. 11, No. 3, 2013, DOI: 10.1109/LGRS.2013.2276936.
Sheeren D., Lefèvre S., Weber J. Binary mathematical morphology for the automatic extraction of buildings in THRS images. Revue internationale de Géomatique, Vol. 17(3-4), 2007, pp. 333-352, DOI:10.3166/geo.17.333-352 (in French).
Weber J. Lefèvre S. and Sheeren D. Detection of buildings in images THRS with mathematical morphology. SAGEO'2006, 2006, pp. 1-4 (in French).
Qian Z. et al. A morphological building detection framework for high-resolution optical imagery over urban areas. IEEE Geoscience And Remote Sensing Letters, Vol. 13, No. 9, 2016, pp. 1-5.
Sellaouti A. et al. Template-based hierarchical building extraction. IEEE geoscience and remote sensing letters, Vol. 11, No. 3, 2013, DOI: 10.1109/LGRS.2013.2276936.
Khan S.N., Urooj Khan S., Nwobodo O.J., Cyran K.A. Iris recognition through edge detection methods: application in flight simulator user identification. International Journal of Advanced Computer Science and Applications, Vol. 14, No. 4, 2023.
Benblidia N., Abdellaoui A., Guessoum A., Bensaid A. Utilisation de la morphologie mathématique pour l'analyse de l'occupation de l'espace en zones urbaines et périurbaines présahariennes: cas de Laghouat (Algérie). Télédétection, Vol. 6, No. 2, 2006, pp. 177-190.
Bres S., Jolion J.M., Lebourgeois F. Traitement et analyse des images numériques. Lavoisier. Hermès, 2003, 410 p.
Hedhli I., Moser G., Zerubia J. Nouvelle méthode en cascade pour la classification hiérarchique multi-temporelle ou multi-capteur d'images satellitaires haute résolution. Revue Française de Photogrammétrie et de Télédétection, Vol. 216, 2018, pp. 3-17.
Sheeren D., Lefèvre S., Weber J. La morphologie mathématique binaire pour l'extraction automatique des bâtiments dans les images THRS. Revue internationale de Géomatique, Vol. 17(3-4), 2007, pp. 333-352, DOI:10.3166/geo.17.333-352.
Weber J. Lefèvre S. et Sheeren D. Détection des bâtiments dans les images THRS avec la morphologie mathématique. SAGEO'2006, 2006, pp. 1-4.

РАЗРАБОТКА НОВОГО RGB-СПЛИТ МЕТОДА ДЛЯ УЛУЧШЕНИЯ ВЫДЕЛЕНИЯ ЗДАНИЙ НА СПУТНИКОВЫХ СНИМКАХ

Бенали А.
Факультет автоматики, Университет наук и технологий Мохамеда Будиафа в Оране, Алжир
UstombBp 1505 El M 'naouer Oran

Резюме. Обработка изображений необходима в различных научных приложениях и областях исследований, особенно в спутниковой съемке. В области дистанционного зондирования, которая является сферой наших интересов, несколько исследователей разработали очень полезные методы классификации и сегментации. Однако их применение ограничено сложностью и разнообразием спутниковых изображений.

В этой статье мы предлагаем оригинальный метод обнаружения зданий на RGB спутниковых снимках. Идея заключается в раздельной обработке трех матриц RGB для точного определения изменений интенсивности пикселей, что обеспечивает лучшее обнаружение контуров зданий. Наш метод в основном основан на применении операторов математической морфологии. Метод представляет собой гибридизацию двух методов, основанных на математической морфологии, а именно: преобразования Hit or Miss и Top Hat. Преобразование Hit or Miss обнаруживает все здания благодаря своей надежной точности в обнаружении сегментов, после применения этого метода мы применяем Top Hat для уточнения результата сегментации и, наконец, четко обнаруживаем все здания на спутниковом изображении.

Мы применили наш метод на нескольких изображениях из многих наборов данных, в основном на изображениях Ikonos и Sentinel-2. Результаты применения нашего метода дали отличные результаты: точность превысила 95 %, отзывы – 89 %. В качестве перспективы, чтобы воспользоваться преимуществами метода, мы можем применить его к медицинским или другим типам изображений.

Ключевые слова: *обработка изображений, математическая морфология, RGB-изображение, классификация*

PEYK ƏKSLƏRİNDƏ BİNALARIN AYRILMASI KEYFİYYƏTİNİN YÜKSƏLDİLMƏSİ ÜÇÜN YENİ RGB-SPLİT METODUNUN İŞLƏNİLMƏSİ

Benali A.
Avtomatika fakültəsi, Oranda Moxamed Budiaf Elm və Texnologiyalar Universiteti, Əlcəzair
UstombBp 1505 El M 'naouer Oran

Xülasə. Təsvirlərin işlənilməsi müxtəlif elmi tədqiqatlarda, xüsusən peyk əkslərində istifadəsi mütləqdir. Bizim maraq sferamızda olan distansiyon zondlama sahəsində bir sıra tədqiqatçılar olduqca faydalı təsnifatlar və seqmentasiya metodları işləmişlər. Lakin onların tətbiqi peyk əkslərinin müxtəlifliyi və mürəkkəbliyi ilə məhdudlaşmışdır.

Bu məqalədə RGB peyk əkslərində (şəkillərində) binaların aşkar edilməsinin orijinal metodunu təklif edirik. İdeyanın məğzi piksellərin dəyişmə intensivliyinin dəqiq təyini üçün üç RGB matrislərinin ayrıca işlənilməsindən ibarətdir ki, bu binaların konturlarının daha yaxşı aşkar ediməsini təmin edir. Bizim metod riyazi morfologiya operatorlarının tətbiqinə əsaslanır. Metod riyazi morfolo-

giyaya əsaslanan, daha doğrusu Hit or Miss və Top Hat operatorlarının dəyişilməsi – 2 metodun hibridləşməsindən ibarətdir. Hit or Miss çevrilməsi seqmentlərin aşkar edilməsində öz etibarlı dəqiqliyinə görə bütün binaları fiksasiya edir, bundan sonra seqmentasiya nəticələrinin dəqiqləşdirilməsi üçün Top Hat metodundan istifadə edilmişdir və nəhayət peyk əkslərində bütün binaları aydın aşkar edirik.

Bizim metod çoxlu çeşidli məlumatlar içərisində, əsasən, Ikonos və Sentinel-2 təsvirlərində tətbiq etdilmişdir. Metodumuzun tətbiqi qiymətləri 95% - dən, daha doğrusu 89% - dən çox dəqiqliklə əla nəticələr verdi. Perspektivdə bu metod tibbi və digər problemlərin həlli üçün istifadə oluna bilər.

Açar sözlər: *təsvirlərin işlənilməsi, riyazi morfologiya, RGB-təsvir, təsnifat*

ANAS Transactions **Earth Sciences** **1 / 2024**

http://www.journalesgia.com

GOLD MINERALIZATION IN OIL FIELDS OF THE SOUTH CASPIAN BASIN*

Huseynov D.A.

Ministry of Science and Education of the Republic of Azerbaijan,
Institute of Geology and Geophysics, Azerbaijan
119, H.Javid ave., Baku, AZ1143: d_huseynov@yahoo.com

Keywords: *gold, oil field, mineralization, noble-metal and oil paragenesis, centers of fluid discharge, geochemical anomaly, stratiform deposits*

Summary. The basis of idea of the gold content of the South Caspian oil-and-gas bearing basin is the notion regarding the forming of gold-bearing catagenic solutions by the oil-gas generating Paleogene – Lower Miocene sediments which within the zone Volga-Don-Pre-Caucasus–Trans Caspian enclose the complex sulphide-phosphatic-rare metal-uranium deposits. In iron sulphides there are constant gold, cobalt, nickel, molybdenum, rhenium, rare copper, zinc, plumbum and arsenic, but in pyritiferous horizons of some regions there are often inclusions of native minerals – gold, bismuth, tin and copper.

The detail geologic-geophysical and isotopic-geohemical studies have showed that in the South-Caspian sedimentary basin in "oil-gas window" the catagenic aqueous solutions enriched with ore components were intensively generated along with formation of liquid and gaseous hydrocarbons. It is proved by high content and constant presence of gold, silver, copper, molybdenum, zinc, arsenic and other metals in oils, bitumens and formation waters. This stimulated the study of possibility of ore accumulations forming in the paleo-sources of the fluids' catagenic discharge and confirmed our predictions regarding the noble metal and oil paragenesis in the South Caspian sedimentary basin.

The top-cut concentrations of gold and palladium as well as the indicators of the epithermal mineralization of gold of the Carlin-type – arsenic and barium – were revealed within the zone.

Such study for gold exploration within the South Caspian basin was performed for the first time. The obtained results open the basin's prospects as the gold-oil-bearing one. The revealed gold-ore mineralization represents a discovery of a new genetic type of gold-ore mineralization in Azerbaijan also known worldwide as stratiform Carlin-type with microdissiminated, low content and significant reserves of gold.

Introduction

Our interest to gold mineralization in hydrocarbon-bearing sedimentary basins is stipulated by the following circumstances:

1. Oil-bearing Carline-type gold deposits of west-central Nevada, US (Gold Point electrum deposits and the Carlin-type gold ore bodies of Yankee basin in the Alligator Ridge mining district) appear as the best example of low temperature gold mineralization.

2. The recently discovery of micro-disseminated gold and gold-base metal alloys in sedimentary rocks of the Western Canada Sedimentary Basin (WCSB) (nearby Athabasca tar mining) has led to the recognition of a new and potentially important occurrence of low temperature sedimentary-hosted gold mineralization named as Prairie-type.

The primary objective of our study was to understand: are these gold deposits types unique or can we find them in other localities in the world including the South Caspian basin and if so, are they similar to **Prairie-type sedimentary Au, Carlin-type Au** or in a class of their own? We need to understand them so that we can be more effective in our exploration for them.

Preliminary integrated investigations carried out in South Caspian basin manifested the intensive mineralization and Au-Pd anomaly that caused the selection of some fields as the object for this study.

We expect that this paper considerably improves our understanding of the industrial gold deposits formation in paragenesis with hydrocarbons in the South Caspian sedimentary basin, which is a new direction for mineral deposits discovering in this oil reach province. This will contribute much to the strategy of noble metals exploration in the South Caspian region as well as other similar hydrocarbon basins all over the world.

Idea justification

Gold mineralization in the Western Canada Sedimentary Basin (WCSB) at Fort MacKay, northeastern Alberta, nearby Athabasca tar sands mining

* Discussion paper

(Prairie formation) occurs as <5 micron-sized grains associated with bitumen in silicified limestone and calcareous sediments within pipe-shaped solution chimneys interpreted to represent focused, paleo-brine discharge sites. Micro-disseminated mineralization is proposed to have occurred by mobilization (scavenge) and transport of gold and other metals in oxidizing, halide-rich brines derived from the halite-bearing Prairie formation at a maximum paleotemperature of about 90°C. Metal deposition was related to changes in redox potential along the flow path and, in part, to the presence of hydrocarbons.

The oil-gold paragenesis is in the best way represented in the Carlin-type gold deposits. Because of abundant oil-saturation some of them have been named oil-bearing Carline-type gold deposits as for instance the Gold Point electrum deposits near Railroad Valley and the Carlin-type gold ore bodies of Yankee basin in the Alligator Ridge mining district, west-central Nevada, US. (Hulen and Collister, 1999).

Carbon and oxygen isotopic systematics of the gold-oil-bearing calcite of the Yankee group deposits show that it is of hydrothermal rather than diagenetic origin; it is quite similar to ore-stage calcite at the Carlin deposit itself located about 100 km to the north. The Yankee fluid-inclusion and fracture-filling "free" oils were clearly involved in the gold-mineralizing hydrothermal system but were not thermally degraded to pyrobitumen, the analogous solid hydrocarbon characteristic of Carlin-type gold deposits. The oil-bearing fluid inclusions all have homogenization temperatures less than 120°C. Temperature-sensitive biomarker transformation ratios both in the fluid-inclusion oils and in the "free" oils, expressed as equivalent vitrinite reflectance (Ro; 0.75–0.95%), suggest peak paleotemperatures no higher than about 145°C (Hulen and Collister, 1999). Thus the Yankee system was cooler than the 175° to 250°C widely cited as typical for Carline-type mineralization. It is very important to note that stable isotopic systematics coupled with fluid-inclusion microthermometry reveal that the Gold Point and the region's premier Grant Canyon oil field thermal waters were otherwise identical in composition and temperature (Hulen et al., 1998). Origin of Carlin-type deposits is enigmatic. Basically recent studies indicate the formation of Carlin-type deposits from relatively low pH, and low-to moderately-saline convective circulated fluids of mixed meteoric and magmatic or metamorphic origin, which leached gold from deep metamorphic or sedimentary rocks (Kuehn and Rose, 1995; Seedorff and Barton, 2004; Ilchik and Barton, 1997).

Carlin-type deposits are large, disseminated, carbonate (calcareous) sediment-hosted gold ore bodies characterized by relatively high Au/Ag, enrichment in As, Sb, Hg, and Tl, and by the dominance of "invisible gold" as ions or submicron-sized particles in iron sulfide. The deposits are under strong structural control of faults and folds (Radtke, 1985; Hofstra and Cline, 2000). In the Carlin systems the physical properties of the host environment place major constraints on ore formation. High porosity host rocks are capped by structural or stratigraphic closures which trap the ore fluid similar to oil accumulation process (Burton et al., 1985).

In addition, Ge X. and colleagues studied the spatial association of hydrocarbons with a Carlin-type gold deposit in detail in Nanpanjiang Basin, South China (Ge X. et al., 2022). Based on complex studies using high-resolution transmission electron microscopy, electron probe microanalysis, and in-situ sulfur isotope analysis of both pyrobitumen and gold-bearing pyrite, they established that liquid hydrocarbons are responsible for the precipitation of metallic gold and could have acted as gold carrier before metal precipitation.

Carlin-type gold deposits are of major economic interest to mining companies because they represent low-cost, bulk-mineable targets. Low grade of gold in the ore is compensated by large size of deposits. For example, Newmont's Gold Quarry deposit is the largest currently known deposit along the Carlin Trend in Nevada, containing 198 million tons grading 1.19 gram/gold per ton, or 259.375 contained tons of gold.

The South Caspian sedimentary basin (SCSB) is generally accepted as one of the richest petroleum province in the world. High-productive oil and gas deposits in the SCSB are concentrated in the Lower Pliocene deposits so called Productive Series (PS) accumulated in the Absheron peninsula, South-East Gobustan, Lower Kura depression, Baku and Absheron archipelagos (Fig. 1). Isotopic-geochemical (biomarker) investigations of oils and organic matter (OM) as well as correlation “oil-oil”, “rock-oil” demonstrate that oils in the PS are derivatives of the Paleogene-Lower Miocene (Maykopian) and Middle-Upper Miocene (Diatomic) oil-generating complexes (Guliyev et al., 2000, 2001; Гулиев и др., 1999; Feyzullayev et al., 2001). In Volga-Don–Pre-Caucasus–Trans-Caspian region the Paleogene-Lower Miocene sedimentary complex is characterized by exclusively high ore-content which is expressed by sheet-like deposits of metalliferous bone detritus of fish and sulfides extending for many kilometers. These sheet deposits are complex sulfide-phosphate-rare metal-uranium deposits of a sedimentary type. In iron sulphides there constantly occur gold, cobalt, nickel, molybdenum, rhenium and rarely, copper, zinc, lead and arsenic. There often occur inclusions of native metals – gold, bismuth, tin and copper in pyritaceous horizons in some regions.

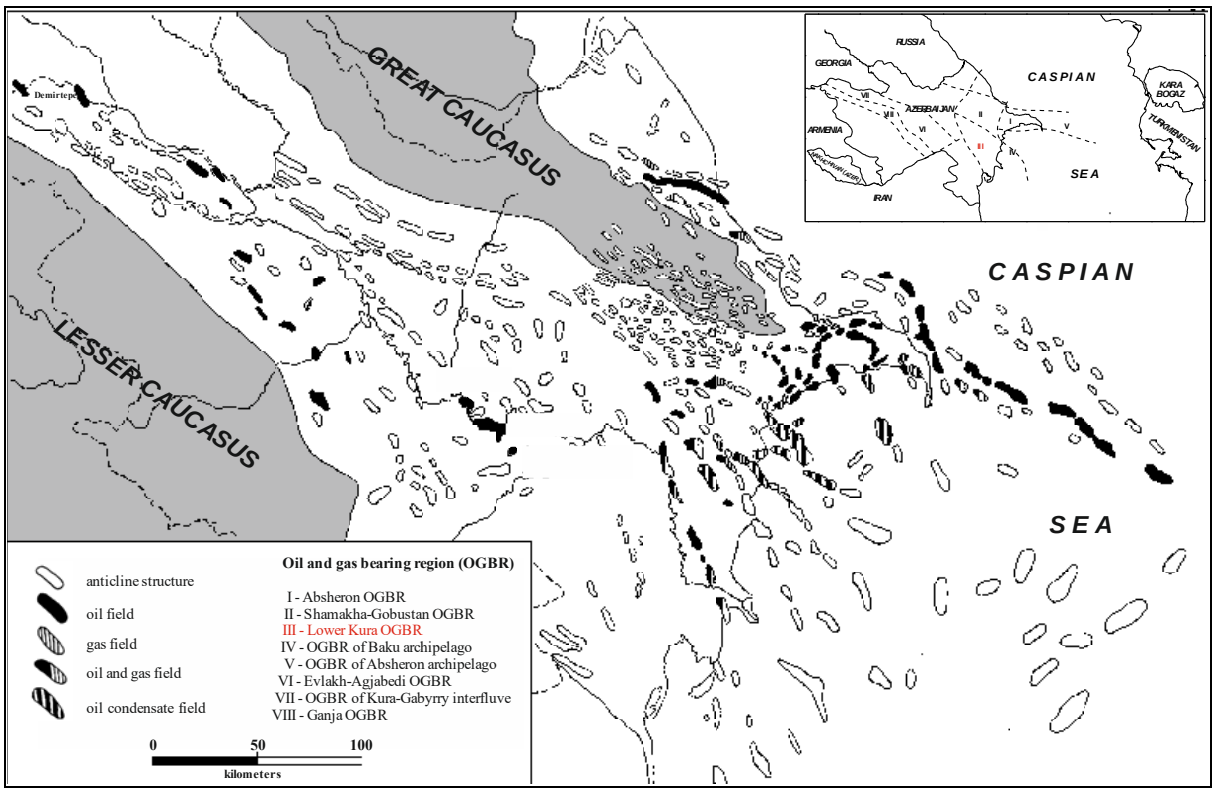

Fig. 1. Location map of oil-gas bearing regions and structures in the South Caspian sedimentary basin

This circumstance initiated investigations of generation of metalliferous catagenic solutions by the Paleogene-Lower Miocene oil-generating series in the SCB and possible formation of the ore-accumulations in zones of fluids' catagenic discharge.

Which data or criteria stipulate successful result?

Isotopic-geochemical (genetic) criteria

A peculiar feature of the oil-generating Paleogene-Miocene deposits in the SCSB is abundance of jarosite in the bedding surfaces of pyrobituminiferous shales with fish remnants. Formation of jarosite (natrojarosite) is, no doubt, associated with the destruction of primary accumulations of iron sulfides during the migration of catagenic heated carbon-dioxide–sodium-chloride solutions through the interlaminar spaces of shales. Process of jarotization is a quite favorable factor for the saturation of water solutions by metals of the decomposing sulfides. For this reason, of a great importance are paleo- and recent centers of gas-water-oil fluids catagenic discharge. In favorable structural-lithological and geochemical environments, accumulations of the ore matter are confined to them. From this point of view of a special interest are zones of tectonic dislocations which control formation of oil-gas anticlinal structures.

The above-mentioned is regularly reflected in the concentration of metals in formation waters of oil-gas bearing fields of the studied region. Investigation of distribution of ore-forming elements (Ag, Cu, Mn, Fe, As, Cd, Mo, Sr, Ba, U, Ra, Th, Ga, Tl, Ge, Zn, Pb, Bi) in formation and pore waters of the Tertiary complex of the South Caspian basin, as well as the comparison of formation waters with the mineral-forming solutions of areas of the recent ore-deposition such as the depressions Discovery and Atlantic II (Red Sea rift), Cheleken peninsula (Turkmenia), active volcanic zone Taupou (New Zealand) show that formation waters of the west flank of the South Caspian basin independently on low mineralization (14-147 g/l) according to metal content are comparable with ore-forming solutions (250-320 g/l) of the above-mentioned areas of the recent ore-formation (Багир-заде и др., 1988; Ахундов и Саппо, 1960; Агаларов и др., 1980; Богашова, 2007; Лебедев и Никитина, 1983; Пушкина, 1965; Эмери и др., 1974; Юшко-Захарова и др., 1986). Comparative analysis is given in Table 1.

The permanent presence and highly concentrations of gold, silver, copper, molybdenum, zinc, arsenic and other metals in the different-facial deposits as well as in oils and bitumens of the South Caspian oil-gas bearing basin (Мирзоев и Харитонов, 1982; Раковский и др., 1985; Бабаев, 1984; Мехтиев и др., 1986; Исраэлян, 1959, 1964; Исраэлян и др., 1975; Багир-заде и др., 1988; Huseynov, 2002) also reflect the metallogenic specialization of the East-Caucasian area of the Paratethys paleobasin in the Paleogene-Miocene time (Table 2).

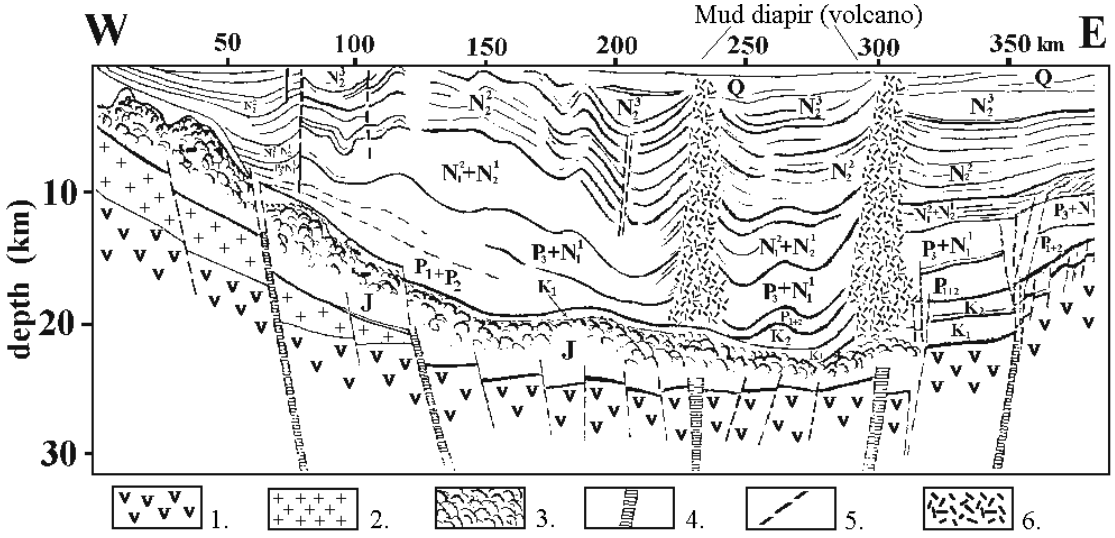

Fig. 2. 12th sec. regional seismic profile cross South Caspian basin (Ализаде и др., 2018). 1 – basaltic layer; 2 – granitic layer; 3 – Mesozoic igneous rock; 4 – crustal faults; 5 – faults; 6 – zone of no seismic information, presumably mud diapir

Results of the conducted studies allow confirming that the southern water area of the Paratethys (within the recent borders of the South Caspian basin) in the Paleogene-Miocene time is also characterized by high metallogenic specialization for some precious, rare and non-ferrous metals and intensive forming of gold-sulphide-rare metal formations in oil-generating complexes.

While choosing the object of investigations, we adhered to the main term that the hydrocarbonaceous fluids have been generated by the Paleogene-Lower Miocene (Maykopian) regional gold-hydrocarbon producing complex.

Isotopic-geochemical investigations of oils in the SCSB and correlation "oil-source rock" and "oil-oil" demonstrate that a share of fluid-generating complexes of different ages in the reservoirs infill is not equal in different oil-gas regions and even in the fields (Гулиев и др., 1999; Guliyev et al., 2001; Huseynov, 2000; Feyzullayev et al., 2004; Фейзуллаев и др., 2022). The highest contribution of the Maykopian complex to the generation of isotopic-light oils was recorded in some regions, and the reservoirs of the individual oil field are infilled with Maykopian fluids in a maximal degree.

Isotopic biomarker criteria
(thermal maturity of fluids)

Oils in the selected oil field according to biomarker features (isomerization of normal sterane C29, correlation of monoaromatic and triaromatic steranes etc.) are the most matured (Ro% – up to 0.75) (Guliyev et al., 2000; Guliyev et al., 2001) which corresponds to paleotemperature of transformation of the OM in the Maykopian complex in the interval (T^0C) 125-135^{0}C. Thermal maturity of hydrocarbonaceous gases calculated on the base of isotopic composition of ethane according to the correlation δ13C(C2H6)(%0)=22.6lgRo(%)-32.2 (Faber, 1987) varies in the interval Ro% 0.95-1.1. This corresponds to paleotemperature transformation of the OM 145^0-150^{0}C. These temperatures are quite favorable for the transformation of montmorillonite into hydromica and release of the interlayer water as well as for the dissolution of the ore minerals there and for their saturation with the ore elements, i.e. for the formation of typical ore hydrotherms.

Structural criteria

Most of the oil-gas structures in the South Caspian basin are controlled by zones of deep regional faults and some oil deposits are tectonically-shielded. Zones of tectonic dislocations are characterized by high fluid activity, mud volcanoes development, gas-oil manifestations and discharge of dehydrated and mineralized elision waters (Guliyev and Huseynov, 2015; Aliyev et al., 2024). Thickness of the Paleogene-Lower Miocene fluid-generating deposits is up to 1500-3000 m from deep seismic data (Fig. 2). Scale of oil-gas content demonstrates the focused fluid flow and high fluid-generating potential of the Paleogene-Lower Miocene complex of the basin. It should be emphasized that the SCB is characterized by a very high elision regime and abnormally high formation pressures in the Paleogene-Pliocene hydrodynamic system.

Table 1

Oreforming elements content in the formation water of the South Caspian oil-gas fields and natural hydrotherms (mg/l)

Element	OIL AND GAS BEARING REGION						OREFORMING SYSTEM				WorldOcean water M 3.5 %
	Shamakha-Gobustan		Absheron		Low Kura	Pricaspian	Red sea rift Atlantis II Discovery M 25-28 %	Cheleken		Active volc.zone Taupo, New Zeland	
Water type Minera-lizat.	Maykop Hydrocarb-at. M 1.39 %	PS Porous solution M 7.8 – 12.5 %	PS_1 Hydrocarbonat. M 1.65-2.86 %	PS_2 Cl-Ca M 5.4-14.7 %	PS_2 Cl-Ca M 12-18 %	Maykop Cl-Ca M 3.2-3.7 %		Cl-Ca M 23.08 %	H_2S M 25.37 %		
Ag	0.014-0.126 0.183-1.647	0.416-3.266 5.47-42.97	0.066 0.868			0.036-0.328 0.48-n,n				0.4 5.26	0,0003 0,004
Cu	0.832 0.00177	2.84-25.15 0.006-0.054	1.15 0.0036	2.59 0.0055		0.221 0.0047	0.3 0.0064	4.7-79.9 0.01-0.17	0.0-4.7 0.0-0.01		0.003 0.000063
Mn	0.41 0.00041		0.126 0.000126	1.5 0.0015		1.1 0.0011		11.0 0.011			0.002 0.000002
Fe	5.04 0.00012			1.26-84 0.00003-0.002		13.02 0.00031		12.6 0.0003	4.2 0.0001		0.01 0.00000024
As								0.430-0.935 0.253-0.55	0.493 0.29	8.0 4.7	0.0 0.00006
Cd								5.98-0.793 46.0-6.1			0.00011 0.00076
Mo	0.0693 0.063	0.78-1.25 0.71-1.14				0.185 0.168		0.297 0.27			0.01 0.009
Sr	1 292 0.038		1.04 0.0041	153 0.45		34 0.1		0.0 2.24			8.0 0.023
Ba	3.45 0.0053		0.48 0.00074	117 0.18		9.1 0.014		24.7 0.038			0.03 0.0003
U	0.0038 0.0015		0.0045 0.0018	0.0004 0.00016	0.0004 0.00016	0.00063 0.00025					0.003 0.0012
Ra	3.2×10^{-8} 0.032		9.6×10^{-8} 0.096	1.2×10^{-7} 0.12	3.6×10^{-7} 0.36	4.9×10^{-7} 0.49					1.010^{-10} 0.0001
Th			0.00083 0.000063		0.0015 0.00011	0.00049 0.000037					0.000032 0.0000024
Ga			0.0034 0.00018	0.0012 0.000065	0.00095 0.00005						0.00007 0.0000016
Tl			0.0021 0.0021	0.00067 0.00067	0.00084 0.00084			2.4 2.4		0.007 0.007	0.00001 0.00001
Ge			0.0042 0.003	0.0034 0.0024	0.0022 0.0016						0.00 0.000042
Zn							4.98 0.06	3.33 0.04	no		0.01 0.00012
Pb		1.33-8.80 0.083-0.55	0.29-0.58 0.018-0.036				0.60 0.0376	4.16 0.26	trace		0.0002 0.0000018
Bi		0.56-10.69 62.22-187.7									

The note: in numerator – contents in water (mg/l); in a denominator – clarke of concentration

Table 2

Distribution of oreforming elements in the South Caspian oils

Element	Clarke	Maykop oils	PS oils
Cu	$5.7x10^{-3}$	$1.55x10^{-4} – 2.2x10^{-4}$	$1.3x10^{-5} – 4x10^{-5}$
U	$3.2x10^{-4}$	$2.2x10^{-6}$	$1.7x10^{-6}$ PS_2
			$2.2x10^{-7}$ PS_1
Ra		$1.1x10^{-13}$	$1.16x10^{-13} – 1.9x10^{-13}$
Ga	$3.0x10^{-3}$	Undeterminated	$12.85x10^{-7}$ PS_2
			$5.85x10^{7}$ PS_1
Tl	$1.0x10^{-4}$	Undeterminated	$9.4x10^{-7}$ PS_2
			$3.7x10^{-7}$ PS_1
Ge	$2.0x10^{-4}$	Undeterminated	$8.82x10^{-7}$ PS_2
			$4.23x10^{-7}$ PS_1
Pb	$2.0x10^{-3}$	$9x10^{-6}$	$6.72x10^{-6}$
Zn	$8.0x10^{-3}$	$0.0 – 5.3x10^{-5}$	$9.3x10^{-5}$
Mo	$2.0x10^{-4}$	$6x10^{-6}$	$3.0x10^{-7} – 5.1x10^{-6}$
Cr	$1.0x10^{2}$	$1.8x10^{-5} – 1.1x10^{-4}$	$7,8x10^{-6}$
Ag	$1.0x10^{-5}$	$4.0x10^{-6}$	$4.7x10^{-7} – 2.0x10^{-6}$
Au	$1.1x10^{-7}$	$4.3x10^{-7}$	$4.4x10^{-7}$

Lithological criteria

The Lower Pliocene deltaic and fluvial oil deposits are successively overlapped by deposits of all stratigraphic units of the Lower, Middle and the Upper Pleistocene (Absheron – 1700-800 Ka, Tyurkyan – 800-700 Ka, Baku – 700-350 Ka, Khazar – 350-75 Ka and Khvalyn – 75-10 Ka horizons). The Pleistocene deposits have been accumulated in isolated basin environment, which was temporarily connected with Evksin (Black Sea). Lithologically the Pleistocene succession is represented by alternative carbonaceous sandy-silty–clayey deposits, marls, detritus limestones, coquina. The thickness of Pleistocene deposits in some place (especially in the near-crust area along the deep faults) is up to 1000 m. Lithologically these deposits are quite favorable for the accumulation of gold (they are carbonaceous geochemical and sorption-mechanical barrier) and are the same type as some oil and gold fields – the Gold Point electrum deposits near Railroad Valley, the Carlin-type gold deposits of the Yankee basin in the southern Alligator Ridge mining district (Nevada, USA) and the "Prairie" type micro-disseminated gold mineralization of the Western Canada Sedimentary Basin at Fort MacKay (northeastern Alberta) in Canada (Hulen and Collister, 1999; Abercrombie, 1997: Fedikow et al., 1996; Fedikow et al., 1997).

Detailed geological-geophysical and isotopic-geochemical investigations demonstrated that there occurred intensive generation of catagenic water solutions saturated by ore components in the SCSB in "oil-gas window" alongside with formation of liquid and gaseous hydrocarbons (Huseynov, 2002; Guliyev et al., 2004).

Idea approbation and Results

The necessity of the investigation of gold-oil paragenesis in South Caspian basin has been proved by the preliminary data. We conducted reconnaissance field studies and geochemical testing of the fault zones within one oil field the thickness of which is more than 100 m. Preliminary testing of one of such zones within distance of 80 m across the strike of the fault showed hurricane concentrations of gold (0.3 to 0.9 g/t), palladium (0.2-0.7 g/t), corresponding to the lower boundary of commercial (cutoff grade) amounts, as well as indicators of the Carlin type epithermal gold mineralization: arsenic on average 1665 g/t, antimony – 30g/t and barium – 1794 g/t, which exceed the Clarke values by 1700, 250-1000 and 170 times respectively (Table 3). There have been also determined abnormally high, relative to the Clarke values, content of the following elements: iron – 10-15 times; manganese and nickel – up to 100 times, copper – 10 times. Zink and lead exceed the Clarke values up to 2 times. Contrary to the above mentioned metals, silver and uranium contents in the investigated zone are tens times below the Clarke value.

Table 3

Distribution of ore elements in the mineralized zone of the fault

№	Fe	Mn	Ti	P	Sb	Cr	Ni	Cu	Zn	As	Zr	Ba	Pb	Au	Pd	Ag	U
	wt. %				g/t												
min	4.28	0.18	0.22	0.05	12	22	144	45	27	161	24	84	11	0,3	0,2	$<1*10^{-4}$	<0.1
max	14.4	0.34	0.3	0.07	48	149	223	64	35	3230	62	3580	15	0,96	0,7	$<1*10^{-4}$	<0.1
mean	**9.39**	**0.29**	0.26	0.06	**25.7**	29.4	**188**	**53.2**	**31.3**	**1665**	38.2	**1794**	**12.7**	**0.57**	**0.35**		
Clarkes by Turekian and Wedepohl, 1961																	
sand	0.98	0.00n	0.15	0.02	0.0n	35	2	n	16	1	220	n*10	7	0.00n	n.d.	0.0n	0.45
carbonate sediments	0.38	0.11	0.04	0.04	0.2	11	20	4	20	1	19	10	9	0.00n	n.d.	0.0n	2.2

** - Fe,Mn,Ti,P,V,Cr,Ni,Cu,Zn,As,Zr,Ba,Mn,Au,Pd,Pb,Ag – were determined by the atomic-absorbtion analysis in the device Analyst –300 (Perki-n Elmer, USA).*

*** - U was determined in the device SARI-2 (limit of sensitivity $1* 10^{-3}$ %)*

As a result of correlation analysis, in the mineralized zone there have been determined three associations of elements: I – Fe-Cu-As-Ba-(Mn); II – Cr-Ti-Zr; III – Au-Pd-Pb. Elements from associations I and III negatively correlate with elements from association II and do not correlate absolutely or weakly with each other. This indicates that Fe, Cu, As, Ba, Mn, Au, Pd and Pb have been delivered to the fault zone and control the balance of Cr, Ti and Zr, which are components of stable in situ accessory minerals of the enclosing sandstones. Superimposed character of the mineralization is confirmed by microscopic investigations of samples from the fault zone.

It should be emphasized that we investigated and tested only the uppermost part of the fault zone which is an area of active circulation of oxygen-rich surficial-atmospheric waters. It is known well enough, that gold, palladium, lead and especially uranium and silver are active migrants in the waters of hypergenesis. For example, palladium is the only member of the PGE that is significantly mobile and dilute surface waters. It forms hydroxyl complexes $Pd(OH)_2$, $Pd(OH)^{3-}$ and $Pd(OH)_4^{2-}$. The results of the field and laboratory studies show that Pd is mobilized from the ore and is carried in solution to be fixed with organic material in sediments, clay minerals and other sorbents (Cameron and Hattori, 2003; Olivo et al., 2001). One can suppose that absence of uranium and silver in the upper near-surface area of the fault zone is a result of their complete leaching whereas the observed amounts of gold (0.3-0.96 g/t) and palladium (0.2-0.7 g/t) although are high but still much more lower than their initial concentrations. Optical microscopic investigations demonstrate that the main bulk of the ore mass mostly composed of aggregates of iron hydroxides formed on pyrite disseminations and phromboides. Pyritization is of a superimposed character (Fig. 3).

Fragmental grains of non-ore minerals are densely impregnated by dotted inclusions and veins of pyrite and in some places they are corroded by it. A visible gold has not been determined (Fig. 3). Absence of correlation of gold, palladium and lead (association III of elements remobilized from oxidation zone) with iron excludes their accumulation in iron hydroxides. At the same time, the strong correlation and high contents of elements association Fe-Cu-As-Ba-Mn are caused by their accumulation in the zone of hypergenesis and iron hydroxides (Fig. 4).

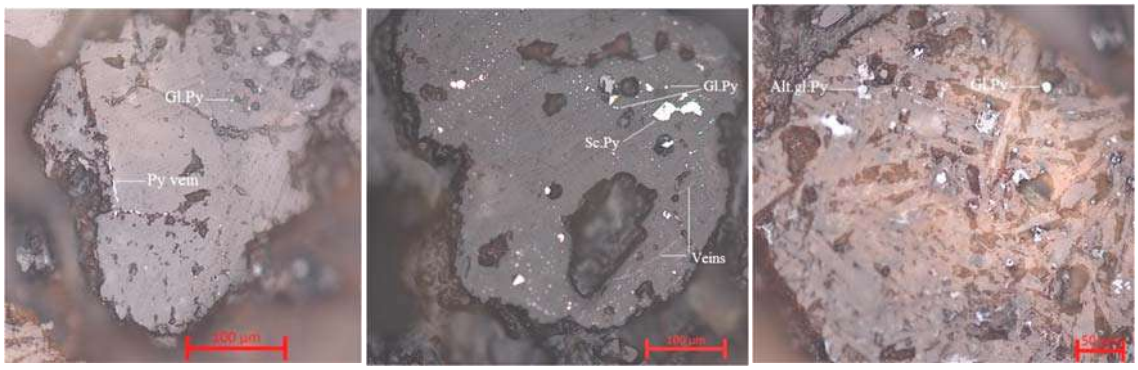

Fig. 3. Photo optical microscopic study of polished sections illustrate a superimposed character of pyritization. Pyrite aggregates: Py vein – vein, Gl Py – globular, Sc Py – secondary, Alt gl Py – alterated globular

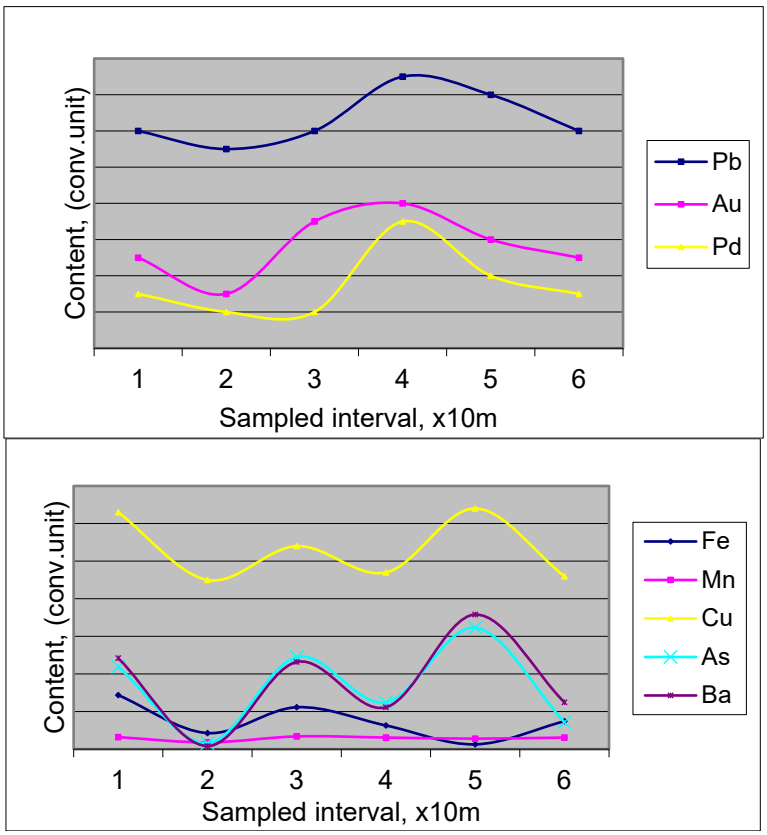

Fig. 4. Distribution and correlation of class I and III element's association within gold-bearing zone

It is very important, that abnormally high amounts of gold and palladium were recorded in calcareous highly-porous sandstones with extremely low amounts of clayey minerals, OM and bitumen, which are the main sorbents, and concentrators of noble metals in stratiform deposits of the Carlin type. This enables to make a conclusion about the existence of commercial concentrations of gold and palladium in the deposits with a high amount of pelitic material and OM, such like clays, silts, silty sandstones, clayey sandstones which constitutes most of the Quaternary section in the studied oil field. At the same time by the analogy with gold epithermal deposits in Nevada and Alberta, one can make a conclusion about the initial concentration of gold in pyrite as well in the studied oil field in SCB. For example, pyrites in the Getchell field contain gold in amount of 2,400 ppm; in the Carlin field – 500 ppm (Cline, 2001; Togashi, 1992; Hausen, 1981; Radtke, 1985; Hausen et al., 1986; Cabri et al., 1989).

SEM analyses of rock samples (Fig. 5) from the mineralization zone of studied oil field show that gold in epigenetic impregnated (ingrained) and vein pyrite aggregates reaches hurricane concentration – from 17,500 ppm (1.75 wt.%) to 21,300 ppm (2.13 wt.%). It is 35-100 times higher than gold concentration in the Getchell's and Carline's pyrites. At magnifying for 10,000-12,000 times by SEM analyses the mineral phase of gold in pyrite aggregates has not been detected (Fig. 6). Thus, one can come to conclusion that gold in pyrite aggregates is in the form of emulsion impregnation.

Chemical re-calculations demonstrate, that accumulation of such amount of iron hydroxides in the zone of oxidation in the investigated fault requires the decomposition of pyrite in amount from 8% to 29% in sediments (without the account of losses for the iron removed from the oxidation zone). This demonstrates intensive initial pyritization of this fragment of the fault and enables to make a supposition, that decomposing pyrites in the hypergenesis zone released significant amount of gold and other metals saturating by these metals the descending oxygen– and SO_4^{2-} containing sulphate waters. Thus, more high gold concentration in the lower horizons of the fault zones in the studied field is beyond all manner of doubt for the following reasons: 1) existence of thick horizons of high-permeable carbonates with high amount of clayey minerals and OM, i.e. favorable combination of carbonate and precipitating barriers; 2) abundance of gold-bearing sulfide disseminations; 3) redeposition in the reduction paleobarrier of gold and palladium, leached out of the upper parts of the mineralized fault zone. Existence of such barrier is proved by the ascending hydrocarbon and hydrogen sulphide fluids.

Element	Weight %	Atomic %
P K	0.77	1.00
S K	54.05	67.35
Ca K	1.24	1.24
Ti K	0.56	0.46
Fe K	41.26	29.52
As L	0.00	0.00
Ag L	0.00	0.00
Au M	2.13	0.43
Total	100.00	

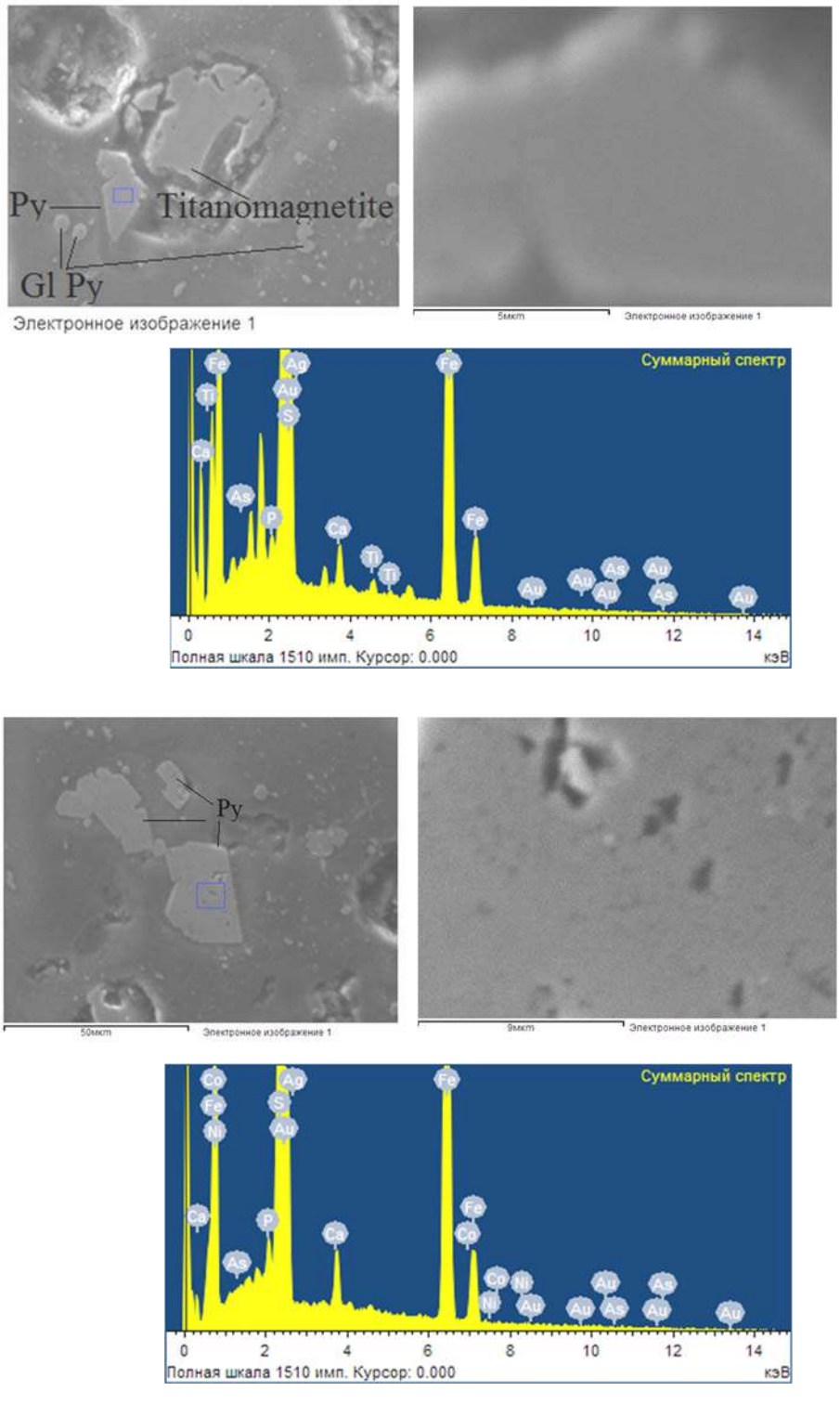

Element	Weight %	Atomic %
P K	0.88	1.14
S K	53.83	66.95
Ca K	1.68	1.67
Fe K	41.86	29.89
Co K	0.00	0.00
Ni K	0.00	0.00
As L	0.00	0.00
Ag L	0.00	0.00
Au M	1.75	0.35
Total	100.00	

Fig. 5. SEM analyses of pyrite aggregates from gold bearing zone in the SCB and spectrograms of distribution gold and other elements (instrument: JEOL 6610-LV)

Existence of a thick (up to 80 m) mineralized fragment composed of gold-paladium-bearing calcareous sandstones and characterized by the intensive hydrothermal activity within regional fault zone in studied oil field enables by analogy with the north Nevada to highly evaluate the potential epithermal gold content of the Carlin type in the great part of area under study.

As a result of this study we expect to estimate the gold and other noble metals potential in studied oil field. It will enable us to assess the gold potential of other hydrocarbon fields in the South Caspian basin, which will give us an unique chance to begin a new era in exploration of mineral resources in the basin which has more than 150 years history as an oil basin.

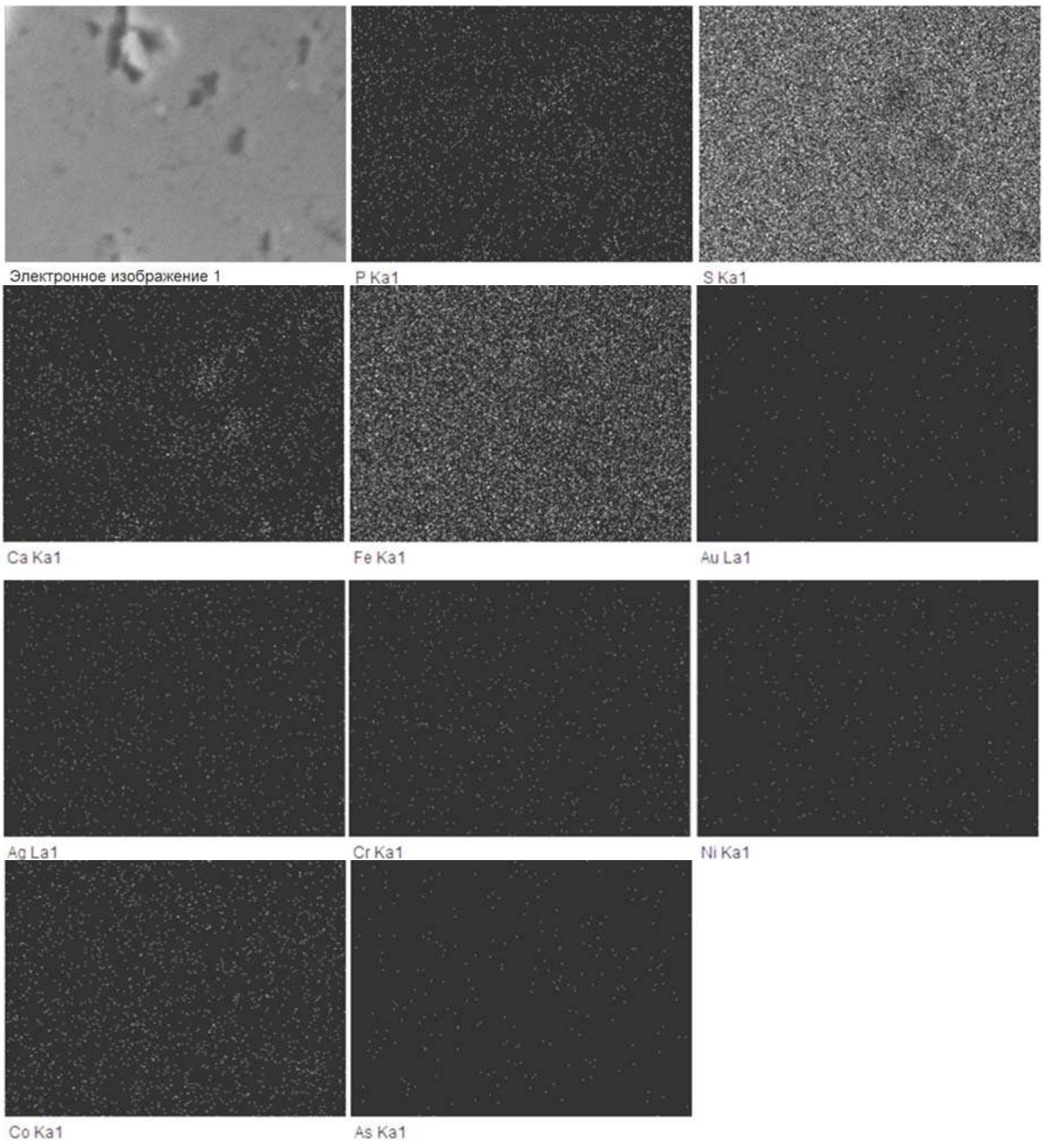

Fig. 6. SEM images of distribution mineral phase in the pyrite aggregate from gold bearing zone in the SCB (instrument: JEOL 6610-LV)

We also expect that this research will give us an opportunity to contribute much in ore industry of Azerbaijan, which is an important step in economic development of our country. The results that we are planning to receive and methodology, which we'll use, might be also applied to other analogous basins in the world.

As a next step, the following studies should be carried out in the study area:

- Determination of linear parameters, occurrence and morphology of mineralized fault zone and its geochemical halo. This should be performed by integration of different geophysical methods – gravimetric, magnetic and radiometric survey.
- Sedimentological investigations based on the integration of field works and data of log diagrams interpretation and aimed to determine facial types of rocks favorable for the ore- mineralization and to trace them in the area and in the vertical section.
- Geochemical testing and mapping aimed to determine Au, Pd contents and accompanying elements and intensity of geochemical anomaly.
- Petrographic investigations of ore-enclosing deposits to determine character of hydrothermal change and degree of mineralization of rocks.
- Mineralogic investigations including microprobe, X-ray spectral, X-ray diffractometric and SEM analyses.

• Isotopic and biomarker analyses to determine the gold-bearing fluid sources.

• 3D modeling of geometry of gold-bearing complexes and estimation of mineralization volume.

Conclusion

The Paleogene-Miocene complex of deposits of the South Caspian basin together with oil-generating potential has high ore (gold)-generating potential. In this connection paleo- and recent centers of katagenic discharging of gas-water-oil fluids have an important meaning. In favorable structural-lithological and geochemical conditions accumulations of ore matter are confined to them. From this viewpoint the mud volcanoes and zones of tectonic faults controlling their location have a special interest. According to geophysical and geochemical data on isotopic composition of oxygen, carbon and hydrogen of mud volcanoes waters and gases, the hearths of mud volcanoes are located on great depths – 10-12 km and their canals serve as the fluids' transportation ways (Fig. 2). Due to such great depth of fluid generation they are heated and saturated with metals.

Preliminary investigations of one of regional zones of tectonic dislocations within one of oil field confirmed our prediction about the possible formation of noble-metal (Au-Pd) and oil paragenesis in the SCB and the discovery of huge gold mineralization within the oil fields. Gold is invisible and micro-disseminated in sulfides (mainly pyrite) and associates with carbonate and clay minerals.

Assessment of the gold potential of other hydrocarbon fields in the South Caspian basin will give us an unique chance to begin a new era in exploration of mineral resources in the basin which has more than 150 years history as an oil basin. We also expect that this research will give us an opportunity to contribute much in ore industry in Azerbaijan, which is an important step economic development of our country.

Investigation like this dealing the search for gold mineralization in the SCB conducted for the first time and result that we got allows us to transform oil-gas bearing basin to *"gold-oil-gas bearing basin"*.

Acknowledgments

The author is deeply grateful to the management of the Institute of Geology and Geophysics represented by academician Akif A.Alizadeh for support and inspiration of the scientific researches as well as his friend and colleague, head of department "Ore-magmatic systems" Dr. Rauf Kerimov and the department staff S.Velizadeh, T.Gadirova and A.Agayev for mineralogic-technologic tests. The author is indebted to N.Sadigov and M.Abdullayev for arrangement of the laboratory and SEM studies.

REFERENCES

Abercrombie H.J. and Feng R. Geological setting and origin of microdisseminated Au-Ag-Cu minerals, Fort Mackay region, northeastern Alberta. Geological Survey of Canada Bulletin, 500, 1997, pp. 247-277.

Agalarov M.S., Israelyan A.D., Sappo P.V., Akhmedova R.A. Content and type of distribution of some chemical elements in the system oil-rock-water within Muradkhanli field. Azerbaijan Oil Economy, 1980, No. 7, pp. 15-18 (in Russian).

Akhundov A.R., Sappo P.V. 1960. On issue of some microelements distribution in the formation waters of Productive Series of Balakhani-Sabunchi-Ramana field. Azerbaijan Oil Economy, No. 8, 1960, pp. 9-11 (in Russian).

Aliyev A.A., Huseynov D.A, Abbasov O., Rashidov T., Kangarli I. Mud volcanoes of Azerbaijan: The unique natural objects of the geoheritage. Geoheritage, Vol. 16(1), article id. 20, 2024, https://doi.org/10.1007/s12371-024-00931-3.

Alizade A.A., Guliyev I.S., Mamedov P.Z., Aliyeva E.G., Feyzullayev A.A., Huseynov D.A. Productive Series of Azerbaijan. In 2 volumes. Publishing House «Nedra», 2018, Vol. 1, 305 p. (in Russian).

Babayev F.R. On geochemistry of oils in Azerbaijan marine deposits. Reports of Academy of Sciences of AzSSR, Vol. XL, No. 8, 1984, pp. 55-57 (in Russian).

Bagir-zade F.M., Narimanov A.A., Babayev F.R. Geologic-geochemical peculiarities of the fields of the Caspian Sea. Nedra. Moscow, 1988 (in Russian).

Bogashova L.G. Role of the halogen waters in forming of the mineral deposits. GEOS. Moscow, 2007, 168 p. (in Russian).

Burton J.C., Lawler J.P., Ayres D.E. Genesis of Carlin-type gold deposits. Geol. Soc. Am., Abstr. Programs; Vol/Issue: 17;/98. Annual meeting of the Geological Society of America; 28 Oct 1985; Orlando, FL, USA.

ЛИТЕРАТУРА

Агаларов М.С., Израэлян А.Д., Саппо П.В., Ахмедова Р.А. Содержание и характер распределения некоторых химических элементов в системе нефть-порода-вода площади Мурадханлы. АНХ, 1980, No. 7, с. 15-18.

Ализаде А.А., Гулиев И.С., Мамедов П.З., Алиева Э.Г., Фейзуллаев А.А., Гусейнов Д.А. Продуктивная толща Азербайджана. В 2-х т. Издательский Дом «Недра». Москва, 2018, Т. 1, 305 с.

Ахундов А.Р., Саппо П.В. К вопросу распределения ряда микроэлементов в пластовых водах ПТ Балаханы-Сабунчи-Раманинского месторождения. АЗНХ, No. 8, 1960, с. 9-11.

Бабаев Ф.Р. К геохимии нефтей морских месторождений Азербайджана. Докл. Акад. Наук. АзССР, Том XL, No.8, 1984, с. 55-57.

Багир-заде Ф.М., Нариманов А.А., Бабаев Ф.Р. Геолого-геохимические особенности месторождений Каспийского моря. Недра. Москва, 1988.

Богашова Л.Г. Роль галогенных вод в формировании месторождений полезных ископаемых. ГЕОС. Москва, 2007, 168 с.

Гулиев И.С., Фейзуллаев А.А., Гусейнов Д.А. Изотопный состав углерода нефтей Южно-Каспийской мегавпадины. Азербайджанское нефтяное хозяйство, No. 6, 1999, с. 3-13.

Израэлян А.Д. Микроэлементы в золе нефтей майкопской свиты Азербайджана. Труды АзНИИ (АзНИПИНефть), 1959, с. 274-281.

Израэлян А.Д. Малые элементы в третичных отложениях нефтеносных областей Азербайджана (по данным спектрального анализа). Автореф. канд. дис., Баку, 1964.

Израэлян А.Д., Ахмедова Р.А., Алиев Г.-М.А. Микроэлементы в золах нефтей ПТ Азербайджана. АНХ, No.10, 1975, с. 6-10.

Cabri L.J., Chryssoulis S.L., DE Villiers J. P.R., Laflamme J.H.G., Buseck R. The nature of "invisible" gold in arsenopyrite. Can. Mineral., Vol. 27, 1989, pp. 353-362.

Cameron E.M. and Hattori K.H. Mobility of palladium in the surface environment: data from a regional lake sediment survey in northwestern Ontario. Geochemistry: Exploration, Environment, Analysis, Vol. 3, 2003, pp. 299-311.

Cline J. Timing of gold and arsenic sulfide mineral deposition at the Getchell Carlin-type gold deposit, North-Central Nevada. Economic Geology, Vol. 96, 2001, pp. 75-89.

Emeri K., Hunt D., Heys E. General review of problem of the thermal solutions and ore sediments of the Red Sea. The modern hydrothermal ore-forming. Mir. Moscow, pp. 7-25 (in Russian).

Faber E.Z. Isotope geochemistry of gaseous hydrocarbons: petroleum, natural gas and coal. Vol. 103, 1987, pp. 210-218 (in German).

Fedikow M.A.F., Bezys R.K., Bamburak J.D., Abercrombie H.J. The geological setting of prairie-type micro-disseminated gold mineralization in Manitoba. Abstracts book of Conference CIM, Vancouver 97, April 27-30, 1997, Vancouver, BC.

Fedikow M.A.F., Bezys R.K., Bamburak J.D., Abercrombie H.J. Prairie-type microdisseminated Au mineralization – a new deposit type in Manitoba's Phanerozoic rocks (NTS 63C/14). In: Manitoba Energy and Mines, Minerals Division, Report of Activities 1996, pp.108-121.

Feyzullayev A.A., Guliyev I.S., Tagiyev M.F. Source potential of the Mesozoic-Cenozoic rocks in the South Caspian Basin and their role in forming the oil accumulations in the Lower Pliocene reservoirs. Petroleum Geoscience, Vol. 7, No. 4, 2001, pp. 409-417.

Feyzullayev A.A., Huseynov D.A., Tagiyev M. Oil source rocks and geochemistry of hydrocarbons in South Caspian basin. In: South Caspian basin: geology, geophysics and gas content. Nafta-Press. Baku, 2004, pp. 286-321.

Feyzullayev A.A. Huseynov D.A., Rashidov T.M. Isotopic composition of the products of the mud volcanoes activity in the South-Caspian basin in connection with petroleum potential of the deeply burried sediments. ANAS Transactions, Earth Sciences No. 1, 2022, pp. 68-80, DOI: 10.33677/ ggianas20220100073 (in Russian).

Ge X., Shen Ch., He P., Jin Y., Li S., Chen Y. The roles of hydrocarbons on the mineralization of Carlin-type gold deposits, Nanpanjiang Basin, South China. Ore Geology Reviews, Vol. 149, 105107, 2022, pp. 1-15.

Guliyev I.S., Feyzullayev A.A., Huseynov D.A. Maturity level of oils contained in different age reservoirs in the South Caspian mega-Basin. Oil and gas geology, Moscow, No. 3, 2000, pp. 41-50.

Guliyev I.S., Feyzullayev A.A., Huseynov D.A. Isotope geochemistry of oils from fields and mud volcanoes in the South Caspian Basin, Azerbaijan. Petroleum Geoscience, Vol. 7, No. 4, 2001, pp. 409-417.

Guliyev I.S., Huseynov D.A., Feyzullayev A.A. Fluids of mud volcanoes in the Southern Caspian sedimentary basin: geochemistry and sources in light of new data on the carbon, hydrogen, and oxygen isotopic compositions. J. Geochemistry International, Moscow, Vol. 42, No. 7, 2004, pp. 688-695.

Guliyev I.S, Feyzullayev A.A., Huseynov D.A. Isotopic composition of carbon of oils of the South-Caspian megadepression. Azerb.Neft.Khozyavstvo, No. 6, 1999, p. 3-13 (in Russian).

Guliyev I.S.and Huseynov D.A. Relics of mud volcanoes in the sedimentary cover of the South Caspian Basin. Lithology and Mineral Resources, Vol. 50, No. 4, 2015, pp. 311-321.

Hausen D.M. Process mineralogy of auriferous pyritic ores at Carlin, Nevada. In: Process Mineralogy (Hausen D.M. and Park W.C., eds.), TMS, Warrendale, PA, 1981, pp. 271-289.

Лебедев Л.М., Никитина И.Б. Челекенская рудообразующая система. Наука. Москва, 1983, 240 с.

Мехтиев Ш.Ф., Раковский Э.Е., Мирзоев Р.Х., Харитонов В.М., Садигов А.М. Металлоносность битуминозных пород Азербайджана. Изв. АН СССР, Серия геологическая, No. 4, 1986, с. 117-123.

Мирзоев Р.Х. и Харитонов В.М. К вопросу изучения следовых содержаний золота в нефтях Азербайджана. АНХ, No. 11, 1982, с. 15-18.

Пушкина З.В. Поровые воды глинистых пород и их изменения по разрезу. Постседиментационные изменения четвертичных и плиоценовых глинистых отложений Бакинского архипелага. Академия Наук СССР, Труды, выпуск 115, Наука. Москва, 1965, с. 160-203.

Раковский Э.Е., Мирзоев Р.Х., Харитонов В.М. К изучению распределения золота в нефтях месторождения Локбатан. АНХ, No. 8, 1985, с. 8-13.

Фейзуллаев А.А., Гусейнов Д.А., Рашидов Т.М. Изотопный состав продуктов деятельности грязевых вулканов Южно-Каспийского бассейна в связи с нефтегазоносностью глубокопогруженных отложений. ANAS Transactions, Earth Sciences, No. 1, 2022, с. 68-80, DOI: 10.33677/ ggianas20220100073.

Эмери К., Хант Д., Хейс Э. Общий обзор проблемы термальных рассолов и рудных осадков Красного моря. Современное гидротермальное рудообразование. Мир. Москва, 1974, с. 7-25.

Юшко-Захарова О.Е., Иванов В.В., Соболева Л.Н. и др. Минералы благородных металлов. Недра. Москва, 1986, 272 с.

Abercrombie H.J. and Feng R. Geological setting and origin of microdisseminated Au-Ag-Cu minerals, Fort Mackay region, northeastern Alberta. Geological Survey of Canada Bulletin, 500, 1997, pp. 247-277.

Aliyev A.A., Huseynov D.A, Abbasov O., Rashidov T., Kangarli I. Mud volcanoes of Azerbaijan: The unique natural objects of the geoheritage. Geoheritage, Vol. 16(1), 20 2024, https://doi.org/10.1007/s12371-024-00931-3.

Burton J.C., Lawler J.P., Ayres D.E. Genesis of Carlin-type gold deposits. Geol. Soc. Am., Abstr. Programs; Vol/Issue: 17;/98. Annual meeting of the Geological Society of America; 28 Oct 1985; Orlando, FL, USA.

Cabri L.J., Chryssoulis S.L., DE Villiers J. P.R., Laflamme J.H.G., Buseck R. The nature of "invisible" gold in arsenopyrite. Can. Mineral., Vol. 27, 1989, pp. 353-362.

Cameron E.M. and Hattori K.H. Mobility of palladium in the surface environment: data from a regional lake sediment survey in northwestern Ontario. Geochemistry: Exploration, Environment, Analysis, Vol. 3, 2003, pp. 299-311.

Cline J. Timing of gold and arsenic sulfide mineral deposition at the Getchell Carlin-type gold deposit, North-Central Nevada. Economic Geology, Vol. 96, 2001, pp. 75-89.

Faber E.Z. Isotopengeochemie gasformiger Kohlenwasserstoffe: Erdole, Erdgas und Kohle. Vol. 103, 1987, pp. 210-218.

Fedikow M.A.F., Bezys R.K., Bamburak J.D., Abercrombie H.J. Prairie-type microdisseminated Au mineralization – a new deposit type in Manitoba's Phanerozoic rocks (NTS 63C/14). In: Manitoba Energy and Mines, Minerals Division, Report of Activities 1996, pp.108-121.

Fedikow M.A.F., Bezys R.K., Bamburak J.D., Abercrombie H.J. The geological setting of prairie-type micro-disseminated gold mineralization in Manitoba. Abstracts book of Conference CIM, Vancouver 97, April 27-30, 1997, Vancouver, BC.

Feyzullayev A.A., Guliyev I.S., Tagiyev M.F. Source potential of the Mesozoic-Cenozoic rocks in the South Caspian Basin and their role in forming the oil accumulations in the Lower Pliocene reservoirs. Petroleum Geoscience, Vol. 7, No. 4, 2001, pp. 409-417.

Hausen D.M., Ahlrichs J.W., Mueller W., Park W.C. Particulate gold occurrences in three Carlin carbonaceous ores. In: Process Mineralogy VI, (Hagni D., ed.), TMS, Warrendale, PA, 1986, pp. 193-214.

Hofstra A.H. and Cline J.S. Characteristics and models for Carlin-type gold deposits. Reviews in Economic Geology, Vol. 13, 2000, pp. 163-220.

Hulen J.B. and Collister J.W. The oil-bearing, Carlin-type gold deposits of Yankee Basin, Alligator Ridge District, Nevada. Economic Geology, Vol. 94, 1999, pp. 1029-1050.

Hulen J.B., Collister J.W., Curtiss D.K. The role of active and ancient geothermal processes in the generation, migration, and entrapment of oil in the Basin and Range Province, Western USA. Grant project DE-FG02-90ER14133 of University Utah. Salt Lake City, Utah, US, 1998.

Huseynov D.A. Origin of oils in the western part of the Kura South Caspian oil-gas bearing basins. Proceedings of 62d EAGE Conference, UK, Glasgow, 2000, P-20, http://dx.doi.org/10.3997/2214-4609-pdb.28.A55.

Huseynov D.A. Paragenesis of metals and oil-generating series in the South Caspian sedimentary basin. Proceedings of 16th Sedimentological Congress, South Africa, 8-12 July 2002, pp. 23-27.

Ilchik R.P. and Barton M.D. An amagmatic origin of Carlin-type gold deposits. Economic Geology and the Bulletin of the Society of Economic Geolocists, Vol. 92, No. 3, 1997, pp. 269-288.

Israelyan A.D. Microelements in ash of oils of the Maykopian formation of Azerbaijan. Proceedings of AzNII (AzNIPINeft), 1959, pp. 274-281 (in Russian).

Israelyan A.D. Trace elements in the Tertiary sediments of oil-bearing provinces of Azerbaijan (by spectral analysis data). Abstract of thesis, Baku, 1964 (in Russian).

Israelyan A.D., Akhmedova R.A., Aliyev G.-M.A. Microelements in ashes of oils of the Productive Series of Azerbaijan. Azerb.Neft.Khozyavstvo, No. 10, 1975, pp. 6-10 (in Russian).

Kuehn C.A. and Rose A.W. Carlin gold deposits, Nevada: Origin in deep zone of mixing between normally pressured and overpressured fluids. Economic Geology, Vol. 90, 1995, pp. 12-36.

Lebedev L.M., Nikitina I.B. Cheleken ore-forming system. Nauka. Moscow, 1983, 240 p. (in Russian).

Mekhtiyev Sh.F., Rakovski E.E., Mirzoyev R.Kh., Kharitonov V.M., Sadigov A.M. Metal content of the bituminous rocks of Azerbaijan. Proceedings of Academy of Sciences of the USSR. Geological series, No. 4, 1986, pp. 117-123 (in Russian).

Mirzoyev R.Kh. and Kharitonov V.M. On issue of study of the gold trace content in Azerbaijan oils. Azerbaijan Oil Economy, No. 11, 1982, pp. 15-18 (in Russian).

Olivo G.R., Gauthier M., Williams-Jones A.E., Levesque M. The Au-Pd mineralization at the Conceição Iron Mine, Itabira District, Southern Sro Francisco Craton, Brazil: an example of a Jacutinga-type deposit. Economic Geology, Vol. 96, 2001, pp. 61-74.

Pushkina Z.V. Porous waters of the clayey rocks and their alterations along the section. Post-sedimentation alterations of quaternary and Pliocene clay deposits of Baku archipelago. Academy of Sciences of the USSR, Transactions, Vol. 115, Nauka. Moscow, 1965, pp. 160-203 (in Russian).

Radtke A.S. Geology of the Carlin gold deposit, Nevada. U.S. Geological Survey Professional Paper 1267, 1985, 124 p.

Rakovski E.E., Mirzoyev R.Kh., Kharitonov V.M. On study of gold distribution in oils of Lokbatan field. Azerb. Neft. Khozyavstvo, No. 8, 1985, pp. 8-13 (in Russian).

Seedorff E. and Barton M.D. Enigmatic origin of Carlin-type deposits: An amagmatic solution? SEG Newsletter, No. 59, 2004, pp. 14-18.

Togashi Y. Geological characteristics of the sediment hosted, disseminated gold deposits in the Western United States of America. In: The series of mineral concentrations and hy-

Feyzullayev A.A., Huseynov D.A., Tagiyev M. Oil source rocks and geochemistry of hydrocarbons in South Caspian basin. In: South Caspian basin: geology, geophysics and gas content. Nafta-Press. Baku, 2004, pp. 286-321.

Ge X., Shen Ch., He P., Jin Y., Li S., Chen Y. The roles of hydrocarbons on the mineralization of Carlin-type gold deposits, Nanpanjiang Basin, South China. Ore Geology Reviews, Vol. 149, 105107, 2022, pp. 1-15.

Guliyev I.S., Feyzullayev A.A., Huseynov D.A. Isotope geochemistry of oils from fields and mud volcanoes in the South Caspian Basin, Azerbaijan. Petroleum Geoscience, Vol. 7, No. 4, 2001, pp. 409-417.

Guliyev I.S., Feyzullayev A.A., Huseynov D.A. Maturity level of oils contained in different age reservoirs in the South Caspian mega-Basin. Oil and gas geology, Moscow, No. 3, 2000, pp. 41-50.

Guliyev I.S.and Huseynov D.A. Relics of mud volcanoes in the sedimentary cover of the South Caspian Basin. Lithology and Mineral Resources, Vol. 50, No. 4, 2015, pp. 311-321.

Guliyev I.S., Huseynov D.A., Feyzullayev A.A. Fluids of mud volcanoes in the Southern Caspian sedimentary basin: geochemistry and sources in light of new data on the carbon, hydrogen, and oxygen isotopic compositions. J. Geochemistry International, Moscow, Vol. 42, No. 7, 2004, pp. 688-695.

Hausen D.M. Process mineralogy of auriferous pyritic ores at Carlin, Nevada. In: Process Mineralogy (Hausen D.M. and Park W.C., eds.), TMS, Warrendale, PA, 1981, pp. 271-289.

Hausen D.M., Ahlrichs J.W., Mueller W., Park W.C. Particulate gold occurrences in three Carlin carbonaceous ores. In: Process Mineralogy VI, (Hagni D., ed.), TMS, Warrendale, PA, 1986, pp. 193-214.

Hofstra A.H. and Cline J.S. Characteristics and models for Carlin-type gold deposits. Reviews in Economic Geology, Vol. 13, 2000, pp. 163-220.

Hulen J.B. and Collister J.W. The oil-bearing, Carlin-type gold deposits of Yankee Basin, Alligator Ridge District, Nevada. Economic Geology, Vol. 94, 1999, pp. 1029-1050.

Hulen J.B., Collister J.W., Curtiss D.K. The role of active and ancient geothermal processes in the generation, migration, and entrapment of oil in the Basin and Range Province, Western USA. Grant project DE-FG02-90ER14133 of University Utah. Salt Lake City, Utah, US, 1998.

Huseynov D.A. Origin of oils in the western part of the Kura South Caspian oil-gas bearing basins. Proceedings of 62d EAGE Conference, UK, Glasgow, 2000, P-20, http://dx.doi.org/10.3997/2214-4609-pdb.28.A55.

Huseynov D.A. Paragenesis of metals and oil-generating series in the South Caspian sedimentary basin. Proceedings of 16th Sedimentological Congress, South Africa, 8-12 July 2002, pp. 23-27.

Ilchik R.P. and Barton M.D. An amagmatic origin of Carlin-type gold deposits. Economic Geology and the Bulletin of the Society of Economic Geolocists. Vol. 92, No. 3, 1997, pp. 269-288.

Kuehn C.A. and Rose A.W. Carlin gold deposits, Nevada: Origin in deep zone of mixing between normally pressured and overpressured fluids. Economic Geology, Vol. 90, 1995, pp. 12-36.

Olivo G.R., Gauthier M., Williams-Jones A.E., Levesque M. The Au-Pd mineralization at the Conceição Iron Mine, Itabira District, Southern Sro Francisco Craton, Brazil: an example of a Jacutinga-type deposit. Economic Geology, Vol. 96, 2001, pp. 61-74.

Radtke A.S. Geology of the Carlin gold deposit, Nevada. U.S. Geological Survey Professional Paper 1267, 1985, 124 p.

Seedorff E. and Barton M.D. Enigmatic origin of Carlin-type deposits: An amagmatic solution? SEG Newsletter, Vol. 59, 2004, pp. 14-18.

drocarbon accumulations in the ESCAP region. Volume 6 – Epithermal gold in Asia and the Pacific (ST/ESCAP/1023). United Nations publication. 1992, 224 p.
Turekian K.K. and Wedepohl K.H. Distribution of the elements in some major units of the Earth's crust. Geological Society of America Bulletin, Vol. 72, 1961, pp. 175-192.
Yushko-Zakharova O.E., Ivanov V.V., Soboleva L.N. et al. Minerals of the noble metals. Nedra. Moscow, 1986, 272 p. (in Russian).
Togashi Y. Geological characteristics of the sediment hosted, disseminated gold deposits in the Western United States of America. In: The series of mineral concentrations and hydrocarbon accumulations in the ESCAP region. Volume 6 – Epithermal gold in Asia and the Pacific (ST/ESCAP/1023). United Nations publication. 1992, 224 p.
Turekian K.K. and Wedepohl K.H. Distribution of the elements in some major units of the Earth's crust. Geological Society of America Bulletin, Vol. 72, 1961, pp. 175-192.

ЗОЛОТОРУДНЫЕ ПРОЯВЛЕНИЯ НА НЕФТЕНОСНЫХ ПЛОЩАДЯХ ЮЖНО-КАСПИЙСКОГО БАССЕЙНА*

Гусейнов Д.А.
Министерство науки и образования Азербайджанской Республики, Институт геологии и геофизики, Азербайджан AZ1143, Баку, просп. Г.Джавида, 119: d_huseynov@yahoo.com

Резюме. В основу идеи золотоносности Южно-Каспийского нефтегазоносного бассейна положено представление о формировании золотоносных катагенных растворов нефтегазопроизводящими палеоген-нижнемиоценовыми отложениями, которые в полосе развития Волга-Дон–Предкавказье–Закаспий характеризуются исключительно высокой рудоносностью и вмещают комплексные сульфидно-фосфатно-редкометально-урановые месторождения осадочного типа. В сульфидах железа постоянно присутствуют золото, кобальт, никель, молибден, рений, реже медь, цинк, свинец и мышьяк, а в пиритоносных горизонтах некоторых регионов часто обнаруживаются включения самородных металлов – золота, висмута, олова и меди.

Детальные геолого-геофизические и изотопно-геохимические исследования показали, что в Южно-Каспийском ОБ в "oil-gas window" наряду с формированием жидких и газообразных углеводородов интенсивно генерировались катагенные водные растворы, насыщенные рудными компонентами, что подтверждено высокими содержаниями и постоянным присутствием в нефтях, битумах и пластовых водах золота, серебра, меди, молибдена, цинка, мышьяка и других металлов. Это обстоятельство стимулировало изучение возможности формирования рудных скоплений в палеоочагах катагенной разгрузки флюидов. Изучение последних на одном из месторождений углеводородов подтвердило наши прогнозы о благородно-металльном и нефтяном парагенезисе в Южно-Каспийском осадочном бассейне.

В пределах зоны выявлены ураганные концентрации золота и палладия, а также индикаторов эпитермального оруденения золота карлинского типа – мышьяка и бария. Выделений золота не обнаружено, оно невидимое, микродисперсное, ассоциирует с сульфидными минералами и рассеяно в породе.

Подобное исследование на предмет поиска золотого оруденения в Южно-Каспийском бассейне проведено впервые и полученные результаты открывают его новые перспективы как золото-нефтегазоносного. Выявленная золоторудная минерализация знаменует открытие нового генетического типа золотого оруденения в Азербайджане, известного в мире как стратиформный карлинский тип с дисперсным и низким содержанием золота, которое компенсируется большой протяженностью минерализованных зон и крупными запасами.

Ключевые слова: *золото, нефтяное месторождение, минерализация, благородно-метальный и нефтяной парагенезис, центры разгрузки флюидов, геохимическая аномалия, стратиформные залежи*

CƏNUBİ XƏZƏR HÖVZƏSİNİN NEFTDAŞIYAN SAHƏLƏRİNDƏ QIZIL FİLİZİ TƏZAHÜRLƏRİ**

Hüseynov D.A.
Azərbaycan Respublikasının Elm və Təhsil Nazirliyi, Geologiya və Geofizika Institutu AZ1143, Bakı, H.Cavid prosp., 119: d_huseynov@yahoo.com

Xülasə. Cənubi Xəzər neft-qaz hövzəsinin qızıllı olma ideyasının əsasını neft-qaz istehsal edən Paleogen-Aşağı Miosen çöküntüləri ilə tərkibində qızıl olan katagen məhlullarının formalaşması təşkil edir. Volqa-Don-Zaqafqaziya-Xəzəryanı regionunun inkişaf zonasında Paleogen-Aşağı Miosen çöküntüləri kompleksi yüksək filiz tərkibi ilə səciyyələnir və mürəkkəb çöküntü tipli sulfid-fosfat-nadirmetal-uran yataqlarının olması ilə ifadə edilir. Dəmir sulfidlərin tərkibində qızıl, kobalt, nikel, molibden, renium, daha az mis, sink, qurğuşun və arsen bəzi regionların piritli horizontlarında isə çox vaxt xalis metallar – qızıl, vismut, qalay və mis aşkar olunur.

Geoloji-geofiziki və izotop-geokimyəvi tədqiqatlar göstərdi ki, Cənubi Xəzər hövzəsində neft-qaz pəncərəsində maye və qaz halında karbohidrogenlərin əmələ gəlməsi ilə yanaşı, filiz komponentləri ilə doymuş katagen sulu məhlulları da intensiv şəkildə əmələ gəlir və bu da neftlərdə, bitumda və lay sularında qızıl, gümüş, mis, molibden, sink, arsen və digər metalların yüksək tərkibi və daimi olması ilə təsdiq edilir. Bu hal flüidlərin katagen boşalmasının paleo-ocaqlarında filiz yığılmalarının əmələ gəlməsinin mümkünlüyünün öyrənilməsinə təkan verdi. Karbohidrogen yataqlarından birində sonuncunun tədqiqi Cənubi Xəzər çöküntü hövzəsində nəcib metal və neft paragenezi ilə bağlı proqnozlarımızı təsdiqlədi.

Zona daxilində qızıl və palladiumun qasırğa konsentrasiyası, karlin tipli epitermal qızıl minerallaşmasının göstəriciləri – arsen və barium aşkar edilmişdir. Qızıl dənələri aşkar edilməmişdir, o, görünməzdir, mikrodispersdir, sulfid mineralları ilə assosiasiya olunur və süxurda səpələnmişdir.

İlk dəfədir ki, Cənubi Xəzər hövzəsində qızıl minerallaşmasının axtarışı üçün belə bir tədqiqat aparılır və əldə edilən nəticələr onun qızıl-neft-qazlı ərazi kimi yeni perspektivlər açır. Müəyyən edilmiş qızıl minerallaşması Azərbaycanda qızıl minerallaşmasının yeni genetik növünün aşkar edilməsini göstərir, dünyada dispers və aşağı qızıl tərkibinə malik stratiform karlin tipi kimi tanınan minerallaşmış zonaların genişliyi və böyük ehtiyatlarla kompensasiya olunur.

Açar sözlər: *qızıl, neft yatağı, minerallaşma, nəcib metal və neft paragenizi, flüid axını mərkəzləri, geokimyəvi anomaliya, qatlı yataqlar*

* Дискуссионная статья

** Müzakirə məqaləsi

ANAS Transactions Earth Sciences 1 / 2024

http://www.journalesgia.com

MÜNDƏRİCAT

CONTENTS

ОГЛАВЛЕНИЕ